Diversity of the biophony of Polynesian photic and mesophotic coral reefs

by **Xavier Raick**

A thesis submitted in conformity with the requirements for the degree of *Philosophiæ doctor* (Faculty of Sciences, Doctoral College in Biology of Organisms and Ecology)

Academic year 2023 – 2024

Laboratory of Functional and Evolutionary Morphology

Department of Biology, Ecology, and Evolution – FOCUS

Faculty of Sciences

University of Liège

Supervisors: Prof. Parmentier[1] and Prof. Di Iorio[2]

[1]Laboratory of Functional and Evolutionary Morphology, FOCUS, University of Liège, Liège, Belgium

[2]CEFREM, CNRS/UMR 1510, University of Perpignan Via Domitia, Perpignan, France

LIÈGE université
Laboratoire de Morphologie Fonctionnelle & Évolutive

CEFREM

Diversity of the biophony of Polynesian photic and mesophotic coral reefs

by **Xavier Raick**

A thesis submitted in conformity with the requirements for the degree of *Philosophiæ doctor*
(Faculty of Sciences, Doctoral College in Biology of Organisms and Ecology)

Academic year 2023 – 2024

Thesis jury:

Prof. Gobert, president (University of Liège, Liège, Belgium)

Prof. Frédérich, secretary (University of Liège, Liège, Belgium)

Dr. Picciulin, member of the jury (Istituto di Scienze Marine, Venice, Italy)

Dr. Bolgan, member of the jury (Ocean Science Consulting Limited, Dunbar, UK)

Prof. Di Iorio, supervisor (University of Perpignan Via Domitia, Perpignan, France)

Prof. Parmentier, supervisor (University of Liège, Liège, Belgium)

Laboratory of Functional and Evolutionary Morphology

Department of Biology, Ecology, and Evolution – FOCUS

Faculty of Sciences

University of Liège

Supervisors: Prof. Parmentier[1] and Prof. Di Iorio[2]

[1]Laboratory of Functional and Evolutionary Morphology, FOCUS, University of Liège, Liège, Belgium

[2]CEFREM, CNRS/UMR 1510, University of Perpignan Via Domitia, Perpignan, France

Cover page: External slope of the barrier reef, Bora Bora, French Polynesia (divers: 90 m, bottom: 120 m) © Franck GAZZOLA / UNDER THE POLE / Zeppelin Network

To forgotten generations of coal miners, may this work be a little light for them in the dark.

To Stacy, may this book be a drop of hope for her in an ocean of sadness.

To Laurent, may this journey be a dive into his memories of these islands.

Contents

Abstract

In the ocean, major biophonic sources include benthic invertebrates, fish, and marine mammals. This acoustic activity can be studied at two levels: at the level of individually identifiable sounds from generally nearby sources of the biophony and at the level of 'mass-phenomena', i.e., continuous noises resulting from the calls of many individuals vocalizing simultaneously. We chose to focus this thesis on French Polynesia for three reasons: the high concentration of coral reefs in the South Pacific, their relatively good preservation, and the scientific knowledge accumulated in Moorea Island. The main objective of this research thesis is to determine how the diversity of the biophony of photic and mesophotic French Polynesian coral reefs varies. We studied the spatiotemporal variation of both the 'mass-phenomena' and individually identifiable sounds of the biophony and we investigated how long-term modifications affect it. The biophony of French Polynesian coral reefs consist primarily of fish sounds and broadband transient sounds emitted by benthic invertebrates. From the reef to the open ocean, this biophony can propagate up to 90 km, although maximal detection distances vary depending on the physical characteristics of the water column and bottom nature, the species and life stage, ranging from less than 0.5 km to 22 km. However, these distances can be reduced due to meteorological conditions and anthropogenic noise. Across the vertical gradient, benthic invertebrate and fish sounds display a stratification primarily determined by depth. We have observed similarities between the sonic morphology of fish species in French Polynesia and well-known temperate sonic species within the same families. Moreover, similarities between sounds from these temperate species and unidentified sounds previously recorded in Polynesian mesophotic coral ecosystems (MCEs) were highlighted. Various methods have been used to study this vocal diversity, among which we have shown that α-acoustic diversity indices are not suitable for inferring marine fish sound diversity. Temporal variations were studied at various time scales. In photic reefs and upper MCEs, sounds produced by benthic invertebrate were louder at night. However, in lower MCEs, the activity rhythms of benthic invertebrates exhibited low or highly variable levels of diel variation. Nonetheless, a distinct peak in the number of BTS was observed between 7 and 9 PM at a depth of 120 m, potentially indicating the presence of cyclic activities of a particular species and supporting the existence of different invertebrate communities in deep mesophotic reefs. Concerning fish sounds, depth has been shown to have an influence on diel cycle and the width of realized acoustic niches. At a longer timescale, changes in the French Polynesian biophony have been observed in response to long-term environmental shifts, such coral degradation following coral bleaching events.

French translation of the abstract

Dans l'océan, les principales sources biophoniques comprennent les invertébrés benthiques, les poissons et les mammifères marins. Cette activité acoustique peut être étudiée à deux égards : au niveau des sons individuellement identifiables provenant généralement de sources biophoniques proches et au niveau des « phénomènes de masse », c'est-à-dire, les bruits continus résultant des vocalisations de nombreux individus qui vocalisent simultanément. Nous avons choisi de centrer cette thèse sur la Polynésie française pour trois raisons : la grande concentration de récifs coralliens dans le Pacifique sud, leur relativement bonne préservation, et les connaissances scientifiques accumulées sur l'île de Moorea. L'objectif principal de cette thèse est de déterminer comment la diversité de la biophonie des récifs coralliens polynésiens, tant photiques que mésophotiques, varie. Nous avons étudié la variation spatiotemporelle à la fois des « phénomènes de masse » et des sources biophoniques proches, et nous avons examiné l'impact des modifications humaines sur cette biophonie. La biophonie des récifs coralliens polynésiens se compose principalement de sons de poissons et de sons large bande émis par les invertébrés benthiques. Du récif vers le large, cette biophonie peut se propager jusqu'à 90 km, bien que les distances maximales de détection varient en fonction de caractéristiques physiques de la colonne d'eau et du fond, des espèces et de leurs stades de vie, allant de moins de 0,5 km à 22 km. Cependant, ces distances peuvent être réduites en raison des conditions météorologiques et du bruit anthropique. D'un point de vue du gradient vertical, les sons des invertébrés benthiques et des poissons présentent une stratification principalement déterminée par la profondeur. Nous avons observé des similitudes entre la morphologie sonique des espèces de poissons en Polynésie française et des espèces tempérées de ces mêmes familles et connues comme étant capables d'émettre des sons. De plus, les sons de ces espèces tempérées ressemblent à des sons non identifiés enregistrés précédemment dans les écosystèmes coralliens mésophotiques (MCE) polynésiens. Diverses méthodes ont été utilisées pour étudier cette diversité vocale, parmi lesquelles nous avons montré que les indices de diversité acoustique α ne sont pas adaptés pour étudier la diversité des sons des poissons marins. Les variations temporelles ont été étudiées à différentes échelles de temps. Dans les récifs photiques et les MCE supérieurs, les sons produits par les invertébrés benthiques étaient plus forts la nuit. Cependant, dans les MCE inférieurs, l'activité des invertébrés benthiques présentait des niveaux de variation journalière faibles ou très variables. Néanmoins, une augmentation du nombre de sons entre 19 h et 21 h à une profondeur de 120 m a été observée, indiquant potentiellement la présence d'activités cycliques d'une espèce particulière et soutenant l'existence de communautés d'invertébrés différentes dans les récifs mésophotiques profonds. En ce qui concerne les sons de poissons, la profondeur influençait le cycle jour/nuit et la largeur des niches acoustiques réalisées. À une échelle temporelle plus longue, des changements dans la biophonie polynésienne ont été observés en réponse à des changements environnementaux, tels que la dégradation des coraux suite à des épisodes de blanchissement corallien.

Preface

Two worlds collide as the boat approaches the pass between the lagoon and the ocean: turquoise meets navy blue. The sound of waves accompanies the heaving motion of the boat, replacing its previous pitching and rolling movement. While brown noddies and frigatebirds watch us perched on buoys and spars, our eyes scan the sky looking for brown boobies and tropicbirds. We arrive at our study site; it is time to prepare. I make sure my diving cylinder is open, put on my BCD, check my regulators, don my mask and fins, and ensure I have all the acoustic equipment with me.

As soon as I enter the water, a new world unfolds before me. From the very beginning, a gentle crackling fills my ears, adding to the sound of the water lapping at the surface and the bubbles from my exhalations. As for the visuals, the sun playing on the water's surface creates a mesmerizing gradient of blue and transparency. Gazing upward reveals a liquid mirror adorned with dancing streams of bubbles. I descend towards the bottom and see shoals of blue triggerfish and black triggerfish swinging their caudal and anal fins in the current, feeding on zooplankton. I shift my focus to observe the play of light on colonial radiolarians drifting in the mass of water. I adjust my eyes to try to spot a blacktip shark, or with a bit of luck, a lemon shark, as long as my horizon is still wide enough.

The seafloor looks like gentle little valleys separated by small hills, all adorned with coral. Solitary *Fungia* corals rest on a carpet of *Pocillopora* colonies. As I descend, the pressure increased and the volume of my BCD decreases. Nevertheless, I continue to descend while carefully injecting air into my BCD to arrive gently near the bottom. Numerous damselfish colonies weave between the branches of coral, entering and emerging as if reflecting a slow breathing of the reef. As I approach the seafloor, I carefully navigate around a colony of fire coral that I spotted on my descent. My eyes behold a kaleidoscope of life in all its abundance: goatfish, Moorish idols, pufferfish, Picasso triggerfish, orange-lined triggerfish, bannerfish, longnose butterflyfish, parrotfish, schools of red and bluestripe snappers, six-banded wrasses, and other wrasses. Perched atop a coral, a lizard fish gracefully glides away, its path crossing with two butterfly fish and an angel fish.

As I approach a coral to observe a hawfish hidden within, I hear the displeasure of a yellowtail dascyllus. This fast staccato makes me smile. I am here partly for it. Upon reaching the desired depth, I search for an optimal location to deploy the acoustic recorder I brought with me.

Today, I will not have time to visit the overhang and see if a hawksbill sea turtle or a nurse shark is resting there among cardinalfish, squirrelfish and soldierfish; or to observe the clownfish in their anemones. It is time to go back up. I ascend slowly, having spent only five minutes underwater, a time that will be well worth the extensive analysis to come.

Acknowledgments

There is no framed content without proper oversight. I could not have undertaken this journey without the invaluable patience and feedback of Prof. Parmentier (Laboratory of Functional and Evolutionary Morphology, ULiège) and Prof. Di Iorio (CEFREM, UPVD). I am also extremely grateful to the other members of my defense committee: Prof. Gobert (*Océanographie biologique*, ULiège) and Prof. Ovidio (*Gestion des Ressources Aquatiques et Aquaculture*, ULiège) for their numerous items of advice and guidance. I would like to thank the members of the final jury: Prof. Di Iorio, Prof. Frédérich, Prof. Gobert, Prof. Parmentier, Dr. Bolgan, and Dr. Picciulin.

On the financial side, this work would not have been possible without the generous support from FOCUS, the University of Liège (*Patrimoine et missions scientifiques*), the *Fondation de l'Université de Liège*, the *Société Royale des Sciences de Liège*, the *Fonds de la Recherche Scientifique* – FNRS (F.R.S. – FNRS), the Wallonia-Brussels Federation (*Subside pour participation à une reunion scientifique de la FWB*), the Royal Academy of Science, Letters and Fine Arts of Belgium (*Fonds Agathon de Potter*), the King Leopold III Fund for Nature Exploration and Conservation, the Royal Belgian Zoological Society, the European Commission, the Aquatic Ecology section of the Ecological Society of America, and the Les Real & Jim Brown Student Travel Award. Thanks to Prof. Grégoire, Dr. Van Goethem, Dr. Lepoint, and Ms. Foguenne for their help during the funding process. I am also grateful to the Intergovernmental Oceanographic Commission (UNESCO) to have endorsed one of my projects as Decade action No.74.4 'Acoustics to Assess the Health Status of Reefs' as part of the UN Decade of Ocean Science for Sustainable Development 2021-2030.

I am also grateful to my colleagues from the laboratory of Prof. Parmentier and the newly established laboratory of Prof. Frédérich. Thank you, Dr. Bolgan, for the very long discussions we had on Bromeliaceae, Mr. Panopoulos, and intangible cultural heritage. Thank you, Dr. Kéver, for always being there to listen to my practice sessions. Thank you, Dr. Gillet, for the tips for the BAEF and Fulbright interviews. Thank you, Dr. Bertucci, for our long collaboration on Polynesian reefs. Thank you, Dr. Colleye, for your explanations on the auditory evoked potential audiometry in fish and on animal welfare. Thank you, Dr. Olivier, for welcoming me to your lab and for your time during the statistics workshop we organized. Thank you, Dr. Dussenne, for being my office neighbor for some months, and for always being cheerful. A big thank you to Dr. Huby for the incredible mission we conducted in Minas Gerais, for having saved my finger following the piranha bite, and for her friendship. Thank you to my co-author,

Dr. Compère, for his assistance with electron microscopy. Thank you, Dr. Henitsoa, for the excellent pies you brought before flying back to Madagascar. I also need to thank Dr. Delaunois, Dr. Gajdzik, Dr. Mélotte, Dr. Salabao, and Dr. Verheye for their scientific advice. In a world where we are always on the go, the efficiency of my schedule would not have been possible without the help of Ms. Lunetta in managing timetable scheduling conflicts. I also need to thank my amphitheater neighbor on Friday afternoons, Ms. Bruls: thank you for our amazing discussions. Thank you, Ms. Banse, one of the four musketeers of the IBAC in Sapporo, for your amazing anecdotes. Thank you, Ms. Laboury, for your assistance during zoology classes and for always keeping me updated with the information you find. Thank you, Ms. Frey, for your physics point of view; it has been useful many times. Thank you, Mr. Van Damme, our stick insect specialist, for our naturalist discussions. Thank you, Mr. Mittelheiser, for sharing the floor with me during the 'Current Issues in Oceanography'. Thank you, Ms. Smeets, for the scuba-diving discussions and for our dive at *La Gombe*. I also need to thank Ms. Henry, Ms. Vignaud, Ms. Eche, Ms. Ravelohasina, and Mr. Braine for all our discussions during midday lunches.

I would like to express my gratitude to the graduate students, whom I supervised during their internship or master's thesis, for the very nice discussions we had: Ms. Solagna, Ms. Millot, Mr. Scalbert, Ms. Koussa, Ms. Laboury, Mr. Leblanc, Ms. Minier, Mr. Collet, Mr. Santoni Guichard, Ms. Krimou, Mr. Campisi, Ms. Cabanne, Ms. Guerin, Ms. Troniseck, Mr. Baccus, and Ms. Vendramme. I am grateful to the *Université de Bretagne Occidentale*, the *Université de Lille* and the *Sciences Sorbonne Université* for their collaboration with us during some of the internships and master's thesis. I had also very good lunch discussions with students I did not supervise. Therefore Ms. Sabbe, Ms. Hourant, Ms. Simonian, Ms. Hamon, Ms. Hanssen, Ms. Huet, Ms. Petrisinec, Ms. Stainier, Mr. Duchesne, Ms. Bertimes, Ms. Leroy, Ms. Greeven, Ms. Soulard, Ms Crucianelli, Ms. Roncali, Ms. Dannemark, Ms. Salbin, and many others who visited us, whether for a day or several months, also deserve special mention.

I wish to express my appreciation to the researchers of Chorus Institute, Sensea, and GIPSA-lab to welcome me in Grenoble several times. I would like to extend my heartfelt thanks to Dr. Gervaise for his help with software and because he always believed in me. I am appreciative to Prof. Mars to allow me to realize an internship in GIPSA-lab and to Dr. Lossent for her help with Chapter 3 and to always choose very good restaurants. I acknowledge the advice of Ms. Audax. Thank you to have undertaken this trip to Geneva with me. I am grateful for the time of

Dr. Desiderà for the many discussions on our theses and on GOT. I would be remiss in not mentioning Ms. Magnin, Mr. Foucher and Mr. Bardet for their friendliness.

I would like to send my heartfelt thanks to the middle of the Pacific Ocean. I would like to express my deepest gratitude to Prof. Lecchini for all the help he provided me during my fieldwork. I am deeply appreciative of the assistance provided by all the administrative staff from the CRIOBE: Dr. Le Guen, Ms. Burns and Ms. Michel. I am indebted to Dr. Caulier, Dr. Lourtie, Ms. Aqua, Ms. Eustache, Mr. Hy, Mr. Iwankow, Mr. Lerouvreur, Ms. Pozas-Schacre, Ms. Léonard, Mr. Schligler, Mr. Espiaux, Mr. Romans, Mr. Morage, Ms. Gairin, Ms. Laboury, and Mr. Gay, for their help during fieldwork. I acknowledge the contribution to Ms. Haguenauer and Mr. Ung for their technical assistance and to Prof. Mann for advice on the equipment. The cover quadrats analyses could not have been completed without the help of Prof. Hédouin, Dr. Rouzé, and Dr. Pérez-Rosales, to whom I am grateful. I am also indebted to all the members of Under the Pole Consortium and all Under The Pole III Expedition members for the positioning of the autonomous recorders. Ms. Boulais deserves my sincere thanks for her help as scientific coordinator of Under the Pole Expéditions. My thanks go to Prof. Mielke and Dr. Sanctorum for their help with micro-CT scan at the University of Antwerp. I am also grateful to Dr. Buscaino and Dr. Farina for her help as academic editor and to Prof. Fine for comments on preliminary versions of several articles. I am grateful to Dr. Riera Vuibert (University of Victoria) for her help with clip submissions and to Ms. Ramos Pamplona and Ms. Biernaux for their time. I had the pleasure of collaborating with Dr. Petersen, Ms. Lilli, Mr. Genten, and Ms. Vastrade. Dr. Pinzone, Dr. Godefroid, and Mr. Kurchevski have my appreciation for their unwavering encouragements and for our good discussions. My sincere thanks go to Mr. Boulanger for his participation to the FOCUS project. I thank Mr. Beguet and Mr. Mamode for providing some fish specimens. My thanks go also to Dr. Fricke (Stuttgart State Museum of Natural History), for the help with fish identification. I am grateful to Dr. Pauwels (IRSNB) and Ms. Bournonville (*Aquarium-Museum de l'Université de Liège*) for their help with administrative procedures for museum collections. My thanks go to Prof. Fonseca and Dr. Amorim (University of Lisbon) for their help with sonic data in controlled environment. I would like to recognize Prof. Haesbroeck and Dr. Klenkenberg for their advice on statistics. I would like to extend my sincere thanks to Dr. Bertucci and Dr. Williams for their help with R codes. Many thanks to the staff from the Belgian scientific diving team, especially Prof. Mallefet, Dr. Norro, Mr. Cox, and Mr. Lefever. The GLUBS group and Dr. Parsons deserve a mention for including me in the WOPAM action. Within this group, I am grateful to Prof. Rice for our

discussions on post-docoral opportunities. Thanks to other researchers from Cornell University, especially Dr. Sugai, Dr. Klinck, Dr. Cohen, Dr. Bouffaut, Ms. Garcia, and Mr. Tessaglia for their advice on my post-doctoral fellowship proposals. Thank you to Dr. Laboury, Dr. Zorzi, Ms. Bertucci, Ms. Clotuche, Mr. Wascotte, Mr. Wanet, and Mr. Donckels for their coaching for postdoctoral fellowships. I would like to thank my colleagues from the *Young Zoologists Group* of the *Royal Belgian Zoological Society*, especially my colleague for workshops organization, Ms. Micha, and our co-president, Mr. Laurent. Special thanks should also be addressed to Dr. Olivier and Mr. Rabasco from the *Universidad Autónoma de Baja California Sur* for the nice discussions we had during fieldwork.

This thesis was realized on an assistant position, i.e., a half time teaching position. Therefore, I would like to thank my teaching colleagues: Prof. Thiry, Dr. Goosse, Dr. Castillo Cabello, Dr. Fanara, Mr. Balthasart, Mr. Brouwers, Mr. Sottiaux, Ms. Compère, and Ms. Mouton. Thanks to Dr. Rougeot and Mr. Prignon for their help with tilapias. Thanks to Prof. Carnol for the interesting discussions we had during the supervision of her exam. Thanks to Prof. Gobert, Dr. Das, Dr. Lejeune, Ms. Lefebvre, and Mr. Delforge for their help at STARESO during these several years. Thanks to the professors and students from the high school present during the *CONCOURS CORSICA*. Thanks to Dr. Roberty for his help with Erasmus Mundus ECT+ and MER students. I also would like to thank all the amazing students I have had the opportunity to teach. I would also like to thank my colleagues from the department board, research unit board, Faculty board, and PhD board. Thank you, Prof. Plumier, for the advice on thesis submission dates. Thanks to my colleagues Ms. Marcq, Ms. Schraepen, and Ms. Dukers for their good mood in Strasbourg.

Thanks should also go to the many professors that help me to arrive to this stage: Ms. Villaverde Vaya, Ms. Dominguez Fernandez, Mr. Lauria, Ms. Thiry, Ms. Stas, Ms. Dethier, and many more. Thanks to my best friend Dr. Benard for all her advice. Thanks to all my scuba-diving colleagues: Ms. Pierard, Mr. Pusic, and many more. Lastly, I would be remiss in not mentioning my family, especially Ms. Granziero, Mr. J-M Raick, Ms. Legenty, Ms. Pérez Nuñez, Ms. Clavier, Mr. G. Clavier, Mr. A. Clavier, Ms. Mertens, Mr. L Raick, Ms. Raick, Mr. Remi, Ms. Bultôt†, Mr. Dubois†, Mr. W. Soto Pérez, Mr. J. Soto Pérez, and Mr. L. Clavier. I would also like to thank Maiko for all the emotional support.

Lastly, I want to express my deepest gratitude to all those I may have unintentionally overlooked in my acknowledgments. Your contributions are equally valued and appreciated.

Abbreviations

2D	two dimensions	**CNES**	*Centre national d'études spatiales*	**H'**	acoustic diversity index
2P	two pulses			**H_2CO_3**	carbonic acid
a	slope coefficient	**CNN**	convolutional neural network	**HDBSCA**	hierarchical density-based
A	Austral Islands	**CNRS**	*Centre national de la recherche scientifique*	**N**	spatial clustering
ACI	acoustic complexity index			**H_f**	spectral entropy, see SE
ACI_f	sub-part of the ACI, opposed to ACI_t	**CO_2**	carbon dioxide	**HI**	pseudo-harmonic interval
		CRIOBE	*Centre de Recherches Insulaires et Observatoire de l'Environnement*	**H_m**	entropy of spectral maxima
ACI_{tot}	total value of the ACI			**H_t**	temporal entropy, see TE
ADI	acoustic diversity index			**H_y**	entropy of spectral variance
ADI_v1	ADI (step = 500 Hz, threshold = −25 dB)	**CS**	complex sound	**HP**	protected habitat area
		D	day	**H.R.**	Héloïze Rouzé
ADI_v2	ADI (step = 100 Hz, threshold = −50 dB)	**dB**	decibel	**HTI**	High Tech Inc.
		df	degree(s) of freedom	**Hz**	hertz
AE	acoustic evenness index, see AEI	**D.L.**	David Lecchini	**IBAC**	International Bioacoustics Congress
		Dr.	doctor		
AEI	acoustic evenness index	**DS**	downsweeping sound	**i.e.**	*id est* (that is)
AEI_v1	AEI (step = 500 Hz, threshold = −25 dB)	**DSG**	digital spectrogram long-term acoustic recorder	**IFRE-COR**	*Initiative Française pour les Récifs Coralliens*
AEI_v2	AEI (step = 100 Hz, threshold = −50 dB)	**E**	East	**Is.**	island
		E2B	*entre deux baies*	**Inc.**	incorporated
AEve	acoustic evenness index, see AEI	**ECT**	environmental contamination and toxicology	**IQR**	interquartile range
				IRSNB	*Institut royal des Sciences naturelles de Belgique*
AI (I)	amplitude index, see M (index)	**EEZ**	exclusive economic zone		
AI (II)	artificial intelligence (general)	**É.P.**	Éric Parmentier	**J.C.**	Julien Campisi
AIC	Akaike information criterion	**EPHE**	*École Pratique des Hautes Études*	**J.L.**	Julie Lossent
AM	*ante meridiem*			**K**	Kiribati Islands
ANCOVA	analysis of covariance	**F**	Statistics of the model	**kHz**	kilohertz
ANH	acoustic niche hypothesis	**edf**	effective degree(s) of freedom	**km**	kilometer
ANL	ambient noise level	**e.g.**	*exempli gratia*	**kn**	knots
ANR	*Agence Nationale de la Recherche*	**FAO**	Food and Agriculture Organization	**kV**	kilovolt(s)
				KW	Kruskal-Wallis
APPPS	alternating pulse period PS	**F.B.**	Frédéric Bertucci	**L**	ligament
AR (I)	acoustic richness index (index)	**Fig**	figure	**LDEO**	Lamont-Doherty Earth Observatory
AR (II)	acoustic release (general)	**FFT**	fast Fourier transform		
ARic	acoustic richness index, see AR	**FL**	Florida	**L.D.I.**	Lucia Di Iorio
		FM	frequency-modulated	**LFFT**	long FFT, see FFT
AS	arched sound	**FOCUS**	Freshwater and Oceanic sCiences Unit of reSearch	**L.H.**	Laetitia Hédouin
b	y-intercept			**log**	logarithm(ic)
BAEF	Belgian American Educational Foundation	**FP**	French Polynesia	**LT**	long tonal call
		FPT	fast pulse train	**m**	meter(s)
BCD	buoyancy control device	**FM_{CS}**	see CS	**M** (I)	amplitude index, see AI (index)
BI	bioacoustic index	**FM_{DS}**	see DS	**M** (II)	Marquesas Islands (geography)
Bio	bioacoustic index, see BI	**FM_{US}**	see US	**MA**	Massachusetts
BP	*boite postale*	**Fpeak**	peak frequency	**M.B.**	Marta Bolgan
BTS	broadband transient sounds	**FRS-FNRS**	*Fonds de la recherche scientifique*	**MCA**	marine control area
BTS Fpeak	peak frequency of BTS			**MCE**	mesophotic coral ecosystem(s)
		FWB	*Fédération Wallonie-Bruxelles*	**MEA**	marine educative area
BTS SPL_{pp}	SPL_{pp} of BTS	**G** (I)	Gambier Islands (geography)	**Mean Sq**	mean square
		G (II)	giant clams protection (protection)	**min**	minute(s)
BW	bandwidth			**misc**	miscellaneous
BY	Benjamini Yekutieli	**GAM**	generalized additive model	**MMA**	marine managed area
C	Cook Islands	**GEBCO**	General Bathymetric Chart of the Oceans	**MN**	Minnesota
°C	degree Celsius			**MPA**	marine protected area
CA (I)	California (geography)	**G.I.**	Guillaume Iwankow	**Mr.**	mister
CA (II)	cycle absent (figures)	**GIPSA**	*Grenoble Images Parole Signal Automatique*	**ms**	millisecond(s)
CBW	critical bandwidth			**MS**	Mississippi
CCA (I)	canonical correspondence analysis (method)	**GIS**	geographic information system	**Ms.**	neutral form for 'Miss' or 'Mrs.'
		GLUBS	Global Library of Underwater Biological Sounds		
CCA (II)	crustose coralline algae (ecology)	**GOT**	Game of Thrones	**N** (I)	Number (general)
		G.P.R.	Gonzalo Pérez-Rosales	**N** (II)	Night (diel cycle)
CTD	conductivity, temperature, and depth	**GPS**	global positioning system	**N** (III)	not present (tables)
		GS	Simpson spectral entropy = Gini Simpson index	**N** (IV)	net fishing prohibited (conservation)
CEFREM	*Centre de Formation et de Recherche sur les Environnements Méditerranéens*			**n°**	number
		G.S.	Gilles Siu	**N/A**	not-applicable
		GU	Guam	**NB**	realized acoustic niche breadth
c.f.	*confer*	**h**	hour(s)	**NB***	standardized NB
C.G.	Cédric Gervaise	**H**	acoustic entropy index = total entropy	**NB_{freq}***	NB* for the frequency axis
cm	centimeter(s)			**NB_{pp}***	NB* for the pulse period axis

NB_{temp}* NB* for the diel axis
ND no data
NDSI normalized difference soundscape index
NGA National Geospatial-Intelligence Agency
nMPA marine non-protected area
NMDS nonmetric multidimensional scaling
No. number of
NOAA National Oceanic and Atmospheric Administration
NoBTS number of detected BTS
NP (I) protected natural area (protection)
NP (II) acoustic complexity index (index)
NP (III) number of peaks (acoustics)
NS not significant
NSF National Science Foundation
NT natural tourist area
N.W. North-West
NY New-York (state)
P fishing prohibited
P *P*-value
Pa Pascal
PAM passive acoustic monitoring
PC principal component
PCA principal components analysis
PerMAN permutational multivariate analysis of variance
OVA
PGEM *Plan de Gestion de l'Espace Maritime*
pH potential of hydrogen
PM *post meridiem*
PMEL Pacific Marine Environmental Laboratory
pp (I) peak-to-peak (for SPL)
pp (I) pulse period (for NB_{pp}*)
PS pulse series
PSD power spectral density
PSD_{Fpeak} highest PSD value
PSL Université Paris Sciences & Lettres
Prof. Professor
Q percentile
r (I) radius (propagation)
r (I) number of resource classes (niche breadth)
R (I) Renyi spectral entropy (index)
R (II) multiple correlation (statistics)
R (III) similarity metric (*anosim* statistic)
R (IV) R Core Team (software)
R (V) fishing restrictions (conservation)
r_0 initial range
R^2 coefficient of determination
RA rahui
r_B dissimilarity between groups
RDA redundancy analysis
re relative
Res reserve
RI integral reserve
RL received level
rms root mean square
r_W dissimilarity within groups
s second
S (I) Shannon spectral entropy = Pielou's evenness (index)
S (II) South (general)
S (III) Salinity (oceanography)
S (IV) fishing restrictions for specific fish species (conservation)
S (V) Society Islands (geography)
SD standard deviation
SE spectral entropy, see H_f
S.E. South-East
SHOM *Service hydrographique et océanographique de la Marine*
SIO Scripps Institution of Oceanography
SL source level
SNR signal-to-noise ratio
sp. unnamed species
spp. more than one unnamed species
SP supplementary
SPL sound pressure level
SPL_{pp} peak-to-peak sound pressure level
SPL_{rms} root-mean-square sound pressure level
SPS slow pulse series
Sq squares
SR sunrise
S/R sound duration / file duration ratio
SS sunset
Sum Sq sum of squares
t statistics of the Student's *t*-test
T (I) Tuamotu Islands (geography)
T (II) special protection for turtles and birds (protection)
TE temporal entropy, see H_t
TL transmission loss
U statistics of the Mann-Whitney U test
UFPS ultra-fast pulse series
UK United Kingdom of Great Britain and Northern Ireland
ULiège University of Liège
UMAP uniform manifold approximation and projection
UMR *Unité mixte de recherche*
UN United Nations
UNESCO United Nations Educational, Scientific and Cultural Organization
UPVD *Université Perpignan Via Domitia*
US upsweeping sound
USA United States of America
U.S. United States, see USA
USB universal serial bus
USR *Unité de Service et de Recherche*
UTP Under The Pole
U.T.P. see UTP
UTP3 Under the Pole Expedition III
v vertebra
V volt
vs. *versus*
W (I) Statistics of the test (Mann-Whitney)
W (II) West (Geography)
WAV waveform audio file format
WAVE see WAV
WOPAM World Oceans Passive Acoustic Monitoring Day
WN white noise
X (I) independent variable (equation)
x (II) indeterminate quantity (example)
x' indeterminate quantity
X.R. Xavier Raick
y (I) dependent variable (equation)
y (II) indeterminate quantity (example)
y' indeterminate quantity
Y yes
Z Statistics of the test (Tukey tests)
ZPR specific fishing regulations area
α (I) species diversity (biodiversity)
α (II) attenuation (acoustics)
α (III) threshold value (statistics)
α (IV) medial bundle (morphology)
β (I) true beta (biodiversity)
β (II) additional bundle (morphology)
δ lateral bundle
δ1 lateral tendon 1
δ2 lateral tendon 2
δA rostral part of δ
δB caudal part of δ
Δ difference
Δ_{20m} difference between the peak frequency at 20 m and a given depth
ΔNB* difference of NB* (60 m – 120 m)
ΔNB_{freq}* ΔNB* for the frequency axis
ΔNB_{temp}* ΔNB* for the diel axis
γ spectral, see PSD
γANL spectral ANL
γFpeak spectral Fpeak
γQ spectral Q
γSPL spectral SPL
ρ Spearman's rank correlation
μ-CT micro-computed tomography
χ^2 (I) χ^2 distribution (ANL)
χ^2 (II) χ^2 statistics (Kruskal-Wallis test)

List of Figures

List of Tables

List of Equations

Remark on the digital art used in the thesis

The cover figure of each chapter is generated by an artificial intelligence. This digital art was created with DALL-E (Open AI; San Francisco, USA).

Remark on the spelling of Polynesian terms

Several Polynesian languages exist in French Polynesia. Among them, Tahitian is the most common one. There are several Tahitian spellings in Latin script. The two common ones are the spelling from the Tahitian Academy and the Raapoto spelling. When the spelling of a Polynesian term differed between these two spellings, the French name has been used. For example, Moorea Island can also be spelled Mo‘ore‘a or Mooreà.

Foreword

Tropical coral reefs can be categorized into two distinct ecosystems: the shallow-water coral reefs, often referred to as photic reefs, and the deeper mesophotic coral ecosystems. Photic reefs are renowned for their rich acoustic environment, hosting a diverse array of benthic invertebrate sounds and various fish vocalizations. These sounds exhibit diel variations, as well as habitat-dependent differences. Although our understanding of the photic biophony has made significant progress, with the exception of aspects such as sound propagation, there remains a considerable knowledge gap when it comes to the mesophotic realm of these reefs. In Polynesia, indications suggest the presence of vocal species in mesophotic reefs, but our understanding of the biophony in this environment, including depth-related and diel cycle variations and species identification, remains virtually non-existent. This lack of information is primarily due to the inherent challenges of accessing this ecosystem.

In addition to natural sounds, anthropogenic noise is widespread in reef environments. A comprehensive understanding of the quantification of boat noise and its potential impact on the biophony is still lacking. Moreover, the effects of conservation measures on the biophony are only beginning to be explored. The long-term consequences of these measures on the resilience of coral reefs, particularly in the face of threats like coral bleaching, remain uncharted territory.

The primary objective of this thesis is to investigate the variability of the biophony in both photic and mesophotic coral reefs in French Polynesia, as well as the threats faced by the biophony. This thesis comprises three fundamental components: (*1*) an examination of spatiotemporal variations in the global biophony, (*2*) a detailed description and identification of spatiotemporal variations in discernible nearby sources of the biophony, and (*3*) an assessment of how human alterations, both positive and negative, impact this biophony.

PART I: INTRODUCTION, METHODS & MATERIALS

Chapter 1. General introduction

Parts of this chapter are adapted from Raick 2023 *À l'écoute des profondeurs des récifs coralliens de Polynésie : le décryptage du whoot.* Bulletin de la Société Royale des Sciences de Liège, 92 (1), p. 171-187

Sections of this chapter and portions of the last chapter are currently being prepared for a review.

Other sections have been used for two educational videos on the MANEA platform: *Introduction aux paysages acoustiques marins – Partie 1 : La géophonie et l'anthropophonie* and *Introduction aux paysages acoustiques marins – Partie 2 : La biophonie*.

KEY INFORMATION

'The Silent World'

- ✓ Each place on Earth possesses a unique soundscape consisting of geophony (non-biological sounds), anthropophony (sounds produced by humans), and biophony (sounds produced by non-human animals).
- ✓ Marine mammals, benthic invertebrates, and fish are major sources of biological sounds in the ocean.
- ✓ Efficient sound propagation underwater and affordable recording systems enable the monitoring of marine soundscapes and species.

'Dive to the depth'

- ✓ Corals form reefs by accumulating skeletons, providing a three-dimensional habitat. MCEs are found at depths ranging from 30/40 m to over 150 m. Limited accessibility has resulted in a lack of knowledge about MCEs.
- ✓ The South Pacific region has the highest concentration of coral reefs globally. The Windward islands of French Polynesia are projected to be climate refugia with less severe coral bleaching.
- ✓ Coral reefs are known for their rich vocalization abilities of many species. PAM has been used to study fish sounds and assess habitats in Polynesian reefs. PAM shows potential for studying MCEs.

'Silent Spring'

- ✓ Bleaching, primarily caused by elevated sea temperatures and high solar irradiance, results in the expulsion of endosymbiotic algae from corals and affects reef ecosystems.
- ✓ Anthropogenic noise impacts marine animals, leading to avoidance behavior, hearing loss, stress, disruptions, altered behaviors, and even stranding events.
- ✓ Well-designed and managed MPAs can be effective in increasing fish biomass, protecting live coral cover, and preserving exploited predatory species.

Objectives

- ✓ The objective of the thesis is to determine how the diversity of the biophony of photic and mesophotic French Polynesian coral reefs varies.
- ✓ The thesis is divided into an introduction, three core parts and a discussion.
- ✓ The three core parts focus on the 'mass-phenomena' biophony, the individually identifiable sources of the biophony, and the human modifications of this biophony.

1. ‘The Silent World’: an introduction to marine soundscapes

1.1. Soundscapes and their components

Over 40 years ago, in the heart of the Amazon Basin, scientists conducted sound recordings in a specific location for several weeks. Although, a seemingly stable acoustic environment was observed, the slightest displacement conducted to a noticeable change in the measured bio-spectrum [1]. This observation exemplified the definition of ‘soundscape’ introduced by Schafer some years before [2]. Soundscapes can be categorized into three components: **geophony** (non-biological sounds), **anthropophony** (sounds produced by humans) and **biophony** (sounds produced by non-human animals) (Figure 1) [1]. These diverse sounds convey valuable information and play a crucial role in the survival of animals [3].

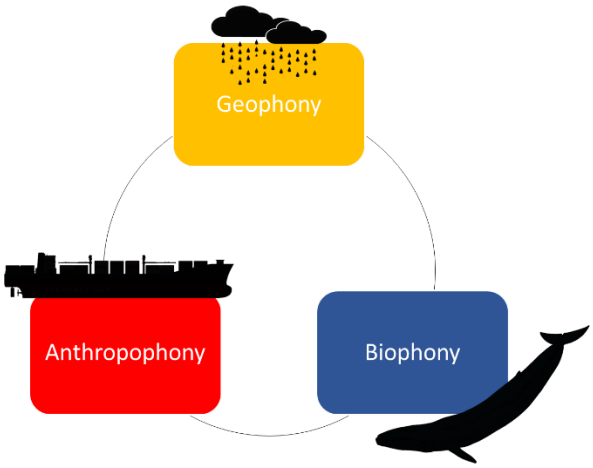

Figure 1 Division of a soundscape into three components: the geophony, the anthropophony, and the biophony.

1.2. Sources of noise in the ocean

In the open ocean, in the absence of local sources (such as the biophony, nearby ships, and local noises), the spectrum of underwater ambient noise can be divided into three frequency bands: low (10 – 500 Hz), medium (500 Hz – 25 kHz), and high (> 25 kHz) [4]. The low-frequency band is predominantly dominated by anthropophony [5]. Sounds in this range experience minimal attenuation, allowing for long-range propagation [4]. The medium-frequency band is primarily attributed to hydrodynamic sources at local or regional scales. This is because higher frequencies in this range cannot propagate over long distances across the sea surface [4–8] (Figure SP1 - 2B). In contract, the high-frequency band experiences extreme acoustic attenuation. As a result, all noise sources in this band, such as thermal agitation [9], are confined to areas in close proximity to the hydrophone [4]. Detailed information about these distinct sources is provided in the following paragraphs.

1.2.1. The geophony: thermal agitation and hydrodynamic sources

Geophony refers to the natural sounds emanating from non-biological sources within the environment. It encompasses a multitude of elements that collectively shape the acoustic landscape of a specific location.

According to the concept of thermal agitation, as the temperature of an object increases, its molecules exhibit more rapid movements (Figure 2). In seawater, this thermal agitation generates noise referred to as '**thermal noise**' [4], whose intensity is logarithmically related to the frequency [9]. Thermal noise dominates marine soundscapes from frequencies above 50 kHz [9] to 60 kHz [4], while below 10 kHz, even the lowest levels of ambient noise surpass the thermal noise levels [5]. In addition to thermal noise, various other acoustic processes continuously occur in the ocean, collectively referred to as hydrodynamic sounds [5].

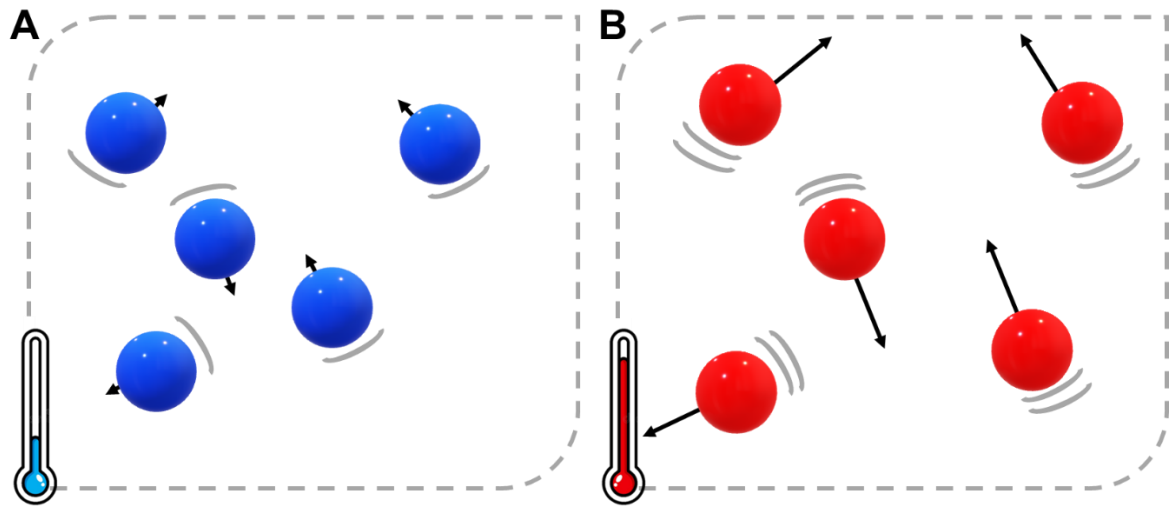

Figure 2 Illustration of thermal agitation for (A) a cold object and (B) a hot object.

Hydrodynamic sources can be classified into four groups: oscillating bubbles, water droplets, surface waves, and turbulence [5]. Many physical objects, such as bubbles, oscillate when disturbed from equilibrium, similar to a pendulum given a push [10]. In the ocean, when air bubbles vibrate, the surrounding medium (i.e., water) dissipates much of the energy as sound [11]. These **oscillations bubbles** can arise from different phenomena (e.g., decaying matter, fish belching, and gas seepages), but they are particularly abundant in surface agitation caused by wind-induced processes [5]. For instance, air can be entrained in the water due to the impact of water droplets on the ocean surface [6] (Figure 3). The second group of sounds is generated by the impact of **water droplets** on the ocean surface. Additionally, fluctuations in the ocean's surface (**surface waves**) induce subsurface pressure variations that influence the underwater ambient noise [7,8]. Lastly, **turbulence** resulting from (*1*) the interaction between water and

the ocean floor, (*2*) surface agitation, and (*3*) internal water movements (advection, convection, and density currents) also contributes to noise production [5].

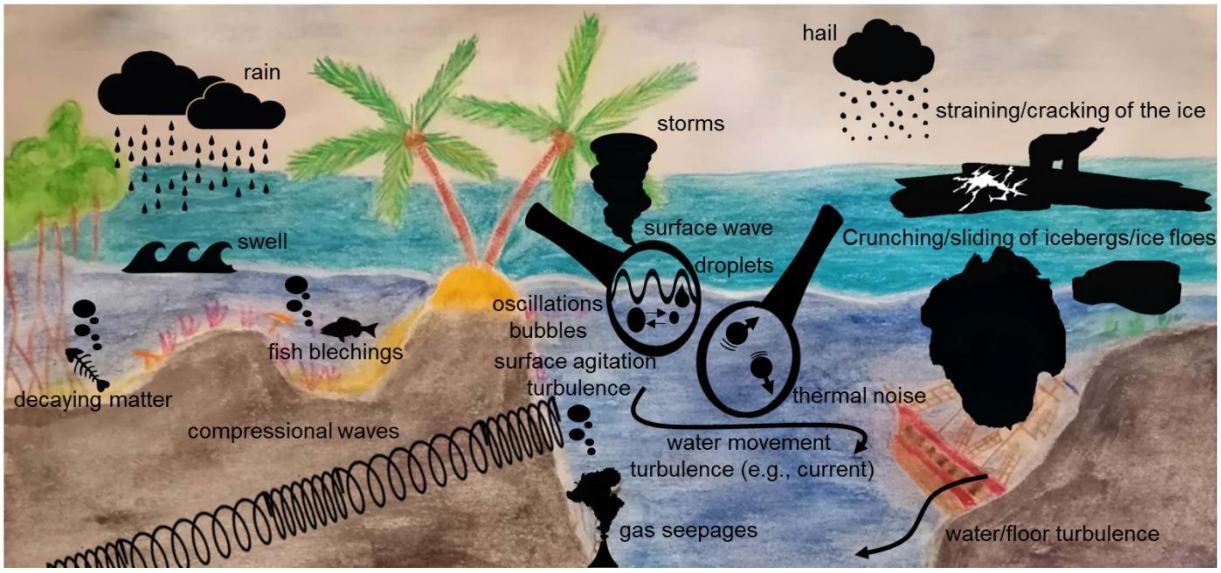

Figure 3 Illustration of the main components of the marine geophony. Decaying matter, fish belching, and gas seepages are source of oscillating bubbles. Swell and storms contribute to the seismic background.

1.2.2. Other components of the geophony

Additional non-biological sounds can be heard in the ocean. These sounds result from volcanic and tectonic sources (compressional waves) [12,13], transient events (storms and swells), precipitation, and sea-ice movements [5] (Figure 3 and Figure 4).

1.2.3. The anthropophony

The most noticeable sounds produced by humans in the ocean are related to ships. These sounds can be divided into two groups: traffic noise and ship noise (Figure 5). **Ship noise** refers to the noise caused by a ship or ships in close proximity, resulting in short-term variations in the soundscape (Figure 4). **Traffic noise**, on the other hand, is the combined effect of all non-immediate ship traffic [5] across an entire basin, even when no ships are visible nearby [4]. Although traffic noise may be less obvious than ship noise, it dominates the low-frequency band (10 – 500 Hz) [14,15]. Ship noise includes broadband noise caused by bubble collapse at the propeller blade tips as well as tonal components associated with blade passages [4]. Furthermore, other sources of ship noise include machinery such as generators, engines, hydraulic power plants, and pumps [4].

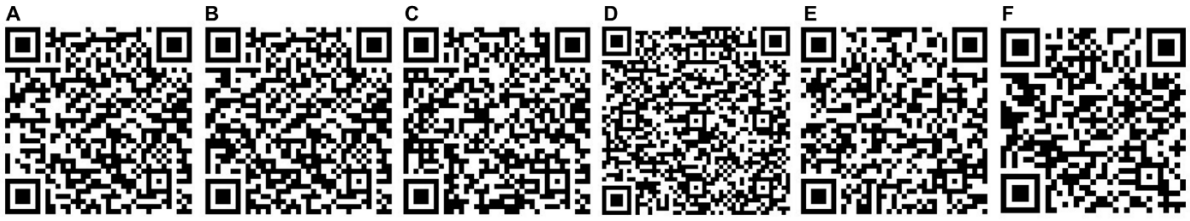

Figure 4 Geophysical and anthropic sounds. (A) Ice calving, (B) ice singing, (C) airguns for seismic exploration (accelerated 10x), (D) pile driving, (E) small vessel, and (F) large vessel. (**A**) NOAA (Fisheries) 2023. 03-ice-calving-clip. https://www.fisheries.noaa.gov/s3/2023-04/Ice-Calving-AWI-Van-Opzeeland-03-ice-calving-clip.mp3 (**B**) NOAA (Fisheries) 2023. 02-ice-singing. https://www.fisheries.noaa.gov/s3/2023-04/Ice-singing-AWI-Van-Opzeeland-02-ice-singing-clip.mp3 (**C**) NOAA (PMEL) 2000. MarcCE-airguns-10x https://www.pmel.noaa.gov/acoustics/env-noise/sounds/airguns_00_03_05_marCE-Airguns-10x.wav (**D**) NOAA (Fisheries) 2023. Pile-driving-high-level-MarthasVineyard https://www.fisheries.noaa.gov/s3/2023-04/Pile-driving-high-level-MarthasVineyardFerryTerminal-NOAA-PAGroup-02-Rowell-pile-driving-clip.mp3 (**E**) NOAA (Fisheries) 2023. 08-Vessel-clip https://www.fisheries.noaa.gov/s3/2023-04/Vess-GRNMS-NOAA-PAGroup-08-vessel-clip.mp3 (**F**) NOAA (Fisheries) 2023. Vess-05-Large-vessel-clip https://www.fisheries.noaa.gov/s3/2023-04/Vess-05-large-vessel-clip.mp3 Used with permission from NOAA PMEL.

Figure 5 Illustration of the main components of the marine anthropophony. Planes and cars serve as examples of terrestrial/aerial acoustic sources that impact coastal waters.

In addition to ship activities, **industrial activities** such as pile driving, hammering, and riveting generate noise, especially in near-shore areas [5,16] (Figure 4). **Explosions**, including the removal of structures, military mines, bombs, and torpedoes [4], also act as significant sources of broadband and highly energetic underwater noise [4]. These events typically occur at regional scales, although some can be detected across multiple ocean basins [17]. Furthermore, smaller explosions are utilized by fishermen to stun or kill fish, or to deter pinnipeds [4]. During **seismic exploration**, air-gun arrays are towed by marine vessels and produce sounds through the expansion and contraction of released air bubbles [18] (Figure 4 and Figure 5).

Sonars are a significant additional source of anthropogenic noise, particularly in the mid-frequency band [4]. **Mid-frequency sonars** are utilized for detecting submarines at moderate ranges, while **low-frequency active sonars** are employed for military surveillance. **Civilian and commercial sonars** operate at higher frequencies that attenuate rapidly, resulting in localized effects [4]. Although they generally produce sounds at lower source levels compared to military sonars, they are more widespread [4]. They are employed for seafloor mapping, with mid-frequencies used in deep-water systems and high-frequencies used in shallow water systems [4]. Sonar are also used to detect plankton and schools of fish [19] and for underwater search and recovery operations. Stationary **modems used for acoustic telemetry** and **acoustic deterrent/harassment devices** (technologies employed to deter marine mammals from fishing gears and aquaculture facilities [20]) also contribute to anthropogenic noise. Finally, **noises originating from other environments**, such as cars and planes, can be detected within the marine anthropophony.

1.2.4. The biophony

Many marine species produce noise or sounds across a wide frequency range, ranging from very low frequencies (< 15 Hz) [21] to very high frequencies (> 100 kHz) [22]. This acoustic activity can be studied at two levels. The first level involves discerning **individually identifiable sounds from generally nearby sources**, requiring the comparison of a diverse range of distinctive acoustic events, often referred to as 'sounds', 'calls', or 'vocalizations', each with limited duration. The second level, referred to as the acoustic '**mass-phenomena'** level, pertains to longer, continuous biological noises that result when many individuals vocalize simultaneously [23–25]. Major sources of biophonic sounds include benthic invertebrates, fish, and marine mammals (Figure 6). The behaviors responsible for sound production by these taxa are variable, encompassing both communication sounds, such as those produced by marine mammals and fish, as well as non-communication sounds, which can occur, for example, when benthic invertebrates move or fish feed.

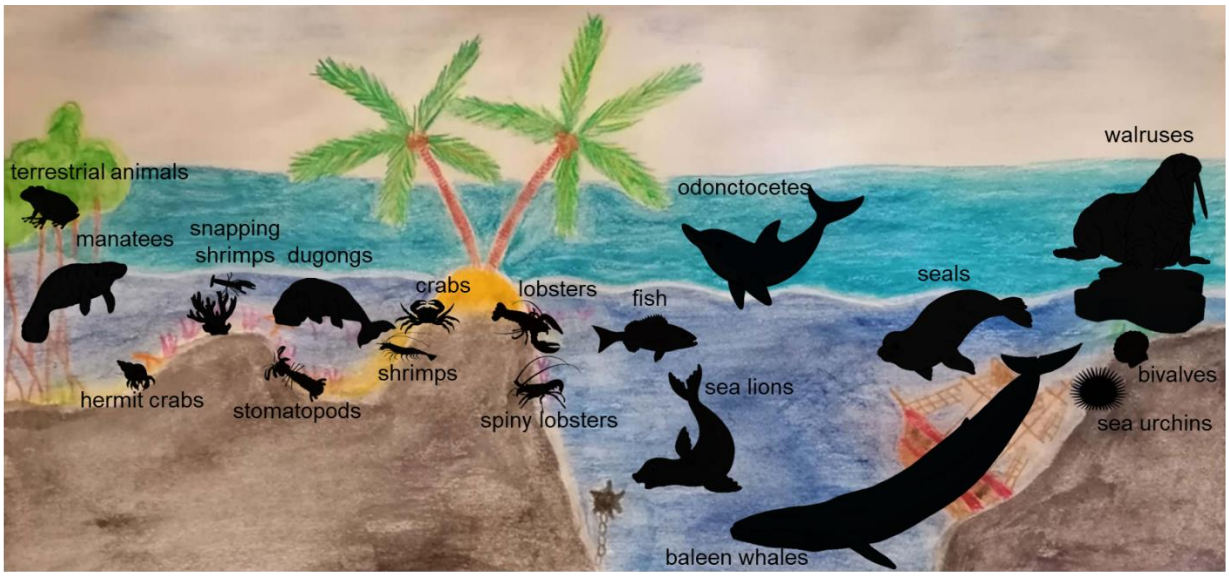

Figure 6 Illustration of the primary sources of the marine biophony. Terrestrial animals can only be detected in coastal shallow waters.

1.2.4.1. Sound emission by marine mammals

All studied marine mammals emit sounds: odontocetes, mysticetes, pinnipeds, and sirenians, as well as some species that are less adapted to marine live, such as the polar bears and two species of otters. Odontocetes, or toothed whales, are capable of producing various types of sounds (Figure 7 and Figure 8), including social sounds such as whistles and burst sounds, as well as broadband clicks [26] (Figure 7). While all studied odontocetes produce clicks and burst pulse sounds, certain species rarely or never produce whistles [3]. **Whistles** are continuous tonal sounds that can cover both the sonic and ultrasonic frequency ranges [27,28]. **Burst pulses** are brief vocalizations characterized by a high repetition rate (> 300 pulses s^{-1}) or short interpulse intervals (< 3 ms), giving them a sqawks/moan-like quality to the human ear [3]. Although less studied than whistles [3], burst pulses play an important role in dolphin sound emissions [29]. There is a fine region of demarcation between burst pulse sounds and **echolocation clicks** [3]. Clicks are short, broadband, and highly directional sounds. Dolphins are thought to produce echolocation signals using their nasal system, with the signals being projected out through the melon [30,31]. Odontocetes emit echolocation signals and receive echoes, enabling them to perceive their environment. These signals are utilized for navigating, prey detection, prey capture, and predator avoidance [3].

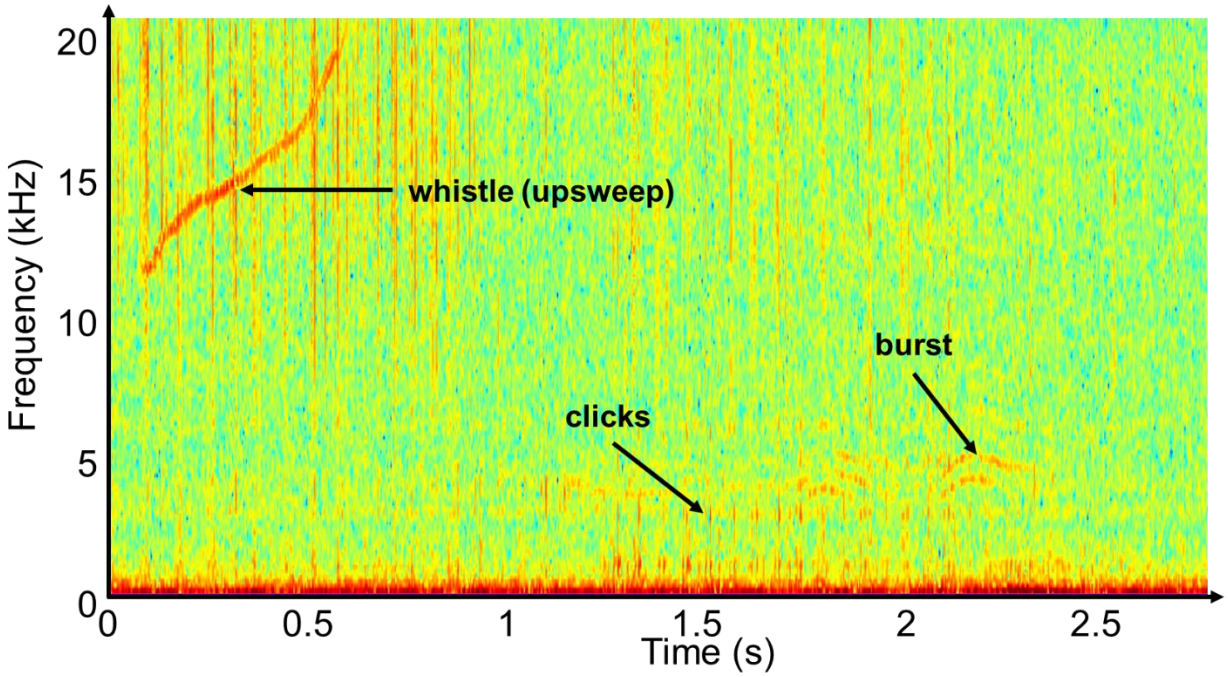

Figure 7 Spectrogram of a segment of the recorded soundscape in French Polynesia at 22.05 kHz (FFT = 256) showing the difference between clicks, bursts, and whistles. The warmer the color, the louder the sound.

A B C D E

Figure 8 Biological sounds. (**A**) *Eubalaena glacialis* (a mysticete), (**B**) *Stenella frontalis* (an odontocete), (**C**) *Erignathus barbatus* (a pinniped), (**D**) *Bairdiella chrysoura* (a teleost), and (**E**) Alpheidae (snapping shrimps). (**A**) NOAA (Fisheries) 2023. Eugl-upcall. https://www.fisheries.noaa.gov/s3/2023-04/Eugl-upcall-NOAA-PAGroup-01-right-clip-1.mp3 (**B**) NOAA (Fisheries) 2023. Stfr-Multisound. https://www.fisheries.noaa.gov/s3/2023-04/Stfr-Multisound-NOAA-PAGroup-01-atlantic-spotted-dolphin-clip.mp3 (**C**) NOAA (Fisheries) 2023. Erba-Multisound. https://www.fisheries.noaa.gov/s3/2023-04/Erba-Multisound-Cornell-OrnithologyLab-01-bearded-seal-clip.mp3 (**D**) NOAA (Fisheries) 2023. Bach-knocks-LGL. https://www.fisheries.noaa.gov/s3/2023-04/Bach-knocks-LGL-Heyman-01-silver-perch-clip.mp3 (**E**) NOAA (Fisheries) 2023. Alsp-snaps. https://www.fisheries.noaa.gov/s3/2023-04/Alsp-snaps-NOAA-PAGroup-02-amplified-snapping-shrimp-clip.mp3 Used with permission from NOAA PMEL.

Among the fourteen extant species of mysticetes, all of them are capable of producing sounds [32–37][1]. These sounds can be categorized into two groups: calls and songs (Figure 8). In contrast, only four species are known to produce songs [38–42]. Songs are defined as 'sequences of notes occurring in a regular sequence and patterned in time' [43]. Songs are related to courtship. Among these four species, the humpback whale (*Megaptera novaeangliae*)

[1] In the literature, a review on the acoustic behavior of mysticete whales was published in 1990. It was previously assumed that ten out eleven species were capable of producing sounds. However, it is now known that the remaining species (*Caperea marginata*) also exhibits vocalizations. Additionally, the three populations that have been elevated to species status are also known to vocalize.

has been extensively studied [44]. **Songs** can vary from one population to another, and singing peaks occurs when humpback whales migrate to warmer waters [44].

Pinnipeds vocalize both in air and underwater (Figure 8). Little is known about their underwater sounds in comparison to their aerial calls [3]. However, it appears that they serve similar social communicative functions. While some **seals** seem to have only one type of vocalization (e.g., *Mirounga* and *Histriophoca* seals) [45,46], others, such as *Leptonychotes weddellii*, are known to produce up to 34 different types of vocalizations [47]. **Sea lions** and **walruses** are also recognized for vocalizing underwater [48–50]. Additionally, underwater vocalizations have been reported in sirenians, both in **dugongs** [51] and **manatees** [52] Nevertheless, these animals are generally known to be very quiet [53].

1.2.4.2. Sound emission by fish

Despite the popular expression ‘dumb like a fish’ that has been popularized since the Renaissance [54,55], the ability of fish to produce sounds has been mentioned since Aristotle [56] and has been exploited by fishermen for centuries [57] (Figure 8). Fish sounds are typically low-frequency sounds (below 2 kHz) [58] and are used in various behavioral contexts, including reproduction, defense, aggression, and perhaps echolocation [59,60].

Out of the more than 34,000 extant species of actinopterygians, over 20,000 species are potentially capable of acoustic communication [61]. The complexity of this vast number of species is further compounded by the fact that fish produce sounds in a wide variety of ways [3]. Sound production is not ancestral but has independently evolved at least 27 times, much more than in tetrapods [61]. Categorizing sonic mechanisms in fish is complicated because one species can use different mechanisms [62]. The two major mechanisms are sonic muscles and stridulation [63] (Figure SP1 - 2D).

1.2.4.3. Sound emission by benthic invertebrates

Many benthic invertebrate taxa, such as bivalves [64], sea urchins [65], and crustaceans [24], are known to be soniferous. Among crustaceans, various taxa including hermit crabs [66], crabs [24], stomatopods [24,67], spiny lobsters [68], lobsters [69], and Palaemonidae shrimps [24] are vocal. However, the most well-known vocal taxa are **snapping shrimps** (Figure 8 and Figure 9) [24,70]. Snapping shrimps, belonging to the *Alpheus* and *Synalpheus* genera [24,71], are small Alpheidae crustaceans ranging in size from a few millimetres to centimetres [72]. The snapping action of their enlarged claw [70] generates a high-velocity water jet that exceeds cavitation conditions [73]. This snapping behaviour is used to stun or kill small preys [74],

injure interspecific opponents [75], engage in agonistic encounters [76,77], or occur spontaneously without any environmental trigger [78,79]. The collapse of the cavitation bubble produces a sharp transient broadband sound [73] with a peak frequency between 2 and 20 kHz [80] and a peak-to-peak amplitude of up to 190 dB re 1 µPa at 1 m [70]. These sounds are considered the most prevalent sounds in coral reefs [24,81,82] and are believed to be constantly present [24,70]. Individual snapping sounds are produced only occasionally, while the combined snapping of a large population results in a continuous loud crackling sound [83].

Figure 9 Snapping shrimps. (**A**) *Alpheus soror*, (**B**) *Alpheus armatus*, and (**C**) *Alpheus randalli.* Pictures taken by the author.

1.3. Passive acoustic monitoring

Due to the abundance of vocal marine taxa, efficient underwater sound propagation (Figure SP1 - 2B), and the increasing affordability of recording systems such as hydrophones and recorders (refer to Chapter 2), listening to these sounds has become a valuable means of quantifying and monitoring marine biodiversity [84]. This approach is known as passive acoustic monitoring (PAM). Beyond complementing visual survey methods for short-term daytime shallow studies, PAM enables the study of environments with limited or no light such as during the night, in the aphotic zone, or in murky waters [82,85]. It also proves beneficial for long-term monitoring [86] and in areas that are poorly accessible by divers.

PAM not only enables the detection of sonic species but also provide information on various behavioral processes, such as courtship [87] or spawning [88,89]. Several studies conducted through PAM have unveiled the presence of cryptic species [90], species misidentification [91], the discovery of new (sub-)species [92], and identification of new spawning/breeding areas for both fish [93] and cetaceans [94,95]. It is particularly important for regulating fishing efforts [96] and for understanding the habitat use strategies of endangered species [84]. Lastly, in coral reefs, PAM emerges as the most effective non-invasive method for studying snapping shrimps [96]. This is particularly important given the known link between biophony alteration and coral reef degradation [97,98].

2. 'Dive to the depth': an introduction to Polynesian photic and mesophotic coral reefs

2.1. Coral reefs

Scleractinian corals are found from the intertidal zone to the abyss [99]. The accumulation of coral skeletons (often cemented by coralline algae) [100] forms a coral reef when they modify sediment deposition, provide a complex three-dimensional habitat, and undergo dynamic processes of growth and erosion [99]. They can be categorized into **cold-water coral reefs** and **tropical coral reefs**. Cold-water coral reefs are associated with colder conditions, often (but not always) in deep offshore waters [99]. The depth at which cold-water corals can be found varies greatly, ranging just 20 m depth in Chilean fjords [101] to over 3000 m depth off the coast of the USA [99].

Despite occupying 'only' 250,000 [102] to 255,000 km^2 [103], tropical coral reefs (also known as light-dependent coral reefs) are one of the largest biodiversity hotspots on Earth [104]. Reefs ranging from the surface to 130/150 m can be divided into **shallow-water coral reefs**, also known as altiphotic or photic reefs[2] (ranging from the surface to 30/40 m depth), and deeper **mesophotic coral ecosystems[3]** (MCEs) [105].

2.2. Mesophotic coral ecosystems

MCEs extend from 30/40 m to/over 150 m [106–108]. Their lower limit is defined as the maximum depth at which there is sufficient sunlight to support photosynthesis and, consequently, the growth of zooxanthellate hermatypic corals [109,110]. In contrast to shallow-water coral reefs, the ecology and population dynamics of MCEs remain largely unknown due to their limited accessibility to humans [108]. However, MCEs are believed to serve as refuges for various reef species and could contribute to the recovery of photic reefs [109,111].

2.3. Polynesian photic and mesophotic coral reefs

2.3.1. Polynesian archipelagos

In the southern Pacific Ocean, French Polynesia spans over 5 million km^2 [112,113] and consists of 118 islands that are divided into five archipelagos: Austral, Gambier, Marquesas, Society, and Tuamotu Islands (Figure 10).

[2] This definition is not equivalent to the (eu)photic zone, i.e., the water column where radiation is degraded down to a maximum of 1%. The euphotic zone can vary from a few centimeters to approximately 200 m.
[3] This definition is not equivalent to the mesopelagic zone, i.e., the water column where radiation is between 1% and 0%. This zone is typically found between 200 and 1000 m in the open ocean.

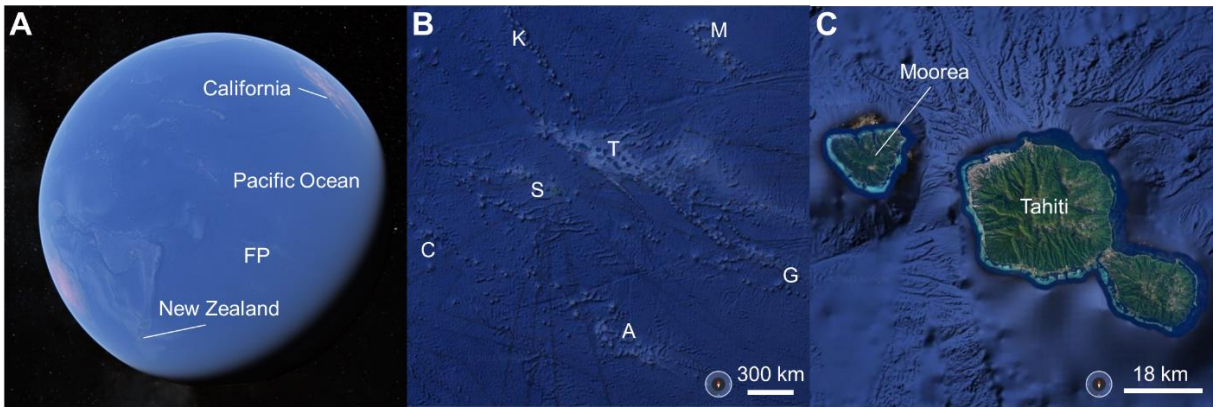

Figure 10 Map of the study area. (**A**) Location of French Polynesia in the Pacific Ocean, (**B**) zoom on French Polynesia (A, G, M, S, and T) and adjacent areas (C and K), and (**C**) zoom on Tahiti and Moorea Islands. FP = French Polynesia, K = Kiribati, C = Cook Islands, M = Marquesas Archipelago, T = Tuamotu Archipelago, S = Society Archipelago, G = Gambier Archipelago, A = Austral Archipelago. Images sourced from SIO, NOAA, U.S. Navy, LDEO-Columbia, NSF (Google Earth).

The Society Archipelago is a 700 km long N.W. – S.E. oriented volcanic archipelago divided into Windward Islands (five islands) and Leeward islands (nine islands). These islands occupy a total land surface of 1,590 km^2, with two-thirds of it belonging to Tahiti Island [114]. The Tuamotu Archipelago follows the same orientation but stretches over a much longer distance of 1,600 km, encompassing 76 islands [113]. Due to its older age, all islands in this archipelago are atolls [115]. On the eastern side of French Polynesia, the Gambier Archipelago consists of eleven islands, with Temoe Island separated from the rest. Finally, Austral and Marquesas Islands comprise seven and ten[4] islands, respectively.

2.3.2. Why focus on Polynesia?

The South Pacific region has the highest concentration of coral reefs, accounting for 35.7% of all tropical coral reefs, surpassing other regions worldwide such as South-East (26.7%), the Indian Ocean (14.1%), the Northern Pacific (6.7%), the Red Sea (6.7%), the Caribbean (7.8%), the Persian Gulf (1.2%), the Northern Atlantic (0.8%), and the Southern Atlantic (0.4%) [103]. The southern areas of French Polynesia, particularly the Windward islands, are projected to serve as 'climate refugia' where coral may experience less severe bleaching in this century due to comparatively lower predicted thermal anomalies (see Section 3.2.1) [116]. Most of the coral reef research in Polynesia focuses on the shallow areas of the Society Archipelago (primarily Moorea and Tahiti) and parts of the Tuamotu Archipelago [117]. Moorea Island is a major research hub for coral reefs in the central Pacific [118]. Surveys to assess the composition of coral reefs in Moorea have been conducted since the 1970s [119,120]. The significance of this

[4] Motu One and Motu Nao are generally not classified as islands but are instead referred to as 'small islands'.

region at a global scale, its relatively well-preserved state, and the wealth of scientific knowledge accumulated on Moorea Island are the primary reasons for choosing Polynesia as the focal point of this thesis.

2.3.3. Structure of Polynesian reefs

Polynesia comprises both coral atolls (also known as low islands) and high islands (volcanic island surrounded by a barrier reef). On young high islands, the coastline consists of rocky areas with a fringe of reef (e.g., Mehetia Island) that develop into a **fringing reef** (e.g., Tahiti Island). Over time, the island subsides [121], resulting in the formation of a **lagoon** surrounded by a **barrier reef** (e.g., Moorea Island) located at the former coastline position (Figure 11). This lagoon expands (e.g., Bora Bora Island) while the central island diminishes, ultimately forming an **atoll** (e.g., Rangiroa Island) (Figure 11). The oceanic side of the reef is referred to as the '**external slope**' (Figure 12). Due to its remarkable richness and diversity [115], this thesis will specifically focus on this particular section of the reef.

In French Polynesia, the external slope is characterized by a high coefficient slope [122]. The external slope varies according to the type of island (Figure 12 and Figure 13). In atolls, the external slope is divided into an **upper slope** consisting of a succession of spurs and grooves followed by a **sloping terrace**, and a more steeply inclined **lower slope** [122]. In high islands, the profile is more variable [122]. Generally, it is divided into three parts: (*1*) the upper slope (up to a depth of 30 m) containing spurs, grooves, terraces, and buttresses; (*2*) a **less inclined slope** (between depths of 30 and 70 m) with a variable nature (predominantly hard bottom coral substrate or a **sandy plain**); and (*3*) a steep slope or **drop off** with a higher inclination (below a depth of 70 m) (Figure 13) [122]. Each part of the external slope can be further divided into smaller zones. For example, in the northwest of Moorea Island, the upper slope is divided into (*1*) algal crest, (*2*) erosion furrows, (*3*) gentle slope, (*4*) superior spur system, (*5*) sand bed, and (*6*) inferior spur system (Figure 13).

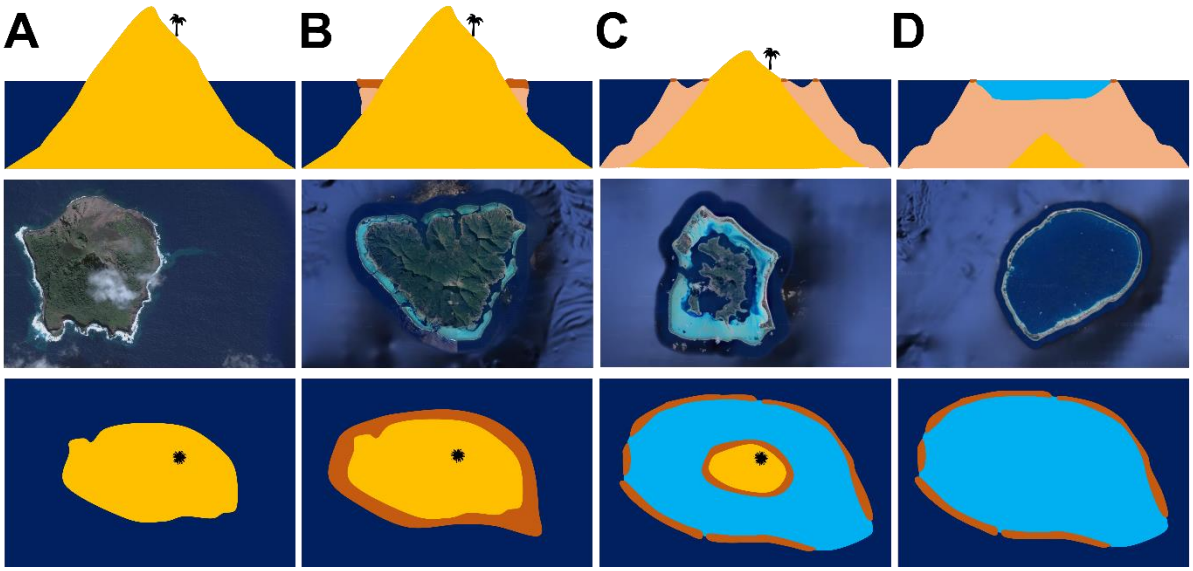

Figure 11 Evolution of island type in French Polynesia. (**A**) Mehetia Island, (**B**) Moorea Island, (**C**) Bora Bora Island, and (**D**) Tikehau Island. The imagery used is from Maxar Technologies Data SIO, NOAA, U.S. Navy, NGA, GEBCO, LDEO-Columbia, NSF, CNES / Airbus and has been modified from Google Earth.

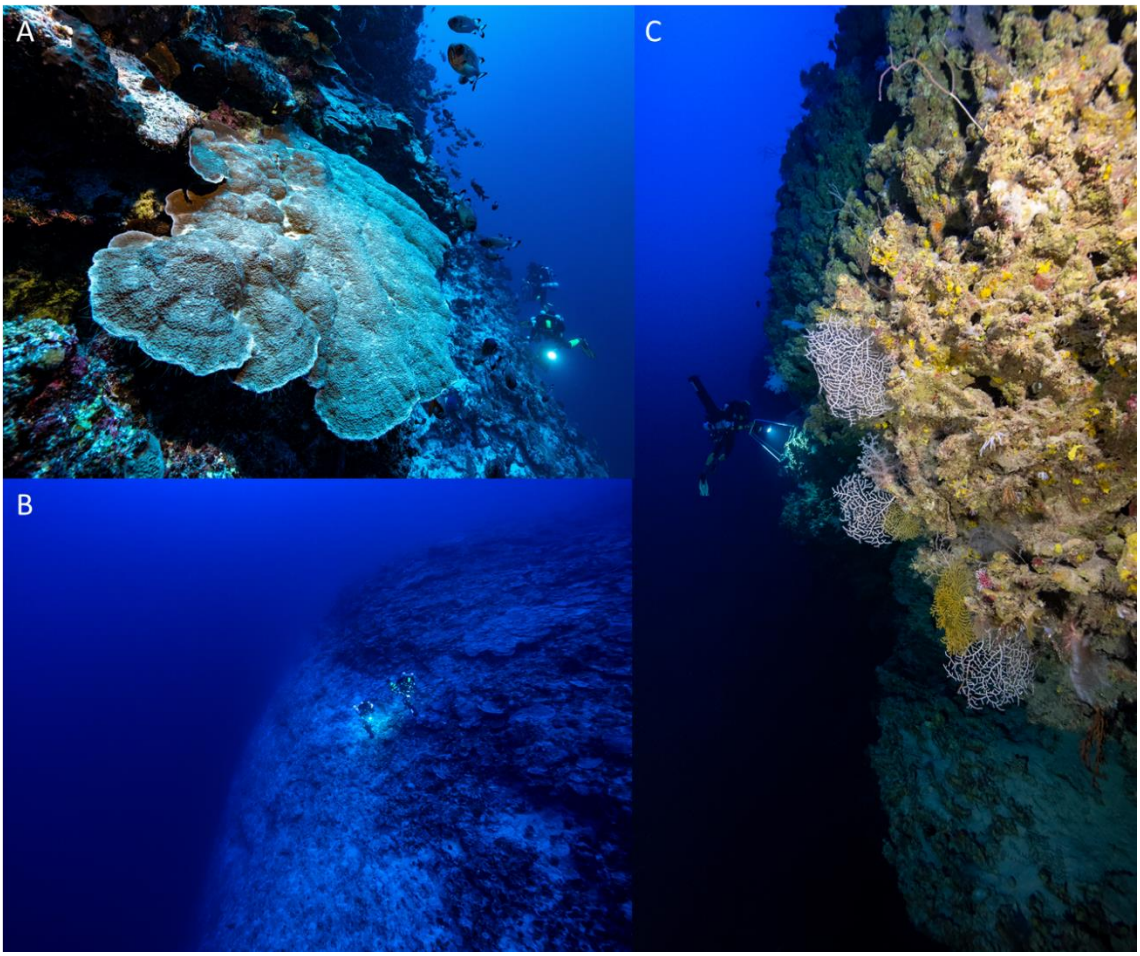

Figure 12 External slope of the barrier reef. (**A**) Tikehau, (**B**) Bora-Bora, and (**C**) Moorea. (**A**) and (**B**): © Franck GAZZOLA / UNDER THE POLE / Zeppelin Network, (**C**): © Ghislain BARDOUT / UNDER THE POLE

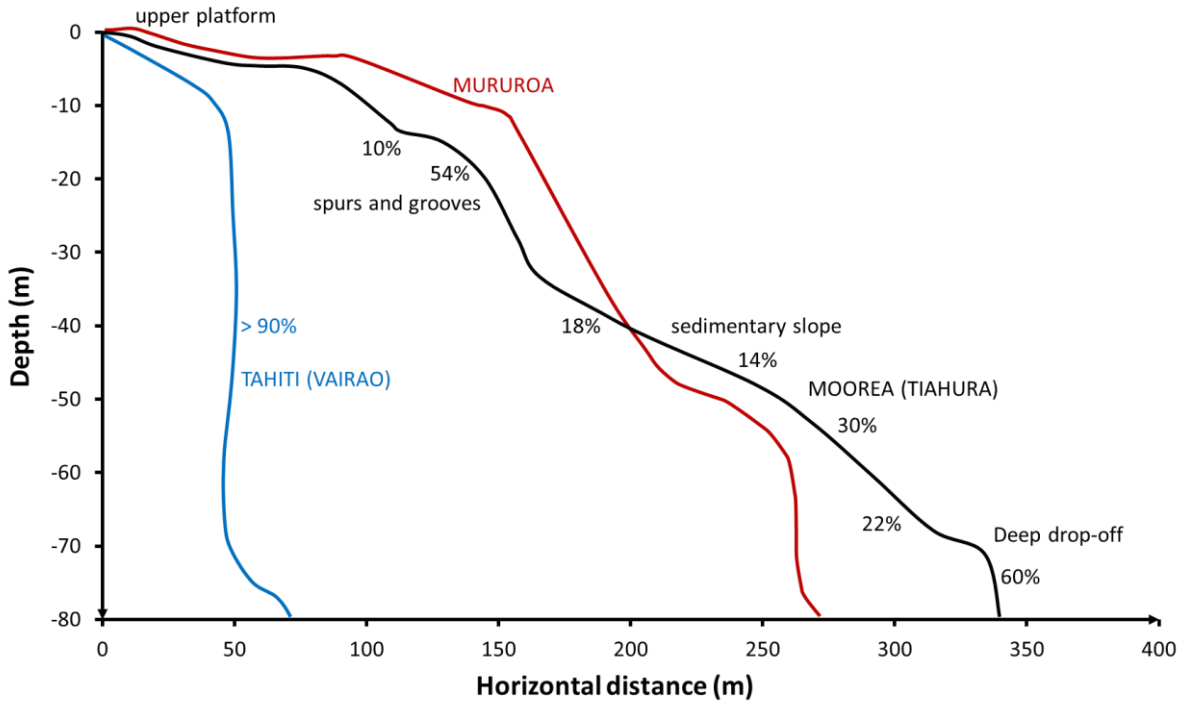

Figure 13 Bathymetric profiles of the outer slope in three Polynesian islands (Tahiti in blue, Mururoa in red, and Moorea in black). Adapted from [122–125].

2.3.4. Fish biodiversity of Polynesian reefs

More than 1,300 fish species are known to occur in French Polynesia [126], with the majority found in the Society Archipelago (67%). The Marquesas Archipelago has the highest proportion of endemic fish species (13.7%), which ranks as the third highest level of endemism for Pacific fish. This significant level of endemism can be attributed to the limited number of reefs in this archipelago, resulting from past modifications in water currents that have led to changes in water temperature and nutrient concentration [115]. These observations primarily focus on the photic zone of the reef because, similar to other regions worldwide, our understanding of MCEs remains limited. This knowledge gap is particularly pronounced below a depth of 80 m [122], where descriptions are generally limited to bottom relief. Only limited information is available regarding fish communities at these depths.

There is an important aspect shared by numerous reef species that needs to be mentioned. In coral reefs, most marine animals (bryozoans, cnidaria, crustaceans, echinoderms, molluscs, polychaetes, sponges, tunicates, teleosts, etc.) exhibit structured life histories with two distinct stages: a relatively benthic/sedentary stage on the reef (usually juveniles and adults) and a pelagic, **dispersal larval stage in the ocean** (Figure 14) [127]. Subsequently, organisms relocate to the reef habitat once they are ready to transition to demersal habitat [128]. To accomplish this, they rely on various cues, which may include vision [129], olfaction [127,130–

132], sounds [128,133,134], turbulence differences [127], gradients of plankton/detritus [127], or a combination of these factors [135–137]. Upon arrival at the reef, larvae undergo metamorphosis and a dietary shift.

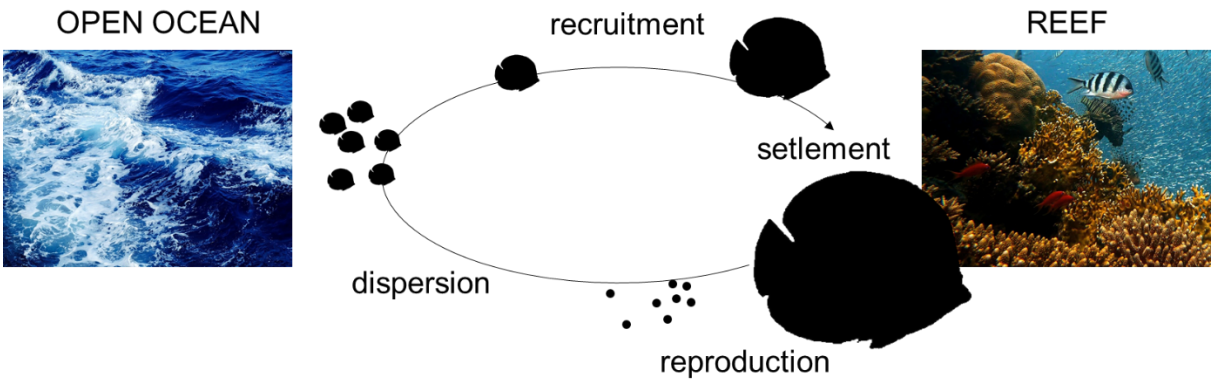

Figure 14 Life cycle of the majority of coral reef fish species. Royalty-free photographs.

2.3.5. Passive acoustic monitoring of Polynesian reefs

Given the diversity of species inhabiting coral reefs, and the known vocalization abilities of many of these species [21,138–140], coral reefs are sometimes referred to as 'choral reefs' [57,138,141]. In French Polynesia, extensive research has been conducted on the characterization of fish sounds from various families, including Balistidae [139,142,143], Carapidae [144–148], Chaetodontidae [149], Ostraciidae [150], Pomacentridae [92,151–153], and Serranidae [154]; while other taxa have received little attention (see [155] for an exception). Since 2015, PAM has been utilized to study Polynesian reefs, primarily for habitat comparisons [156,157] and site assessments [158,159]. It has also been employed to examine temporal patterns of fish sounds in the photic reef [141] and to investigate the impact of noise on taxa such as gastropods [160], rays [161], and sharks [162]. Preliminary studies suggest that PAM is a valuable tool for studying reefs in conjunction with or as a replacement for other techniques (Figure SP1 - 1). In Moorea Island, closely related habitats located within 1 km of each other exhibited significant differences in their spectral composition [156]. Furthermore, there are indications that vocal species can also be found in deeper habitats (75 to 90 m) [157]. Thus, passive acoustics could serve as a proxy for studying MCEs [138,163,164]. However, despite its usefulness in reef research, there is limited knowledge regarding (*1*) the range of sound propagation in the open ocean, (*2*) the depth-related variations in reef sounds, (*3*) the temporal patterns of MCE sounds, and (*4*) the impact of anthropogenic pressures on the biophony. This is particularly important as the health of Polynesian coral reefs is currently or will be increasingly threatened by rising anthropogenic pressures [165].

3. ‘Silent Spring’: an introduction to the Anthropocene

3.1. What is the Anthropocene?

The Anthropocene refers to the current geological time interval during which Earth is profoundly impacted by humans activities, typically since the mid-twentieth century [166]. Human activities have a significant impact on the marine environment through five major pathways: (*1*) extraction of living resources, (*2*) pollution, (*3*) physical alteration (such as bottom fishing, seabed mining, or coastal structures [167], Figure 15), (*4*) biological invasions, and (*5*) global climate change [168,169]. Threats from global changes include invasives (Figure 16) [170], coral bleaching (Figure 17), increasing levels of CO_2, and increasing/new diseases.

Figure 15 Illustration of typical artificial embankments, part of the coastal development in French Polynesia. (**A**) Embankment at Raiatea Island; (**B**) embankment for littoral privatization at Moorea Island. Pictures taken by the author.

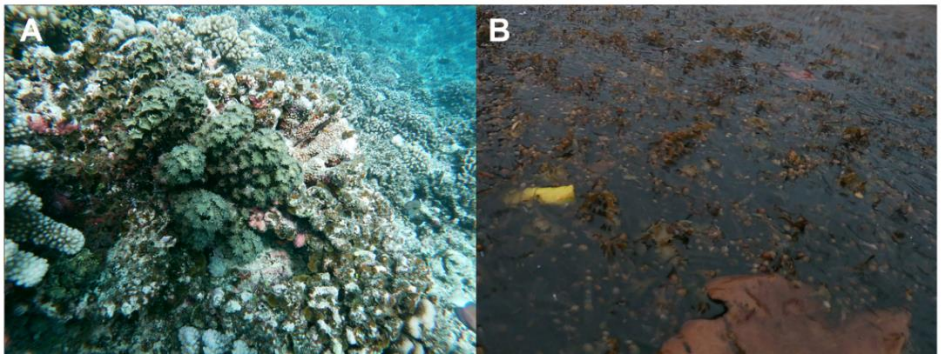

Figure 16 Illustration of increasingly abundant invasive opportunistic macroalgae on Polynesian coral reefs. (**A**) Genus *Turbinaria* on the external slope (8.4 m) at Moorea Island; (**B**) floating assemblages of macroalgae (mainly *Sargassum* and to a lesser extent *Turbinaria*) in the lagoon, Moorea Island. Pictures taken by the author.

3.2. Negative impacts on the biophony of coral reefs

Human activities alter marine soundscapes by adding anthropogenic noise and by impacting the geophony and the biophony [16]. Climate change leads to an increase in the energy of tropical storms, causing an increase in associated waves, wind, and rain and therefore increasing the geophony level [16]. These events are also associated with the degradation of reefs leading to reduced associated biophonies [171]. This reduction is also reinforced by the direct

degradation of their habitat and the resulting lower species abundance [172,173]. In addition to these alterations of the vocalization patterns of animals, climate change cause the ocean to be warmer leading to an alteration in the acoustic detectability, and the auditory capabilities of animals [174]. These changes can result in the changes or loss of choruses due to community alterations [174] and changing sea-surface temperature [175,176].

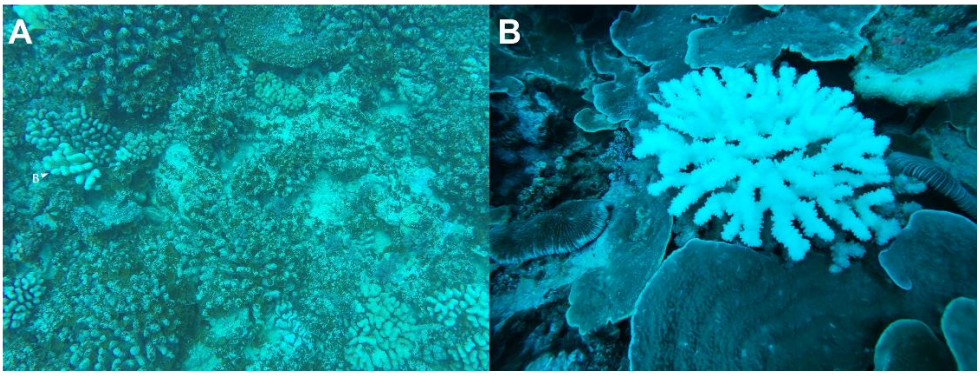

Figure 17 Illustration of dead and bleached coral. (**A**) Underwater photography at Moorea Island (site: E2B, depth: 10 m) in January 2021, depicting a significant proportion of dead coral partially covered by macroalgae, as well as bleached coral. (**B**) Coral bleaching in MCEs at Moorea Island. Pictures taken by the author.

3.2.1. Coral bleaching and the loss of biophony

In the long-term, human-induced climate change may represent the greatest threat to marine ecosystems [167,177]. Anomalously high sea temperatures are linked to coral bleaching events [178,179]. Coral bleaching occurs when corals expel their endosymbiotic algae, resulting in a reduction in their density and the concentration of photosynthetic pigments within them (Figure 17) [180,181]. Although various stressors can contribute to initiating bleaching [182–184], the primary cause of mass bleaching events is elevated sea temperatures [182–184] and/or high solar irradiance [185–187].

Mass bleaching events alter the ecological process of reefs [188]. Coral declines have been accompanied by changes in the structure, diversity, and trophic composition of reef fish communities [189]. Furthermore, degraded reef sounds are less attractive to young fish during their recruitment process, see section 2.3.4), resulting in reduced settlement rates and posing a threat to the recovery of degraded reefs [97,190]. Preliminary reports on Australian reefs have shown that soundscapes can be degraded when severe damages occur on the reef [97].

3.2.2. Acoustic pollution

In addition to climate change related impacts, another stressor for marine animals from coral reefs is anthropogenic noise [16]. Over the past few decades, shipping has significantly contributed to the increase in ambient noise levels by up to 12 dB [4]. Marine mammals are

well-documented to be impacted by various sources of anthropogenic noise, including military sonars [191], seismic surveys [192–196], detonations [197], pile driving [198,199], and ship noise [200–204]. These impacts can lead to avoidance behavior [198,201,203], hearing disabilities/loss [197,199], stress [204], disruptions [200], increased vocalizations [202], delayed migrations [195], or even stranding events [191–194]. Fish and invertebrates are also affected by anthropogenic noise. Studies have reported impacts on these groups from seismic surveys sounds [205–211] and ship noise [160,161,212–218], resulting in mortality [209–211], hearing loss or behavioral changes [206,207,219,220], and alterations in factors such as predation risk [216], offspring survival [215] or settlement patterns [212,217]. It is important to note that a minority of studies have found no impact of seismic surveys on fish [221] and invertebrates [222,223] to provide a comprehensive perspective.

3.3. Protection measures

The publication of Rachel Carson's 'Silent Spring' in 1962 [224] raised greater environmental awareness among the general public. Despite this, there is currently no international treaty specifically dedicated to coral reef conservation [167]. However, due to the high inertia nature of ocean-atmosphere systems, coral reefs can benefit from other international agreements, such as the 'Global Programme of Action for the Protection of the Marine Environment from Land-Based Activities', the 'International Convention for the Prevention of Marine Pollution from Ships' or the FAO's 'Code of Conduct for Responsible Fisheries' [167]. At the local and regional level, Marine Protected Areas (MPAs) primarily focus on fisheries management and biodiversity conservation.

3.3.1. Coral reef MPAs

When properly designed and managed, MPAs can be effective, particularly for species with limited mobility [167]. The biomass of resident fish within MPAs is generally two times higher compared to areas outside MPAs [225]. Exploited predatory species, in particular, tend to be more abundant and larger in size within 'no-take' MPAs [226,227]. Additionally, MPAs can help prevent the loss of live coral cover [228,229]. However, it should be noted that there can be significant time delay before coral cover responds to protection measures due to the slow growth rate of corals [167]. An attempt to quantify this protection measure showed an increase in coral cover of 0.05 – 0.08% per year within MPAs, while outside MPAs, there was a decline of 0.27 – 0.43% per year [228].

3.3.2. MPAs in French Polynesia

In 2018, the entire exclusive economic zone (EEZ) of French Polynesia was designated as a marine managed area (MMA), called 'Tainui Atea', covering an area of nearly 4.9 million km^2 [230,231]. It is important to note that this MMA is not classified as an MPA. The 'management goals' of the MMA focus on 'the sustainable exploitation of fishery resources' and 'the rational use of marine resources for sustainable development' [230]. In French Polynesia, marine protection measures are governed by two distinct legislations: environment laws and spatial planning laws [232] (Table 1). This results in a complex situation with some MPAs allowing fishing activities and specific areas designated as 'Specific fishing regulations areas' where fishing is prohibited (Table SP1 - 1). The main protection measures in place include two integral reserves (Manuae and Motu One Islands) and two major spatial planning plans (PGEM) in Moorea Island and the Fakarava Municipality, which is part of the Fakarava Biosphere Reserve (Table SP1 - 1) [232,233].

Table 1 Levels of protection in French Polynesia based on legislative code.

Level	Local name	Translation
Code de l'environnement		
I	Réserve intégrale et zone de nature sauvage	Integral reserve and wilderness area
II	Parc territorial	Territorial Park
III	Monument naturel	Natural monument
IV	Aire de gestion des habitats et des espèces	Habitat and species managed area
V	Paysage protégé	Protected countryside
VI	Aire protégée de ressources naturelles gérées	Managed area
Code de l'aménagement		
Maritime space management plan of Fakarava Island		
RI	Réserve intégrale	Integral reserve
NP	Zone naturelle protégée	Protected natural area
HP	Zone à habitat protégé	Protected habitat area (e.g., nesting turtles)
RA	Rahui	Traditional alternating fishing area
NT	Zone naturelle à vocation touristique	Natural tourist area
Maritime space management plan of Moorea Island		
MPA	Aire marine protégée	Marine protected area
ZPR	Zone reglementée de pêche	Specific fishing regulations area
Other spatial planning legislations		
ZPR	Zone reglementée de pêche	Specific fishing regulations area
-	Rahui	Traditional alternating fishing area

3.3.3. Passive acoustic monitoring of Polynesian MPAs

Moorea Island has eight MPAs. In MPAs, fishing is prohibited, the harvesting of any species is forbidden, as well as any modification of the beach and lagoon, and any activity leading to degradation of the marine environment, including the discharge of wastewater and waste, and the collection of substrate. However, mooring on permanent anchors and swimming are allowed. Regarding fishing regulations, there are three exceptions, one of which applies to an

MPA studied in this thesis (MPA_{East}), where line fishing and specific fishing, such as for Gobiidae, some Scrombidae, and juveniles of some Mullidae, is allowed. This island has the advantage of containing marine control areas (MCAs) which are non-protected areas that are used as 'controls' in the monitoring of MPAs [234]. When comparing the soundscapes of MPAs and MCAs, it has been shown that MPAs had a higher ambient sound pressure level than MCAs [158]. This preliminary observation highlights the significance of acoustics as a tool in monitoring MPAs [158]. However, the long-term resilience of these MPAs and how it is transposed into their biophony is still unknown.

4. Objectives of the research thesis

In French Polynesia, the current knowledge on the biophony mainly focused on fish vocalizations from photic reefs. It highlights a gap on our understanding of (*1*) the high-frequency part of the biophony, and more broadly of the 'mass-phenomena' biophony, and on (*2*) the biophony in MCEs, including its depth-related and diel cycle variations, as well as species identification. A comprehensive understanding of the long-term consequences of protection measures on the resilience of coral reefs, particularly in the face of threats such as coral bleaching, is still lacking.

The main objective of this research thesis is to determine how the diversity of the biophony of photic and mesophotic French Polynesian coral reefs in the Anthropocene varies. In order to achieve this objective, the thesis is divided into an introduction (**Part I**), three core parts (**Parts II**, **III**, and **IV**) and a discussion (**Part V**). The three core parts focus on (*I*) the 'mass-phenomena' of the biophony, (*2*) the individually identifiable sources of the biophony, and (*3*) the human modifications of this biophony. Each part is associated to a specific objective. The first specific objective is to describe the spatiotemporal variation of the 'mass-phenomena' biophony. The second specific objective is to describe and identify the spatiotemporal variation of the 'indivividually identifiable sounds from generally nearby sources' of the biophony. The third specific objective is to determine how human modifications, both positive and negative, affects this biophony.

5. Overview of thesis parts and chapters

The first part contains two chapters. The **first chapter** is devoted to the general introduction of theoretical concepts important for understanding the research thesis. You have almost finished reading this first chapter. The **second chapter** serves as a general overview of the materials and methods. Its purpose is to provide explanations of the various methodologies

(sampling and acoustic analysis) that have been utilized in several chapters. Following these two introductory chapters, the thesis chapters are organized into three parts (Figure 18).

The second part of the thesis focuses on the 'mass-phenomena' of the biophony described in chapters 3 and 4 (Figure 18). The **third chapter** describes the mass phenomena composed of fish and benthic invertebrate sounds in Moorea Island, as well as their propagation into the open ocean. In addition, the propagation distances are compared to audiograms of different taxa. This comparison is particularly important to understand to which extent pelagic larvae can capture the detection of the reef (see 2.3.4). The **fourth chapter** explores the sounds produced by photic and mesophotic benthic invertebrates. This 'mass-phenomena' of the biophony as well as the individually identifiable BTS were studied in six different Polynesian islands. They were compared along a depth gradient (from 20 m to 120 m), between atolls and high islands, and at different periods of the day (nigh, sunrise, day, and sunset).

The third part focuses on individually identifiable sources of the biophony (Figure 18). In this part, fish sounds will be explored in more detail. There are two reasons why we decided to focus on fish sounds. The first reason is that they are continually present on the reefs (unlike cetacean sounds) and they can be species-specific (unlike benthic invertebrate sounds). The second reason is that these sounds are primarily involved in communication. This second part of the thesis is detailed in chapters 5, 6, 7 and 8. Firstly, we tested an automatic approach using α-acoustic diversity indices to evaluate the diversity of fish sounds (**fifth chapter**). However, these indices were originally developed for terrestrial soundscapes, and their application to marine soundscapes appears to be influenced by fundamental differences between the two environments. Therefore, in the following chapters, fish sounds were identified by manual inspection. The **sixth chapter** studies the spatial variation of fish sounds along the same depth gradient and types of islands used in Chapter 4. The **seventh chapter** explains how these fish sounds vary diurnally. Finally, the **eighth chapter** focuses on identifying the emitters of fish sounds recorded in Polynesian mesophotic reefs. For the sixth and eighth chapters, we focused on the mesophotic part of the reef because there is significantly less scientific knowledge compared to the photic part of the reefs.

The fourth part of the thesis investigates the influence of human modifications on the biophony. The **ninth chapter** is dedicated to the modifications of the biophony following bleaching events to determine a possible effect of the protection status (MPA vs. MCA). To accomplish this, the biophony was recorded in four MPAs and four MCAs in 2015 and 2021, respectively, before and after the bleaching events that occurred in 2016 and 2019.

The last part of this thesis (**Chapter 10**) is dedicated to the general discussion and main conclusions. The goal of this chapter is to provide answers to the biological questions posed in this thesis by integrating the results from the previous chapters. Additionally, this chapter includes perspectives for further research.

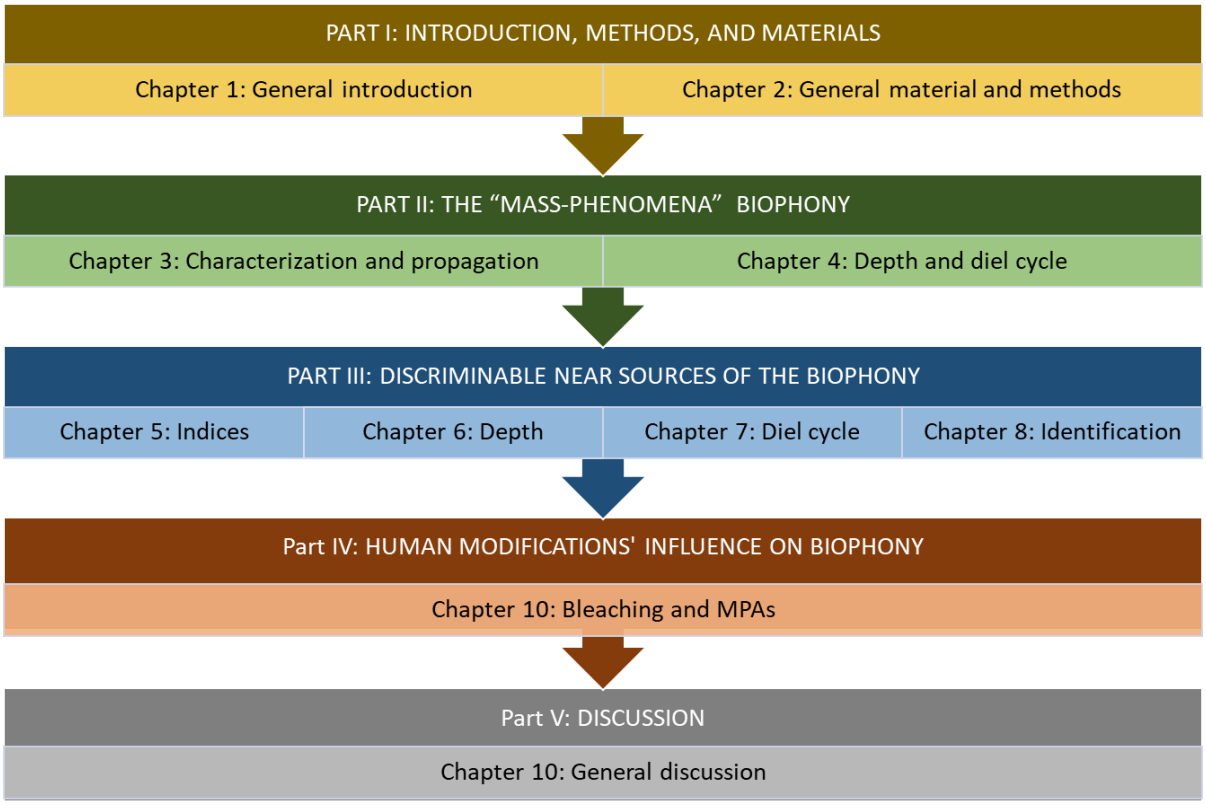

Figure 18 Articulation of the different parts and chapters of the thesis.

Creative inspirations

Thanks to Jacques-Yves Cousteau, Nathalie Imbruglia, and Rachel Carson for their contributions through film, music, and literature, respectively, which served as inspiration for the subtitles of this chapter.

Chapter 2. General material and methods

Sections of this chapter have been used for an educational video on the MANEA platform: *Outils d'étude de la biophonie – Partie 3 : Autres techniques.*

KEY INFORMATION

Sampling places

- ✓ The research thesis utilizes data from multiple scientific missions.
- ✓ Acoustic data was collected at six different islands. Data were collected mainly on the external slope of the barrier reef and in the open ocean.
- ✓ Fishing sessions were conducted in Moorea and Bora Bora.

Data

- ✓ All data were collected using acoustic recording systems, which consist of three components: a hydrophone, an amplifier, and a recorder. The hydrophone converts acoustic energy into an electric signal using a piezoceramic material, while the amplifier amplifies the voltage of the signal.
- ✓ Fixed acoustic recorders were used to collect data on the reef, while recorders attached to drifting antennas were used for data collection in the open ocean.
- ✓ Two datasets of biological data were utilized in the thesis: benthic cover and fish species identification data.

Acoustic analyses

- ✓ The thesis involves various acoustic analyses with recurring steps outlined.
- ✓ Software programs used include Matlab®, RavenPro Sound Analysis Software, RavenLite Sound Analysis Software, Avisoft SAS Lab Pro, R software, Adobe Audition, and PamGuard software.
- ✓ Subsampling at 4 kHz was performed for chapters focusing on fish sounds.

Representations

- ✓ Oscillograms represent amplitude as a function of time, power-spectra represent amplitude as a function of frequency, and spectrograms represent frequency as a function of time using a color code.
- ✓ Fourier transform is used to transform data from the temporal domain to the frequency domain, and the FFT algorithm is employed for efficient computation.
- ✓ Parameters such as overlap, FFT length, and the type of window are important in the switch from the temporal to the frequency domain. Different FFT lengths were used depending on the type of sounds and sampling rate.

1. Sampling

1.1. Sampling places

Since the thesis aims to understand the variations in the biophony, it was decided to obtain acoustic data at (*1*) different distances from the reef, (*2*) different depths, and (*3*) different times of the day. Additionally, (*1*) pre- and post-bleaching data within and outside MPAs were sampled. The goal was to obtain enough data to address our biological questions with statistical support.

To know how the biophony propagates from the reef, we used data sampled both on the external slope of the barrier reef but also in the open ocean off the external slope (mission CHORUS-16). Concerning the vertical variations of the biophony, we needed both acoustic data from the photic part of the reefs and from MCEs (Table SP2 - 1). We obtained acoustic data from MCEs through a collaboration with Under The Pole Expedition (https://underthepole.org). During the Under The Pole Expedition III (UTP3), acoustic data were collected at six different islands (Figure 19). The data obtained during UTP3 were used in Chapters 4 and 5. Specifically, the data from Tuamotu Archipelago were employed to assess fish diel cycles[5]. Additionally, data from Raroia Island were reused for a section of Chapter 7, along with play-back recordings from Temae (Moorea Island, Table SP2 - 1) and recordings from a pool (refer to Chapter 7). In addition to acoustic data, fishing sessions were conducted (ULIEGE-22 mission) to obtain specimens for morphological studies (Chapter 8). Moreover, during this mission, a preliminary investigation of the lower rariphotic zone [235] was carried out in Moorea Island (refer to the General discussion section). To meet the last objectives of the thesis, focusing on the effect of human modifications on the biophony, we realized a specific field trip (ULIEGE20-21) to Moorea (Figure 19, Table SP2 - 1). To assess the resilience of the reefs within and outside MPAs, we used data from a previous mission led by Dr. Bertucci during my master's thesis fieldwork (CRIOBE-15). The data collected on the North coast of Moorea Island during ULIEGE20-21 were used in Chapters 9. Specifically, data from eight sites (four MPAs and four nMPAs) were used for Chapter 9.

[5] The data from the other archipelagos were used in another study, which is not included in this final document (see Chapter 6, 'remark').

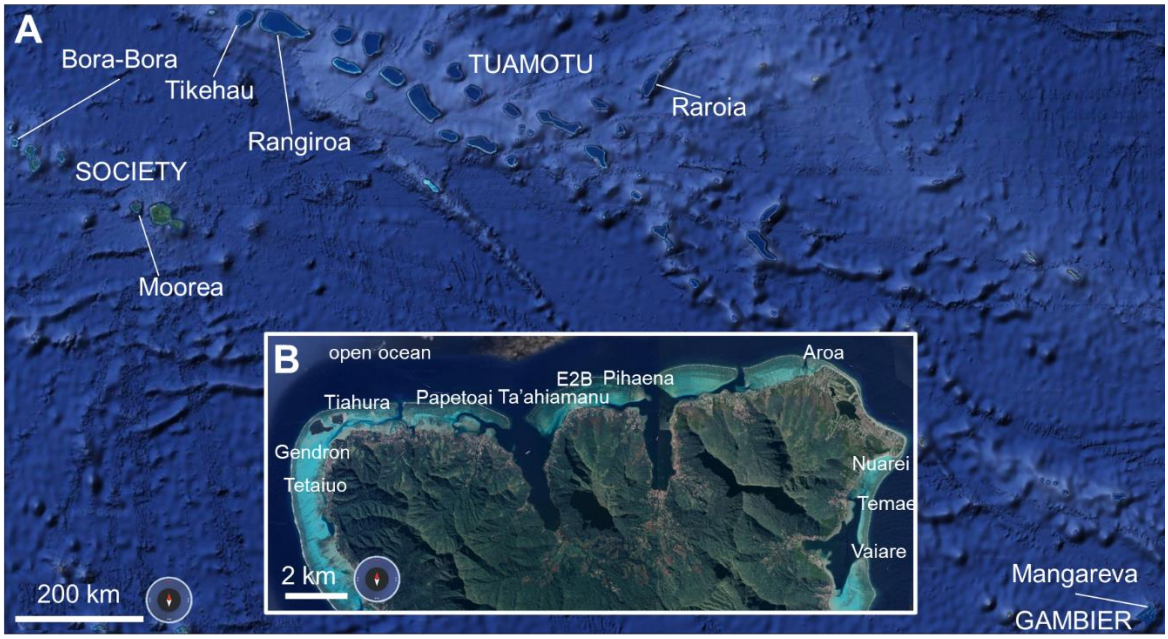

Figure 19 Map of the sampling sites used in this thesis. (**A**) Central part of French Polynesia. (**B**) Zoomed-in view of the North coast of Moorea Island indicating all the sampled locations. The 'open ocean' location encompasses 78 stations between Tiahura and E2B from 50 m off the reef crest to 10 km in the open ocean.

1.2. Recording systems

All the data were collected using acoustic recording systems. These systems consist of three components: a hydrophone (i.e., an underwater microphone), an amplifier (usually integrated into the hydrophone), and a recorder. The **hydrophone** converts acoustic energy into an electric signal by using a piezoceramic material that produces a voltage when mechanically stressed. The **amplifier** then amplifies the voltage of this signal to ensure it falls within the range that can be processed by the recorder. Lastly, the **recorder** digitizes the signal. All the data were recorded in an uncompressed format called Waveform Audio File Format (WAV = WAVE).

The data collected on the reef were obtained using fixed acoustic recorders, while the data collected in the open ocean (refer to Chapter 3) were collected using recorders attached to drifting antennas. Two types of fixed recorders were used. The first type is an autonomous underwater digital spectrogram (DSG) recorder (Loggerhead Instruments, Sarasota, FL, USA). This particular recorder was exclusively used during the CRIOBE-15 mission and is no longer commercially available. All other missions used SNAPs recorders (Loggerhead Instruments, Sarasota, FL, USA; Figure 20). Both systems were connected to HTI96 hydrophones (High Tech Inc., Long Beach, MS, USA) with variable sensitivities (expressed in dB re 1 V for a sound pressure of 1 µPa). Two different schedules (continuous and 1-minute intervals every 10 minutes) were employed based on the apparatus's autonomy and the duration of the recording

period. The recorders can be either deployed fixed to the seafloor or vertically on a tripod above the seafloor. The latter method is privileged due to the three-dimensional complexity of reefs and the presence of local acoustic hotspots [236]. Therefore, during the UTP3 and ULIEGE-22 missions, the recorders were fixed to a vertical pole. However, during the ULIEGE-20/21 mission, the recorders were placed horizontally on the seafloor to ensure comparability with previous studies (CRIOBE-15 mission) [141,157,158]. For drifting deployments, EA-SDA14 recorders (RTSys®, Caudan, France) connected to wideband low-noise HTI-92 hydrophones (High Tech Inc., Long Beach, MS, USA) were deployed. This system was positioned on a floating antenna. In addition, specific equipment such as loudspeakers was used for play-back experiments (see Chapter 5 – 2.1).

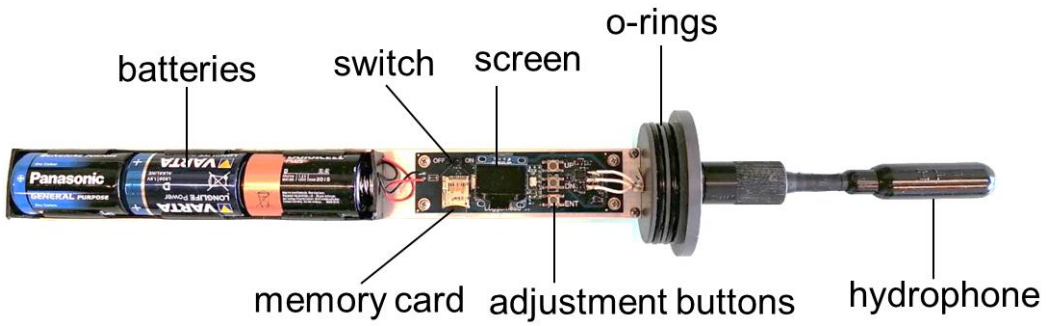

Figure 20 SNAP acoustic recorder (Loggerhead Instruments, Sarasota, FL, USA) connected to an HTI96 hydrophone (High Tech Inc., Long Beach, MS, USA). Picture taken by the author.

1.3. Biological data

Two datasets of biological data were used in this thesis. The first set pertains to benthic cover data (Figure 21) collected during the UTP3 mission (refer to Chapter 5). The second dataset encompasses both benthic cover and fish species identification data at Moorea Island, as part of the scientific monitoring program called *Service National d'Observation CORAIL* (http://observatoire.criobe.pf) (refer to Chapter 10).

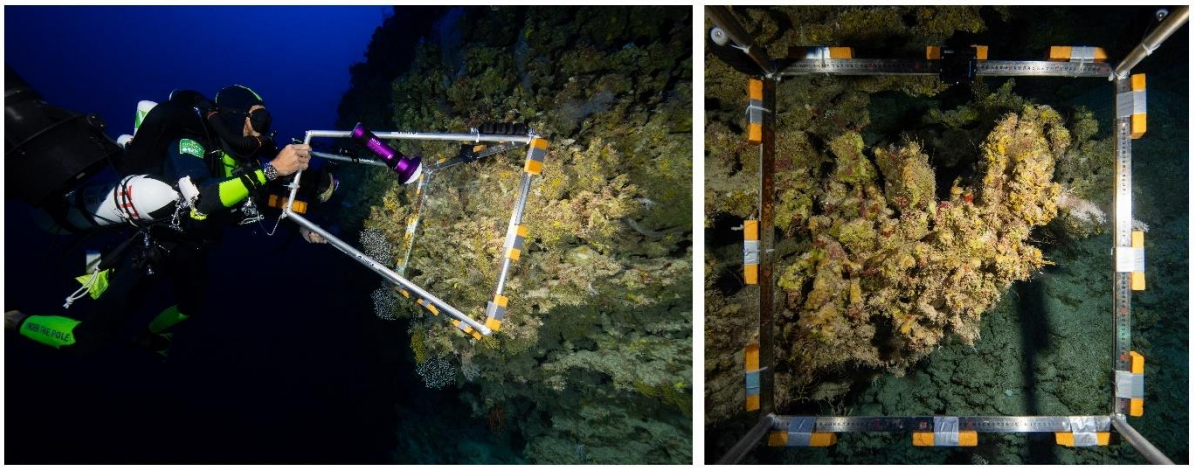

Figure 21 Photoquadrats for characterizing the benthic cover. © Ghislain BARDOUT / UNDER THE POLE.

2. Acoustic analyses

2.1. Steps and software

In this thesis, various acoustic analyses were performed, involving several steps outlined in Figure 22. One key step that is consistently applied is subsampling (see 2.2). While the steps differ when studying the 'mass-phenomena' biophony and the discriminable near sources of the biophony, there are recurring concepts shared between the two throughout the thesis. Therefore, the creation of oscillograms, power-spectra, and spectrograms is detailed in section 2.3.

Several software programs were used for the acoustic analyses. Subsampling, spectra, spectrograms, and Wenz modeling, as well as pretreatments and spectra comparisons, were performed using Matlab® R2014b (MathWorks, Natick, MA, USA). In Chapter 9, version R2022b was used due to the introduction of the poctave function in 2018. Manual scrolling and cleaning were conducted using RavenPro Sound Analysis Software 1.5 and RavenLite Sound Analysis Software 2 (Cornell Lab of Ornithology, Ithaca, NY, USA). Manual measurements of isolated fish sounds were carried out using Avisoft SAS Lab Pro (Avisoft Bioacoustics; Glienicke/Nordbahn, Germany). Testing of indices (chapter 7) and statistical analyses were performed using R software versions 3.3.0. to 4.1.1 (R Core Team, 2016 to 2021). Other bioacoustics software programs, such as Adobe Audition 3.0 (Adobe Systems Inc., Mountain View, CA, USA) and PamGuard software [237], were used on specific occasions.

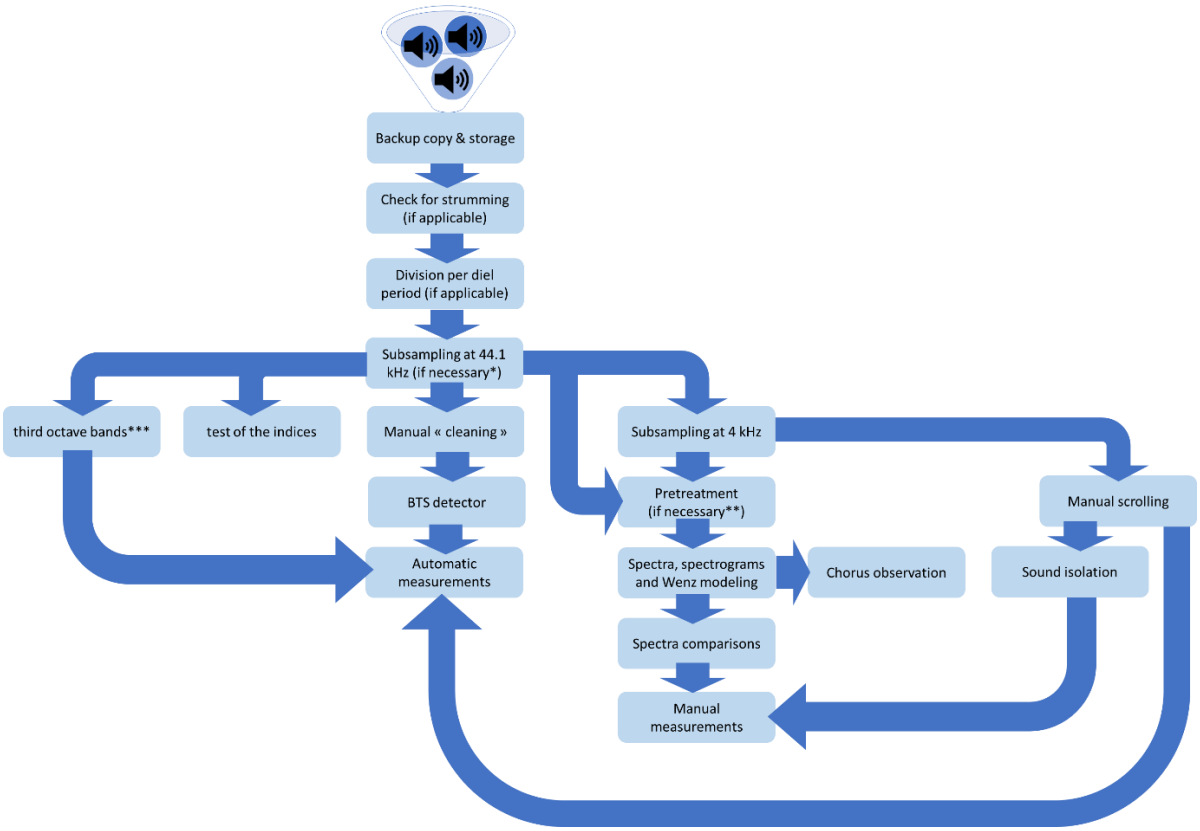

Figure 22 Main recurrent steps in the acoustic analyses used in the thesis. * Applicable only to data with a sampling frequency of 96 kHz or 48 kHz. ** Not applicable to Chapter 3. *** Not presented in the final document.

2.2. Oscillograms, power-spectra, and spectrograms

Sounds can be characterized at three scales: temporal, frequency, and amplitude/sound pressure (Figure 23). However, 2D representations allow us to depict only two of these scales simultaneously. **Oscillograms** represent amplitude as a function of time (Figure 23). Power-spectra represent amplitude as a function of frequency. Finally, spectrograms represent frequency as a function of time using a color code to indicate the amplitude (Figure 23). Recordings are performed in the time domain by measuring voltage changes. To obtain a **power spectrum**, it is necessary to transform the data from the temporal domain to the frequency domain (Figure SP2 - 1). This is achieved through the **Fourier transform** (= Fourier analysis), which decomposes complex waveforms into an infinite sum of simple waveforms, each with its own frequency [238]. Due to the time-consuming nature of the Fourier transform, the **fast Fourier transform** (FFT) algorithm is employed to compute parallel Fourier transforms [239]. The limitation of power-spectra lies in the lack of temporal information. By applying Fourier transforms to shorts segments of the original signals, the **spectrogram** is constructed. The spectrogram can be viewed as numerous consecutive partially overlapping power-spectra (Figure SP2 - 1 and Figure SP2 - 2).

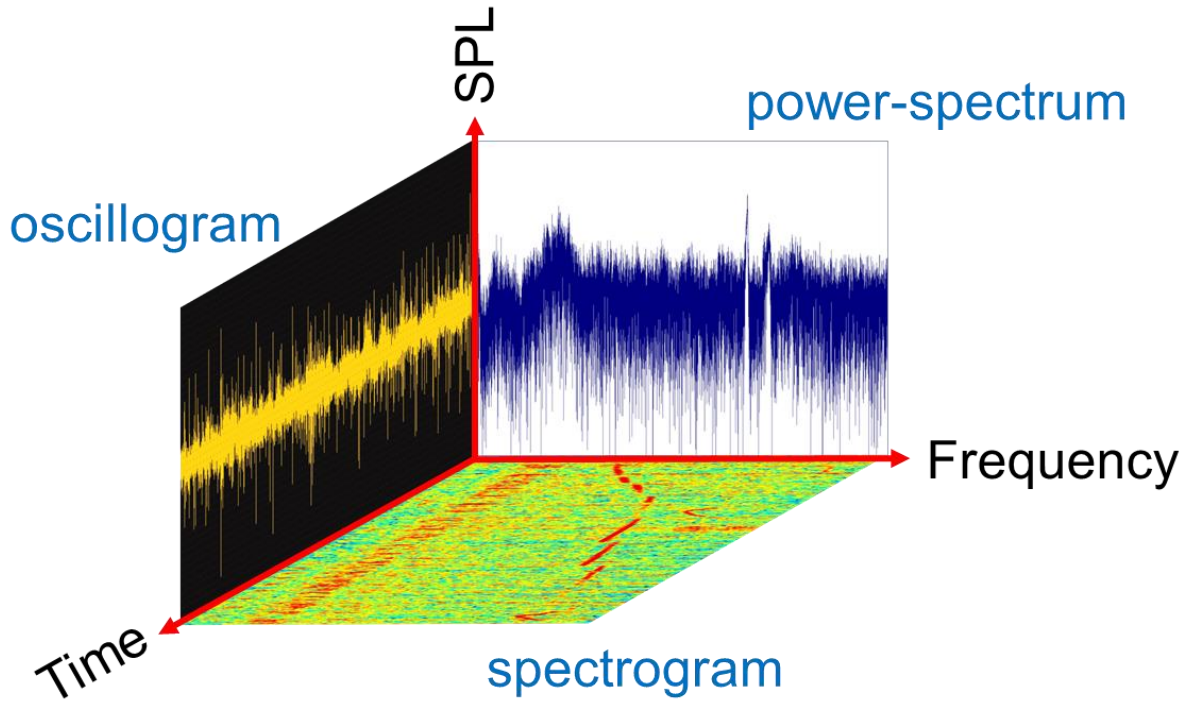

Figure 23 Schematization of the links between an oscillogram, a power-spectrum, and a spectrogram. Data: dolphin vocalizations from French Polynesia.

PART II: THE ‘MASS-PHENOMENA’ BIOPHONY

Chapter 3. From the reef to the ocean: revealing the acoustic range of the biophony of a coral reef (Moorea Island, French Polynesia)

Xavier Raick[1,2], Lucia Di Iorio[2], Cédric Gervaise[2], Julie Lossent[2], David Lecchini[3,4] and Éric Parmentier[1]

[1] Laboratory of Functional and Evolutionary Morphology, Freshwater and Oceanic Science Unit of Research, University of Liège, Liège, Belgium

[2] Chorus Institute, Grenoble, France

[3] Centre de Recherches Insulaires et Observatoire de l'Environnement, USR 3278, EPHE-UPVD-CNRS-PSL University, Moorea, French Polynesia

[4] Laboratoire d'Excellence 'CORAIL', Perpignan, France

This chapter has been published in *Journal of Marine Science and Engineering*. Additionally, sections of this chapter have been used for an educational video on the MANEA platform: *Portée de la biophonie vers le large : cas d'étude d'un récif corallien*.

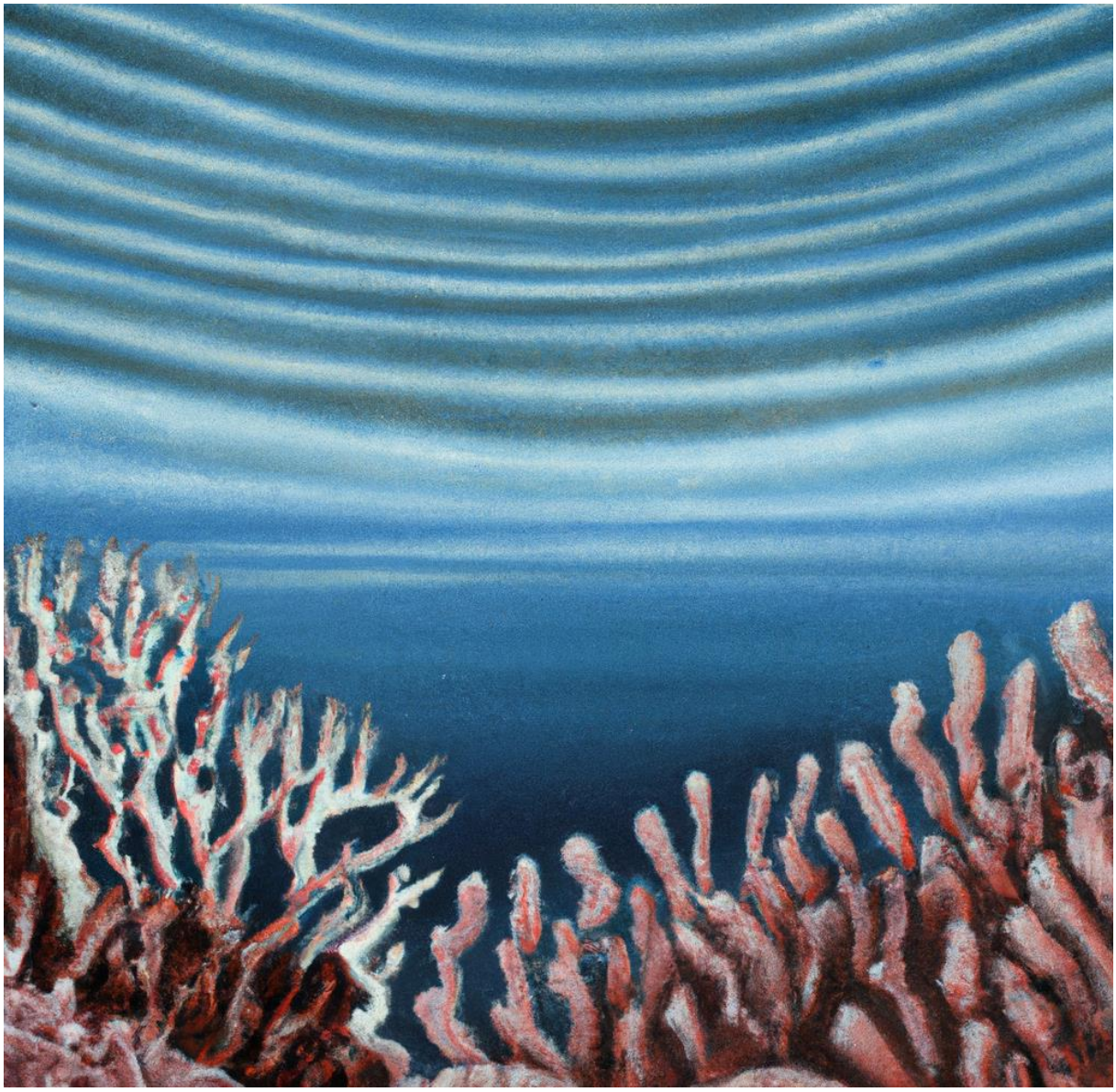

MAJOR RESULTS

Benthic invertebrate sounds

- ✓ The soundscape of the barrier reef of Moorea is characterized by a high number of broadband transient sounds between 3.5 and 17 kHz.
- ✓ NoBTS was 8% greater at night in the 3.5–5.5 kHz band, 14% smaller at night in the 6–8 kHz band, and 5% smaller at night in the 10–13 kHz band. It was similar between day and night in the 14–17 kHz band.
- ✓ SPL and ANL of all BTS bands were significantly higher at night, with a 6.7 to 9.2 dB difference between 5 and 6 p.m.

Fish sounds

- ✓ The soundscape of the barrier reef of Moorea is characterized by fish sounds between 200 and 500 Hz.
- ✓ The frequency band between 200 and 500 Hz showed a diel pattern with higher sound pressure spectrum levels during the day.
- ✓ The spectra in the 200-500 Hz band showed differences between day and night. A peak between 400 and 500 Hz was present during the day for intense sounds and median sounds, while peaks between 250 and 280 Hz were observed at night for intense sounds but not for median sounds.

Propagation distances

- ✓ Transmission loss (TL) estimates varied from −8.99 to −16.80 dB decade−1 for BTS, depending on noise levels and the frequency band used.
- ✓ The ANL of the BTS between 570 and 2000 Hz was detectable up to 55 km during the day and up to 90 km at night under calm sea conditions. The distance of detection for fish chorus frequencies was found to be between 1322 m and 1501 m with no wind.
- ✓ Wind speed and ship traffic influenced the propagation distances of BTS bands.

Comparisons with audiograms

- ✓ Using audiograms of different taxa, we estimated that fish post-larvae and invertebrates likely hear the reef at distances up to 0.5 km.
- ✓ Post-larval reef fish have their best hearing sensitivity between 200 and 600 Hz. The detection distances are generally smaller at night, except for species like M. kuntee, which can hear higher frequencies.
- ✓ Odontocetes have their maximum hearing sensitivity around 40 and 64 kHz. However, the frequency range that allows them to perceive reef sounds from a greater distance is between 5.6 and 20 kHz. The maximal detection distances of median reef sounds range from 7 - 9 km (day) to 15 - 19 km (night).

Key question for the objective of the thesis

What is the 'mass-phenomena' biophony and how it propagates into the open ocean?

Abstract

The ability of different marine species to use acoustic cues to locate reefs is known, but the maximal propagation distance of coral reef sounds is still unknown. Using drifting antennas (made of a floater and an autonomous recorder connected to a hydrophone), six transects were realized from the reef crest up to 10 km in the open ocean on Moorea Island (French Polynesia). Benthic invertebrates were the major contributors to the ambient noise, producing acoustic mass phenomena (3.5–5.5 kHz) that could propagate at more than 90 km under flat/calm sea conditions and more than 50 km with an average wind regime of 6 knots. However, fish choruses, with frequencies mainly between 200 and 500 Hz would not propagate at distances greater than 2 km. These distances decreased with increasing wind or ship traffic. Using audiograms of different taxa, we estimated that fish post-larvae and invertebrates likely hear the reef at distances up to 0.5 km and some cetaceans would be able to detect reefs up to more than 17 km. These results are an empirically based validation from an example reef and are essential to understanding the effect of soundscape degradation on different zoological groups.

1. Introduction

A soundscape is a collection of sounds composed of three acoustic sources: geophony, anthrophony, and biophony that reflect important ecosystem processes and human activities [240,241]. In the ocean, the biophony consists of sounds from marine fauna. Fish [242] and invertebrate [243] sounds constitute the most persistent part and the majority of coastal biophonies. Coral reefs are considered to be hotspots of biodiversity [244] and acoustic hotspots [57,141]. In these environments, snapping shrimps tend to dominate reef soundscapes at frequencies above 1 kHz [245], while a band attributed to damselfish is found around 400 Hz [246]. Numerous studies have estimated that these soundscapes may offer a reef orientation cue at relatively large distances [128,133,134], but there is a lack of empirical studies on reef sound propagation. Measuring the distance over which reef sounds propagate is necessary to determine their relative importance as cues for long-range orientation and habitat choice. However, as reef soundscapes are composed of sounds of different frequencies, they propagate over different distances. Since different species have different hearing frequency ranges, the detection distance (the maximum distance at which a species can perceive a sound above ambient background noise) does not automatically correspond to the propagation distance (the maximum distance at which the ambient background noise masks reef sounds) of the reef sound. The effective use of acoustic cues to detect the reef requires (*1*) a loud reef soundscape, (*2*) low ambient noise (wind and boats), (*3*) hearing ability in the relevant frequency bands and (*4*) sound localization.

Propagation and detection distances have been mainly assessed using theoretical spreading models with distances varying from a few hundred meters to a few kilometers [247–250]. In addition, some authors observed a so-called 'reef effect'; i.e., sound levels decrease more slowly than expected from a cylindrical spreading model over a distance approximately equal to the length of the reef (≈ 20 km). The supporting reason is that the reef sound is not located in a single point but results from a series of sources. The high variability in the theoretically estimated propagation distances has highlighted the need to conduct empirical measurements of the soundscape at different distances from a reef [247]. Such empirical studies are fundamental for estimating the distances at which reef sounds can be perceived by marine organisms because they can be useful for many taxa. Many species of cetaceans are known to roam over great distances, for example between mating and feeding areas [251,252]. As lighting conditions are often a constraint, water has excellent sound transmission properties, so the sounds of biotic and abiotic origin can be exploited as

acoustic cues for orientation [253]. The routes that cetaceans travel are, in fact, exposed to elevated levels of biological and nonbiological ambient noise [254], and it has been suggested that cetaceans use reef sounds for navigation [254,255].

Many fish species are also known to migrate between spawning and feeding areas [253] or to have distinct migration cycles related to life stages [256]. In coral reefs, most marine organisms (bryozoans, cnidaria, crustaceans, echinoderms, molluscs, polychaetes, sponges, tunicates, teleosts, etc.) have structured life histories with two distinct stages: a relatively benthic/sedentary stage on the reef (usually juveniles and adults), and a pelagic, dispersal larval stage in the ocean [127]. While some species are known to disperse to a maximum of hundreds of meters, other species would travel up to hundreds of kilometers [257]. Their dispersal depends both on hydrodynamic processes and on species-specific behavioral responses to environmental cues [258]. One of the greatest challenges faced by these organisms is relocation to the patchily distributed reef habitats in a vast oceanic matrix once they are ready to transition to demersal habitat [128]. For effective orientation, animals require cues that are heterogeneous in the environment and contain reliable information about potential settlement sites [135,259]. These potential cues include vision [129], olfaction [127,130–132], sounds emanating from reefs [128,133,134], differences in wind- or wave-induced turbulence [127], gradients in abundance of fish, plankton or reef detritus [127] or a combination of several of them [135–137]. Many of these cues, such as vision, are effective only at small distances from the reef [260–262] (a few tens of meters) [127], whereas sounds from the reef (e.g., from benthic invertebrates and fish) are potential cues for larval orientation over long distances. They are thought to assist pelagic larvae of cnidaria [263–265], mollusks [266,267] , crustaceans [268–270] and fish [271–276] to locate and orient toward settlement habitat. However, the distances over which pelagic individuals can detect and localize sounds from reefs are still unassessed [247]. A first set of theoretical approaches calculated the distances of detection to be less than 1 km [247] to more than 5 km depending on the hearing ability of the studied species [248,249]. Other studies suggested a distance of detection of 20 km based on the audiogram of a Pomacentridae species on rocky habitats of New Zealand [271].

The aims of the present study are to describe the biophony (sounds of fish and benthic invertebrates) of the barrier reef at Moorea Island (French Polynesia) to (*1*) measure its propagation distance in the ocean empirically, (*2*) describe how abiotic and anthropic factors interfere with it and (*3*) estimate the detection distance based on known audiograms.

2. Materials and methods

2.1. Sampling

Data sampling was conducted 13 – 17 May 2016, on the north coast of Moorea (French Polynesia) (17.5 S, 149.9 W, Figure 24). Recordings were realized with drifting antennas made of a floater and an autonomous EA-SDA14 recorder (RTSys®, Caudan, France) connected to a wideband low-noise HTI-92 hydrophone (High Tech Inc., Long Beach, MS, USA) with a sensitivity of −155 ± 3 dB re 1 V µPa^{-1} and a flat frequency response from 2 Hz to 50 kHz. It was placed on a vertical rope at ≈ 5 m from the surface to minimize sea-surface noise. Sounds were acquired continuously at a 156 kHz sampling rate and 32 bits resolution. Six transects were realized during daytime (8:30 AM – 5:30 PM) with recordings of approximately 600 s duration recorded at 50, 100, 200, 400, 600, 800, 1500, 2000, 3000, 4000, 5000, 7000, and 10,000 m from the reef crest; i.e., a total of 78 stations corresponding to 13 h of recordings (Figure 24). The mean depth varied from 9 to 2580 m. Water depth was measured for each transect using a portable echosounder. These data were completed with bathymetric data obtained from the French Naval Hydrographic and Oceanographic Service (reference: LOTS BATHY S201208100-08, SHOM, France).

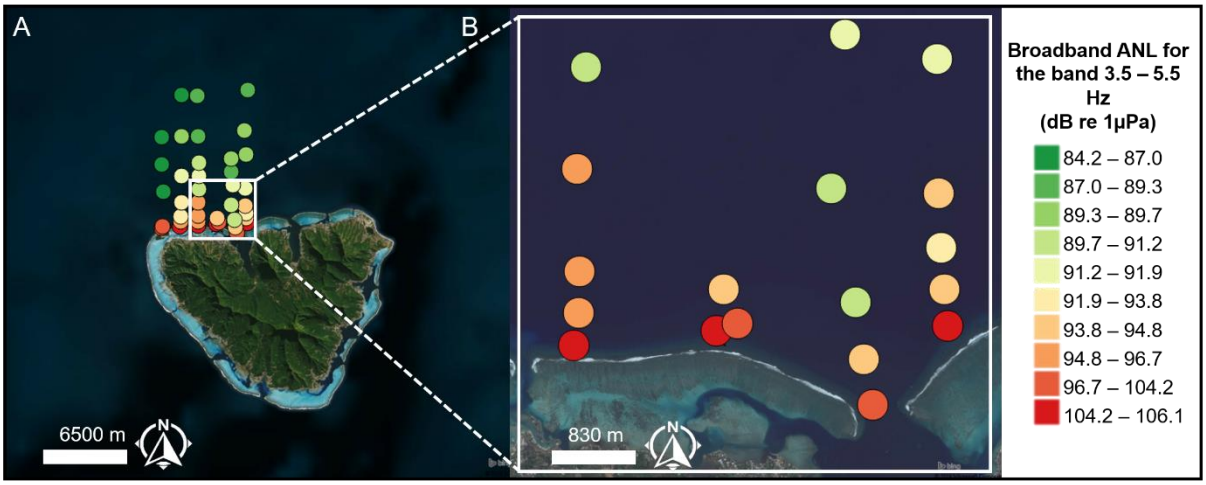

Figure 24 Distribution of the ambient noise level (ANL) of the broadband transient sounds (BTS) between 3.5 and 5.5 kHz on (A) the 40 stations and (B) zoom of the proximal part of the transects. Color scale indicates ambient noise levels.

GPS positions of the drifting antennas were recorded both when they were deployed and when they were recovered. The drift distances were not uniform, but the error caused by the uncertainty of the hydrophone position due to drift was inferior to 1.8 dB for all the data. In addition, to record the diel variability of the biophony during the recording period, a fixed recording station, composed of the same type of recorder and hydrophone, was bottom-moored

on the external slope, at a depth ≈ 12 m and 127 m distant from the reef crest on the same dates as the transects.

2.2. Analyses

The recordings were visually and aurally inspected with RavenPro Sound Analysis Software 1.5 (Cornell Lab of Ornithology, Ithaca, NY, USA). Only transect stations with low noise levels from buoy strumming (e.g., not in the presence of high swells) were considered (40 out of 79). For each of the selected stations, only sections without boat noises were analysed. Long-term spectrograms, sound pressure spectrum levels and graphics were realized with custom-made Matlab® R2014b routines (MathWorks, Natick, MA, USA).

2.3. Benthic invertebrate sounds

To assess the temporal variability of the benthic invertebrate biophony (the sum of the many isolated broadband transient sounds (BTS) produced by benthic invertebrates [277] (Figure 25A) recordings from the fixed station were analysed (Figure 24 and Figure 25). BTS were grouped into four frequency 'bands' (3.5–5.5 kHz, 6–8 kHz, 10–13 kHz and 14–17 kHz). These bands were chosen based on peaks in 24 h power spectra. An automatic BTS detector (see [278] for details of the algorithm) was run for each of the selected bands. In addition to the four bands, the same algorithm was run on the BTS between 570 and 2000 Hz, because these frequencies corresponded to sounds that appeared to be more attractive to larvae of different fish families [259]. The three features calculated were the number of detected BTS (NoBTS) having a minimal signal-to-noise ratio (SNR) of 10 dB, the peak-to-peak sound pressure level (SPL), and the ambient noise level (ANL), both in dB re 1 µPa for each band (Figure 25A). The ANL is the background SPL modelled with a χ^2 distribution on the 20th percentile (*cf.* [279] for the definition and [280] for the formula). It represented the overall energy of distant BTS emanating from the reef without the discriminable near sources of high- energetic BTS. The SPL is the sum of both discriminable near sources of the biophony and the ANL. Wenz's ambient noise curves [5], calculated on the same bands as the BTS, were superposed to the sound levels to estimate attenuation due to wind regime or ship traffic [201]. The flat sea state condition corresponded to a wind speed of 0 kn while the average condition corresponded to 6 kn; that is, the average wind speed of the study area (annual mean at the Tahiti Island meteorological station between 2008 and 2019). To compare the different acoustic features between day and night recordings of the fixed station at the barrier reef, Student's *t*-tests were realized using the R software version 3.3.0. (R Core Team, 2016).

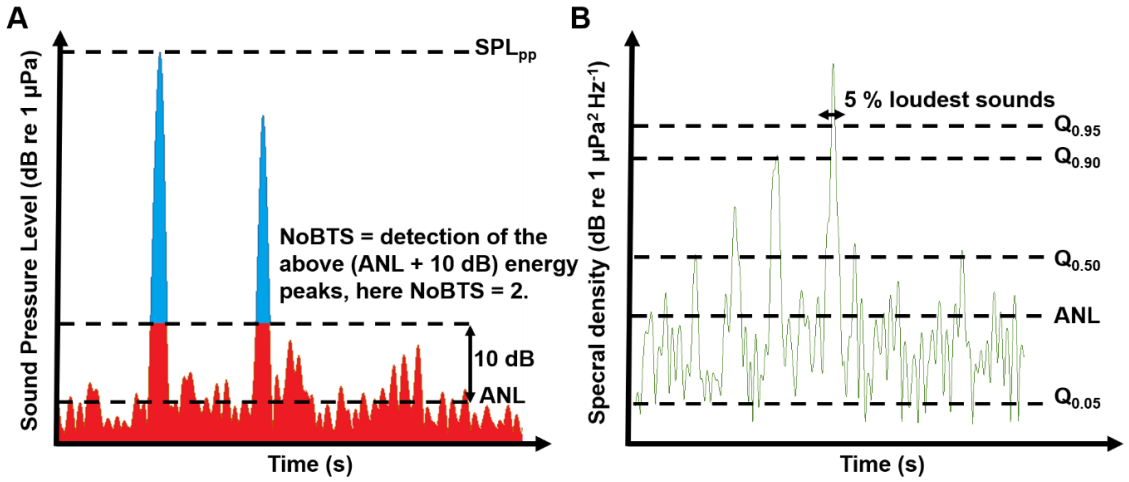

Figure 25 Description of the acoustic features for (A) benthic invertebrates sounds (for each BTS band) and (B) fish sounds (200–500 Hz). In blue: nearby sources producing loud and short discriminable near sources of the biophony's energy peaks; in red, a collection of a large number of distant unidentified sources producing a background chorus. SPL = Sound Pressure Level, pp = peak to peak, NoBTS = number of broadband transient sounds, ANL = ambient noise level, Q = percentile, with $Q_{0.05}$ = 5% faintest sounds, $Q_{0.50}$ = median levels, $Q_{0.90}$ = 10% loudest sounds and $Q_{0.95}$ = 5% loudest sounds.

2.4. Fish Sounds

To characterize fish sounds, the mean sound pressure level of the frequency band comprised between 200 and 500 Hz was analysed because it corresponded to the frequency band in which a fish chorus [58,281] was present. The features measured were the spectral ANL, the 50th percentile ($Q_{0.50}$), the 90th percentile ($Q_{0.90}$) (representative of the 10% loudest sounds), and discriminable near sources of the biophony, represented as the 90th percentile with 10 dB above the Wenz background noise ($Q_{0.90}$ −10) in dB re 1 µPa^2 Hz^{-1} (Figure 25B). Wenz's ambient noise spectra were superposed to the calculated spectra [201] to estimate the wind- or shipping noise-dependent effect on reef sound propagation. To compare the different acoustic features between day and night recordings of the fixed station at the barrier reef, Mann-Whitney *U* tests were conducted using the R software version 3.3.0. (R Core Team, 2016).

2.5. Propagation distances of reef sounds

To account for complex local conditions of propagation near the shore, logarithmic linear regressions were obtained from sound levels measured in situ from the reef up to 10 km offshore as $y = a \log_{10} r + b$ for $r < 10$ km. Sounds below 200 Hz were affected by the strumming noise produced by the drifting systems and were not considered. Distances between locations of the drifting recording devices and the reef crest were measured using QGIS 2.14.3 (Open Source Geospatial Foundation Project).

For distances greater than 10 km, a theorical cylindrical propagation loss (= transmission

loss, TL) was calculated from 10 km to range r, with $TL = 10 \log (r \cdot r_0^{-1}) + \alpha (r - r_0)$ for $r \geq 10$ km and $r_0 = 10$ km. The attenuation of sound in seawater (α in dB km^{-1}) was calculated using the model of Ainslie and McColm [282] to fit the average temperature of 26 °C. Reference values were used for the pH and salinity (pH = 8; S = 35) [282]. This propagation model was chosen because the majority of the regression equations for distances shorter than 10 km were closer to a cylindrical than a spherical propagation (Table SP3 - 2). The difference between day and night recordings of the fixed station were used to infer the difference between diurnal and nocturnal propagation.

2.6. Comparisons with audiograms

Regressions of the biophony reef spectra against distance from the reef (Table SP3 - 2) were compared to audiograms from cetaceans, invertebrates and (post-)larval fish in the literature. Polynesian coral reef species were used except when little data were available, in which case we used audiograms reported for other species (e.g., *Stenella coeruleoalba* was used instead of the one of *S. longirostris*). Values in particle motion from the literature were converted to pressure values assuming a plane-wave propagation [283]. To compare audiogram values at one given frequency (dB re 1 µPa) to the spectra (dB re 1 μPa^2 Hz^{-1}), it was necessary to adjust the audiogram thresholds [284] by lowering them by 10 $\log_{10}$ (critical bandwidth, CBW) [285,286] with CBW estimated to 10% of the center frequency as in Egner and Mann 2005. According to the literature [287,288], for both fish and invertebrates, a correction factor of 10 to 30 dB was applied to compare methods. In contrast, in cetaceans, the results of the different methods were comparable [289]. The biophony spectra used were the 90th percentile ($Q_{0.90,}$ the 10% loudest sounds), the 50th percentile (the median) and the ANL on the basis of the regressions (calculated on each frequency used in the audiograms, Figure 25B). When propagation distances were beyond 10 km (i.e., the greatest distance at which recordings were acquired), the theoretical TL model was used with an α calculated for each frequency of the audiograms. The distances obtained were compared to the background noise of the Wenz model.

3. Results

The soundscape of the barrier reef of Moorea was characterized by fish sounds between 200 and 500 Hz and by a high number of broadband transient sounds (NoBTS) between 3.5 and 17 kHz (Figure 26).

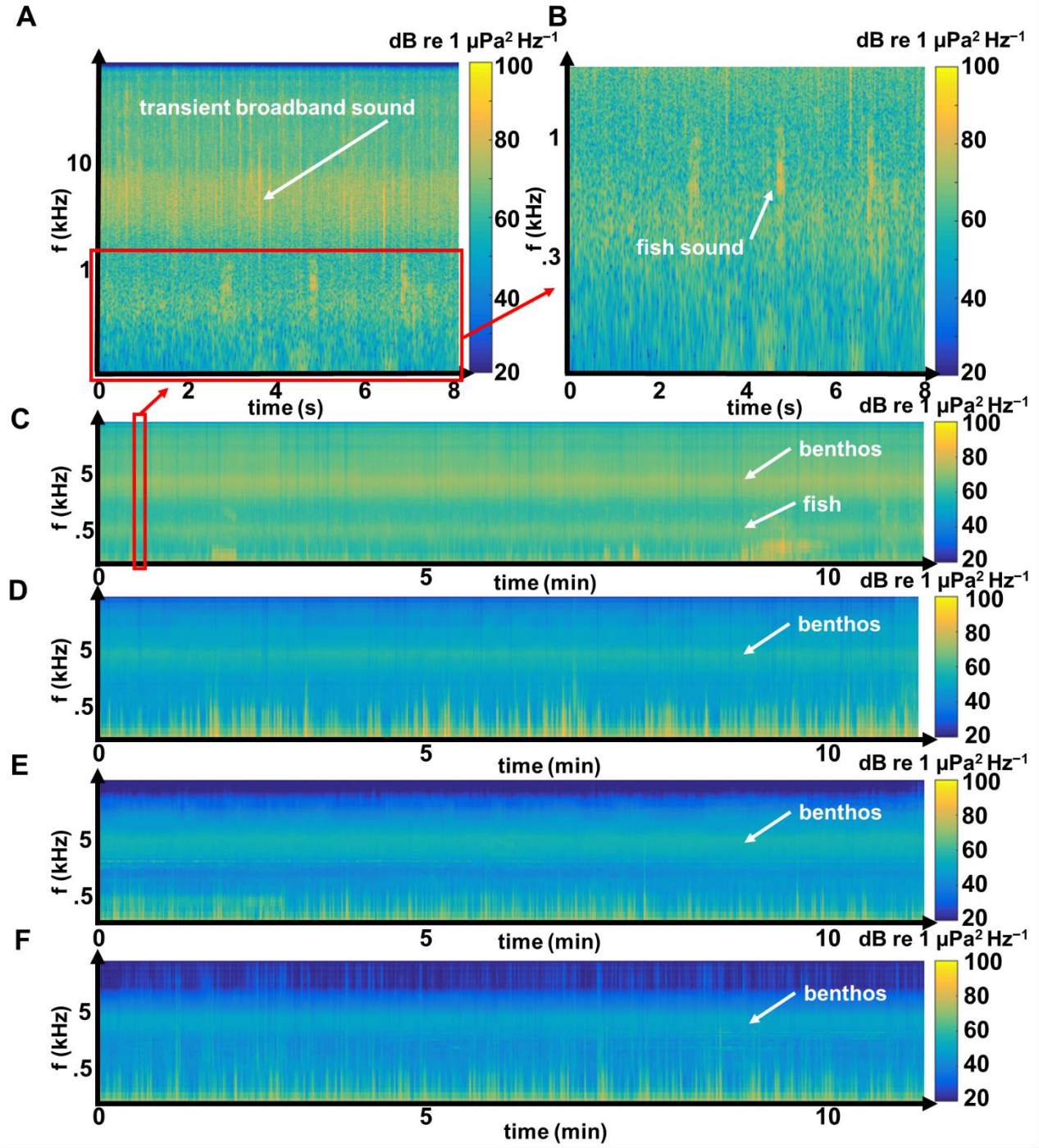

Figure 26 Spectrograms of the soundscapes recorded at different distances from the reef. (**A**) and (**B**) illustrate subsections of spectrogram (**C**) highlighting (**A**) invertebrate and (**B**) fish sounds. **C** was recorded at 138 ± 11 m from the reef, (**D**) 964 ± 138 m, (**E**) 3896 ± 3 m, and (**F**) 9866 ± 43 m from the reef crest. For **A** and **B**: LFFT = 16,384, overlap = 75%, window = Kaiser. For C, D, E and F: LFFT = 65,536, overlap = 50%, window = Kaiser.

3.1. Benthic invertebrate sounds

The NoBTS ranged from 106 ± 6 (mean ± SD) per second in the 3.5–5.5 kHz band; 96 ± 9 per second in the 6 – 8 kHz; 86 ± 4 in the 10 – 13 kHz and 83 ± 3 in the 14–17 kHz. The NoBTS was 8% greater during the night for the band 3.5–5.5 kHz (Δ = 8.12, t = –5.64, df =

23, $P < 10^{-5}$, Student's *t*-test), 14% and 5% smaller during the night within the band 6–8 kHz ($\Delta = 14.05$, t = 7.67, df = 23, $P < 10^{-6}$, Student's *t*-test) and the band 10–13 kHz respectively ($\Delta = 4.42$, t = 3.15, df = 22, $P = 0.0046$, Student's *t*-test), and similar for the band 14–17 kHz (t = 0.59, df = 23, $P = 0.56$, Student's *t*-test, Figure 26A and Figure 27).

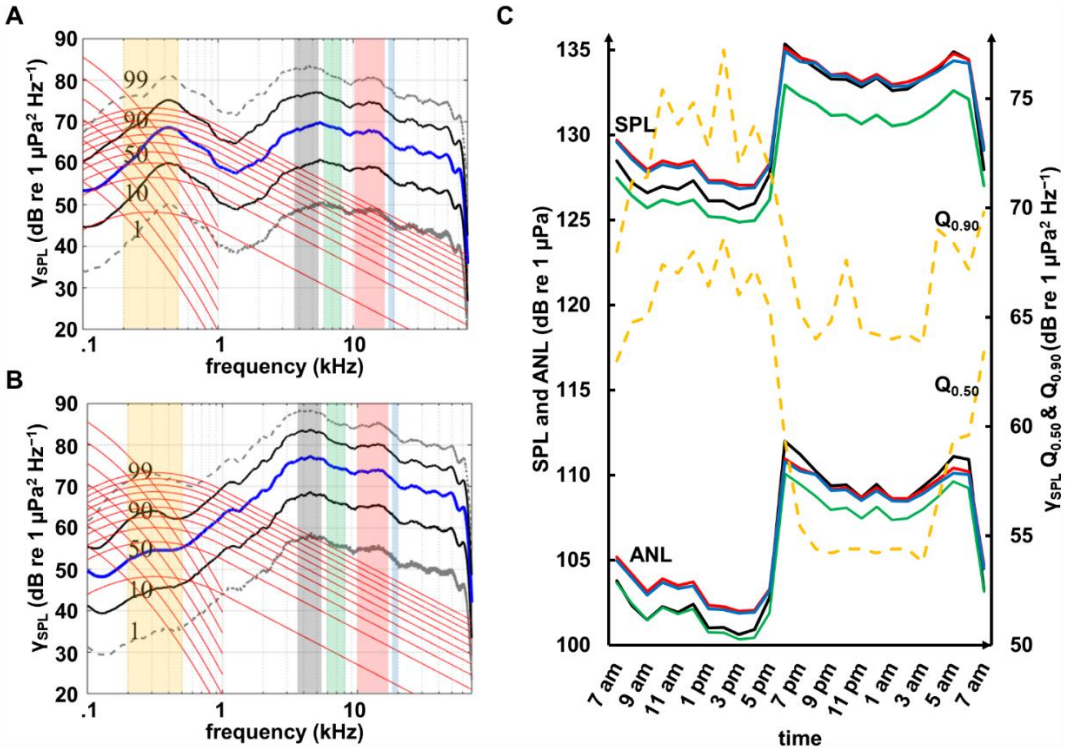

Figure 27 Power spectral density at the fixed recording station at –12 m depth and 127 m distance from the reef crest at (A) 2 PM and (B) midnight. In dashed grey, percentiles $Q_{0.01}$ and $Q_{0.99}$; in black, percentiles $Q_{0.10}$ and $Q_{0.90}$; in bold blue, the median $Q_{0.50}$ and in red, Wenz background noise for wind speeds between 0 and 30 kn and ship traffic index between 1 and 7. (C) Diel pattern of sound pressure level (SPL) and ambient noise level (ANL) (left scale) for benthic BTS bands (3.5–5.5 kHz, 6–8 kHz, 10–13 kHz and 14–17 kHz) highlighted respectively in black, green, red, and blue non-dashed lines, also highlighted in the vertical rectangles in (A) and (B). Diel pattern of $Q_{0.50}$ and $Q_{0.90}$ of power spectral density (γSPL) (right scale) for the frequency band between 200 and 500 Hz corresponding to the daytime fish chorus highlighted in orange (dashed lines).

The SPL and ANL of all the bands of BTS were significantly higher during the night (for all: t < −16.79, 20 < df < 23, $P < 10^{-13}$, Student's *t*-test) with a 6.7 to 9.2 dB difference between 5 and 6 PM (Figure 27C). This means that sounds were four to eight times louder at dusk. There was a peak at dusk and dawn with a higher difference between day and night for BTS in the 3.5–5.5 Hz band (SPL: 126.90 ± 0.86 dB re 1 µPa during the day and 133.72 ± 0.88 dB re 1 µPa during the night) (Figure 27C). The SPL and the ANL of the 6–8 kHz band were always smaller than those of the other bands (Figure 27C).

3.2. Fish sounds

The band between 200 and 500 Hz presented a diel pattern with higher values of sound pressure spectrum level during the day: $Q_{0.50}$ = 66.02 ± 1.74 dB re 1 µPa^2 Hz^{-1} (day) and

55.92 ± 2.40 dB re 1 µPa^2 Hz^{-1} (night); $Q_{0.90}$ = 72.58 ± 2.29 dB re 1 µPa^2 Hz^{-1} (day), and 65.76 ± 2.12 dB re 1 µPa^2 Hz^{-1} (night) (W = 918 and 901; both $P < 10^{-5}$, Mann–Whitney U test for $Q_{0.50;}$ Figure 27). The spectra presented differences between day and night: a peak between 400 and 500 Hz was present during the day both for intense (percentile $Q_{0.99}$) and median sounds ($Q_{0.50}$), while during the night, peaks were always observed between 250 and 280 Hz for $Q_{0.99}$ and were never observed for $Q_{0.50}$ (Figure 27) Other peaks were punctually observed at dusk and dawn, especially for lower frequencies. This suggests that vocal species produce sounds with different diel patterns.

3.3. Propagation distances of reef sounds

A decrease of the sound spectrum level from the shore to the open ocean was observed for sounds between 200 and 70,000 Hz (Figure 24 and Figure 26). ANL and SPL of BTS showed a constant logarithmic decrease with distance from the reef crest (Figure 28A). From the slope of the regressions, TL was estimated to vary from −8.99 to −16.80 dB decade^{-1} (a decade corresponds to a factor-of-ten increase) for BTS depending on the noise levels (i.e., SPL or ANL) and the band of BTS used (Table 2). There was a positive relationship between TL and frequency except for frequencies between 600 and 2100 Hz, for which a decrease in TL was observed. At 10 km, the measured ANL of the four bands of BTS was between 70 and 86 dB re 1 µPa and the SPL between 93 and 107 dB re 1 µPa (Figure 28).

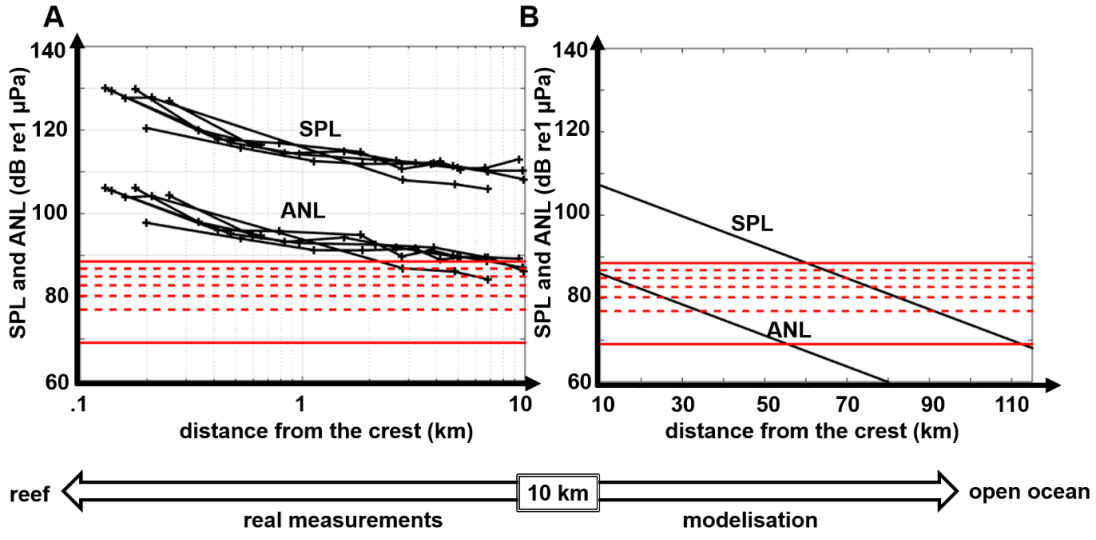

Figure 28 In situ measurements and subsequent modelled regression. (**A**) In situ measurements of the sound pressure level (SPL) and ambient noise level (ANL) for the band 3.5–5.5 kHz for each of the six transects up to 10 km. (**B**) Logarithmic regression with a modelled propagation loss (= transmission loss, TL): $\boldsymbol{TL = 10 \log (r \cdot r_0^{-1}) + \alpha(r - r_0)}$ with $\boldsymbol{r_0}$ = 10 km and $\boldsymbol{\alpha = 0.274}$ dB km^{-1} for distances beyond 10 km. In red, Wenz background noise for wind speeds between 0 and 18 kn (from bottom to top: 0, 3, 6, 9, 12, 15 and 18 kn).

Table 2 Regressions of broadband transient sounds (BTS) levels (dB re 1 µPa) at 1 m and 10 km from the reef crest for the ambient noise level (ANL) and the sound pressure level (SPL). Equations correspond to propagation loss regression equations assessed form the empirical data.

Band (kHz)	Feature	Equation	R^2	Value at 1 m	Value at 10 km	Δ night
				(dB re 1 µPa)		
3.5–5.5	ANL	$y = -8.99 \log_{10}x + 121.97$	0.85	121.97	86.01	7.92
	SPL	$y = -10.01 \log_{10}x + 147.23$	0.83	147.23	107.19	6.81
6–8	ANL	$y = -10.22 \log_{10}x + 121.79$	0.88	121.79	80.91	6.73
	SPL	$y = -11.13 \log_{10}x + 146.72$	0.84	146.72	102.20	5.60
10–13	ANL	$y = -13.84 \log_{10}x + 130.29$	0.94	130.29	74.93	6.22
	SPL	$y = -14.50 \log_{10}x + 155.64$	0.93	155.64	97.64	5.72
14–17	ANL	$y = -16.42 \log_{10}x + 135.74$	0.96	135.74	70.06	6.24
	SPL	$y = -16.80 \log_{10}x + 160.45$	0.95	160.45	93.25	5.71

At 10 km, the ANL of the dominant BTS band 3.5–5.5 Hz was 86.01 dB re 1 µPa (Table 2). Its estimated propagation range was 65 km under a low wind regime (0 kn) and decreased to 28 km with a 6 kn wind (Figure 28). During the day, the SPL of the BTS in the 3.5–5.5 kHz band under 0 kn wind conditions was 10 dB re 1 µPa above the background noise and detectable by hydrophone at 101 km. During the night, the intensity of these BTS was higher. Consequently, the estimated distances were higher: 90 km for the ANL under flat-sea conditions and 54 km with a 6 kn wind.

Propagation distances decreased with increasing BTS frequency band (Table 3). The ANL of the BTS between 570 and 2000 Hz (the band described to be attractive to fish larvae [259]) was detectable up to 55 km (day) and up to 90 km (night) with 0 kn of wind and to 0.9 km (day) and 3.4 km (night) with an average wind speed of 6 kn. Similar results were obtained for the spectral density values (Table 2) except for the 570–2000 Hz band. Propagation distances of all analysed BTS bands were likely poorly affected by ship traffic. In fact, based on Wenz's ship traffic spectra, if the index increased from 0 to 2, the ANL of the 570–2000 Hz band decreased by less than 1% (Figure 29) while with an index of 6, the ANL decreased by 50% (Figure 29A).

Table 3 Distance of detection (km) of the investigated Broadband Transient Sounds (BTS) frequency bands at day and night under different wind regimes as reported by Wenz (1962). ANL = ambient noise level, SPL = sound pressure level, both measured in dB re 1 µPa, kn = knot. γANL, $\gamma Q_{0.50}$ = 50th percentile and $\gamma Q_{0.90}$ = 90th percentile, measured as dB re 1 µPa^2 Hz^{-1} from the power spectra.

		Distance from the Reef Crest (km)									
		Day					Night				
Band (kHz)	**Feature**	**0 kn**	**3 kn**	**6 kn**	**9 kn**	**12 kn**	**0 kn**	**3 kn**	**6 kn**	**9 kn**	**12 kn**
3.5–5.5	ANL	65	39	28	20	13	90	65	54	46	39
	SPL	134	108	97	90	82	156	130	120	111	104
	SPL–10	101	75	65	56	50	123	97	87	79	72
	γANL	59	33	22	15	8.4	81	55	45	36	30
	γQ0.50	54	28	18	9.8	6.0	76	50	39	31	24
	γQ0.90	71	46	35	27	20	92	66	56	47	40
6–8	ANL	43	26	19	13	< 10	58	40	33	28	23
	SPL	90	72	65	60	55	102	84	77	72	67
	SPL–10	68	50	43	38	33	80	63	55	50	45
	γANL	40	22	15	9.7	7.0	52	35	27	22	17
	γQ0.50	36	19	12	6.1	4.4	48	31	24	18	14
	γQ0.90	48	30	23	18	13	59	42	35	29	25
10–13	ANL	23	14	< 10	< 10	< 10	31	21	17	14	12
	SPL	50	41	37	34	31	57	48	44	41	38
	SPL–10	38	29	25	22	19	45	36	32	29	26
	γANL	21	12	7.5	5.0	3.5	28	18	15	12	< 10
	γQ0.50	19	10	5.9	4.0	2.8	26	17	13	< 10	< 10
	γQ0.90	26	16	13	9.6	6.9	32	23	19	16	14
14–17	ANL	16	10	< 10	< 10	< 10	21	15	13	11	< 10
	SPL	34	28	26	24	22	38	32	30	28	26
	SPL–10	26	20	18	16	14	31	25	22	20	19
	γANL	15	9.0	5.7	4.0	3.0	20	14	11	< 10	< 10
	γQ0.50	14	7.4	4.7	3.3	2.5	19	13	10	< 10	< 10
	γQ0.90	19	13	10	7.5	5.6	23	17	14	13	11

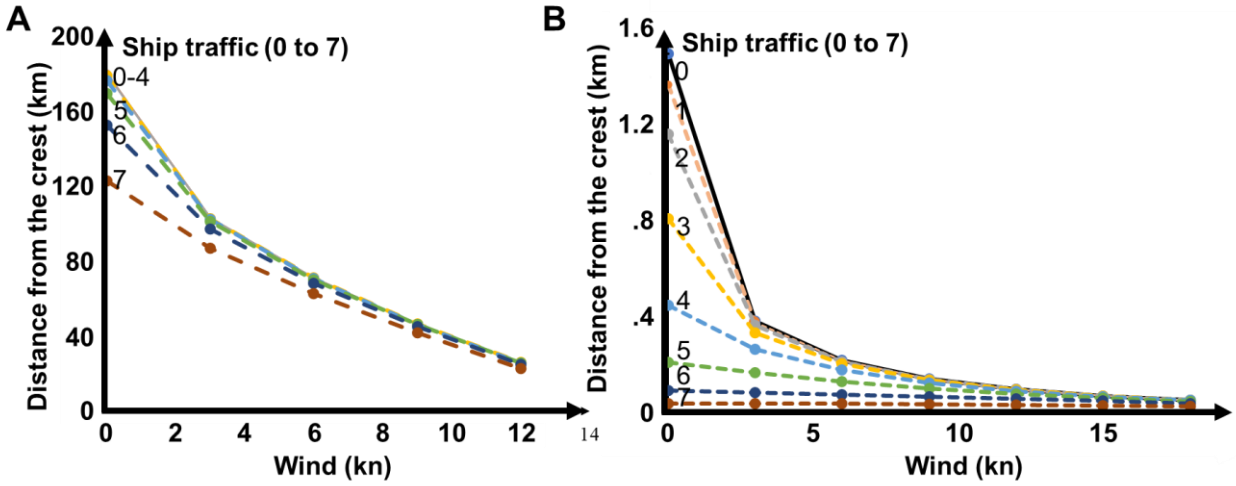

Figure 29 Detection distances as a function of the wind in knots of (A) the discriminable near sources of the biophony represented as the 90th percentile with 10 dB above the Wenz background noise ($Q_{0.90}$ – 10) between 570 and 2000 Hz and (B) fish ambient noise level (ANL). The solid line is without considering boats and dashed lines are when considering ship traffic from the Wenz model; each colour corresponds to a ship traffic regime also numbered from 1 (upper line) to 7 (bottom line).

Diurnal fish sounds (between 200 and 500 Hz) presented a logarithmic decrease in both ANL and $Q_{0.50}$, up to 1 km from the reef crest. Between 1 and 10 km, a logarithmic decrease of the sound pressure spectrum level was observed only in calm sea conditions. In presence of high swells up to 2 m, the sound pressure spectrum level of the transects was higher because it included hydrodynamic noises. Therefore, only transects under a calm sea state were used for the analyses (40 out of 79). This result indicated a limitation of the drifting method for low-frequency sounds in the presence of a significant swell. For the flattest sea-state transect, the distance of detection of the fish chorus frequencies (200–500 Hz) was found between 1322 m (for $Q_{0.50}$) and 1501 m (for ANL) with no wind ($y = -13.00 \log_{10} x + 91.82$, $R^2 = 0.96$, for $Q_{0.50}$, and $y = -13.42 \log_{10} x + 93.87$, $R^2 = 0.95$, for ANL; between the crest and 2 km, Table SP3 - 1). The 10% loudest sounds ($Q_{0.90}$) were detected at 3.5 km from the crest and discriminable near sources of the biophony ($Q_{0.90}$ with 10 dB above the Wenz background noise, named $Q_{0.90}-10$) at 793 m front the crest ($y = -14.62 \log_{10} x + 103.63$, $R^2 = 0.94$ between the crest and 1 km on the descending portions of all the transects, Table SP3 - 1). Propagation distance decreased by a factor ≈4 (for $Q_{0.50}$ & ANL) or 3.5 (for $Q_{0.90}$) with a 3 kn increase in wind speed (Table SP3 - 1). With an average wind speed of 6 kn, these four distances decreased to 180, 217, 654 and 134 m for $Q_{0.50}$, ANL, $Q_{0.90}$ and $Q_{0.90}-10$ respectively. Under no-wind conditions, the increase of the level of Wenz's ship traffic index from 1 to 2 decreased the distance between 187 and 207 m (for $Q_{0.50}$ & ANL) and 491 to 102 m (for $Q_{0.90}$ and $Q_{0.90}$–10); however, this decrease was less important when wind speeds were higher as there was a combined effect of wind and boats on detection distance during the day (Figure 29B, Table SP3 - 1).

3.4. Comparisons with audiograms: fish

In post-larval reef fish, audiograms based on sound pressure showed that the best hearing sensitivity is between 200 and 600 Hz [249,284,287,290–292]. The frequencies that allowed them to hear the reef from the greatest distance during daytime were in the same frequency range. Based on the audiograms (SPL) of post-larval reef fish [249,284,287,288,290–292], the estimated detection distances ranged from 0 to 65 m (median) and 80 m (ANL) for the six species of Pomacentridae, 8 to 336 m (median) and 11 to 401 m (ANL) for *Myripristis kuntee* (Holocentridae); 4 to 191 m (median) and 6 to 234 m (ANL) for *Acanthurus triostegus* (Acanthuridae); 23 to 455 m (median) and 28 to 560 m (ANL) for *Chaetodon citrinellus* (Chaetodontidae); 19 to 392 m (median) and 24 to 482 m (ANL) for *Rhinecanthus aculeatus* (Balistidae) and 0 to 4–5 m for the two Lutjanidae and the four Serranidae species analyzed

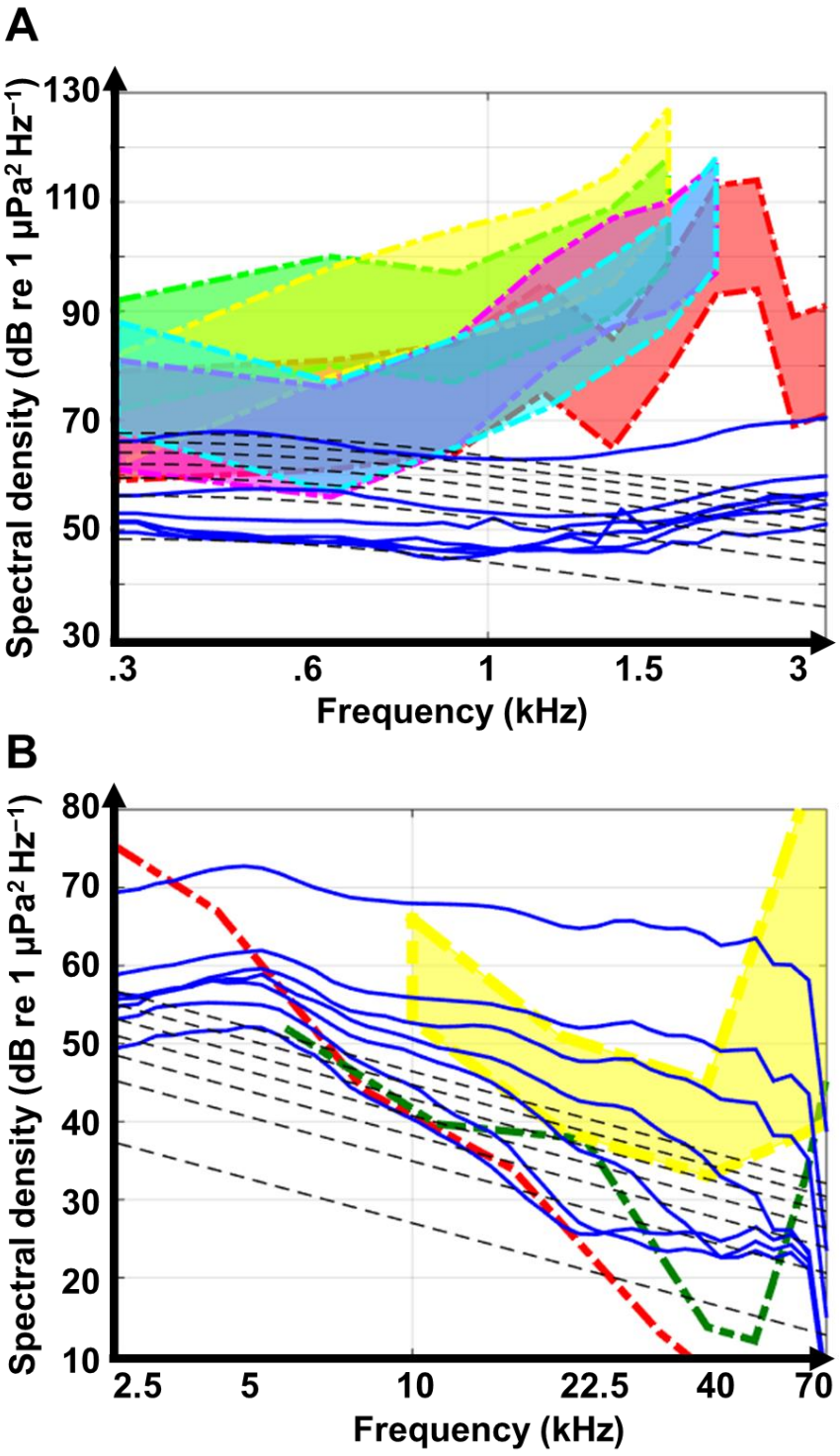

Figure 30 Audiograms compared to spectrum level of ambient noise level (ANL) at different distances from the barrier reef for (A) fish post-larvae and (B) cetaceans. Solid blue line: measured ANL on one of the six transects; from top to bottom: at 138, 476, 964, 2134, 3896, 6831, 9866 m from the reef crest. Dashed black line: Wenz's ambient noise curves; from bottom to top: 0, 3, 6, 9, 12, 15 and 18 kn of wind. Equivalent threshold (for details of the transformations, see Table SP3 - 3). (**A**) Red: *Myripristis kuntee*, green: *Abudefduf vaigiensis*, yellow: *Acanthurus triostegus*, magenta: *Chaetodon citrinellus* and cyan: *Rhinecanthus aculeatus*; (**B**) Red: *Stenella coeruleoalba*, green: *Mesoplodon densirostris* and yellow: *Globicephala macrorhynchus* [292–295].

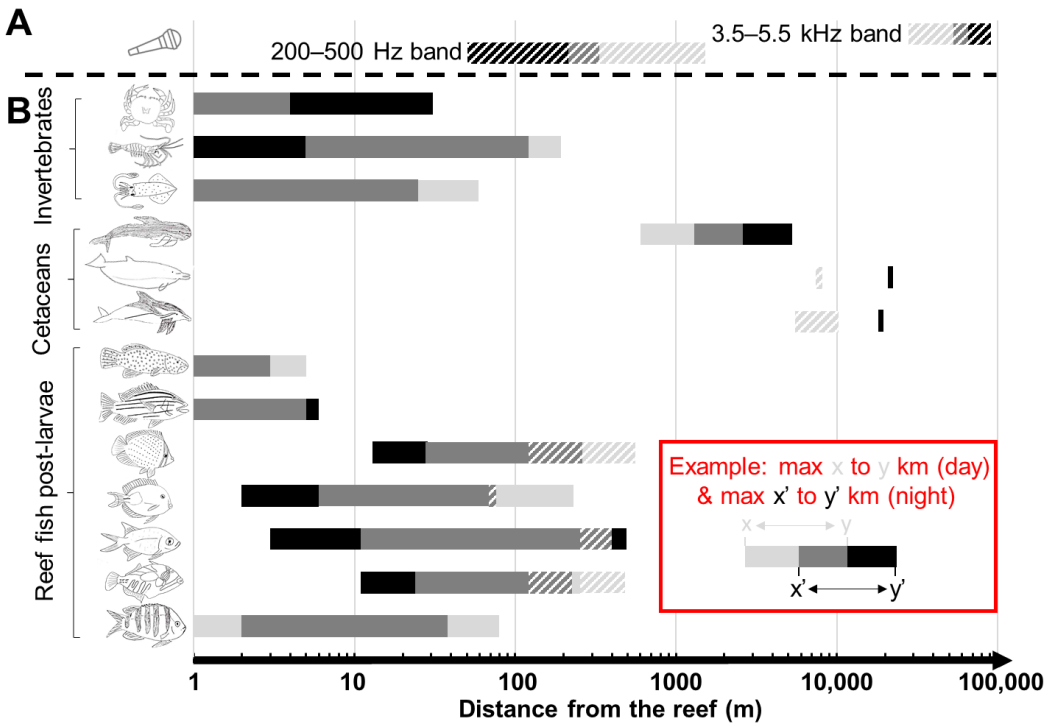

Figure 31 (A) Maximal distance of detection of the ambient noise level (ANL) of the fish chorus (200–500 Hz) and benthic invertebrate (3.5–5.5 kHz) bands and (B) maximal distance of detection of the ANL of the reef by different species from the literature. From bottom to top: fish (Pomacentridae, Balistidae, Holocentridae, Acanthuridae, Chaetodontidae, Lutjanidae and Serranidae), cetaceans (*Stenella*, *Mesoplodon* and *Globicephala*) and invertebrates (squid *Loligo*, shrimp *Palaemon* and crab *Ovalipes*). See Table SP3 - 3 for details of the individuals used. Light grey = diurnal values, black = nocturnal values, dark grey = overlap between diurnal and nocturnal values. Hatched parts correspond to values possible only when the wind is less than 6 knots, the average speed in Polynesia). The red box is an example to show how to read the figure.

(Figure 27, Table SP3 - 2, and Table SP3 - 3). These distances were smaller during the night except for species such as *M. kuntee*, which are able to hear higher frequencies (Figure 30 and Figure 31). For this species, frequencies between 2.7 and 3 kHz were the ones showing the greatest detection distances ranging from 2 to 337 m (median) and from 3 to 498 m for the ANL. For fish, the detection of low frequencies 300 and 600 Hz was limited by ambient noise values, as maximal detection distances both at day and night for an average wind of 6 kn can decrease up to 54% (Figure 30 and Figure 31).

However, for the majority of fish species, particle motion seems to be more appropriate for evaluating hearing thresholds [296]. As only little is known about particle motion perception on fish post-larvae, adult thresholds [297–299] were also used for comparisons with soundscape data (particle motion thresholds converted to pressure thresholds) as assumed in several studies [271,297]. Distances below 13 m were found for all the considered species except for the temperate *Sciaena umbra* (Sciaenidae): 13 to 344 m (median) and 16 to 430 m (ANL) at 500 Hz (maximum 217 and 271 if there are 6 kn of wind). For adult fish

hearing specialist species, these distances are higher; for example, *Pempheris adspersa* (Pempheridae) could detect the pressure component of the reef at 49 to 1389 m (median) and 59 to 1710 m (ANL) (maximum 207 and 258 m in a 6 kn wind).

3.5. Comparisons with audiograms: cetaceans

Odontocetes have their maximum hearing sensitivity around 40 and 64 kHz [293–295]. However, the audiogram comparison [293–295] indicated that the frequency range that would allow them to perceive reef sounds from a greater distance is between 5.6 and 20 kHz (Figure 30). The maximal detection distance of the median reef sounds ($Q_{0.50}$) ranged between 7.6 km (day) and 15.9 km (night) for the striped dolphin *Stenella coeruleoalba*, while the ambient noise level (ANL) emanating from the reef could be heard up to 9.2 km (day) to 19.0 km (night) (Figure 30 and Figure 31). With an average wind of 6 kn, diurnal values decreasedto 4.5 km and 5.5 km while nocturnal values did not change (Figure 31). Similar results were obtained for the Blainville's beaked whale *Mesoplodon densirostris* (median: 6.4 km (5.8 km if 6 kn of wind (day)) to 17.5 km (night); ANL: 8.2 km (7.3 km if 6 kn of wind (day)) to 21.8 km (night)) while smaller maximum distances were estimated for the short- finned pilot whale *Globicephala macrorhynchus* [median: 0.5 to 2.2 km (day) to 1.1 to 4.5 km (night); ANL: 0.6 to 2.6 km (day) to 1.3 to 5.3 km (night)] (Figure 27B, Table SP3 - 2, and Table SP3 - 3). In contrast to odontocetes, mysticetes are sensitive to lower frequencies, around 0.7 to 10 kHz with best values between 2 and 6 kHz [300]. However, as the exact auditory sensitivity of mysticetes is unknown (the frequency range is based on a mathematical function describing frequency sensitivity by the position along the basilar membrane coupled with data from other mammals [300]), detection range estimates could not be calculated.

3.6. Comparisons with audiograms: invertebrates

To the best of our knowledge, there are no available audiograms of post-larval marine invertebrates. Based on audiograms of adult individuals from the literature [301–306], different detection distances were estimated: some species such as *Panopeus* spp. crabs could perceive reef sounds with a maximal detection distance smaller than 1 m. Other species such as the crab *Ovalipes catharus* likely attained higher maximal detection distances at high frequencies (2000 Hz) and during the night (median: 0–21 m, ANL: 0–31 m) (Figure 31). For cephalopods, the maximal detection distances were found for lower frequencies between 200 and 600 Hz. These distances were estimated between 0 and 59 m. Finally, some species such as the prawn *Palaemon serratus* were likely capable of detecting reef sounds at 4–159 m (median) and 5–195 m (ANL) at 300 Hz during the day (Figure 31). During the night, maximal

distances could be achieved for higher frequencies (3 kHz; between 1 and 121 m) (Figure 27B, Table SP3 - 2, and Table SP3 - 3).

4. Discussion

4.1. Diel pattern

Sounds emitted by coral reefs are complex signals since they are generated by numer- ous species and affected by physical processes [247]. The source level of the barrier reef of Moorea (SPL at 1 m) was estimated to be 147 dB re 1 µPa for the most energetic frequency band 3.5–5.5 kHz and was of 136 dB re 1 µPa for larger BTS band (1–70 kHz). These values are within the range of source levels usually found in coral reefs [81] and healthy temperate rocky reefs [277]. In this study, there was an increase in low frequency sounds emitted by fish (200–500 Hz) during the day and an increase of high frequencies emitted by benthic invertebrates (3.5–5.5 kHz) during the night. Moreover, a peak in this higher frequency band was observed at both dawn and dusk. Similar diel patterns have been previously described from Polynesian [141,156] and non-Polynesian coral reefs [246,307].

4.2. Propagation distances

In the literature, the estimation of the propagation distances of biogenic reef sounds varies greatly according to the use of a spherical or cylindrical spreading model [308]. Moreover, different studies [271,308] assumed, without experimental demonstration, that acoustic cues could be detected at several tens of kilometers (see Mann et al. (2007) and Kaplan and Mooney (2016) for exceptions). Therefore, measurements of sound fields at different distances from the reef were required to establish an empirical propagation model based on in situ noise measurements [247]. This was the scope of this study. We showed that sound pressure and ambient noise levels decreased linearly. Transmission losses up to 10 km from the reef crest were intermediate between values from cylindrical and spherical models. On average, transmission losses up to 10 km from the reef crest varied between −9 and −17 dB decade^{-1}, depending on the source level and frequency band. The differences between these empirically estimated transmission losses and the ones of cylindrical or spherical models were likely a consequence of the acoustic reef effect [271]. This effect is observed because the recorder placed near the reef mainly records the nearby sounds, whereas a hydrophone placed further away from the reef records sounds coming from a larger portion of the reef.

Based on the empirical models, we found distinct propagation distances according to the nature of the sounds that form the reef soundscapes, i.e., fish choruses or the sum of broadband transient sounds (BTS). BTS from Moorea reefs (band: 3.5–5.5 kHz, ambient noise

level) at 65 km (day) propagated up to 90 km (night) in optimal sea state conditions. In comparison, for the lower frequency band corresponding to fish choruses (200–500 Hz, spectral ambient noise level), the propagation distance in optimal sea state conditions was 1.5 km. These empirically assessed propagation distances are necessary to understand how the species could use reef sound and to provide a first prediction of detection distance of sounds by marine organisms.

4.3. Wind and anthropogenic noise

In the ocean off Moorea reef, with an average wind regime of 6 kn, propagation distances of BTS (band: 3.5–5.5 kHz, ANL) decreased by a factor between 2.3 (day) and 1.7 (night) while fish sounds (200–500 Hz, spectral ANL) propagation distances decreased by a factor of 6.9 compared to optimal sea state conditions. Propagation distances with a Wenz's ship traffic index of 2 decreased by less than 1% for BTS (band: 3.5–5.5 kHz, ANL)and of a factor of 8 for fish sounds (200–500 Hz, spectral ANL). Moreover, the fact that the fish chorus occurred during the day, when vessel traffic and noise is highest, impliesa greater impact on the propagation distances of the low-frequency component of the reef's biophony. The quantification of this influence is important because previous studies have shown that soundscape degradation by boat noise can reduce settlement success in different larvae of coral reef fish [212,213]. Increases in ambient background noise levels caused by wind speed or anthropogenic noise may also interfere with the localization of suitable habitats as they reduce the intensity of natural reef sound that limits or impairs perception by marine organisms [309].

4.4. Comparisons with audiograms

Detection distances of reef sounds do, however, depend not only on geophysical or bathymetric conditions that affect propagation loss and on background noise masking, but also on the hearing sensitivity of the animal (e.g., auditory threshold) and the sensory mechanisms of signal perception that determine the ability of aurally detecting reef sounds from the ocean (e.g., critical bands). These distances are automatically lower than propagation distances. In our study, comparisons with audiograms indicated detection distances of less than 22 km for odontocetes and less than 0.5 km for fish post-larvae and invertebrates. The detection distances for fish reported here are in accordance with a previous study on the damselfish *Abudefduf saxatilis* (Pomacentridae), where Egner & Mann (2005) have estimated that reef sounds from the Great Barrier Reef can be aurally detected at a distance between 0.54 km and 2.15 km [284].

Previous studies, based on soundscapes recorded in New Zealand temperate waters, suggested greater detection distances up to 50 km [271]. The soundscapes of the two environments showed important differences. Typical soundscapes of New Zealand rocky reefs have peak intensities between 1 and 1.9 kHz [65]. These peaks are generally absent in coral reefs soundscapes [141,156,246,307] where they usually occupy frequencies between 3 and 6 kHz. As these peaks in temperate water are within the audible range of several of species of fish, cetaceans, and invertebrates, they likely affect detection distances.

The uncertainty in estimating the detection distance of numerous species is largely the result of a lack of information on their hearing abilities. Although fish and invertebrate species use particle motion and to some extent sound pressure, current audiograms are mainly based on sound pressure [298] and few studies described the contribution of direct particle motion and pressure detection separately in the auditory response [298,310,311]. In Hawaii, Kaplan and Mooney (2016) measured reef particle acceleration in the field. Average levels were found to be generally below these published hearing thresholds, meaning that particle motion may not play a major role as long-range orientation and settlement cue [307]. Because particle motion will attenuate more rapidly than acoustic pressure and is therefore not as likely to propagate as far as acoustic pressure, the estimated distances should likely be considered maximal values. Nevertheless, discriminable near sources of the biophony that exceed the mean ambient noise values, may also play a role in reef detection [307]. For example, when considering SPL of high-energetic BTS (3.5–5.5 kHz), propagation distances increased by a factor of 1.6 to 2.1 (day) and 1.4 to 1.7 (night) under flat sea state conditions.

Not only larvae use reef sound to detect suitable habitats. In the 1960s, Norris speculated that migrating cetaceans could use consistent sound sources as acoustic marks [312]. Subsequent observations showed that cetaceans may use the sound of snapping shrimp to orient themselves toward shallow water [254]. Depending on the species' audiograms and wind regimes, we found maximal detection distances for odontocetes (*Globicephala macrorhynchus*, *Mesoplodon densirostris*, and *Stenella coeruleoalba*) in a range from 2 to 22 km for sounds between 5.6 and 20 kHz, which represents the frequency range of best hearing for reef sounds. In odontocetes, maximum hearing sensitivities between 34 and 55 dB re 1 µPa are found between 3 and 35 kHz and between 30 and 110 kHz [3]. Consequently, cetaceans are able to hear higher frequencies than fish and their frequency range of audition overlaps with the intense BTS emitted by benthic invertebrates from the coral reef, which are the ones for which we reported the greatest propagation distances (up to 20 km). Although the attenuation in seawater increases with increasing frequency (e.g., α =

0.005 dB km^{-1} at 300 Hz vs. α = 0.3 dB km^{-1} at 4.5 kHz), ambient noise is naturally lower at high frequencies (e.g., 51 dB re 1 μPa^2 Hz^{-1} at 300 Hz vs. 36 dB re 1 μPa^2 Hz^{-1} at 4.5 kHz; both with a wind regime of 0 kn). As a consequence, detection distances are higher for cetaceans than for fish and invertebrates. To which extent different species of cetaceans use reef sounds for orientation remains unknown [253]. But considering their responses to playbacks of biological and industrial sounds [309] and considering their hearing abilities, it constitutes an interesting subject for investigation.

5. Conclusions

In conclusion, Moorea reef biophony can propagate up to 90 km from the coast, but depending on the species and life stage, maximal detection distances range from less than 0.5 km to 22 km. Furthermore, these distances can be reduced if reef noise is masked by meteorological conditions and anthropic noise. Therefore, the reduction of the distance of detection both by changing the soundscape or by masking can directly affect a variety of biological processes and reduce habitat sustainability.

6. Author contributions

Conceptualization, É.P., D.L., C.G., J.L., L.D.I. and X.R.; methodology, C.G., L.D.I., J.L., É.P. and X.R.; software, C.G.; validation, É.P., L.D.I., X.R. and C.G.; formal analysis, X.R.; investigation, X.R., L.D.I., C.G., J.L. and É.P.; resources, C.G. and L.D.I.; data curation, X.R.; writing—original draft preparation, X.R..; writing—review and editing, X.R., É.P., L.D.I., C.G. and J.L.; visualization, X.R., C.G., J.L. and L.D.I.; supervision, É.P., L.D.I., X.R. and C.G.; project administration, X.R., É.P. and L.D.I.; funding acquisition, É.P., D.L. and X.R. All authors have read and agreed to the published version of the manuscript.

Chapter 4. Invertebrate sounds from photic to mesophotic coral reefs reveal vertical stratification and diel diversity

Xavier Raick[1*], Éric Parmentier[1], Cédric Gervaise[2], David Lecchini[3,4], Under The Pole Consortium[5], Gonzalo Pérez-Rosales[3], Frédéric Bertucci[1,3] and Lucia Di Iorio[7]

[1] Laboratory of Functional and Evolutionary Morphology, FOCUS, University of Liège, Liège, Belgium

[2] Chorus Institute, Grenoble, France

[3] PSL University, EPHE-UPVD-CNRS, USR 3278 CRIOBE, Papetoai, Moorea, French Polynesia

[4] Laboratoire d'Excellence 'CORAIL', Perpignan, France

[5] Under the Pole Expéditions. Concarneau, France. Members : G. Bardout, J. Fauchet, A. Ferucci, F. Gazzola, G. Lagarrigue, J. Leblond, E. Marivint, A. Mittau, N. Mollon, N. Paulme, E. Périé-Bardout, R. Pete, S. Pujolle & G. Siu.

[6] Marine Laboratory, University of Guam, Mangilao, USA

[7] Université de Perpignan Via Domitia, CNRS, CEFREM UMR 5110, Perpignan, France

This chapter has been submitted in *Oecologia* in November 2022.

MAJOR RESULTS

Depth variability

- ✓ All acoustic features were significantly influenced by depth.
- ✓ Frequency features variability was higher in MCEs.
- ✓ The highest power spectral density value, the number of BTS, and their SPL decreased with increasing depth.

Link between BTS and benthic cover

- ✓ BTS peak frequency appears to be associated to features such as non-encrusting sponges, sand, hydroids, sessile invertebrates, black coral and gorgonians, as well as to greater depths.
- ✓ Other features such as BTS SPL and PSD features were grouped together and associated with features such as macroalgae, scleractinian, and dead coral.
- ✓ NoBTS tended to be associated with shallow reefs. It reflects the lower benthic activity observed in deep mesophotic reefs.

Diel variability

- ✓ Diel patterns of acoustic features were notably variable at 120 m depth.
- ✓ At 20 m, no significant differences were found in BTS Fpeak between night and day; whereas, in MCEs, diurnal and nocturnal BTS Fpeak differed.
- ✓ At 7 PM, NoBTS levels surged for two hours at three islands, with a peak frequency of BTS around 5.4 kHz, signifying increased activity by a specific species during this timeframe.

Differences between islands

- ✓ Depth effect on acoustic features was not equivalent at all the islands: Moorea and Bora Bora showed extreme contrasted patterns.
- ✓ The pattern of decreasing NoBTS with increasing depth was not found at all the islands.
- ✓ The peak frequency was constant all along the day at all depths in some islands while diel cycles were observed in some mesophotic reefs with higher frequencies during the night or during the day.

Key question for the objective of the thesis

How does the 'mass-phenomena' biophony vary along a depth gradient and diurnally?

Abstract

Although mesophotic coral ecosystems account for approximately 80% of coral reefs, they remain largely unexplored due to their challenging accessibility. The combined snapping of benthic invertebrates results in a continuous loud crackle. The acoustic richness within reefs has led scientists to consider passive acoustic monitoring as a reliable method for studying both photic and mesophotic coral reefs. We investigated the relationship between benthic invertebrate sounds (1.5–22.5 kHz), depth, and benthic cover composition, key ecological factors that determine differences between photic and mesophotic reefs. Diel patterns of snaps and peak frequencies were also explored at different depths to assess variations in biorhythms. Acoustic recorders were deployed at 20 m, 60 m, and 120 m depths across six islands in French Polynesia. The results indicated that depth is the primary driver of differences in broadband transient sounds (BTS) soundscapes, with sound intensity decreasing as depth increases. At 20 and 60 m, sounds were louder at night displaying clear diel patterns. At 120 m depth, benthic activity rhythms exhibited low or highly variable levels of diel variation, likely a consequence of reduced solar irradiation. On three islands, a peculiar peak in the number of BTS was observed every day between 7 and 9 PM at 120 m, suggesting the presence of cyclic activities of a specific species. It supports the existence of different invertebrate communities or distinct behaviors, particularly in deep mesophotic reefs. Overall, this study strongly supports the use of passive acoustic monitoring to describe and understand ecological patterns in mesophotic reefs.

1. Introduction

Most marine habitats are filled with biological sounds, which can be either communication signals and/or sounds emitted as by-products of animal activities such as feeding or movement [313]. The composition of sounds within a given habitat depends on the presence of species, their behavior, and activities, which, in turn, are influenced by ecological and environmental factors [241,314] (Chapter 6). The study of animal sounds within an ecological framework is the core objective of ecoacoustics [315]. It represents an innovative and effective monitoring technique for non-invasively acquiring information on biodiversity, behaviors, and biorhythms, irrespective of water turbidity, temperature, or depth [316–319]. Soundscapes, encompassing all sounds emanating from an ecosystem, also provide information on cryptic species and their activities 24 hours a day, making them suitable for assessing cryptic biodiversity. Recording these sounds and their variability is therefore promising, particularly for studying less accessible ecosystems such as Mesophotic Coral Ecosystems (MCEs) [320] (Chapter 6).

Mesophotic coral ecosystems, extending from depths of 30/40 m to/over 150 m [106–108], constitute approximately 80% of coral reefs [321]. Despite their significant contribution to reef ecosystems, little is known about their ecology and functioning [108] (Chapter 6), primarily due to the challenges in accessing and collecting scientific data at such depths. The limited studies conducted in mesophotic reefs have documented high spatial heterogeneity and structural complexity, providing shelter to a myriad of species [322–324]. Knowledge of mesophotic soundscapes, including the diversity of biological sounds and their variability, remains very limited. It is largely unknown whether acoustic composition and patterns are specific to MCEs, to what extent they differ from photic reefs, and whether lower light conditions influence biorhythms. Most studies on coral reef sounds have, in fact, been conducted in the photic zone [141,325,326]. The major sources of biological sounds in these photic coral reefs are benthic invertebrates, fish, and cetaceans. Fish and whales vocalize mainly in the low-frequency band (below 2 kHz) while dolphins and benthic invertebrates emit Broadband Transient Sounds (BTS) generally at higher frequencies (> 2 kHz) [84]. To provide ecologically relevant information about specific environments, the biogenic sound composition and/or acoustic patterns of a soundscape should be linked to habitat features.

Depth is an important driver influencing the composition of animal communities [327,328]. The depth-dependent composition and abundance of fish sounds has been documented in coral and temperate red-algae coralligenous reefs, likely reflecting the vertical stratification observed in fish assemblages [318] (Chapter 6). Furthermore, the acoustic community composition of

fish is strongly linked to benthic cover composition (e.g., the percentage of living fixed organisms) in temperate red-algae coralligenous reefs, as well as photic and mesophotic coral reefs [158,318] (Chapter 6). This indicates that acoustic cues can be associated with habitat-specific features. Depth-dependent distributions of benthic assemblages have been described for various coral reefs based on visual data [327,329–332]. Additionally, the three-dimensional structure of coral reefs and the presence of specific organisms such as sponges or octocorals provides shelter to a variety of often invisible invertebrate species, known to significantly contribute to the high biodiversity of coral reefs [333,334]. Acoustic footprints emitted by these sheltered invertebrate species reflect the activities of animal communities and may serve as proxies of biodiversity and density of benthic organisms [171]. Most sounds produced by benthic invertebrates are broadband transient sounds (BTS) extending over tens of kilohertz, dominating coastal soundscapes day and night [23,83]. These sounds can be emitted by numerous species from different taxonomic groups, such as sea urchins [65,243], bivalves [64] or numerous crustaceans such as hermit crabs [66], crabs, stomatopods, Palaemonidae shrimps [24], and snapping shrimps, specifically species from *Alpheus* and *Synalpheus* genera (Alpheidae) [24,70–72]. Despite documented decreases in snapping shrimp sounds below a depth of 55 m, which are among the most prevalent sounds in coral reefs [24,81,82], our understanding of depth-related differences in BTS is limited. Furthermore, there is a dearth of studies exploring the composition and contribution of BTS to soundscapes, as well as their correlation with benthic cover in mesophotic reefs.

Sounds produced by benthic invertebrates can serve as indicators of different habitats [335,336]. Moreover, BTS, particularly those emitted by snapping shrimps, respond to environmental changes such as temperature or pH [72,337,338] and exhibit distinct biorhythms. In fact, in many photic reefs, BTS display diel variations [23,72,79] (Chapter 3), with peaks typically observed around sunrise and/or sunset [24,82] (Chapter 3). Different diel cycles can co-occur at a specific site [79,82] and are known to depend on the peak frequency of BTS, potentially indicating differences in underlying communities (Chapter 3).

In this study, we investigated the relationship between benthic invertebrate sounds, depth, and benthic cover composition, key ecological factors determining differences between photic and mesophotic coral reefs. Our aim was to establish whether specific BTS are found in MCEs, and whether they are possibly related to the community compositions of benthic invertebrates. Additionally, we explored the diel cycles of BTS at different depths to assess whether different light regimes affect biorhythms. Three predictions were tested: (1) photic and

mesophotic reefs are characterized by distinct BTS that may contribute biodiversity differences; (2) BTS show a strong relationship to benthic cover composition, suggesting the presence of specific BTS in MCEs; (3) depth affects diel patterns of BTS, suggesting an influence on biorhythms. To test these three predictions, we used a unique dataset collected from six islands in French Polynesia, a group of islands that extends over 5 million km^2 in the South Pacific Ocean [112,113], at three different depths (20 m, 60 m, and 120 m) coupling passive acoustic recordings with benthic sessile cover inventories.

2. Materials and methods

2.1. Data collection

Data sampling was conducted between March 2018 and April 2019 on six islands in French Polynesia: Bora Bora, Moorea (both in the Society Archipelago), Teauaone Islet near Mangareva (Gambier Archipelago), Rangiroa, Raroia, and Tikehau (all three in the Tuamotu Archipelago) (Figure 32, Table 4). The first three islands are high volcanic islands, while the last three are atolls. At each island, three different depths were studied concurrently on the external slope, one in the photic reef (20 m) and two in the mesophotic reef (60 m and 120 m). At Mangareva, only the two shallower depths were studied due to an issue with the recorder.

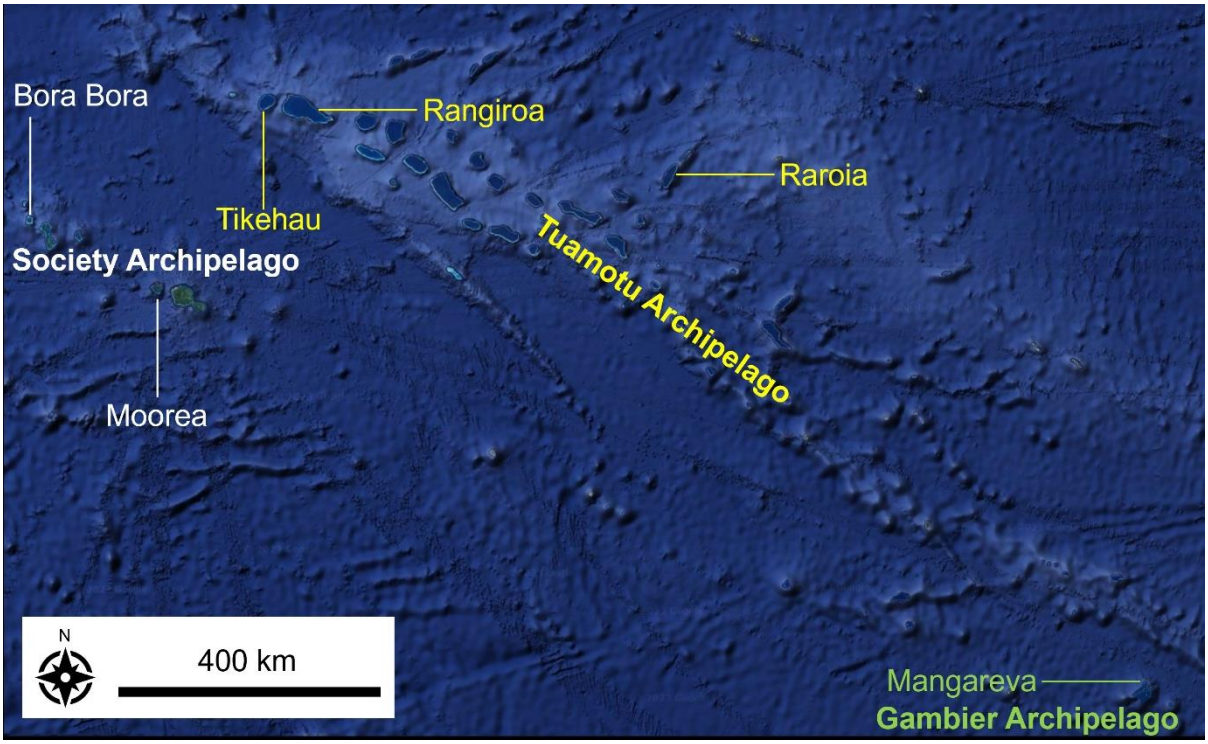

Figure 32 Map of the central part of French Polynesia: Society Archipelago (in white), Tuamotu Archipelago (in yellow), and Gambier Archipelago (in green) with the six studied islands highlighted.

Table 4 Localization and period of sampling for each island. For all the islands, three depths were sampled: 20 m, 60 m, and 120 m except at Mangareva where only the two shallower depths were studied.

Island	Type	Lat (S)	Long (W)	Year	Month	Day
Tuamotu Archipelago						
Rangiroa	Atoll	14.980°	147.613°	2018	Oct - Nov	$30^{th} – 2^{nd}$
Raroia	Atoll	16.023°	142.463°	2018	March	$2^{nd} – 5^{th}$
Tikehau	Atoll (Raised atoll)	15.017°	148.287°	2018	October	$15^{th} – 18^{th}$
Society Archipelago						
Bora Bora	High island (Almost atoll)	17.477°	149.851°	2018	September	$21^{st} – 24^{th}$
Moorea	High Island	16.437°	151.754°	2018	September	$4^{th} – 7^{th}$
Gambier Archipelago						
Mangareva (Teauaone)	High Island	23.001°	134.960°	2019	April	$16^{th} – 19^{th}$

Tripod structures, each equipped with 4 kg and measuring 60 cm, were deployed on the sea bottom of the barrier reef at depths of 20 m, 60 m, and 120 m on each island. On the vertical pole of each tripod, an acoustic recorder SNAP / HTI96 hydrophone (Loggerhead Instruments, Sarasota, FL, USA) was attached. The recorder operated for 62 hours (1 min on / 9 min off, flat frequency response between 2 and 30,000 Hz, sampling frequency: 44.1 kHz, resolution: 16-bit, gain: +2.05 dB, sensitivity: −170.5 to −169.7 dB re 1 V for a sound pressure of 1 µPa. The recorded files were categorized into four temporal periods: day (07 AM – 04:59 PM, n = 2 per depth and island), sunset (05 PM – 06:59 PM, n = 3), night (07 PM – 04:59 AM, n = 3), and sunrise (05 AM – 06:59 AM, n = 3).

To assess benthic cover, we used photo-quadrats from Chapter 6. For each island, photo-quadrats were realized during each deployment and employed to characterize the benthic sessile cover. At each depth, ten non-superimposed 0.75 x 0.75 m photo-quadrats were taken along four 10 m-long lines leaving a constant of 25 cm between quadrats following the methodology described by Pérez-Rosales et al. [339]. Subsequently, 90 pictures out of 120 (30 pictures out of 40 per depth) were randomly selected. The benthic cover was categorized into 16 classes: (1) sand, (2) dead coral, (3) rubble, (4) consolidated substrate, (5) scleractinian, (6) black coral and gorgonians, (7) Anthoathecata, (8) other hydroids, (9) encrusting sponges, (10) non encrusting sponges, (11) turf, (12) calcifying algae, (13) fleshy algae, (14) macroalgae including *Halimeda* algae, (15) encrusting algae and (16) other sessile invertebrates (Chapter 6). The photo-quadrats were analyzed using Photoquad 1.4 software (University of the Aegean, Mytilene, Greece), following the methodology developed by Pérez-Rosales et al. [339]. Percentages of each category per quadrat were averaged to obtain mean values for each depth

and island. This data was then used for the redundancy analysis (see 'Link between BTS and benthic cover' section).

2.2. Acoustic analysis

2.2.1. Spectral density

To assess patterns of mass phenomena of BTS production, we calculated Power Spectral Densities (PSD) using custom-made Matlab routines (version R2014b) with parameters set to FFT = 256, Kaiser window, and overlap = 50% (MathWorks, Natick, MA, USA). Median ($Q_{0.50}$) spectra were generated for each depth (20 m, 60 m, and 120 m), each period (day, night, sunrise, and sunset) and each replicate (Bora Bora, Mangareva, Moorea, Rangiroa, Raroia, and Tikehau). Two features were measured on each spectrum: the highest power spectral density value (**PSD_{Fpeak}**, in dB re 1 µPa^2 Hz^{-1}) and the corresponding frequency (**γFpeak**, in kHz, Figure 33), representing the frequency at which the power spectral density is maximal [340]. To compare PSD values corresponding to the same frequency at different depths, the difference between the peak frequency at 20 m was compared to the corresponding frequency at 60 m and 120 m and referred to as **Δ_{20m}** (in dB re 1 µPa^2 Hz^{-1}) (Figure 33).

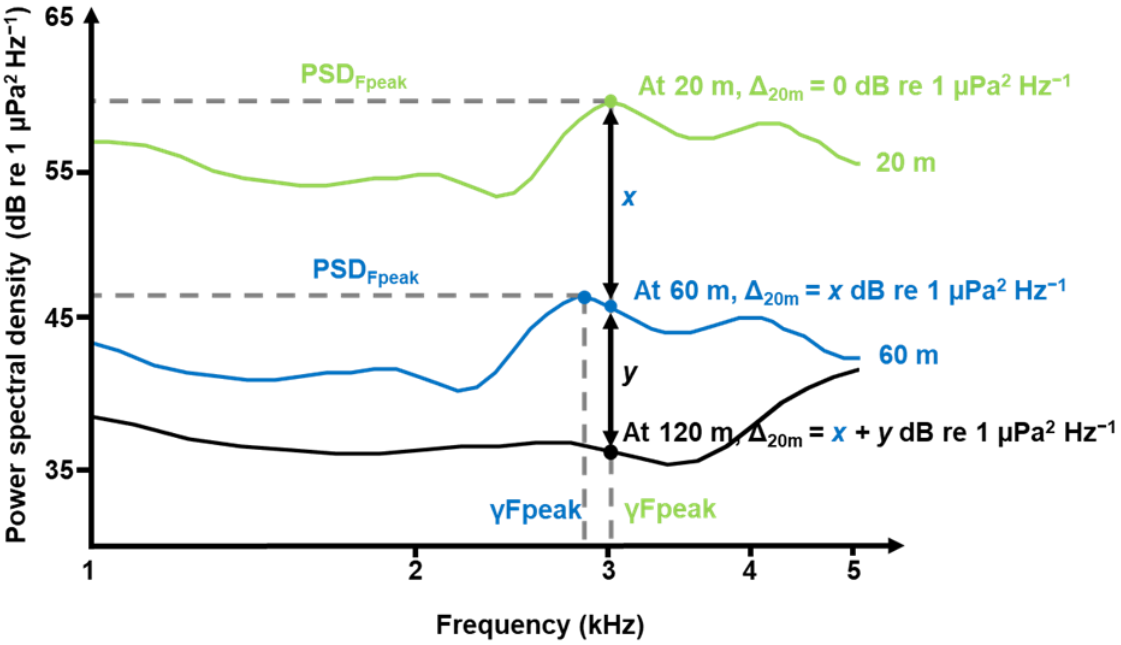

Figure 33 Graphical representation of the parameters measured on Power Spectral Densities (PSD) graphs. Green line: median at 20 m, blue line: median at 60 m, and black line: median at 120 m. The horizontal axis is frequency in logarithmic scale. PSD_{Fpeak} = highest power spectral density value, γFpeak = corresponding frequency, and Δ20m = difference between the peak frequency at 20 m compared to the corresponding frequency at 60 or 120 m.

2.2.2. Acoustic features of single BTS

In addition to the acoustic description of the mass phenomena, acoustic features were also extracted from single BTS, selected using an automatic BTS detector [278] that was run on the audio recordings using a custom-made Matlab (version R2014b) routine (MathWorks, Natick, MA, USA). To avoid inclusion of sounds other than from benthic invertebrates, the recordings were first visually and aurally inspected with RavenPro Sound Analysis Software 1.5 (Cornell Lab of Ornithology, USA) for frequencies between 1.5 and 22.5 kHz to remove the recordings containing echolocation clicks of odontocetes and masking anthropogenic noise. For each 1-minute file, three features were calculated: (*1*) the number of detected BTS per second (**NoBTS**, in BTS s^{-1}) with a minimal signal-to-noise ratio of 10 dB, (*2*) their peak frequency (**BTS Fpeak**, in kHz) and (*3*) the broadband-peak to-peak Sound Pressure Level (SPL_{pp}) (**BTS SPL_{pp}**, in dB re 1 µPa) (Chapter 3).

In addition to the acoustic characterization of the mass phenomena, acoustic features were extracted from each BTS, selected using an automatic BTS detector [278] applied to the audio recordings through a custom-made Matlab routine (version R2014b, MathWorks, Natick, MA, USA). The signal was filtered, and its energy was calculated. Subsequently, the ambient noise level (ANL) was estimated, and based on this ANL and a target false alarm probability, a detection threshold was computed using the energy of the signal [278]. If the local energy exceeded the detection threshold, a BTS was identified [278]. To avoid inclusion of sounds other than those produced by benthic invertebrates, the recordings were first visually and aurally inspected with RavenPro Sound Analysis Software 1.5 (Cornell Lab of Ornithology, USA) for frequencies between 1.5 to 22.05 kHz, with the aim of removing recordings containing echolocation clicks of odontocetes and masking anthropogenic noise. For each 1-minute file, three features were computed: (*1*) the number of detected BTS per second (**NoBTS**, in BTS s^{-1}) with a minimum signal-to-noise ratio of 10 dB, (*2*) their peak frequency (**BTS Fpeak**, in kHz) and (*3*) the broadband peak-to-peak Sound Pressure Level (SPL_{pp}) (**BTS SPL_{pp}**, in dB re 1 µPa) (Chapter 3). γFpeak reflects mass-phenomena differences, while BTS Fpeak provides an indication on the diversity of individual BTS.

2.3. Statistical analysis

2.3.1. Depth variability of BTS

To evaluate the depth variability of BTS, the power spectra of each depth (20 m, 60 m, and 120 m) were initially compared visually. Five linear mixed-effect models (function *lme*, package *nlme*) were then employed: one for each acoustic feature derived from the power

spectra (PSD_{Fpeak} and γFpeak), as well as individual BTS features (NoBTS, BTS Fpeak, and BTS SPL_{pp}). Depth (20 m, 60 m, and 120 m) and temporal periods (sunset, night, sunrise, and day) were designated as fixed factors, nested within the season (as a random effect). For spectral features (PSD_{Fpeak}, γFpeak, and Δ_{20}), 187 datapoints were used (11 temporal replicates per island and per depth). For the acoustic features of individual BTS (NoBTS, BTS Fpeak and BTS SPL_{pp}), the dataset comprised between 5465 and 5752 data points (one value per file was used, i.e., 36 for sunset and sunrise periods, 120 for the day, and 180 for the night). The variation in data points is due to some files lacking sufficient BTS to determine BTS SPL_{pp} and BTS Fpeak. The significance level was set to $\alpha = 0.05$. Subsequent between-depth comparisons were conducted with Tukey tests (function *glht*, package *multcomp*, with Bonferroni correction). Bonferroni corrections were applied to counteract the multiple comparisons problem and avoid Type I errors. Following this, acoustic features were compared between islands to investigate spatial variability. Non-parametric Kruskal-Wallis tests (with Dunn's test as *post-hoc* analysis, employing a Benjamini-Hochberg correction on *P*-values) were separately conducted for each island to compare the three depths (20 m, 60 m, and 120 m). In Mangareva, a Mann-Whitney-U test was used instead to compare the two sampled depths (20 and 60 m). These tests were chosen due to non-compliance with normality and/or homoscedasticity of variances. All statistical analyses were performed using R software version 3.6.1. (R Core Team, 2019).

2.3.2. Link between BTS and benthic cover

A redundancy analysis (RDA) was performed to examine the relationship between benthic sessile cover features and acoustic characteristics (library *vegan*, function *rda;* *https://cran.r-project.org/web/packages/vegan/vegan.pdf*) [341]. RDA, commonly applied in ecology [342], employs multiple linear regressions to assess the variation between independent features (explanatory variables) and dependent features (response variables). It captures the primary patterns of species variation and presents correlation coefficients between each independent and dependent feature [343,344]. It can be considered as an extension of Principal Component Analysis (PCA), in which components are constrained to linear combinations of environmental features [345]. Acoustic features (PSD_{Fpeak}, γFpeak, Δ_{20m}, NoBTS, BTS Fpeak, BTS SPL_{pp}) were standardized (to zero mean and unit variance) and used as response variables, while cover features were used as explanatory variables. To aid in interpretating *site constraints*, Spearman correlations, with associated *P*-values adjusted by Holm's method, were calculated between *site constraints* and acoustic features.

2.3.3. Diel variability of BTS

Spectrograms and PSD graphs between 1 and 20 kHz were generated with custom-made Matlab routines (version R2014b) for the temporal periods (day, night, sunrise, and sunset). These were visually compared to evaluate the diel variability of BTS. In addition, time series analyses (with 1 data point per 10 min) were performed on the 62 h of recordings for NoBTS, BTS Fpeak and BTS SPL_{pp} and the results were graphically presented.

To assess the influence of the different acoustic features, a linear mixed-effect model (function *lme*, package *nlme*) was performed for each studied depth (20 m, 60 m, and 120 m) and acoustic feature (PSD_{Fpeak}, γFpeak, NoBTS, BTS Fpeak, and BTS SPL_{pp}). Temporal period (sunset, night, sunrise, or day) was used as fixed-effects factor, nested within the season (considered as random effect). For the spectral features (PSD_{Fpeak}, γFpeak and Δ_{20}), we used between 55 (120 m) and 66 data points (20 and 60 m). In the case of acoustic features of BTS (NoBTS, BTS Fpeak and BTS SPL_{pp}), the dataset comprised between 1341 and 2152 data points. The significance threshold was set at $\alpha = 0.05$. Diagnostic plots were employed to verify model assumptions. Multiple comparisons (Tukey tests) between depths were conducted with Bonferroni corrections (function *glht*, package *multcomp*). Additionally, acoustic features were compared among islands to explore inter-island variability. Mann-Whitney U tests and Kruskal-Wallis tests (followed by Dunn's test as *post-hoc* with a Benjamini-Hochberg correction on *P*-values) were employed to compare temporal periods at each depth.

3. Results

3.1. Depth variability

3.1.1. General pattern

The spectrograms and PSD graphs revealed that the soundscape at the frequency range [1.5, 22 kHz] was predominantly characterized by broadband transient sounds (BTS) produced by benthic invertebrates (Figure SP4 - 1). When considering all depths and all islands, the highest values of power spectral density (PSD_{Fpeak}) were found between 3 and 10 kHz, displaying variations in both the number and intensity of spectral peaks. As depicted in Figure 34, at a depth of 20 m, γF_{peak} predominantly ranged between 5 and 6 kHz, aligning with the characteristic spectral increase associated with snapping shrimp [23,80]. The variability in γF_{peak} was more pronounced at 60 and 120 m depths. At 60 m, γF_{peak} seemed to fluctuate between 4 and 10.5 kHz, depending on the island, while at 120 m, γF_{peak} exhibited variations from 2.9 to 6.4 kHz (Figure 34). BTS beyond 2 to 4 kHz consistently surpassed the average

Wenz ambient noise level, i.e., the ambient noise level in the presence of a 6-knot wind (Chapter 3).

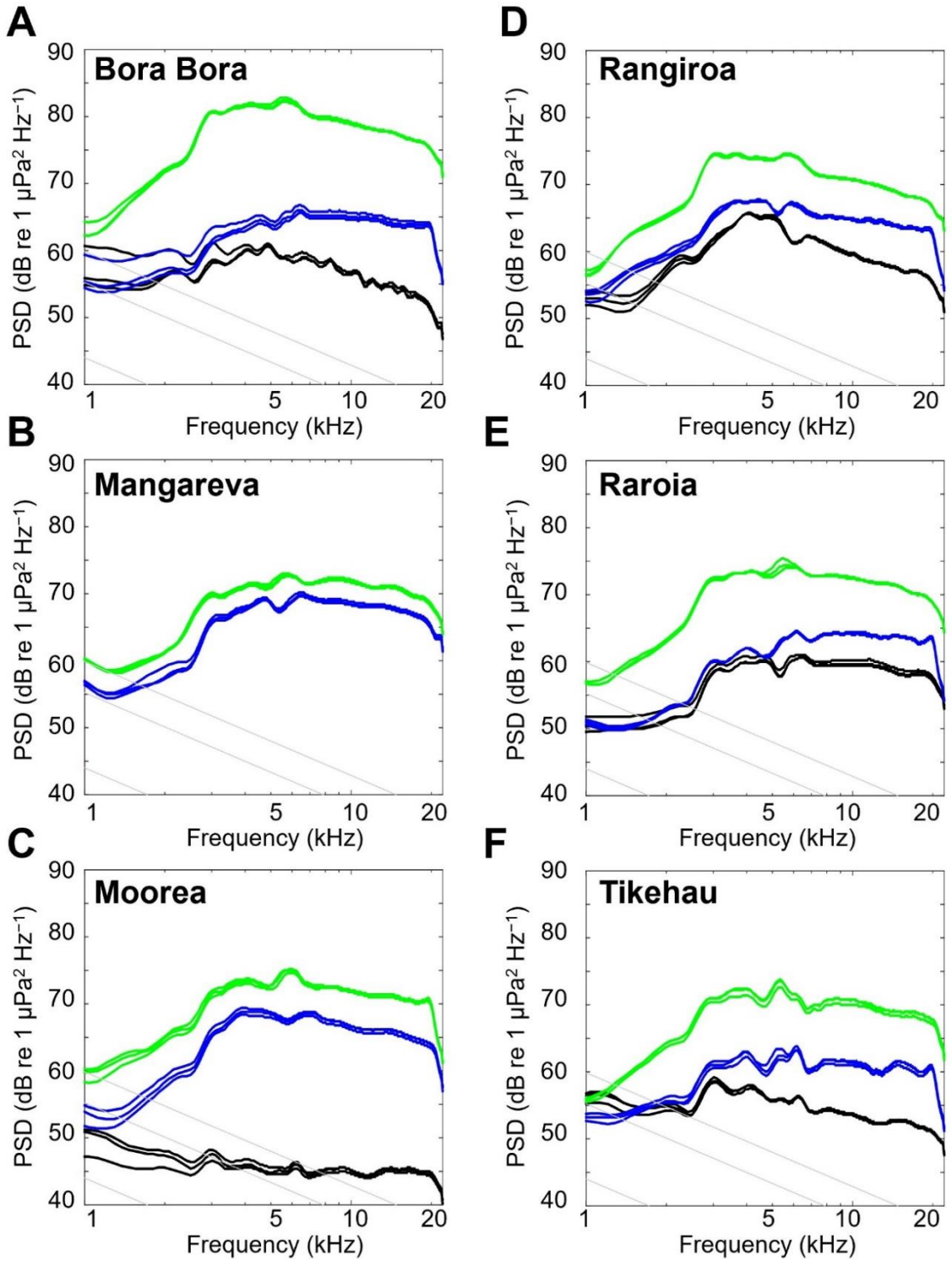

Figure 34 Median Power Spectral Density (PSD) during the night per island. (**A**) Bora Bora, (**B**) Mangareva, (**C**) Moorea, (**D**) Rangiroa, (**E**) Raroia, and (**F**) Tikehau. In green: 20 m, in blue: 60 m, and in black: 120 m. Each line is a replicate (night n°1, n°2 and n°3). In grey, Wenz ambient noise level curves for wind speeds 0 kn, 6 kn and 12 kn (from bottom to top). The horizontal axis is frequency in logarithmic scale.

The spectral acoustic features of the mass phenomena of BTS and those extracted from individual BTS events identified using the automatic detector were significantly influenced by depth (Figure 34, Table 5). The highest power spectral density value (PSD_{Fpeak}) decreased with increasing depth (71.7, 63.7 and 57.8 dB re 1 $\mu Pa^2\ Hz^{-1}$ at 20, 60 and 120 m, respectively). The difference was statistically significant between 20 and 60 m but not between 60 and 120 m (Table 5). The frequency corresponding to the highest power spectral density value (γF_{peak}) also varied with depth; it was consistent between 20 and 60 m but approximately 2 kHz lower between 60 and 120 m. Both BTS SPL_{pp} and the number of BTS decreased with increasing depth, while the opposite trend was observed for BTS Fpeak (Table 5, Figure 35). γFpeak and BTS Fpeak were equivalent at 20 m (5.50 kHz vs. 5.37 kHz) and at 60 m (5.88 kHz vs. 5.98 kHz) but showed a substantial difference at 120 m (3.89 kHz vs. 8.22 kHz). This discrepancy between γFpeak and BTS Fpeak is likely attributed to the low number of detections at 120 m.

Table 5 Linear mixed-effect model results with multiple comparisons (Tukey tests) to access depth variability. *P*-values are adjusted with Bonferroni corrections. PSD_{Fpeak} = highest power spectral density value, γFpeak = corresponding frequency, Δ20m = difference between the peak frequency at 20 m compared to the corresponding frequency at 60 or 120 m, BTS SPL_{pp} = peak-to-peak sound pressure level of the broadband transient sounds, NoBTS = number of broadband transient sounds, and BTS Fpeak = peak frequency of the broadband transient sounds. α = 0.05

		Z value	***P***
PSD_{Fpeak} (F = 212.16, *P* < .0001)	20 vs. 60	−4.64	**< .0001**
n = 187	20 vs. 120	−6.06	**< .0001**
	60 vs. 120	−1.64	0.30
γFpeak (F = 48.21, *P* < .0001)	20 vs. 60	−0.18	≈ 1.00
n = 187	20 vs. 120	−4.30	**< .0001**
	60 vs. 120	−4.13	**0.00011**
Δ_{20} (F = 306.15, *P* < .0001)	20 vs. 60	−5.62	**< .0001**
n = 187	20 vs. 120	−8.90	**< .0001**
	60 vs. 120	−3.55	**0.0012**
BTS SPL_{pp} (F = 9342.4, *P* < .0001)	20 vs. 60	−38.73	**< .0001**
n = 5732	20 vs. 120	−64.71	**< .0001**
	60 vs. 120	−27.39	**< .0001**
NoBTS (F = 1445.14, *P* < .0001)	20 vs. 60	−6.72	**< .0001**
n = 5752	20 vs. 120	−37.38	**< .0001**
	60 vs. 120	−30.23	**< .0001**
BTS Fpeak (F = 640.171, *P* < .0001)	20 vs. 60	6.66	**< .0001**
n = 5465	20 vs. 120	23.41	**< .0001**
	60 vs. 120	17.02	**< .0001**

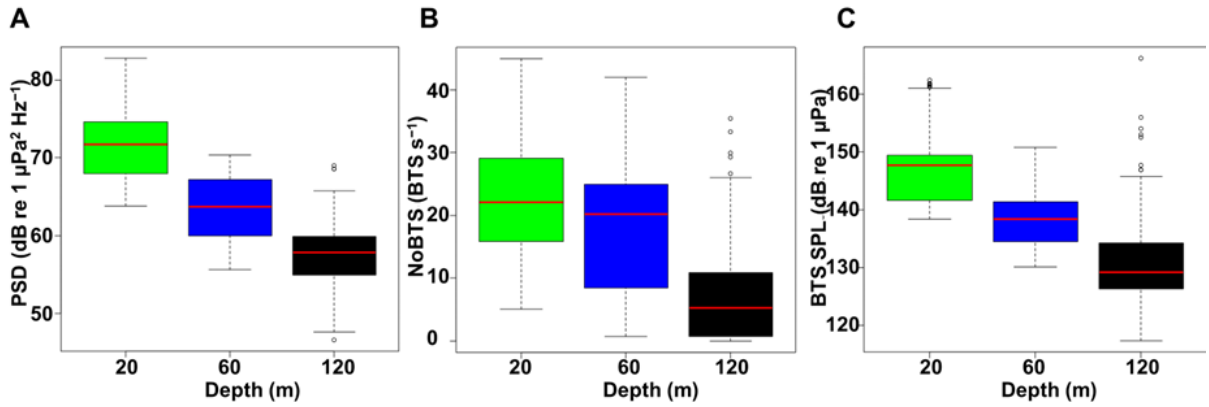

Figure 35 Depth variation of acoustic features. (**A**) PSD_{Fpeak} = highest power spectral density value. (**B**) NoBTS = number of broadband transient sounds, and (**C**) BTS SPL_{pp} = peak-to-peak sound pressure level of the broadband transient sounds. In green: 20 m, in blue: 60 m and in black: 120 m. Whiskers represent 1.5 inter-quartile range. Data falling outside the Q1 – Q3 range are plotted as outliers of the data.

3.1.2. Differences between islands

The depth effect on acoustic features was not consistent across all islands. Moorea and Bora Bora exhibited highly contrasting patterns. In Moorea, similar values for PSD_{Fpeak}, Δ20, and BTS SPL_{pp} values were observed between 60 m and 20 m, whereas in Bora Bora, the similarity was between 60 m and 120 m (Figure 34, Table SP4 - 1). These differences may be attributed to three factors: slope, temperature (Figure SP4 - 2), and/or substrate composition.

The pattern of a decreasing number of BTS with increasing depth was not consistently observed across all islands. In Bora Bora and Raroia, the number of BTS was 1.3 to 1.5 times higher at 60 m than at 20 m depth. At 120 m, a high number of BTS was observed for Raroia and Tikehau, while a lower number of BTS was recorded for Bora Bora, Moorea, and Rangiroa.

3.2. Link between BTS and benthic cover

The redundancy analysis (RDA) indicated that acoustic features were primarily influenced by depth. Inspection of the RDA plot enables the association of benthic cover features, sites, and acoustic features (Figure 36, Table 6, Table SP4 - 3). Positive RDA1 values were predominantly explained by non-encrusting sponges, sand, hydroids, other sessile invertebrates, 'black coral and gorgonians' (RDA1 scores: 0.70, 0.67, 0.67, 0.62, and 0.58, respectively). BTS peak frequency appears to be associated with these features as well as with greater depths (Figure 36). In contrast, negative RDA1 values were primarily explained by macroalgae, scleractinians, and dead coral (−0.64, −0.55, and −0.50, respectively). PSD_{Fpeak}, Δ20, and BTS SPL_{pp} features were grouped together and significantly negatively correlated with RDA 1 (ρ = −0.95, −0.92 and −0.96, all $P < .0001$). In addition, the number of BTS tended to be associated

with shallow reefs (Figure 36). This reflects the lower benthic acoustic activity observed in deep mesophotic reefs. RDA2 to RDA6 did not correlate with any acoustic features.

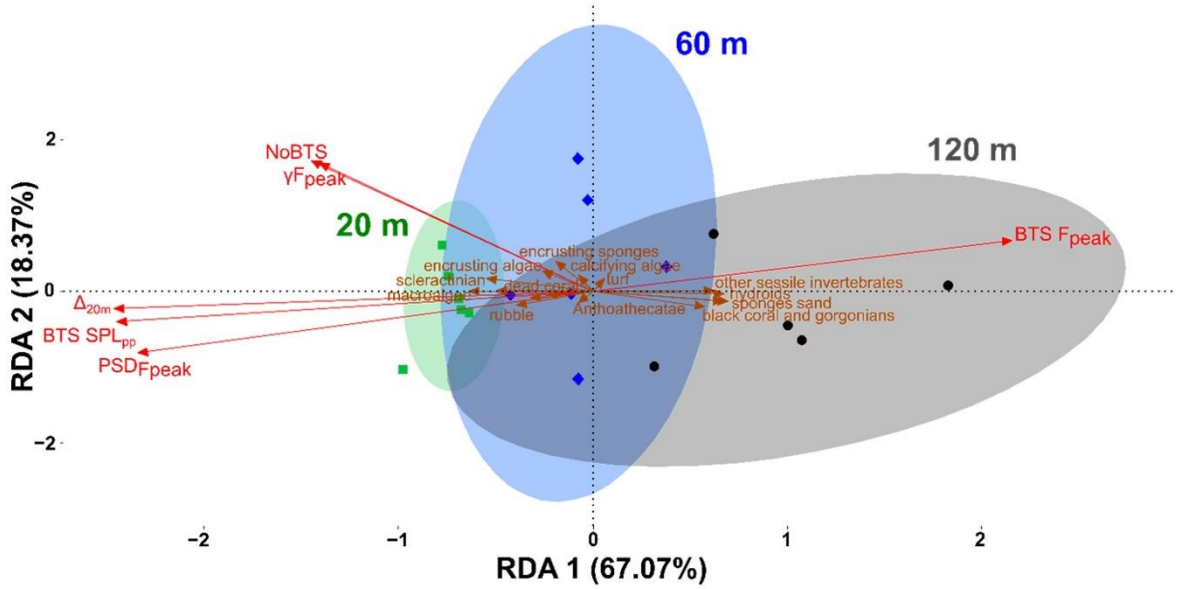

Figure 36 Redundancy analysis (RDA) plot examining the link between benthic cover features and acoustic features. Ellipses are 95% confidence interval. Red arrows indicate acoustic features while brown arrows indicate benthic cover features. In green: 20 m, in blue: 60 m, and in black: 120 m. PSD_{Fpeak} = highest power spectral density value, γFpeak = corresponding frequency, Δ20m = difference between the peak frequency at 20 m compared to the corresponding frequency at 60 or 120 m, BTS SPL_{pp} = peak-to-peak sound pressure level of the broadband transient sounds, NoBTS = number of broadband transient sounds, and BTS Fpeak = peak frequency of the broadband transient sounds.

3.3. Diel variability

3.3.1. General pattern

Diel cycles were clearly evident (Figure SP4 - 1). Variations in diel variation were observed for most acoustic features. PSD_{Fpeak} was generally higher at night than during the day, except at a depth of 120 m, where the patterns varied between islands (Table 7, Figure 37A, Figure SP4 - 2, Figure SP4 - 3, and Figure SP4 - 4). Photic reefs exhibited the highest PSD values, followed by mesophotic reefs at depths of 60 and 120m. BTS Fpeak displayed consistent diel patterns at 20 m and 60 m depth, but with higher variability at 120 m depth (Figure 37) At 20 m, BTS Fpeak differed at sunset compared to daytime and night. However, no significant differences were found between night and day (Table 7). In contrast, in mesophotic reefs (60 and 120 m) diurnal and nocturnal BTS Fpeak differed significantly (Table 7), indicating potential activity switches in the communities of the emitting species. Finally, the number of BTS and the BTS SPL_{pp} presented diel variations at all depths, but distinct patterns were observed. Particularly at 120 m depth, diel variability was highly variable between islands (Table 7, Figure 37).

Table 6 Mean percentage of benthic cover per island and per depth.

		Sand	Non encrusting sponges	Turf	Consolidated substrate	Black coral and gorgonians	Calcifying algae	Anthoathecata	Encrusting sponges	Other sessile invertebrates	Rubble	Other hydroids	Scleractinian	Macroalgae including *Halimeda*	Dead coral	Fleshy	Encrusting algae
Bora Bora	**20 m**	9	1.2	0	30.3	0	0.5	0	0.2	0	22.4	0	35.1	1	0.4	0	0
	60 m	0.6	5.5	0	16.8	0	6	0.3	1.6	0	0.1	0	68.3	0.5	0	0	0
	120 m	42.3	12.8	6.2	19.4	7.1	4.4	0	0.4	0	5.6	0.6	1.2	0	0	0	0.1
Mangareva	**20 m**	0.8	0	0	39.8	0	8.2	0.5	0	0	1	0	43.6	3.1	2.7	0	0.4
	60 m	18.1	0.1	5.6	22.3	0	2.5	0	0.1	0	1.6	0	9.4	1.2	1.9	0	36.9
Moorea	**20 m**	7.8	0.4	0	32.9	0	6.4	0	0.5	0	10.3	0	38	3.3	0.1	0	0
	60 m	23.4	0.7	0	45.4	0	14	0	0	0	0.7	0	15.3	0	0	0	0.4
	120 m	29.6	21.9	11	22.1	2.9	3.3	0	0	2.9	2.9	2.8	0.3	0	0	0	0
Rangiroa	**20 m**	4	1	0	35.1	0	3.8	0	2	0	23	0	11.1	0.6	0.1	0	19.2
	60m	42	8.6	4.1	15.8	0	1.1	0	4.2	0	1.9	0	22	0	0	0	0.2
	120 m	50.1	21.9	12.5	12.5	0.2	0.5	0.3	0.3	0.2	0.1	0.1	0	0	0	0	0
Raroia	**20 m**	0	0	0	19.1	0	8.7	0	9.6	0	0	0	56.1	1.8	4.6	0	0
	60 m	16.9	0.5	0	44.1	0	4.2	0	11	0	4.7	0	18.5	0	0	0	0
	120 m	57.9	8.7	0	20.8	0	10.7	0	0.9	0	0.6	0	0.3	0	0	0	0
Tikehau	**20 m**	2.2	5.1	28.1	11.2	0	6.1	0	0	0.2	7.6	0	32.1	1.9	3.3	0.6	1.2
	60 m	28.9	6.3	12.8	3.8	0	11.2	0	0	0.1	3.6	0	32.4	0	0.1	0.1	0.4
	120 m	79.8	1.8	0	9.2	0.1	3.4	0	0	0.2	5.2	0	0	0	0	0	0

At 120 m depth, the number of BTS did not show a general diel pattern, as indicated by the highly variable time series, suggesting no generalizable diel rhythms in the activity of benthic invertebrates. (Figure 37, Table SP4 - 8).

Table 7 Linear mixed-effect model (per depth) results with multiple comparisons (Tukey tests) to access diel variability. *P*-values are adjusted with Bonferroni corrections. PSD_{Fpeak} = highest power spectral density value, γFpeak = corresponding frequency, Δ20m = difference between the peak frequency at 20 m compared to the corresponding frequency at 60 or 120 m, BTS SPL_{pp} = peak-to-peak sound pressure level of the broadband transient sounds, NoBTS = number of broadband transient sounds, and BTS Fpeak = peak frequency of the broadband transient sounds. α = 0.05, SR = sunrise, SS = sunset.

Feature	Comparison	20 m		60 m		120 m	
		Z value	***P***	**Z value**	***P***	**Z value**	***P***
PSD_{Fpeak}		F =18.58, ***P* < .0001**, n = 66		F = 19.84, ***P* < .0001**, n = 66		F = 1.63, *P* = 0.19, n = 55	
	Night – day	7.00	**< .0001**	7.05	**< .0001**		
	SR − day	3.36	**0.0047**	2.86	**0.026**		
	SS – day	5.64	**< .0001**	5.65	**< .0001**		
	SR – night	−4.07	**0.00028**	−4.69	**< .0001**		
	SS – night	−1.52	0.78	−1.56	0.71		
	SS − SR	2.55	0.064	3.13	**0.011**		
γFpeak		F = 2.82, ***P* = 0.0465**, n = 66		F = 1.96, *P* = 0.13, n = 66		F = 1.87, *P* = 0.15, n = 55	
	Night – day	−1.97	0.29				
	SR − day	−0.030	≈ 1.00				
	SS – day	−1.92	0.33				
	SR – night	2.17	0.18				
	SS – night	0.049	≈ 1.00				
	SS − SR	−2.12	0.20				
Δ_{20}				F = 0.12, *P* = 0.95, n = 66		F =1.26, *P* = 0.30, n = 55	
BTS SPL_{pp}		F = 608.98, ***P* < .0001**, n = 2152		F = 987.58, ***P* < .0001** n = 2028		F = 106.73, ***P* < .0001**, n = 1552	
	Night – day	42.34	**< .0001**	53.60	**< .0001**	17.20	**< .0001**
	SR − day	13.39	**< .0001**	16.67	**< .0001**	3.80	**0.00086**
	SS – day	20.62	**< .0001**	28.13	**< .0001**	9.87	**< .0001**
	SR – night	−14.08	**< .0001**	−19.44	**< .0001**	−7.57	**< .0001**
	SS – night	−6.55	**< .0001**	−7.22	**< .0001**	−1.24	≈ 1.00
	SS − SR	5.86	**< .0001**	9.50	**< .0001**	4.94	**< .0001**
NoBTS		F = 52.37, ***P* < .0001**, n = 2152		F = 69.20, ***P* < .0001** n = 2028		F = 7.41, ***P* = 0.0001**, n = 1552	
	Night – day	12.46	**< .0001g**	−14.24	**< .0001**	4.31	**< .0001**

	SR − day	−3.77	**0.00099**	−4.02	**0.00035**	3.06	**0.013**
	SS – day	−5.35	**< .0001**	−5.30	**< .0001**	3.00	**0.016**
	SR – night	4.32	**< .0001**	5.60	**< .0001**	0.33	≈ 1.00
	SS – night	2.68	**0.044**	4.23	**0.00014**	0.23	≈ 1.00
	SS − SR	−1.28	≈ 1.00	−1.06	≈ 1.00	−0.082	≈ 1.00
BTS Fpeak		F = 4.52, ***P* = 0.0036**, n = 2130		F = 23.26, ***P* < .0001** n = 1994		F = 6.89, **P = 0.0001**, n = 1341	
	Night – day	−1.25	≈ 1.00	−8.28	**< .0001**	−4.44	**< .0001**
	SR − day	−14.47	0.85	−3.18	**0.0087**	−0.92	≈ 1.00
	SS – day	−3.61	**0.0018**	−4.38	**< .0001**	−2.04	0.25
	SR – night	−0.72	≈ 1.00	2.35	0.11	1.97	0.29
	SS – night	−2.98	**0.018**	1.02	≈ 1.00	0.80	≈ 1.00
	SS − SR	−1.75	0.48	1.02	≈ 1.00	−0.91	≈ 1.00

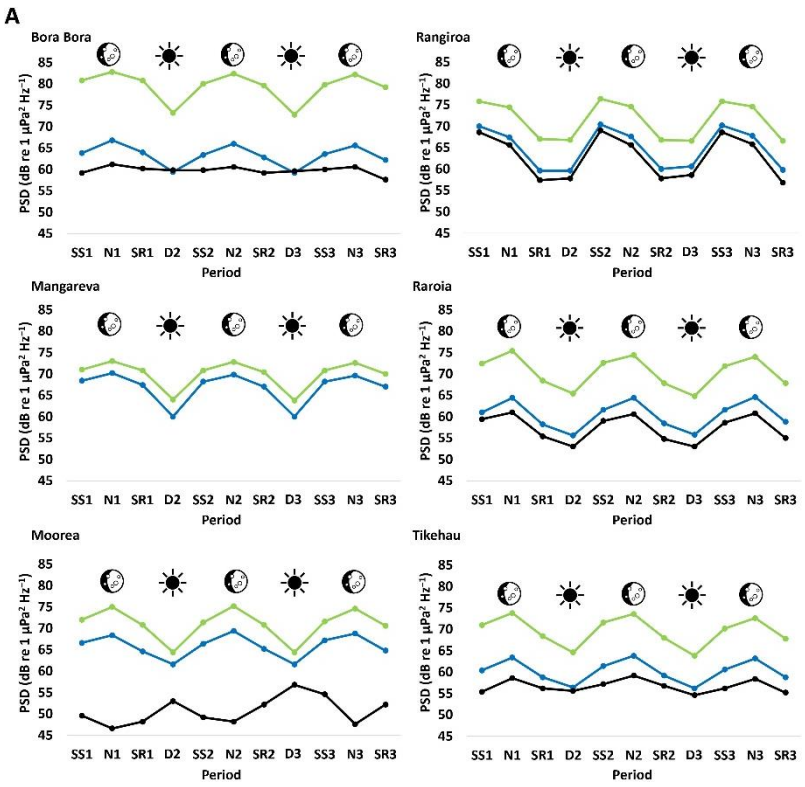

Figure 37 Diel pattern of the BTS. (**A**) the highest power spectral density value (PSDFpeak) (**B**) peak-to-peak sound pressure level of the broadband transient sounds (BTS SPL_{pp}) and (**C**) number of broadband transient sounds (NoBTS). Depths are indicated as following: green 20 m, blue 60 m, and black 120 m. Sun and moon symbols indicate day and night periods respectively. For panel **A**, periods are used (SS = sunset, N = night, SR = sunrise, and D = day) while time series are showed for panels **B** and **C**.

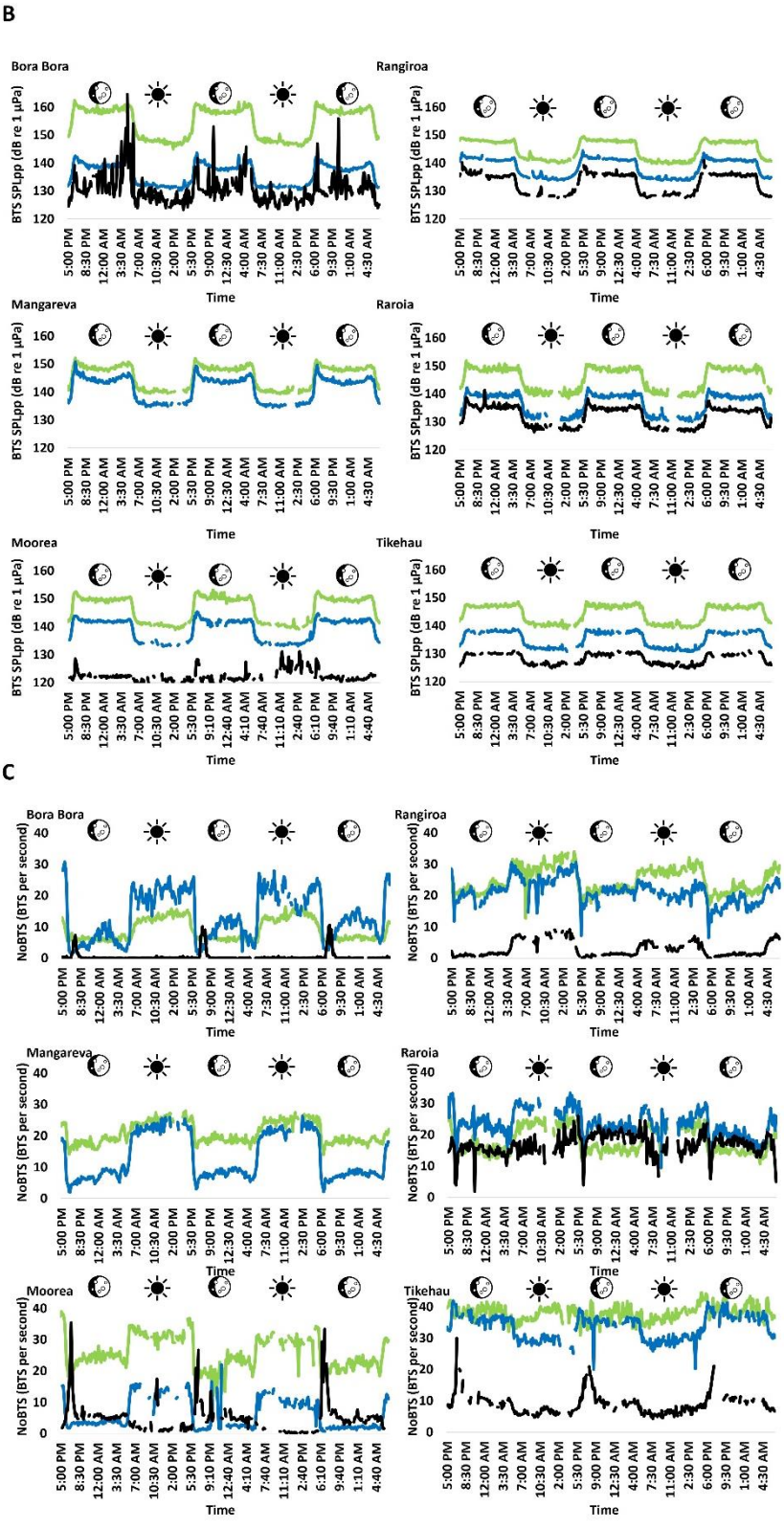

(continuation) Diel pattern of the BTS. (**A**) the highest power spectral density value (PSDFpeak) (**B**) peak-to-peak sound pressure level of the broadband transient sounds (BTS SPL_{pp}) and (**C**) number of broadband transient sounds (NoBTS). Depths are indicated as following: green 20 m, blue 60 m, and black 120 m. Sun and moon symbols indicate day and night periods respectively. For panel **A**, periods are used (SS = sunset, N = night, SR = sunrise, and D = day) while time series are showed for panels **B** and **C**.

There was an increase in the number of BTS around 7 PM that lasted for two hours at the three islands of Bora Bora (6:50 – 7 to 8:30 – 8:50 PM), Moorea (6:30 to 7:40 – 7:50 PM), and Tikehau (6:30 – 6:40 to 8:00 – 9 PM). Indeed, the number of BTS was 37.7% to 97.7% higher during this period compared to the 2 hours before and after (Table SP4 - 15). The peak frequency of the BTS during this 2-hour increase was around 5.4 kHz, significantly different from the peak frequency of the BTS the 2 hours before and after (Table SP4 - 15). This suggests an activity onset of a specific species peaking between 7 and 9 PM. When examining the variation in PSD graphs at a depth of 120 m in detail, peaks of 10 to 20 min in duration are observed. For example, at Bora Bora, an increase of 5 dB re 1 $\mu Pa^2\ Hz^{-1}$ between 7.3 and 8 kHz is observed at 6:40 PM – 6:50 PM (Figure 38), while a less intense but longer increase was observed from 7:10 PM to 7:50 PM between 4.6 and 5 kHz (Figure 38). These observations likely represent activities of species specific to the deep part of mesophotic reefs (120 m).

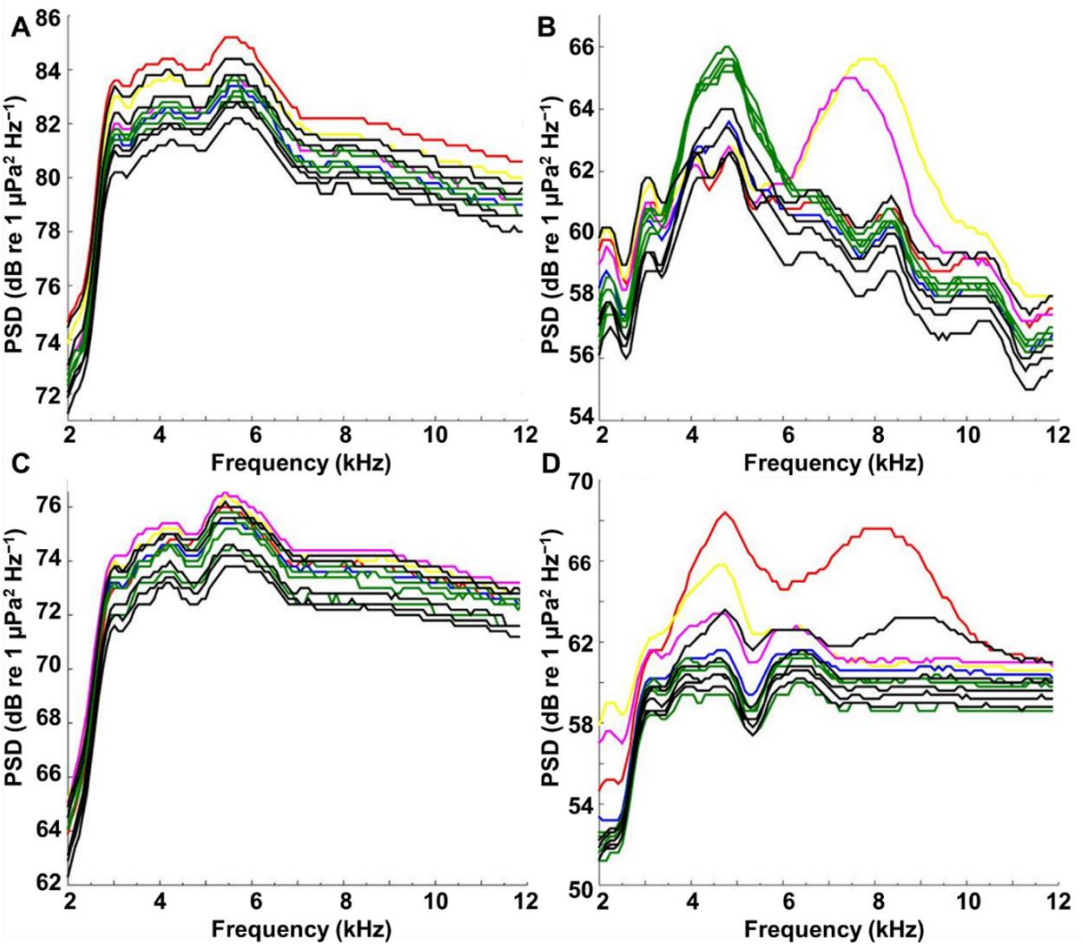

Figure 38 Examples of the detailed variation of Power Spectral density (PSD) between 6:20 PM and 8:30 PM for two islands (Bora Bora and Raroia). Graphs are median PSD between 2 and 12 kHz. (**A**) Bora Bora 20 m, (**B**) Bora Bora 120 m, (**C**) Raroia 20 m, (**D**) Raroia 120 m. Red: 6:30 PM, yellow: 6:40 PM, magenta: 6:50 PM, blue: 7 PM, green: 7:10 to 7:40 PM, black: 7:50 to 8:30 PM.

3.3.2. Differences between islands

Overall, PSD_{Fpeak} diel patterns at 20 m and 60 m depth were similar across islands. At 120 m, some islands (e.g., Rangiroa and Raroia) exhibited PSD_{Fpeak} patterns resembling those at 20 m while others (e.g., Moorea) displayed opposite patterns (not statistically supported) (Figure 37A, Figure SP4 - 3, Table SP4 - 4). γF_{peak} remained constant throughout the day at all depths on some islands, whereas diel cycles were observed in certain mesophotic reefs, with a higher γF_{peak} during the night or day, suggesting that acoustic mass phenomena vary, or not, depending on the site/island (Figure SP4 - 4 and Figure SP4 - 5). The diel variation of the number of BTS at 20 and 60 m was relatively consistent across islands, with generally higher values during the day than at night, (but see Bora Bora and Raroia, Figure 37C, Table SP4 - 6, and Table SP4 - 7).

4. Discussion

4.1. Depth variability

The underwater acoustic survey conducted at three different depths across six islands in French Polynesia revealed significant differences in the sounds emitted by benthic invertebrates. Despite the brief sampling period, it was evident that depth was the primary factor influencing benthic transient sounds, as indicated by depth-related differences in almost all acoustic parameters.

The acoustic features of benthic invertebrate sounds were found to be correlated with the sessile benthic cover structure. At a depth of 120 m, marked differences in peak frequencies were observed compared to the BTS recorded at 60 and 20 m depth, likely reflecting distinct benthic communities. Thus, the sounds emitted by benthic invertebrates varied along the depth gradient, ranging from photic reefs to the upper part of mesophotic reefs, and notably in the lower part of mesophotic reefs. These depth-related differences may be associated with a decrease in temperature [338], an increase in the distance from shore [318], and the transition from a light-dependent scleractinian-dominated reef with macroalgae to a sandy reef with a higher number of sponges, black corals, and gorgonians [172]. However, not all measured acoustic features showed linear trends. For sound pressure level features (SPL_{pp} and PSD_{Fpeak}), the greater the depth, the lower the sound pressure levels, with an average decrease of 6 to 8 dB re 1 μPa^2Hz^{-1} at 60 m compared to 20 m, and at 120 m compared to 60 m). In contrast, regarding the number of BTS, the number of nocturnal BTS was generally higher at 60 m than at 20 m. This might seem counterintuitive, as a higher number of sounds would typically be associated with higher sound pressure levels. ‘Intensity features’ (i.e., PSD and BTS SPL_{pp}) and NoBTS

may thus provide different information related to differences in biodiversity or invertebrate communities. Higher coral genus diversity in French Polynesia has been reported at 60 m compared to 20 m depth [332], which could consequently explain a higher diversity of sessile benthic invertebrate fauna and the increased BTS observed at 60 m depth. There are also alternative explanations. On one hand, the upper part of the mesophotic reefs (60 m) could shelter more sound-emitting specimens or species producing more sounds than in photic reefs. On the other hand, photic reefs seem to shelter species producing louder sounds than in the upper part of the mesophotic reefs, as indicated by the highest levels of SPL_{pp} and $PSD_{Fpeak.}$ Photic reefs are dominated by snapping shrimp sounds, which are among the loudest marine sounds emitted by benthic invertebrates [70]. Therefore, even in smaller numbers, they could be responsible for the observed increase in sound levels at 20 m depth. Alternatively, snapping shrimp sounds create mass phenomena that elevate ambient noise levels, potentially reducing the signal-to-noise ratio and thus negatively biasing the outcomes of the automatic detector in the photic zone.

Unlike the reefs at 20 and 60 m, the deeper part of the mesophotic reef (120 m) exhibited considerably lower acoustic activity. This finding aligns with Everest et al. (1948), who reported that beyond a depth of 55 m, and regardless of environmental suitability [24], the noise levels of snapping shrimp sounds decrease. Below 61 to 91 m, the presence of snapping shrimp noise is unlikely, unless transmitted from nearby shallower areas [83]. The absence of snapping shrimp sounds may therefore account for the absence of the continuous crackle typically found in shallow habitats [24]. The lower concentration of deep living species [24,83,346,347] also likely contributes to the reduction of BTS recorded at 120 m depth. It has been hypothesized that the increased number of invertivores in the mesophotic reefs may explain the decrease in crustacean sound intensity with depth observed in Japanese reefs [348]. The reduction of canopy-forming algae has also been suggested as a potential cause for the decrease in snapping shrimp sound production, favouring opportunistic turf-forming algae [337,349,350].

Acoustic variables also differed between islands. For instance, in Moorea, the most significant decrease in PSD_{Fpeak} occurred between 60 and 120 m. At a depth of 120 m, Moorea diverged from other islands due toa higher percentages of black coral (1.3% vs. 0 to 0.09%), hydroids (2.8% vs. 0 to 0.6%) and sessile invertebrates (2.9% vs. 0 to 0.18%), as well as a lower temperature. Temperature has been reported as positively correlated with the number of snap sounds [72,338]. Previous studies have demonstrated that differences in bottom types can influence sounds. At equivalent depths, less intense sounds have been observed from non-

favourable bottom types compared to favorable ones for snapping-shrimps (e.g., coral, rock, stone, and shell) [83]. Additionally, at Rangiroa; PSD_{Fpeak} values at 20 m were significantly higher than in the other islands. This might be explained by the unique geomorphological features of the site [23]. However, further investigation is necessary for a comprehensive understanding.

The differences observed in spectral frequencies (γFpeak) suggest the presence of distinct mass phenomena. However, a consistent trend specific to depth was not identified. These variations may be associated with differences in associated crustaceans communities, given that peak frequencies vary depending on the emitting species [70,351–353]. They could also result from differences in the abundances of species present with sounds of varying peak frequencies. Alternatively, single BTS can have multiple frequency peaks [23,243] leading to distinct spectral increases. The broadband nature of snapping shrimp sounds complicates the association between specific species and the identification of recorded peak frequencies.

In reefs, high-frequency sounds other than those of snapping shrimp, which predominantly fall within the 2 to 20 kHz range [83], can also be recorded. For instance, interactions between hard-shelled benthic macro-organisms and the coral substrate contribute to a peak between 11 and 17 kHz, centred at 14.3 and 14.6 kHz [66]. Higher frequencies can be emitted by certain species of Palinuridae [354]. Conversely, lower frequencies are known to be produced by some species of Palinuridae [68,355–357] and Penaeidae [358–360]. In temperate areas, bivalves are known to produce high frequency sounds [64], while sea urchins are known to emit lower-frequency sounds (between 0.7 and 2.8 kHz) with relatively lower peak frequencies during feeding [65]. However, in Polynesian reefs, this frequency range does not correspond to a spectral increase (Chapter 3).

4.2. Diel variability

Overall, benthic activity rhythms at 120 m exhibited low or highly variable levels of diel variation, likely due to reduced solar irradiation. Between-island variability was most pronounced at 120 m. Notably, distinctive rhythmic patterns were observed in terms of number of BTS. One particular observation in the soundscapes at 120 m in Bora Bora, Moorea, and Tikehau was a daily peak in the number of BTS around 5.4 kHz, consistently occurring at 7 PM. Since the sounds forming the peak shared the same peak frequency, it is likely that these peaks represent cyclic activity of a specific species. To our knowledge, this sound has not been previously described, and its peak frequency does not match descriptions of animals in mesophotic reefs. Moreover, its presence on different islands from different archipelagos and

during various nights indicates it is not anecdotical but reflects a cyclic biological activity of a particular species or deep-adapted ecological groups. At 20 and 60 m depths, benthic activity rhythms were more similar compared to those at 120 m depth. They also exhibited pronounced diel variations with higher PSD and BTS SPL_{pp} during the night. This aligns with studies in the Caribbeans [79] and Polynesia (Chapter 3). The number of BTS showed opposite trends, with higher values during the day. In Moorea, recordings made at 12 m revealed that the number of BTS could vary differently between day and night depending on the frequency band (Chapter 3). During the night, the number of BTS in the 3.5 – 5.5 kHz band was 8% higher, while in higher frequency bands (6 – 8 kHz and 10 – 13 kHz), it was 14% to 5% lower compared to the day (Chapter 3).

5. Conclusions

This study identifies for the first-time acoustic patterns from photic to mesophotic coral reefs associated with the activity of benthic invertebrates. The observed differences can reflect community composition or different behaviors. The findings emphasize the marked differences in the deeper part of the mesophotic reefs compared to the upper part at 60 m depth and the photic zone, likely indicative of variations in biodiversity or community composition linked to benthic sessile cover features such as hydroids, sponges, black corals and gorgonians. These features create animal forests, three-dimensional structures hosting a variety of small cryptic organisms [361,362] . Furthermore, the limited occurrence of diel patterns at 120 m suggests that reduced light regimes influence biorhythms. Studies linking habitat variables to acoustics are still scarce but necessary to understand habitat-specific patterns and the drivers of acoustic variations [318] (Chapter 6). The results presented here support the use of passive acoustics for the study and monitoring of mesophotic reefs. In these challenging-to-access environments, where species are often cryptic, ecoacoustic approaches offer unprecedented opportunities for assessing the spatio-temporal dynamics of mesophotic reefs.

6. Author contributions

Conceptualization, X.R.; methodology, X.R. and L.D.I.; software, C.G.; validation, X.R., L.D.I. and É.P.; formal analysis, X.R.; investigation, X.R. and U.T.P.; resources, G.P.R., F.B., and H.R.; data curation, X.R.; writing—original draft preparation, X.R..; writing—review and editing, X.R., É.P., L.D.I., F.B., G.P.R., and H.R.; visualization, X.R.; supervision, X.R. and L.D.I.; project administration, X.R.; funding acquisition, D.L.. All authors have read and agreed to the published version of the manuscript.

PART III: INDIVIDUALLY IDENTIFIABLE SOURCES OF THE BIOPHONY

Chapter 5. ‘To be, or not to be’: critical assessment of the use of α-acoustic diversity indices to evaluate the richness and abundance of coastal marine fish sounds

Xavier Raick[1], Lucia Di Iorio[2,3], David Lecchini[4,5], Marta Bolgan[1], & Éric Parmentier[1]

[1] Laboratory of Functional and Evolutionary Morphology, FOCUS, University of Liege, Liege, Belgium

[2] Université de Perpignan Via Domitia, CNRS, CEFREM UMR 5110, Perpignan, France

[3] Chorus Institute, 5 Rue Gallice, Grenoble, France

[4] PSL University, EPHE-UPVD-CNRS, USR 3278 CRIOBE Moorea, French Polynesia

[5] Laboratoire d’Excellence ‘CORAIL’, Perpignan, France

Two research studies have been conducted. The first one focused on fish sounds and is presented in this thesis, having been published in the *Journal of Ecoacoustics*. Additionally, sections of this chapter have been utilized for two educational videos on the MANEA platform: *Outils d’étude de la biophonie – Partie 1 : Les indices de diversité acoustique* and *Outils d’étude de la biophonie – Partie 2 : Problématique de l’utilisation des indices acoustiques en milieu marin.* The second study, which investigates benthic invertebrate sounds, has not been included in the final document of this thesis. It is currently in the final stages of preparation.

MAJOR RESULTS

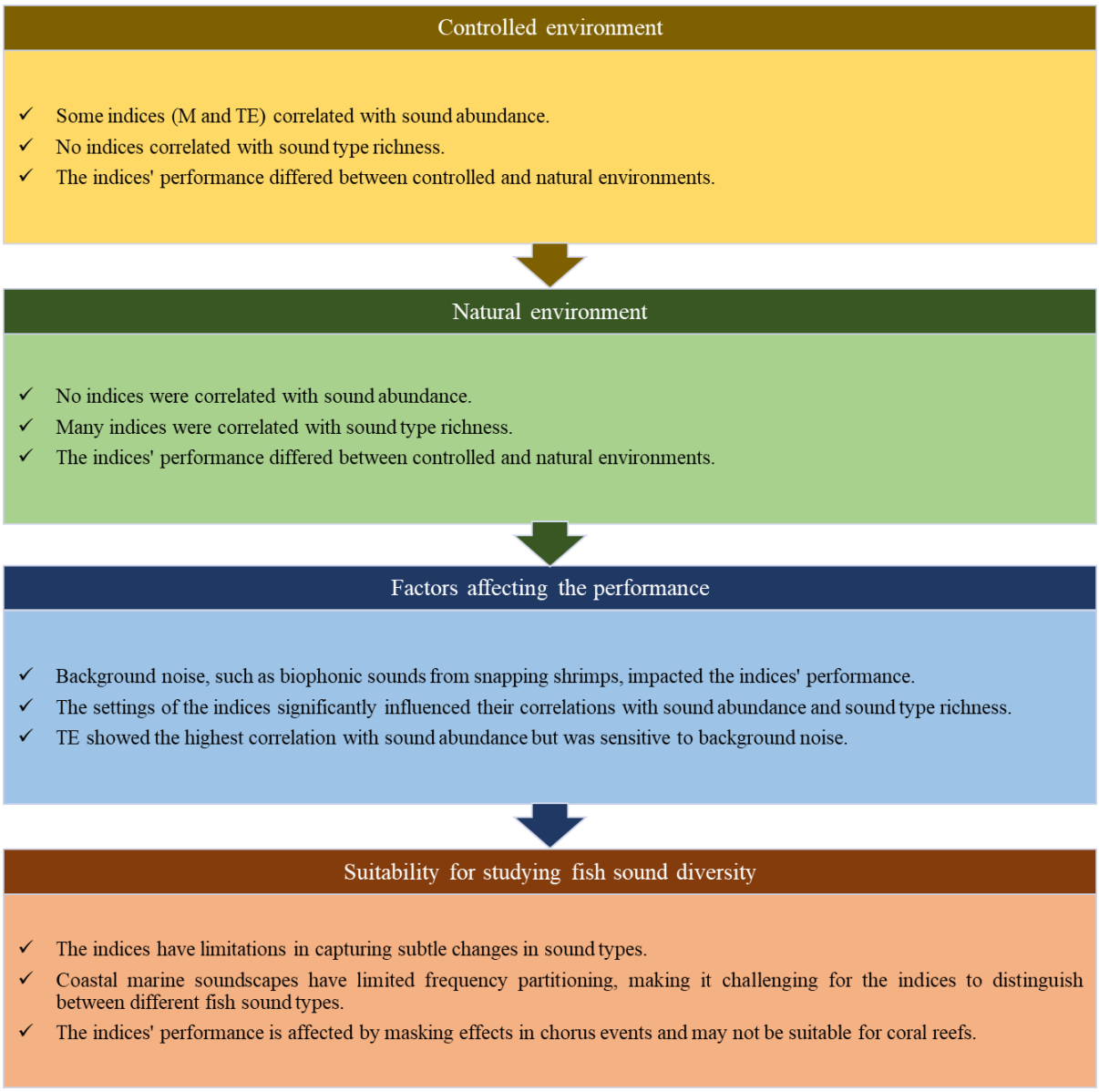

Key question for the objective of the thesis

Can we use 'α-acoustic diversity indices' to study this discriminable near sources of the biophony?

Abstract

Passive acoustic monitoring can be used to assess the presence of vocal species. Automatic estimation of such information is critical for allowing diversity monitoring over long time spans. Among the existing tools, α-acoustic indices were originally designed to assess the richness/complexity of terrestrial soundscapes. However, their use in marine environments is impacted by fundamental differences between terrestrial and marine soundscapes. The aim of this study was to determine how they vary depending on the abundance and sound type richness of fish sounds. Fourteen indices used in terrestrial environments were tested. The indices were calculated for files from three sources: a controlled environment (playback of artificial tracks in a pool), in situ playbacks (playback of natural soundscapes), and a natural environment (only natural sounds). The controlled experiment showed that some indices were correlated with the sound abundance but not with the sound type richness, implying that they are not capable of distinguishing the different types of fish sounds. In the in situ playbacks, the indices were not able to capture differences, both in terms of the sound abundance and sound type diversity. In the natural environment, there was no correlation between most of the indices and the abundance of sounds. They were impacted by mass phenomena of biological sounds (e.g., the Pomacentridae sounds in shallow reefs) that cannot inform on fish acoustic diversity. Indices are appropriate when soundscapes are divided into bands. In contrast to terrestrial environments, frequency bands in coastal marine soundscapes do not provide ecologically relevant information on diversity. Overall, indices do not appear to be suitable for inferring marine fish sound diversity.

1. Introduction

Biodiversity is directly linked to the resilience of ecosystems [363], and it is declining in many ecosystems around our planet [177,364]. Therefore, there is a need to monitor biodiversity trends over large spatio-temporal scales and to collect comparable and standardized measurements. Biodiversity can be measured by counting the number of different species in a given area, or by taking into account their relative abundance [365]. The first metric is known as species richness, while the second involves the calculation of diversity indices. In the last 20 years, technological developments in remote sensing have boosted our ability to detect species and to monitor their distribution together with the ecological state of understudied ecosystems [84]. Among remote sensing techniques, monitoring the biological sounds present in a habitat is an effective way of measuring biodiversity [366]. The two fundamental aspects of species biodiversity (abundance and richness) are encoded in the biological component of the acoustic environment of a habitat (i.e., the biophony), and they can be measured as the number of different sound types (acoustic richness) and their relative abundances [84,163,367] (Chapter 6). Technological advancements allow recording for long time periods at large spatial scales, thus requiring the development of adequate standardized, automatic, and quick processing methods, which can inform on biodiversity trends [84]. This is a fundamental requirement for meeting international targets of biodiversity monitoring [368]. In this context, many α-acoustic indices, representing the α-diversity measures in a single habitat or sampling unit, have been developed to describe the sonic biodiversity of a soundscape [369]. These indices are classically divided into three groups: those describing the intensity of the acoustic scene, those characterizing its complexity, and those on soundscape components [369]. **Intensity indices** are based on the measurement of sound intensity, i.e., the ratio of sound pressure relative to a reference value. The *sound pressure level* (**SPL**) is a logarithmic measure of the ratio of the sound pressure of a sound to a reference sound pressure. Intensity indices have been used for noise level assessment or in ecological studies, for example, to assess avian biophonies in various environments [370–374]. The inconvenience of these indices is that they do not provide any information on the number/identity of sound sources or on the frequency composition of the soundscape, which makes them unsuitable for estimating acoustic richness. This has led to the birth of the first complexity indices based on the frequency composition of the soundscape. These indices postulate that a biophony is more complex when the number of vocal individuals/species increases. **Complexity indices** are computed *(1)* within precise frequency ranges, leading to the creation of the *bioacoustic index* (= *relative abundance*, **BI** =

Bio) [375], *(2)* on the *amplitude index* (**M** = **AI**) based on the median of the amplitude envelope [376], and (*3*) on the *acoustic entropy index* (= *total entropy*, **H**) related to the evenness of the acoustic environment [377]. It is calculated by multiplying the *temporal entropy* (**TE** = $\mathbf{H_t}$), i.e., measurement of the Shannon evenness of the amplitude envelope, by the *spectral entropy* (**SE** = $\mathbf{H_f}$), i.e., measurement of the Shannon evenness of the frequency spectrum [377]. Different indices have also been developed based on entropy: the *Shannon spectral entropy* (= *Pielou's evenness index*, **S**), the *Simpson spectral entropy* (= *Gini Simpson spectral entropy* = *Gini Simpson index*, **GS**), the *Renyi spectral entropy* (**R**), the *entropy of spectral variance* ($\mathbf{H_v}$), the *entropy of spectral maxima* ($\mathbf{H_m}$), and the *acoustic diversity index* (**ADI** = **H'**) [377–379]. More recently, other indices have been created to account for soundscapes that might not be dominated by a biophony and to study noise-like sounds produced by single species (e.g., cicadas). These new indices include the *acoustic richness (index)* (**AR** = **ARic**) [376], the *acoustic evenness index* (**AEI** = **Aeve** = **AE**) [380], the *acoustic complexity index* (**ACI**) [381] and the *number of peaks* (= *frequency peak number*, sometimes confusedly named the *acoustic complexity index*, **NP**) [382]. This list is not exhaustive, as other indices (e.g., *mid-band activity*, *spectral diversity* and *spectral persistence*) have also been developed to determine avian richness [378]. The third category of α-acoustic diversity indices, **soundscape indices**, works on soundscape components by analyzing the biophony (sounds of biological origin) alone or in relation to the anthropophony (sounds produced by humans). To calculate these indices, terrestrial soundscapes are generally split into a frequency band between 0.2 and 2 kHz dominated by the anthropophony, and one between 2 and 8 kHz, generally characterized by the biophony. Some indices use the ratio of anthropophony to biophony such as the *normalised difference soundscape index* (**NDSI**) [383], while others are based only on the biophony, such as *biophony* or *biophony peak* (**bioPeak**) [380,384].

Because indices are quick and easy to use, they have been widely adopted to study the biophony in a variety of different terrestrial/aerial environments, such as in the Amazon rainforest [385], tropical wet evergreen forests [386], dry tropical forests [387], the Valdivian [388] or Atlantic rainforest [389,390], savannas [390,391], Mediterranean forests [392], pastures [393], temperate woodlands [376], cities [394,395], and mangroves [395]. In comparison to terrestrial soundscapes, sounds at sea include ambient noise caused by thermal agitation, oscillating bubbles, water droplets, surface waves, turbulence, seismic sources, precipitation, and sea-ice movements [5]. Except for sea-ice movements, these sources are less frequency-modulated than sources in terrestrial soundscapes (e.g., birds) and often create broadband noises (similar to white noises) [396]. The soundscapes of marine coastal

environments are generally dominated by sounds emitted by invertebrates, such as snapping shrimps or sea urchins, in the frequency band between 1.5 and 40 kHz [24,243]. Below 2 kHz, that is, within a very narrow frequency band, marine coastal biophonies are dominated by fish and marine mammal sounds [397]. This makes coastal marine soundscapes profoundly different from terrestrial soundscapes. Despite these considerations, indices have been used in different environments such as mangroves [398], streams [399], ponds [400], seagrass meadows [398,401], sandy bottoms [398,401], deep seamounts [402], temperate reefs [403], and coral reefs [158,236,398].

Although highly informative, one of the biggest challenges with the use of acoustic indices, particularly in the marine environment, is identifying the extent to which they are representative of the acoustic richness and diversity of an environment. Among all indices, the **ACI**, **H**, **AEI** and **ADI** have often been applied to study acoustic fish communities. However, controlled experiments have shown the difficulty in discriminating between sound abundance and sound type richness [396]. Furthermore, the ACI, for instance, has been shown to be unrelated to fish sound diversity [404,405]. Depending on the settings, the **ACI** increases or decreases when the sound abundance increases, but **H** always decreases [405]. For Indonesian reefs, the **AEI** and **ADI** (band: 1.2 – 11 kHz) are considered good predictors of fish abundance and/or richness (explaining 19% to 40% of the deviance) [406]. However, it is difficult to fully appreciate these relationships since the band used for the analysis (1.2 – 11 kHz) does not correspond to the frequency band of fish vocalizations, but to the frequency band of invertebrate activity. Similar to what has been carried out in terrestrial environments [407], experimental tests of acoustic indices are required [408] to understand if they are representative of fish biophony diversity. In this work, we focused on fish sounds, because fish are the only taxa with species-specific vocalizations that are always present on reefs (contrary to marine mammals). The aim of this study was to experimentally determine if α-acoustic diversity indices can reflect the abundance and sound type richness of marine fish sounds.

2. Materials and methods

2.1. Experimental conditions

The α-acoustic indices were studied under three experimental conditions: a controlled environment (with artificial tracks only), in situ playbacks (with artificial tracks played back over natural sounds), and a natural environment (only with natural sounds) (Figure 39).

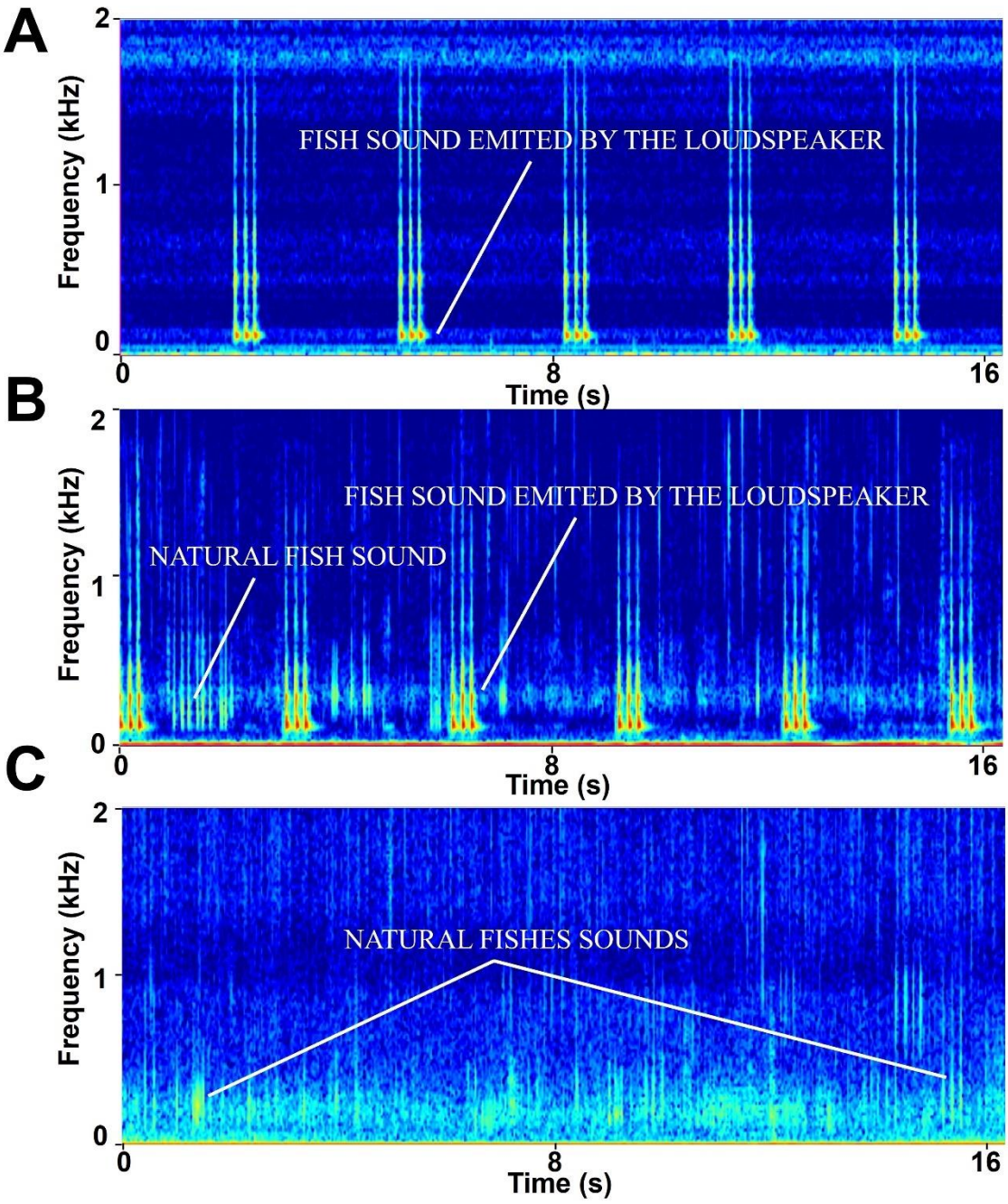

Figure 39 Acoustic background variation depending on the environment: (A) controlled environment, (B) in situ playbacks, and (C) natural environment. For all the spectrograms: files were subsampled at 4 kHz, FFT = 256, window = Hann, overlap = 0.50.

2.1.1. Controlled environment

Trials were conducted in a large pool during the experiment presented in Bolgan et al. (2018). We focused only on stimuli emitted by a single loudspeaker, which were recorded as part of a broader experiment, but were not presented in the resulting article. An HTI-94 SSQ hydrophone (High Tech INC; Long Beach, MS, USA; sensitivity −162 dB re 1 V μPa^{-1})

connected to a USB A-D converter (Edirol U25-EX, 48 kHz, 16 bits) and controlled by a laptop running Adobe Audition 3.0 (Adobe Systems Inc., Mountain View, CA, USA) was placed in the middle of the pool (6 m × 9 m × 1.30 m) at 0.9 m from a UW-30 loudspeaker (Electrovoice, Burnsville, MN, USA) attached to a GTA 260 amplifier (Blaupunkt, Hildesheim, Germany) connected to a U25-EX USB D-A converter (Edirol, Hamamatsu, Japan) controlled by a laptop running Adobe Audition 3.0 (Adobe Systems Inc., Mountain View, CA, USA), which produced the sound stimuli (Figure 40A). The sound stimulus was a sound file (WAV format, 48 kHz, 16 bit) composed of 10 blocks of 2 min duration. The first block was white noise (WN) [396]. The other nine blocks had a known sound abundance and a known sound type richness (Table SP5 - 1). Three ranges of sound abundance were tested: low (20 sounds min^{-1} in total, regardless of the number of sound types), medium (60 sounds min^{-1}), and high (100 sounds min^{-1}), as well as three ranges of sound type richness: low (one sound type), medium (two sound types) and high (three sound types, Table SP5 - 1) [396]. The sound types used were isolated fish calls from three different species [396]. All the sounds had the same amplitude (see Bolgan et al. (2018) for the complete procedure). Within each block, fish sounds were separated by white noise (signal-to-noise ratio > 48 dB). The durations of the three sound types were equalized in order to occupy the same period of time (for details, see [396]).

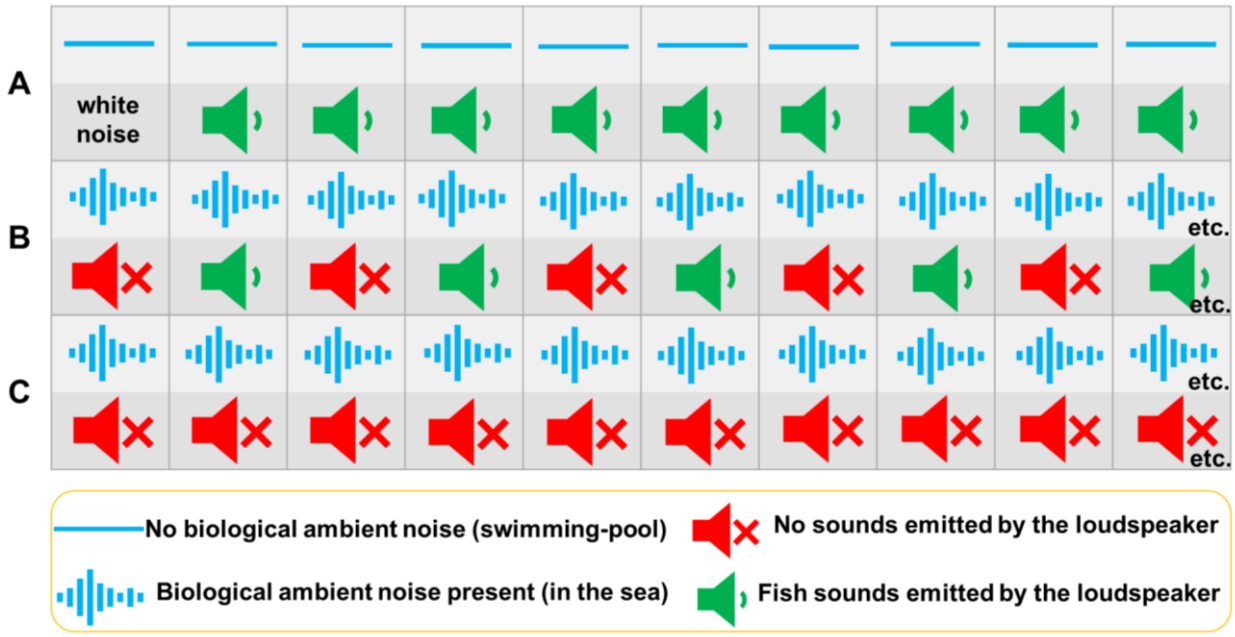

Figure 40 Schematization of the experimental design. (**A**) Controlled environment. (**B**) In situ playbacks. (**C**) Natural environment. Blocks are indicated by the gray cases. For **A**, within each block, fish sounds were separated by white noise, while for **B**, they were separated by silence.

2.1.2. In situ playback

Trials were conducted in December 2020 in coral reefs at Moorea Island (Temae lagoon, French Polynesia; 17.50° S; 149.76° W, 2 to 4 m depth). This area was chosen because this part of the lagoon has a reduced anthropophony because of the absence of a boat channel. The loudspeaker was attached to a GTA 260 amplifier (Blaupunkt, Hildesheim, Germany) connected to a DR5 recorder (TASCAM, Wiesbaden, Germany) playing back the recorded soundtrack. The soundtrack was a sound file (WAV format, 44.1kHz, 16 bit) composed of 9 blocks of 6 min duration each. Replicates were realized at five locations in the lagoon (Table SP5 - 2). The sounds used in the playbacks were the same as those used in the experimental design of the controlled environment (Table SP5 - 1). However, because the ambient noise of in situ playbacks could vary between the beginning and the end of the session, each block was composed of 3 min of silence followed by 3 min of sounds, thus allowing for pairwise comparisons (Figure 40B). The order of the blocks was random and was always different from one replicate to another.

A SNAP autonomous underwater acoustic recorder (Loggerhead Instruments, Sarasota, USA; sensitivities of the hydrophones: −169.6 to −169.7 dB re 1 V for a sound pressure of 1 µPa, flat frequency response 2 Hz to 30 kHz, WAV format, 44.1 kHz, 16 bit) was placed on the bottom at 1 m from a UW-30 loudspeaker (Electrovoice, Burnsville, MN, USA). It recorded during the entire session to obtain acoustic recordings with both natural sounds (emitted by fishes present on the reef) and sounds broadcasted by the loudspeaker. The signal-to-noise ratios of the broadcasted sounds were overall equivalent to those of natural sounds. All the identifiable discriminable near sources of fish sounds were selected and classified through visual and aural inspection using RavenPro Sound Analysis Software 1.5 (Cornell Lab of Ornithology, Ithaca, NY, USA). Then, the natural fish sound abundance (total number of sounds per minute) and sound type richness (one value per minute) were calculated.

2.1.3. Natural environment

Acoustic recordings were collected in March 2018 on the external slope of Raroia Island (French Polynesia) (S 16.02310°, W 142.46327°) during the study presented in Chapter 6. Three SNAP autonomous underwater acoustic recorders (Loggerhead Instruments, Sarasota, USA; sensitivities of the hydrophones: −170.5, −170.2 and −169.7 dB re 1 V for a sound pressure of 1 µPa, flat frequency response 2 Hz to 30 kHz, WAV format, 44.1 kHz, 16 bit) were deployed during three consecutive sunsets (05:00 PM – 06:59 PM) at −20 m, −60 m, and −120 m. A total of 108 recording files of 1 min were visually and aurally inspected with RavenPro

Sound Analysis Software 1.5 (Cornell Lab of Ornithology, Ithaca, NY, USA) to assess the fish sound abundance and sound type richness (Figure 40C). Fish sounds were classified into 45 different sound types (Chapter 6).

2.2. Acoustic indices of α-diversity

Fourteen α-acoustic diversity indices were calculated for tracks from the controlled environment, in situ playbacks, and natural environment: two intensity indices, eleven complexity indices, and one soundscape index. The used indices are summarized in Table 8, along with their bibliographic references: *(1)* the peak-to-peak sound pressure level (**SPL_{pp}**); *(2)* the root mean square sound pressure level (**SPL_{rms}**); *(3)* the amplitude index, calculated as the median of the amplitude envelope (**M** = AI); *(4)* the bioacoustic index, which measures the area under the power spectrum (**BI** = Bio); *(5)* the temporal entropy (**TE** = H_t), which measures the envelope complexity; *(6)* the spectral entropy (also named the Shannon spectral entropy and Pielou's evenness index, **SE** = S = H_f), which measures the spectral complexity; *(7)* the Gini Simpson spectral entropy (also named the Simpson spectral entropy, Gini Simpson spectral index, or Simpson spectral index, **GS**), which is derived from the spectral entropy; *(8)* the acoustic entropy index (also named total entropy or acoustic entropy, **H**), which measures both the envelope and spectrum; *(9)* the acoustic richness index (also named acoustic richness, **AR**), which measures the envelope complexity and intensity; *(10)* the acoustic diversity index (**ADI** = H'), which measures the spectrum complexity; *(11)* the acoustic evenness index (**AEI** = AEve = AE), which applies the Gini index to a frequency spectrum; *(12)* the number of peaks in a frequency spectrum (also named frequency peak number, **NP**); *(13)* the acoustic complexity index (**ACI**); and *(14)* the normalized difference soundscape index (**NDSI**), which measures the ratio between two frequency bands (Table 8 and Equation SP5 - 1 to SP5 - 5). All the indices were calculated in R software version 3.6.1. (R Core Team, 2019) with the libraries seewave, signal, sound, and soundecology. The functions used are detailed in Table 8.

2.3. Calculation of the indices

Prior to analysis, the files recorded by the hydrophone in the controlled environment were subsampled at 44.1 kHz to be comparable with the soundtracks recorded during the in situ playbacks, and in the natural environment.

Table 8 α-Acoustic diversity indices calculated in this study.

	Name	Library	Function	Reference
Intensity indices				
SPL_{pp}	*Peak to peak sound pressure level*			
SPL_{rms}	*Root mean square sound pressure level*			
Complexity indices				
M	*Amplitude index = median of the amplitude envelope*	Seewave	M	[376]
BI	*Bioacoustic index = relative abundance*	Soundecology	bioacoustic_index	[375]
TE	*Temporal entropy*	Seewave	Th	[377]
SE	*(Shannon) spectral entropy*	Seewave	Sh	[377]
GS	*(Gini) Simpson spectral entropy*	Seewave	Sh	[377]
H	*Acoustic entropy index = total entropy*	Seewave	H	[377]
AR	*Acoustic richness (index)*	Seewave	AR	[376]
ADI	*Acoustic diversity index*	Soundecology	acoustic_diversity	[379,409]
AEI	*Acoustic evenness index*	Soundecology	acoustic_evenness	[409]
NP	*Number of peaks*	Seewave	fpeaks	[382]
ACI	*Acoustic complexity index*	Seewave	ACI	[381]
Soundscape indices				
NDSI	*Normalised difference soundscape index*	Seewave	NDSI	[383]

The indices were calculated for the 50 – 2000 Hz frequency band. For the **NDSI**, the so-called 'anthropophony band' was the band of interest (fish sounds, 50 – 2000 Hz), while the so-called 'biophony band' was the band occupied by benthic invertebrate snaps (mainly snapping shrimps, 2.5 – 8.5 kHz). Out of the eleven tested complexity indices, specific settings were necessary for three of them (**ACI**, **ADI**, and **AEI**). To examine the effect of the settings on the **ADI** and **AEI**, the following frequency bandwidths and threshold were tested: 10, 50, 100, 500 and 1000 Hz; −10, −25, −50, and −75 dB. These tests were realized on the three datasets (controlled, in situ playbacks, and natural environments). The effect of the settings was not tested on the **ACI** because it had already been done by Bolgan et al. (2018). For the **ADI** and **AEI**, two 'optimal' settings, obtained from the controlled environment, were kept because one of them was more representative of the sound abundance, while the other was more representative of the sound type richness. Consequently, the following settings were used for the calculations: FFT window = 2048, window name = Hanning, size of frequency bands (for the **ADI** and **AEI**) = step = 100 and 500 Hz, threshold (for the **ADI** and **AEI**) = −25 and −50 dB (referred to as '**ADI_v1**, **ADI_v2**, **AEI_v1**, and **AEI_v2**' throughout the document; v1 = 100 Hz and −50 dB and v2 = 500 Hz and −25 dB), overlap = 75%, number of windows (for the **ACI**) = 120 for 1 min files and 360 for 3 min files.

The indices were calculated for each file, i.e., each block from the controlled environment (Figure 40), five replicates of each block for the in situ playbacks, and 108 files of 1 min for the natural environment (Figure 40). In addition, for the in situ playbacks, a second analysis was realized: the indices were calculated for each 'background block' (i.e., natural acoustic

environment without playbacks) and for each 'playback block' (i.e., blocks with both natural acoustic environment and playback sounds) from each replicate. Then, the values from each 'background block' were subtracted from those of the adjacent 'playback block' to obtain a delta, referred to as 'delta sounds' throughout the document. For graphical visualization, the deltas of all the replicates were averaged together.

2.4. Graphical representation and statistics

The values of the different indices were standardized between 0 and 1 with the formula 'standardized(x) = [(x − min(x)) (max(x) − min(x))$^{-1}$]'. These standardized values were plotted as 'bubble graphs'. Standard Z-scores greater than |3| were considered as outliers. The correlation between each index with both the sound abundance and the sound type richness was assessed using Spearman's rank correlation ρ with the associated p-values corrected with the Benjamini-Yekutieli method. This method was used rather than the Benjamini-Hochberg method because of the non-independence of the tests. Then, the coefficient of multiple correlation (R) was calculated for each index (Equation 1). For the in situ playbacks, both the artificial abundance/richness (from the stimuli) and the total abundance/richness (including both stimuli and natural sounds) were examined.

$$R^2_{i,a,d} = \frac{\rho^2_{a,i} + \rho^2_{d,i} - 2\rho_{a,i}\,\rho_{d,i}\,\rho_{a,d}}{1 - \rho^2_{a,d}}$$

Equation 1 Calculation of the coefficient of multiple correlation (R). *i* = index; *a* = sound abundance; *d* = sound type richness.

3. Results

3.1. Controlled environment

In the controlled environment, no index was significantly correlated with the sound type richness (Table 9). The **ACI**, **GS**, **H**, and **SE** showed positive correlations with the sound type richness that were, however, not statistically significant (Table 9). The **ADI**, **M**, and **TE** were strongly correlated with the sound abundance (ρ = 0.95, 0.90, and 0.90, *P* = 0.0062, 0.036, and 0.036), while a negative correlation was observed for the **AEI** (ρ = −0.95, *P* = 0.0062, Table 9). The correlation between sound the abundance and **ADI** was observed with a threshold of −50 dB, but not with smaller (−10 or −25 dB) or higher thresholds (−75 dB) (ρ = 0.95, *P* = 0.0044, Table SP5 - 3). No effect of the step (i.e., the size of the frequency bands) was observed. No correlation was observed with the default settings. The same results were obtained for the **AEI (**Figure 41**,** Table SP5 - 4).

Table 9 Correlation coefficients and associated *P*-values between α-acoustic indices, sound abundance, and sound type richness in the controlled environment. Statistically significant *P*-values are in bold. Both = both abundance and richness. BY = Benjamini Yekutieli.

	Correlation			Non-adjusted *P*		BY-adjusted *P*	
	ρ		R				
	Abundance	**Richness**	**Both**	**Abundance**	**Richness**	**Abundance**	**Richness**
ACI	−0.05	0.84	0.84	0.89	**0.0043**	1.00	0.11
ADI_v1	0.95	0.11	0.96	< **0.0001**	0.79	**0.0062**	1.00
ADI_v2	0.32	0.58	0.66	0.41	0.10	1.00	1.00
AEI_v1	−0.95	−0.16	0.96	< **0.0001**	0.68	**0.0062**	1.00
AEI_v2	−0.32	−0.58	0.66	0.41	0.10	1.00	1.00
AR	0.19	0.48	0.52	0.63	0.19	1.00	1.00
BI	0.37	0.26	0.45	0.33	0.49	1.00	1.00
GS	−0.16	0.74	0.76	0.68	**0.023**	1.00	0.38
H	0.16	0.69	0.71	0.68	**0.042**	1.00	0.60
M	0.90	0.32	0.96	**0.0011**	0.41	**0.036**	1.00
NDSI	−0.32	−0.63	0.71	0.41	0.07	1.00	0.80
NP	−0.74	−0.16	0.76	**0.022**	0.68	0.38	1.00
SE	−0.21	0.79	0.82	0.59	**0.011**	1.00	0.24
SPL_{pp}	0.05	0.63	0.63	0.89	0.07	1.00	0.80
SPL_{rms}	0.47	0.42	0.63	0.20	0.26	1.00	1.00
TE	0.90	0.32	0.96	**0.0011**	0.41	**0.036**	1.00

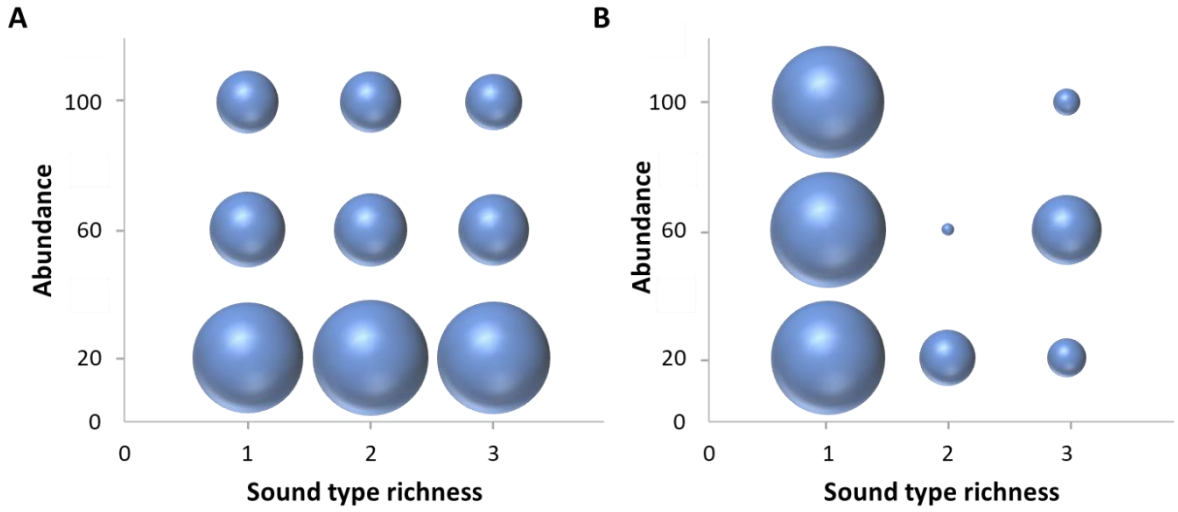

Figure 41 Bubble graph for the standardized AEI as a function of the sound abundance and sound type richness. (**A**) Step = 1000 Hz, threshold = −50 dB; (**B**) step = 500 Hz, threshold = −25 dB. Range: between 0 and 1. This figure highlights the importance of the settings. In panel **A**, the sound type richness does not affect the AEI, while the contrary is shown in panel **B**.

3.2. In situ playback

In the in situ playbacks, **M** and **TE** were both correlated with the play back sound abundance (both ρ = 0.82, both $P < 0.0001$; Table SP5 - 5), and total sound abundance (i.e., playback and natural fish sounds) (ρ = 0.84 and 0.80, both $P < 0.0001$; Table 10). In contrast, **NP** was negatively correlated with the total sound abundance (ρ = −0.56, $P = 0.0032$; Table 10). When considering the 'delta sounds', only **M** was correlated with the sound abundance (ρ = 0.90, $P <$

0.0001; Table SP5 - 6). In all cases, the **ADI** never correlated with the sound abundance or sound type richness (Table SP5 - 7, Table SP5 - 8, and Table SP5 - 9). Similar observations were obtained for the **AEI,** but with negative signs (Table SP5 - 10, Table SP5 - 11, and Table SP5 - 12).

Table 10 Correlation coefficients and associated P-values between α-acoustic indices, sound abundance, and sound type richness per minute (natural + played back) for the in situ playbacks. Statistically significant P-values are in bold. Both = both abundance and richness; BY = Benjamini Yekutieli. The correlation between the sound abundance and sound type richness was almost null (ρ = 0.045).

	Correlation			Non-adjusted *P*		BY-adjusted *P*	
	ρ		R				
	Abundance	**Richness**	**Both**	**Abundance**	**Richness**	**Abundance**	**Richness**
ACI	−0.28	0.38	0.48	0.063	**0.011**	0.85	0.35
ADI_v1	0.21	0.26	0.33	0.16	0.082	1	0.97
ADI_v2	−0.17	−0.16	0.23	0.27	0.29	1	1
AEI_v1	−0.22	−0.23	0.31	0.14	0.13	1	1
AEI_v2	0.20	0.13	0.23	0.20	0.39	1	1
AR	−0.28	−0.057	0.28	0.066	0.71	0.85	1
BI	0.058	−0.30	0.31	0.71	**0.047**	1	0.76
GS	−0.32	0.018	0.32	0.034	0.91	0.73	1
H	−0.15	0.18	0.24	0.31	0.25	1	1
M	0.84	0.047	0.84	**<.0001**	0.76	**<.0001**	1
NDSI	−0.14	−0.18	0.23	0.35	0.24	1	1
NP	−0.56	−0.076	0.56	**<.0001**	0.62	**0.0032**	1
SE	−0.31	0.14	0.35	**0.039**	0.35	0.73	1
SPLpp_	−0.0055	−0.041	0.042	0.97	0.79	1	1
SPLrms_	−0.16	−0.31	0.34	0.31	**0.039**	1	0.73
TE	0.80	−0.0077	0.80	**<.0001**	0.96	**<.0001**	1

3.3. Natural environment

In the natural environment, when considering the optimal settings, no index showed any statistically significant correlation with the sound abundance (Figure 42, Table 11). Four indices (**ADI_v1**, **NP**, **SPL$_{rms}$** and **TE**) were negatively correlated with sound type richness (ρ = −0.43, −0.52, −0.35, and −0.57, all $P < 0.001$), while six indices (**ACI**, **AEI_v1**, **BI**, **M**, **NDSI**, and **SPL$_{pp}$**) were positively correlated with the sound type richness (ρ = 0.53, 0.43, 0.36, 0.55, 0.35, 0.47, all $P < 0.05$; Figure 42, Table 11). In the natural environment, sound abundance and sound type richness were not independent (ρ = 0.53, $P < 0.0001$). When considering a broader range of settings, the **ADI** was positively correlated with the sound abundance (ρ = 0.33 to 0.34, all $P < 0.006$), but only with a low threshold (−10 dB) and low step values (10, 50 and 100 Hz). With this low threshold (−10 dB), a positive correlation with the sound type richness was found (ρ = 0.29, $P = 0.031$), but only with low step values (10 and 100 Hz). In contrast, with high thresholds (−50 and −75 dB), the correlations between the sound type richness and **ADI** were generally all negative (−0.51 < ρ < −0.34, all $P < 0.004$) (Table SP5 - 13). Similar results were obtained for the **AEI** (Table SP5 - 14). When using a low threshold (−10 dB) with low step

values (10, 50, and 100 Hz), the **AEI** appeared to be negatively correlated with the sound abundance ($\rho = -0.32$, $P = 0.012$), while with higher thresholds, it was generally positively correlated with the sound type richness ($0.36 < \rho < 0.51$, all $P < 0.004$) (Table SP5 - 14).

Table 11 Correlation coefficients and associated P-values between α-acoustic indices, sound abundance, and sound type richness in the natural environment. Statistically significant P-values are in bold. Both = both abundance and richness; BY = Benjamini Yekutieli.

	Correlation			**Non-adjusted *P***		**BY-adjusted *P***	
	ρ		**R**				
	Abundance	**Richness**	**Both**	**Abundance**	**Richness**	**Abundance**	**Richness**
ACI	0.060	0.53	0.60	0.54	**< 0.0001**	1	**< 0.0001**
ADI_v1	−0.066	−0.43	0.47	0.50	**< 0.0001**	1	**< 0.0001**
ADI_v2	−0.018	0.10	0.14	0.85	0.28	1	1
AEI_v1	0.066	0.43	0.47	0.50	**< 0.0001**	1	**< 0.0001**
AEI_v2	0.038	−0.10	0.15	0.70	0.30	1	1
AR	−0.15	−0.024	0.17	0.12	0.81	0.95	1
BI	0.13	0.36	0.37	0.19	**0.0001**	1	**0.0016**
GS	0.073	0.27	0.29	0.45	**0.0043**	1	0.051
H	0.014	0.092	0.10	0.89	0.35	1	1
M	0.21	0.55	0.55	0.030	**< 0.0001**	0.30	**< 0.0001**
NDSI	0.031	0.35	0.40	0.75	**0.0002**	1	**0.026**
NP	−0.21	−0.52	0.52	0.029	**< 0.0001**	0.30	**< 0.0001**
SE	0.055	0.19	0.20	0.57	**0.043**	1	0.40
SPL_{pp}	0.018	0.47	0.54	0.86	**< 0.0001**	1	**< 0.0001**
SPL_{rms}	0.16	−0.35	0.54	0.11	**0.0002**	0.93	**0.0026**
TE	−0.13	−0.57	0.60	0.20	**< 0.0001**	1	**< 0.0001**

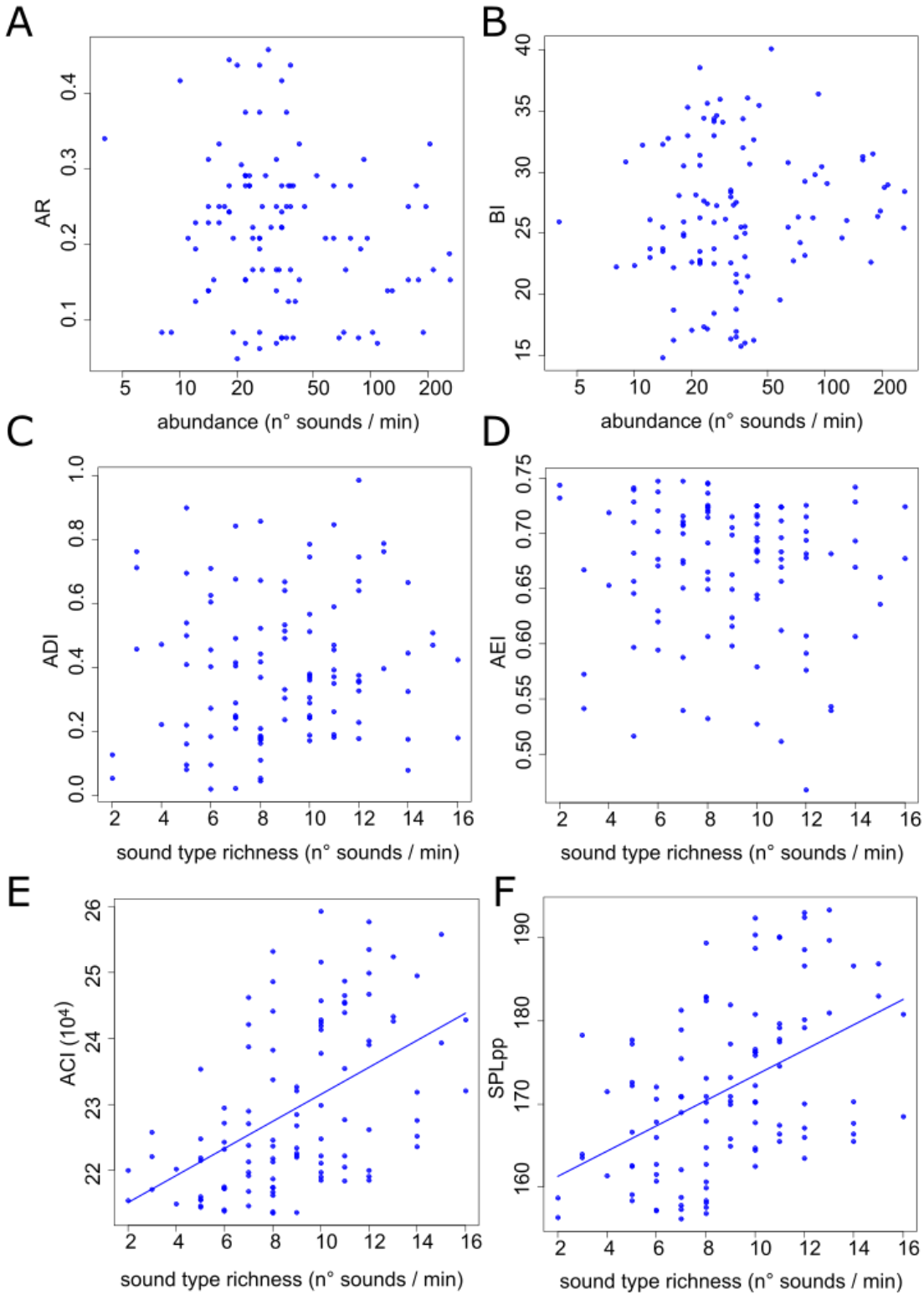

Figure 42 Scatterplots of the indices as a function of the sound abundance or sound type richness, in the natural environment. (**A**) AR and (**B**) BI as a function of the sound abundance (logarithmic scale). (**C**) ADI_v2 (step = 500 Hz, threshold = −25 dB), (**D**) AEI_v2 (step = 500 Hz, threshold = −25 dB), (**E**) ACI, and (**F**) SPL_{pp} as a function of the sound type richness. Regression lines are presented for cases where a significant correlation was observed.

4. Discussion

The aim of this study was to determine whether, and how, α-acoustic diversity indices, which are easily and rapidly applicable on large datasets, discriminate between the sound abundance and sound type richness of coastal marine fish sounds, and whether they are appropriate as proxies of species diversity for environmental monitoring.

4.1. Use of α-acoustic diversity indices to assess sound abundance and sound type richness

In both the controlled environment and in situ playbacks, no index was correlated with the sound type richness. **M** and **TE** were correlated with the sound abundance in both the controlled environment and with in situ playbacks. Similarly, the **ADI** and **AEI** were also correlated with the sound abundance, but only in the controlled environment. In the natural environment, the opposite was observed: no indices were correlated with the sound abundance, but many (**ACI**, **ADI**, **AEI**, **BI**, **M**, **NDSI**, **NP**, **SPL_{rms}**, **SPL_{pp}**, and **TE**) were correlated with the sound type richness. These results are therefore contradictory and can lead to misinterpretation.

The controlled experiments showed that the indices were correlated with the sound abundance but not with the sound type richness, implying that they are sensitive to the number of sounds but are not capable of distinguishing the different types of fish sounds. In the in situ playbacks, the indices were not able to capture those differences, both in terms of the sound abundance and sound type diversity of the played-back and naturally occurring fish sounds. This is of critical importance, because it clearly shows that indices are incapable of discerning subtle modifications of a subset of a soundscape (i.e., fish frequency band), being intended, rather, to describe soundscape phenomena over a wide and often diverse frequency bandwidth. The disappearance of a species or the arrival of an invasive species within the fish frequency band would therefore be difficult to assess, unless it produced mass phenomena. Marine coastal soundscapes are always noisy and distinct from terrestrial soundscapes because they show limited frequency partitioning. In contrast, in terrestrial soundscapes, frequency partitioning is often linked to species or a group of animals (Figure 43) [410]. Coastal biological soundscapes are dominated by a broad band range (> 30 kHz) of short transient snaps of invertebrates, with a low frequency resolution [277] and a narrow (< 2 kHz) low-frequency band occupied mainly by fish sounds. Coastal soundscapes, especially in coral reefs, are therefore characterized by mass biophonic phenomena with little frequency partitioning (Figure 43).

In some terrestrial environments, indices are not suitable for biodiversity monitoring without prior removal of biasing sounds, such as the anthropophony [394] or anuran sounds in tropical forests [411]. In a study on terrestrial soundscapes conducted in Japan, the comparison between acoustic indices and acoustic richness (i.e., the number of different sounds produced by animals) under different sonic conditions (e.g., presence or absence of wind, rain, and anthropophony) revealed that only two (**AR** and **TE**) out of the eleven tested indices reflected the measured richness across all the sonic conditions. Moreover, none of these indices correlated with the measured richness when masked by broadband insect stridulations [412]. In our study, the indices were affected by background noise (Figure 39). In coral reefs, the major contributor to background noise is the biophony, such as sounds from snapping shrimps that are always present [24,70]. Although their peak frequency is above 2 kHz, these sounds are usually broadband sounds and overlap the fish band (0.05 – 2 kHz). These broadband sounds affect indices, particularly those detecting peaks, such as **NP**. In addition, in coral reefs, a diurnal 'background noise' band around 400 to 500 Hz is present and composed of transient short pulses attributed to Pomacentridae sounds (Figure 39 and Chapter 6) [246]. This mass phenomenon in the fish band influences the indices. In the Polynesian Islands, the intensity of this 'fish noise' was higher in shallow reefs than in deeper reefs (Chapter 6), but the indices did not show the same trends depending on the depth. For example, the **ACI** and $\mathbf{SPL_{pp}}$, which were positively correlated with the sound type richness, were higher at shallow depths, while the contrary was found for the $\mathbf{SPL_{rms}}$, which was negatively correlated with the sound type richness. The indices that were positively correlated with the sound type richness, i.e., the number of fish sound types that were clearly identified and into which the detected sounds were classified, did not reflect this sound type richness, but they did quantify biological mass phenomena (e.g., the Pomacentridae sounds in shallow reefs). Consequently, none of the acoustic indices tested can inform on fish acoustic diversity. Even a combination of indices [413] within such a small, poorly stratified frequency band dominated by biophonic background noise cannot inform on fish sound acoustic diversity because it is not suitable for depicting subtle changes in sound types.

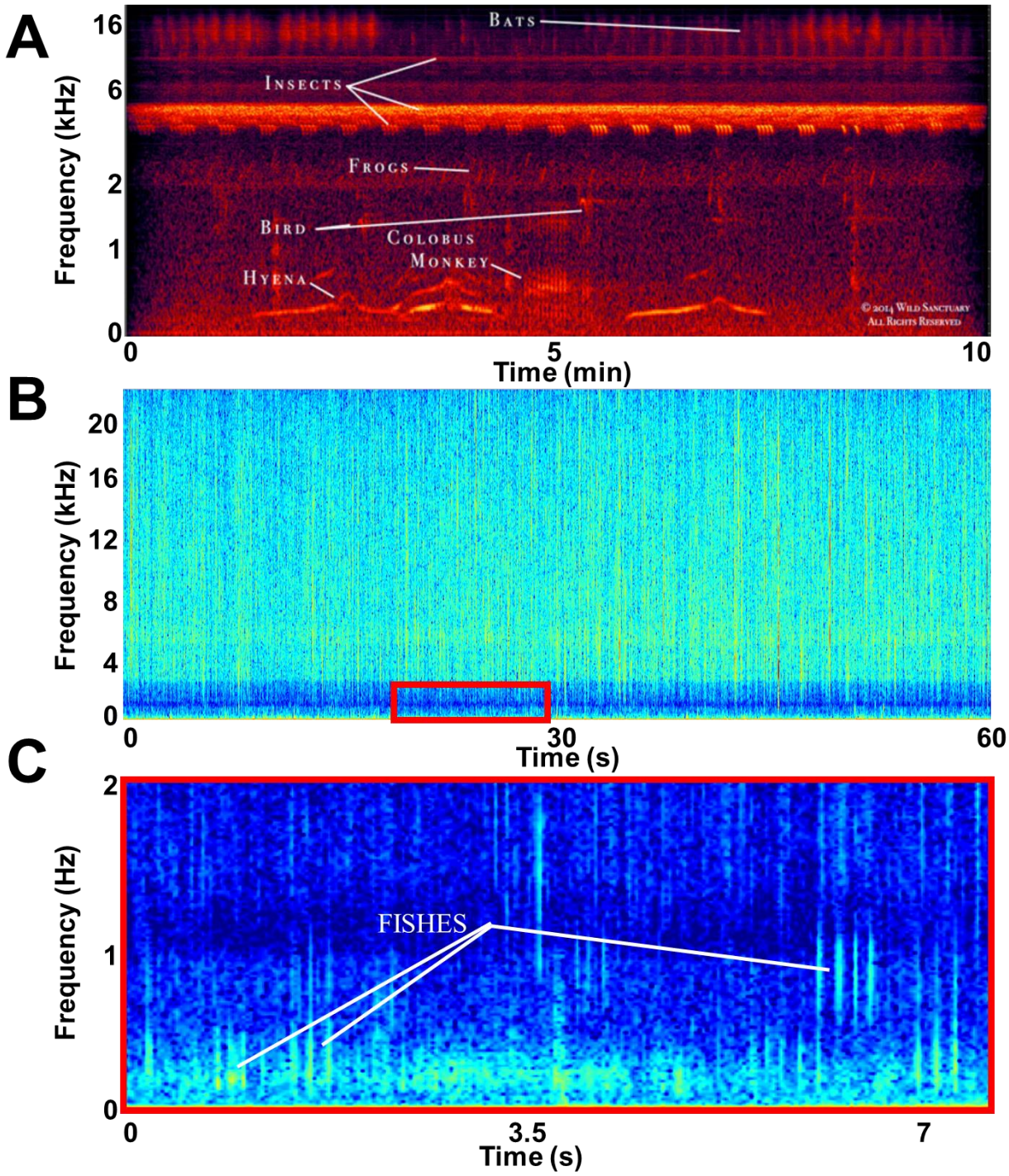

Figure 43 Difference between terrestrial and coastal marine soundscapes. (**A**) Spectrogram in a savanna (Courtesy Bernie Krause. © 2021 Wild Sanctuary. All Rights Reserved [410]); (**B**) a coral reef dominated by broadband transient sounds mainly produced by snapping shrimps; (**C**) zoom-in of the low-frequency part (0 – 2 kHz) of the spectrogram, dominated by fish sounds (subsampled at 4 kHz, FFT = 256).

In addition, there was no correlation between most of the indices and the measured sound abundance in the natural environment. This is because the number of sounds in the background noise was higher than the number of sounds manually selected to measure the abundance and

richness, i.e., those with a high signal-to-noise ratio allowing for the identification and classification of sounds into types. When testing the settings of the ADI and AEI, the only threshold that showed a link with the sound abundance was −10 dB, while in the controlled environment, this threshold was −50 dB, which implies an influence of the presence of mass acoustic phenomena. Moreover, to establish a link with the sound abundance the ADI and AEI frequency bands (i.e., steps) had to be small (bandwidths of 10 to 100 Hz). Small bands also better correlated with the sound type richness, but both positively and negatively depending on the threshold. However, indices that work on frequency bands, such as the AEI or ADI, are appropriate when soundscapes are divided into bands, which is not the case in marine coastal soundscapes (or only partly the case). Indeed, coastal marine soundscapes, contrary to terrestrial soundscapes, are generally divided into a few overlapping bands: a low-frequency band (mainly fish sounds, some crustacean sounds, and sometimes whale sounds) and a high-frequency band (broadband transient sounds, and occasionally small cetacean sounds) (Figure 42). The band occupied by fish sounds (mainly below 2 kHz) is narrow and shows little frequency partitioning. Contrary to terrestrial environments, frequency bands in coastal marine soundscapes provide only poor ecologically relevant information on diversity.

Moreover, the use of the tested indices to assess fish sound diversity is problematic because fish sounds are typically drum-like sounds, of similar frequencies, composed of pulses or (pseudo-)harmonic sounds. If the frequency bands chosen in the settings are too small, such sounds would be detected in several bands. Bands would therefore ‘decompose’ a sound type in different bands but would not be representative of different fish sound types. The type of fish sounds (e.g., knocks and herbivorous sounds vs. grunts, buzzes, and chirps) has been shown to impact some indices’ values [396,404]. Similarly, in fish and frogs, indices have been suggested to be more limited with harmonic sounds than with single-pulsed sounds [396,414]. Therefore, as dominating fish sounds are not the same everywhere, this can impact the indices and comparisons between sites. For example, in French Polynesia, the proportion of pulse series is known to vary between the photic and mesophotic reefs (Chapter 6). Therefore, caution is needed when comparing the values of indices from one environment to another.

These different considerations lead to the conclusion that acoustic indices are not appropriate for studying fish sound diversity in marine coastal environments such as coral reefs. Indices, for example, may be used to report on the anthropophony, to study the geophony, to focus on high-frequency sounds produced by benthic invertebrates, or to study fish mass phenomena, but such usage was not inspected in the present study.

4.2. Effect of the settings

In this study, the use of manually chosen settings compared to default settings considerably increased the values of the correlations. Depending on the settings used, indices such as the **ADI** or the **AEI** could be correlated with the sound abundance or with the sound type richness. In addition, the sign of the correlation changed depending on the settings, and more importantly, the threshold used: low (around −10 dB) or high (under −50 dB). The same observations were made by Bohnenstiehl et al. (2018) with the **ACI**. They found negative correlations between the **ACI** and sound abundance of harmonic fish calls with a low frequency resolution (47 – 94 Hz), and positive correlations with a high frequency resolution (23 Hz). This is in agreement with other studies showing the high sensitivity of the **ACI** to settings such as the frequency resolution [396,404]. When comparing the results of the controlled experiment in this study with those reported in 2018 for similar tracks [396], the correlation between the **ACI** and the sound abundance is completely different ($\rho = 0.66$ vs. $\rho = -0.05$). The differences could be due to slight changes in the softwares used (R vs. SoundscapeMeter [415]), which measure different **ACI** metrics (e.g., ACI_f vs. ACI_{tot}) and allow slightly different settings (e.g., presence or absence of a noise filter). In addition, the settings that allow the best representation of the sound abundance and sound types richness vary depending on the environment, e.g., temperate seas vs. coral reefs [404]. This high sensitivity of the settings would pose a risk if acoustic diversity indices were to be widely used for habitat management or for informing on marine spatial planning.

4.3. Comparison of the different indices

TE was one of the two indices correlated with the sound abundance in both the controlled environment and in situ playbacks. In the natural environment, this index was the most impacted by biological 'background' noise (i.e., the highest correlation observed with the sound type richness). The higher performance of **TE** compared to other indices and the impact of background noise have been underlined in terrestrial environments too [412]. **TE** is known to perform well in the presence of a geophony [412] and anthropophony [376,412], which appear as temporally invariable low-frequency patterns in the soundscape [381]. On the other hand, **TE** is known to be affected by background noise, the sound duration, and overlap [416].

Correlations between H and the fish sound type richness were not observed, not even in the natural environment, where many of the indices were impacted by biological 'background' noise. Similar observations were made in temperate reefs [403]. These results are not caused by the absence of a link but by the intrinsic calculation of the index. H is designed to have low

values for pure tones and high values for almost silent soundscapes or, on the contrary, noisy soundscapes across frequency bands. In the in situ playbacks, the values of H were always higher when the loudspeaker was silent. In addition, when the number of sound types emitted by the loudspeaker was increased from 1 to 2, H increased, but when the number of sounds was increased from 2 to 3, H decreased (Figure SP5 - 1). This was observed for all the sound abundances tested. This shows that this index is not representative of the sound type richness because there is no linear relation between them.

The ADI and AEI were only correlated with the sound abundance in the controlled environment. In Indonesian coral reefs, the ADI and AEI were correlated with fish species richness (19% to 24% of the deviance explained), when calculated for a higher-frequency band: 1.2 – 11 kHz [406], which is the frequency band covered by benthic invertebrates' snapping sounds [417] (Chapter 3). Similar to what is observed with H, low values of the AEI could relate to a near-silent, saturated, or windy terrestrial soundscape, while high values of the ADI could relate to a completely silent or a noisy soundscape.

At low frequencies (band: 0.1 – 1.2 kHz), Peck et al. (2021) found that only the ACI was affected by fish abundance (38% of the deviance explained). However, the use of the ACI in coral reefs is known to be impacted by a masking effect [404], for example, in chorus events [398]. Therefore, a single fish species can have a considerable effect on indices because they respond to mass phenomena [396,398]. Moreover, when considering higher-frequency bands, typically dominated by snapping shrimps' broadband sounds, indices such as the ACI saturate at high snap rates [405].

Using simulated bird recordings, Gasc et al. (2015) showed that some indices are affected by the sound duration in comparison to the file duration (S/R ratio; **H**, **SE**, **TE**, **M**, and **ACI**), background noise (**H**, **SE**, **TE**, **M**, **AR**, and **ACI**), type of sound (**NP** and **ACI**), relative amplitude (**AR**), and overlap (**H**, **SE**, **TE**, **M**, and **ACI**) [418]. Therefore, to correctly reflect the acoustic biodiversity, particularly of a group of animals, indices should be insensitive to the *(1)* S/R ratio, *(2)* background noise, *(3)* type of sound (i.e., should be equally sensitive to different types of sounds (e.g., pulse series vs. upsweeps)) , *(4)* relative amplitude of the sounds and *(5)* sound overlap [418].

5. Conclusions

In coral reefs, which are hotspots of biodiversity, indices do not appear to be suitable for inferring information on fish acoustic diversity, because they are affected by naturally highly abundant sounds. In this sense, indices rather describe mass phenomena, and thus the activity of a group of sound-producing organisms (e.g., Pomacentridae or snapping shrimps), that are limited in diversity. Overall, this study clearly suggests that the use of acoustic indices to study fish sound diversity is inappropriate.

6. Author contributions

Conceptualization, X.R. and É.P.; Methodology, X.R. and É.P.; Software, X.R.; Validation, X.R., L.D.I. and É.P.; Formal Analysis, X.R.; Investigation, X.R.; Resources, X.R., M.B., D.L., É.P.; Data Curation, X.R.; Writing—Original Draft Preparation, X.R.; Writing—Review & Editing, X.R., É.P. and L.D.I.; Visualization, X.R.; Supervision, X.R., É.P. and L.D.I.; Project Administration, X.R.; Funding Acquisition, X.R. and D.L. All authors have read and agreed to the published version of the manuscript.

Chapter 6. Fish sounds of photic and mesophotic coral reefs: variation with depth and type of island

Xavier Raick[1,2], Lucia Di Iorio[3,2], David Lecchini[4,5], Cédric Gervaise[2], Laetitia Hédouin[4,5], Under The Pole Consortium[6], Gonzalo Pérez-Rosales[4], Héloïse Rouzé[4,7], Frédéric Bertucci[1,4] & Éric Parmentier[1]

[1] Laboratory of Functional and Evolutionary Morphology, FOCUS, University of Liège, Liège, Belgium

[2] Chorus Institute, Grenoble, France

[3] Université de Perpignan Via Domitia, CNRS, CEFREM UMR 5110, Perpignan, France

[4] PSL University, EPHE-UPVD-CNRS, USR 3278 CRIOBE, Papetoai, Moorea, French Polynesia

[5] Laboratoire d'Excellence 'CORAIL', Perpignan, France

[6] Under the Pole Expéditions. Concarneau, France. Members : G. Bardout, J. Fauchet, A. Ferucci, F. Gazzola, G. Lagarrigue, J. Leblond, E. Marivint, A. Mittau, N. Mollon, N. Paulme, E. Périé-Bardout, R. Pete, S. Pujolle & G. Siu.

[7] Marine Laboratory, University of Guam, Mangilao, USA

This chapter has been published in *Coral Reefs.* Additionally, parts have been used for an educational video on the MANEA platform: *Diversité des sons des poissons des récifs mésophotiques : cas d'étude en Polynésie*.

MAJOR RESULTS

Fish sounds description

- ✓ The most abundant fish sound type recorded in the study was an arched sound (AS) referred to as AS4, which appeared as pseudo-harmonic arched sounds in spectrograms.
- ✓ Among the frequency-modulated (FM) sounds, the most abundant sound types were DS1, US1, and CS1.
- ✓ The pulse series (PS) stricto sensu category included at least 25 different sound types. It comprised seven sound types characterized by an average pulse period between 19 and 40 ms, grouped as Fast Pulse Train (FPT) sounds.

Influence of depth and island type on sound abundance

- ✓ Acoustic fish community composition differed between depths, with PS sounds dominating at 20 m and AS and FM sounds being more abundant at 120 m.
- ✓ The abundance of certain sound types increased with depth, while others decreased.
- ✓ The number of AS4 sounds increased with depth, along with their signal-to-noise ratio and bandwidth, suggesting they are mainly produced in the deep part of the reef.

Shannon acoustic diversity

- ✓ The highest Shannon acoustic diversity was found at 20 m at Moorea. The lowest diversity was observed at 60 m at Rangiroa.
- ✓ For most islands, the Shannon acoustic diversity decreased between 20 and 60 m. However, the trend varied between 60 and 120 m.
- ✓ The overlap of α-diversity was higher between 60 and 120 m compared to the overlaps between 20 and 60 m or between 20 and 120 m. This indicates stronger similarities between mesophotic environments. Atolls generally showed a higher within island-type overlap than high islands.

Fish sound types community composition

- ✓ The similarity statistic revealed that comparing depths of 20 and 60 m had higher similarity within sites compared to comparing depths of 60 and 120 m.
- ✓ Depth had the strongest influence on acoustic community. The type of island also had a significant but lesser effect. Certain sound types were associated with specific depths or island types.
- ✓ The CCA revealed that the acoustic community composition, based on sound types, was influenced by depth and the type of island, with benthic cover features explaining the variation in acoustic communities at different depths and islands.

Key question for the objective of the thesis

How does the discriminable near sources of the biophony vary along a depth gradient?

Abstract

Mesophotic Coral Ecosystems remain largely unexplored. The aim of this study was to determine how the acoustic fish biodiversity varied depending on the depth and the type of island in six Polynesian islands. The link between benthic cover and fish sound diversity was established. In most islands, acoustic fish α-diversity decreased between 20 and 60 m but not between 60 and 120 m. Fish sound types community composition was more driven by depth, likely due to benthic coral cover differences, than by the type of island. These results show fish sounds exhibit a bathymetric stratification and can reflect different habitat features. It opens perspectives in the monitoring of mesophotic coral ecosystems using passive acoustics.

1. Introduction

Coral reefs are one of the biggest biodiversity hotspots on Earth. However, species richness and diversity are not homogeneous in coral reefs as they vary depending on the depth [108] and the type of island, i.e. coral atolls (also named low islands) or high islands (volcanic island surrounded by a barrier reef) [419].

Light-dependent coral reefs can be divided into shallow-water coral reefs (between the surface and 30/40 m) and Mesophotic Coral Ecosystems (MCEs) [105] that extend from 30/40 m to/over 150 m [106–108]. The lower limit is defined as the maximum depth at which there is sufficient sunlight to support photosynthesis and, consequently, the growth of zooxanthellate hermatypic corals [109,110]. Contrarily to shallow-water coral reefs, the ecology and population dynamics of MCEs remains largely unknown because they are not easily accessible to humans [108]. MCEs are, however, thought to serve as refuges for different reef species and could contribute to the recovery of photic reefs [109,111]. Depth gradients in coral reefs are described for fish assemblages. Upper (30 to 60 m) mesophotic fish communities share similarities with shallow-water (surface to 30 m) coral reef communities [105,420], while the lower mesophotic zone (between 60 and 150 m) has unique fish assemblages [105,421]. The faunal shift between the upper and lower MCEs fauna is generally found between 60 and 90 m [107,108,421].

Differences in coral cover and fish assemblages have also been reported in relation to the type of island [419]. In Polynesian atolls, the barrier reef appears to be divided into an upper slope made of a succession of spurs and grooves followed by a sloping terrace, and a lower slope which is more steeply inclined [122]. In high islands, the profile is more variable because of more recent volcanic formations [122]. Generally, it is divided into three parts: (1) the upper slope (until 30 m) containing spurs, grooves, terraces, buttresses; (2) a less inclined slope (between 30 and 70 m) of variable nature (predominantly hard bottom coral substrate or a sandy plain); and (3) a steep slope or drop off with a higher inclination (bellow 70 m) [122]. The substrate is important since most fish species between 30 and 70 m are found where hard substrates are dominant, while the central sandy part of the slope has low fish diversity and abundance [123,422].

French Polynesia extends over 5 million km^2 [112,113] and is divided into five archipelagos: Austral, Gambier, Marquesas, Society and Tuamotu Islands. Some islands are coral atolls, like all the islands in the Tuamotu Archipelago [117], while most islands from other archipelagos

are high islands [122]. The majority of the Polynesian coral reef research is focused on the shallow part of the islands of the Society Archipelago and regions of the Tuamotu Archipelago [117,122]. Like in other parts of the world, little is known about MCEs. This is particularly true below 80 m [122], where descriptions are generally limited to bottom relief. Only sparse information is available on the fish communities at these depths. Reefs are often named 'choral reefs' because their shallow parts are known to be acoustic hotspots [57,138,141]. Many fish species from the photic reef are known to be vocal [21,138–140], and there are indications that deeper habitats (75 to 90 m) also host vocal fish species [157]. Therefore, passive acoustics could be used as a proxy to investigate fish communities [138,163,164] in deeper reefs. However, despite being a useful tool to study the diversity of fish assemblages, there is little knowledge on the association between acoustic diversity with depth, the type of island or benthic cover features in coral reefs.

The aim of this study is to describe the acoustic fish biodiversity from the photic reef to the MCE in six Polynesian locations, i.e., three atolls (Rangiroa, Raroia, and Tikehau) and three high islands (Bora Bora, Mangareva, and Moorea), to determine if and how the acoustic fish biodiversity varies depending on the depth (20, 60 and 120 m), the type of island, and how this is related to habitat features.

2. Materials and methods

2.1. Sampling

Data sampling was conducted between March 2018 and April 2019 in six Polynesian islands from three archipelagos: Society Islands, Gambier Islands and Tuamotu Islands (Figure 44A, Table SP6 - 1). Three islands were high islands (Bora Bora, Moorea, and Mangareva) and three were atolls (Rangiroa, Raroia, and Tikehau) (Figure 44B, Table SP6 - 1). The sampling was realized by deep divers from Under the Pole Expeditions (Concarneau, France). At each island, three different depths were sampled simultaneously on the external slope of the reef, one in the photic reef (20 m) and two in the mesophotic reef (60 m and 120 m) (except at Mangareva, where only 20 m and 60 m depths were sampled).

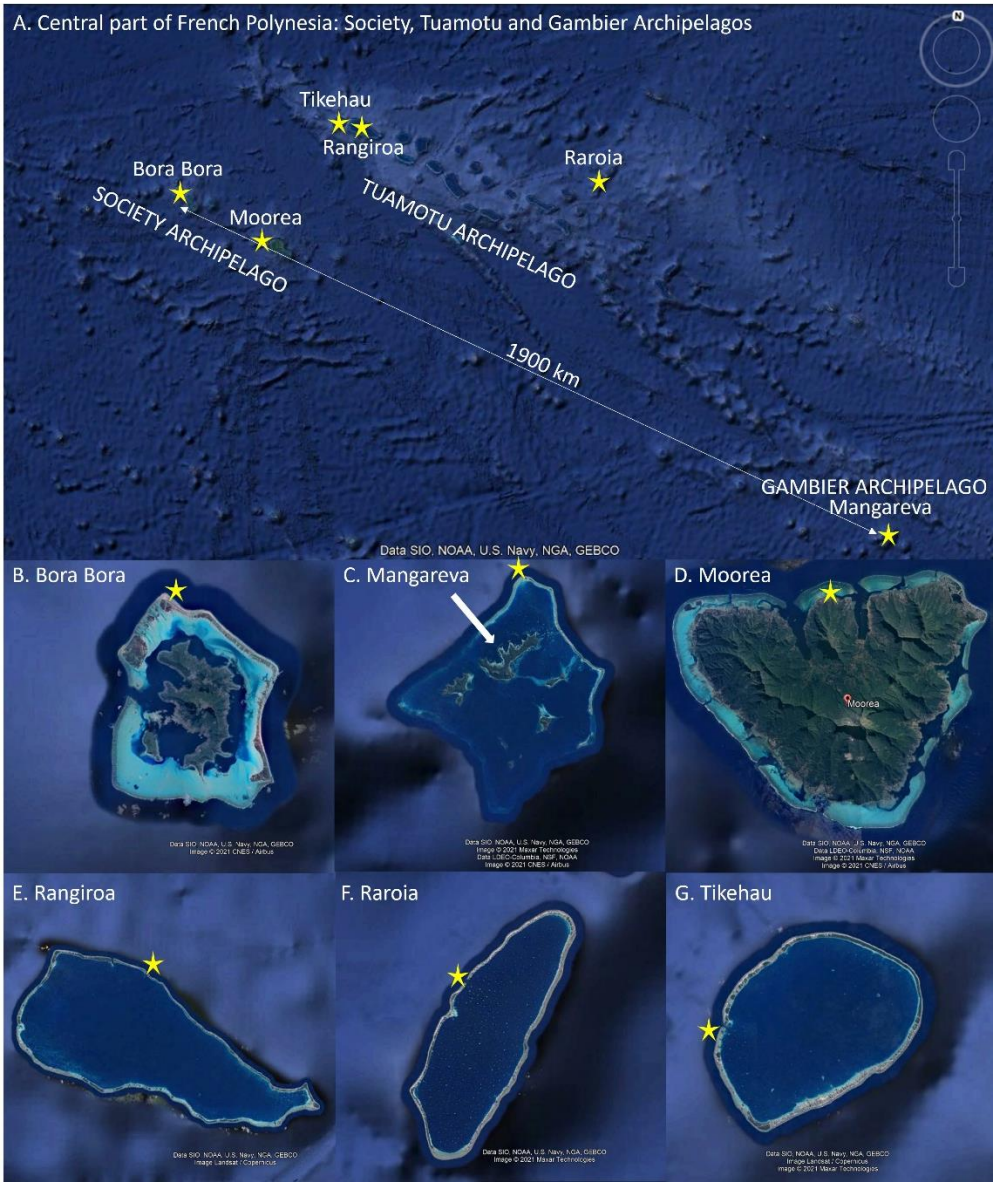

Figure 44 Location of sampling sites (A) Central part of French Polynesia: Society, Tuamotu, and Gambier Archipelagos. (**B**) Bora Bora, (**C**) Gambier Archipelago with Mangareva in the center, (**D**) Moorea (these three islands are high islands), (**E**) Rangiroa, (**F**) Raroia, and (**G**) Tikehau (these three islands are atolls). Yellow stars indicate sampling sites. Images from SIO, NOAA, U.S. Navy, NGA, GEBCO 2021 Maxar Technologies Data LDEO-Columbia NSF, NOAA 2021 CNES / Airbus.

At each depth, an autonomous underwater long-term acoustic recorder SNAP (Loggerhead Instruments; Sarasota, FL, USA) connected to a HTI96 hydrophone (sensitivities: −170.5, −170.2 and −169.7 dB re 1 V for a sound pressure of 1 µPa, flat frequency response from 2 Hz to 30 kHz) was deployed during 72 h. The recorders were attached vertically to the pole of a 4 kg weighted tripod structure (60 cm high) placed on the sea bottom. All the recorders were scheduled to record sounds for 1 minute every 10 minutes at a sampling rate of 44.1 kHz (16-bit resolution), with a + 2.05 dB gain.

In addition, for each island, a total of 90 photo-quadrats (i.e., 30 quadrats per depth) 0.75 x 0.75 m^2 were realized during each deployment (Figure SP6 - 1) and used to characterize the benthic cover. The benthic cover was divided in 16 categories: (1) sand, (2) dead coral, (3) rubble, (4) consolidate substrate, (5) scleractinians, (6) black coral and gorgonians, (7) hydroids, (8) Anthoathecatae, (9) encrusting sponges, (10) non encrusting sponges, (11) turf, (12) calcifying algae, (13) fleshy algae, (14) macroalgae including *Halimeda* algae, (15) encrusting algae and (16) other sessile invertebrates. Values of the quadrats (percent cover) of each of these categories were averaged to obtain mean values for each depth and each island. Finally, temperature was sampled with a MIDAS CTD (Valeport; Totnes, UK) between the surface and 130 m at all the islands except for Mangareva. The thermocline was generally between 60 and 120 m (Figure SP6 - 2).

2.2. Fish sounds selection

The audio files were subsampled at 4 kHz in order to focus on the low-frequency (0 – 2 kHz) part of the sound files, because fish are known to vocalize in this frequency band [58] (Chapter 3). Because sunset is the time of the day with the highest acoustic activity of Polynesian coral reef fishes (Chapter 3) and sound type identification is time-consuming, inspection of the files was focused on the hours of civil sunsets only (measured at Faanui, Papeete and Rikitea; https://www.sunrise-and-sunset.com/fr/). Files from three consecutive days were therefore visually and aurally inspected between 05:00 PM and 07:00 PM using RavenPro Sound Analysis Software 1.5 (Cornell Lab of Ornithology; Ithaca, NY, USA).

Fish sounds were classified into categories (referred to as sound types) with a dichotomous key (see KeySP6 - 1) based on qualitative and quantitative acoustic properties [163]. A sound type is defined as a category that contains sounds that share similar acoustic features. On the one hand, a sound type is likely usually produced by one species and/or contain sounds from multiple, sometimes closely related species. On the other hand, different sound types could also be produced by the same species [143,150,423,424].

2.3. Fish sounds description

A detailed description of ten sounds with a good signal-to-noise ratio allowing sounds to be characterized was realized for each sound type. Measurements were conducted on oscillograms and power spectra with Avisoft SAS Lab Pro (Avisoft Bioacoustics; Glienicke/Nordbahn, Germany). For each sound, the following features were manually measured: total duration of the sound (ms), peak frequency (Hz), number of pulses and pulse period (ms); (pseudo-) harmonic interval (if applicable, Hz), i.e., the frequency range between two consecutive

harmonics or pseudo-harmonics (i.e., a harmonic of the amplitude-modulated function); frequency interquartile interval (Hz); or presence of several peaks in the power spectra (if applicable). In addition, the 90% frequency bandwidth (BW, in Hz) was measured on the spectrograms on RavenPro Sound Analysis Software as the difference between the 5% and 95% frequency of the signal selection. For each sound type, the mean value and the standard deviation (SD) of the features were calculated.

2.4. Influence of depth and island type on sound abundance

To assess differences in fish sound abundance related to depth, the relative abundance (%) and the number of fish sounds (sounds per hour) of each sound types were compared between the three depths (20 m, 60 m, and 120 m) and the six islands. Normality and homoscedasticity were tested with Shapiro–Wilk and Bartlett tests. Kruskal–Wallis tests (KW) with Dunn's *post-hoc* tests with a Benjamini–Hochberg correction were used to compare BW of three sound types between the three studied depths. All statistics were realized using the R software version 3.6.1. (R Core Team 2019) and the significance level was $\alpha = 0.05$.

2.5. Shannon acoustic diversity

The Shannon index of acoustic α-diversity was determined based on the established sound type repertoire for each depth of each island. Three temporal replicates for each recording position were used (sunset of day 1, day 2 and day 3) (library *vegan*, function *Shannon*). Then, the overlap of α-diversity was determined between the three depths and between the three pairs of depths to investigate acoustic similarities between depth ranges. The overlap is a measurement based on a ratio of α-diversity over γ-diversity [425].

To test whether the Shannon acoustic diversity differs between depths and the types of islands, an analysis of variance was performed (function *aov*). Depth (20, 60 or 120 m) and the type of island (atoll or high island) were set as factors nested within seasons (i.e., the period of sampling: March/April or September/October, Table SP6 - 1). Diagnostic plots were used to verify assumptions. Because temperature data was not available for all the islands, the effect of temperature could not be tested, but it was discussed, as it is known to influence fish assemblage composition [426].

Finally, to test the influence of benthic cover features on Shannon acoustic diversity, a linear model was used. Only influencing benthic cover variables were included in the model and chosen using a forward stepwise method based on the AIC [427].

2.6. Acoustic community composition

Acoustic community composition was compared using Bray–Curtis distance matrices (function *vegdist*) that quantify the dissimilarity between two sites based on counts of each sound type at each site [428]. For all the tests, a log-standardization was used to reduce the influence of abundant sound types. The dispersion was calculated (function *betadisper*) and permutation based-tests of multivariate homogeneity of group variances were implemented on the results.

2.6.1. Similarity of acoustic communities

The similarities in acoustic fish community composition between depths (20, 60 and 120 m) and types of islands (atolls vs. high islands) were tested using analyses of similarities (function *anosim*, number of permutations: 999). Significant differences between groups were tested based on the Bray-Curtis dissimilarity matrices. The *anosim* statistic R, i.e., the metric quantifying similarities between groups, was determined by examining the mean ranks of the dissimilarities both between groups (r_B) and within groups (r_W) and was calculated as $R = (r_B - r_W)\ divisor^{-1}$ with *divisor* calculated to obtain R in the interval [−1, 1]. Positive R values indicate more similarity within groups, null values indicate random grouping, and negative R values indicate more similarity between than within groups [429].

2.6.2. Influence of depth and island type on the acoustic community composition

To test whether the acoustic community composition differs with depth and the type of island, permutational multivariate analyses of variance (PerMANOVA) based on the calculated distance matrices were carried out (function *adonis*) [430]. Depth (20, 60, or 120 m) and type of island (atoll or high island) were set as factors, islands (Bora Bora, Mangareva, Moorea, Rangiroa, Raroia or Tikehau) were set as random factor nested within season. A permutation-based test was used to test the multivariate homogeneity of group variances (Table SP6 - 8). Finally, Nonmetric Multidimensional Scaling (NMDS) was performed (function *metaMDS*) to represent acoustic communities in relation to the type of island and depth.

2.6.3. Influence of benthic cover on the acoustic community composition

A canonical correspondence analysis (CCA) was conducted to test the influence of benthic cover features on acoustic community composition (function *cca*). The CCA was used to find the best dispersion of sound types, and to relate them to combinations of benthic cover features [431]. A model-building process was used to reduce the number of explanatory variables and select the most effective CCA model. A forward stepwise variable selection method was applied, which gradually adds significant variables based on the Akaike information criterion

(AIC) to help determine which are most relevant for the model [427]. Grouping variables (depth and type of island) were added to the ordination plot to see their relationships to acoustic community composition and coral cover variables (function *ordiellipse*, *vegan* package with a 95% confidence interval). All statistics were realized using the R software version 3.6.1. (R Core Team, 2019).

3. Results

A total of 17,574 fish sounds were detected during sunsets at all depths and at all islands (Table SP6 - 4). Among the defined sound types, only those with at least ten selections were kept for the analyses. Consequently, 45 different fish sound types were used, representing 92% of all the identified sounds (Figure 45).

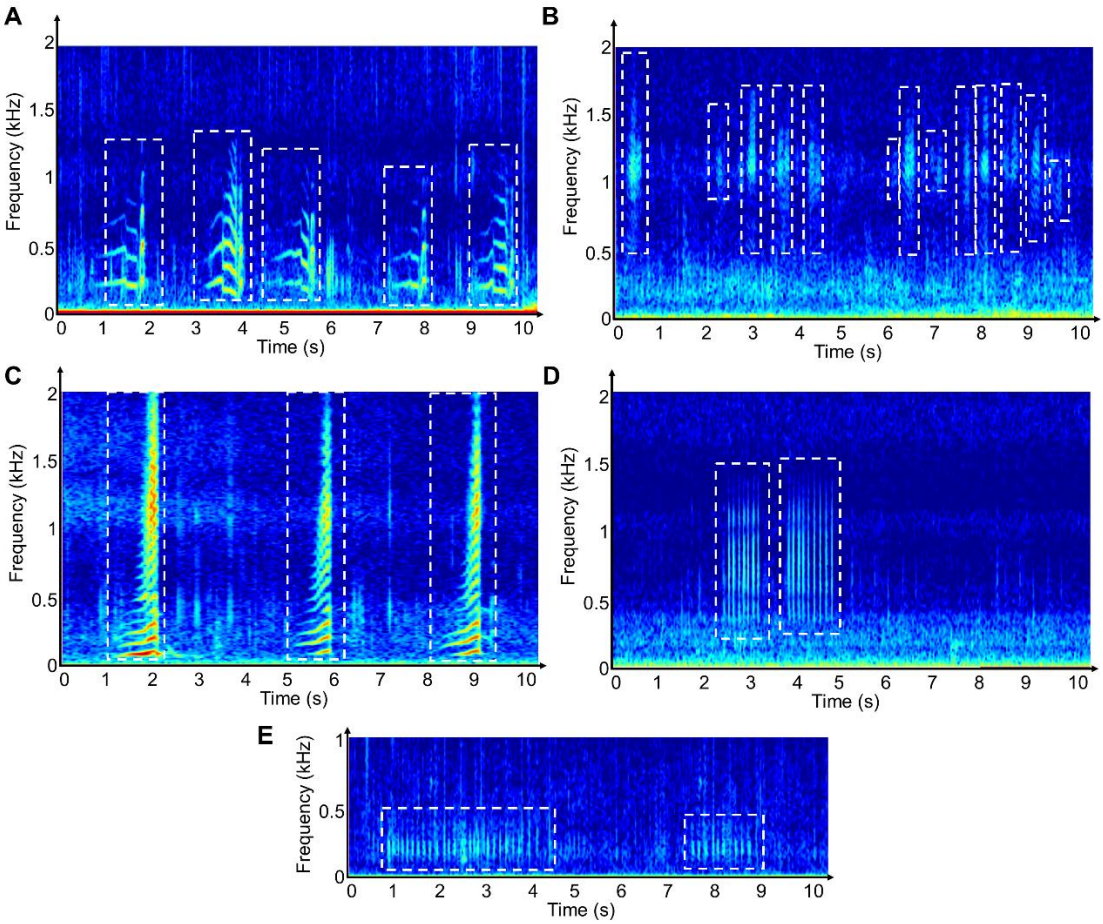

Figure 45 Illustration of five abundant sound types. (**A**) CS1, (**B**) AS4, (**C**) US1, (**D**) PS16, and (**E**) PS17. FFT = 256 for all the spectrograms. Sampling frequency = 4 kHz.

3.1. Fish sounds description

According to Desiderà et al. (2019), fish sounds could be divided into two main categories: frequency-modulated signals (FM) and pulse series (PS) *lato sensu*, i.e., series of at least three short broadband transient pulses. Polynesian PS sounds were divided into two sub-categories: PS *stricto sensu*, sounds with distinguishable pulses and without (pseudo-)harmonics, and arched sounds (AS), i.e., sounds with ultra-short pulse periods that appear as (pseudo-)harmonics in the spectrographic representation (Figure 46). The AS sound type category comprises ultra-fast pulse series (UFPS) and long tonal non-frequency modulated calls (LT) described by Desiderà et al. (2019).

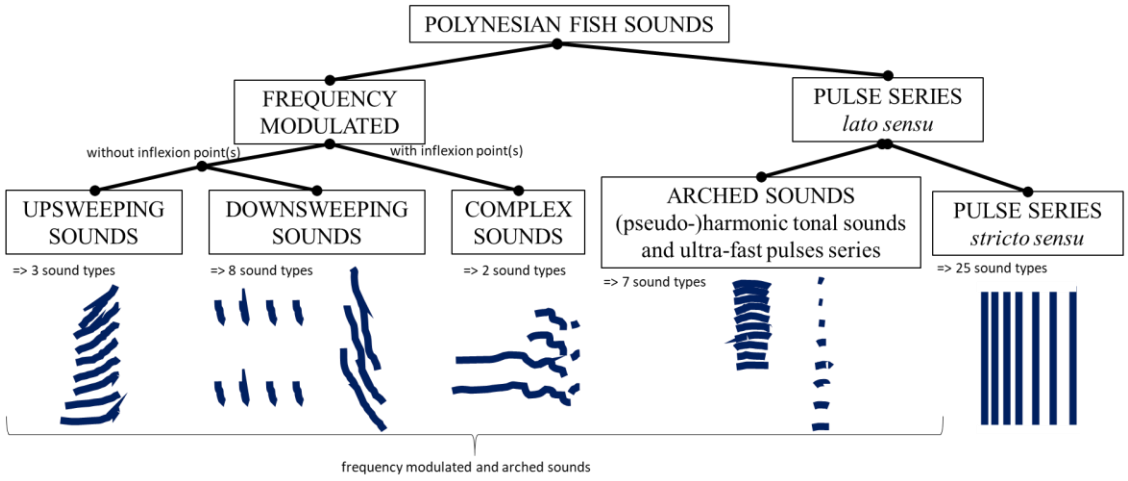

Figure 46 Dichotomous classification of Polynesian fish sounds with graphical illustrations of a few sound types.

The most abundant sound type (42% of the total number of sounds) was an arched sound referred to as AS4 sound that shares similarities with the ultra-fast pulse series, also known as *kwa* sound recorded in the Mediterranean Sea [281]. The AS4 sound type was a pulse train of 183 ± 7 ms (mean ± standard deviation) duration, characterized by 12 ± 1 pulses and a pulse period of 15 ± 1 ms. In the spectrograms, they appeared as pseudo-harmonic arched sounds. In the power-spectra, mean pseudo-harmonic interval (HI) was around 68 ± 4 Hz with an interquartile interval of 393 ± 20 Hz. Their waveforms were characterized by a peak frequency of 847 ± 148 Hz modulated in amplitude by a periodic envelope with HI^{-1} oscillations (Figure SP6 - 3M).

Frequency-modulated (FM) sounds were divided in downsweeping (DS), upsweeping (US) and complex sweeps (CS), i.e., with more than one frequency modulation (mix of downsweeps and upsweeps). When considering the total occurrence, the most abundant sound type of each

sub-category was, respectively, the DS1, US1 and CS1. CS1 was a long complex frequency modulated sound also referred to as whoot because of its high similarity with the '*whoot*' described by Bertucci et al. (2020). The main features of each type of FM sound are detailed in the Table SP6 - 3, as well as in oscillograms and power spectra in the Figure SP6 - 3.

US1 sounds were harmonic upsweeping sounds of 335 ± 80 ms duration, characterized by a waveform with 32 ± 6 pulses and a pulse period of 11 ± 0.2 ms. The peak frequency was 225 ± 49 Hz and corresponded to the fundamental frequency or to the first harmonic. The mean harmonic-interval was 94 ± 2 Hz (Figure SP6 - 3J). CS1 were pulse trains of 940 ± 174 ms duration, characterized by 168 ± 66 peaks and a peak period of 5 ± 0.3 ms. Their waveform was characterized by two consecutive parts (first part: 756 ± 291 ms with 150 ± 65 peaks of 5 ± 0.5 ms; second part: 84 ± 9 ms with 18 ± 2 peaks of 5 ± 0.3 ms). Their power-spectra presented a complex harmonic structure with two peaks around 200 Hz (one at 190 ± 6 Hz and one at 227 ± 9 Hz) and two peaks around 400 Hz (one at 363 ± 11 Hz and one at 423 ± 35 Hz) with a mean harmonic-interval of 183 ± 19 Hz (Figure SP6 - 3T).

The PS *stricto sensu* category comprised at least 25 different sound types. Seven sound types were characterized by an average pulse period between 19 and 40 ms. These seven sound types can be group in the *Fast Pulse Train* (FPT) category described by Desiderà et al. (2019). One sound type was a slow pulse series (pulse period: 822 ± 289 ms, SPS). The 17 others sound types had intermediate pulse period values. Sounds lasted from 86 ± 45 ms (for FPT5) to 5.68 ± 7.71 s (for PS6). The main features (duration, number of peaks, peak frequency and period) of each type of PS sound are detailed in Table SP6 - 2, whereas the oscillograms and power spectrum of each sound are presented in Figure SP6 - 2.

3.2. Influence of depth and island type on sound abundance

Acoustic fish community composition differed between depths (Figure SP6 - 4). PS sounds dominated at 20 m while AS and FM sounds were more abundant at 120 m. However, the number of some sound types (e.g., AS4, US1 and CS1) increased with depth while the opposite was observed for other sound types (e.g., FPT4, FPT5, PS16, PS17, DS1 and DS4) (Figure 47, Figure SP6 - 6). The ten most abundant sound types represented 78% of the overall sound type abundance (Figure 47, Table SP6 - 4). They were found in all islands. The abundance of six of them (DS1, DS4, FPT4, FPT5, PS16 and PS17) decreased with depth, while it increased for three other sound types (AS4, US1 and CS1) (Figure SP6 - 5, Table SP6 - 5). Among the sounds that 'decreased with depth', the most abundant ones at 20 m were short pulse series and fast pulse trains (see Table SP6 - 2): PS16, FPT5, PS17 and FPT4 sound types (Figure 47). Among

the sounds that ‘increased with depth’, the most abundant ones at 120 m were the AS4 (= *kwa*-like sound), the US1 and the CS1(= whoot) sound types (Figure 47, Figure SP6 - 6). At all depths, the most abundant sound type in atolls was the AS4 (average occurrence between 22 to 78%, Figure SP6 - 6). In high islands, the most abundant sounds were AS4, FPT5, PS16 and PS17 sound types (Table SP6 - 4, Figure SP6 - 6). Noticeably, the number of AS4 sounds increased with depth (n = 229 per hour at 20 m, n = 684 per hour at 60 m, and n = 1077 per hour at 120 m, Figure 47, Figure SP6 - 5, Figure SP6 - 6, Table SP6 - 5), so did their signal-to-noise ratio, and their bandwidth (BW = 350, 402 & 478 Hz; KW: χ^2 =374, df = 2, $P < 0.0001$; Dunn: $Z = 18$, 11 & −10, all $P < 0.0001$) suggesting they are mainly produced in the deep part of the reef. At Moorea, Rangiroa, Raroia, and Tikehau, the number of AS4 sounds was higher at 120 m while it was higher at 60 m at Bora Bora (Table SP6 - 5). At Bora Bora, Moorea, Rangiroa, and Raroia, the bandwidth of AS4 was greater at 120 m than at other depths ranges (KW: χ^2 = 18, 111, 89, 171, df = 2, all $P < 0.001$; Dunn: Z = 2, 4, 4, 10, 8, 7, 13, 6, $P = 0.02$, < 0.001, < 0.001, all others $P < 0.0001$) while at Tikehau, the bandwidth was higher at 60 m compared to the other depths (KW: χ^2 = 148, df = 2, $P < 0.0001$; Dunn: Z = −2 and −12, P = 0.02 and < 0.0001).

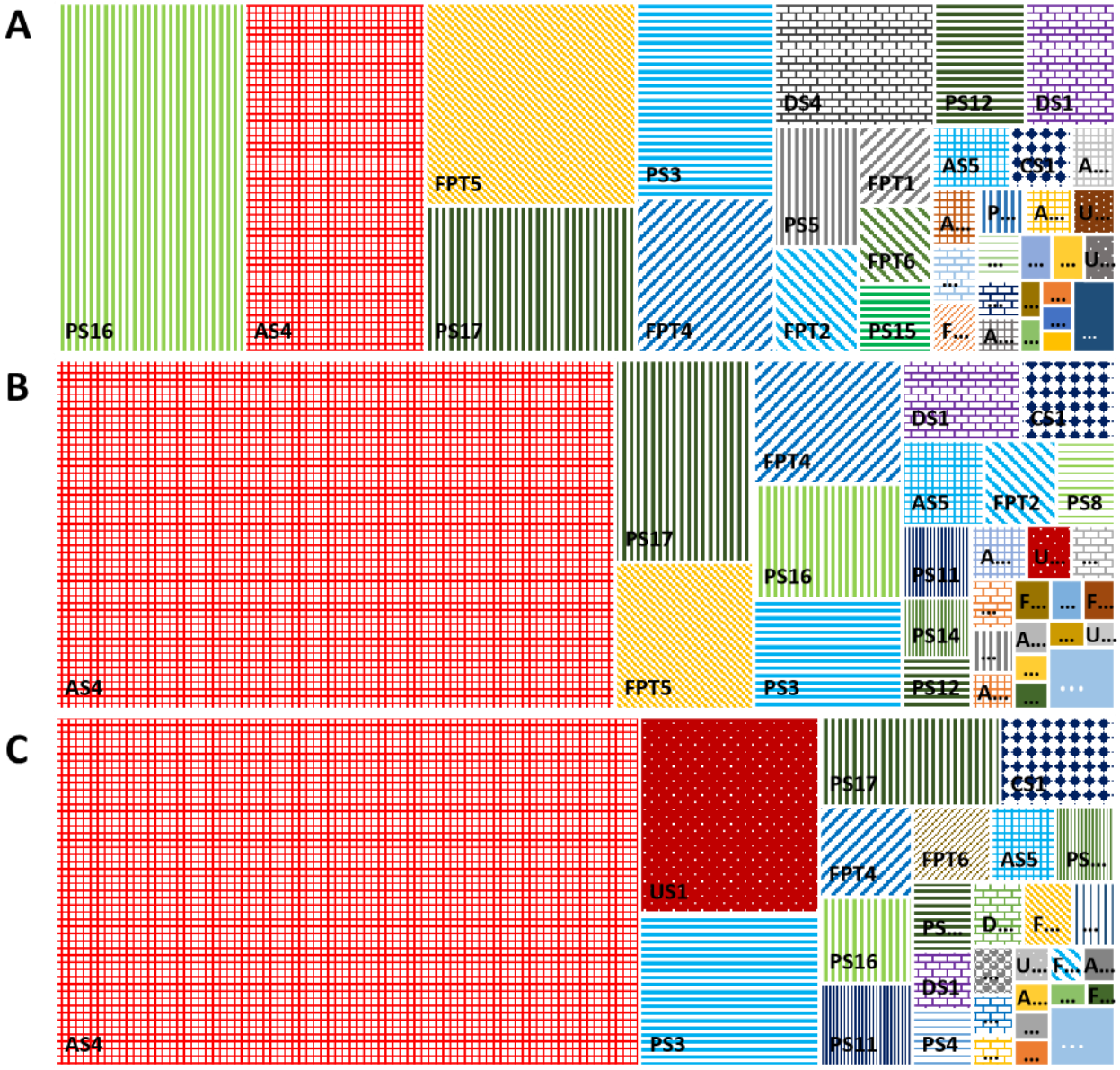

Figure 47 Treemaps of the number of sound types per depth: (A) 20 m, (B) 60 m and (C) 120 m. Stripes = FM, diagonal stripes = FPT, dots = US, bricks = DS, checkerboard = CS sound types.

Similar patterns were observed for other FM sounds. For example, the number of US1 increased with depth (n = 7 per hour at 20 m, n = 9 per hour at 60 m and n = 187 per hour at 120 m, Figure 47). This was also the case for CS1 sounds (n = 9 per hour at 20 m, n = 23 per hour at 60 m and n = 54 per hour at 120 m). Moorea was the only island where the number of CS1 was higher at 60 m than at 120 m (73 vs. 15 per hour). The bandwidth of CS1 increased with depth (BW = 229, 379 and 418 Hz at 20, 60 and 120 m respectively; KW: $\chi^2 = 30$, df = 2, $P < 0.0001$; Dunn: $Z = 5, 3, -3$, all $P < 0.01$).

3.3. Shannon acoustic diversity

The highest Shannon acoustic diversity was found at 20 m at Moorea (Shannon: 2.77 ± 0.02, median ± 0.5 IQR, Table SP6 - 6), while the lowest value was observed at 60 m at Rangiroa (Shannon: 0.99 ± 0.05). For all the islands except for Mangareva, the Shannon acoustic diversity decreased between 20 and 60 m (Figure 48). Between 60 and 120 m, either it increased again (e.g., Rangiroa), decreased (e.g., Tikehau) or showed no differences (e.g., Moorea) (Table SP6 - 6, Table SP6 - 7).

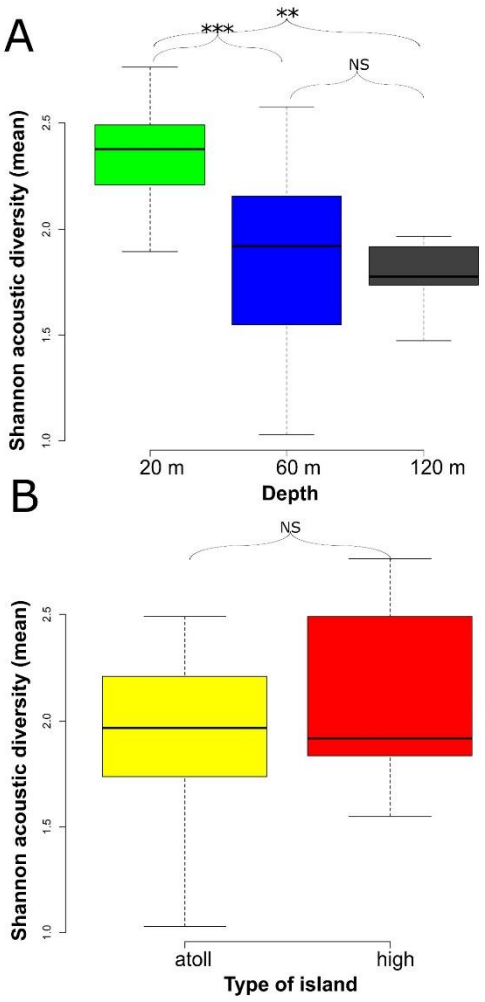

Figure 48 Boxplot of the Shannon acoustic diversity depending on (A) depth (20, 60 or 120 m) and (B) the type of island (atoll vs. high island). Boxes represent the median ± interquartile range (IQR) and lines represent Q1 –1.5 IQR and Q3 + 1.5 IQR. *** $P < 0.0001$, ** $0.0001 < P < 0.001$, NS = not significant (Analysis of variance, Table SP6 - 7).

The overlap of α-diversity was higher between 60 and 120 m (74%) than between 20 and 60 m or between 20 and 120 m (60% in both cases, Table SP6 - 7), indicating stronger similarities between mesophotic environments. The overlap of α-diversity between the two

types of islands (atolls and high islands) was 62%. Atolls generally showed a higher within island-type overlap than high islands (75% vs 46%).

The Shannon acoustic diversity differed with depth (analysis of variance, F = 8.59, *P* = 0.00068, Table SP6 - 7). The Shannon acoustic diversity differed between 20 and 60 m (Tukey test, *P* = 0.00079) but not between 60 m and 120 m (*P* = 0.82). All the benthic cover variables influenced the Shannon acoustic diversity (Table SP6 - 7).

3.4. Fish sound types community composition

3.4.1. Similarity of acoustic communities

The similarity statistic R indicated a higher similarity within sites when comparing 20 and 60 m (R = 0.30, *P* < 0.001) than when comparing 60 and 120 m (R = 0.17, *P* = 0.004). Atolls and high islands showed higher similarities in acoustic community composition than depths (R = 0.29 and 0.26, *P* = 0.015 and 0.001, respectively).

3.4.2. Influence of depth and island type on the acoustic community composition

Permutational multivariate analyses of variance (PerMANOVA) on acoustic β-diversity revealed that depth had the strongest effect on acoustic community composition (df = 5, Sum Sq = 1.58, Mean Sq = 0.32, F = 4.79, R^2 = 0.32, *P* = 0.001) (Figure 49). To a lesser extent, the type of island had also an effect (df = 2, Sum Sq = 0.59, Mean Sq = 0.29, F = 4.46, R^2 = 0.12, *P* = 0.002) (Figure 49, Table SP6 - 9). Some sound types, such as the pulse sequence PS1 and the downsweeping sound DS8, appeared to be strongly associated with deep reefs as they were only recorded at 120 m. Other sound types, including the complex sound CS2 (Figure SP6 - 3, Table SP6 - 3) were only found at 20 m, or in the case of PS7 only at 20 and 60 m. Some sounds, such as the fast pulse train FPT7 were only found in atolls while others, such as the upsweeping sound US3 were only recorded at high islands. In addition, when visualizing acoustic community composition, atolls appeared clearly separated from high islands at 20 m (Figure SP6 - 7), suggesting island-type differences in the shallow part of the coral reefs.

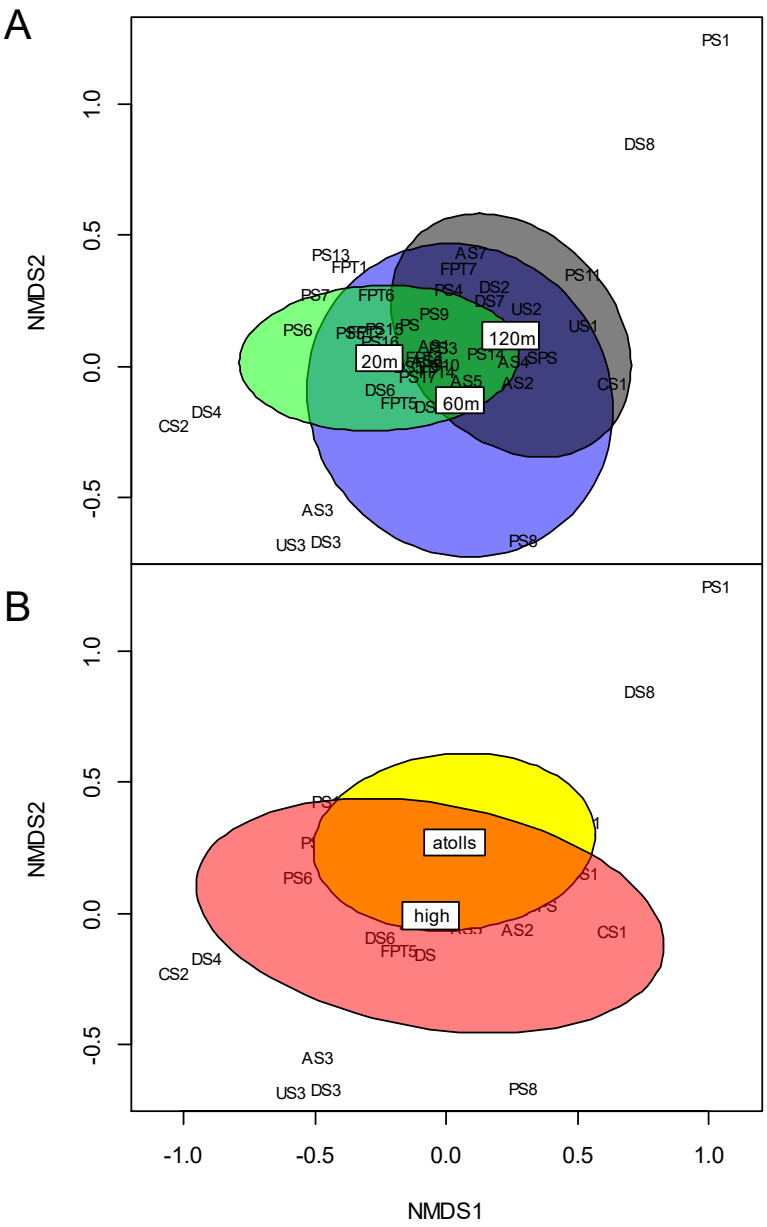

Figure 49 'Nonmetric Multidimensional Scaling' ordination plot of centroids based on Bray-Curtis distance representing the effect of (A) depth and (B) type of island on acoustic fish communities assessed on sound types (c.f. Table SP6 - 2 and Table SP6 - 3 for sound type abbreviations). Groupings are presented with ellipses (95% confidence around the centroid).

3.4.3. Influence of benthic cover on the acoustic community composition

The Canonical Correspondence Analysis (CCA) indicated that the acoustic community composition, based on sound types, was influenced by depth and the type of island. Inspection of the CCA ordination plot allows the association of sound types to benthic cover features (Figure 50, Table SP6 - 10, Table SP6 - 11). Positive CCA1 values are mainly explained by non-encrusting sponges, sand, and to a lesser extent by black coral / gorgonians and hydroids (CCA1 scores: 0.75, 0.62, 0.38 and 0.32, respectively). Negative CCA1 values are mainly

explained by macroalgae, scleractinians, and dead coral (−0.80, −0.68, and −0.57 respectively). The benthic cover explains part of the difference between islands.

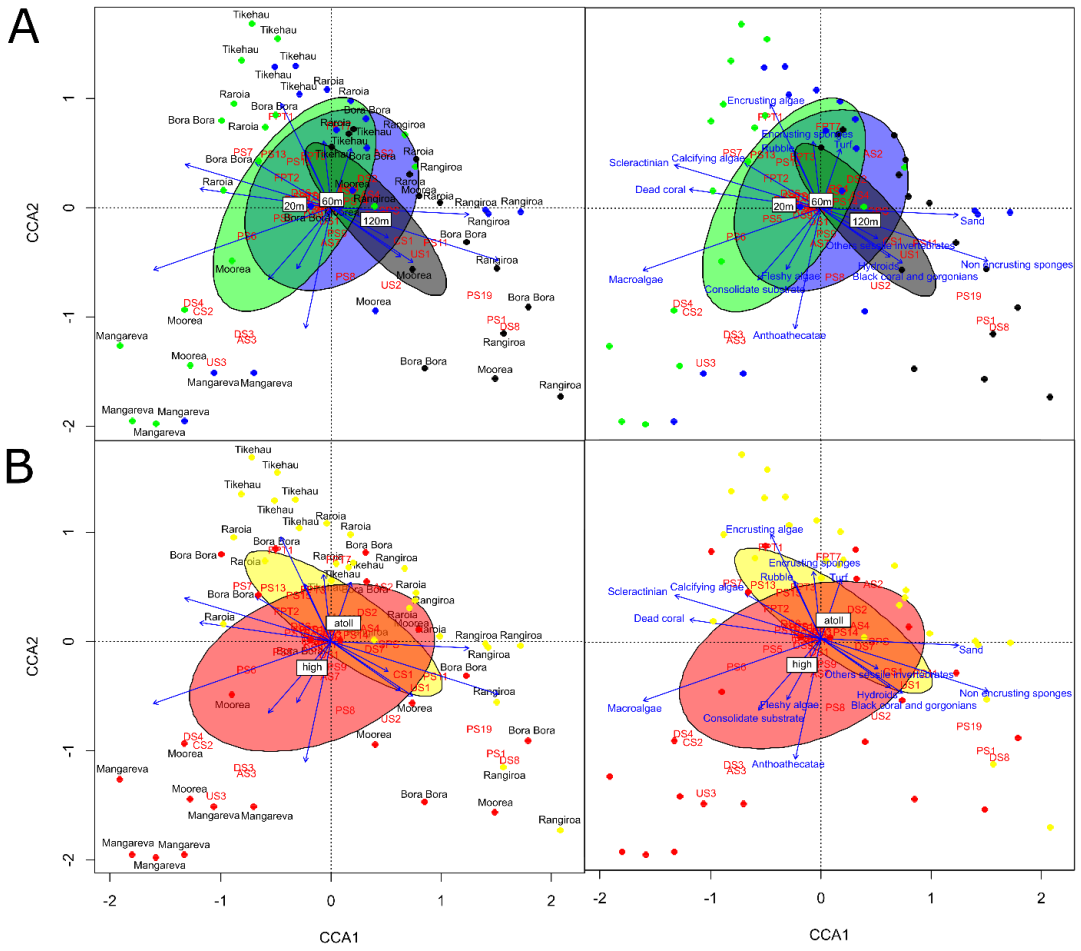

Figure 50 Canonical correspondence analysis ordination plots of the acoustic fish community composition based on Bray−Curtis dissimilarities of relative abundance of n = 45 sound types (in red) at (A) three depths (green: 20 m, blue: 60 m, black: 120 m) and (B) for two types of islands (yellow: atolls, red: high islands). Blue arrows show the influence of benthic cover features. Ellipses are 95% confidence interval. For better visualisation figures have been split in two pannels with islands labels on the left and benthic cover labels on the right.

At 20 m, the most present benthic cover is scleractinians for all the islands (between 32% and 56%; except for Rangiroa, with more consolidate substrate: 35% vs 11%). Despite a domination by scleractinians, a variability is observed at 20 m between the different islands (Figure 69). In Tikehau reef (atoll), turf accounts for more than 28%, while rubble account for more than 20% in Bora Bora and Rangiroa. In Moorea (high island), when comparing with sounds, the presence of CS2 in the photic reef seems to be associated with the presence of consolidate substrate, fleshy algae and macroalgae, while PS7 seems to be rather linked to the presence of scleractinians, calcifying and encrusting algae (Figure 69). At 60 m benthic cover composition was highly variable. Some islands are dominated by scleractinians (e.g.,

Mangareva and Tikehau), others by consolidate substrate (e.g., Moorea and Raroia) and sand dominates the reef of Rangiroa. This is also visible in the CCA ordination plot, where the reef of Rangiroa at 60 m is located within deeper reefs (Figure 69). This greater variability in the benthic cover could explain why 60 m appears to be a transition depth for acoustic fish communities. Finally, at 120 m, the most present benthic cover is sediment substrate and sand for all the islands. However, differences exist. For example, at 120 m in Bora Bora, there is 59% to 100% more black coral compared to the other islands.

4. Discussion

Polynesian underwater soundscapes were rich, even at depth, with at least 45 non-occasional fish sound types recorded during sunset. It is worth mentioning the fish sound type diversity reported here is only part of the complex biophony found in the low-frequency part of the soundscape (i.e., below 2 kHz) in coral reefs, that can also comprise vocalizations from other taxa such as whales [432] or tonal rumble sounds of mantis shrimps [67,356].

In French Polynesia, the acoustic fish community of the deep part of the reefs and the shallow part of the atolls was dominated by a single fish sound: the AS4 that shows high similarities with the */kwa/* sound, suspected to be produced by nocturnal benthic Mediterranean *Scorpaena* spp. [281,433]. Although AS4 and AS5 sounds share similar features, they differ in terms of peak frequency. These two sound types could therefore be produced by two different species of Scorpaenidae, a group well represented in French Polynesia, with 37 to 39 sp. [126]. Among the other sound types, PS10 is composed of a long succession of low-frequency pulses and it shares similarities with sounds from temperate Ophidiidae [434], and may thus be emitted by fish of this family known to inhabit coral reefs [140]. FPT2 is a long fast pulse train that presents similarities with Cottidae sounds [435]. FPT5 sounds could be attributed to Pomacentridae recorded in coral reefs [151,153,436], while FPT6 shares similarities with the 'Pomacentridae' sound type described previously in Moorea [141]. Finally, AS1 was a low-frequency (i.e., below 700 Hz) long tonal call that was similar to Serranidae sounds (e.g., *Epinephelus adscensionis*) [21]. This family is very diverse in French Polynesia, with at least 68 to 69 species [126]. Other sound types like the US1 and the CS1, two abundant sounds at 120 m could not be attributed to a clade. CS1 seems to correspond to the *whoot* previously recorded at Moorea [141].

Acoustic fish diversity and calls composition showed a depth dependence. Both FM and PS sounds were recorded at all the depths, but PS *stricto sensu* were more abundant at 20 m where

they constituted 67% of all the sounds vs. only 27% at 120 m. The soundscape was dominated by AS sounds at 120 m (57% of all the sounds at 120 m but only 21% at 20 m). However, US and CS sound types were, respectively, 9.79x and 1.96x more abundant at 120 m than at 20 m. In a study conducted in South Africa, frequency of sounds made during daytime overlap, whereas there was a clear distinction between nocturnal sounds [437] suggesting that diurnal fishes living in the photic zone would mainly use sounds to support visual behaviours such as courtship rituals, aggressive attitudes, or colour pattern changes. At night, in the dark, or in an environment with more colour absorption (like MCEs), vision is progressively substituted by other senses like hearing. In this context, it becomes more important for their vocal inhabitants to produce more stereotyped sounds. Bertucci et al. (2017) reported a higher sound level in the photic reef compared to the mesophotic reef in Moorea Island. Similar observations were made for all the studied reefs. However, the acoustic diversity reported in this study was not necessarily lower in deeper environments. MCEs showed distinct acoustic communities with sound types strongly associated or only found in this deeper ecosystem (e.g., US1 and CS1) (Figure 50 and Figure 69). This is in accordance with the hypothesis suggesting that the sonic environment in the mesophotic zone is not composed of sounds propagated from the upper part of the reef [157]. This is also in line with depth gradients found in temperate acoustic communities [318]. This study also indicates that acoustic fish communities, from the surface to 120 m, are divided into two parts with a buffer zone around 60 m. This buffer zone seems to coincide with a zone showing a higher fish species richness on the drop-off [157]. In addition, another explanation of this division is likely related to temperature and more precisely to the presence of one to several thermoclines, known to influence fish assemblage composition [426]. Finally, depth-dependent differences in acoustic fish communities are also related to changes in the benthic cover composition [318]. Different studies have demonstrated the existence of a positive relationship between acoustic metrics and coral cover in shallow reefs [158,417,438]. In this study, deep sites were characterized by an increase in the percentage of sponges, sand, black corals and gorgonians, and a decrease in the percentage of macroalgae and scleractinians. The transition zone in the upper part of MCEs is acoustically closer to the deep part of the MCEs than to the photic part of the reefs, showing a greater overlap between MCEs. However, the level of dissimilarities of acoustic fish communities appeared different within the two MCEs depths: a small dissimilarity was found at 120 m while the highest one was observed at 60 m (Figure 50A and Figure 69A), indicating a higher variability at 60 m than 120 m. This could be explained by the highest diversity of benthic cover composition at 60 m and by the transition from one assemblage of coral species to another one. For example, around 60 to 70 m at Tikehau

a shift occurs from *Pachyseris speciosa* assemblages by assemblages dominated by *Leptoseris* and *Echinophyllia* species [122,439]. In addition, within a single island the reef at 60 m can be dominated by a monospecific coral cover (e.g., 70 to 80% of *Pachyseris speciosa* at Moorea) or by sedimentary deposits.

In addition to differences linked to the depth and related benthic cover, part of the acoustic variability can also be explained by the type of island (Figure 49B and Figure 50B). Dissimilarities are higher in high islands than in atolls. Atolls are known to exhibit less habitat diversity compared to high islands with greater habitat diversity [419]. Moreover, reefs with similar degrees of habitat diversity, are known to have similar fish fauna [440,441], and shifts in habitat structure are reflected in changes in the diversity of the fish fauna (Anderson et al 1981). Another potential explanation for the similarity results between island types may be because three of the studied atolls belong to Tuamotu Archipelago, while the three studied high islands do not belong to the same archipelago (Bora Bora and Moorea are part of the Society Archipelago whereas Mangareva belongs to Gambier Archipelago). However, acoustic fish communities of Moorea's photic reef appeared to be closely related to the ones at Mangareva, suggesting that differences are rather explained by the type of island than the archipelago. Moreover, the acoustic composition of the photic reef of Bora Bora shared more similarities with the one of atolls like Raroia and Tikehau. Bora Bora's peculiarity could be linked to the fact that this island has an intermediate status between an atoll and a high island. Indeed, this island is sometimes called an almost-atoll due to its large lagoon [112].

This study suggests that acoustic fish community composition and diversity reflects habitat characteristics and can be indicative of subtle differences in vertical gradients, buffer zones and benthic cover. The occurrence of abundant and specific sound types of the MCEs makes acoustic monitoring of fish assemblages a promising tool to follow temporal changes in MCEs.

5. Author contributions

Conceptualization, X.R.; methodology, X.R. and L.D.I.; software, C.G.; validation, X.R., L.D.I. and É.P.; formal analysis, X.R.; investigation, X.R. and U.T.P.; resources, G.P.R., F.B., L.H., and H.R.; data curation, X.R.; writing—original draft preparation, X.R..; writing—review and editing, X.R., É.P., L.D.I., F.B., and G.P.R.; visualization, X.R.; supervision, X.R. and L.D.I.; project administration, X.R.; funding acquisition, L.H. and D.L.. All authors have read and agreed to the published version of the manuscript.

Chapter 7. Depth shapes diel cycles and realized acoustic niches of fish sounds

Xavier Raick[1], Julien Campisi[1], Under The Pole Consortium[2], Frédéric Bertucci[3], David Lecchini[4,5], Lucia Di Iorio[6], and Eric Parmentier[1]

[1] Laboratory of Functional and Evolutionary Morphology, Freshwater and Oceanic Science Unit of Research, B6c allée du 6 août, University of Liège, 4000 Liège, Belgium

[2] Under the Pole Expeditions, 1 Rue des Senneurs, Concarneau, France. Members: G. Bardout, J. Fauchet, A. Ferucci, F. Gazzola, G. Lagarrigue, J. Leblond, E. Marivint, A. Mittau, N. Mollon, N. Paulme, E. Périé-Bardout, R. Pete, S. Pujolle and G. Siu.

[3] UMR MARBEC, IRD-CNRS-IFREMER-INRAE-University of Montpellier, Sète, France

[4] PSL University, EPHE-UPVD-CNRS, USR 3278 CRIOBE, BP 1013 98729 Papetoai, Moorea, French Polynesia

[5] Laboratoire d'Excellence 'CORAIL', 58 avenue Paul Alduy, 66860 Perpignan, France

[6] CEFREM, CNRS/UMR 1510, University of Perpignan Via Domitia, Perpignan, France

This chapter has been the subject of a Master's 2 thesis and is currently in the final stages of preparation for submission to a scientific journal. A similar study, undertaken as part of a Master's 1 internship, has already been published in 2023 in *Scientia Marina*. It was not included in the final document of this thesis.

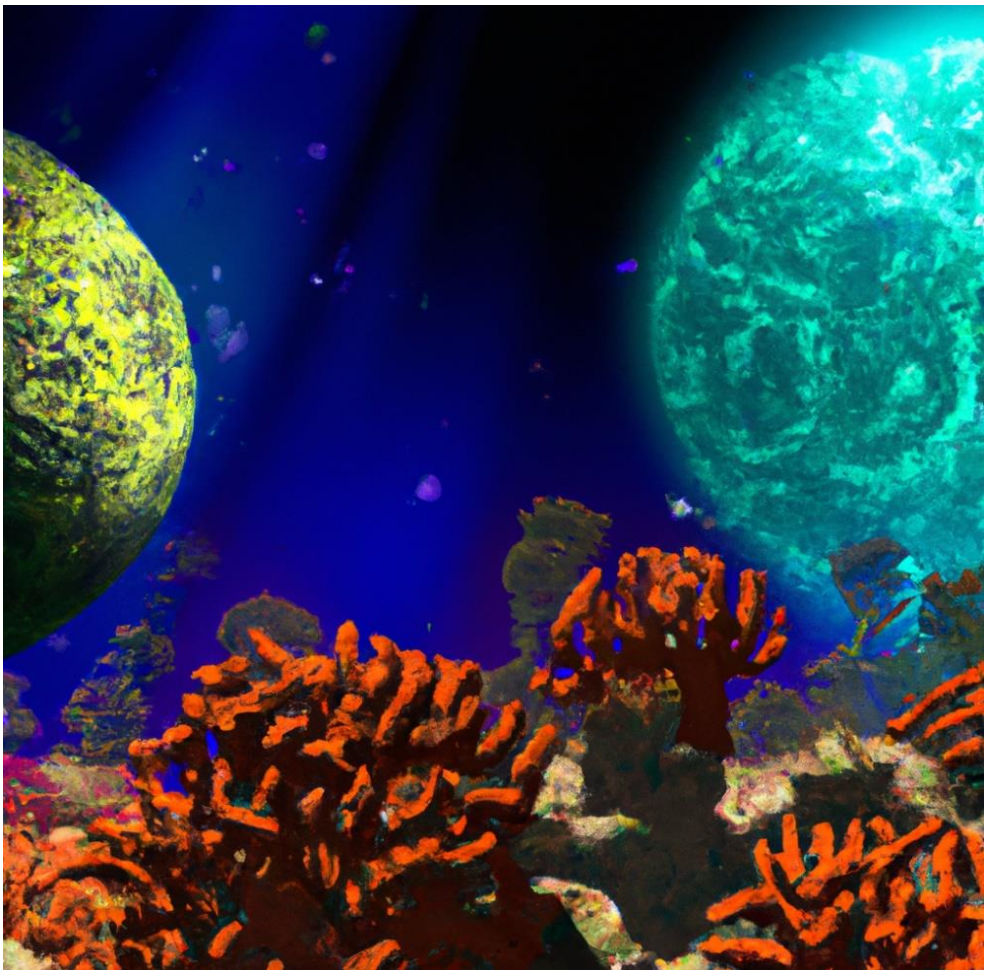

MAJOR RESULTS

Diel cycle (1/2)

- ✓ The acoustic community is divided into a diurnal and a nocturnal community.
- ✓ The nocturnal community is subdivided into several sub-communities.
- ✓ The diurnal community was dominated by PS while the first nocturnal community was dominated by AS. FM sounds reached their maximum abundance around the midpoint of the night.

Diel cycle (2/2)

- ✓ AS4 played a major role in the global abundance in the first nocturnal community,
- ✓ When depth increases, there was more FM detected during the night and less during the day, while it was not true for PS.
- ✓ When the number of sound types is examined during specific periods (e.g., during the night) less PS types are present at greater depth.

Acoustic niches (1/2)

- ✓ All sound types had different acoustic niches.
- ✓ AS and FM sound types mainly differentiated along the temporal and the frequency axes, while PS sound types primarily differentiated based on their pulse period.
- ✓ The predominance of FM sounds types at depth and the larger niches for FM sound types at depth could indicate an additional difference for FM sound types in addition to a distinction on the three other axes.

Acoustic niches (2/2)

- ✓ Contrary to FM sound types, the niche widths for frequency resources decreased with depth for all the studied AS sound types: they exhibit frequency-based specialization at depth.
- ✓ The overall niche widths were similar for most PS sound types, but some particular PS had temporal niche width narrower with depth.
- ✓ When exploring the community level, the temporal niche width is narrower with depth, while the frequency niche width is wider with depth. At greater depths, acoustic activity becomes more focused during specific time periods, and there is a broader exploitation of the frequency spectrum.

Key question for the objective of the thesis

How depth affects the diel variations of the individually identifiable fish sounds?

Abstract

The sound spectrum is a limited resource shared to minimize acoustic competition. However, how abiotic factors shape this partitioning is poorly known. This research focuses on the ecological role of depth on the acoustic behavior of fish. The study focused on lower and upper mesophotic coral reefs from the Tuamotu Archipelago, pursuing three key objectives: investigating how depth shapes the diel cycle of fish sounds with GAM models, studying the difference in their frequency distribution in relation to time, depth, and acoustic features; and analyzing their acoustic niches. The study reveals that depth exerts a significant influence on the community dynamics of fish sounds. As depth increases, the nocturnal character of frequency modulated sounds is more pronounced while the contrary is observed for pulse series. Depth also affects realized acoustic niches. At the community level, at greater depths acoustic activity becomes more focused during specific time periods, particularly during the night, and there is a broader exploitation of the frequency spectrum. At the opposite, for certain sound types, acoustic niches become narrower for frequency resources at deeper depths. Overall, these findings emphasize the intricate interplay between depth, and fish acoustic communities.

1. Introduction

Based on their depth, tropical coral reefs can be divided into two parts: a shallow part called the euphotic reef (ranging from the surface to ~30-40 m deep), from which extends a deeper part known as mesophotic coral ecosystems (MCEs, ~30-40 m to over 170 m deep) [105,110]. MCEs represent approximately 80% of global tropical coral reef ecosystems [324]. Within MCEs, the presence of variations in ichthyological diversity based on depth has been highlighted [442]. MCEs consist of an 'upper' zone (from 30 to 60 meters) where ichthyological communities are similar to those of shallow reefs [105,420], and a 'lower' zone (from 60 to over 150 meters) that possesses its own fish assemblages [105,421]. The boundary between the upper and lower zones of MCEs is an interval between 60 and 90 meters deep, within which a shift in faunal community is observable [107,108,421]. Some authors even propose subdividing MCEs into three zones (upper, middle, and lower), but the definitions of these zones vary across studies [443–445]. The study of MCEs remains highly challenging due to numerous logistical, human, and financial constraints [108,446]. As a result, our knowledge about these ecosystems and their functioning has significant gaps in various areas, particularly in ecology [324]. Today, advancements in underwater technology enable the study of MCEs through less invasive methods [447]. Approaches that do not involve the visual field, such as acoustic methods, have been developed to study the ichthyological communities of these ecosystems.

Passive Acoustic Monitoring (PAM) is a technique used to non-intrusively and with high temporal resolution collect various types of sounds (e.g., fish sounds) to infer ecological data [84,448]. PAM can be used to study a specific species [423,449,450], a group of species [281,451], or the entire vocal fish community living in a particular location [141,326,397,437] (Chapters 3 and 6). The production of various types of sounds might lead to the assumption that the acoustic landscape in an environment inhabited by numerous populations of sound-producing fish would be so noisy that species would be unable to hear each other properly and could risk misidentification [437]. However, fish can adopt different strategies to cope with this. First, the 'Lombard effect' is a strategy in which fish increase the intensity of their emitted sounds [452–454] to enhance reception by the receiver and avoid masking effects caused by background noise. A second strategy involves producing sounds at different times. Although fish acoustic activity is often higher at specific times such as dusk and night [451,455–457], vocalizations are generally not produced at the same time within the same site [141,437]. Indeed, some species vocalize more during the day [93,246], others vocalize both day and night [141,458], and some vocalize primarily at night [397,459]. Within this distribution, there can

be further subdivisions for each part of the day, with some species producing sounds only for a few hours [141,460]. This partitioning within a community aims to prevent misidentification between different species in challenging conditions or a cacophony that masks the emitted signals [437,461]. This is the foundation of the acoustic niche hypothesis (ANH) [462].

The ‘acoustic niche’ can be defined as ‘a multidimensional abstraction encompassing spectral and temporal features of a sound type, as well as its diel pattern of occurrence’ while the ‘realized acoustic niche' can be defined as ‘the range of acoustic resources exploited by a specific sound type along three axes: diel timing of calling activity, call spectral features and call temporal features’ [460] observed at a specific moment and location. The realized acoustic niche is always a subset of the acoustic niche. According to the ANH, the sound spectrum is a limited resource that species or communities share to minimize acoustic competition [462]. It has been demonstrated in birds [463–465], frogs [466–468], and arthropods [469,470]. Concerning marine ichthyofauna, it is known that fish do not occupy the same temporal periods [141,437] and can be partitioned into nocturnal and diurnal acoustic communities [437]. Within the nocturnal acoustic community, which is more diverse than the diurnal one [141,437], the sounds show less overlap in certain acoustic characteristics (e.g., dominant frequency and pulse period) [437]. In marine temperate ecosystems, the allocation of acoustic resources (both temporal and frequency ranges) increases when the acoustic richness increase [460]. Unfortunately, the number of studies on how an entire ichthyological community occupies the acoustic landscape in coral reefs remains relatively low [141,397,471], and our knowledge on this topic in MCEs is extremely limited [472] (Chapter 6).

Although there are still few studies on the ichthyological biophony of MCEs, several recent studies have focused on the biophony of MCEs in French Polynesia (Chapter 6). The composition of acoustic communities varies with depth (Chapter 6). The relative proportions of acoustic categories vary with depth, and it has been observed that pulse series (PS) sounds are dominant in the photic zone, while frequency-modulated (FM) sounds are more abundant in the lower mesophotic zone (Chapter 6). Regarding the temporal distribution of fish sounds in MCEs, a recent preliminary study focusing on the two most abundant FM sounds in the MCEs of French Polynesia [472] (Chapter 6) showed a greater presence of these sounds during the night [472]. However, how the fish community share the soundscape within MCEs has never been studied. The objective of this research is to study the depth-related difference in the soundscape sharing among fish in MCEs from three islands in the Tuamotu archipelago (French Polynesia). Specifically, two lines of investigation were pursued. (*1*) Assessing how depth

shapes the diel cycle of fish sounds in the upper (60 m) and lower (120 m) parts of the MCEs. (*2*) Analyzing the realized acoustic niche of the most abundant sound types at both depths.

2. Materials and methods

2.1. Sampling

The acoustic data collection was conducted between March and November 2018 at three atolls in the Tuamotu Archipelago (French Polynesia): Rangiroa, Raroia, and Tikehau. During fielwork, sunrise was between 5:50 and 6:09 AM and sunset was between 5:21 and 5:43 PM. Sampling was carried out as part of the Under The Pole III expedition (https://underthepole.org) by divers using closed-circuit rebreathers. Recordings were simultaneously conducted at depths of 60 m and 120 m along the outer slope as detailed in Raick et al. (2023). At each depth, a SNAP autonomous acoustic recorder (Loggerhead Instruments; Sarasota, FL, USA) connected to an HTI96 hydrophone (sensitivity ranging from −170.5 to −169 dB re 1 V for an acoustic pressure of 1 µPa, flat frequency response from 2 Hz to 30 kHz) was deployed. The recorders were vertically mounted on a 60 cm tripod, weighted with 4 kg, and placed on the seafloor. All recorders were programmed to capture 1-minute recordings every 10 minutes over a 62-hour period, with a sampling frequency of 44.1 kHz (16-bit resolution) and a gain of +2.05 dB.

2.2. Data analysis

The audio files were downsampled to 4 kHz as the range below 2 kHz corresponds to the frequency range dominated by fish sounds (Chapters 3, 5, and 6). The audio files (totaling 37.2 hours) were visually and audibly inspected using the acoustic analysis software Raven Pro 1.5. (Cornell Lab of Ornithology; Ithaca, NY, USA). The audio files included three replicates between 5 PM and 7 AM and two replicates between 7 AM and 5 PM.

Fish sounds were classified into categories referred to 'sound types' (Figure 45 and Figure 51) as using a dichotomous key adapted from a pre-existing key from Chapter 6 (Figure 46, Figure SP7 - 1, KeySP7 - 1). A sound type encompasses sounds with similar acoustic characteristics, such as dominant frequency or pulse period, and can either be produced by a single species [473] or can contain sounds from multiple related species [281,424,474]. In total, 52,867 fish sounds were detected in MCEs of the three studied atolls. Among those described in the identification key, only sound types with at least ten occurrences were used for analyses. Consequently, 52,824 sounds classified into 69 different fish sound types were used, representing 99.92% of all identified sounds. For the interpretation, sounds types were grouped into three broad sound categories referred to as ‘acoustic categories’ (Figure SP7 - 1): pulse

series (PS), frequency modulations (FM), and arched sounds (AS, grouping non-FM tonal calls and ultra-fast pulse series with pulses too closely spaced to be perceived as PS) like described in Chapter 6. FM can be subdivided into of upsweeping sounds (FM_{US}), downsweeping sounds (FM_{DS}), and complex sounds (i.e., sounds with both upsweeping and downsweeping parts, FM_{CS}).

All the sounds were used to examine the general pattern of the diel cycle. In contrast, for the diel cycle per sound type and the niches analyses, we specifically focused on sounds with a minimum of 1,000 observations. Out of all the sounds detected in the MCEs of the three atolls, 13 met this criterion. These 13 types comprised a total of 42,578 sounds, representing ca. 80% of the total sounds detected. Among the 13 types, there were three AS (AS4, AS5, and AS1), seven PS (PS3, PS17, PS16, PS18, FPT1, FPT2, and FPT4), and three FM sound types: one FM_{CS} (CS1), one FM_{DS} (DS2), and one FM_{US} (US1). Among these 13 sound types, 12 had already been described (Chapter 6). A detailed description of ten sounds with a good signal-to-noise ratio allowing sounds to be characterized was realized for each of the 13 sound types. The pulse period was measured on oscillograms with Avisoft SAS Lab Pro (Avisoft Bioacoustics; Glienicke/Nordbahn, Germany). This feature was needed for the realized acoustic niche analysis, and it was not automatically measured by Raven. The thirteenth sound, named PS18, is an undescribed sound type composed of two distinct parts separated by a time interval. The first part consists of a single pulse with multiple peaks, while the second part is a series of regular pulses (i.e., constant pulse period) with a single peak. For each of the 13 sound types, the mean and standard deviation of the aforementioned acoustic characteristics were calculated.

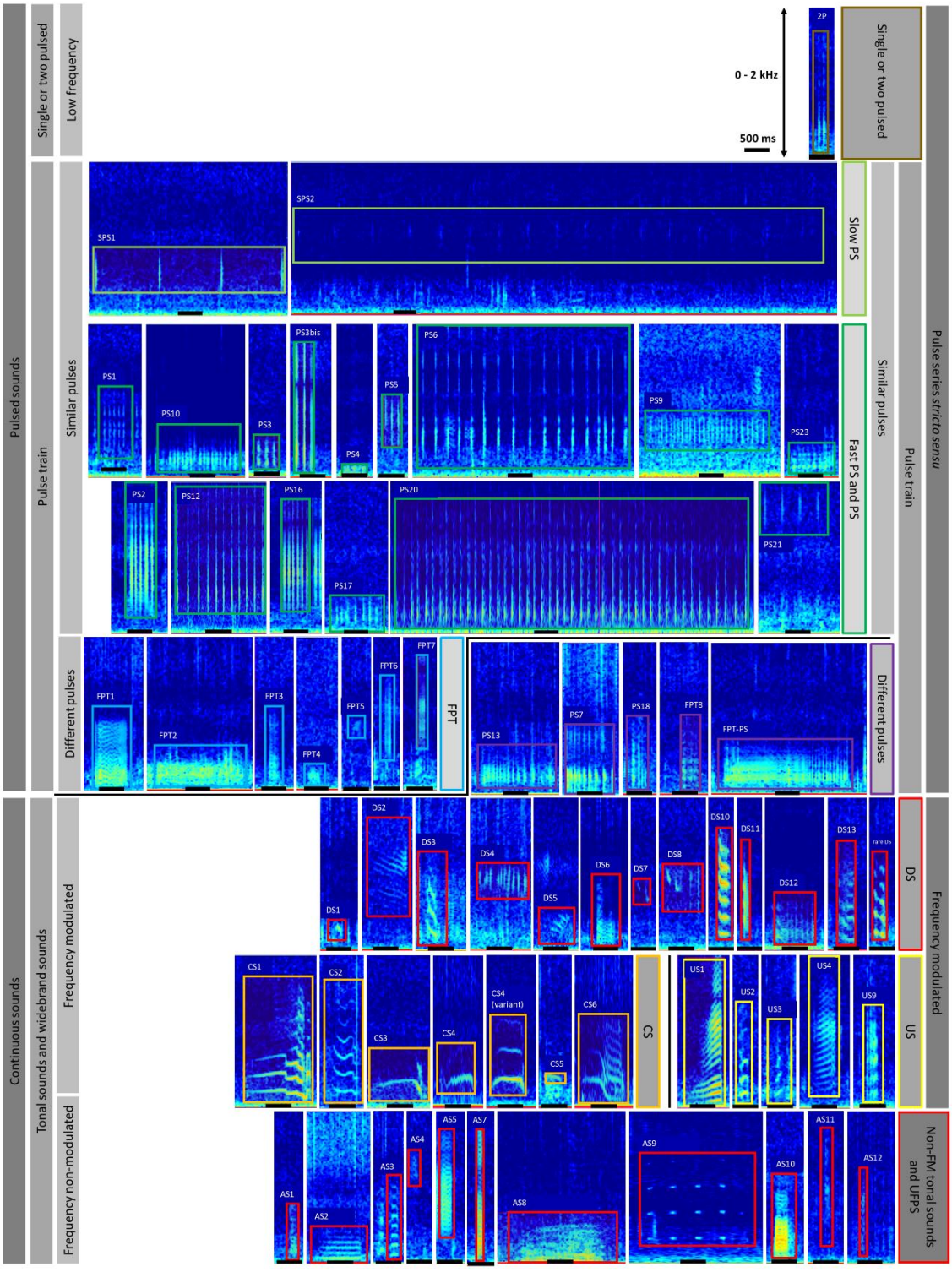

Figure 51 Diversity of fish sounds in Polynesian mesophotic reefs. The classification on the right of the figure is adapted from Chapter 6 and 7, while the classification from Puebla-Aparicio et al. (2024) [475] is presented on the left side of the figure. Sampling frequency: 4 kHz. FFT = 256. PS = pulse series, FPT = fast pulse train. DS = downsweeping sound. US = upsweeping sound. CS = complex sound. UFPS = ultra-fast pulse series. The structure of the figure is inspired by [475] (Fig. 3). 'kwa-like' sounds are a sub-category of 'arched sounds' also named 'non-FM tonal sounds and UFPS'.

2.3.Statistical analyses

To address the various objectives of this study, the analyses were divided into the study of the depth effect on (1) the diel cycle, and (2) realized acoustic niches. All statistical analyses were conducted using R software version 4.2.1 (R Core Team, 2022), and a significance level of $\alpha = 0.05$ was used.

2.3.1. Diel cycle

The first axis of the study aimed to examine the temporal dimension of the acoustic activity for each sound type (Figure 51) in order to investigate a potential depth relationship in diel cycles.

Raw abundance data of each sound type were converted into average abundance per minute. For each studied depth, cumulative graph of average abundance over time was generated for sound types. To enhance visualization of rarer sounds, in addition to the graph of original values on a linear scale, graphs of relative values and the logarithm of abundance were employed.

Generalized Additive Models (GAMs) were used to assess the presence of trends. GAMs are commonly used to study diel cycles [476,477]. The *gam* function from the *mcgv* package was used to create a model for the 13 aforementioned sound types. For each model, we only used data with a minimum of 30 sounds per depth per island. If this condition was not met, the depth/island with less than 30 sounds was not used in the model. The model predicted the average abundance of sounds based on the spline of time by depth, the depth itself, and the island. Poisson distributions were initially used for all the models [478]. Subsequently, the dispersion of residuals was computed using the model's residuals, the number of observations, and the number of predictors in the model. When the dispersion of residuals was below 1.5, the Poisson model was retained. When it was not the case, the same model was employed, but with a negative binomial distribution. Thus, all final models exhibited appropriate residual dispersion (minimum value obtained: 0.59, maximum value obtained: 1.23). The relationship between predictors and the dependent variable (i.e., the abundance of each sound) is described in part through the effective degrees of freedom (edf), which estimate the 'complexity' of each smooth term (spline). An edf value close to 1 implies a linear relationship, while a higher value indicates a non-linear relationship (complex and undulating curve). Finally, the model-predicted values along with a 95% confidence interval were exponentiated (due to the log link used in the model) and represented alongside the original abundance data.

2.3.2. Realized acoustic niches

The acoustic resources used to define the realized acoustic niche of each sound included: (1) the period of acoustic activity (time), (2) the dominant frequency, and (3) the pulse period [460]. The realized acoustic niche was studied for each of the two depths, focusing on the 13 most abundant sound types. Because only two replicates (i.e., two days of data) were available for each island/depth from 7 AM to 5 PM, only two replicates from 5 PM to 7 AM were used. Each hour of the day represented a temporal resource. The number of frequency dominant resource classes was obtained by dividing the range of frequencies (i.e., the difference between the highest and lowest frequency data) by the frequency range of each class (100 Hz classes ranging from 15 to 1815 Hz). The number of resources for pulse period was obtained by dividing the range of pulse periods (i.e., the temporal difference between maximum and minimum periods) by the temporal range of each class (logarithmic scale 0.1 ms classes ranging from 0.1 to 2.9 ms). The number of acoustic resource classes used varied according to the three axes: 24 for the temporal axis (axis I), 18 for the frequency axis (axis II), and 28 classes for the pulse period axis (axis III). The sizes of each resource class (1 h, 100 Hz, and 0.1 ms respectively for axes I, II, and III) were identical to those of Bolgan et al. (2022).

For the third axis, the pulse period data for each regular sound type (all types except PS18) were estimated by dividing the total sound duration (automatically measured in Raven) by the average number of pulses (manually measured in Avisoft). Because of its irregularity, only the regular part of the PS18 was considered for the measurement.

The data for each axis were organized into a resource matrix, where each row represented a sound type and each column represented a resource class. For each sound type and resource axis, the number of sounds belonging to each resource class was calculated and displayed with a relative percentage color scale. Furthermore, the acoustic community space (i.e., the range of acoustic resources exploited by the entire acoustic community) was calculated by summing all sound types present in each resource class across the three axes [460]. Finally, the realized acoustic niche breadth (NB), measuring the level of resource class occupation, was calculated using the inverse of the Simpson diversity index (using the *diversity* function from the *vegan* package) and standardized (NB*) as follows: $NB^* = (NB - 1) / (r - 1)$, where r is the number of resource classes. When NB* is zero, the sound type is considered a specialist meaning it only exploits one resource class, while when NB* is 1, the sound type exploits all resource classes [467,479]. The standardized realized acoustic niche width for each sound type was calculated separately for each niche axis (NB_{temp}* = standardized realized acoustic niche width for the

temporal axis; NB_{freq}* = standardized realized acoustic niche width for the frequency axis; NB_{pp}* = standardized realized acoustic niche width for the pulse period axis), as well as for the overall realized acoustic niche (NB_{tot}*).

3. Results

3.1. Diel cycle

The GAM models performed on the most abundant sound types demonstrated a significant influence of the time of day on the abundance of all studied sound types at both depths (all $P < 0.001$; Figure 52 and Table SP7 - 1). 11 out of 13 sound types can be characterized as nocturnal. Among them, some such as the AS4, are part of the first nocturnal community, while others such as the CS1 and AS5 are part of the second nocturnal acoustic community (Figure 53 and Figure SP7 - 1). It is observed that more PS types are present at 60 m than at 120 m during this period (Figure 53 and Figure SP7 - 1). Other sound types, such as PS3 and PS17 have one abundance peak before 7:40 PM and another during the second half of the night (Figure 52 and Table SP7 - 2), placing them in both the first and second nocturnal acoustic communities. At 120 m, the two most abundant sound types during the daytime are PS17 and PS3 (Figure 53) while the three most abundant PS at 60m are PS18, PS17, and FPT4 (Figure SP7 - 2). It shows that some sounds such as the PS18 are associated with one depth (Figure 52 and Table SP7 - 2). Additionally, Some PS exhibits abundance peaks at different times depending on the depth (Figure 52 and Table SP7 - 2). The PS16 is part of the first community at 60 m and the second community at 120 m. The FPT2 sound type is a nocturnal type at 120 m, in contrast to its more diurnal behavior observed at 60 m (Figure 52 and Table SP7 - 2).

When examining all the sound types (Figure 51) together, we discern a general tendency with average abundance peaks generally after sunset and/or before sunrise. Regardless of the depth, the abundance gradually increased during sunset (Figure 53).

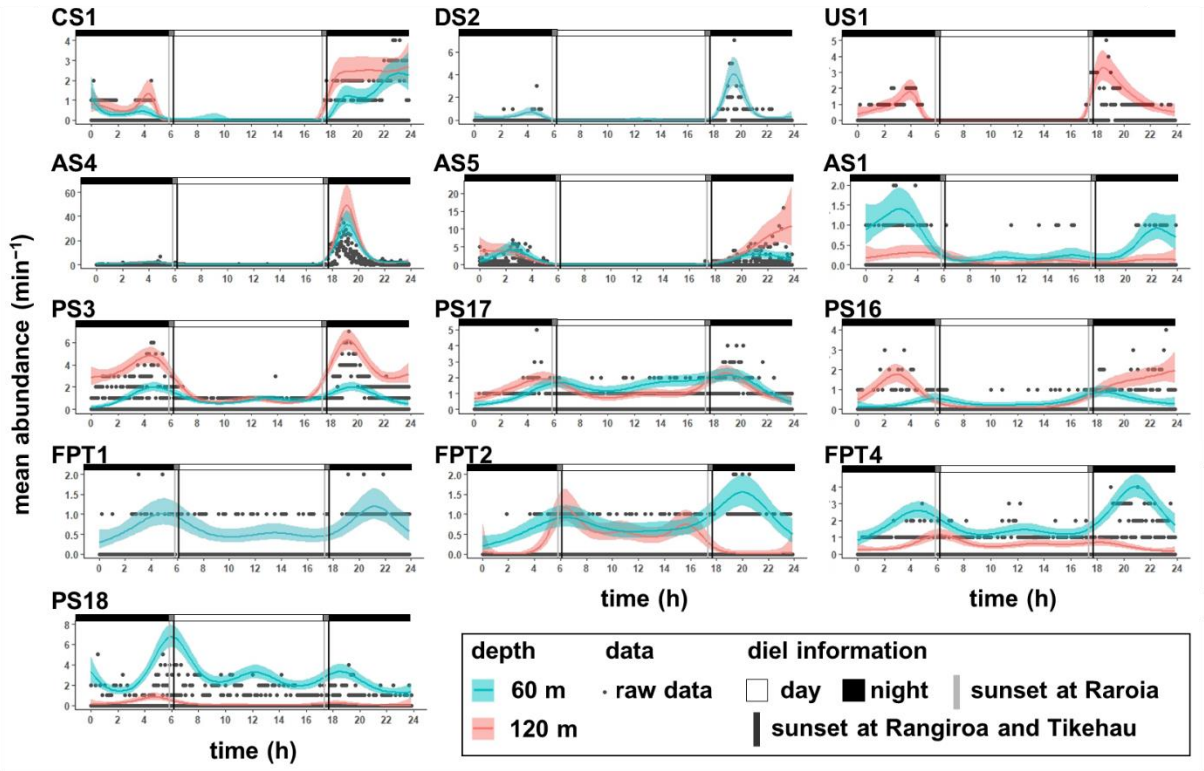

Figure 52 Temporal variations in sound type abundance. Predicted values from GAM models depicted by curves, with blue curves representing 60 m depth and red curves representing 120 m depth. Each curve is accompanied by a band illustrating the corresponding 95% confidence interval. Dots signify raw data points. Vertical grey lines denote sunrise and sunset at Raroia (5:50 AM and 5:21 PM), while black lines indicate corresponding hours at Tikehau and Rangiroa (6:09 AM and 5:43 PM).

During this period, a shift in the acoustic community was observed: from a 'diurnal acoustic community' dominated by PS sound types to a 'first nocturnal acoustic community' dominated by the AS4 (+27% AS increase at 120 m, +23% AS increase at 60 m between 5:40 and 5:50 PM). Subsequently, this acoustic activity decreased, marking the transition to the 'second nocturnal community' starting later deeper and characterized by an increase in FM_{CS} sounds such as CS1. During sunrise, there was a re-increase in the average abundance of PS sound types to a level almost as high as the first peak. The second abundance peak was reached an hour earlier at 120 m and was equal to the first one. Following sunrise, the abundance of PS sounds types gradually returned to daytime values. The abundance and relative proportion of PS sounds during the daytime decreased with depth. Inversely, the predominance of FM sounds during nighttime/sunset was more pronounced at greater depth.

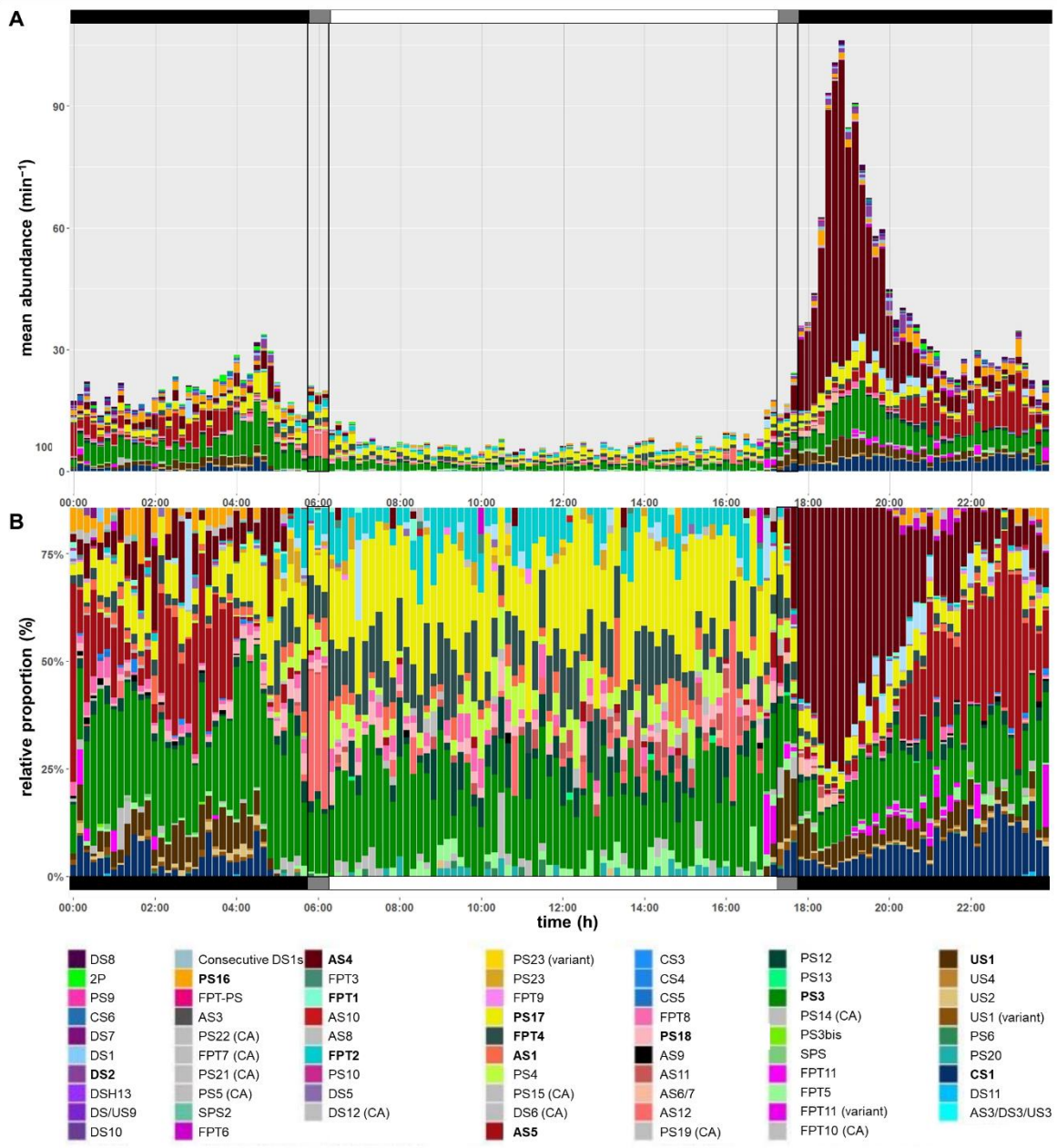

Figure 53 Cumulative graph of mean abundance over time for all sound types at 120 m depth: absolute values (A) and relative proportion (B). Less abundant sound types lacking a clear diel cycle are colored in grey for ease of interpretation. The legend includes the annotation 'CA' (Cycle Absent) for such sounds. The 13 most abundant sound types, utilized in the models, are highlighted in bold.

3.2. Realized acoustic niches

3.2.1. Composition of the realized acoustic niches

The 13 most abundant sound types differentiated along (at least) one of the three axes of their realized acoustic niche. AS sound types differentiated well along both the temporal axis (Axis I) and the frequency axis (Axis II) but exhibited comparable pulse periods (Figure 54). This was true for both 60 m and 120 m depths (Figure 54). Among PS at 60 m, the PS18, FPT1, and FPT4 sound types exhibited different activity periods (Axis I) compared to other PS types, while at 120 m, only the FPT2 and FPT4 types differed in their temporal axis (Figure 54).

Unlike AS, PS exhibited similar frequency spectrum exploitations at both depths, except for the PS16. At 120 m, PS16 had higher frequencies more prominently (Figure 54). PS primarily differentiated based on their pulse period (Axis III), regardless of depth (Figure 54). Concerning FM, the CS1 sound type stood temporally apart from the other two FM sound types which had more similar acoustic activity and pulse periods (Axis I and Axis III, respectively). However, this temporal resource competition was compensated for at the frequency level. Specifically, the DS2 sound type distinguished itself from the other two FM sound types by a different frequency spectrum exploitation.

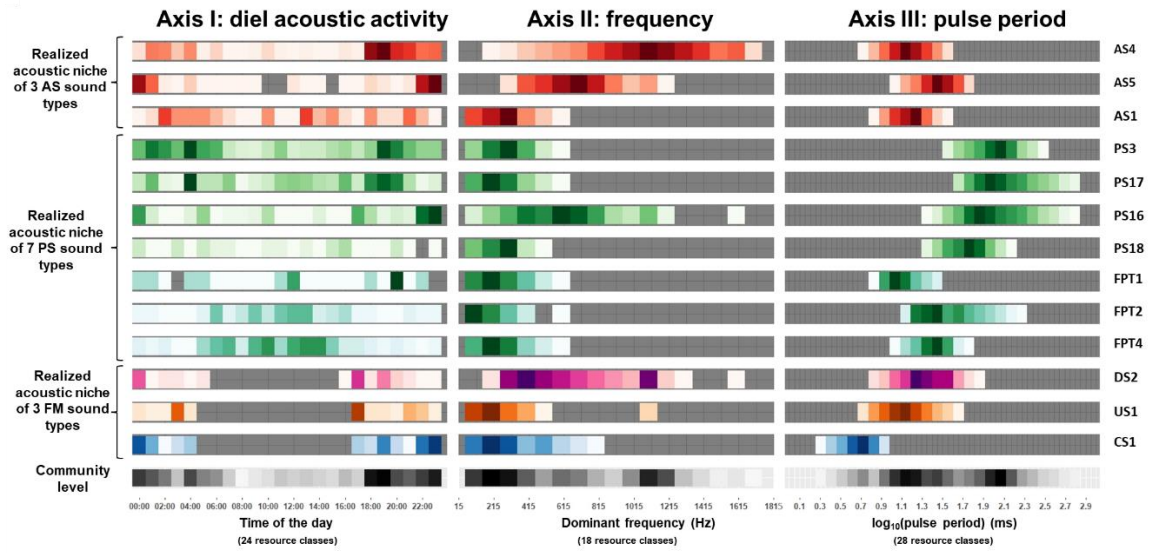

Figure 54 Realized acoustic niche analysis of the 13 most abundant sound types and the entire community level at 120 m depth. Each vertical panel represents an axis of the realized acoustic niche (axis I: diel, 24 resource classes; axis II: frequency, 18 resource classes; axis III: pulse period, 18 resource classes). Data for each axis were organized in a resource matrix, where each row represented a sound type and each column a resource class. For each sound type and resource axis, the number of sounds associated with each resource class was calculated and is presented with a color scale as a relative percentage. The range of acoustic resources utilized by the entire acoustic community was calculated from the sum of all sounds present in each resource class for each of the three axes.

3.2.2. Comparison of the width of the realized acoustic niches

The realized acoustic niche breadth, and therefore the 'specialization' of the sound types, varied depending on the sound types and the depth. The 13 sound types occupy distinct realized acoustic niches. The overall realized acoustic niche width of the AS4 type was narrower than that of the other two AS sound types (AS5 and AS1), which had more similar overall realized acoustic niche widths (Table SP7 - 3). This was due to the fact that the realized temporal niche of the AS4 sound type was narrower than that of the other two sound types at both depths (Table SP7 - 3). The same pattern was observed at 120 m (Figure 54, Table SP7 - 3). However, comparing the two depths revealed that the realized niche widths for frequency resources

decreased with depth for all AS sound types (Table SP7 - 3). AS occupy fewer resource classes and exhibit frequency-based specialization at depth.

The overall realized acoustic niche widths were similar for most PS types at both depths (Table SP7 - 3). However, two out of the seven PS sound types exhibited different realized acoustic niche widths along specific axes at certain depths. A distinctive PS type is PS3. Its overall realized acoustic niche width at 120 m was narrower than the average width of all PS types (NB_{tot}* = 0.22 vs 0.33 ± 0.06). This trend was less evident at 60 m (NB_{tot}* = 0.30 vs 0.34 ± 0.036). Furthermore, its realized acoustic niche width along the temporal axis at 120 m was narrower compared to 60 m. This suggests that the PS3 type is more 'specialized' and exhibits more focused acoustic activity at 120 m compared to 60 m, where its activity is more spread out over time (Figure 54).

Finally, CS1, US1, and DS2 exhibited similar overall realized acoustic niche widths among themselves at each depth. However, the values differed between the two depths. At 120 m, the realized temporal niche width values were all higher than at 60 m ($NB_{temp}*_{60m}$ = 0.24 ± 0.10, $NB_{temp}*_{120m}$ = 0.36 ± 0.021). This is related to the fact that acoustic activity of FM sounds was more prominent at 120 m than at 60 m.

Globally, FM sounds (CS1, US1, and DS2) had realized temporal niche widths that increased with depth (Figure 55). It could be interpreted as the temporal window of vocalization being broader due to the presence of individuals vocalizing outside the mean vocalizing time. On the other hand, most PS (FPT2, FPT1, PS18, PS16, PS17, and PS3) had their realized temporal niche widths decreasing with depth. The realized temporal niche widths of AS (AS1, AS5, and AS4) decreased slightly. Concerning the frequency axis, the contrary was observed: the realized niche widths of FM and AS, whose abundance increased with depth, decreased with depth and the ones of PS, whose abundance decreased with depth increased. This suggests that the more individuals are vocalizing, the more there is need to restrict the frequency range to avoid overlap. With depth, the specialization of FM and AS sounds appears accentuated on the frequency axis, while the specialization of PS sounds is more pronounced along the diel axis.

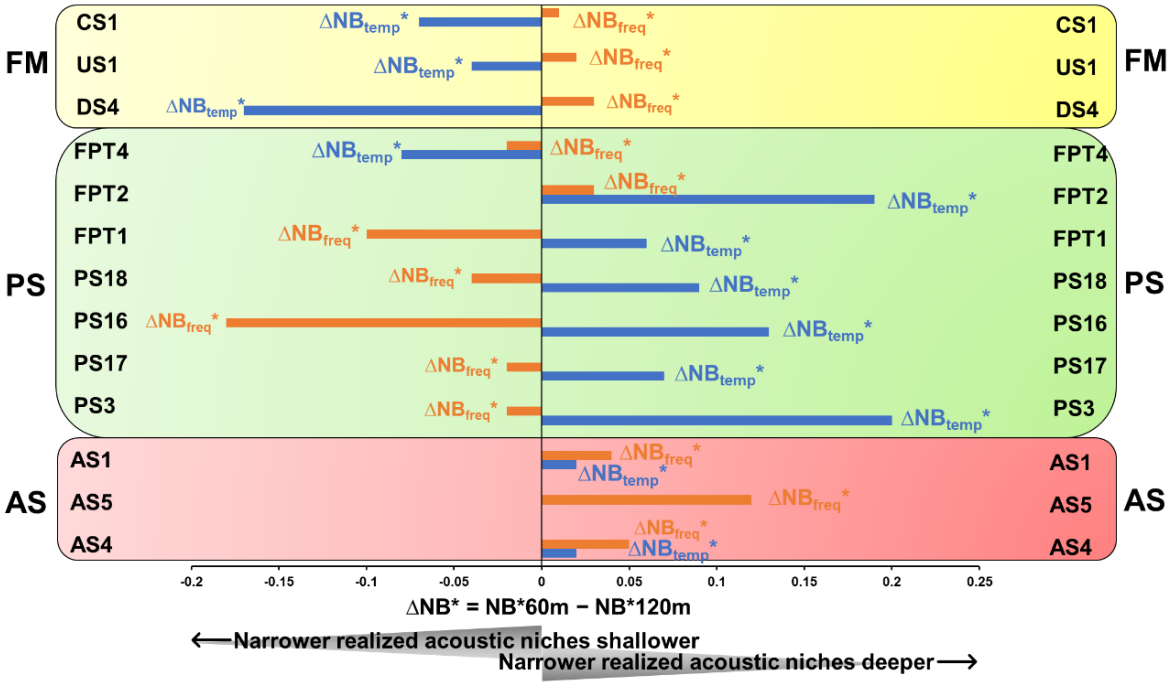

Figure 55 Illustration of the difference in the widths of the realized acoustic niches, diversity, and abundance. Difference in the width of the diel realized acoustic niche (ΔNB^*_{temp}, in blue) and the frequency realized acoustic niche (ΔNB^*_{freq}, in orange) for the 13 most abundant sound types between 60 and 120 m.

When examining the realized acoustic niches at the community level, it becomes evident that there is a difference in terms of both temporal and frequency axes between the two depths. Specifically, the realized temporal niche width at 120 m is narrower than at 60 m ($NB_{temp}*_{120m}$ = 0.32 vs $NB_{temp}*_{60m}$ = 0.40), while the realized frequency niche width at 120 m is wider than at 60 m ($NB_{freq}*_{120m}$ = 0.43 vs $NB_{temp}*_{60m}$ = 0.31). This indicates that at greater depths, acoustic activity becomes more focused during specific time periods, particularly during the night, and there is a broader exploitation of the frequency spectrum, particularly at higher frequencies.

4. Discussion

4.1. Diel cycle

The analysis of the selected sound types revealed diverse trends in their distribution. This includes the identification of sounds that are predominantly made during the day [93] or at night [472,480]. Notably, the periods of sunset [151,481–485] and sunrise [151,486] emerge as critical times periods when specific sounds are produced, highlighting the importance of these transitional times in the daily rhythm of sound emission. Within these sounds, the most abundant sound in MCEs, named AS4 or 'kwa-like' is particularly interesting since it shares acoustic characteristics with the 'kwa' sound type recorded in the Mediterranean Sea, such as pseudo-harmonics, pulse periods, and a very similar nychthemeral cycle (Chapter 6). The latter reference illustrates the production of AS-type sounds called 'kwa' at a frequency of 747 Hz,

which occupies the acoustic scene for 2 h, 2 h after sunset. This sound production is remarkably similar to the one of AS4. The AS4 dominates the acoustic environment for 50 to 100 min 80 to 90 min after sunset. The ‘kwa’ in temperate shallow-water of the Mediterranean Sea is attributed to scorpionfish of the genus *Scorpaena* (Scorpaenidae) [433]. Consequently, the AS4 sound detected in French Polynesian MCEs could plausibly be produced by one or more species of scorpionfish from the Scorpaenidae family that inhabit this region. In French Polynesia, the frequency range near the dominant frequency of ‘kwa-like’ sounds (around 1 kHz) is not occupied by center frequencies of sounds from invertebrates (Chapter 3), unlike in other reefs around the world [65]. As a result, this sound can be heard without being masked by invertebrate sounds.

The conducted GAMs provided a deeper insight into the temporal partitioning of the entire acoustic community of MCEs. The temporal segregation serves as a primary means for fish to communicate, avoiding interference between signals and minimizing competition for temporal resources [462]. The division of the acoustic community into a diurnal and a nocturnal community aligns with observations made in other marine environments [141,437]. However, beyond this general result, our study demonstrates that the nocturnal community itself can further subdivide into two sub-communities, and the (sub-)acoustic categories associated with each community are not identical.

FM sounds reached their maximum abundance around the midpoint of the night. The predominance of FM sounds during the night could be related to the need to produce a sufficiently distinctive sound. There are several examples of fish producing FM during reproductive-related behaviors [89,487]. The need for stereotypy becomes more pronounced at night, a period conducive to reproduction due to the reduced light intensity, aiding in the avoiding and minimization of predation risks [488]. This contrasts with daytime conditions [151], where the absence of light means sounds cannot be augmented by visual stimuli, as they can be during daylight hours [437]. The absence of light at night requires sounds to have more distinctive characteristics for differentiation. Auditory signals must be clear enough to facilitate effective communication in nocturnal conditions. Thus, the more stereotyped a sound is, the more it minimizes the risk of not being recognized by conspecifics. Incorporating frequency modulations could serve as a method to enhance its stereotypical nature. Unlike amplitude modulations, the propagation of frequency modulations seems to be less affected by noise. This could be because in an FM signal, information is transmitted by varying the frequency, not the amplitude, and noise primarily affects amplitude.

The obtained results not only highlighted the presence of nychthemeral cycles, but also revealed a depth-related difference. When depth increases, there was more FM detected during the night and less during the day, while it was not true for PS. In addition, when the number of sound types is examined during specific periods (e.g., during the night) less PS types are present at greater depth. This last depth difference is similar to the depth-related effect on the abundance of PS and FM highlighted by a previous study during sunset (Chapter 6).

Sounds more prevalent in deeper waters exhibit more frequency modulations (e.g., CS1). This prevalence is true for the night period compared to the daytime when considering each depth separately. The transition from day to night and from shallow to deep environments shares the common factor of decreasing light intensity. Thus, a single factor (light intensity) acting in two different ways has a similar effect on the acoustic community. We believe that the primary reason for this could be the difference in the role of sounds between night and day, which could also explain the depth-related difference.

4.2. Realized acoustic niches

All sound types had different realized acoustic niches. The studied AS sound types and the studied FM sound types mainly differentiated along the temporal and the frequency axes, while the studied PS sound types primarily differentiated based on their pulse period. At 113 m depth, it has previously been observed that fish sounds are temporally and frequentially partitioned while a significant difference in terms of pulse period was not highlighted [437]. In other taxa, the third axis can encompass other acoustic features such as sound duration. In South America, the red howler monkey vocalizes both during the day and night, but the vocalizations are generally longer at night than during the day [489]. In addition to these three axes, differences could occur in the modulated character of the sound. In marine mammals, sound modulation has also been demonstrated as an adaptation to exploit a new acoustic niche by killer whales when leopard seals (another predator vocalizing at the same frequencies) are acoustically present during a part of the year. In our case, the predominance of the studied FM sound types at depth and the larger realized acoustic niches for the studied FM sound types at depth could indicate an additional difference based on this fourth axis (modulation type). This is in addition to the distinctions observed on the three other axes. Contrary to the studied FM sound types, the realized niche widths for frequency resources decreased with depth for all the three studied AS sound types: they exhibit frequency-based specialization at depth. The overall realized acoustic niche widths were similar for most PS types but some particular PS had temporal niche width narrower with depth.

When all three axes are considered together, it becomes apparent that each sound type tends to occupy a distinct acoustic niche. ANH is a concept that has started to be explored in fish [460], but it has been studied for a longer time in other zoological groups, particularly mammals [490], birds [464], and amphibians [466–468]. However, the results are not equivalent across taxa and environments. While in tropical birds, partitioning has primarily been observed at the temporal level [465], reverse results (frequency partitioning but not temporal) have been shown in frogs [491]. In anurans, differentiation of niches involves not only frequency but also frequency modulation [492]. Overall, caution is needed when extrapolating from acoustic niches to ecological niches. The minimization of the competition for different resources within the soundscape assumes that these sound types are produced by different species. Some sound types could encompass sounds produced by several close-related species emitting sounds at different frequencies. This is because, when a fish species emits different types of sounds, they often share the same fundamental/dominant frequency [163]. Concerning depth, when exploring the whole community, the realized temporal niche width is narrower with depth, while the realized frequency niche width is wider with depth. This indicates that at greater depths, acoustic activity becomes more focused during specific time periods, particularly during the night, and there is a broader exploitation of the frequency spectrum, particularly at higher frequencies.

In general ecology, there is an assumption that low abundances and narrow niches (i.e., specialization) are positively correlated [493,494]. This correlation may also extend to acoustic niches [460]. However, at least one example contradicts this assumption for fish, suggesting that different levels of sonic system plasticity may be linked to various strategies for sharing the acoustic space [460]. To gain a more comprehensive understanding of community dynamics, it is essential to consider ecological context, such as species hearing capabilities, along with phylogenetic niche conservatism [495] and morpho-allometric constraints.

In conclusion, this study reveals that depth has a significant influence on the acoustic characteristics and community dynamics of fish sounds in MCEs. Overall, these findings emphasize the intricate interplay between depth, and the fish acoustic communities, deepening our understanding of MCEs' dynamics.

5. Author contributions

Conceptualization, X.R.; methodology, X.R.; software, X.R.; validation, X.R. and É.P.; formal analysis, X.R. and J.C.; investigation, X.R. and J.C.; resources, U.T.P. and F.B.; data curation, X.R.; writing—original draft preparation, X.R. and J.C.; writing—review and editing, X.R., L.D.I., É.P., and J.C.; visualization, X.R. and J.C.; supervision, X.R.; project administration, X.R.; funding acquisition, D.L.

Chapter 8. Analyzing the origins of fish sounds in Polynesian lower mesophotic coral reefs: hypothesizing potential sound producers and related sonic morphology

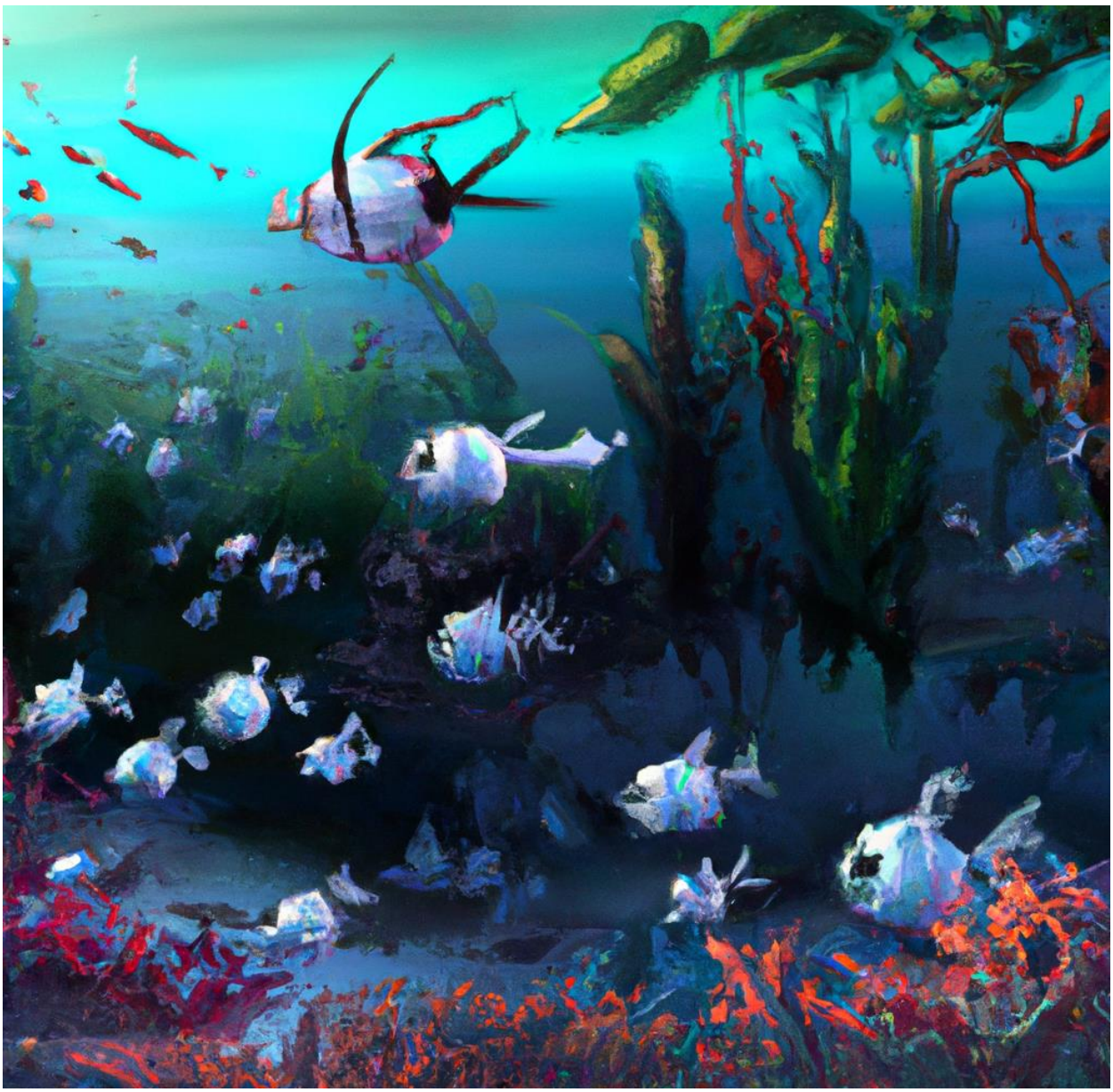

MAJOR RESULTS

Presence of vocal species

- ✓ In French Polynesia, 39 vocal families were identified as potentially present at a depth of 120 m.
- ✓ This number decreases to 23 sonic families when only the species from known vocal genera are considered.
- ✓ The highest number of species were found in Serranidae (17.7%), followed by Lutjanidae (12.9%), Gobiidae (5.6%), Scorpaenidae (4.8%), and Carangidae (4.8%).

Link between taxa present and sounds recorded

- ✓ The most abundant sound recorded in Polynesian MCEs is a high frequency pseudoharmonic sounds that exhibit similarities to sounds produced by Mediterranean *Scorpaena* species (Scorpaenidae).
- ✓ Specific sounds recorded in Polynesian MCEs share similarities with those generated by temperate grouper species.
- ✓ Other sounds from Polynesian MCEs share similarities with those generated by Ophidiidae. *Brotula multibarbata* was therefore examinated as it is the only species of this family present in Society and Tuamotu MCEs according to the literature review.

Sonic morphology: Scorpaenidae

- ✓ The sonic morphology of *Scorpaenopsis* is similar to that of *Scorpaena*: no swim bladder; a main muscle inserted into the skull, prolonged by tendons attached to the vertebrae, and a narrower medial bundle passing above Baudelot's ligaments.
- ✓ In *Dendrochirus*, an extrinsic sonic muscle was found on each side of the fish.
- ✓ We did not observe any evident sonic structures in *Pontinus*.

Sonic morphology: Serranidae and Ophidiidae

- ✓ *Saloptia powelli* (Serranidae) has a swim bladder closely associated with the ribs, muscle connecting the first rib to the neurocranium, intercostal ligaments and muscle, and no muscle directly attached to the swim bladder.
- ✓ The rib-associated morphology observed in all the other Serranidae species closely resembled that described in *S. powelli*.
- ✓ *Brotula multibarbata* possess a thick swim bladder divided into a small anterior part and a larger posterior part separated by a bottleneck area where a pair of sonic muscles is inserted.

Key question for the objective of the thesis

Which species emit the individually identifiable fish sounds recorded in lower MCEs?

Abstract

Mesophotic coral reefs host unique fish assemblages and a highly diverse biophony. However, many of the sources of these sounds remain unknown. The objectives of this study are as follows: *(1)* to identify, based on the literature, the vocal fish species present in the deep part of mesophotic coral reefs in French Polynesia; *(2)* to infer the sounds produced by the species present to link them with previously recorded sounds; and (*3*) to identify the sonic structures used by species from these families to produce sounds. A total of 42 fish families able to produce sounds were found to be possibly present at 120 m depth. The most abundant sound recorded in Polynesian mesophotic reefs exhibites similarities to sounds produced by Mediterranean *Scorpaena* species (Scorpaenidae). Specific sounds recorded in Polynesian MCEs share similarities with those generated by temperate grouper species. Finally, other sounds from Polynesian MCEs share similarities with those generated by Ophidiidae. In addition to Scorpanidae and Serranidae, *Brotula multibarbata* was therefore examinated as it is the only species of this family present in Society and Tuamotu MCEs according to the literature review. Some Polynesian Scorpaenidae lack a swim bladder and have a sonic muscle composed of bundles originating into the skull and long tendons attached to the vertebrae. The studied Serranidae have a swim bladder closely related to the ribs, a muscle attached to the neurocranium and the first ribs, and series of intercostal ligament in addition to classic intercostal muscles. Finally, *Brotula multibarbata* (Ophidiidae) had a thick swim bladder with a small anterior part separated from a large posterior part by a bottleneck area. A pair of sonic muscles originated anteriorly on the neurocranium and posteriorly on the bottleneck area. This study provides initial insights into which vocal fish taxa are present in Polynesian MCEs and to their corresponding sonic structures.

1. Introduction

Sound production is presently documented in 37% of fish families [496] with an estimated independent evolution of sound production occurring approximately 33 times among Actinopterygii. In contrast to tetrapods, fish use a wide variety of mechanisms to produce sounds, including for example intrinsic swim bladder muscles [497–499], fast extrinsic swim bladder muscles [424,500–505], slow extrinsic swim bladder muscles [146], muscles not attached to the swim bladder [149,424,506–509], buckling of modified scales [139,142,143], sonic-ligament causing jaw-snapping [510,511], stridulation [512,513], or a combination of several of these mechanisms [143,150,514].

Fish acoustic communication can be used for passive acoustic monitoring (PAM) in various underwater environments, including coral reefs [141,515,516] (Chapter 3 and 6). In French Polynesia, fish diversity [105,421] and its corresponding call composition have been shown to vary with depth (Chapter 6), with differences between mesophotic and photic compartments of coral reefs. The recorded sound types were diverse, including both pulse series and frequency-modulated sounds (Chapter 6). Frequency-modulated sounds were found to be in higher proportion in mesophotic coral reefs than in photic reefs but the majority of fish species responsible for producing these sound types remains unknown. Discovering which species produce them would be an advantage because it would allow for studies to determine the presence or absence of a species. Such studies have been conducted for shallow temperate species and species from photic reefs, mainly through aquarium-based [139,142,517], mesocosm-based [433], and field-based methods using cameras [87,518–520] or hydrophones held by rebreathing divers [138]. However, employing these techniques in lower mesophotic reefs is impractical, primarily due to challenges such as the difficulty of prolonged dives at significant depths and the disturbance caused to nocturnal fish by artificial lighting. Furthermore, bringing these fish to the surface alive for study is highly challenging, given that the pressure differential induces irreversible damage to their swim bladders.

Our study focuses in lower mesophotic coral reefs, found between 60 and 150 m deep, that host unique fish communities [105,421], which are reflected in their biophony (Chapter 6). More precisely, we focused on the diversity of sounds previously reported at 120 m in French Polynesia [472] (Chapter 6), with the aim of identifying the fish species responsible for some of these sounds and hypothesizing the potential sonic morphology associated to this sound production. This study has been conducted in three phases. *(1)* Initially, a literature review was performed to identify teleost species inhabiting the deep regions (at 120 m) of mesophotic coral

reefs in the Society and Tuamotu Archipelagos in French Polynesia, with the specific goal of pinpointing taxa known to be vocal. *(2)* Subsequently, we investigated the sounds produced by the identified species by examining the literature to understand the types of sounds each selected species is known to generate. We then compared these identified sounds with those recorded at a depth of 120 m in Polynesia. (*3*) Lastly, we selected the most relevant sonic families based on the literature review and conducted dissections of previously fished specimens to identify the sonic structures employed by species within these families for sound production.

2. Materials and methods

2.1. Vocal species present

Bibliographic research was conducted in five steps as detailed below, resulting in a categorized list of species: *(I)* species certainly present (listed as '1' in Table 12), *(II)* species probably or possibly present (listed as 2a if excluded at Step 3 and as 2b if excluded at Step 1), and *(III)* species considered unlikely to be present and therefore excluded from consideration.

Step 1: Check for the presence of fish species in French Polynesia by using the Fishbase database (https://www.fishbase.de) and Siu et al.'s (2017) updated list of Polynesian fish [126]. The search criteria for Fishbase were set as *count_native$Country=="French Polynesia" OR "Marquesas Is." OR "Tahiti" OR "Tuamotu Is."*. Any species found in Fishbase but not included in Siu et al.'s (2017) list were classified as 'possibly present' and duly noted.

Step 2: Exclusion of freshwater species and Elasmobranchs.

Step 3: Selection of species confirmed to be only present at a depth of 120 m. Species with a depth range shallower than 60 m (based on the minimum occurrence depth in Fishbase) or deeper than 200 m (based on the maximum occurrence depth in Fishbase) were omitted. Species indicated as 'not present below 60 m' in Siu et al. (2017) were also removed. Species known to occur at 120 m were retained, while those found between 60 and 119 m or between 121 and 200 m were categorized as 'probably present'. Species with conflicting data (i.e., species not reported to occur deeper than 60 m according to Siu et al. (2017) but with records at greater depths in Fishbase) were cross-referenced with the literature. If these species were confirmed to be present at 120 m, they were included in the 'probably present' category. Species with incomplete information were retained in the same category.

In addition, all species from French Polynesia were automatically extracted from the French National Museum of Natural History's list. Specimens captured between 60 and 200 m,

belonging to vocal families and not already present in our list, were included. Specimens captured within a depth range overlapping the '60 – 200 m range' (e.g., 42 – 70 m range), belonging to vocal families, and not yet on our list, were classified as 'probably present'. Larval specimens were excluded. Additionally, the depth of all specimens was cross-referenced with Fishbase to identify any potential new species for inclusion.

Step 4: Retain potential vocal species by selecting species belonging to known vocal families (identified from scientific literature or qualitative descriptions) or families with a known sonic structure [496]. The presence of these species in the soniferous fish inventory from Looby et al. (2022) was verified. Four species with uncertain vocalization status, namely *Aphareus furca* [138], *Decapterus macarellus* [521,522], *Mulloidichthys vanicolensis*, and *Naso hexacanthus* [138], were excluded from the list. Within the output list, we specified whether the studies referred to the exact species or to other species within the same genus, or to species from another genus within the same family.

Step 5: Complete the information regarding the archipelagos. Each species was individually assessed for its occurrence in the Society and Tuamotu Archipelagos.

2.2. Connection between present taxa and recorded sounds

The sound types previously recorded at a depth of 120 m in Polynesian mesophotic reefs (Chapter 6) were compared to the sounds of the species from the literature. For each retained species, we conducted a literature review to determine their sonic morphology and/or the types of sounds they produce. If information was unavailable for a species, we examined other species within the same genus. In cases where information was lacking for a genus, we investigated other genera within the same family. The lists provided by Rice et al. (2022) and Looby et al. (2022) were used as starting points to locate references for family-level and species-level information, respectively. Additional literature was consulted for families with conflicting information (designated as non-sonic families according to Looby et al. (2022) but identified as sonic by Rice et al. (2022): Apogonidae, Caesionidae, Leiognathidae, Lethrinidae, Myctophidae, and Uranoscopidae).

2.3. Sonic morphology

2.3.1. Specimen origin and permissions

Three families were selected for the investigation of their sonic morphology: Scorpaenidae, Serranidae, and Ophidiidae. For the last family, only the species *Brotula multibarbata* was studied. It was a male obtained from the Biodiversity Research Center (Academia Sinica,

Taiwan) while all the other species were obtained from French Polynesia. They were procured from local fishermen, in Bora Bora and Moorea, or from the fish market in Papeete (Tahiti). The specimens were fixed in 5% formaldehyde for several days, depending on their size, before being transferred to 70% alcohol for long-term preservation. The species used for the morpho-anatomical study were the ophidiid *Brotula multibarbata*, the scorpaenids *Dendrochirus biocellatus*, *Pontinus macrocephalus*, *Scorpaenopsis diabolus*, *S. papuensis*, and the serranids *Cephalopholis argus*, *Cephalopholis igarashiensis*, *Epinephelus tauvina*, *Liopropoma lunulatum*, *Plectranthias taylori*, *Saloptia powelli*, and *Variola louti*. This research was conducted with the authorization of the Environment Department of the Ministry of Culture, Environment, and Marine Resources (permit No. 1137/MCE/ENV).

2.3.2. µCTscan

To visualize mineralized tissues such as the neurocranium, vertebrae, ribs, spines, and rays, as well as the swim bladder position, specimens underwent microCT scanning at the dynxlab platform (University of Antwerp) using a custom-made UnitimXL X-ray CT scanner (Tescan, [523]) operating at 60 to 80 kV. The isotropic voxel size ranged from 0.038 to 0.080 µm. Segmentation and surface rendering of bones were performed using Amira version 2019.2 (Thermo Fisher Scientific; Waltham, MA, USA). Automatic thresholding was applied to identify bones, while manual outlining was used for the swim bladder membrane when present.

2.3.3. Dissections

Dissections were conducted using a Wild M10 stereoscopic microscope (Leica, Wetzlar, Germany) equipped with a camera lucida. The examination focused on the region close to the swim bladder, when present. In cases where the swim bladder was absent, the entire area between the posterior part of the neurocranium and the ribs was examined. Muscles, ligaments, and tendons were delineated on printed µCT scan reconstructions.

3. Results

3.1. Presence of vocal species

In total, species from 39 vocal families were identified as potentially present at a depth of 120 m (Table 12), with the highest number of species found in Serranidae (17.7%), followed by Lutjanidae (12.9%), Gobiidae (5.6%), Scorpaenidae (4.8%), and Carangidae (4.8%). This number decreases to 23 sonic families when only the species from known vocal genera are considered.

According to what is known in euphotic reefs, among the different vocal species found in MCEs, the probability to record their sounds in PAM studies is not equivalent. For example, include if numerous species of Gobiidae are known to produce sounds; their sounds are usually very faint and can typically only be heard at distances of a few centimeters [524], and are therefore not frequently used in PAM studies. On the other hand, other taxa such as Carangidae, are fast-swimming predators found in the waters above the reef and in the open sea. The two vocal genera found in the area (*Alectis* and *Selar*) are known to produce scratchy bursts (*Alectis* genus [21,522]) and sustained or irregular series of toothy grating sounds (*Selar* genus [21]). These sounds are not easy to distinguish in PAM studies and are typically not considered during manual scrolling processes [163] (Chapter 6). On the other hand, other families (e.g., Carapidae, Ophidiidae, Scorpaenidae, or Serranidae) appears to be highly vocal based on the numerous studies that described their sounds, including in PAM contexts (Table 12).

Table 12 State of the art of the vocal species present in the study area. The column 'Type' separates species certainly present (1) and species probably and possibly present (2a and 2b). The column 'Level' separates known vocal species (species), species likely vocal but with references known only at the genus level (genus) and species likely vocal but with references known only at the family level (i.e., in another genus from the family). Additionally, genera for which the exact species present in MCEs is uncertain are also indicated as 'genus'. Families for which the exact genus present in MCEs is uncertain are also indicated as 'family'. * = families with conflicting information (non-sonic families according to [525] but sonic according to [496]), ** = only morphological evidence, S = Society Archipelago, T = Tuamotu Archipelago, Y = Yes, N = Not present.

Family	Species	S	T	Type	Level	Reference
Acanthuridae	*Naso hexacanthus*	Y	Y	2a	family	[138]
Apogonidae*	*Foa fo*	Y	N	2b	family	[138,526]
Balistidae	*Xanthichthys auromarginatus*	Y	Y	1	species	[138]
Balistidae	*Xanthichthys caeruleolineatus*	Y	Y	2a	genus	
Blenniidae	*Petroscirtes xestus*	Y	N	2a	family	[527–529]
Bythitidae	*Tuamotuichthys bispinosus*	N	Y	2b	family	[530]
Caesionidae*	*Caesionidae*	N	N	2b	family	[531]
Caesionidae*	*Pterocaesio* sp.	N	N	1	family	
Caproidae	*Antigonia capros*	Y	N	1	family	[532]
Carangidae	*Alectis indica*	Y	Y	2b	genus	[21,522]
Carangidae	*Atule mate*	Y	N	2b	family	[21,164,512,521,522,526,532–542]
Carangidae	*Decapterus macarellus*	Y	Y	2a	family	
Carangidae	*Decapterus tabl*	Y	N	2b	family	
Carangidae	*Selar boops*	Y	N	2b	genus	[21]
Carangidae	*Uraspis helvola*	N	N	2b	family	[21,164,512,521,522,526,532–542]
Carapidae	*Carapus mourlani*	Y	Y	2a	species	[145,146]
Chaetodontidae	*Chaetodon* sp.	N	N	1	genus	[21,138,526,543,544]
Chaetodontidae	*Heniochus singularius*	N	N	2b	genus	[149]
Congridae	*Ariosoma scheelei*	Y	N	2a	family	[521,522]
Congridae	*Ariosoma sereti*	N	N	1	family	

Congridae	*Bathyuroconger vicinus*	N	N	1	family	
Congridae	*Congriscus marquesaensis*	N	N	1	family	
Congridae	*Uroconger* sp.			1	family	
Dactylopteridae	*Dactyloptena* sp.	N	N	1	family	[21,164,545]
Diodontidae	*Diodontidae*	N	N	1	family	[21,138,164,512,521,522,526]
Gobiidae	*Gnatholepis anjerensis*	Y	Y	2a	family	[520,546]
Gobiidae	*Gunnellichthys monostigma*	Y	N	2a	family	
Gobiidae	*Kraemeria bryani*	Y	N	2b	family	
Gobiidae	*Oxyurichthys notonema*	Y	N	2a	family	
Gobiidae	*Priolepis farcimen*	Y	Y	2b	family	
Gobiidae	*Priolepis* sp.	N	N	1	family	
Gobiidae	*Valenciennea strigata*	Y	Y	2a	family	
Holocentridae	*Myripristis chryseres*	Y	Y	1	genus	[21,138,547–549]
Holocentridae	*Ostichthys archiepiscopus*	Y	N	1	family	[21,138,526,534,547–553]
Holocentridae	*Ostichthys ovaloculus*	Y	N	1	family	
Holocentridae	*Pristilepis sp.*			2b	family	
Labridae	*Bodianus bilunulatus*	N	N	2b	genus	[21,138]
Labridae	*Bodianus paraleucosticticus*	Y	N	2a	genus	
Labridae	*Cirrhilabrus claire*	Y	N	2a	family	[21,138,521,522,526,539,554–557]
Labridae	*Oxycheilinus lineatus*	Y	N	2a	family	
Labridae	*Polylepion russelli*	Y	N	1	family	
Leiognathidae*	*Deveximentum insidiator*	Y	N	2b	family	[537,558]
Leiognathidae*	*Gazza minuta*	Y	N	2b	family	
Lethrinidae*	*Gymnocranius* confer *grandoculis*	N	Y	1	family	[559]
Lethrinidae*	*Lethrinus rubrioperculatus*	Y	N	1	family	
Lutjanidae	*Aphareus furca*	Y	Y	1	family	[21,138]
Lutjanidae	*Aphareus rutilans*	Y	N	1	family	
Lutjanidae	*Etelis carbunculus*	Y	Y	1	family	
Lutjanidae	*Etelis coruscans*	Y	Y	1	family	
Lutjanidae	*Etelis radiosus*	Y	N	1	family	
Lutjanidae	*Lutjanus kasmira*	Y	Y	1	species	[138]
Lutjanidae	*Lutjanus argentimaculatus*			2b	genus	[21,138,526,560]
Lutjanidae	*Lutjanus* sp.	N	N	1	genus	
Lutjanidae	*Parapristipomoides squamimaxillaris*	N	N	2a	family	[21,138]
Lutjanidae	*Pristipomoides argyrogrammicus*	Y	Y	1	family	
Lutjanidae	*Pristipomoides auricilla*	Y	N	1	family	
Lutjanidae	*Pristipomoides filamentosus*	Y	Y	1	family	
Lutjanidae	*Pristipomoides flavipinnis*	Y	N	1	family	
Lutjanidae	*Pristipomoides sieboldii*	N	N	1	family	
Lutjanidae	*Pristipomoides zonatus*	Y	Y	1	family	
Lutjanidae	*Randallichthys filamentosus*	Y	N	2a	family	
Macrouridae	*Malacocephalus laevis***	N	N	2a	species	[561]
Macrouridae	*Malacocephalus nipponensis*	Y	N	1	genus	

Macrouridae	*Malacocephalus* sp.	Y	N	1	genus	
Mullidae	*Mulloidichthys pfluegeri*	Y	N	2a	genus	[21,138]
Mullidae	*Mulloidichthys* sp.	N	N	1	genus	
Mullidae	*Mulloidichthys vanicolensis*	Y	Y	1	genus	[138]
Mullidae	*Parupeneus* sp.	N	N	1	genus	
Myctophidae*	*Benthosema fibulatum*	N	N	2b	family	[562]
Myctophidae*	*Diaphus splendidus*	Y	N	1	family	
Myctophidae*	*Lampadena luminosa*	Y	N	1	family	
Myctophidae*	*Symbolophorus evermanni*	N	N	2b	family	
Ophidiidae	*Brotula multibarbata*	Y	Y	2a	family	[90,163,434,451,530,563–581]
Ophidiidae	*Ophidion muraenolepis*	N	N	1	genus	[564,567,568,573,574]
Ostraciidae	*Lactoria* sp.	N	N	1	genus	[514]
Ostraciidae	*Ostracion* sp.	N	N	1	genus	[138,150,582]
Ostraciidae	*Tetrosomus* sp.	N	N	1	family	[21,150,514,533,582,583]
Peristediidae	*Satyrichthys* sp.			1	genus	[532]
Pleuronectidae	*Nematops nanosquama*	N	N	1	family	[21,521,522]
Pomacanthidae	*Centropyge boylei*	N	N	1	genus	[138]
Pomacanthidae	*Centropyge narcosis*	Y	Y	1	genus	
Pomacanthidae	*Genicanthus bellus*	Y	Y	1	family	[21,138,526]
Pomacentridae	*Chromis* sp. 2 (Tahiti Island)	Y	N	1	genus	[138,584,585]
Pomacentridae	*Pomacentridae* sp. (Rapa Is.)	N	N	1	family	
Priacanthidae	*Cookeolus japonicus*	N	N	1	family	[586–588]
Priacanthidae	*Priacanthus hamrur*	Y	Y	1	genus	[588]
Scombridae	*Thunnus maccoyii*	N	N	1	genus	[589]
Scombridae	*Thunnus obesus*	Y	Y	1	genus	
Scorpaenidae	*Neomerinthe naevosa*	N	N	1	genus	[590]
Scorpaenidae	*Pontinus macrocephalus*	Y	Y	2a	genus	
Scorpaenidae	*Pteroidichthys amboinensis*	N	N	1	family	[21,433,590,591]
Scorpaenidae	*Pteroidichthys caussei*	N	N	1	family	
Scorpaenidae	*Scorpaena lacrimata*	Y	N	2b	genus	[21,433,526,590]
Scorpaenidae	*Scorpaenopsis pusilla*	N	N	1	genus	[21,532]
Serranidae	*Cephalopholis aurantia*	Y	Y	2a	genus	[21,138,592]
Serranidae	*Cephalopholis igarashiensis*	Y	Y	1	genus	
Serranidae	*Cephalopholis polleni*	Y	Y	2a	genus	
Serranidae	*Cephalopholis sexmaculata*	Y	Y	1	genus	
Serranidae	*Epinephelus morrhua*	N	N	1	genus	[21,352,458,526,553,593–596]
Serranidae	*Epinephelus retouti*	Y	Y	1	genus	
Serranidae	*Epinephelus tuamotuensis*	Y	Y	1	genus	
Serranidae	*Hyporthodus octofasciatus*	Y	N	2a	genus	[21]
Serranidae	*Belonoperca pylei*	N	Y	1	family	[21,89,93,138,154,163,164,352,423,458,471,484,485,521,522,526,533,534,553,592–594,596–607]
Serranidae	*Gracila albomarginata*	Y	Y	2a	family	
Serranidae	*Liopropoma erythraeum*	Y	N	1	family	
Serranidae	*Liopropoma lunulatum*	Y	N	1	family	
Serranidae	*Odontanthias tapui*	Y	N	1	family	
Serranidae	*Plectranthias bennetti*	Y	N	2a	family	

Serranidae	*Plectranthias kamii*	Y	N	2a	family	
Serranidae	*Plectranthias rubrifasciatus*	N	Y	1	family	
Serranidae	*Plectranthias* sp.	Y	Y	1	family	
Serranidae	*Plectranthias taylori*	Y	Y	1	family	
Serranidae	*Pogonoperca punctata*	Y	Y	1	family	
Serranidae	*Saloptia powelli*	Y	Y	1	family	
Serranidae	*Pseudanthias privitera*	Y	N	2a	genus	[138]
Serranidae	*Pseudanthias ventralis*	Y	Y	1	genus	
Setarchidae	*Setarches guentheri***			2a	species	[590]
Sphyraenidae	*Sphyraena acutipinnis*			2b	genus	[21,138,526]
Syngnathidae	*Hippocampus kuda*	Y	N	2b	genus	[608,609]
Syngnathidae	*Hippocampus* sp.	N	N	1	genus	
Tetraodontidae	*Sphoeroides pachygaster*	Y	N	1	genus	[21,512,521,522,526]
Uranoscopidae*	*Genyagnus monopterygius*	Y	N	2b	family	[21]
Zanclidae	*Zanclus cornutus*	Y	Y	2a	species	[138]
Zeidae	*Cyttomimus affinis*	N	Y	1	family	[545,610,611]

3.2. Link between present taxa and recorded sounds

More than 65 fish sound types are known from Polynesian mesophotic reefs (Chapters 6 and 7, Figure 51). Each category of sound is examined and comparing to the sounds emitted by the species from the literature (Table SP8 - 1) in the following sub-sections.

3.2.1. Frequency modulated sounds

In Polynesian mesophotic reefs, several frequency-modulated (FM) have been recorded (Chapter 6). FM sounds are present in diverse clades of marine fish, including Batrachoididae [497,498,612], Gobiidae [613], and Serranidae [89,163,423]. Only the two last families are present in French Polynesia. FM sounds can be categorized as downsweeps (DS), upsweeps (US), and complex sounds (CS; a combination of DS and US). Each category will now be examined in more detail.

3.2.1.1. Downsweeps

Some of the DS sounds recorded in Polynesian MCEs exhibit similarities to sounds produced by certain species of groupers (e.g., *Epinephelus* spp.). For example, *E. marginatus*, a temperate grouper species, is known to produce low-frequency DS [163,423]. In the area of study, eleven genera of Serranidae are present: *Belanoperca*, *Cephalopholis*, *Epinephelus*, *Gracila*, *Hyporthodus*, *Liopropoma*, *Odontanthias*, *Plectranthias*, *Pogonoperca*, *Pseudanthias*, and *Saloptia*.

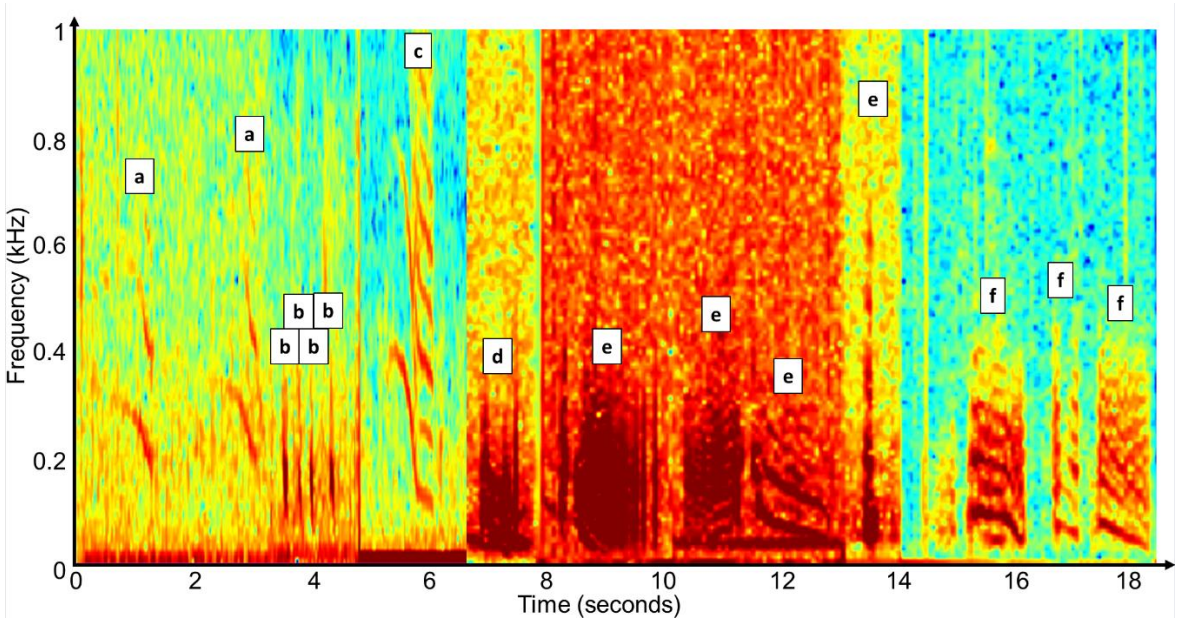

Figure 56 Comparison of fish downsweeping sounds recorded in Polynesian photic and mesophotic reefs, (a) DS5, (b) rare series of low DS, and (c) CS6 (Chapters 6 and 7) and downsweeping sounds from three groupers species from the literature: (d) *Epinephelus adscensionis*, (e) *Epinephelus guttatus*, and (f) *Epinephelus striatus.*

3.2.1.2. Upsweeps

US sounds are well known to occur in Batrachoididae and Triglidae. However, these two families are not known to inhabit Polynesian mesophotic reefs. Some Ophidiidae, such as *Genypterus maculatus*, are also known to produce US growls but with a less pronounced FM pattern and at much lower frequencies than the US observed in Polynesian MCEs [579].

3.2.1.3. Complex sounds

The CS2 sounds recorded in Polynesia share similarities with those recorded offshore in the Atlantic Ocean (40 – 200 m depth), referred to as the '300 Hz FM harmonic single' [451]. CS3 is highly identical to the 'sound #46' from the Indian Ocean [475]. Concerning CS1 (Chapter 6), it is identical to the 'whoot' described in Society Islands [141] and highly similar to the 'sound #13' described in Mozambique [475]. In both studies, it is a non-abundant sound. There is currently no valid scientific identification on the emitter of this peculiar sound type [472].

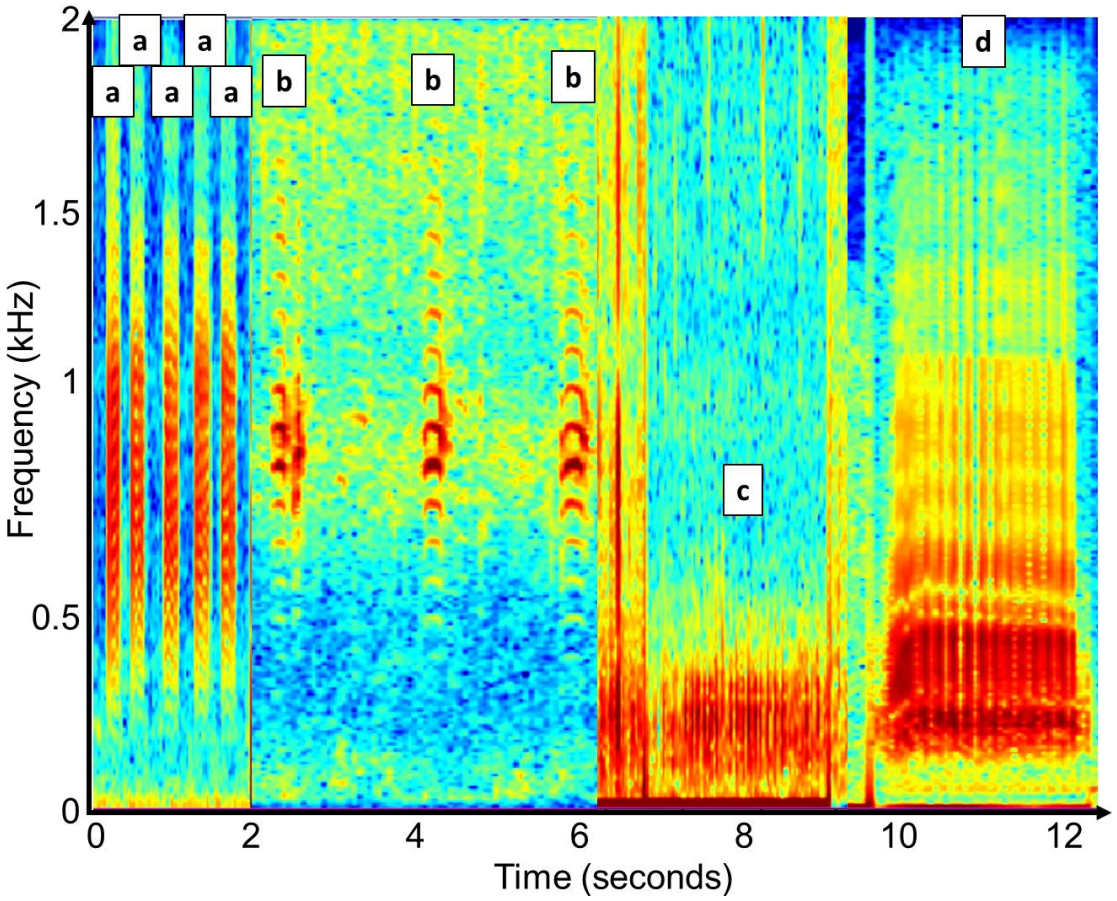

Figure 57 Comparison of fish complex, arched, and pulse series sounds. (**a** and **b**) arched sounds, and (**c** and **d**) and pulse series recorded in Polynesian photic and mesophotic reefs (**a**) AS4, and (**c**) PS10 and similar sounds from the literature: (**b**) '/kwa/' [281], and (**d**) *Ophidion rochei* male.

3.2.2. 'kwa-like' sounds

In MCEs, the most abundant sound is a sound named AS4 (Chapter 6 and 7) and shares similarities with a sound described in the Mediterranean Sea and named '/*kwa*/' [281]. Both sounds are pulse train characterized by a similar number of pulses (/*kwa*/: 13 ± 6 vs. AS4: 12.3 ± 1.2). On the spectrograms, they appear as pseudo-harmonics around a 800 Hz contour (/*kwa*/: 747 ± 136 Hz vs. AS4: 846.9 ± 147.6 Hz). Their contour is characterized by a similar initial and final frequency giving them a generally arch-shaped contour. For both sound types, the peak sound emission occurs at the beginning of the night [281] (Chapter 7). In the Mediterranean Sea, /*kwa*/ are attributed to *Scorpaena* species (Scorpaenidae). MCEs from Society and Tuamotu Islands seems to inhabit several genera of Scorpaenidae such as *Pontinus*, *Scorpaena*, and *Scorpaenopsis*.

In addition to AS4, a second 'kwa-like', named AS5 (Chapter 6), is found in MCEs, with its peak sound production following that of AS4 (Chapter 7). This sound is 72 ms shorter, has 5 fewer peaks, and its peak frequency is 203 Hz lower than that of AS4.

3.2.3. Pulse series and fast pulse trains

Some PS recorded in Polynesian MCEs exhibit similarities with sounds described in Carapidae. Sounds produced by *Carapus boraborensis* (duration: 3-14 s, 10-83 pulses, pulse period: 180-212 ms, [614]) share temporal similarities with PS6 sounds from MCEs (duration: 5.7 ± 7.7 s, 26 ± 24 pulses, pulse period: 185 ± 69 ms; mean ± SD) but not in terms of peak frequency (200 Hz vs. 640 ± 438 Hz).

Carapus mourlani, a species present in Polynesian MCEs, is able to produce double-pulse sounds highly similar to a sound observed in MCEs and named '2P'. This sound was not considered in Chapter 6 because of its rarity but was examined in Chapter 7, where it represented 1.26% of sounds recorded in MCEs. In the literature, some *C. mourlani* sounds are described as having two pulses, with the second one being lower in amplitude [146]. 2P was also composed of 2 ± 0 pulses, with the second one being generally lower in amplitude by 1,08 ± 1,14 dB re 1 µPa. However, the pulse period (67,77 ms ± 10,04 ms) was higher than in *C. mourlani* sounds (theoretically around 31.3 ms by summing a described pulse duration of 22 ± 4.2 ms and an interpulse interval: 9.26 ± 2.2 ms [146]). The peak frequency is higher in *C. mourlani* (765 ± 124 Hz, [146]) than in 2P (471 ± 224 Hz).

PS10 (duration: 1.5 ± 0.5 s, 18 ± 6 pulses, pulse period: 85 ± 21 ms, peak frequency: 221 ± 25 Hz) recorded in Polynesian MCEs exhibits similarities with sounds described in shallower species of Ophidiidae [434,572,574] (Chapter 6). A close zoom on the oscillograms of PS10 reveals a series of pulses dominated by a high-amplitude peak (Figure SP6 - 3F). In the inter-pulse interval, smaller peaks can be observed. This configuration is similar to the one observed in some species from genus *Ophidion*. However, the main difference between PS10 and sounds from *Ophidion* species is the difference in frequency range, with a lower frequency for PS10. At the contrary, PS10 has a higher frequency compared to *Genypterus*, a species of bigger Ophidiidae from the Southern Hemisphere. In MCEs from the Society and Tuamotu Islands, the literature review highlighted only one species of Ophidiidae: *Brotula multibarbata*.

3.2.4. Selected candidates

Three soniferous families were selected for sonic morphology investigation. Firstly, Scorpaenidae was chosen due to its presence in the studied archipelagos, and sounds from temperate species exhibited similarities with the most prevalent sounds recorded in MCEs. Secondly, Serranidae was included as this family is present in Polynesian MCEs, and sounds from other grouper species shared similarities with downsweep sounds from MCEs. Finally, *Brotula multibarbata* was the only species of Ophidiidae present in Society and Tuamotu MCEs

according to the literature review. It was examined because this family is known to produce low click trains similar to some recorded in MCEs.

3.3. Sonic morphology

3.3.1. Scorpaenidae

3.3.1.1. *Scorpaenopsis* spp.

Similar sonic structures were observed in both *Scorpaenopsis diabolus* and *S. papuensis*. Both species lack a swim bladder. There is a sonic apparatus on each side of the fish, consisting of two main muscle bundles and three tendons. The main muscle bundle, referred to as the lateral bundle (δ) is divided into two parts by Baudelot's ligament, which connects the basioccipital and the supracleithrum. The rostral part (δA) originates from the skull and inserts onto Baudelot's ligament, while the caudal part (δB) originates from Baudelot's ligament and is connected to two tendons, the lateral tendons (δ1 and δ2), which insert onto ventral plate-shaped parapophyses of the seventh vertebra (V7) and the eighth vertebra (V8), respectively (Figure 58). The medial bundle (α) is narrower than the lateral bundle and is taller than wide. It covers a portion of the δ bundle, originating from the skull, passing above Baudelot's ligament, and extending via the α tendon, which is inserted onto the sixth vertebra (V6). Neither V5 nor V6 has a plate-shaped structure like V7. Vertebrae anterior to V6 do not possess developed parapophyses. Contrary to the anterior ones, V5 had ribs with intermusculars. In addition to the primary description provided above, a narrow proximal part of δB (named β) detaches from the rest of the bundle to connect to α tendon. None of the muscles or tendons are directly attached to the pectoral girdle.

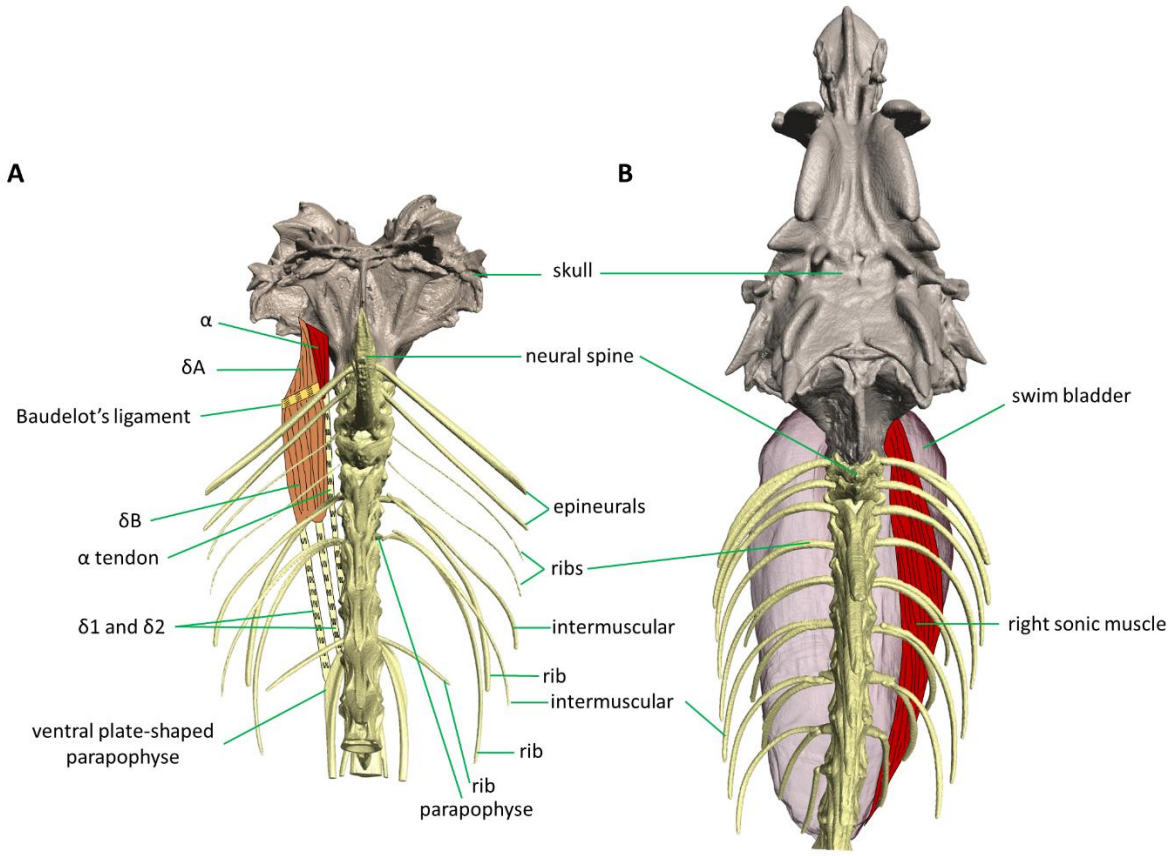

Figure 58 µCTscan reconstructions of two Scorpaenidae species with a sonic morphology. (**A**) Dorsal view of *Scorpaenopsis diabolus*. (**B**) Dorsal view of the shallower species *Dendrochirus biocellatus*. The muscles involved in the sound production are illustrated in one side of the specimen. α: medial bundle. δ: lateral bundle. δA: rostral part of the lateral bundle. δB: caudal part of the lateral bundle. δ1 and δ2: lateral tendons.

3.3.1.2. *Pontinus macrocephalus*

This species has a swim bladder. We did not observe any structures typically associated with sound production.

3.3.1.3. *Dendrochirus biocellatus*

This species has a swim bladder. Like in *Scorpaenopsis*, we found neural spines and then ribs associated with accessory ribs. However, the sonic muscles configuration was completely different. The origin of the sonic muscle is on the posterior portion of the neurocranium and its insertion is on the posterior part of the swim bladder below the ribs (Figure 58).

3.3.2. Serranidae

In *Saloptia powelli*, the first six ribs are connected laterally by ligaments, namely L1 (connecting the first rib to the second rib), L2 (connecting the second rib to the third rib), and so on, up to L5 (Figure 59). In addition to these five ligaments, there is a longer ligament (L1-6) that originates from the first rib, passes beneath the second rib, and extends over the third, fourth, and fifth rib before attaching to the sixth rib. These ligaments are only present on the

dorsal section of the ribs. Additionally, a very thin ligament is attached to the second rib and runs beneath the third rib.

A muscle connects the first rib to the neurocranium (Figure 59). This muscle shares the same color as the epaxial and hypaxial musculature. The swim bladder is closely associated with the ribs. Moving the first two muscles does not seem to affect the swim bladder, whereas the opposite is observed for the subsequent muscles. The first two muscles do not make direct contact with the swim bladder and appear to enhance the movement of the third muscle. Importantly, no muscle is directly attached to the swim bladder.

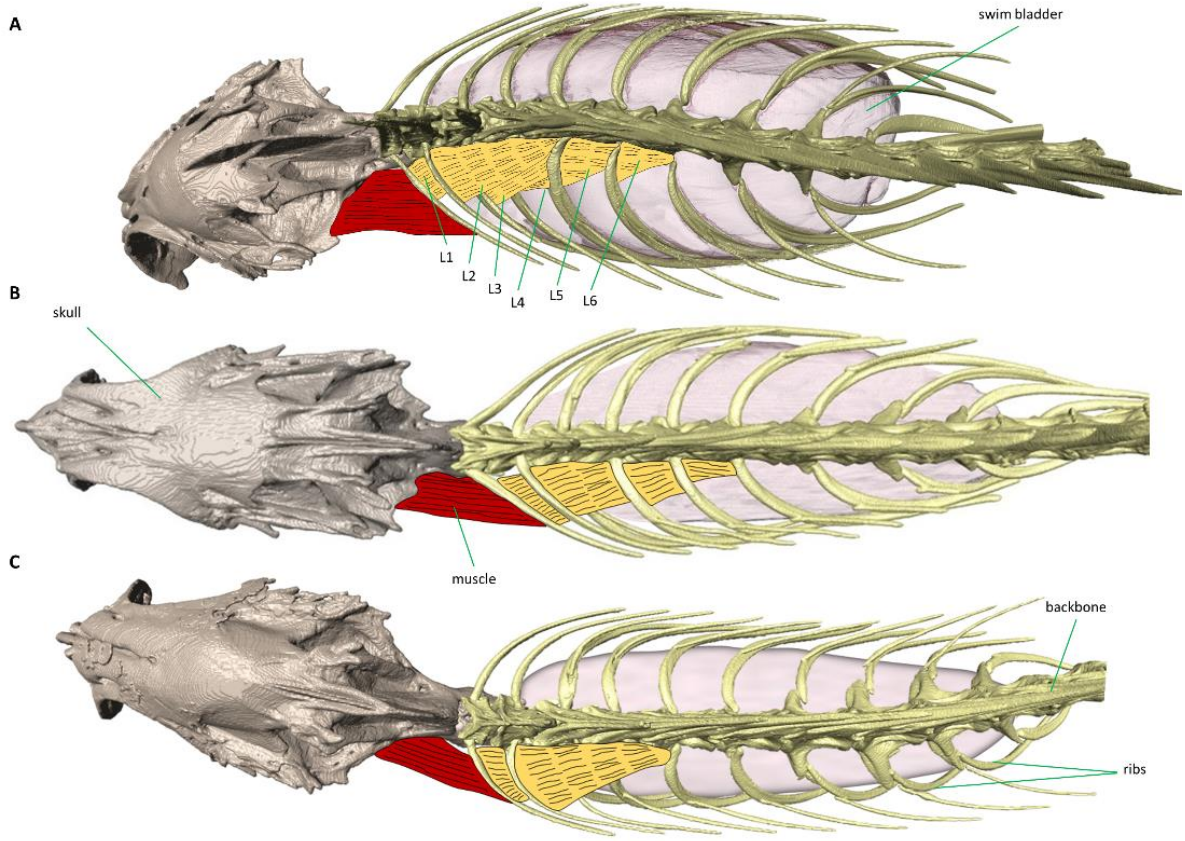

Figure 59 Dorsal view of µCTscan reconstructions of three Serranidae species with the muscle connecting the neurocranium to the first rib and the intercostal ligaments represented. (**A**) *Plectranthias taylori*, (**B**) *Saloptia powelli*, and (**C**) *Liopropoma lunulatum*. The intercostal muscles are not represented. L = ligament.

The rib-associated morphology observed in all the other species closely resembled that described in *S. powelli* (Figure 59, Note SP8 - 1).

3.3.4. *Brotula multibarbata*

Brotula multibarbata possess a thick swim bladder, which is divided into a small anterior part and a larger posterior part separated by a bottleneck area. While the posterior part of the

swim bladder has a typical appearance, the wall of the anterior part exhibited a different color, non-homogeneous texture, and softer consistency (Figure SP8 - 1). The swim bladder was welded to the vertebra. A pair of sonic muscles were originated anteriorly to the neurocranium and posteriorly to the bottleneck area.

4. Discussion

The two main sonic families encountered at a depth of 120 m in the Society and Tuamotu Islands were Serranidae and Lutjanidae, collectively constituting 30.6% of all fish species present. These two families also represent the dominant groups among the '*paru*', a local Polynesian term for fish inhabiting depths ranging from 100 to 600 m [615]. However, the most abundant and diverse taxa in terms of species richness are typically not the most prominent contributors to the underwater biophony. While Serranidae are highly vocal, very little is known about sound production in Lutjanidae, with the existing knowledge primarily focused on Lutjaninae species. Their sounds have been described as 'low-pitched', 'feeble', or 'possible' [21], and these descriptions are limited to non-FM non-harmonic pulse(s)-like sounds [21,138].

In lower MCEs, AS4 accounts for 40% to 66% of all sound types (measured at 120 m during sunset, Chapter 6). This pseudoharmonic sound closely resembles the /kwa/ vocalizations produced by *Scorpaena* spp. *Scorpaena* is not a monophyletic taxon. According to phylogeny, *Scorpaena* and *Scorpaenopsis* species are grouped together in a monophyletic group. These two genera are known to inhabit lower MCEs in Polynesian waters [126]. A comparison of the sonic morphology between *Scorpaenopsis* (as determined in this study) and *Scorpaena* (as documented in the literature [433,590]) reveals striking similarities: several muscles prolonged by tendons including one that has a more unusual configuration because it is divided into two bundles by Baudelot's ligament. Bolgan et al. (2019) hypothesized the rostral part of the muscle could modify the tendon tension modifying the frequency during sound production while the caudal part of the muscle could produce vibrations in the tendons. Despite the high similarity, minor differences exist between the two configurations like the subdivisions of the medial bundle in *Scorpaenopsis* and presence of an intermediate bundle in *Scorpaena*. The medial bundle of *Scorpaenopsis* could be homologous of the α or the β bundles observed in *Scorpaena*. In contrast to these genera, both *Dendrochirus* and *Pontinus* possess swim bladders. *Pontinus* forms a monophylic genus while *Dendrochirus* does not. Within the clade containing *Dendrochirus* spp., which includes species from the genera *Pterois* and *Brachypterois*, many species have two large extrinsic muscles attached to the neurocranium and the swim bladder [590]. Species within this group, such as *Pterois volitans*, are recognized for producing

repetitive pulse calls and hums with intermittent pulses [591]. These sounds markedly differ from the AS sounds recorded in MCEs. Concerning *Pontinus*, other species within this genus are known to feature extrinsic muscles connecting to the vertebrae and the neurocranium [590], a morphology that is not known to be associated with the production of AS sounds such as AS4 contrary to what was observed in the *Scorpaenopsis*/*Scorpaena* group.

The presence of at least two 'kwa-like' sounds in MCEs, as opposed to one in the Mediterranean Sea, may be linked to the existence of two genera exhibiting a similar unusual sonic configuration (*Scorpaena* and *Scorpaenopsis*), in contrast to the Mediterranean Sea where only *Scorpaena* is present.

Within Serranidae, a wide array of species have been documented as producing non-FM non-harmonic pulse(s)-like sounds, which have been described using various terms such as thumps, knocks, single pulses, pulse series, single booms, serial booms, loud booms, deep booms, low-frequency pulse sequences, pulse train calls, hollow knocks [21,138,163,423,458,534,593,596,598], or a combination of PS and tonal elements [484,485,606]. Additionally, tonal and downsweeps (DS) sounds have been identified in several genera, including *Epinephelus* [163,423,593,596], *Hypoplectrus* [89], and *Mycteroperca* [484,485,606,607]. At least one of them, the long tonal call of *E. adscensionis* [21], resembles a low-frequency tonal AS sound recorded in MCEs (Chapter 6). These genera are not clustered together in the phylogeny tree but are distributed across both the Anthiinae/Serraninae and Epinephelinae taxa. Across all the species examined in this study, a similar sonic morphology was observed: (*1*) a muscle connecting the first rib to the neurocranium, (*2*) intercostal ligaments in addition to the intercostal muscles positioned between the ribs, (*3*) the swim bladder closely associated with the ribs, and (*4*) no muscle directly attached to the swim bladder. Differences were primarily observed in terms of the presence/absence and arrangement of intercostal ligaments. The presence of this configuration appears to align with the fundamental sonic structures description found in the literature, where it is generally assumed that swim bladder vibrates due to the contraction of associated axial muscles [21,352,526]. High-frequency DS from MCEs do not resemble grouper sounds but are highly similar to an unknown sound previously documented in the Atlantic Ocean and referred to as 'unknown sound 365 Hz harmonic' [451]. Conversely, Polynesian species of Serranidae have the morphological capacity to produce sounds. More investigation is needed to know which low-frequency DS and certain tonal calls from MCEs (Chapter 6) are produced by which species of Serranidae.

Given the substantial number of groupers found at greater depths than MCEs [615], it is highly probable that similar sound types still exist in the rariphotic zone.

The last species studied was *Brotula multibarbata*, a member of the monophyletic taxon Brotulinae within the paraphyletic Ophidiidae taxon. This family is well-known for its sonic capabilities, exhibiting a high diversity of mechanisms and distinct sounds not only between related species but also between males and females of the same species [568,575,578,616,617]. *Brotula multibarbata* possesses a swim bladder with tough tendinous walls, making it challenging to compress [618]. Some adaptations, such as its solid attachment to the vertebral column and its division into two chambers [618], are shared with other species and taxa [21,498,576,619]. However, the peculiar feature is the bottleneck separation [618]. In certain Ophidiidae species, it has been demonstrated that the separation of the swim bladder can decouple the movement of the anterior part of the swim bladder from the rest of the structure [576]. A more rigid posterior section of the swim bladder could concentrate pressure from sound production and reflect it back to a less rigid anterior portion, where it might potentially re-excite other structures [576]. Additionally, attaching part of the swim bladder to the vertebral column is known to isolate part of the swim bladder from muscles contractions. Moreover, the high resistance to movement of a segment of the swim bladder renders it ineffective as a sound radiator [576]. Conversely, it has also been hypothesized that wing-like processes could store strain energy [620]. Include if *B. multibarbata* possesses the morphological capacity to produce sounds with low fundamental frequencies determined by the rate of muscle contraction [621–624], the observation of sonic muscles during the dissection of *B. multibarbata* is not sufficient to have an idea of the sounds produced. To know if this species produces low-frequency long fast pulse trains or other sounds such as long-duration harmonic tonal sounds, as previously hypothesized, more investigation is needed to. In this species, it is likely that the peculiar bottleneck of the swim bladder plays a central role in the sound production. A two-step system is also found in terrestrial animals using resonators modelled as Helmholtz resonators [625,626]. Analogies with this system are known to exist in related fish (Carapidae, Ophidiiformes) [627]. Generally, in such sounds, frequencies above the peak frequency are generated by higher-order vibrations of the swim bladder [576].

In conclusion, this study offers preliminary insights into which vocal fish taxa are present in Polynesian MCEs and to their corresponding sonic structures. Notably, it highlights the connection between *Scorpaenopsis* morphology and the one of *Scorpaena* (a genus known to produce pseudo-harmonic AS sounds) as well as the relationship between the morphology of

Polynesian Serranidae and temperate species known to produce long tonal and DS sounds. Additionally, the study reports an unusual swim bladder morphology in *B. multibarbata*, a suspected soniferous species in MCEs.

PART IV: HUMAN MODIFICATIONS' INFLUENCE ON BIOPHONY

Chapter 9. Passive acoustic monitoring reveals the resilience effect of marine protected areas to coral bleaching events

Xavier Raick[1], Éric Parmentier[1], David Lecchini[2,3], Cédric Gervaise[4], Frédéric Bertucci[5], Guillaume Iwankow[2], Gilles Siu[2], and Lucia Di Iorio[6]

[1] Laboratory of Functional and Evolutionary Morphology, FOCUS, B6c allée du 6 août, University of Liège, 4000 Liège, Belgium

[2] PSL University, EPHE-UPVD-CNRS, USR 3278 CRIOBE, BP 1013 98729 Papetoai, Moorea, French Polynesia

[3] Laboratoire d'Excellence 'CORAIL', 58 avenue Paul Alduy, 66860 Perpignan, France

[4] Chorus Institute, 5 rue Gallice, 38100 Grenoble, France

[5] Institute of Research for Development, 87 Av. Jean Monnet, 34200 Sète, France

[6] Université de Perpignan Via Domitia, CNRS, CEFREM UMR 5110, 52 avenue Paul Alduy, 66860 Perpignan, France

This chapter is currently in the final stages of preparation for submission to a scientific journal. The continuation of this research has been the subject of two Master's 2 thesis that will be grouped for publication to a scientific journal. This content has not been included in the final document of this thesis.

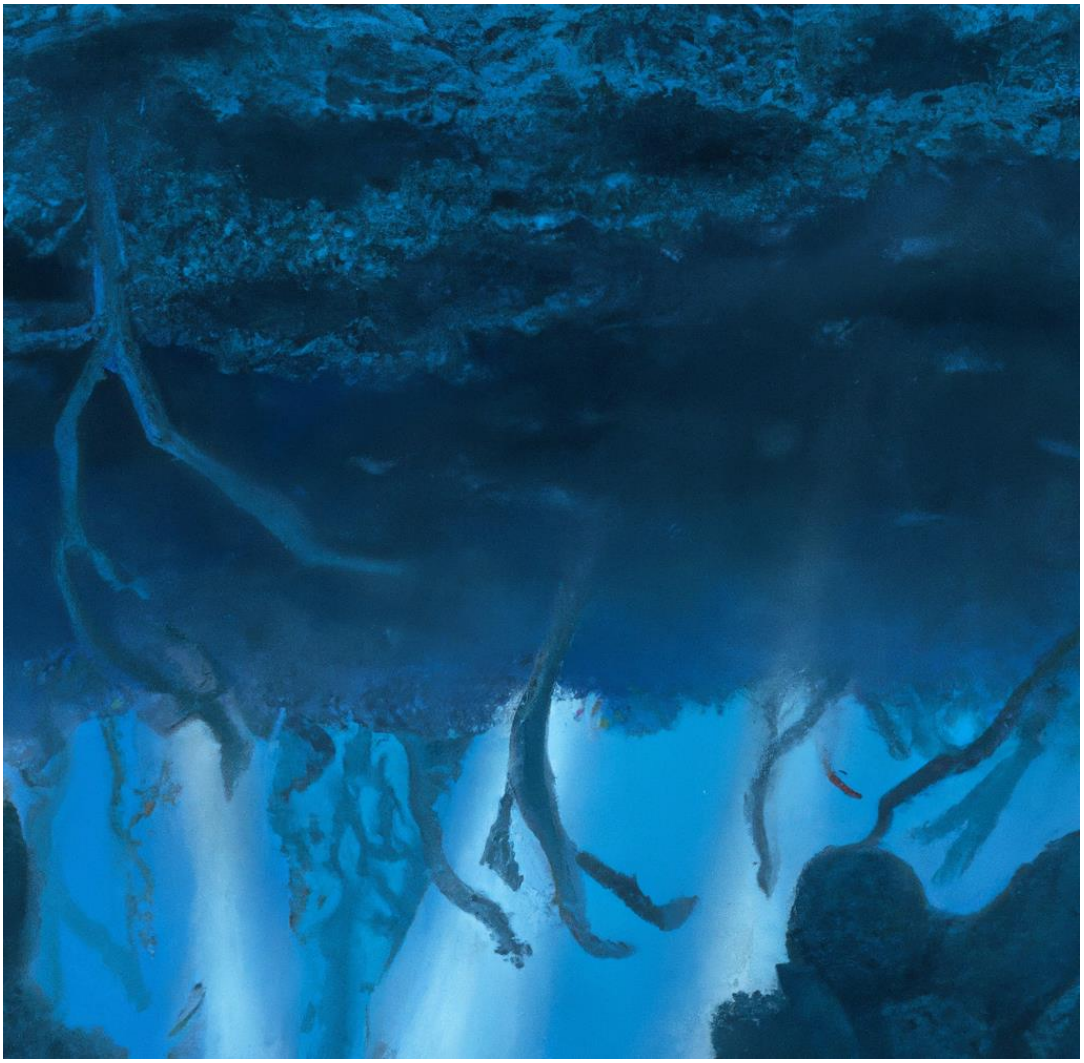

MAJOR RESULTS

MPA vs. nMPA: low frequencies

- ✓ Fish abundance was equivalent between MPAs and nMPAs, but MPAs showed a higher fish species richness, and a higher percentage of coral and algae cover than nMPAs. A transition from the east coast to the west coast was observed.
- ✓ PSD was lower in MPAs than in nMPAs, both during the day and night.
- ✓ Diurnal PSD displayed an opposite trend compared to the percentage of algae, meaning the diurnal acoustic mass phenomenon produced by fish was louder in sites with a low algae cover. Nocturnal PSD values were related to the presence of the majority of Holocentridae species.

MPA vs. nMPA: high frequencies

- ✓ PSD values were not statistically different between MPAs and nMPAs while spectral Fpeak was lower in MPAs than in nMPAs.
- ✓ The percentage of coral cover was higher on eastern sites.
- ✓ The total percentage of corals did not explain PSD. PSD values were associated with the presence of Porites, a genus of stony corals, known to inhabit snapping shrimps.

Pre-bleaching vs. post bleaching: low frequencies

- ✓ Diurnal PSD did not statistically differ when considering all the sites together.
- ✓ Only nocturnal PSD varied, with an average increase of 4.07 dB re 1µPa2 Hz−1. This increase was observed at all sites and was higher in MPAs than in nMPAs.
- ✓ All the sites, except eastern sites, had a reduction in coral cover. Eastern sites were the only two with an increase in coral cover. On the CCA, there were smaller changes for eastern sites.

Pre-bleaching vs. post bleaching: high frequencies

- ✓ Significant nocturnal PSD increases were only observed on the eastern sites.
- ✓ There was an interaction between protection status and the year both for diurnal and nocturnal PSD.
- ✓ A significant diurnal PSD decrease was only observed at one site. It was associated with a loss in coral cover by a factor of 3 and an increase in algae by a factor of 6,

Key question for the objective of the thesis

How does the biophony vary because of bleaching and protection measures?

Abstract

Marine Protected Areas (MPAs) can increase the resilience of coral reef communities to natural disturbances, playing a role in sheltering biodiversity from climate-related impacts and in the recovery of corals from bleaching events. The objective of this study is to determine if Passive Acoustic Monitoring (PAM) can assess a resilience effect of MPAs to coral bleaching events. To reach this goal, the biophony of the external slope of the coral reefs of different longstanding MPAs in Moorea Island were recorded in 2021 and compared to the one of adjacent zones outside the MPAs. Then, acoustic data from 2021 were compared to those from the same locations sampled in 2015, i.e., after and before two bleaching events (2016 and 2019). Our hypothesis is that the difference of the biophony between these two periods varies within and outside MPAs. The main result of this study is an increase in the nocturnal high-frequency (2 – 22 kHz) mass-phenomena of benthic invertebrates, observed only at sites with higher coral cover post-bleaching compared to the pre-bleaching periods. When assessing the mass-phenomena with PAM, the observed effect in 2021 is not a global effect of the MPAs. Instead, it reflects an interaction between time and the protection effect, associated with an east-west gradient in coral cover resulting from bleaching events. Therefore, PAM is not only effective in correlating coral cover with sounds but also in assessing the resilience effect of MPAs to bleaching events.

1. Introduction

In this century, mass bleaching events caused by extended high water temperatures due to climate change are a major and increasing cause of degradation of coral reef ecosystems [177–179,182–184,628]. They alter ecological processes of coral reefs (e.g., photosynthesis, reproduction, herbivory or predator-prey dynamics) [188] and can cause changes in the size, diversity and composition of the reefs and their associated fauna [189]. In Moorea (French Polynesia), regular monitoring of coral cover has revealed that bleaching events have occurred every 2-5 years over the last four decades [118] (Figure 60), resulting in a variation of the coral cover that oscillates from <10% to >80%. [629]. Between 2006 and 2010, a combination of bleaching events, crown-of-thorns sea star (*Acanthaster planci*) outbreaks and cyclones caused a loss of coral cover of around 60%, followed by a low restoration. In 2016, global warming combined to the El Niño event [630] affected coral reefs again [631], resulting in bleaching rates up to 44.4 to 61.2% [632]. However, the mortality was under 1% [632,633] and did not affect recruitment, [633], and consequent coral cover increase. In 2019, high-sea temperatures provoked a new severe bleaching event [634] in Moorea Island. This time, bleaching was associated with a significant decrease in coral cover (Figure 60).

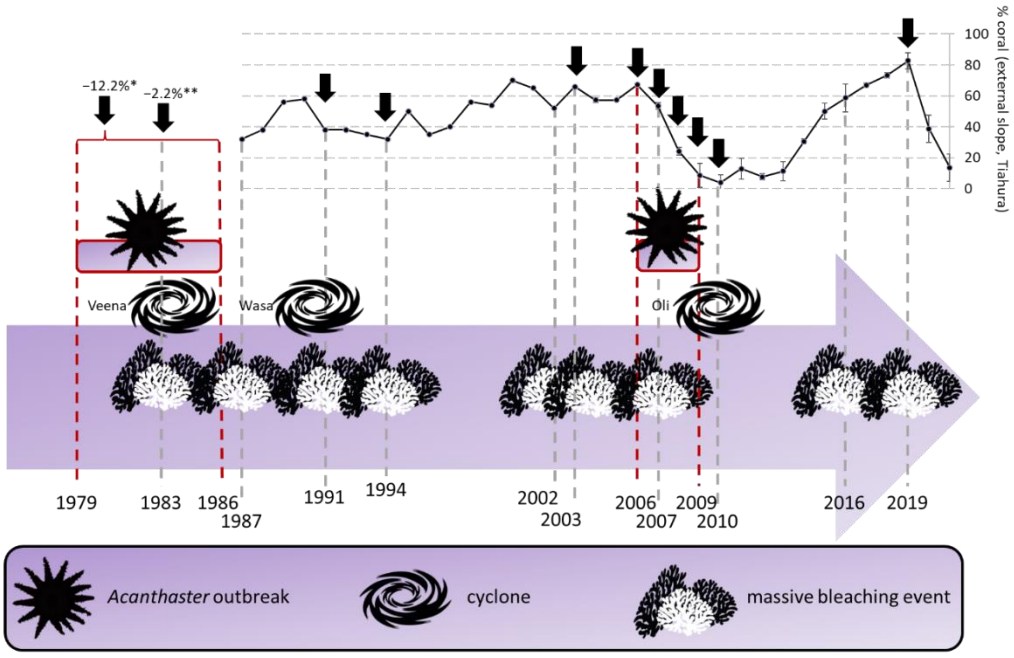

Figure 60 Timeline of negative events affecting the reefs of Moorea Island since 1979 and percentage of corals at the external slope of Tiahura (Northwest) since 1987. Black arrows indicate decreases in coral cover related to the presented events. The presence of a single event can cause a decrease in coral cover but not always. References: 1979-1986: [120,635], 1983: [178,636–638], 1987: [178,637,638], 1991: [628,638,639], 1994: [639–641], 2002: [639,641,642]; 2003: [642] Carroll et al. (unpulished data) IN [118], 2006-2009: [643–645], 2007: [639,644,646]; 2010: [188,645], 2016: [632,633,647], 2019: [634], coral cover between 1987 and 2003: [648]. *: [120,635] **: [636]. Vertical bars since 2004 are Standard Deviation.

Marine Protected Areas (MPAs) have been promoted as effective management tools to protect biodiversity at local and global scales [629]. They are known to increase the resilience of coral reef communities to natural disturbances, including coral bleaching, coral diseases, *Acanthaster* outbreaks and cyclones [649]. Therefore, MPAs can play an important role in protecting biodiversity from climate-related impacts and in the recovery of corals from massive bleaching events [650]. The *Plan de Gestion de l'Espace Maritime* (PGEM) is a network of eight MPAs on the island of Moorea. It was initiated in the early 90s and finalized in 2004 [651]. To promote spillover of fish densities outside the MPAs and to integrate the several 'associated communes', the decision was made to create small MPAs instead of a single large MPA [652]. Therefore, the largest width of these MPAs is 2 km. These MPAs are the only ones in French Polynesia for which an initial state has been described [652]. This island has the advantage of containing marine control areas (MCAs) which are non-protected areas that are used as 'controls' in the monitoring of MPAs [233]. Regulations within these MPAs include reduced boat speed, specific anchoring regulations, prohibitions on fishing, prohibition of shell collecting, protection of coral, prohibition of littering and discharging wastewater, and probation of modification of the shoreline. These MPAs cover various marine habitats such as typical lagoons of high volcanic islands, fringing reef, reef channel, and the external slope down to 70 m depth [652]. De loma et al. (2008) suggest that inside these MPAs, protection effects would be better detected in the outer slope habitat than in the barrier and fringing reefs, probably due to its less-variable geomorphology [629]. Despite the existence of these precise rules regulating marine spaces and the collection of specific resources, there are few resources deployed to enforce sanctions in case of violations [651]. This is both because of the difficulty of observing the infractions and the absence of penalties [651].

While classic monitoring involves visual scuba-diving observations, recent advances developed Passive Acoustic Monitoring (PAM) as a complementary method [158] (Chapter 6). Recording sounds is well suited for non-invasive long-term ecosystem-based monitoring as it provides information about abiotic, biological, and anthropogenic processes simultaneously [84]. Sounds emitted by animals can inform scientists on the presence, diversity and distribution of species, the phenology of biological events (e.g., diel, lunar and seasonal cycles of activity), and habitat quality [70,72,79,163,242,317,338,448,455,653–656]. Soundscapes of coastal reef ecosystems are dominated by passively emitted transient sounds form benthic invertebrates (BTS) and fish sounds that form mass phenomena [417] (Chapter 3). Sound pressure level (SPL) and acoustic indices generally applied to the coastal environment do not differentiate between different mass phenomena (Chapters 5 and 6). However, it has been shown that

different habitats show different combinations of mass phenomena [156,277,317,336], and that these features can differ between species and behaviors [65,243]. Also, the level of these mass phenomena is related to the abundance of sound-producing species.

In coral reefs, correlations have been found between the biophony (i.e., sounds emitted by animals within a particular ecosystem) and the coral cover [158]. The SPL of the coral reefs' biophony has been shown to differ between MPAs and non-protected areas, with higher SPLs in MPAs, possibly reflecting higher abundance of sound-producing species [158]. On the other hand, soundscape alteration has been shown to correlate with coral reef degradation [97,98]. PAM has therefore the potential to highlight differences in positive effects linked to protection measures and negative effects of coral reef degradation. However, these studies generally focus on very extreme reefs (e.g., pristine reef vs. very degraded reef). It remains largely unknown if soundscapes reflect combined effects of protection measures and impact of bleaching events. The objective of this study is to determine if PAM can be used to assess a resilience effect of MPAs to coral bleaching events. To do so, the biophony of the external slope of the coral reefs of different longstanding MPAs in Moorea Island were recorded in 2021 and compared to the one of adjacent zones outside the MPAs. Then, acoustic data from 2021 were compared to acoustic data from the same locations sampled in 2015, just before two bleaching events (2016 and 2019) that caused a mean coral cover loss of 10.2%. Our hypothesis is that the difference of the biophony between these two periods would vary within and outside MPAs.

2. Materials and methods

2.1. Data collection

The study was conducted on the outer slope of the coral reefs of Moorea Island (Society Archipelago, French Polynesia). Two different periods were investigated: pre-bleaching events, i.e., before the bleaching events of 2016 and 2019, and post-bleaching events. The initial sampling was carried out for 24 h in 2015 [158]. The second sampling took place over a period of 14 days in 2021. Both data collections were performed between the end of January and the beginning of May, corresponding to the warm season (Table SP9 - 1). For both sampling periods, the same eight sites were surveyed at a depth of 10 m: four located within MPAs (MPA_{West}, $MPA_{Northwest}$, MPA_{North}, MPA_{East}) and four outside MPAs ($nMPA_{West}$, $nMPA_{Northwest}$, $nMPA_{North}$, $nMPA_{East}$). These sites, namely Tetaiuo, Tiahura, Pihaena, Nuarei, Gendron, Papetoai, Entre-deux-baies, and Temae, were selected for the study (Figure 61).

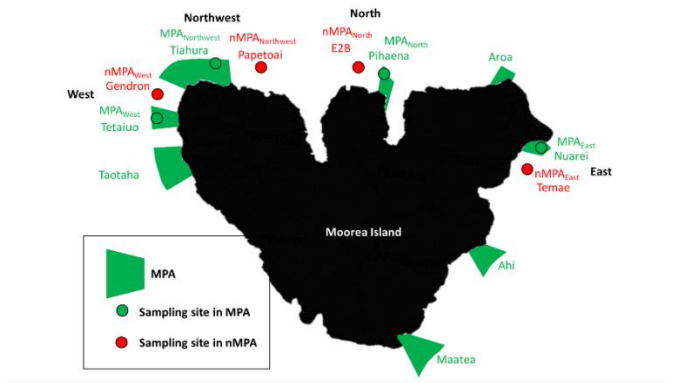

Figure 61 Sampling sites around Moorea Island: two on the west coast, two on the north-west coast, two on the north coast, and two on the east coast. MPA = marine protected area.

In 2015, an acoustic recorder miniDSG (Loggerhead Instruments; Sarasota, FL, USA) connected to an HTI-96 hydrophone (sensitivity: −181 dB re 1 V µPa^{-1}, gain: 10 dB) recorded sounds for 4.4 min per hour at a sampling rate of 48 kHz [158]. In 2021, acoustic recorders SNAP (Loggerhead Instruments; Sarasota, FL, USA) connected to HTI-96 hydrophones (sensitivity between −170.1 and −169.6 dB re 1 V µPa^{-1}, gain between 2 and 2.05 dB) continuously recorded sounds at a sampling rate of 44.1 kHz. For each site, data from 2021 were compared to the 24-hour recording from 2015. In 2021, four sites were sampled simultaneously (first set: MPA_{North}, $nMPA_{North}$, MPA_{East}, and $nMPA_{East}$; second set: $MPA_{NorthWest}$, $nMPA_{NorthWest}$, MPA_{West}, and $nMPA_{West}$) whereas opportunistic data were used during the 2015 campaign. In all the MPA except MPA_{East} fishing is prohibited as well as anyactivity leading to degradation of the marine environment. In MPA_{East}, fishing is allowed only with a line or for specific taxa (Gobiidae, Mullidae, and some Scrombidae). The $MPA_{NorthWest}$ includes a scientific reserve that has been protected since 1993.

2.2. Benthic cover and fish species

Benthic cover and fish diversity data were collected twice, once in February 2015 and again in February 2021, as part of the scientific monitoring program *Service National d'Observation CORAIL* (http://observatoire.criobe.pf). Data were available for all sites except for $nMPA_{Northwest}$. Surveys were conducted five days before the full moon and always during daytime [657]. At each site, three transect lines were laid parallel to the reef crest at a depth of 10 m (between 7 and 12 m). Each transect line was surveyed twice: once for fish diversity and once for benthic cover. Three replicates were completed for each transect [652]. The transect lines were 25 m long and 2 m wide (i.e., 50 m²).

Fish were surveyed from the surface to the bottom. All observed fishes were identified to the species level. The entire transect line was surveyed to record the occurrence of very large or highly mobile fishes, while smaller individuals and more territorial species were counted in 5 m subsections. This process was repeated five times to cover the entire 25 m transect. This method ensured equal observation time for each portion of the transect [629].

The benthic cover was quantified every 50 cm using the *Point Intercept Transect* method [658]. It was divided into ten categories (sand, rubble, dead coral, pavement, *Asparagopsis* algae, *Halimeda* algae, *Turbinaria* algae, others macroalgae, *Millepora* fire coral, and scleractinian corals, see Table SP9 - 2 for details) according to the procedure developed by Lison de Loma et al. (2008). Additionally, scleractinians were recorded to the genus level. The proportion (%) represented by each substrate type was calculated as the mean of the three transects. The total percentage of algae and the total percentage of coral cover were then calculated.

2.3. Acoustic analyses

To assess the mass phenomena produced by fish sounds, we focused on the low-frequency part of the soundscapes (bellow 2 kHz) because fish mainly emit sounds in this frequency range [246] (Chapters 3, 5, and 6). Separately, to assess the mass phenomena produced by benthic invertebrates, we focused on the high-frequency part of the soundscape (between 2 and 22 kHz) because this frequency range is known to contain BTS (Chapter 4) mainly produced by snapping shrimps [23,71,83]. In addition, soundscapes were divided into daytime (7 AM to 5 PM) and nigh-time (7 PM to 5 AM). The protection effect was first assessed using the data from 2021, and then compared to the ones from 2015. Each calendar day for each site was considered as a replicate.

To study low-frequency fish sounds, all the files were subsampled at 4 kHz. For the analyses of mass phenomena of high-frequency benthic invertebrate sounds, the files from 2015 were subsampled at 44.1 kHz. For the files from 2021, no sub-sampling was applied. Then, sound pressure spectrum levels graphs were generated with custom-made MatLab® routines (MathWorks, Natick, MA, USA) (LFFT = 256 and 64, overlap = 75% and 50% for low- and high-frequencies respectively, window = Kaiser). We decided to focus on the power spectral density (PSD) rather than on SPL because the SPL calculated between 0 and 2 kHz, as sometimes found in the literature to study fish sounds, is affected by the low-frequency part of BTS. PSD plots provide an overview of the levels of energy likely to occur at a given frequency and are source-specific if the source is abundant [84]. The calculation of PSD on frequency

bands that correspond to animals' vocalizations is, therefore, linked to the abundance of the vocal activity of these animals.

Two commonly used features were then measured on each median spectrum: the highest power spectral density value (PSD_{Fpeak}, in dB re 1 $\mu Pa^2\,Hz^{-1}$) and the corresponding frequency (γFpeak, in kHz). The γFpeak is defined as the frequency at which the power spectral density is maximal [340]. The recording system has an error of 3 dB. Therefore, changes below |3 dB| were considered as non-significant.

2.4. Statistical analyses: (1) MPAs vs. nMPAs in the low frequency fish sounds

All statistics were performed using the R software version 4.1.1. (R Core Team, 2021) with the significance level set at $\alpha = 0.05$. Acoustic data were averaged to obtain one data per site per day. Analyses of covariance (ANCOVA) (function *lme*) followed by type II tests (function *Anova*) were conducted for each response variable (diurnal PSD_{Fpeak}, nocturnal PSD_{Fpeak}, diurnal γFpeak, and nocturnal γFpeak) on the data collected in 2021 to estimate the presence or absence of protection as main effect [*protection* (two levels: MPA or nMPA)], site as random effect [*location* (West, Nort-West, North and East)] with *moon* phase as covariate. Analyses of variance (ANOVA) were used to compare fish abundance, fish species richness (number of different species present), and percentage of cover features between MPAs and nMPAs with *location* as a random factor. Violins plots were used for visualization (package *ggplot2*, function *geom-violin*). A Canonical Correspondence Analysis (CCA) was conducted to investigate the influence of benthic cover features (percentage of coral and percentage of algae) and acoustic features (diurnal PSD_{Fpeak}, nocturnal PSD_{Fpeak}, diurnal γFpeak, and nocturnal γFpeak) on fish assemblages (package *vegan*, function *cca*). The CCA was used to understand the link between fish species, and to relate these species to combinations of the features [431].

2.5. Statistical analyses: (2) MPAs vs. nMPAs in the high frequency BTS band

The same ANCOVAs and violin plots that were used for the low-frequency band were performed for the high-frequency band. A CCA was conducted to investigate the influence of benthic cover features (percentage of coral and percentage of algae) and acoustic features (diurnal PSD_{Fpeak}, nocturnal PSD_{Fpeak}, diurnal γFpeak, and nocturnal γFpeak) on coral cover composition (package *vegan*, function *cca*).

2.6. Statistical analyses: (3) pre- vs. post-bleaching in the low frequency fish sounds

ANCOVAs were carried for each response variable (diurnal PSD_{Fpeak}, nocturnal PSD_{Fpeak}, diurnal γFpeak, and nocturnal γFpeak). The complete dataset [2015 (n = 8) and 2021 (n = 112)] was used to assess the interaction effect of *year* and *protection* [*year* (two levels: 2015 or 2021)

* *protection* (two levels: MPA or nMPA), random = *location* (West, North, Northwest, and East) and *moon* phase = covariate]. Each calendar day for each site was considered as a temporal replicate. Only differences greater than |3| dB, i.e., the internal measurement error, were considered significant. Violins plots were used for visualization (package *ggplot2*, function *geom-violin*). A CCA on all the data was conducted to test the influence of benthic cover features (percentage of coral and percentage of algae) and acoustic features (diurnal PSD_{Fpeak}, nocturnal PSD_{Fpeak}, diurnal γFpeak, and nocturnal γFpeak) on fish community composition (package *vegan*, function *cca*). Protection (MPA or nMPA) and the year (2015 or 2021) were added as grouping variables to the ordination plot to visualize their relationships to fish community and features (function *ordiellipse*, with a 95% confidence interval).

2.7. Statistical analyses: (4) pre- vs. post-bleaching in the high frequency BTS band

The same ANCOVAs and violin plots that were used for the low-frequency band were applied to the high-frequency band. A CCA was performed to test the influence of benthic cover features (percentage of coral, algae, pavement, rubble, or sand) and acoustic features (diurnal PSD_{Fpeak}, nocturnal PSD_{Fpeak}, diurnal γFpeak, and nocturnal γFpeak) on coral cover composition (package *vegan*, function *cca*). The protection variable (MPA or nMPA) and the year (2015 or 2022) were added to the ordination plot to visualize their relationships with coral genera and features (function *ordiellipse*, with a 95% confidence interval).

3. Results

3.1. MPAs vs. nMPAs: low frequency fish sounds

In the low-frequency band (below 2 kHz) in 2021, diurnal γFpeak was lower in MPAs than in nMPAs (χ^2 = 111.62, df = 1, $P < 0.0001$, Table SP9 - 3). PSD_{Fpeak} was lower in MPAs than in nMPA, both during the day and night (χ^2 = 110.51 and 19, df = 1, both $P < 0.0001$, Figure 62). In 2021, fish abundance was equivalent between MPAs and nMPAs (χ^2 = 0.31, df = 1, P = 0.58, Figure 63, Table SP9 - 4), but MPAs showed a higher fish species richness (χ^2 = 4.45, df = 1, P = 0.035) and a higher percentage of coral and algae cover (χ^2 = 21.86 and 48.47, df = 1, both $P < 0.0001$) than nMPAs. The examination of the CCA ordination plot reveals that diurnal PSD_{Fpeak} displayed an opposite trend compared to the percentage of algae, implying that fish mass phenomena were louder in sites with a low algae cover (Figure 64). Some taxa like Chaetodontidae (Figure 64, cyan polygon) were clearly reef-associated. The majority of Holocentridae species (83.3%) were restricted to the upper left corner of the plot (Figure 64, blue polygon). This area coincides with intense nocturnal PSD_{Fpeak} values. These results coincide with a known high nocturnal feeding activity of Holocentridae [659]. Positive CCA1

values are associated with the West coast while negative CCA1 values are associated with the East coast.

3.2. MPAs vs. nMPAs: the high frequency BTS band

In the high-frequency band (between 2 and 22 kHz) in 2021, γFpeak was lower in MPAs than in nMPAs both during the day and the night (χ^2 = 145.74 and 103.84, both $P < 0.0001$, Figure 62). This difference is still within the known range of snapping shrimps' sound emissions. PSD_{Fpeak} values were not statistically different between MPAs and nMPAs (χ^2 = 0.27 and 1.69, P = 0.60 and 0.19). Positive CCA1 values were associated with the total percentage of corals and the presence of *Acropora*, a genus of usually arborescent/caespitose or tabular corals (Figure 65). The percentage of coral cover was higher on eastern sites (Figure 65). The total percentage of corals did not explain PSD_{Fpeak}. Negative values of CCA2 were associated with PSD_{Fpeak} and the presence of *Porites*, a genus of stony corals, known to host snapping shrimps [660].

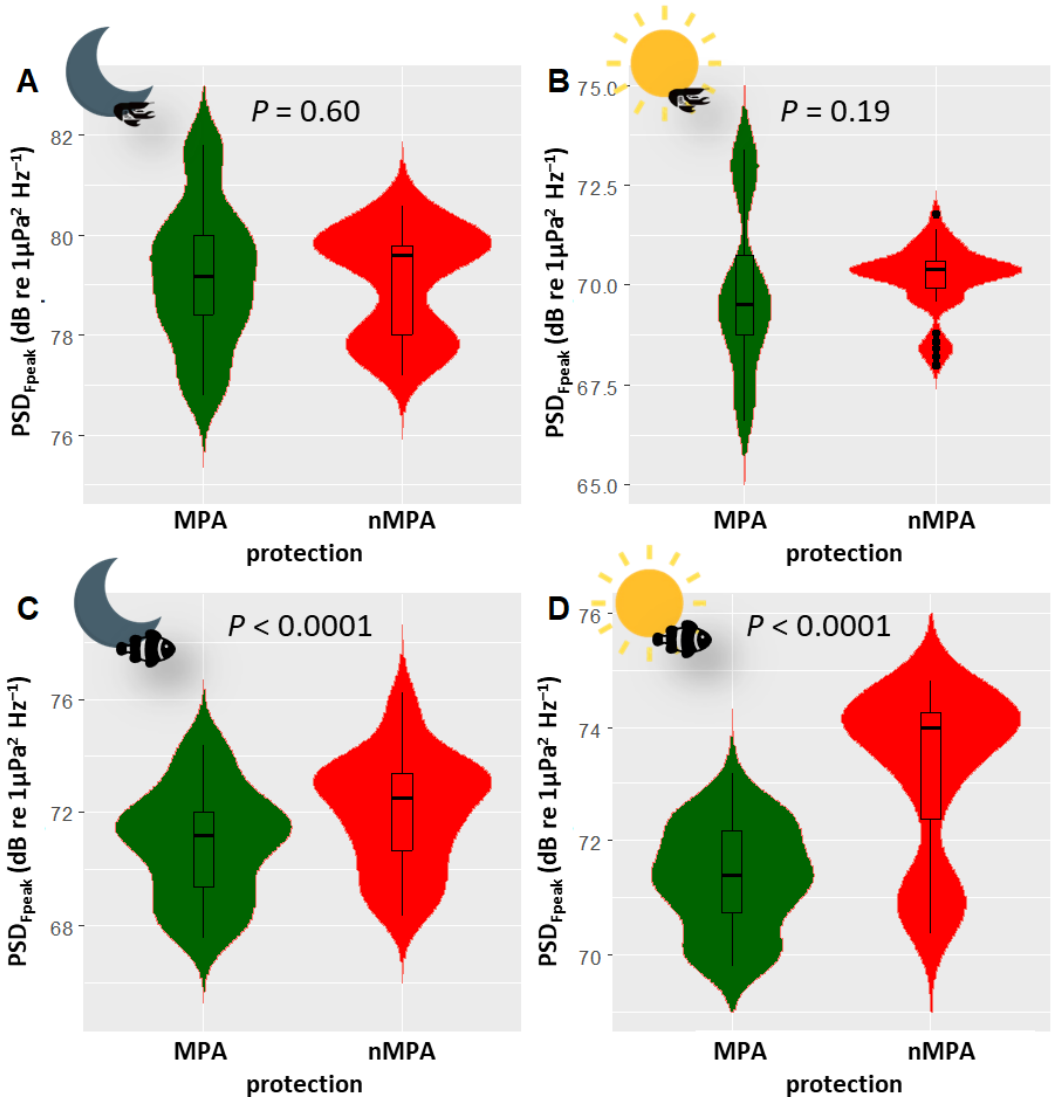

Figure 62 Violin plots of PSD_{Fpeak} in MPAs and nMPAs in 2021. (**A**) nocturnal high-frequency band, (**B**) diurnal high-frequency band, (**C**) nocturnal low-frequency band, and (**D**) diurnal low-frequency band.

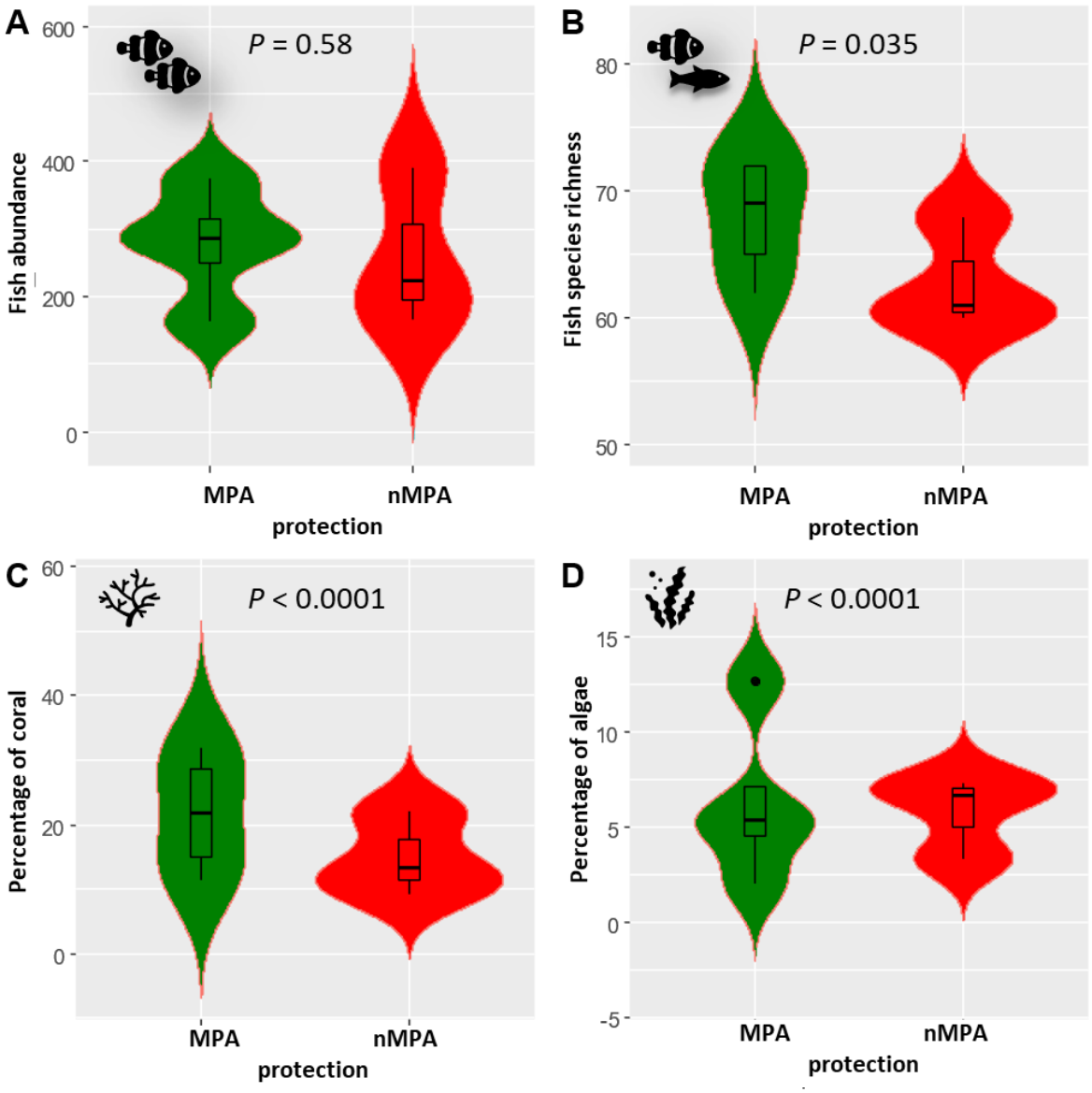

Figure 63 Violin plots of ecological features. (**A**) fish abundance, (**B**) fish species richness, (**C**) % of coral cover and (**D**) % of algae cover. MPA = marine protected area. nMPA = non-marine protected area.

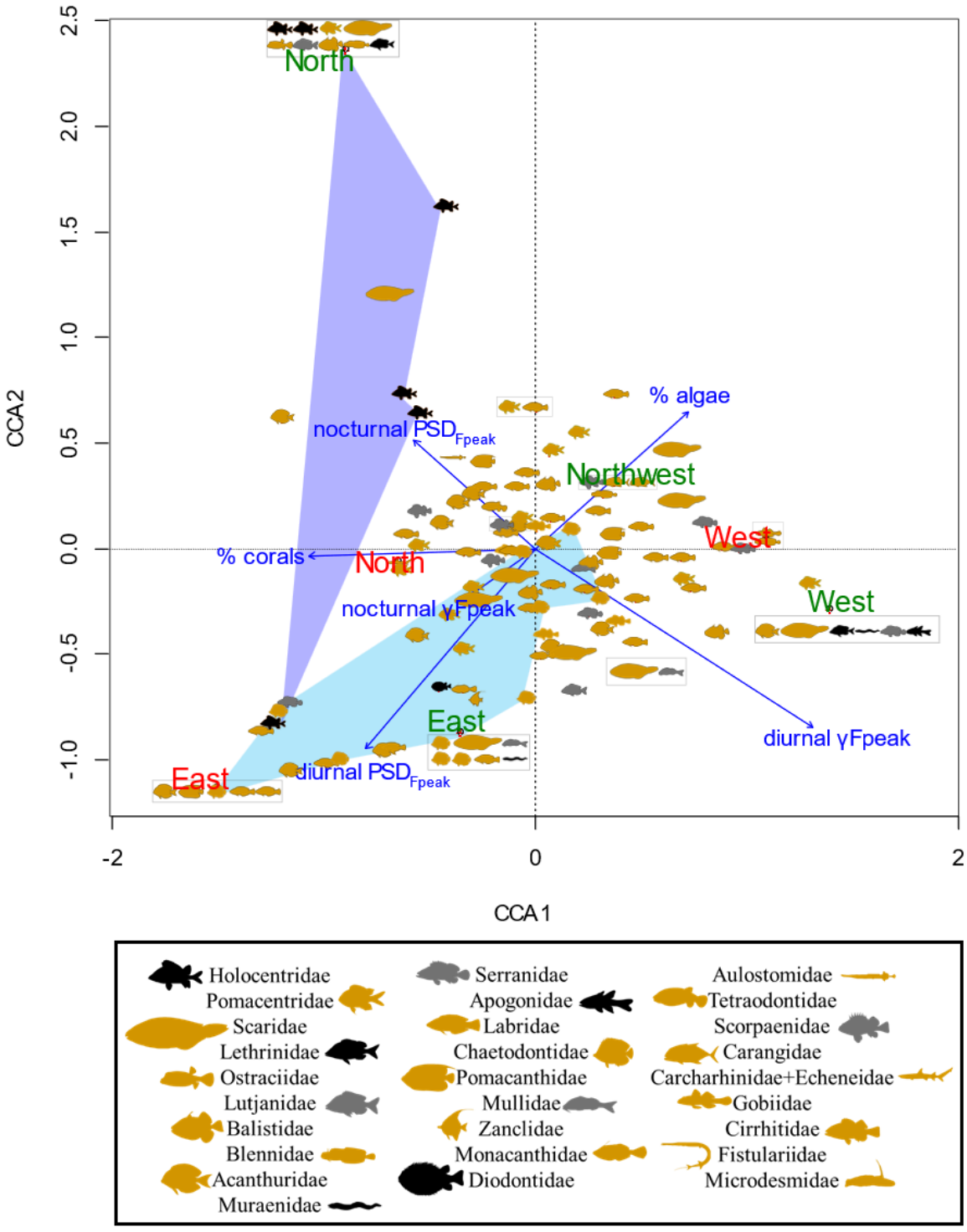

Figure 64 Canonical correspondence analysis ordination plot of fish assemblages based on Bray-Curtis dissimilarities of relative abundances of fish species. Acoustic features were calculated in the low-frequency band (< 2 kHz). Blue arrows show the influence of benthic cover and acoustic low-frequency features. Shapes were used per fish family (one datapoint per species). In yellow: diurnal families, in grey: diurnal and nocturnal families, in black: nocturnal families. Grey boxes gather species with the same CCA coordinates. Chaetodontidae appeared to be reef associated on the graph (cyan polygon) while the majority of Holocentridae species were restricted to the upper left corner of the plot (blue polygon) coinciding with intense nocturnal PSD_{Fpeak} values. Sites are indicated in green (MPAs) and red (nMPAs).

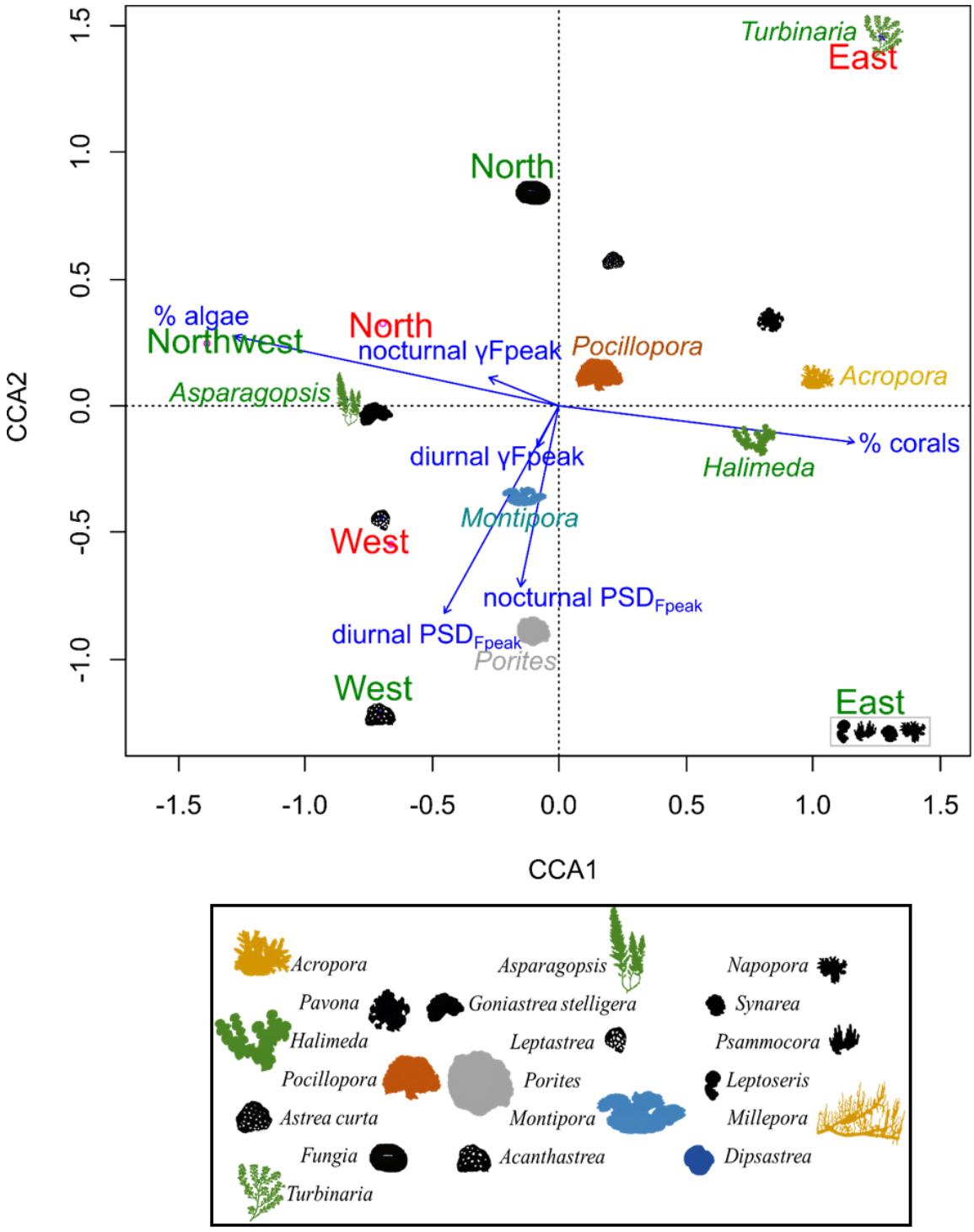

Figure 65 Canonical correspondence analysis ordination plot of the coral/algae assemblages based on Bray-Curtis dissimilarities of relative abundances of coral/algae genera. Acoustic features were calculated in the high-frequency band (2 – 22 kHz). Shapes were used per coral/algae genus. Blue arrows show the influence of benthic cover and acoustic high-frequency features. Sites are indicated in green (MPAs) and red (nMPAs).

3.3. Pre-bleaching vs. post-bleaching: low frequency fish sounds

In the low-frequency band, only nocturnal PSD_{Fpeak} varied between the two years ($\chi^2 = 44.82$, df = 1, n = 120, $P < 0.0001$), with an average increase of 4.07 dB re 1µPa^2 Hz^{-1} in 2021 (Table SP9 - 5 and Table SP9 - 6). This increase was observed at all sites (between 2.56 and 6.44 dB re 1µPa^2 Hz^{-1}) with maximal values at $MPA_{Northwest}$. This increase was higher in MPAs than in nMPAs (4.55 vs. 3.58 dB re 1 µPa^2 Hz^{-1}, Figure 66). Diurnal PSD_{Fpeak} did not statistically differ between 2015 and 2021 when considering all the sites together. A significant difference (i.e., higher than |3| dB) was observed only for $MPA_{Northwest}$ (3.83 dB re 1µPa^2 Hz^{-1}). Between 2015 and 2021, the CCA highlighted smaller changes for eastern sites than for all the other sites (Figure 67). This displacement is related to a decrease in coral cover and an increase in algae and pavement percentage. All the sites, except eastern sites, had a reduction in coral cover (between −34% and −3%). Eastern sites were the only two with an increase in coral cover (between +10% and +21%). All the sites had an increase in algae cover. All the sites, except the eastern sites, had an increase in pavement cover.

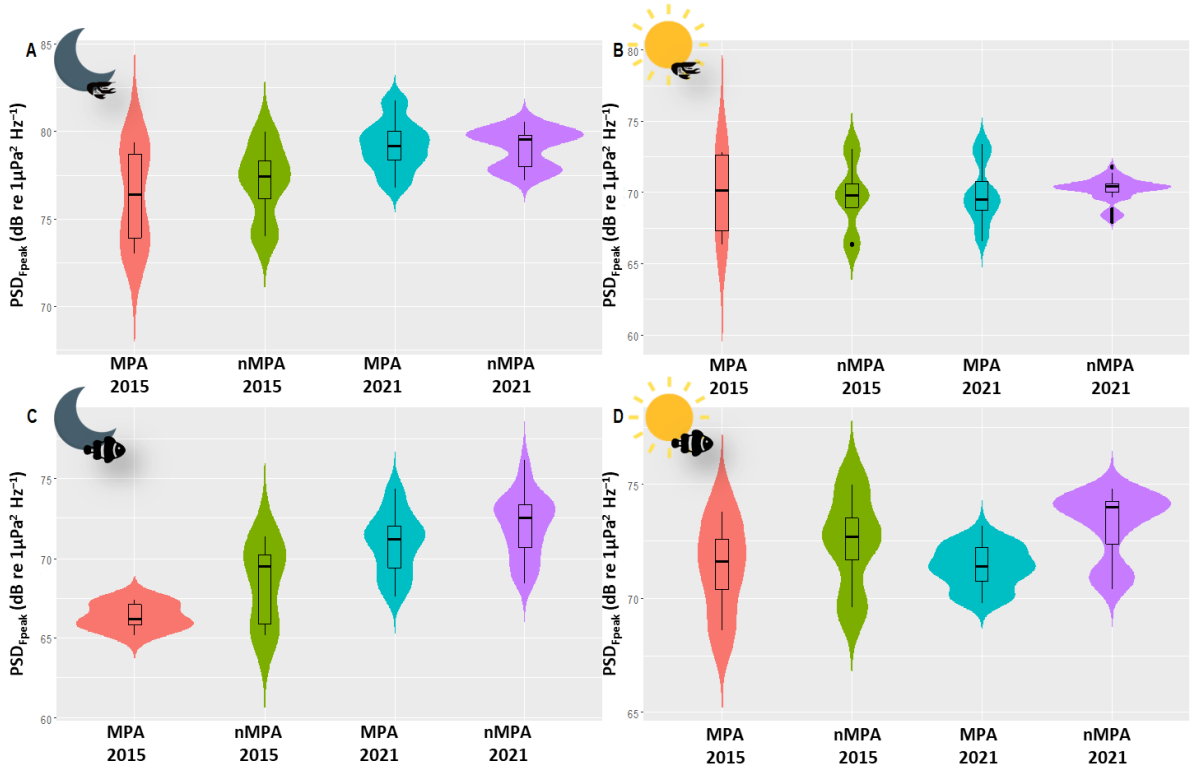

Figure 66 Violin plots of PSDFpeak in MPAs and nMPAs in 2015 and 2021. (**A**) nocturnal high-frequency band, (**B**) diurnal high-frequency band, (**C**) nocturnal low-frequency band, and (**D**) diurnal low-frequency band.

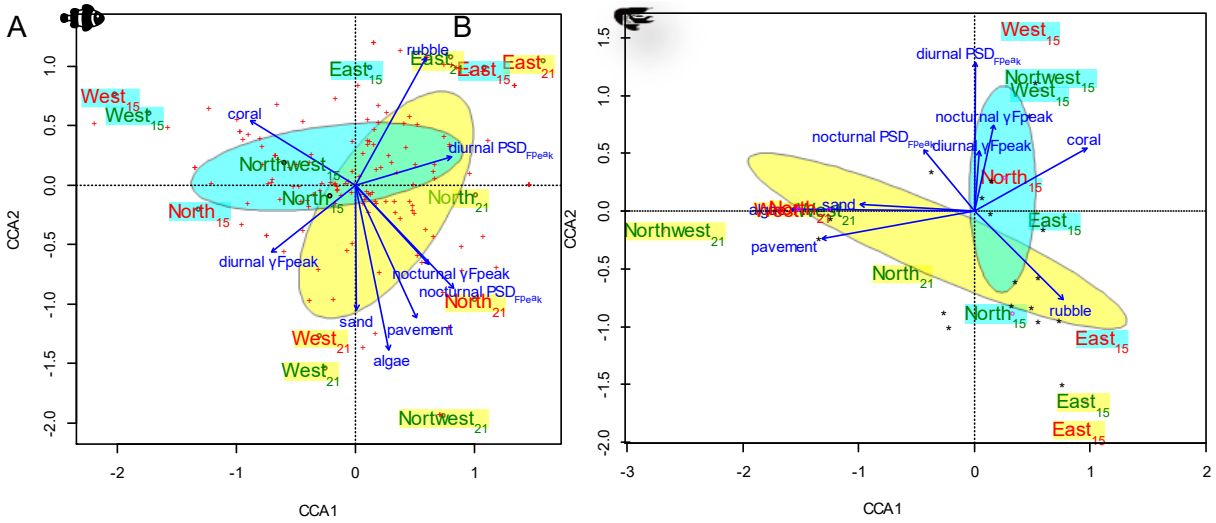

Figure 67 Canonical correspondence analysis ordination plot of (A) the fish and (B) coral/algae assemblages based on Bray-Curtis dissimilarities of relative abundances of (A) fish species and (B) coral/algae genera between 2015 (green) and 2021 (pink). Crosses show (**A**) fish species and (**B**) coral/algae genera. Blue arrows show the influence of benthic cover and (**A**) acoustic low-frequency features (**B**) high-frequency features. Sites are indicated in green (MPAs) and red (nMPAs). Ellipses are 95% interval: in cyan (2015) and yellow (2021).

3.4. Pre-bleaching vs. post-bleaching: the high frequency BTS band

In the high-frequency band, nocturnal PSD_{Fpeak} and γFpeak varied between 2015 and 2021 (χ^2 = 23.35 and 5.62, df = 1, n = 120, $P < 0.0001$ and = 0.018 respectively). The variation of nocturnal PSD_{Fpeak} was higher in MPAs than in nMPAs (increase of 2.88 vs. 1.96 dB re 1µPa^2 Hz^{-1}) but within the |3| dB error of the system. Nocturnal PSD_{Fpeak} variations > |3| dB were only observed on the three eastern sites (increase of 3.41, 4.79 and 5.93 dB re 1µPa^2 Hz^{-1}, Figure 68). There was an interaction between protection status and the year both for diurnal and nocturnal PSD_{Fpeak} (χ^2 = 40.90, df = 1, n = 120, $P < 0.0001$). Diurnal PSD_{Fpeak} variations > |3| dB were only observed at $MPA_{Northwest}$, with a decrease of 3.13 dB re 1µPa^2 Hz^{-1}. The examination of the CCA ordination plot reflects this decrease, also associated with a loss in coral cover by a factor of 3 and an increase in algae by a factor of 6. Diurnal PSD_{Fpeak} seems to be more associated with coral cover than nocturnal PSD_{Fpeak}.

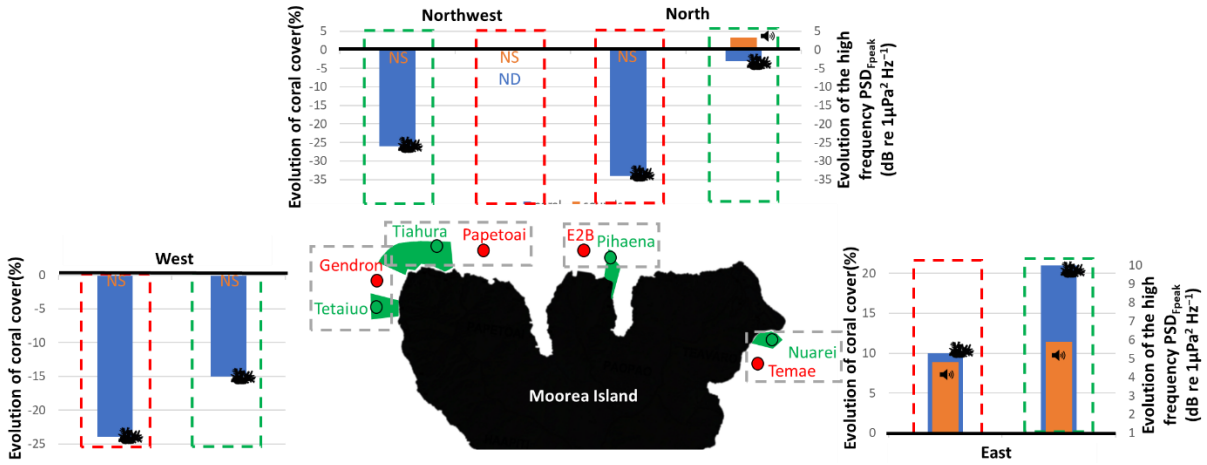

Figure 68 Schematization of the distribution of loss/gain in coral cover and high-frequency PSD_{Feak} (respectively in blue and orange) between 2015 and 2021. NS = non-significative. ND = no data.

4. Discussion

This study suggests that high-frequency soundscapes reflect a protection effect on coral cover after bleaching events. In fact, an increase in nocturnal high-frequency mass-phenomena of benthic invertebrates was observed only at sites with higher coral cover after the bleachings. The observed effect is not a global one, but rather an interaction between time and protection. This observation is also associated with an east-west gradient in coral cover resulting from varying bleaching histories. Therefore, PAM is not only effective in correlating coral cover via the biophony but it is also in comparing the evolution of coral cover between pre-bleaching and post-bleaching events. This is true both within and outside MPAs.

4.1. MPAs vs. nMPAs

In the high-frequency BTS band (between 2 and 22 kHz), no differences in PSD_{Fpeak} were found between MPAs and nMPAs. However, a difference of coral cover was observed between MPAs and nMPAs in 2021 (21.7% vs. 14.9%, respectively). This difference was not significant enough to be reflected acoustically when measuring only two parameters of the BTS mass-phenomena. In terms of fish mass-phenomena, diurnal PSD_{Fpeak} was lower in MPAs. It was also lower in sites with high algae cover. To understand this result, it is necessary to consider that, in addition to higher coral cover and greater fish species richness in MPAs, MPAs in Moorea had a higher percentage of algae cover as well. In addition, the comparison between MPAs and nMPAs is complicated by the violations related to prohibited fishing [651] reducing the observation of a MPA effect. Finally, γFpeak differed between MPAs and nMPAs. These last pattern may reflect differences in the species present responsible for the mass phenomenon. Further investigation is needed to better understand this result.

Correlations between low-frequency SPL and coral cover have been described in the literature, specifically at night [158]. However, caution is needed when using the SPL calculated between 0.02 and 2 kHz to infer fish acoustic behaviour, as it can be affected by the low-frequency component of broadband transient sounds produced by benthic invertebrates. This is not the case when using PSD_{Fpeak} measurements.

4.2. Pre-bleaching vs. post-bleaching

When comparing pre-bleaching and post-bleaching soundscapes, a significant increase in the nocturnal high-frequency biophony was found on the eastern sites. These findings are in agreement with visual observations showing that Eastern sites were the only ones with a higher coral cover in the post-bleaching period compared to the pre-bleaching period. In 2016, bleaching was more severe on the west coast (up to 100% *Acropora* colonies bleached) and on the north coast (twice the number of *Pocillopora* colonies bleached compared to the other coasts) [647]. The situation was more mitigated in the north coast than in the west coast [632,633]. In 2019, the bleaching event seems to have been shorter on the east coast compared to the west and north coasts [634]. Consequently, this resulted in a higher coral mortality on the north coast, intermediate mortality on the west coast, and lower mortality on the east coast. During the day, a significative decrease in PSD_{Fpeak} was observed at $MPA_{Northwest}$. This is consistent with the high coral mortality observed in this area (Service National d'Observation CORAIL). This positive relationship between high PSD_{Fpeak} values and coral cover agrees with the SPL observations made by Bertucci et al. (2021).

The impact of these bleachings was not equivalent across MPAs and nMPAs. In 2015, the MPAs had less coral cover than the surrounding areas, while in 2021, the MPAs had a higher percentage of coral compared to nMPAs. This change in coral cover highlights a resilience effect of Moorea's MPAs, an effect that can be effectively assessed using PAM. In the eastern sites, the resilience is clearly evident with PAM, whereas for the western sites, we can hypothesize that if the destruction of coral cover was too significant, more time is needed to observe a resilience effect.

4.3. Effectiveness of passive acoustics monitoring

In this study, we focused on the acoustic mass-phenomena produced by both fish and benthic invertebrates, mainly snapping shrimps [23,24,71]. It appears that the mass phenomena produced by fish may be less dependent of the health of the coral reef compared to the broadband transient sounds produced by snapping shrimps. It is known that Pomacentridae contribute significantly to the low-frequency mass phenomenon [397], and certain abundant

vocal species (e.g. *Stegastes* spp.) primarily feed on filamentous algae [661], which can also be found on degraded reefs. To obtain more information about the link between fish sounds and the health of the reef, it is likely necessary to study the diversity of fish sounds and not only two features of their mass phenomena (Chapter 6).

Among the various acoustic features tested, high-frequency PSD_{Fpeak} values demonstrated the strongest correlation with temporal changes in coral cover in Polynesian scleractinian-dominated habitats. Compared to fish sounds, benthic invertebrate sounds exhibit several advantages: (*1*) they are less masked by the geophony (which is crucial as the geophony level is known to increase due to a rise in storm frequency [16]) and the increasing anthropophony levels [662], (*2*) they more accurately reflect changes in coral cover and, (*3*) they are easier to assess with automatic methods. We suggest including a measurement of nocturnal benthic invertebrate sounds in long-term coral reef monitoring studies due to its cost-effectiveness and complementary nature with respect to classical monitoring methods.

5. Author contributions

Conceptualization, X.R.; methodology, X.R. and L.D.I.; software, C.G.; validation, X.R., L.D.I. and É.P.; formal analysis, X.R.; investigation, X.R.; resources, G.I., G.S. and F.B.; data curation, X.R. and F.B.; writing—original draft preparation, X.R..; writing—review and editing, X.R., É.P., L.D.I., F.B., and G.P.R.; visualization, X.R.; supervision, X.R., E.P., and L.D.I.; project administration, X.R.; funding acquisition, X.R.. All authors have read and agreed to the published version of the manuscript.

PART V: DISCUSSION

Chapter 10. General discussion

KEY INFORMATION

Variation and propagation of the 'mass-phenomena' biophony from coral reefs in the Anthropocene

- ✓ The use of acoustic cues is dependent of the loudness of the sounds from the reef that is impacted both by the anthropophony and by the modification of the biodiversity.
- ✓ They also depend on the non-loudness of the ambient noise off the reef that is impacted by ship traffic and by the geophony that is also impacted by (*1*) an increase in storm energy because of climate change, (*2*) sound absorption decrease caused by ocean acidification and (*3*) increasing anthropophony levels.
- ✓ Daytime and night-time sound levels, detection distances and impacts are not equivalent.

Production and variation of the biophony from photic and mesophotic reefs

- ✓ Depth was a major driver of differences of the types of biophony and their diel cycles.
- ✓ SPL was less intense at depth but peculiar peaks of BTS and many fish sound types were recorded in MCEs. The most abundant sounds were pseudo harmonic sounds sharing similarities with those produced by temperate species of Scorpaena.
- ✓ MCEs have their own communities which is reflected in their biophony.

Main conclusions

- ✓ The biophony can propagate up to 90 km, although maximal detection distances vary from less than 0.5 km to 22 km. Boat noise, bleaching events, and protection measures have been shown to impact the biophony and its detection distance.
- ✓ The biophony exhibited a vertical stratification. Similarities have been found between the sonic morphology of Polynesian species and known temperate sonic species from the same families producing sounds similar to those from Polynesian MCEs. Depth affected sound types, diel cycles, and sound specialization.
- ✓ Cyclic activities were found in deep MCEs; fish sound cycles and biophony changes after bleaching events were also noted.

Perspectives for further works

- ✓ To assess which sound types can serve as ecological indicators and to actively pursue the automatic detection of these sounds in Polynesian reefs.
- ✓ To test acoustic enrichment in Polynesian nMPAs.
- ✓ To enhance the identification of the sonic species by deploying cameras and networks of hydrophones in MCEs and in the reef-faunal zone below it, named the rariphotic zone.

General discussion

Coral reefs, being one of the most significant biodiversity hotspots on Earth, unsurprisingly exhibit a very rich biophony. All three primary vocal groups at sea (marine mammals, fish, and benthic invertebrates) are present in French Polynesian coral reefs. This thesis focuses on the study of sounds emitted by both fish and benthic invertebrates, revealing that these two taxa produce distinct sounds (low-frequency sounds in the case of fish, and broadband transient sounds at higher frequencies for benthic invertebrates).

In instances where a multitude of fish vocalize simultaneously or when the distance between the emitter and the acoustic recorder increases, fish sounds manifest as a 'mass phenomenon'. The methods employed to study 'mass phenomena' differ from those used to investigate discernable near sources of fish sounds. Consequently, these two categories were examined separately in this thesis.

1. Variation and propagation of the 'mass-phenomena' of the biophony from coral reefs in the Anthropocene

In the Anthropocene, this biophony is influenced by both anthropogenic acoustic and non-acoustic phenomena, which were examined in Chapters 3 and 9. When investigating the horizontal variations of the acoustic 'mass-phenomena' (Chapter 3), the reported propagation/detection distances were affected by anthropogenic factors (such as ship traffic), and by geophony. Additionally, in the Anthropocene, soundscapes are impacted, resulting in changes due to the globally increasing background noise caused by *(1)* elevated geophony levels linked to increased storm energy from climate change [16], *(2)* decreased sound absorption caused by ocean acidification [663,664] and *(3)* rising anthropophony levels [662] (Figure 69). Through this thesis, we performed a case study on these modifications on Polynesian photic reefs.

The 'mass-phenomena' of the biophony encompasses both numerous BTS (e.g., exceeding 100 s^{-1} in the 3.5 – 5.5 kHz band in the photic reef) and fish sounds at lower frequencies. These two phenomena contribute to the distinctive 'camel humps' pattern observed in PSD graphs in coral reefs (Figure 27A).

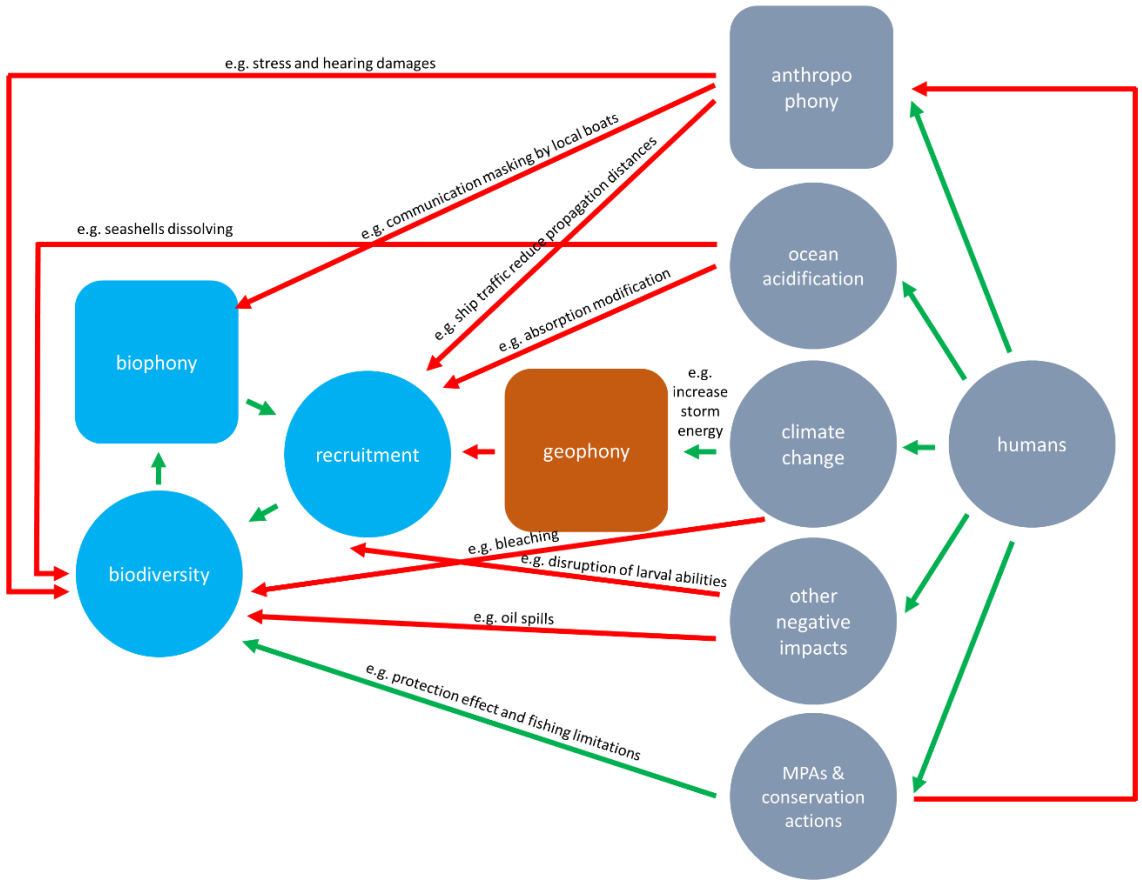

Figure 69 Relationships between human impacts, the biotope, and the biocenosis (in grey, brown, and blue respectively). Arrows indicate positive correlations (green) and negative correlations (red). The three main components of soundscapes (i.e., the biophony, geophony, and anthropophony) are represented by squares.

Understanding the (variation in) propagation of the biophony to the open ocean is crucial, as soundscapes are recognized to provide orientation and/or habitat choice cues for many taxa [128,133,134], including invertebrates [263–270], fish [271–276], and cetaceans [254,255]. In the literature, propagation and detection distances have been assessed using theoretical models [247–250]. In this thesis, in situ measurements revealed that benthic invertebrate sounds between 3.5 and 5.5 kHz could propagate over 50 km under an average wind regime of 6 kn. In contrast, fish sounds (200 to 500 Hz) would not propagate beyond 2 km.

When comparing these results with audiograms of different taxa, two distinct ranges emerge. The first is a long-distance range (up to more than 17 km) for cetacean orientation. The second is an intermediate distance range (up to 500 m) for fish and invertebrates post-larvae habitat choice. For the latter, sounds from the reef appear to be essential, along with other cues such as vision [129] and olfaction [127,130–132]. This multi-cue approach has been demonstrated in field experiments for fish larvae [665–667] and adults [668]. For instance, Lecchini et al. (2005) showed that detection distances increased when olfactory cues were added to visual/acoustic

cues. In the literature, this flexibility in cue choice is hypothesized to enhance fitness by increasing successful settlement [135]. Other studies suggest that larvae may orient differently depending on the distance to the reef [669,670]. Initially, they might orient by magnetic cues, polarized light, sun compass, or 'swim towards a particular cardinal direction maintaining an angle relative to the mean direction of surface capillary waves' [135,669]. Subsequently, they could use acoustic and olfactive cues [669]. Finally, vision becomes effective close to the reef for habitat-selection [135].

In the context of global change, the rise in atmospheric CO_2 levels resulted in increased H_2CO_3. This ocean acidification causes a decreased sound absorption at low frequencies (mainly below 500 Hz) due to absorption by borate ions only as the absorption due to magnesium sulfate is not pH-dependent [671]. In fine, the absorption decrease leads to amplified levels of ocean ambient noise [672], which impact propagation distances. The effective use of acoustic cues depends on the loudness of sounds originating from the reef and the absence of ambient noise beyond the reef. Unfortunately, in the Anthropocene, both conditions are impacted (Figure 69). The biophony is affected both directly by the anthropophony and indirectly by changes in biodiversity. Ship noises are categorized as traffic noise and passing ship's noise. Ship noise, generated by ship(s) in close proximity, causes short-term variations in the soundscape [5]. Traffic noise, on the other hand, results from the combined impact of all non-immediate ship traffic [5] across an entire basin, persisting even when no ships are visible nearby [4]. In Polynesia, the impact of ship noises is present but limited compared to other global regions. In addition, traffic noise affects propagation distances [212][213]. This thesis reveals that the impact is lower for BTS than for fish sounds. With a Wenz's ship traffic index of 2, propagation distances decreased by less than 1% for BTS (band: 3.5–5.5 kHz, ANL) and by a factor of 8 for fish sounds (200–500 Hz, γANL). Additionally, acoustic fish 'mass-phenomena' were louder during the daytime (a period with a higher local anthropophony) leading to diel differences in detection distances, with fish generally experiencing shorter detection ranges at night, but not for hearing specialist (e.g., Holocentridae, see Chapter 3). From a biological point of view, these differences are important as fish larvae move offshore at night [134,260,673] and are more abundant near reef waters at night [674]. However, fish settlement is complex with many species settling predominantly at night [673,675,676], but others during daytime [261,677] or both [673]. The nocturnal vocal activity in reefs should be even more important during some period, such as new moon periods, because it is known that moon phase has an influence on ichtyoplankton

near reef crest [678] with a tendency to settle at new moon periods [679] coinciding with peaks in reef biophony [680].

Biodiversity positively influences the biophony, which, in turn, positively influences recruitment. Ultimately, a higher recruitment rate contributes to increased biodiversity on the reef, sustaining a virtuous circle [681,682]. However, the difference between *virtuous* and *vicious* is subtle. An altered ecosystem will be acoustically modified, resulting in modified recruitment [190]. A major cause of coral reef degradation is climate change [177], as elevated sea temperatures are associated with mass bleaching events [178,179,182–184]. In Moorea Island, bleaching events have occurred every 2-5 years [118]. This includes the 'third global coral bleaching event' [630,631] in 2016.

In this thesis, we examined how PAM could be employed to assess the resilience of MPAs to long-term changes resulting from mass bleaching events. Recorders were deployed on the reefs in 2015 and again in 2020/2021, following the 2019 bleaching event that had a severe impact on Moorea reefs, causing colony mortality ranging from 11 to 42% within four months [634]. The most affected colonies were mainly those exceeding 30 cm in diameter, revealing a significant impact on the overall reef structure [634]. Our study on the impact of this event on biophony using PAM showed benthic invertebrate sounds were not only effective in correlating coral cover with sounds but also in assessing the resilience effect of MPAs to bleaching events. Among the advantages, we identified a lower impact by the geophony and anthropophony levels and a better suitability for automatic detectors. Regarding management strategies, incorporating measurements of benthic invertebrate sounds in coral reefs would allow to have a cost-effective method that could be used for long term assessment with a high temporal resolution both during daytime and night-time.

2. Production and variation of the biophony from photic and mesophotic reefs

To understand the variation in the biophony of Polynesian coral reefs, it was crucial to consider also the acoustic vertical aspect of the reefs. Therefore, we conducted for the first time different acoustic studies on the mesophotic part, which constitutes approximately 80% of coral reefs surface [321]. These studies focused both on benthic invertebrate sounds – examining their diel cycles and vertical stratification (Chapter 4) – and fish sounds. Fish sounds from MCEs were examined to understand (*1*) their variation with depth and type of island, (*2*) how depth influenced diel cycles and realized acoustic niches, and (*3*) which species could produce

them (see Chapters 6, 7, and 8, respectively). For both sounds of benthic invertebrates and fish, depth emerged as the primary driver of differences. When solely considering the SPL of the biophony, it was less intense at greater depth. However, distinctive peaks of BTS and many fish sound types were recorded in MCEs with a transition from the euphotic compartment to lower MCEs (Figure 70). Depth also influenced fish diel cycles and the temporal partitioning of the acoustic scene, leading to sound specialization with more specific time periods. The differences in the biophony of photic and mesophotic reefs also impact on α-acoustic indices, which exhibit variations in performance with harmonic sounds compared to PS sounds [396,414] (Chapter 5). For benthic invertebrate sounds, differences in terms of diel cycle were also highlighted between the lower MCEs and upper compartments.

In addition to vertical stratification, a quick look at Figure 70 also shows that one sound type clearly dominates the biophony of MCEs. This sound type, named AS4, is a pseudo harmonic ultrafast pulse series that account for 40 to 66% of all sound types during sunset in lower MCEs. AS4 is similar to a sound produced by temperate species of *Scorpaena* (Scorpaenidae). In Polynesia, lower MCEs host both *Scorpaena* and *Scorpaenopsis*, two closely related genera. These genera exhibit a similar sonic morphology, characterized by muscles prolonged by tendons including one with an unusual division into two bundles by the Baudelot's ligament. This sonic morphology markedly differs from that observed in other Scorpaenidae genera (e.g., *Dendrochirus*, *Pterois*, and *Pontinus*), further emphasizing the diversity in fish sonic morphology.

In the field of MCEs' ecology and conservation, the protection of MCEs has been grounded in their role as refugia for photic reefs based on the 'deep reef refuge' hypothesis [109,111,683]. Due to an overlap between MCEs and photic communities, some species that had disappeared in photic reefs may persist in MCEs [684,685], subsequently recovering in photic reefs via vertical connectivity [686,687]. However, recent studies emphasize that MCEs are biologically diverse [688,689] with a high level of endemism [690] and unique communities [691,692], constituting a new argument for their protection [693]. The peculiarities of the MCEs' biophony in Polynesia align with the findings of this second set of studies.

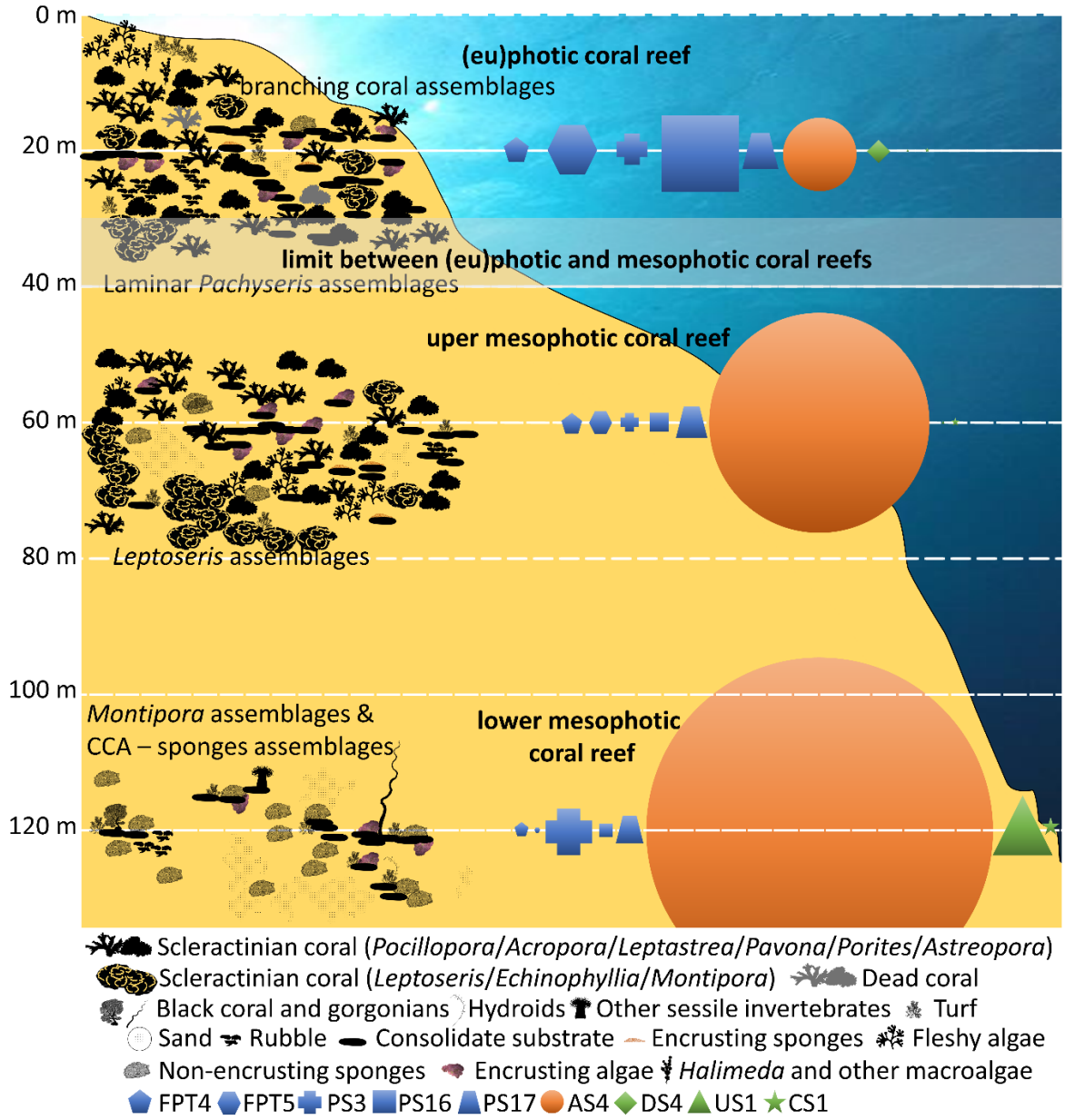

Figure 70 Schematization of vertical differences in fish sound types in Polynesian coral reefs during sunset. Slope between the surface and 80 m is based on Moorea Island (Tiahura) [122–125]. Benthic cover assemblages are based on biological data from Chapter 4 and 6 except for the diversity of scleractinian which is based on [332]. The superior depth limit of mesophotic coral reefs is based on [106–108]. Shapes represent the most abundant fish sounds recorded between 5 and 7 PM (see Chapter 4) colored by acoustic category: pulse series *stricto sensu* (in blue), ultrafast pulse series (arched sound, in orange), and frequency modulated sounds (in green). Sound types are named according to Chapter 4. FPT = fast pulse train, PS = pulse series, AS = arched sound, DS = downsweep, US = upsweep, CS = complex sound, CCA = crustose coralline algae.

3. Main conclusions

The biophony of French Polynesian coral reefs encompasses both fish and benthic invertebrate sounds. It varies along horizontal axes (both offshore and lateral) and a vertical axis. In addition, these axes are subject to temporal variations.

From the reef to the open ocean, the biophony can propagate up to 90 km, although maximal detection distances vary depending on the species and life stage, ranging from less than 0.5 km to 22 km. In the Anthropocene, however, these distances can be diminished due to both meteorological conditions and anthropogenic noise. Lateral variations in the biophony depend on features such as benthic cover (e.g., coral or algae percentage).

Along the vertical gradient, both benthic invertebrate and fish sounds exhibit stratification primarily driven by depth. Several sounds from MCEs shared similarities with those emitted by species from other environments. The sonic morphology of those species shared similarities with the ones found in species from Polynesian MCEs.

The temporal axis can be studied at various time scales. In photic reefs and upper MCEs, sounds produced by benthic invertebrates were louder at night but more abundant during the daytime. However, in lower MCEs, the activity rhythms of benthic invertebrates exhibited low or highly variable levels of diel variation. Nevertheless, a distinct peak in the number of BTS was observed between 7 and 9 PM at a depth of 120 m, potentially indicating cyclic activities of a particular species and supporting the existence of different invertebrate communities, particularly in deep mesophotic reefs. Diel cycles of fish sounds were also influenced by depth. At a longer time scale, changes in the biophony have been observed between bleaching events in French Polynesia, attributed to variations in coral cover.

4. Perspectives for further works

4.1. Ecological indicators and automatic detection of discriminable near sources of fish sounds

In this thesis, high-frequency (i.e., 2 to 22 kHz) PSD measurements were shown to be effective in accessing changes in coral cover over time. This effectiveness was not observed for low-frequency (i.e., below 2 kHz) PSD measurements. Differences in γFpeak and PSD_{Fpeak} were observed between MPAs and nMPA (Chapter 9). These differences are presumed to be linked to variations in species composition, but further investigations are required for a comprehensive understanding. To delve deeper into these distinctions, we are examining different fish sound types at the level of the individually identifiable sounds of the biophony, using the methodology described in Chapter 6 and data from Chapter 9 [694]. Comparing sound types between MPAs and nMPAs will help identify which sound types can provide insights into the reef's condition (e.g., high coral cover). In the Mediterranean Sea, a sound type named /*kwa*/ has proven to be relevant for monitoring seagrass meadows. This sound has a higher

frequency compared to other concomitant fish sounds and, therefore, was the only sound detectable under anthropogenic noise conditions [281]. Similar studies have not yet been conducted in coral reefs.

Once the relevance of a sound type as an ecological indicator will have been established in coral reefs, automatic detection methods could be employed to circumvent time-consuming manual work. For acoustic data, automatic methods, such as machine learning techniques, have the potential for a significant impact and have recently gained more attention [695]. However, until recently, many of these methods were constrained by the requirement for large amounts of data for testing and training [695]. Moreover, the training dataset should encompass all variability within the sound type under study [696]. For these two reasons, it is challenging to use machine learning techniques for rare sounds, that are pertinent in acoustic biodiversity assessment [84]. Thus, the need has been expressed by the scientific community to develop a web-based reference library and a training platform for artificial intelligence algorithms [697].

Currently, various methods have proven successful in detecting temperate fish sounds in their natural environment. These methods have been independently developed by different teams to detect sounds produced by one or several taxa, such as Batrachoididae [698,699], Labridae [700], Sciaenidae [701–704], Serranidae [595,705], or Ophidiidae [706]. However, not all algorithms are universally effective for all species. For instance, the algorithm developed for *Halobatrachus didactylus* sounds does not perform well for other concomitant sound types [698]. Conversely, the algorithm developed by Le bot et al. (2015) [707] is suitable for PS sounds (e.g., for UFPS = *kwa*, PS and APPPS [163]) but not for FM. Sounds produced by *H. didactylus* share several similarities with FM sounds from Polynesian mesophotic reefs (e.g., CS1), even if they are not produced by the same fish family (see Chapter 6 for the sound description and Chapter 8 for shared similarities). On the other hand, UFPS, PS, and APPPS are highly similar to sounds like AS4, PS7, and PS10, respectively. Due to their similarity, we suggest testing such methods on coral reefs sounds. Preliminary testing of the method developed by Le bot et al. (2015) for detecting Polynesian fish sounds was carried out. The algorithm was tested under five conditions: (*1*) only high SNR sounds of interest, (*2*) a mix of low and high SNR sounds of interest, (*3*) a mix of sounds of interest and other fish sounds, (*4*) only other fish sounds, and (*5*) a mix of fish sounds and anthropogenic noise (Figure SP10 - 1). Preliminary results indicate good potential of this method for AS4 sounds from MCEs. Further research needs to be conducted to apply existing algorithms developed for temperate fish sounds to more coral reefs fish sounds. More recently, the automation process in bioacoustics

research has been standardized through convolutional neural networks (CNN) – for an exception example see hidden Markov models [698] – a methodology derived from image processing [708–710]. In fish, examples of CNN use are found in diverse taxa such as Pomacentridae [711], Scianidae [704], and Serranidae [705]. When the study does not center on a specific species, the uniform manifold approximation and projection (UMAP) followed by hierarchical density-based spatial clustering (HDBSCAN) could be an approach to study fish sounds over extended time periods [712].

4.2. Automatic methods for the 'mass-phenomena' biophony

In this thesis, the 'mass-phenomena' biophony was investigated using long-term spectrogram analysis and power spectral density plots, both of which are influenced by continuous signals. To enhance the detection of transient signals, an existing method involves calculating the difference between a classical spectrogram (combining background ambient noise and transient sounds, denoted as RL) and a spectrogram of the background noise only (ANL) [84,280]. This calculation results in a spectrogram highlighting only the transient sounds (RL – ANL) [84]. Automatic methods to suppress environmental and anthropogenic noise to focus on fish choruses without a need for training data [703,713,714] and with CNNs are being developed [715]. Similarly, SoundScape Learning uses unsupervised automated method through integration of both unsupervised clustering and a neural network to detect fish chorus [716].

In Polynesian reefs, within a low frequency band (10 – 800 Hz), pattern recognition algorithms successfully differentiated sound sources into four groups: geophony, anthropophony, biophony, and unidentified sounds [325]. In addition, based on preliminary results with data from Polynesian coral reefs, UMAP appears capable of detecting boats, whales, and depth-induced variations. Further investigation is necessary to assess how these software tools could be employed for studying the complex underwater biophony present in coral reefs.

4.3. In mesophotic reefs

In this thesis, bathymetric and diel differences were explored in mesophotic reefs. While both fish and benthic invertebrate were studied as the two main categories of sonic species, the focus of identification was on fish. Nevertheless, distinctive sonic cycles of high frequency sounds were observed around 7 PM at a depth of 120 m. This finding warrants further investigation to identify the (group of) species responsible for this sonic activity. However, identifying this taxon poses a significant challenge. One approach could involve sampling

various benthic invertebrates at 120 m and recording them in aquaria. Both the capture of specimens and their transfer to the surface have a high failure rate. Another option would be to use cameras for in situ filming. However, light interference could affect this nocturnal sound emission, and the probability that the emitting species is small and/or cryptic is very high. In my opinion, a more effective strategy would be to introduce an additional step prior to the identification process. I recommend employing a network of hydrophones to obtain more precise information regarding the microhabitat type used by this taxon.

4.4. Below mesophotic reefs

This thesis delves into a wide depth range, extending from the surface down to 120 m. This span encompasses both the (alti)photic (0 to 30/40 m) and the mesophotic zone (30/40 to 130/150 m) of the reefs. However, tropical photosymbiotic reefs extend beyond the 120-m mark. Current knowledge places the lower limit of photosymbiotic scleractinian corals at 172 m [110], as demonstrated by *Leptoseris hawaiiensis* in the Gambier Archipelago (French Polynesia), thriving in an environment with less than 1% surface irradiance [110]. The reef-faunal zone immediately below the mesophotic but above the deep aphotic is termed rariphotic [107]. The rariphotic zone forms a continuum of reef fishes with the altiphotic and mesophotic zones [107]. Despite this continuity, the rariphotic fish assemblage exhibits distinct characteristics [717]. Regarding benthic communities, connectivity to shallow reefs from the rariphotic zone is limited [718]. This underscores the importance of managing deep reefs as separate entities from shallow reefs [718].

Nothing is known about the biophony of the rariphotic zone in French Polynesia. For this thesis, data on MCEs were collected with rebreather scuba-divers. However, this technique is not suitable to study the rariphotic zone. Depths below 150 m have been researched mostly with submersibles and unmanned vehicles [719]. For PAM, a more cost-effective option involves employing an acoustic release, comprising a hydrophone, a battery, and a hook. An acoustic signal is used to remotely open the hook, triggering the release of the anchor. A preliminary investigation into the biophony of the lower rariphotic zone (240 – 319 m, [235]) was conducted on Moorea Island during the ULIEGE-22 mission. A SNAP recorder (Loggerhead Instruments, Sarasota, FL, USA) connected to a HTI96 hydrophone (High Tech Inc., Long Beach, MS, USA) was affixed to an Acoustic Release AR701 (iXblue, Saint-Germain-en-Laye, France) (Figure SP10 - 2). After ten days of continuous recording, it was retrieved with a TT701 telecomand (iXblue, Saint-Germain-en-Laye, France).

Preliminary spectrogram observations reveal boat passages during the daytime, while transient sounds, characterized by a peak frequency of approximately 9 kHz, are detected 30 minutes after sunset for approximately 15 minutes (Figure 71 and Figure 72). In the low-frequency band (i.e., below 2 kHz), there is an abundance of whale vocalizations and fish sounds (Figure SP10 - 3 and Figure SP10 - 4). These fish sounds appear to share similarities with some sound types found in mesophotic reefs. Further in-depth investigations are necessary to gain better understanding of the biophony of the rariphotic zone.

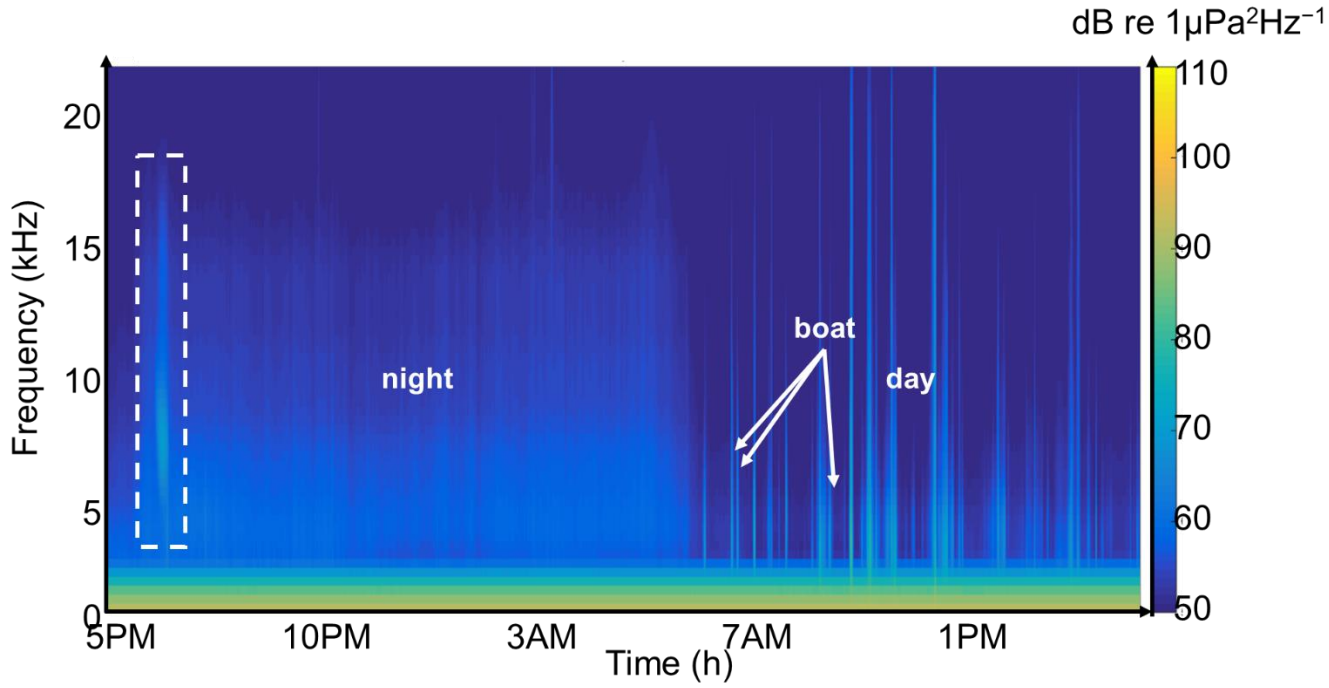

Figure 71 Spectrogram of the soundscape recorded at 300 m at Moorea (24h, from 5PM to 4:59 PM). LFFT = 64, overlap = 50%, window = Kaiser. The white dotted box highlights a sound production during ca. 15 min from ca. 6:10PM with a peak frequency around ca. 9 kHz.

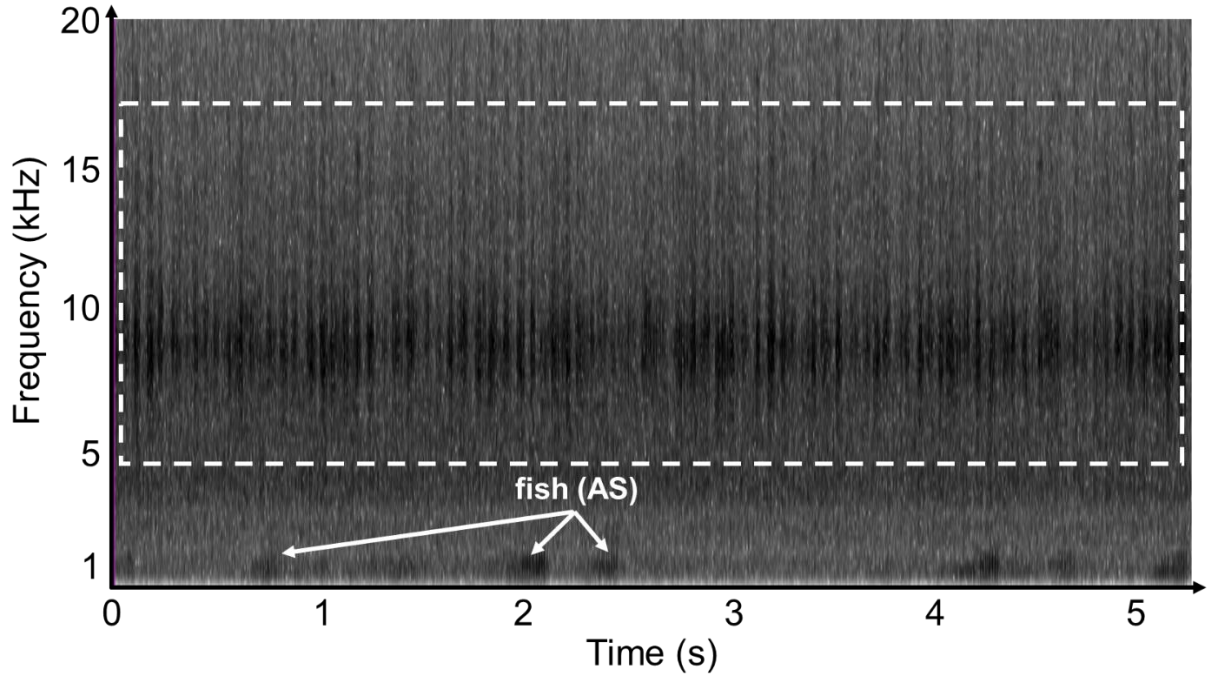

Figure 72 Spectrogram of the soundscape recorded at 300 m at Moorea around 6:15 PM between 1 and 20 kHz. FFT = 256. The white dotted box highlights a sound production during ca. 15 min from ca. 6:10PM with a peak frequency around ca. 9 kHz.

References

1. Krause, B. Bioacoustics: Habitat Ambience & Ecological Balance. *Whole Earth Rev.* **1987**, *57*, 14–16.
2. Schafer, R.M. *The Tuning of the World*; Knopf, Ed.; 1977; ISBN 9780394409665.
3. Au, W.W.L.; Hastings, M.C. *Principles of Marine Bioacoustics*; Springer US: New York, NY, 2008; ISBN 978-0-387-78364-2.
4. Hildebrand, J. Anthropogenic and natural sources of ambient noise in the ocean. *Mar. Ecol. Prog. Ser.* **2009**, *395*, 5–20, doi:10.3354/meps08353.
5. Wenz, G.M. Acoustic Ambient Noise in the Ocean: Spectra and Sources. *J. Acoust. Soc. Am.* **1962**, *34*, 1936–1956, doi:10.1121/1.1909155.
6. Franz, G.J. Splashes as Sources of Sound in Liquids. *J. Acoust. Soc. Am.* **1959**, *31*, 1080–1096, doi:10.1121/1.1907831.
7. Neumann, G. *On ocean wave spectra and a new method of forecasting wind-generated sea*, *U. S. Army, Corps of Engineers, Beach Erosion Board, Tech. Memo. No. 43*; 1953;
8. Pierson, W.J. Wind Generated Gravity Waves. *Adv. Geophys.* **1955**, *2*, 93–178, doi:10.1016/S0065-2687(08)60312-X.
9. Mellen, R.H. The Thermal-Noise Limit in the Detection of Underwater Acoustic Signals. *J. Acoust. Soc. Am.* **1952**, *24*, 478–480, doi:10.1121/1.1906924.
10. Dawson, P. The physics of the oscillating bubble made simple. *Eur. J. Radiol.* **2002**, *41*, 176–178, doi:10.1016/S0720-048X(02)00023-2.
11. Strasberg, M. Gas Bubbles as Sources of Sound in Liquids. *J. Acoust. Soc. Am.* **1956**, *28*, 20–26, doi:10.1121/1.1908212.
12. Tolstoy, I.; Ewing, M. The T phase of shallow-focus earthquakes. *Bull. Seismol. Soc. Am.* **1950**, *40*, 25–51, doi:10.1785/BSSA0400010025.
13. Shurbet, D.H. Bermuda T phases with large continental paths. *Seism. Soc. Am. Bull* **1955**, *45*, 23–25, doi:10.1785/BSSA0450010023.
14. Ross, D. *Mechanics of underwater noise*; Pergamon Press: New York, 1976; ISBN 978-0-08-021182-4.
15. Andrew, R.K.; Howe, B.M.; Mercer, J.A.; Dzieciuch, M.A. Ocean ambient sound: Comparing the 1960s with the 1990s for a receiver off the California coast. *Acoust. Res. Lett. Online* **2002**, *3*, 65–70, doi:10.1121/1.1461915.
16. Duarte, C.M.; Chapuis, L.; Collin, S.P.; Costa, D.P.; Devassy, R.P.; Eguiluz, V.M.; Erbe, C.; Gordon, T.A.C.; Halpern, B.S.; Harding, H.R.; et al. The soundscape of the Anthropocene ocean. *Science (80-.).* **2021**, *371*, doi:10.1126/science.aba4658.
17. Munk, W.H.; O'Reilly, W.C.; Reid, J.L. Australia-Bermuda Sound Transmission Experiment (1960) Revisited. *J. Phys. Oceanogr.* **1988**, *18*, 1876–1898, doi:10.1175/1520-0485(1988)018<1876:ABSTER>2.0.CO;2.
18. Dragoset, W.H. A comprehensive method for evaluating the design of air guns and air gun arrays. *Lead. Edge* **1984**, *3*, 52–61, doi:10.1190/1.1439027.
19. Simmonds, E.J.; MacLennan, D.N. *Fisheries acoustics: theory and practice*; Blackwell Publishing: London, 2005; ISBN 9780632059942.
20. Pepper, P.A.; Turner, V.L.G.; Goodson, A.D.; Black, K.D. Source levels and spectra emitted by three commercial aquaculture anti-predation devices. In *Proc 7th European Conf on Underwater Acoustics, ECUA 2004. Commission of the European Communities*; Simons, D.G., Blackquiere, G., Eds.; Delft, 2004.
21. Fish, M.P.; Mowbray, W.H. *Sounds of western North Atlantic fishes: a reference file of biological underwater sounds*; Press, J.H., Ed.; Baltimore, 1970; ISBN 9780801811302.

22. Kellogg, W.N.; Kohler, R.; Morris, H.N. Porpoise Sounds as Sonar Signals. *Science (80-.).* **1953**, *117*, 239–243, doi:10.1126/science.117.3036.239.

23. Everest, F.A.; Young, R.W.; Johnson, M.W. Acoustical Characteristics of Noise Produced by Snapping Shrimp. *J. Acoust. Soc. Am.* **1948**, *20*, 137–142, doi:10.1121/1.1906355.

24. Johnson, M.W.; Everest, F.A.; Young, R.W. The role of snapping shrimp (*Crangon* and *Synalpheus*) in the production of underwater noise in the sea. *Biol. Bull.* **1947**, *93*, 122–138, doi:10.2307/1538284.

25. Knudsen, V.O.; Alford, R.S.; Emling., J.W. Underwater ambient noise. *J. Mar. Res.* **1948**, *7*, 410–429.

26. Evans, W.E. Vocalization among marine animals. In *Marine Bioacoustics, vol. 2*; Tavolga, W.N., Ed.; Pergamon: New York, 1967; pp. 159–186.

27. Lammers, M.O.; Au, W.W.L. Broadband recording of social acoustic signals of the Hawaiian spinner and spotted dolphins. *J. Acoust. Soc. Am.* **1996**, *100*, 2609–2609, doi:10.1121/1.417642.

28. Bazua-Duran, M.C. Comparisons of whistles among different groups dolphins (*Tursiops truncatus*) from the Gulf of Mexico, Universidad Nacional Autónoma de México, 1997.

29. Herman, L.M.; Tavolga, W.N. The Communication Systems of Cetaceans. In *Cetacean behavior: Mechanisms and Function*; Herman, L.H., Ed.; Wiley-Interscience: New York, 1980; pp. 149–209.

30. Cranford, T.W. In search of impulse sound sources in odontocetes. In *Hearing by Whales and Dolphins*; Au, W.W.L., Popper, A.N., Fay, R.R., Eds.; Springer-Verlag: New York, 2000; p. 155.

31. Cranford, T.W. Functional morphology of the odontocete forehead: implications for sound generation, University of California, 1992.

32. Acoustic behavior of mysticete whales. In *Sensory Abilities of Cetaceans*; Thomas, J., Kastelein, R., Eds.; Plenum: New York, 1990; pp. 571–583.

33. Dawbin, W.H.; Cato, D.H. Sounds of a pygmy right whale (*Caperea marginata*). *Mar. Mammal Sci.* **1992**, *8*, 213–219, doi:10.1111/j.1748-7692.1992.tb00405.x.

34. McDonald, M.A.; Moore, S.E. Calls recorded from North Pacific right whales (*Eubalaena japonica*) in the eastern Bering Sea. *J. Cetacean Res. Manag.* **2002**, *4*, 261–266, doi:10.47536/jcrm.v4i3.838.

35. Dominello, T.; Širović, A. Seasonality of Antarctic minke whale (*Balaenoptera bonaerensis*) calls off the western Antarctic Peninsula. *Mar. Mammal Sci.* **2016**, *32*, 826–838, doi:10.1111/mms.12302.

36. Risch, D.; Gales, N.J.; Gedamke, J.; Kindermann, L.; Nowacek, D.P.; Read, A.J.; Siebert, U.; Van Opzeeland, I.C.; Van Parijs, S.M.; Friedlaender, A.S. Mysterious bio-duck sound attributed to the Antarctic minke whale (*Balaenoptera bonaerensis*). *Biol. Lett.* **2014**, *10*, 20140175, doi:10.1098/rsbl.2014.0175.

37. Cerchio, S.; Andrianantenaina, B.; Lindsay, A.; Rekdahl, M.; Andrianarivelo, N.; Rasoloarijao, T. Omura's whales (*Balaenoptera omurai*) off northwest Madagascar: ecology, behaviour and conservation needs. *R. Soc. Open Sci.* **2015**, *2*, 150301, doi:10.1098/rsos.150301.

38. Alling, A.K.; Payne, R. Song of the Indian Ocean blue whale in *Balaenoptera musculus*. In *Cetaceans and Cetacean Research in the Indian Ocean Sanctuary, United Nations Environment Programme, Marine Mammal Technical No. 3. Report*; 1991; pp. 33–65.

39. Alling, A.K.; Dorsey, E.M.; Gordon, J.C. Blue Whales (*Balaenoptera musculus*) off the Northeast Coast of Sri lanka. In *Cetaceans and Cetacean Research in the Indian Ocean Sanctuary, United Nations Environment Programme, Marine Mammal Technical No. 3. Report*; 1991; pp. 247–258.

40. Watkins, W.A.; Tyack, P.; Moore, K.E.; Bird, J.E. The 20-Hz signals of finback whales (*Balaenoptera physalus*). *J. Acoust. Soc. Am.* **1987**, *82*, 1901–1912, doi:10.1121/1.395685.

41. Ljungblad, D.K.; Thompson, P.O.; Moore, S.E. Underwater sounds recorded from migrating bowhead whales, *Balaena mysticetus*, in 1979. *J. Acoust. Soc. Am.* **1982**, *71*, 477–482, doi:10.1121/1.387419.

42. Payne, R.S.; McVay, S. Songs of Humpback Whales. *Science (80-.).* **1971**, *173*, 585–597, doi:10.1126/science.173.3997.585.

43. Clark, C.W. Acoustic behavior of mysticete whales. In *Sensory Abilities of Cetaceans*; Thomas, J., Kastelein, R., Eds.; Plenum: New York, 1990; pp. 571–583.

44. Helweg, D.A.; Frankel, A.S.; Mobley, J.J.R.; Herman, L.M. Humpback whale song: our current understanding. In *Sensory Abilities of Aquatic Mammals*; Thomas, J.A., Kastelein, R., Supin, A., Eds.; Plenum: New York, 1992; pp. 459–483.

45. Rogers, T.; Cato, D.H.; Bryden, M.M. Underwater vocal repertoire of the leopard seal (*Hydrurga leptonyx*) in Prydz Bay, Antartica. In *Sensory Systems of Aquatic Mammals*; Kastelein, R.A., Thomas, J.A., Nachtigall, P.E., Eds.; De Spil, Woerden, The Netherlands, 1995; pp. 223–236.

46. Watkins, W.A.; Ray, G.C. Underwater sounds from ribbon seal, *Phoca* (*Histriophoca*) *fasciata*. *Fish. Bull.* **1977**, *75*, 450–453.

47. Thomas, J.A.; Kuechle, V. Quantitative analysis of the underwater repertoire of the Weddell seal (Leptonychotes weddelli). *J. Acoust. Soc. Am.* **1982**, *72*, 1730–1738, doi:10.1121/1.388667.

48. Schevill, W.E.; Watkins, W.A.; Ray, C.G. Analysis of underwater Odobenus calls with remarks on the develoment and function of the pharyngeal pouches. *Zoologica* **1966**, *51*, 103–106, doi:10.5962/p.203287.

49. Stirling, I.; Calvert, W.; Spencer, C. Evidence of stereotyped underwater vocalization of male Atlantic walruses (Odobenus rosmarus rosmarus). *Can. J. Zool.* **1987**, *65*, 2311–2321, doi:10.1139/z87-348.

50. Schusterman, R.J.; Gentry, R.L.; Schmook, J. Underwater sound production by captive California sea lions, *Zalophus californianus*. *Zool. Sci. Contrib. New York Zool. Soc.* **1967**, *52*, 21–24, doi:10.5962/p.203257.

51. Nishiwaki, M.; Marsh, H. Dugong *Dugong dugon* (Müller, 1776). In *Handbook of Marine Mammals Vol. 3*; Ridgway, S.H., Harrison, R., Eds.; Academic Press: London, 1985; pp. 1–31.

52. Hartman, D.S. *Ecology and behavior of the Manatee (Trichechus manatus) in Florida*; The American Society of Mammalogists: Pittsburgh, 1979;

53. Richardson, W.J.; Green Jr., C.R.; Malme, C.I.; Thomson, D.H. *Marine Mammals and Noise*; Academic Press: San Diego, 1995; ISBN 978-0-08-057303-8.

54. de Cholières, N. *Les Après-Disnées du seigneur de Cholières*; Chez Jean Richer: Paris, 1587;

55. Rabelais, F. *Tiers livre des faits et dits Héroïques du noble Pantagruel : composés par M. François Rabelais, Docteur en Médecine, et Calloier des Iles d'Hyeres*; 1546;

56. Ἀριστοτέλης (Aristotle) *Περὶ τὰ ζῷα ἱστορίαι (History of Animals) IX*; 343BC;

57. Lobel, P.S.; Kaatz, I.M.; Rice, A.N. Acoustical behavior of coral reef fishes. In *Reproduction and Sexuality in Marine Fishes*; Cole, K.S., Ed.; University of California Press: Berkeley, 2010; pp. 307–348 ISBN 9780520264335.

58. Cato, D.H. Marine biological choruses observed in tropical waters near Australia. *J. Acoust. Soc. Am.* **1978**, *64*, 736, doi:10.1121/1.382038.

59. Tavolga, W.N. Acoustic orientation in the sea catfish Galeichthys felis. *Ann. N. Y. Acad. Sci.* **1971**, *188*, 80–97, doi:10.1111/j.1749-6632.1971.tb13091.x.

60. Tavolga, W.N. Acoustic obstacle detection in the sea catfish *Arius felis*. In *Sound Reception in Fish*; Schuijf, A., Hawkins, A.D., Eds.; Elsevier: Amsterdam, 1976; pp. 185–204.

61. Rice, A.N.; Farina, S.C.; Makowski, A.J.; Kaatz, I.M.; Lobel, P.S.; Bemis, W.E.; Bass, A.H. Evolution and Ecology in Widespread Acoustic Signaling Behavior Across Fishes. *Prepr. BioRxiv*, doi:10.1101/2020.09.14.296335.

62. Ladich, F.; Fine, M.L. Sound-generating mechanisms in fishes: a unique diversity in vertebrates. In *Communication in Fishes*; Collin, S., Moller, P., Kappor, B., Eds.; Science Publishers: Enfield, 2006; pp. 3–34.

63. Fine, M.L.; Parmentier, E. Mechanisms of Fish Sound Production. In *Sound Communication in Fishes*;

Ladich, F., Ed.; Animal Signals and Communication; Springer Vienna: Vienna, 2015; Vol. 4, pp. 77–126 ISBN 978-3-7091-1845-0.

64. Di Iorio, L.; Gervaise, C.; Jaud, V.; Robson, A.A.; Chauvaud, L. Hydrophone detects cracking sounds: Non-intrusive monitoring of bivalve movement. *J. Exp. Mar. Bio. Ecol.* **2012**, *432–433*, 9–16, doi:10.1016/j.jembe.2012.07.010.

65. Radford, C.; Jeffs, A.; Tindle, C.; Montgomery, J.C. Resonating sea urchin skeletons create coastal choruses. *Mar. Ecol. Prog. Ser.* **2008**, *362*, 37–43, doi:10.3354/meps07444.

66. Freeman, S.E.; Rohwer, F.L.; D'Spain, G.L.; Friedlander, A.M.; Gregg, A.K.; Sandin, S.A.; Buckingham, M.J. The origins of ambient biological sound from coral reef ecosystems in the Line Islands archipelago. *J. Acoust. Soc. Am.* **2014**, *135*, 1775–1788, doi:10.1121/1.4865922.

67. Patek, S.N.; Caldwell, R.L. The stomatopod rumble: Low frequency sound production in *Hemisquilla californiensis*. *Mar. Freshw. Behav. Physiol.* **2006**, *39*, 99–111, doi:10.1080/10236240600563289.

68. Moulton, J.M. Sound Production in the Spiny Lobster *Panulirus argus* (Latreille). *Biol. Bull.* **1957**, *113*, 286–295, doi:10.2307/1539086.

69. Henninger, H.P.; Watson, W.H. Mechanisms underlying the production of carapace vibrations and associated waterborne sounds in the American lobster, *Homarus americanus*. *J. Exp. Biol.* **2005**, *208*, 3421–3429, doi:10.1242/jeb.01771.

70. Au, W.W.L.; Banks, K. The acoustics of the snapping shrimp *Synalpheus parneomeris* in Kaneohe Bay. *J. Acoust. Soc. Am.* **1998**, doi:10.1121/1.423234.

71. Johnson, M.W. *Underwater noise and the distribution of snapping shrimp with special reference to the asiatic and the southwest and central Pacific areas.*; 1944;

72. Lillis, A.; Mooney, T.A. Snapping shrimp sound production patterns on Caribbean coral reefs: relationships with celestial cycles and environmental variables. *Coral Reefs* **2018**, *37*, 597–607, doi:10.1007/s00338-018-1684-z.

73. Versluis, M.; Schmitz, B.; Von der Heydt, A.; Lohse, D. How snapping shrimp snap: Through cavitating bubbles. *Science (80-.).* **2000**, *289*, 2114–2117, doi:10.1126/science.289.5487.2114.

74. MacGinitie, G.E. Notes on the natural history of several marine crustacea. *Am Midl Nat* **1937**, *18*, 1031–1036, doi:10.2307/2420601.

75. Schultz, S.; Wuppermann, K.; Schmitz, B. Behavioural interactions of the snapping shrimp (*Alpheus heterochaelis*) with conspecifics and sympatric crabs (*Eurypanopeus depressus*). *Zool. - Anal. Complex Syst.* **1998**, *101*, 85.

76. Nolan, B.A.; Salmon, M. The behavior and ecology of snapping shrimp (Crustacea: *Alpheus heterochelis* and *Alpheus normanni*). *Forma Funct.* **1970**, *2*, 289–335.

77. Hazlett, B. Aspects of the biology of snapping shrimp (Alpheus and Synalpheus). *Crustaceana* **1962**, *4*, 82–83, doi:10.1163/156854062X00094.

78. Lillis, A.; Perelman, J.N.; Panyi, A.; Aran Mooney, T. Sound production patterns of big-clawed snapping shrimp (*Alpheus* spp.) are influenced by time-of-day and social context. *J. Acoust. Soc. Am.* **2017**, *142*, 3311–3320, doi:10.1121/1.5012751.

79. Lillis, A.; Mooney, T.A. Loudly heard, little seen, and rarely understood: Spatiotemporal variation and environmental drivers of sound production by snapping shrimp. *Proc. Meet. Acoust.* **2016**, *27*, doi:10.1121/2.0000270.

80. Ferguson, B.G.; Cleary, J.L. In situ source level and source position estimates of biological transient signals produced by snapping shrimp in an underwater environment. *J. Acoust. Soc. Am.* **2001**, *109*, 3031–3037, doi:10.1121/1.1339823.

81. Piercy, J.J.B.; Codling, E.A.; Hill, A.J.; Smith, D.J.; Simpson, S.D. Habitat quality affects sound production and likely distance of detection on coral reefs. *Mar. Ecol. Prog. Ser.* **2014**, *516*, 35–47, doi:10.3354/meps10986.

82. Lammers, M.O.; Brainard, R.E.; Au, W.W.L.; Mooney, T.A.; Wong, K.B. An ecological acoustic recorder (EAR) for long-term monitoring of biological and anthropogenic sounds on coral reefs and other marine habitats. *J. Acoust. Soc. Am.* **2008**, *123*, 1720–1728, doi:10.1121/1.2836780.

83. *Underwater noise caused by snapping shrimp*; University of California and Division of war research, 1946;

84. Mooney, T.A.; Di Iorio, L.; Lammers, M.; Lin, T.-H.H.; Nedelec, S.L.; Parsons, M.; Radford, C.; Urban, E.; Stanley, J. Listening forward: Approaching marine biodiversity assessments using acoustic methods: Acoustic diversity and biodiversity. *R. Soc. Open Sci.* **2020**, *7*, 201287, doi:10.1098/rsos.201287.

85. McCauley, R.D.; Thomas, F.; Parsons, M.J.G.; Erbe, C.; Cato, D.H.; Duncan, A.J.; Gavrilov, A.N.; Parnum, I.M.; Salgado-Kent, C.P. Developing an Underwater Sound Recorder: The Long and Short (Time) of It... *Acoust. Aust.* **2017**, *45*, 301–311, doi:10.1007/s40857-017-0113-8.

86. Tittensor, D.P.; Mora, C.; Jetz, W.; Lotze, H.K.; Ricard, D.; Berghe, E. Vanden; Worm, B. Global patterns and predictors of marine biodiversity across taxa. *Nature* **2010**, *466*, 1098–1101, doi:10.1038/nature09329.

87. Mann, D.A.; Lobel, P.S. Propagation of damselfish (Pomacentridae) courtship sounds. *J. Acoust. Soc. Am.* **1997**, *101*, 3783–3791, doi:10.1121/1.418425.

88. Hawkins, A.D.; Amorim, M.C.P. Spawning sounds of the male haddock Melanogrammus aeglefinus. *Environ. Biol. Fish* **2000**, *59*, 29–41, doi:10.1023/A:1007615517287.

89. Lobel, P.S. Sounds produced by spawning fishes. *Environ. Biol. Fishes* **1992**, *33*, 351–358, doi:10.1007/BF00010947.

90. Picciulin, M.; Kéver, L.; Parmentier, E.; Bolgan, M. Listening to the unseen: Passive acoustic monitoring reveals the presence of a cryptic fish species. *Aquat. Conserv. Mar. Freshw. Ecosyst.* **2018**, *29*, 202–210, doi:10.1002/aqc.2973.

91. Raick, X.; Huby, A.; Kurchevski, G.; Godinho, A.L.; Parmentier, É. Use of bioacoustics in species identification: piranhas from genus Pygocentrus (Teleostei: Serrasalmidae) as a case study. *PLoS One* **2020**, *15*, e0241316, doi:10.1371/journal.pone.0241316.

92. Parmentier, E.; Scalbert, R.; Raick, X.; Gache, C.; Frédérich, B.; Bertucci, F.; Lecchini, D.; Parmentier, É.; Scalbert, R.; Raick, X.; et al. First use of acoustic calls to distinguish cryptic members of a fish species complex. *Zool. J. Linn. Soc.* **2022**, *195*, 964–975, doi:10.1093/zoolinnean/zlab056.

93. Wall, C.C.; Lembke, C.; Mann, D.A. Shelf-scale mapping of sound production by fishes in the eastern Gulf of Mexico, using autonomous glider technology. *Mar. Ecol. Prog. Ser.* **2012**, *449*, 55–64, doi:10.3354/meps09549.

94. Lammers, M.; Fisher-Pool, P.; Au, W.; Meyer, C.; Wong, K.; Brainard, R. Humpback whale *Megaptera novaeangliae* song reveals wintering activity in the Northwestern Hawaiian Islands. *Mar. Ecol. Prog. Ser.* **2011**, *423*, 261–268, doi:10.3354/meps08959.

95. Salisbury, D.P.; Clark, C.W.; Rice, A.N. Right whale occurrence in the coastal waters of Virginia, U.S.A.: Endangered species presence in a rapidly developing energy market. *Mar. Mammal Sci.* **2016**, *32*, 508–519, doi:10.1111/mms.12276.

96. Hughes, T.P. Climate Change, Human Impacts, and the Resilience of Coral Reefs. *Science (80-.).* **2003**, *301*, 929–933, doi:10.1126/science.1085046.

97. Gordon, T.A.C.; Harding, H.R.; Wong, K.E.; Merchant, N.D.; Meekan, M.G.; McCormick, M.I.; Radford, A.N.; Simpson, S.D. Habitat degradation negatively affects auditory settlement behavior of coral reef fishes. *Proc. Natl. Acad. Sci.* **2018**, *115*, 5193–5198, doi:10.1073/pnas.1719291115.

98. Simmons, K.R.; Eggleston, D.B.; Bohnenstiehl, D.R. Hurricane impacts on a coral reef soundscape. *PLoS One* **2021**, *16*, e0244599, doi:10.1371/journal.pone.0244599.

99. *Cold-Water Corals and Ecosystems*; Freiwald, A., Roberts, J.M., Eds.; Springer Berlin Heidelberg: Berlin, Heidelberg, 2005; ISBN 978-3-540-24136-2.

100. Wood, R. *Reef evolution*; Oxford Univ Press: Oxford, 1999; ISBN 9780198577843.

101. Försterra, G.; Beuck, L.; Häussermann, V.; Freiwald, A. Shallow-water *Desmophyllum dianthus* (Scleractinia) from Chile: characteristics of the biocoenoses, the bioeroding community, heterotrophic interactions and (paleo)-bathymetric implications. In *Cold-Water Corals and Ecosystems*; Springer-Verlag: Berlin/Heidelberg; pp. 937–977.

102. Burke, L.; Reytar, K.; Spalding, M.; Perry, A. *Reefs at risk revisited*; World Resources Institute: World Resources Institute, 2011;

103. Spalding, M.D.; Grenfell, A.M. New estimates of global and regional coral reef areas. *Coral Reefs* **1997**, *16*, 225–230, doi:10.1007/s003380050078.

104. Roberts, C.M.; McClean, C.J.; Veron, J.E.N.; Hawkins, J.P.; Allen, G.R.; McAllister, D.E.; Mittermeier, C.G.; Schueler, F.W.; Spalding, M.; Wells, F.; et al. Marine Biodiversity Hotspots and Conservation Priorities for Tropical Reefs. *Science (80-.).* **2002**, *295*, 1280–1284, doi:10.1126/science.1067728.

105. Kahng, S.E.; Copus, J.M.; Wagner, D. Mesophotic Coral Ecosystems. In *Marine Animal Forests*; Rossi, S., Bramanti, L., Gori, A., Orejas, C., Eds.; 2017; pp. 185–206 ISBN 9783319170015.

106. Hinderstein, L.M.; Marr, J.C.A.; Martinez, F.A.; Dowgiallo, M.J.; Puglise, K.A.; Pyle, R.L.; Zawada, D.G.; Appeldoorn, R. Mesophotic Coral Ecosystems: Characterization, Ecology, and Management. *Coral Reefs* **2010**, *29*, 247–251, doi:10.1007/s00338-010-0614-5.

107. Baldwin, C.C.; Tornabene, L.; Robertson, D.R. Below the Mesophotic. *Sci. Rep.* **2018**, *8*, 4920, doi:10.1038/s41598-018-23067-1.

108. Pyle, R.L.; Boland, R.; Bolick, H.; Bowen, B.W.; Bradley, C.J.; Kane, C.; Kosaki, R.K.; Langston, R.; Longenecker, K.; Montgomery, A.; et al. A comprehensive investigation of mesophotic coral ecosystems in the Hawaiian Archipelago. *PeerJ* **2016**, *2016*, 1–45, doi:10.7717/peerj.2475.

109. Bongaerts, P.; Ridgway, T.; Sampayo, E.M.; Hoegh-Guldberg, O. Assessing the "deep reef refugia" hypothesis: Focus on Caribbean reefs. *Coral Reefs* **2010**, *29*, 1–19, doi:10.1007/s00338-009-0581-x.

110. Rouzé, H.; Galand, P.E.; Medina, M.; Bongaerts, P.; Pichon, M.; Pérez-Rosales, G.; Torda, G.; Moya, A.; Raina, J.-B.; Hédouin, L. Symbiotic associations of the deepest recorded photosynthetic scleractinian coral (172 m depth). *ISME J.* **2021**, *15*, 1564–1568, doi:10.1038/s41396-020-00857-y.

111. Van Oppen, M.J.H.; Bongaerts, P.; Underwood, J.N.; Peplow, L.M.; Cooper, T.F. The role of deep reefs in shallow reef recovery: an assessment of vertical connectivity in a brooding coral from west and east Australia. *Mol. Ecol.* **2011**, *20*, 1647–1660, doi:10.1111/j.1365-294X.2011.05050.x.

112. Rougerie, F.; Fichez, R.; Déjardin, P. Geomorphology and hydrogeology of selected islands of French Polynesia: Tikeahau (atoll) and Tahiti (barrier reef). In *Geology and Hydrogeology of Carbonate Islands. Developments in Sedimentology 54*; 1997; pp. 475–502.

113. Rancher, J.; Rougerie, F. L'environnement océanique de l'archipel des Tuamotu (Polynésie Française). *Oceanol. Acta-* **1994**, *18*, 43–60.

114. Jamet, R. *Les sols de Moorea et des îles Sous-le-Vent : Archipel de la Société : Polynésie française*; IRD: Paris, 2000;

115. Bachet, P.; Zysman, T.; Lefèvre, Y. *Guide des poissons de Tahiti et ses îles*; Au vent de.; Pirae (Tahiti), 2010; ISBN 978-2-36734-148-4.

116. van Hooidonk, R.; Maynard, J.; Tamelander, J.; Gove, J.; Ahmadia, G.; Raymundo, L.; Williams, G.; Heron, S.F.; Planes, S. Local-scale projections of coral reef futures and implications of the Paris Agreement. *Sci. Rep.* **2016**, *6*, 39666, doi:10.1038/srep39666.

117. Purkis, S.; Dempsey, A.; Carlton, R.D.; Andréfouët, S.; Samaniego, B.; Rauer, E.M.; Renaud, P.G. *Global Reef Expedition: French Polynesia. Final Report*; 2017; Vol. 5; ISBN 978-0-9975451-1-1.

118. Trapon, M.L.; Pratchett, M.S.; Penin, L. Comparative Effects of Different Disturbances in Coral Reef Habitats in Moorea, French Polynesia. *J. Mar. Biol.* **2011**, *2011*, 1–11, doi:10.1155/2011/807625.

119. Chevalier, J.-P.; Kuhlmann, D.H.H. Les scléractiniaires de Moorea. Ile de la Société (Polynésie française). *J. Soc. Ocean.* **1983**, *77*, 55–75.

120. Bouchon, C. Quantitative study of Scleractinian Coral Communities of Tiahura Reef, Moorea Island, French Polynesia. In Proceedings of the The Fifth International Coral Reef Symposium; Tahiti, 1985; pp. 279–284.

121. Darwin, C. *Geological Observations on Coral Reefs, Volcanic Islands, and on South America: Being the Geology of the Voyage of the Beagle, Under the Command of Captain Fitzroy, R.N., During the Years 1832 to 1836*; Smith, E. and co., Ed.; Steward and Murray: London, 1878;

122. Pichon, M. French Polynesia. In *Marine Animal Forests: The Ecology of Benthic Biodiversity Hotspots*; Loya, Y., Puglise, K.A., Bridge, T.C.L., Eds.; 2019; pp. 425–444 ISBN 9783319210124.

123. Vigliola, L. *Etude des peuplements ichtyologiques benthiques de la plaine sableuse de la pente externe de Tiahura (Ile de Moorea, Polynésie Française)*; 1993; p. 72;.

124. Jaubert J, Thomassin BA, V.P. Morphologie et étude bionomique préliminaire de la pente externe du récif de Tiahura, Ile de Moorea (Polynésie Française). *Cah Pacifique* **1975**, *19*, 299–323.

125. Montaggioni, L.F. Mururoa Atoll. In *Encyclopedia of modern coral reefs: structure, form and process*; D, H., Ed.; 2011; pp. 713–716.

126. Siu, G.; Bacchet, P.; Bernardi, G.; Brooks, A.J.; Carlot, J.; Causse, R.; Claudet, J.; Clua, É.; Delrieu-Trottin, E.; Espiau, B.; et al. Shore fishes of French Polynesia. *Cybium* **2017**, *41*, 245–278, doi:10.26028/cybium/2017-413-003.

127. Leis, J.M.; McCormick, M.I. The Biology, Behavior, and Ecology of the Pelagic, Larval Stage of Coral Reef Fishes. In *Coral Reef Fishes*; 2002; pp. 171–199.

128. Myrberg, A.A.; Fuiman, L.A. The Sensory World of Coral Reef Fishes. In *Coral Reef Fishes*; Elsevier, 2002; pp. 123–148.

129. Havel, L.N.; Fuiman, L.A. Depth Preference of Settling Red Drum (*Sciaenops ocellatus*) Larvae in Relation to Benthic Habitat Color and Water-Column Depth. *Estuaries and Coasts* **2017**, *40*, 573–579, doi:10.1007/s12237-016-0160-7.

130. Dixson, D.L.; Jones, G.P.; Munday, P.L.; Pratchett, M.S.; Srinivasan, M.; Planes, S.; Thorrold, S.R. Terrestrial chemical cues help coral reef fish larvae locate settlement habitat surrounding islands. *Ecol. Evol.* **2011**, *1*, 586–595, doi:10.1002/ece3.53.

131. Dixson, D.L.; Jones, G.P.; Munday, P.L.; Planes, S.; Pratchett, M.S.; Srinivasan, M.; Syms, C.; Thorrold, S.R. Coral reef fish smell leaves to find island homes. *Proc. R. Soc. B Biol. Sci.* **2008**, *275*, 2831–2839, doi:10.1098/rspb.2008.0876.

132. Gerlach, G.; Atema, J.; Kingsford, M.J.; Black, K.P.; Miller-sims, V. Smelling home can prevent dispersal of reef fish larvae. *Proc. Natl. Acad. Sci.* **2007**, *104*, 858–863, doi:10.1073/pnas.0606777104.

133. Leis, J.; Sweatman, H.; Reader, S. What the Pelagic Stages of Coral Reef Fishes Are Doing out in Blue Water: Daytime Field Observations of Larval Behavioural Capabilities. *Mar. Freshw. Res.* **1996**, *47*, 401, doi:10.1071/MF9960401.

134. Stobutzki, I.C.; Bellwood, D.R. Nocturnal orientation to reefs by late pelagic stage coral reef fishes. *Coral Reefs* **1998**, *17*, 103–110, doi:10.1007/s003380050103.

135. Barth, P.; Berenshtein, I.; Besson, M.; Roux, N.; Parmentier, E.; Lecchini, D. From the ocean to a reef habitat : how do the larvae of coral reef fishes find their way home ? A state of art on the latest advances. *Vie Milieu* **2015**, *65*, 91–100.

136. Lecchini, D.; Mills, S.C.; Brié, C.; Maurin, R.; Banaigs, B. Ecological determinants and sensory mechanisms in habitat selection of crustacean postlarvae. *Behav. Ecol.* **2010**, *21*, 599–607, doi:10.1093/beheco/arq029.

137. Lecchini, D.; Planes, S.; Galzin, R. Experimental assessment of sensory modalities of coral-reef fish larvae in the recognition of their settlement habitat. *Behav. Ecol. Sociobiol.* **2005**, *58*, 18–26, doi:10.1007/s00265-004-0905-3.

138. Tricas, T.C.; Boyle, K.S. Acoustic behaviors in Hawaiian coral reef fish communities. **2014**, doi:10.3354/meps10930.

139. Raick, X.; Lecchini, D.; Kéver, L.; Colleye, O.; Bertucci, F.; Parmentier, É. Sound production mechanism in triggerfish (Balistidae): a synapomorphy. *J. Exp. Biol.* **2018**, *221*, jeb168948, doi:10.1242/jeb.168948.

140. Parmentier, E.; Bertucci, F.; Bolgan, M.; Lecchini, D. How many fish could be vocal? An estimation from a coral reef (Moorea Island). *Belgian J. Zool.* **2021**, *151*, doi:10.26496/bjz.2021.82.

141. Bertucci, F.; Maratrat, K.; Berthe, C.; Besson, M.; Guerra, A.S.; Raick, X.; Lerouvreur, F.; Lecchini, D.; Parmentier, E. Local sonic activity reveals potential partitioning in a coral reef fish community. *Oecologia* **2020**, doi:10.1007/s00442-020-04647-3.

142. Parmentier, E.; Raick, X.; Lecchini, D.; Boyle, K.; Vanwassenbergh, S.; Bertucci, F.; Kéver, L. Unusual sound production mechanism in the triggerfish *Rhinecanthus aculeatus* (Balistidae). *J. Exp. Biol.* **2017**, *220*, 186–193, doi:10.1242/jeb.146514.

143. Raick, X. Production de sons chez le baliste Picasso *Rhinecanthus aculeatus* (Linnæus , 1758), University of Liège, 2015.

144. Parmentier, E.; Fine, M.L.; Berthe, C.; Lecchini, D. Taxonomic validation of *Encheliophis chardewalli* with description of calling abilities. *J. Morphol.* **2018**, *279*, 864–870, doi:10.1002/jmor.20816.

145. Parmentier, E.; Colleye, O.; Lecchini, D. New insights into sound production in *Carapus mourlani* (Carapidae). *Bull. Mar. Sci.* **2016**, *92*, 335–342, doi:10.5343/bms.2016.1014.

146. Parmentier, E.; Fine, M.; Vandewalle, P.; Ducamp, J.-J.; Lagardère, J.-P. Sound production in two carapids (*Carapus acus* and *C. mourlani*) and through the sea cucumber tegument. *Acta Zool.* **2006**, *87*, 113–119, doi:10.1111/j.1463-6395.2006.00221.x.

147. Kéver, L.; Colleye, O.; Lugli, M.; Lecchini, D.; Lerouvreur, F.; Herrel, A.; Parmentier, E. Sound production in Onuxodon fowleri (Carapidae) and its amplification by the host shell. *J. Exp. Biol.* **2014**, *217*, 4283–4294, doi:10.1242/jeb.109363.

148. Parmentier, E.; Lagardère, J.P.; Chancerelle, Y.; Dufrane, D.; Eeckhaut, I. Variations in sound-producing mechanism in the pearlfish Carapini (Carapidae). *J. Zool.* **2008**, *276*, 266–275, doi:10.1111/j.1469-7998.2008.00486.x.

149. Parmentier, E.; Boyle, K.S.; Berten, L.; Brié, C.; Lecchini, D. Sound production and mechanism in Heniochus chrysostomus (Chaetodontidae). *J. Exp. Biol.* **2011**, *214*, 2702–2708, doi:10.1242/jeb.056903.

150. Parmentier, E.; Solagna, L.; Bertucci, F.; Fine, M.L.; Nakae, M.; Compère, P.; Smeets, S.; Raick, X.; Lecchini, D. Simultaneous production of two kinds of sounds in relation with sonic mechanism in the boxfish *Ostracion meleagris* and *O. cubicus*. *Sci. Rep.* **2019**, *9*, 4962: 1–13, doi:10.1038/s41598-019-41198-x.

151. Parmentier, E.; Kéver, L.; Casadevall, M.; Lecchini, D. Diversity and complexity in the acoustic behaviour of *Dacyllus flavicaudus* (Pomacentridae). *Mar. Biol.* **2010**, *157*, 2317–2327, doi:10.1007/s00227-010-1498-1.

152. Colleye, O.; Vandewalle, P.; Lanterbecq, D.; Lecchini, D.; Parmentier, E. Interspecific variation of calls in clownfishes: degree of similarity in closely related species. *BMC Evol. Biol.* **2011**, *11*, doi:10.1186/1471-2148-11-365.

153. Parmentier, E.; Lecchini, D.; Frederich, B.; Brie, C.; Mann, D. Sound production in four damselfish (*Dascyllus*) species: Phyletic relationships? *Biol. J. Linn. Soc.* **2009**, *97*, 928–940, doi:10.1111/j.1095-8312.2009.01260.x.

154. Jublier, N.; Bertucci, F.; Kéver, L.; Colleye, O.; Ballesta, L.; Nemeth, R.S.; Lecchini, D.; Rhodes, K.L.; Parmentier, E. Passive monitoring of phenological acoustic patterns reveals the sound of the camouflage grouper, *Epinephelus polyphekadion*. *Aquat. Conserv. Mar. Freshw. Ecosyst.* **2020**, *30*, 42–52, doi:10.1002/aqc.3242.

155. Garland, E.C.; Goldizen, A.W.; Rekdahl, M.L.; Constantine, R.; Garrigue, C.; Hauser, N.D.; Poole, M.M.; Robbins, J.; Noad, M.J. Dynamic Horizontal Cultural Transmission of Humpback Whale Song at the Ocean Basin Scale. *Curr. Biol.* **2011**, *21*, 687–691, doi:10.1016/j.cub.2011.03.019.

156. Bertucci, F.; Parmentier, E.; Berten, L.; Brooker, R.M.; Lecchini, D. Temporal and spatial comparisons of underwater sound signatures of different reef habitats in Moorea Island, French Polynesia. *PLoS One* **2015**, *10*, 1–12, doi:10.1371/journal.pone.0135733.

157. Bertucci, F.; Parmentier, E.; Berthe, C.; Besson, M.; Hawkins, A.D.; Aubin, T.; Lecchini, D. Snapshot recordings provide a first description of the acoustic signatures of deeper habitats adjacent to coral reefs of Moorea. *PeerJ* **2017**, *2017*, doi:10.7717/peerj.4019.

158. Bertucci, F.; Parmentier, E.; Lecellier, G.; Hawkins, A.D.; Lecchini, D. Acoustic indices provide information on the status of coral reefs: An example from Moorea Island in the South Pacific. *Sci. Rep.* **2016**, *6*, 1–9, doi:10.1038/srep33326.

159. Bertucci, F.; Guerra, A.S.; Sturny, V.; Blin, E.; Sang, G.T.; Lecchini, D. A preliminary acoustic evaluation of three sites in the lagoon of Bora Bora, French Polynesia. *Environ. Biol. Fishes* **2020**, *103*, 891–902, doi:10.1007/s10641-020-01000-8.

160. Nedelec, S.L.; Radford, A.N.; Simpson, S.D.; Nedelec, B.; Lecchini, D.; Mills, S.C. Anthropogenic noise playback impairs embryonic development and increases mortality in a marine invertebrate. *Sci. Rep.* **2014**, *4*, 13–16, doi:10.1038/srep05891.

161. Berthe, C.; Lecchini, D. Influence of boat noises on escape behaviour of white-spotted eagle ray *Aetobatus ocellatus* at Moorea Island (French Polynesia). *C. R. Biol.* **2016**, *339*, 99–103, doi:10.1016/j.crvi.2016.01.001.

162. Nelson, D.R.; Johnson, R.H. *Acoustic studies on sharks, Rangiroa Atoll, July, 1969*; Long Beach, 1970;

163. Desiderà, E.; Guidetti, P.; Panzalis, P.; Navone, A.; Valentini-Poirrier, C.A.; Boissery, P.; Gervaise, C.; Iorio, L. Di Acoustic fish communities: Sound diversity of rocky habitats reflects fish species diversity. *Mar. Ecol. Prog. Ser.* **2019**, *608*, 183–197, doi:10.3354/meps12812.

164. Carriço, R.; Silva, M.A.; Meneses, G.M.; Fonseca, P.J.; Amorim, M.C.P. Characterization of the acoustic community of vocal fishes in the Azores. *PeerJ* **2019**, *7*, e7772, doi:10.7717/peerj.7772.

165. Hédouin, L.; Berteaux-Lecellier, V. Traditional vs new approaches for assessing coral health: A global overview and the paradigm of French polynesia. *J. Mar. Sci. Technol.* **2014**, *22*, 25–35, doi:10.6119/JMST-013-0813-2.

166. Subramanian, M. Anthropocene now: influential panel votes to recognize Earth's new epoch. *Nature* **2019**, doi:10.1038/d41586-019-01641-5.

167. Probert, P.K. *Marine Conservation*; Cambridge University Press: Cambridge, 2017; ISBN 9781139043588.

168. *Global Marine Biological Diversity: a Strategy for Builiding Conservation into Decision Making*; Norse, E.A., Ed.; Island Press: Washington D.C., 1993;

169. Thorne-Miller, B. *The Living Ocean: Understanding and Protecting Marine Biodiversity*; Island Press: Washington D.C., 1999; ISBN 1559636777.

170. Wilkinson, C. Status of coral reefs of the world: summary of threats and remedial action. In *Coral Reef Conservation*; Coté, I.M., Reynolds, J.D., Eds.; Cambridge University Press: Cambridge, 2006; pp. 3–39.

171. Kennedy, E.V.; Holderied, M.W.; Mair, J.M.; Guzman, H.M.; Simpson, S.D. Spatial patterns in reef-generated noise relate to habitats and communities: Evidence from a Panamanian case study. *J. Exp. Mar. Bio. Ecol.* **2010**, *395*, 85–92, doi:10.1016/j.jembe.2010.08.017.

172. Butler, J.; Butler, M.J.; Gaff, H. Snap, crackle, and pop: Acoustic-based model estimation of snapping shrimp populations in healthy and degraded hard-bottom habitats. *Ecol. Indic.* **2017**, *77*, 377–385, doi:10.1016/j.ecolind.2017.02.041.

173. Rossi, T.; Connell, S.D.; Nagelkerken, I. The sounds of silence: regime shifts impoverish marine soundscapes. *Landsc. Ecol.* **2017**, *32*, 239–248, doi:10.1007/s10980-016-0439-x.

174. Armarego-Marriott, T. Calling out and listening in. *Nat. Clim. Chang.* **2021**, *11*, 292–292, doi:10.1038/s41558-021-01025-6.

175. Siddagangaiah, S.; Chen, C.-F.; Hu, W.-C.; Danovaro, R.; Pieretti, N. Silent winters and rock-and-roll summers: The long-term effects of changing oceans on marine fish vocalization. *Ecol. Indic.* **2021**, *125*, 107456, doi:10.1016/j.ecolind.2021.107456.

176. McWilliam, J.N.; McCauley, R.D.; Erbe, C.; Parsons, M.J.G. Patterns of biophonic periodicity on coral reefs in the Great Barrier Reef. *Sci. Rep.* **2017**, *7*, 17459, doi:10.1038/s41598-017-15838-z.

177. Hoegh-Guldberg, O.; Mumby, P.J.; Hooten, A.J.; Steneck, R.S.; Greenfield, P.; Gomez, E.; Harvell, C.D.; Sale, P.F.; Edwards, A.J.; Caldeira, K.; et al. Coral Reefs Under Rapid Climate Change and Ocean Acidification. *Science (80-.).* **2007**, *318*, 1737–1742, doi:10.1126/science.1152509.

178. Glynn, P.W. Coral reef bleaching in the 1980s and possible connections with global warming. *Trends Ecol. Evol.* **1991**, *6*, 175–179, doi:10.1016/0169-5347(91)90208-F.

179. Jokiel, P.L.; Coles, S.L. Response of Hawaiian and other Indo-Pacific reef corals to elevated temperature. *Coral Reefs* **1990**, *8*, 155–162, doi:10.1007/BF00265006.

180. Kleppel, G.S.; Dodge, R.E.; Reese, C.J. Changes in pigmentation associated with the bleaching of stony corals. *Limnol. Oceanogr.* **1989**, *34*, 1331–1335, doi:10.4319/lo.1989.34.7.1331.

181. Hoegh-Guldberg, O.; Smith, G.J. The effect of sudden changes in temperature, light and salinity on the population density and export of zooxanthellae from the reef corals *Stylophora pistillata* Esper and *Seriatopora hystrix* Dana. *J. Exp. Mar. Bio. Ecol.* **1989**, *129*, 279–303, doi:10.1016/0022-0981(89)90109-3.

182. Hoegh-Guldberg, O. Climate change, coral bleaching and the future of the world's coral reefs. *Mar. Freshw. Res.* **1999**, doi:10.1071/MF99078.

183. Glynn, P.W. Coral reef bleaching: ecological perspectives. *Coral Reefs* **1993**, *12*, 1–17, doi:10.1007/BF00303779.

184. Brown, B.E. Coral bleaching: causes and consequences. *Coral Reefs* **1997**, *16*, S129–S138, doi:10.1007/s003380050249.

185. Brown, B.; Dunne, R.; Scoffin, T.; Le Tissier, M. Solar damage in intertidal corals. *Mar. Ecol. Prog. Ser.* **1994**, *105*, 219–230, doi:10.3354/meps105219.

186. Dunne, R.; Brown, B. The influence of solar radiation on bleaching of shallow water reef corals in the Andaman Sea, 1993–1998. *Coral Reefs* **2001**, *20*, 201–210, doi:10.1007/s003380100160.

187. Hill, R.; Frankart, C.; Ralph, P.J. Impact of bleaching conditions on the components of non-photochemical quenching in the zooxanthellae of a coral. *J. Exp. Mar. Bio. Ecol.* **2005**, *322*, 83–92, doi:10.1016/j.jembe.2005.02.011.

188. Carroll, A.G.; Harrison, P.L.; Adjeroud, M. Susceptibility of coral assemblages to successive bleaching events at Moorea, French Polynesia. *Mar. Freshw. Res.* **2017**, *68*, 760–771, doi:10.1071/MF15134.

189. Graham, N.A.J.; McClanahan, T.R.; MacNeil, M.A.; Wilson, S.K.; Polunin, N.V.C.; Jennings, S.; Chabanet, P.; Clark, S.; Spalding, M.D.; Letourneur, Y.; et al. Climate Warming, Marine Protected Areas and the Ocean-Scale Integrity of Coral Reef Ecosystems. *PLoS One* **2008**, *3*, e3039, doi:10.1371/journal.pone.0003039.

190. Gordon, T.A.C.; Radford, A.N.; Davidson, I.K.; Barnes, K.; McCloskey, K.; Nedelec, S.L.; Meekan, M.G.; McCormick, M.I.; Simpson, S.D. Acoustic enrichment can enhance fish community development on degraded coral reef habitat. *Nat. Commun.* **2019**, *10*, 1–7, doi:10.1038/s41467-019-13186-2.

191. Parsons, E.C.M. Impacts of Navy Sonar on Whales and Dolphins: Now beyond a Smoking Gun? *Front. Mar. Sci.* **2017**, *4*, doi:10.3389/fmars.2017.00295.

192. McGeady, R.; McMahon, B.J.; Berrow, S. The effects of seismic surveying and environmental variables on deep diving odontocete stranding rates along Ireland's coast. In Proceedings of the Fourth International Conference on the Effects of Noise on Aquatic Life; Acoustics, P. of M. on, Ed.; Dublin, 2016; p. 14.

193. Castellote, M.; Llorens, C. Review of the effects of offshore seismic surveys in cetaceans: Are mass strandings a possibility? In *The Effects of Noise on Aquatic Life II (Advances in Experimental Medicine*

and Biology Series, vol. 875); Popper, A., Hawkins, A., Eds.; Springer, 2016; pp. 133–143.

194. Taylor, B.; Barlow, J.; Pitman, R.; Ballance, L.; Klinger, T.; Hildebrand, J.; Urban, J.; D.Palacios; Mead, J. A call for research to assess risk of acoustic impact on beaked whale populations. In Proceedings of the 56th Meeting of the International Whaling Commission; Sorrento, Italy, 2004.

195. Heide-Jørgensen, M.P.; Hansen, R.G.; Westdal, K.; Reeves, R.R.; Mosbech, A. Narwhals and seismic exploration: Is seismic noise increasing the risk of ice entrapments? *Biol. Conserv.* **2013**, *158*, 50–54, doi:10.1016/j.biocon.2012.08.005.

196. Ahonen, H.; Stafford, K.M.; de Steur, L.; Lydersen, C.; Wiig, Ø.; Kovacs, K.M. The underwater soundscape in western Fram Strait: Breeding ground of Spitsbergen's endangered bowhead whales. *Mar. Pollut. Bull.* **2017**, *123*, 97–112, doi:10.1016/j.marpolbul.2017.09.019.

197. Aarts, G.; von Benda-Beckmann, A.; Lucke, K.; Sertlek, H.; van Bemmelen, R.; Geelhoed, S.; Brasseur, S.; Scheidat, M.; Lam, F.; Slabbekoorn, H.; et al. Harbour porpoise movement strategy affects cumulative number of animals acoustically exposed to underwater explosions. *Mar. Ecol. Prog. Ser.* **2016**, *557*, 261–275, doi:10.3354/meps11829.

198. Carstensen, J.; Henriksen, O.; Teilmann, J. Impacts of offshore wind farm construction on harbour porpoises: acoustic monitoring of echolocation activity using porpoise detectors (T-PODs). *Mar. Ecol. Prog. Ser.* **2006**, *321*, 295–308, doi:10.3354/meps321295.

199. Kastelein, R.A.; Gransier, R.; Marijt, M.A.T.; Hoek, L. Hearing frequency thresholds of harbor porpoises (*Phocoena phocoena*) temporarily affected by played back offshore pile driving sounds. *J. Acoust. Soc. Am.* **2015**, *137*, 556–564, doi:10.1121/1.4906261.

200. Blair, H.B.; Merchant, N.D.; Friedlaender, A.S.; Wiley, D.N.; Parks, S.E. Evidence for ship noise impacts on humpback whale foraging behaviour. *Biol. Lett.* **2016**, *12*, 20160005, doi:10.1098/rsbl.2016.0005.

201. Gervaise, C.; Simard, Y.; Roy, N.; Kinda, B.; Ménard, N. Shipping noise in whale habitat: Characteristics, sources, budget, and impact on belugas in Saguenay–St. Lawrence Marine Park hub. *J. Acoust. Soc. Am.* **2012**, *132*, 76–89, doi:10.1121/1.4728190.

202. Holt, M.M.; Noren, D.P.; Veirs, V.; Emmons, C.K.; Veirs, S. Speaking up: Killer whales (*Orcinus orca*) increase their call amplitude in response to vessel noise. *J. Acoust. Soc. Am.* **2009**, *125*, EL27–EL32, doi:10.1121/1.3040028.

203. Erbe, C.; Marley, S.A.; Schoeman, R.P.; Smith, J.N.; Trigg, L.E.; Embling, C.B. The Effects of Ship Noise on Marine Mammals—A Review. *Front. Mar. Sci.* **2019**, *6*, doi:10.3389/fmars.2019.00606.

204. Rolland, R.M.; Parks, S.E.; Hunt, K.E.; Castellote, M.; Corkeron, P.J.; Nowacek, D.P.; Wasser, S.K.; Kraus, S.D. Evidence that ship noise increases stress in right whales. *Proc. R. Soc. B Biol. Sci.* **2012**, *279*, 2363–2368, doi:10.1098/rspb.2011.2429.

205. McCauley, R.D.; Fewtrell, J.; Popper, A.N. High intensity anthropogenic sound damages fish ears. *J. Acoust. Soc. Am.* **2003**, *113*, 638–642, doi:10.1121/1.1527962.

206. Popper, A.N.; Smith, M.E.; Cott, P.A.; Hanna, B.W.; MacGillivray, A.O.; Austin, M.E.; Mann, D.A. Effects of exposure to seismic airgun use on hearing of three fish species. *J. Acoust. Soc. Am.* **2005**, *117*, 3958–3971, doi:10.1121/1.1904386.

207. Løkkeborg, S.; Ona, E.; Vold, A.; Salthaug, A. Sounds from seismic air guns: gear- and species-specific effects on catch rates and fish distribution. *Can. J. Fish. Aquat. Sci.* **2012**, *69*, 1278–1291, doi:10.1139/f2012-059.

208. Day, R.D.; McCauley, R.D.; Fitzgibbon, Q.P.; Hartmann, K.; Semmens, J.M. Exposure to seismic air gun signals causes physiological harm and alters behavior in the scallop *Pecten fumatus*. *Proc. Natl. Acad. Sci.* **2017**, *114*, E8537–E8546, doi:10.1073/pnas.1700564114.

209. Day, R.D.; McCauley, R.; Fitzgibbon, Q.P.; Semmens, J.M. *Assessing the impact of marine seismic surveys on southeast Australian scallop and lobster fisheries (FRDC Report 2012/008, University of Tasmania, Hobart)*; 2016;

210. Guerra, A.; González, A.F.; Rocha, R. A review of the records of giant squid in the northeastern Atlantic

and severe injuries in *Architeuthis dux* stranded after acoustic explorations. In Proceedings of the e ICES Annual Science Conference, Vigo, Spain; 2004.

211. Day, R.D.; McCauley, R.D.; Fitzgibbon, Q.P.; Hartmann, K.; Semmens, J.M. Seismic air guns damage rock lobster mechanosensory organs and impair righting reflex. *Proc. R. Soc. B Biol. Sci.* **2019**, *286*, 20191424, doi:10.1098/rspb.2019.1424.

212. Simpson, S.D.; Radford, A.N.; Holles, S.; Ferarri, M.C.O.; Chivers, D.P.; Mccormick, M.I.; Meekan, M.G. Small-boat noise impacts natural settlement behavior of coral reef fish larvae. In *The Effects of Noise on Aquatic Life II*; 2016; Vol. 875, pp. 1041–1048 ISBN 978-1-4939-2980-1.

213. Holles, S.H.; Simpson, S.D.; Radford, A.N.; Berten, L.; Lecchini, D. Boat noise disrupts orientation behaviour in a coral reef fish. *Mar. Ecol. Prog. Ser.* **2013**, *485*, 295–300, doi:10.3354/meps10346.

214. González Correa, J.M.; Bayle Sempere, J.-T.T.; Juanes, F.; Rountree, R.; Ruíz, J.F.; Ramis, J. Recreational boat traffic effects on fish assemblages: First evidence of detrimental consequences at regulated mooring zones in sensitive marine areas detected by passive acoustics. *Ocean Coast. Manag.* **2019**, *168*, 22–34, doi:10.1016/j.ocecoaman.2018.10.027.

215. Nedelec, S.L.; Radford, A.N.; Pearl, L.; Nedelec, B.; McCormick, M.I.; Meekan, M.G.; Simpson, S.D. Motorboat noise impacts parental behaviour and offspring survival in a reef fish. *Proc. R. Soc. B Biol. Sci.* **2017**, *284*, 20170143, doi:10.1098/rspb.2017.0143.

216. Simpson, S.D.; Radford, A.N.; Nedelec, S.L.; Ferrari, M.C.O.; Chivers, D.P.; McCormick, M.I.; Meekan, M.G. Anthropogenic noise increases fish mortality by predation. *Nat. Commun.* **2016**, *7*, 10544, doi:10.1038/ncomms10544.

217. Jolivet, A.; Tremblay, R.; Olivier, F.; Gervaise, C.; Sonier, R.; Genard, B.; Chauvaud, L. Validation of trophic and anthropic underwater noise as settlement trigger in blue mussels. *Sci. Rep.* **2016**, *6*, 33829, doi:10.1038/srep33829.

218. Nedelec, S.L.; Mills, S.C.; Lecchini, D.; Nedelec, B.; Simpson, S.D.; Radford, A.N. Repeated exposure to noise increases tolerance in a coral reef fish. *Environ. Pollut.* **2016**, *216*, 428–436, doi:10.1016/j.envpol.2016.05.058.

219. Slotte, A.; Hansen, K.; Dalen, J.; Ona, E. Acoustic mapping of pelagic fish distribution and abundance in relation to a seismic shooting area off the Norwegian west coast. *Fish. Res.* **2004**, *67*, 143–150, doi:10.1016/j.fishres.2003.09.046.

220. Engås, A.; Løkkeborg, S.; Ona, E.; Soldal, A. V Effects of seismic shooting on local abundance and catch rates of cod (*Gadus morhua*) and haddock (*Melanogrammus aeglefinus*). *Can. J. Fish. Aquat. Sci.* **1996**, *53*, 2238–2249, doi:10.1139/f96-177.

221. Miller, I.; Cripps, E. Three dimensional marine seismic survey has no measurable effect on species richness or abundance of a coral reef associated fish community. *Mar. Pollut. Bull.* **2013**, *77*, 63–70, doi:10.1016/j.marpolbul.2013.10.031.

222. Day, R.D.; McCauley, R.D.; Fitzgibbon, Q.P.; Semmens, J.M. Seismic air gun exposure during early-stage embryonic development does not negatively affect spiny lobster *Jasus edwardsii* larvae (Decapoda:Palinuridae). *Sci. Rep.* **2016**, *6*, 22723, doi:10.1038/srep22723.

223. Christian, J.R.; Mathieu, A.; Thompson, D.H.; White, D.; Buchanan, R.A. *Effect of seismic energy on snow crab (*Chionoecetes opilio*) (Environmental Funds Project No. 144, Fisheries and Oceans Canada)*; Calgary, 2003;

224. Carson, R. *Silent spring*; Houghton Mifflin Company: Boston, 1962; ISBN 0618249060.

225. MacNeil, M.A.; Graham, N.A.J.; Cinner, J.E.; Wilson, S.K.; Williams, I.D.; Maina, J.; Newman, S.; Friedlander, A.M.; Jupiter, S.; Polunin, N.V.C.; et al. Recovery potential of the world's coral reef fishes. *Nature* **2015**, *520*, 341–344, doi:10.1038/nature14358.

226. Roberts, C.M.; Polunin, N.V.C. Are marine reserves effective in management of reef fisheries? *Rev. Fish Biol. Fish.* **1991**, *1*, 65–91, doi:10.1007/BF00042662.

227. Friedlander, A.M.; Brown, E.K.; Monaco, M.E. Coupling ecology and GIS to evaluate efficacy of marine protected areas in Hawaii. *Ecol. Appl.* **2007**, *17*, 715–730, doi:10.1890/06-0536.

228. Selig, E.R.; Bruno, J.F. A Global Analysis of the Effectiveness of Marine Protected Areas in Preventing Coral Loss. *PLoS One* **2010**, *5*, e9278, doi:10.1371/journal.pone.0009278.

229. Hargreaves-Allen, V.; Mourato, S.; Milner-Gulland, E.J. A Global Evaluation of Coral Reef Management Performance: Are MPAs Producing Conservation and Socio-Economic Improvements? *Environ. Manage.* **2011**, *47*, 684–700, doi:10.1007/s00267-011-9616-5.

230. ARRETE n° 507 C M du 3 avril 2018 portant classement de la zone économique exclusive de la Polynésie française en aire marine gérée.

231. Diazabakana, A.; Binet, T.; Rochette, J. *Etude d'optimisation d'une aire marine gérée à l'échelle de la ZEE polynésienne. Recommandations et orientations*; 2016;

232. Verducci, M.; Benet, A.; Aubanel, A.; Monier, C.; Tatarata, M.; Garganta, E.; Salvat, B. Les aires marines protégées en Polynésie française. In Proceedings of the 1er colloque national sur les aires marines protégées. Quelle stratégie pour quels objectifs ?; Boulogne-sur-Mer, 2007.

233. Aubanel, A.; Monier, C.; Benet, A.; Di Jorio, J.-A.; Salvat, B.M. Management plan for marine environment in French Polynesia. *Oceanis* **2003**, *29*, 375–395.

234. Galzin, R.; Emmanuelli, E.; Ferraris, J.; Mellado, T. *Polynésie française - Suivi des Aires Marines Protégées de Moorea, apport IRD/CRIOBE pour le SPE et l'Urbanisme, Services Territoriaux de Polynésie française*; 2006;

235. Weijerman, M.; Grüss, A.; Dove, D.; Asher, J.; Williams, I.; Kelley, C.; Drazen, J. Shining a light on the composition and distribution patterns of mesophotic and subphotic fish communities in Hawai'i. *Mar. Ecol. Prog. Ser.* **2019**, *630*, 161–182, doi:10.3354/meps13135.

236. Élise, S. Développement d'indices écoacoustiques pour caractériser et suivre l'état et le fonctionnement des écosystèmes coralliens, Université de la Réunion, 2019.

237. Gillespie, D.; Mellinger, D.K.; Gordon, J.; McLaren, D.; Redmond, P.; McHugh, R.; Trinder, P.; Deng, X.; Thode, A. PAMGUARD: Semiautomated, open source software for real-time acoustic detection and localization of cetaceans. *J. Acoust. Soc. Am.* **2009**, *125*, 2547–2547, doi:10.1121/1.4808713.

238. Hartmann, W. *Signals, sound, and sensation*; Springer.; New York, 1998; ISBN 978-1-56396-283-7.

239. Cooley, J.W.; Tukey, J.W. An algorithm for the machine calculation of complex Fourier series. *Math. Comput.* **1965**, *19*, 297–301, doi:10.1090/S0025-5718-1965-0178586-1.

240. Krause, B. Anatomy of the soundscape: evolving perspectives. *J. Audio Eng. Soc.* **2008**, *56*, 73–80.

241. Pijanowski, B.C.; Farina, A.; Gage, S.H.; Dumyahn, S.L.; Krause, B.L. What is soundscape ecology? An introduction and overview of an emerging new science. *Landsc. Ecol.* **2011**, *26*, 1213–1232, doi:10.1007/s10980-011-9600-8.

242. Rountree, R.A.; Grant Gilmore, R.; Goudey, C.A.; Hawkins, A.D.; Luczkovich, J.J.; Mann, D.A. Listening to Fish: Applications of Passive Acoustics to Fisheries Science. *Fisheries* **2006**, *31*, 433–446, doi:10.1577/1548-8446(2006)31.

243. Coquereau, L.; Grall, J.; Chauvaud, L.; Gervaise, C.; Clavier, J.; Jolivet, A.; Di Iorio, L. Sound production and associated behaviours of benthic invertebrates from a coastal habitat in the north-east Atlantic. *Mar. Biol.* **2016**, *163*, 127, doi:10.1007/s00227-016-2902-2.

244. Stuart-Smith, R.D.; Bates, A.E.; Lefcheck, J.S.; Duffy, J.E.; Baker, S.C.; Thomson, R.J.; Stuart-Smith, J.F.; Hill, N.A.; Kininmonth, S.J.; Airoldi, L.; et al. Integrating abundance and functional traits reveals new global hotspots of fish diversity. *Nature* **2013**, *501*, 539–542, doi:10.1038/nature12529.

245. Au, W.W.L.; Banks, K. The acoustics of the snapping shrimp *Synalpheus parneomeris* in Kaneohe Bay. *J. Acoust. Soc. Am.* **1998**, *103*, 41–47, doi:10.1121/1.423234.

246. Staaterman, E.; Rice, A.N.; Mann, D.A.; Paris, C.B. Soundscapes from a Tropical Eastern Pacific reef and a Caribbean Sea reef. **2013**, 553–557, doi:10.1007/s00338-012-1007-8.

247. Mann, D.A.; Casper, B.M.; Boyle, K.S.; Tricas, T.C. On the attraction of larval fishes to reef sounds. *Mar. Ecol. Prog. Ser.* **2007**, *338*, 307–310, doi:10.3354/meps338307.

248. Phillips, B.F.; Penrose, J.D. *The puerulus stage of the spiny (rock) lobster and its ability to locate the coast. School of Physics and Geosciences, Western Australian Institute of Technology, Report SPG 374/1985/AP92.*; 1985;

249. Wright, K.J.; Higgs, D.M.; Cato, D.H.; Leis, J.M. Auditory sensitivity in settlement-stage larvae of coral reef fishes. *Coral Reefs* **2010**, *29*, 235–243, doi:10.1007/s00338-009-0572-y.

250. Thilges, K.; Potty, G.; Freeman, S.; Freeman, L.; Van Uffelen, L. Measurements and models of acoustic transmission loss on two Hawaiian coral reefs. *179th Meet. Acoust. Soc. Am.* **2021**, *42*, 070005, doi:10.1121/2.0001336.

251. Stevick, P.; McConnell, B.; Hammond, P. Patterns of Movement. In *Marine Mammal Biology: an evolutionary approach*; Hoelzel, A.R., Ed.; Blackwell, 2002; pp. 185–216.

252. Silva, M.A.; Prieto, R.; Magalhães, S.; Seabra, M.I.; Santos, R.S.; Hammond, P.S. Ranging patterns of bottlenose dolphins living in oceanic waters: implications for population structure. *Mar. Biol.* **2008**, *156*, 179–192, doi:10.1007/s00227-008-1075-z.

253. van Opzeeland, I.; Slabbekoorn, H. Importance of Underwater Sounds for Migration of Fish and Aquatic Mammals. In *Advances in experimental medicine and biology*; 2012; Vol. 730, pp. 357–359.

254. Crane, N.L.; Lashkari, K. Sound production of gray whales, *Eschrichtius robustus*, along their migration route: A new approach to signal analysis. *J. Acoust. Soc. Am.* **1996**, *100*, 1878–1886, doi:10.1121/1.416006.

255. Ann Nichole, A. An investigation of the roles of geomagnetic and acoustic cues in whale navigation and orientation, Joint Program in Oceanography/Applied Ocean Science and Engineering (Massachusetts Institute of Technology, Department of Biology; and the Woods Hole Oceanographic Institution), 2013.

256. van den Thillart, G.; Dufour, S.; Rankin, J.C. *Spawning Migration of the European Eel*; van den Thillart, G., Dufour, S., Rankin, J.C., Eds.; Springer Netherlands: Dordrecht, 2009; ISBN 978-1-4020-9094-3.

257. Shanks, A.L. Pelagic Larval Duration and Dispersal Distance Revisited. *Biol. Bull.* **2009**, *216*, 373–385, doi:10.1086/BBLv216n3p373.

258. Nozais, C.; Duchêne, J.C.; Bhaud, M. Control of position in the water column by the larvae of *Poecilochaetus serpens*, (Polychaeta): The importance of mucus secretion. *J. Exp. Mar. Bio. Ecol.* **1997**, *210*, 91–106, doi:10.1016/S0022-0981(96)02693-7.

259. Simpson, S.D.; Meekan, M.G.; Jeffs, A.; Montgomery, J.C.; McCauley, R.D. Settlement-stage coral reef fish prefer the higher-frequency invertebrate-generated audible component of reef noise. *Anim. Behav.* **2008**, *75*, 1861–1868, doi:10.1016/j.anbehav.2007.11.004.

260. Leis, J.M.; Carson-Ewart, B.M. Complex behaviour by coral-reef fish larvae in open-water and near-reef pelagic environments. *Environ. Biol. Fishes* **1998**, *53*, 259–266, doi:10.1023/A:1007424719764.

261. Leis, J.M.; Carson-Ewart, B.M. In situ swimming and settlement behaviour of larvae of an Indo-Pacific coral-reef fish, the coral trout *Plectropomus leopardus* (Pisces: Serranidae). *Mar. Biol.* **1999**, *134*, 51–64, doi:10.1007/s002270050524.

262. Lecchini, D.; Peyrusse, K.; Lanyon, R.G.; Lecellier, G. Importance of visual cues of conspecifics and predators during the habitat selection of coral reef fish larvae. *Comptes Rendus - Biol.* **2014**, *337*, 345–351, doi:10.1016/j.crvi.2014.03.007.

263. Vermeij, M.J.A.; Marhaver, K.L.; Huijbers, C.M.; Nagelkerken, I.; Simpson, S.D. Coral larvae move toward reef sounds. *PLoS One* **2010**, *5*, 3–6, doi:10.1371/journal.pone.0010660.

264. Lillis, A.; Bohnenstiehl, D.; Peters, J.W.; Eggleston, D. Variation in habitat soundscape characteristics influences settlement of a reef-building coral. *PeerJ* **2016**, *4*, e2557, doi:10.7717/peerj.2557.

265. Apprill, A.; Lillis, A.; Suca, J.J.; Llopiz, J.K.; Mooney, T.A.; Becker, C. Soundscapes influence the settlement of the common Caribbean coral *Porites astreoides* irrespective of light conditions. *R. Soc. Open Sci.* **2018**, *5*, 181358, doi:10.1098/rsos.181358.

266. Lillis, A.; Eggleston, D.B.; Bohnenstiehl, D.R. Oyster larvae settle in response to habitat-associated underwater sounds. *PLoS One* **2013**, *8*, 21–23, doi:10.1371/journal.pone.0079337.

267. Eggleston, D.B.; Lillis, A.; Bohnenstiehl, D.R. Soundscapes and Larval Settlement: Larval Bivalve Responses to Habitat-Associated Underwater Sounds. In *The Effects of Noise on Aquatic Life II*; 2016; pp. 255–263.

268. Hinojosa, I.A.; Green, B.S.; Gardner, C.; Hesse, J.; Stanley, J.A.; Jeffs, A.G. Reef sound as an orientation cue for shoreward migration by pueruli of the rock lobster, *Jasus edwardsii*. *PLoS One* **2016**, *11*, 1–15, doi:10.1371/journal.pone.0157862.

269. Radford, C.A.; Jeffs, A.G.; Montgomery, J.C. Directional swimming behavior by five species of crab postlarvae in response to reef sound. *Bull. Mar. Sci.* **2007**, *80*, 369–378.

270. Jeffs, A.; Tolimieri, N.; Montgomery, J.C. Crabs on cue for the coast: The use of underwater sound for orientation by pelagic crab stages. *Mar. Freshw. Res.* **2003**, *54*, 841–845, doi:10.1071/MF03007.

271. Radford, C.A.; Tindle, C.T.; Montgomery, J.C.; Jeffs, A.G. Modelling a reef as an extended sound source increases the predicted range at which reef noise may be heard by fish larvae. *Mar. Ecol. Prog. Ser.* **2011**, *438*, 167–174, doi:10.3354/meps09312.

272. Simpson, S.D.; Meekan, M.; Montgomery, J.; McCauley, R.; Jeffs, A. Homeward sound. *Science (80-.).* **2005**, *308*, 221, doi:10.1126/science.1107406.

273. Tolimieri, N.; Jeffs, A.; Montgomery, J.C. Ambient sound as a cue for navigation by the pelagic larvae of reel fishes. *Mar. Ecol. Prog. Ser.* **2000**, *207*, 219–224, doi:10.3354/meps207219.

274. Leis, J.M.; Carson-Ewart, B.M.; Cato, D.H. Sound detection in situ by the larvae of a coral-reef damselfish (Pomacentridae). *Mar. Ecol. Prog. Ser.* **2002**, *232*, 259–268, doi:10.3354/meps232259.

275. Leis, J.M.; Carson-Ewart, B.M.; Hay, A.C.; Cato, D.H. Coral-reef sounds enable nocturnal navigation by some reef-fish larvae in some places and at some times. *J. Fish Biol.* **2003**, *63*, 724–737, doi:10.1046/j.1095-8649.2003.00182.x.

276. Parmentier, E.; Berten, L.; Rigo, P.; Aubrun, F.; Nedelec, S.L.; Simpson, S.D.; Lecchini, D. The influence of various reef sounds on coral-fish larvae behaviour. *J. Fish Biol.* **2015**, *86*, 1507–1518, doi:10.1111/jfb.12651.

277. Lossent, J.; Di Iorio, L.; Valentini-Poirier, C.; Boissery, P.; Gervaise, C. Mapping the diversity of spectral shapes discriminates between adjacent benthic biophonies. *Mar. Ecol. Prog. Ser.* **2017**, *585*, 31–48, doi:10.3354/meps12370.

278. Gervaise, C.; Lossent, J.; Valentini-Poirier, C.A.; Boissery, P.; Noel, C.; Di Iorio, L. Three-dimensional mapping of the benthic invertebrates biophony with a compact four-hydrophones array. *Appl. Acoust.* **2019**, *148*, doi:10.1016/j.apacoust.2018.12.025.

279. *Ocean Noise and Marine Mammals (National Research Council; Division on Earth and Life Studies; Ocean Studies Board; Committee on Potential Impacts of Ambient Noise in the Ocean on Marine Mammals)*; Washington, DC, 2003;

280. Kinda, G.B.; Simard, Y.; Gervaise, C.; Mars, J.I.; Fortier, L. Under-ice ambient noise in Eastern Beaufort Sea, Canadian Arctic, and its relation to environmental forcing. *J. Acoust. Soc. Am.* **2013**, *134*, 77–87, doi:10.1121/1.4808330.

281. Di Iorio, L.; Raick, X.; Parmentier, E.; Boissery, P.; Valentini-Poirier, C.-A.; Gervaise, C. '*Posidonia* meadows calling': a ubiquitous fish sound with monitoring potential. *Remote Sens. Ecol. Conserv.* **2018**, *4*, 248–263, doi:10.1002/rse2.72.

282. Ainslie, M.A.; McColm, J.G. A simplified formula for viscous and chemical absorption in sea water. *J. Acoust. Soc. Am.* **1998**, *103*, 1671–1672, doi:10.1121/1.421258.

283. Nedelec, S.L.; Campbell, J.; Radford, A.N.; Simpson, S.D.; Merchant, N.D. Particle motion: the missing link in underwater acoustic ecology. *Methods Ecol. Evol.* **2016**, *7*, 836–842, doi:10.1111/2041-210X.12544.

284. Egner, S.A.; Mann, D.A. Auditory sensitivity of sergeant major damselfish Abudefduf saxatilis from post-settlement juvenile to adult. *Mar. Ecol. Prog. Ser.* **2005**, *285*, 213–222, doi:10.3354/meps285213.

285. Yost, W.A. *Fundamentals of Hearing*; Academic Press: San Diego, 2000; ISBN 9780127756950.

286. Zwicker, E.; Flottorp, G.; Stevens, S.S. Critical Band Width in Loudness Summation. *J. Acoust. Soc. Am.* **1957**, *29*, 548–557, doi:10.1121/1.1908963.

287. Wright, K.J.; Higgs, D.M.; Belanger, A.J.; Leis, J.M. Auditory and olfactory abilities of pre-settlement larvae and post-settlement juveniles of a coral reef damselfish (Pisces: Pomacentridae). *Mar. Biol.* **2005**, *147*, 1425–1434, doi:10.1007/s00227-005-0028-z.

288. Wright, K.J.; Higgs, D.M.; Leis, J.M. Ontogenetic and interspecific variation in hearing ability in marine fish larvae. *Mar. Ecol. Prog. Ser.* **2011**, *424*, 1–13, doi:10.3354/meps09004.

289. Taylor, K.A.; Nachtigall, P.E.; Mooney, T.A.; Supin, A.Y.; Yuen, M.M.L. A Portable System for the Evaluation of the Auditory Capabilities of Marine Mammals. *Aquat. Mamm.* **2007**, *33*, 93–99, doi:10.1578/AM.33.1.2007.93.

290. Kenyon, T.N. Ontogenetic changes in the auditory sensitivity of damselfishes (pomacentridae). *J. Comp. Physiol. - A Sensory, Neural, Behav. Physiol.* **1996**, *179*, 553–561, doi:10.1007/BF00192321.

291. Wright, K.J.; Higgs, D.M.; Belanger, A.J.; Leis, J.M. Auditory and olfactory abilities of larvae of the Indo-Pacific coral trout *Plectropomus leopardus* (Lacepède) at settlement. *J. Fish Biol.* **2008**, *72*, 2543–2556, doi:10.1111/j.1095-8649.2008.01864.x.

292. Colleye, O.; Kéver, L.; Lecchini, D.; Berten, L.; Parmentier, E. Auditory evoked potential audiograms in post-settlement stage individuals of coral reef fishes. *J. Exp. Mar. Bio. Ecol.* **2016**, *483*, 1–9, doi:10.1016/j.jembe.2016.05.007.

293. Pacini, A.F.; Nachtigall, P.E.; Quintos, C.T.; Schofield, T.D.; Look, D.A.; Levine, G.A.; Turner, J.P. Audiogram of a stranded Blainville's beaked whale (*Mesoplodon densirostris*) measured using auditory evoked potentials. *J. Exp. Biol.* **2011**, *214*, 2409–2415, doi:10.1242/jeb.054338.

294. Greenhow, D.R.; Brodsky, M.C.; Lingenfelser, R.G.; Mann, D.A. Hearing threshold measurements of five stranded short-finned pilot whales (*Globicephala macrorhynchus*). *J. Acoust. Soc. Am.* **2014**, *135*, 531–536, doi:10.1121/1.4829662.

295. Kastelein, R.A.; Hagedoorn, M.; Au, W.W.L.; de Haan, D. Audiogram of a striped dolphin (*Stenella coeruleoalba*). *J. Acoust. Soc. Am.* **2003**, *113*, 1130–1137, doi:10.1121/1.1532310.

296. Montgomery, J.C.; Jeffs, A.; Simpson, S.D.; Meekan, M.; Tindle, C. Sound as an Orientation Cue for the Pelagic Larvae of Reef Fishes and Decapod Crustaceans. *Adv. Mar. Biol.* **2006**, *51*, 143–196, doi:10.1016/S0065-2881(06)51003-X.

297. Wysocki, L.E.; Codarin, A.; Ladich, F.; Picciulin, M. Sound pressure and particle acceleration audiograms in three marine fish species from the Adriatic Sea. *J. Acoust. Soc. Am.* **2009**, *126*, 2100, doi:10.1121/1.3203562.

298. Radford, C.A.; Montgomery, J.C.; Caiger, P.; Higgs, D.M. Pressure and particle motion detection thresholds in fish: A re-examination of salient auditory cues in teleosts. *J. Exp. Biol.* **2012**, *215*, 3429–3435, doi:10.1242/jeb.073320.

299. Chapman, C.J.; Sand, O. Field studies of hearing in two species of flatfish *Pleuronectes platessa* (L.) and *Limanda limanda* (L.) (family pleuronectidae). *Comp. Biochem. Physiol. Part A Physiol.* **1974**, *47*, 371–385, doi:10.1016/0300-9629(74)90082-6.

300. Houser, D.S.; Helweg, D.A.; Moore, P.W.B. A bandpass filter-bank model of auditory sensitivity in the humpback whale. *Aquat. Mamm.* **2001**, *27*, 82–91.

301. Hughes, A.R.; Mann, D.A.; Kimbro, D.L.; Randall Hughes, A.; Mann, D.A.; Kimbro, D.L. Predatory fish sounds can alter crab foraging behaviour and influence bivalve abundance. *Proc. R. Soc. B Biol. Sci.* **2014**, *281*, 20140715, doi:10.1098/rspb.2014.0715.

302. Breithaupt, T.; Tautz, J. Vibration sensitivity of the crayfish statocyst. *Naturwissenschaften* **1988**, *75*, 310–312, doi:10.1007/BF00367325.

303. Lovell, J.M.; Findlay, M.M.; Moate, R.M.; Yan, H.Y. The hearing abilities of the prawn *Palaemon serratus*. *Comp. Biochem. Physiol. - A Mol. Integr. Physiol.* **2005**, *140*, 89–100, doi:10.1016/j.cbpb.2004.11.003.

304. Hu, M.Y.; Yan, H.Y.; Chung, W.S.; Shiao, J.C.; Hwang, P.P. Acoustically evoked potentials in two cephalopods inferred using the auditory brainstem response (ABR) approach. *Comp. Biochem. Physiol. - A Mol. Integr. Physiol.* **2009**, *153*, 278–283, doi:10.1016/j.cbpa.2009.02.040.

305. Mooney, T.A.; Hanlon, R.T.; Christensen-Dalsgaard, J.; Madsen, P.T.; Ketten, D.R.; Nachtigall, P.E. Sound detection by the longfin squid (Loligo pealeii) studied with auditory evoked potentials: sensitivity to low-frequency particle motion and not pressure. *J. Exp. Biol.* **2010**, *213*, 3748–3759, doi:10.1242/jeb.048348.

306. Budelmann, B.U.; Bleckmann, H. A lateral line analogue in cephalopods: water waves generate microphonic potentials in the epidermal head lines of *Sepia* and *Lolliguncula*. *J. Comp. Physiol. A* **1988**, *164*, 1–5, doi:10.1007/BF00612711.

307. Kaplan, M.B.; Mooney, T.A. Coral reef soundscapes may not be detectable far from the reef. *Sci. Rep.* **2016**, *6*, 1–10, doi:10.1038/srep31862.

308. Stanley, J.A.; Radford, C.A.; Jeffs, A.G. Behavioural response thresholds in New Zealand crab megalopae to ambient underwater sound. *PLoS One* **2011**, *6*, doi:10.1371/journal.pone.0028572.

309. Moore, S.E.; Clarke, J.T. Potential impact of offshore human activities on gray whales. *J. Cetacean Res. Manag.* **2002**, *4*, 19–25.

310. Fay, R.R. The goldfish ear codes the axis of acoustic particle motion in three dimensions. *Science (80-.).* **1984**, *225*, 951–954, doi:10.1126/science.6474161.

311. Horodysky, A.Z.; Brill, R.W.; Fine, M.L.; Musick, J.A.; Latour, R.J. Acoustic pressure and particle motion thresholds in six sciaenid fishes. *J. Exp. Biol.* **2008**, *211*, 1504–1511, doi:10.1242/jeb.016196.

312. Norris, K.S. Some observations on the migration and orientation of marine mammals. In Proceedings of the Animal Orientation and Navigation. Proceedings of the Twenty-Seventh Annual Biology Colloquium.; Storm, R.M., Ed.; Oregon State University Press: Corvallis, 1967; p. ix+134pp.

313. Ladich, F. Communication in fishes. In *Sound Communication in Fishes*; 2015; pp. 127–148 ISBN 9783709118450.

314. Desjonquères, C.; Rybak, F.; Castella, E.; Llusia, D.; Sueur, J. Acoustic communities reflects lateral hydrological connectivity in riverine floodplain similarly to macroinvertebrate communities. *Sci. Rep.* **2018**, *8*, 14387, doi:10.1038/s41598-018-31798-4.

315. Sueur, J.; Farina, A. Ecoacoustics: the Ecological Investigation and Interpretation of Environmental Sound. *Biosemiotics* **2015**, *8*, 493–502, doi:10.1007/s12304-015-9248-x.

316. Gibb, R.; Browning, E.; Glover-Kapfer, P.; Jones, K.E. Emerging opportunities and challenges for passive acoustics in ecological assessment and monitoring. *Methods Ecol. Evol.* **2019**, *10*, 169–185, doi:10.1111/2041-210X.13101.

317. Bolgan, M.; Gervaise, C.; Di Iorio, L.; Lossent, J.; Lejeune, P.; Raick, X.; Parmentier, E. Fish biophony in a Mediterranean submarine canyon. *J. Acoust. Soc. Am.* **2020**, *147*, 2466–2477, doi:10.1121/10.0001101.

318. Di Iorio, L.; Audax, M.; Deter, J.; Holon, F.; Lossent, J.; Gervaise, C.; Boissery, P. Biogeography of acoustic biodiversity of NW Mediterranean coralligenous reefs. *Sci. Rep.* **2021**, *11*, 16991, doi:10.1038/s41598-021-96378-5.

319. Favaro, L.; Cresta, E.; Friard, O.; Ludynia, K.; Mathevon, N.; Pichegru, L.; Reby, D.; Gamba, M. Passive acoustic monitoring of the endangered African Penguin (*Spheniscus demersus*) using autonomous recording units and ecoacoustic indices. *Ibis (Lond. 1859).* **2021**, *163*, 1472–1480, doi:10.1111/ibi.12970.

320. Lin, T.-H.; Chen, C.; Watanabe, H.K.; Kawagucci, S.; Yamamoto, H.; Akamatsu, T. Using Soundscapes to Assess Deep-Sea Benthic Ecosystems. *Trends Ecol. Evol.* **2019**, *34*, 1066–1069, doi:10.1016/j.tree.2019.09.006.

321. Loya, Y.; Puglise, K.A.; Bridge, T.C.L. *Mesophotic Coral Ecosystems*; Loya, Y., Puglise, K.A., Bridge, T.C.L., Eds.; Coral Reefs of the World; Springer International Publishing: Cham, 2019; ISBN 978-3-319-92734-3.

322. Lesser, M.; Slattery, M.; Leichter, J. Ecology of mesophotic coral reefs. *J. Exp. Mar. Bio. Ecol.* **2009**, *375*, 1–8, doi:10.1016/j.jembe.2009.05.009.

323. Weinstein, D.K.; Klaus, J.S.; Smith, T.B. Habitat heterogeneity reflected in mesophotic reef sediments. *Sediment. Geol.* **2015**, *329*, 177–187, doi:10.1016/j.sedgeo.2015.07.003.

324. Pyle, R.L.; Copus, J.M. Mesophotic Coral Ecosystems: Introduction and Overview. In *Mesophotic Coral Ecosystems*; 2019; pp. 3–27.

325. Minier, L.; Bertucci, F.; Raick, X.; Gairin, E.; Bischoff, H.; Waqalevu, V.; Maueau, T.; Sturny, V.; Blin, E.; Parmentier, E.; et al. Characterization of the different sound sources within the soundscape of coastline reef habitats (Bora Bora, French Polynesia). *Estuar. Coast. Shelf Sci.* **2023**, *294*, 108551, doi:10.1016/j.ecss.2023.108551.

326. Minier, L.; Raick, X.; Gairin, E.; Maueau, T.; Sturny, V.; Blin, E.; Parmentier, E.; Bertucci, F.; Lecchini, D. 'Habitat-associated soundscape' hypothesis tested on several coral reefs within a lagoon (Bora-Bora Island, French Polynesia). *Mar. Biol.* **2023**, *170*, 61, doi:10.1007/s00227-023-04206-3.

327. Kahng, S.E.; Kelley, C.D. Vertical zonation of megabenthic taxa on a deep photosynthetic reef (50–140 m) in the Au'au Channel, Hawaii. *Coral Reefs* **2007**, *26*, 679–687, doi:10.1007/s00338-007-0253-7.

328. Milligan, R.J.; Spence, G.; Roberts, J.M.; Bailey, D.M. Fish communities associated with cold-water corals vary with depth and substratum type. *Deep Sea Res. Part I Oceanogr. Res. Pap.* **2016**, *114*, 43–54, doi:10.1016/j.dsr.2016.04.011.

329. Goreau, T.; Goreau, N. The ecology of Jamaican coral reefs. II. Geomorphology, zonation, and sedimentary phases. *Bull Mar Sci* **1973**, *23*, 399–464.

330. Liddell, W.D.; Ohlhorst, S.L. Hard Substrata Community Patterns, 1-120 M, North Jamaica. *Palaios* **1988**, *3*, 413, doi:10.2307/3514787.

331. Lesser, M.P.; Slattery, M.; Laverick, J.H.; Macartney, K.J.; Bridge, T.C. Global community breaks at 60 m on mesophotic coral reefs. *Glob. Ecol. Biogeogr.* **2019**, *28*, 1403–1416, doi:10.1111/geb.12940.

332. Pérez-Rosales, G.; Hernández-Agreda, A.; Bongaerts, P.; Rouzé, H.; Pichon, M.; Carlot, J.; Torda, G.; Parravicini, V.; Hédouin, L. Mesophotic depths hide high coral cover communities in French Polynesia. *Sci. Total Environ.* **2022**, *844*, 157049, doi:10.1016/j.scitotenv.2022.157049.

333. Chin, Y.-Y.; Prince, J.; Kendrick, G.; Abdul Wahab, M.A. Sponges in shallow tropical and temperate reefs are important habitats for marine invertebrate biodiversity. *Mar. Biol.* **2020**, *167*, 164, doi:10.1007/s00227-020-03771-1.

334. Díaz, M.C.; Rützler, K. Sponges: An essential component of caribbean coral reefs. *Bull. Mar. Sci.* **2001**, *69*, 535–546.

335. Radford, C.A.; Stanley, J.A.; Hole, W.; Montgomery, J.C.; Jeffs, A. Localised coastal habitats have distinct underwater sound signatures. *Mar. Ecol. Prog. Ser.* **2010**, *401*, 21–29, doi:10.3354/meps08451.

336. Radford, C.A.; Stanley, J.A.; Jeffs, A.G. Adjacent coral reef habitats produce different underwater sound signatures. *Mar. Ecol. Prog. Ser.* **2014**, *505*, 19–28, doi:10.3354/meps10782.

337. Rossi, T.; Connell, S.D.; Nagelkerken, I. Silent oceans: Ocean acidification impoverishes natural soundscapes by altering sound production of the world's noisiest marine invertebrate. *Proc. R. Soc. B Biol. Sci.* **2016**, *283*, doi:10.1098/rspb.2015.3046.

338. Watanabe, M.; Sekine, M.; Hamada, E.; Ukita, M.; Imai, T. Monitoring of shallow sea environment by using snapping shrimps. *Water Sci. Technol.* **2002**, *46*, 419–424, doi:10.2166/wst.2002.0772.

339. Pérez-Rosales, G.; Pichon, M.; Rouzé, H.; Villéger, S.; Torda, G.; Bongaerts, P.; Carlot, J.; Parravicini, V.; Hédouin, L. Mesophotic coral ecosystems of French Polynesia are hotspots of alpha and beta generic diversity for scleractinian assemblages. *Divers. Distrib.* **2022**, *28*, 1391–1403, doi:10.1111/ddi.13549.

340. Jézéquel, Y.; Bonnel, J.; Coston-Guarini, J.; Guarini, J.; Chauvaud, L. Sound characterization of the European lobster *Homarus gammarus* in tanks. *Aquat. Biol.* **2018**, *27*, 13–23, doi:10.3354/ab00692.

341. Oksanen, J.; Blanchet, F.G.; Kindt, R.; Legendre, P.; Minchin, P.R.; O'Hara, R.B.; Simpson, G.L.;

Solymos, P.; Stevenes, M.H.H.; Wagner, H. *Vegan: Community Ecology Package. R package version 2.0-2*; 2012;

342. Kopp, D.; Bouchon-Navaro, Y.; Louis, M.; Legendre, P.; Bouchon, C. Spatial and Temporal Variation in a Caribbean Herbivorous Fish Assemblage. *J. Coast. Res.* **2012**, *278*, 63–72, doi:10.2112/JCOASTRES-D-09-00165.1.

343. Ramette, A. Multivariate analyses in microbial ecology. *FEMS Microbiol. Ecol.* **2007**, *62*, 142–160, doi:10.1111/j.1574-6941.2007.00375.x.

344. ter Braak, C.J.F. Canonical community ordination. Part I: Basic theory and linear methods. *Écoscience* **1994**, *1*, 127–140, doi:10.1080/11956860.1994.11682237.

345. Rao, C.R. The Use and Interpretation of Principal Component Analysis in Applied Research. *Sankhyā Indian J. Stat. Ser. A* **1964**, *26*, 329–358.

346. Hurley, K.K.C.; Timmers, M.A.; Godwin, L.S.; Copus, J.M.; Skillings, D.J.; Toonen, R.J. An assessment of shallow and mesophotic reef brachyuran crab assemblages on the south shore of O'ahu, Hawai'i. *Coral Reefs* **2016**, *35*, 103–112, doi:10.1007/s00338-015-1382-z.

347. Anker, A. On two new deep-water snapping shrimps from the Indo-West Pacific (Decapoda: Alpheidae: *Alpheus*). *Zootaxa* **2020**, *4845*, 393–409, doi:10.11646/zootaxa.4845.3.5.

348. Lin, T.-H.; Akamatsu, T.; Sinniger, F.; Harii, S. Exploring coral reef biodiversity via underwater soundscapes. *Biol. Conserv.* **2021**, *253*, 108901, doi:10.1016/j.biocon.2020.108901.

349. Connell, S.D.; Kroeker, K.J.; Fabricius, K.E.; Kline, D.I.; Russell, B.D. The other ocean acidification problem: CO2 as a resource among competitors for ecosystem dominance. *Philos. Trans. R. Soc. B Biol. Sci.* **2013**, *368*, 20120442, doi:10.1098/rstb.2012.0442.

350. Nagelkerken, I.; Russell, B.D.; Gillanders, B.M.; Connell, S.D. Ocean acidification alters fish populations indirectly through habitat modification. *Nat. Clim. Chang.* **2016**, *6*, 89–93, doi:10.1038/nclimate2757.

351. Knowlton, R.E.; Moulton, J.M. Sound production in the snapping shrimps *Alpheus* (*Crangon*) and *Synalpheus*. *Biol. Bull.* **1963**, *125*, 311–331, doi:10.2307/1539406.

352. Hazlett, B.; Winn, H.E. Sound Producing Mechanism of the Nassau Grouper *Epinephelus striatus*. *Copeia* **1962**, *2*, 447–449, doi:10.2307/1440928.

353. Readhead, M.L. Snapping shrimp noise near Gladstone, Queensland. *J. Acoust. Soc. Am.* **1997**, *101*, 1718–1722, doi:10.1121/1.418153.

354. Buscaino, G.; Filiciotto, F.; Gristina, M.; Bellante, A.; Buffa, G.; Di Stefano, V.; Maccarrone, V.; Tranchida, G.; Buscaino, C.; Mazzola, S. Acoustic behaviour of the European spiny lobster *Palinurus elephas*. *Mar. Ecol. Prog. Ser.* **2011**, *441*, 177–184, doi:10.3354/meps09404.

355. Mulligan, B.E.; Fischer, R.B. Sounds and Behavior of the Spiny Lobster *Panulirus argus* (Latreille, 1804) (Decapoda, Palinuridae). *Crustaceana* **1977**, *32*, 185–199.

356. Patek, S.N.; Shipp, L.E.; Staaterman, E.R. The acoustics and acoustic behavior of the California spiny lobster (*Panulirus interruptus*). *J. Acoust. Soc. Am.* **2009**, *125*, 3434, doi:10.1121/1.3097760.

357. Hazlett, B.A.; Winn, H.E. Characteristics of a Sound Produced by the Lobster *Justitia longimanus*. *Ecology* **1962**, *43*, 741–742, doi:10.2307/1933469.

358. Berk, I.M. Sound production by white shrimp (*Penaeus setiferus*) analysis of another crustacean-like sound from the Gulf of Mexico, and the possible use of passive sonar for dedication and stock assessment of shrimp, Texas A&M University, 1997.

359. Silva, J.F.; Hamilton, S.; Rocha, J.V.; Borie, A.; Travassos, P.; Soares, R.; Peixoto, S. Acoustic characterization of feeding activity of *Litopenaeus vannamei* in captivity. *Aquaculture* **2019**, *501*, 76–81, doi:10.1016/j.aquaculture.2018.11.013.

360. Wei, M.; Lin, Y.; Chen, K.; Su, W.; Cheng, E. Study on Feeding Activity of *Litopenaeus vannamei* Based on Passive Acoustic Detection. *IEEE Access* **2020**, *8*, 156654–156662,

doi:10.1109/ACCESS.2020.3019529.

361. Rossi, S.; Bramanti, L.; Gori, A.; Orejas, C. An Overview of the Animal Forests of the World. In *Marine Animal Forests*; Springer International Publishing: Cham, 2017; pp. 1–26.

362. Poupin, J.; Barathieu, G.; Konieczny, O.; Mulochau, T. Crustacés (Decapoda, Stomatopoda) dans la zone mésophotique corallienne de Mayotte (Sud-Ouest Océan Indien). *Naturae* **2022**, *2022*, doi:10.5852/naturae2022a8.

363. Oliver, T.H.; Heard, M.S.; Isaac, N.J.B.; Roy, D.B.; Procter, D.; Eigenbrod, F.; Freckleton, R.; Hector, A.; Orme, C.D.L.; Petchey, O.L.; et al. Biodiversity and Resilience of Ecosystem Functions. *Trends Ecol. Evol.* **2015**, *30*, 673–684, doi:10.1016/j.tree.2015.08.009.

364. Marques, L. Collapse of Biodiversity in the Aquatic Environment. In *Capitalism and Environmental Collapse*; Springer International Publishing: Cham, 2020; pp. 275–301.

365. Whittaker, R.H. Evolution and measurement of species diversity. *Taxon* **1972**, *21*, 213–251, doi:10.2307/1218190.

366. Blumstein, D.T.; Mennill, D.J.; Clemins, P.; Girod, L.; Yao, K.; Patricelli, G.; Deppe, J.L.; Krakauer, A.H.; Clark, C.; Cortopassi, K.A.; et al. Acoustic monitoring in terrestrial environments using microphone arrays: applications, technological considerations and prospectus. *J. Appl. Ecol.* **2011**, *48*, 758–767, doi:10.1111/j.1365-2664.2011.01993.x.

367. Celis-Murillo, A.; Deppe, J.L.; Allen, M.F. Using soundscape recordings to estimate bird species abundance, richness, and composition. *J. F. Ornithol.* **2009**, *80*, 64–78, doi:10.1111/j.1557-9263.2009.00206.x.

368. Maron, M.; Juffe-Bignoli, D.; Krueger, L.; Kiesecker, J.; Kümpel, N.F.; ten Kate, K.; Milner-Gulland, E.J.; Arlidge, W.N.S.; Booth, H.; Bull, J.W.; et al. Setting robust biodiversity goals. *Conserv. Lett.* **2021**, *14*, doi:10.1111/conl.12816.

369. Sueur, J.; Farina, A.; Gasc, A.; Pieretti, N.; Pavoine, S. Acoustic indices for biodiversity assessment and landscape investigation. *Acta Acust. united with Acust.* **2014**, *100*, 772–781, doi:10.3813/AAA.918757.

370. Rodriguez, A.; Gasc, A.; Pavoine, S.; Grandcolas, P.; Gaucher, P.; Sueur, J. Temporal and spatial variability of animal sound within a neotropical forest. *Ecol. Inform.* **2014**, *21*, 133–143, doi:10.1016/j.ecoinf.2013.12.006.

371. Gage, S.H.; Axel, A.C. Visualization of temporal change in soundscape power of a Michigan lake habitat over a 4-year period. *Ecol. Inform.* **2014**, *21*, 100–109, doi:10.1016/j.ecoinf.2013.11.004.

372. Barber, J.R.; Crooks, K.R.; Fristrup, K.M. The costs of chronic noise exposure for terrestrial organisms. *Trends Ecol. Evol.* **2010**, *25*, 180–189, doi:10.1016/j.tree.2009.08.002.

373. Francis, C.D.; Paritsis, J.; Ortega, C.P.; Cruz, A. Landscape patterns of avian habitat use and nest success are affected by chronic gas well compressor noise. *Landsc. Ecol.* **2011**, *26*, 1269–1280, doi:10.1007/s10980-011-9609-z.

374. González-Oreja, J.A.; De La Fuente-Díaz-Ordaz, A.A.; Hernández-Santín, L.; Bonache-Regidor, C.; Buzo-Franco, D. Can human disturbance promote nestedness? Songbirds and noise in urban parks as a case study. *Landsc. Urban Plan.* **2012**, *104*, 9–18, doi:10.1016/j.landurbplan.2011.09.001.

375. Boelman, N.T.; Asner, G.P.; Hart, P.J.; Martin, R.E. Multi-trophic invasion resistance in Hawaii: Bioacoustics, field surveys, and airborne remote sensing. *Ecol. Appl.* **2007**, *17*, 2137–2144, doi:10.1890/07-0004.1.

376. Depraetere, M.; Pavoine, S.; Jiguet, F.; Gasc, A.; Duvail, S.; Sueur, J. Monitoring animal diversity using acoustic indices: Implementation in a temperate woodland. *Ecol. Indic.* **2012**, *13*, 46–54, doi:10.1016/j.ecolind.2011.05.006.

377. Sueur, J.; Pavoine, S.; Hamerlynck, O.; Duvail, S. Rapid Acoustic Survey for Biodiversity Appraisal. *PLoS One* **2008**, *3*, e4065, doi:10.1371/journal.pone.0004065.

378. Towsey, M.; Wimmer, J.; Williamson, I.; Roe, P. The use of acoustic indices to determine avian species richness in audio-recordings of the environment. *Ecol. Inform.* **2014**, *21*, 110–119,

doi:10.1016/j.ecoinf.2013.11.007.

379. Pekin, B.K.; Jung, J.; Villanueva-Rivera, L.J.; Pijanowski, B.C.; Ahumada, J.A. Modeling acoustic diversity using soundscape recordings and LIDAR-derived metrics of vertical forest structure in a neotropical rainforest. *Landsc. Ecol.* **2012**, *27*, 1513–1522, doi:10.1007/s10980-012-9806-4.

380. Joo, W.; Gage, S.H.; Kasten, E.P. Analysis and interpretation of variability in soundscapes along an urban–rural gradient. *Landsc. Urban Plan.* **2011**, *103*, 259–276, doi:10.1016/j.landurbplan.2011.08.001.

381. Pieretti, N.; Farina, A.; Morri, D. A new methodology to infer the singing activity of an avian community: The Acoustic Complexity Index (ACI). *Ecol. Indic.* **2011**, *11*, 868–873, doi:10.1016/j.ecolind.2010.11.005.

382. Gasc, A.; Sueur, J.; Pavoine, S.; Pellens, R.; Grandcolas, P. Biodiversity Sampling Using a Global Acoustic Approach: Contrasting Sites with Microendemics in New Caledonia. *PLoS One* **2013**, *8*, e65311, doi:10.1371/journal.pone.0065311.

383. Kasten, E.P.; Gage, S.H.; Fox, J.; Joo, W. The remote environmental assessment laboratory's acoustic library: An archive for studying soundscape ecology. *Ecol. Inform.* **2012**, *12*, 50–67, doi:10.1016/j.ecoinf.2012.08.001.

384. Krause, B.; Gage, S.H.; Joo, W. Measuring and interpreting the temporal variability in the soundscape at four places in Sequoia National Park. *Landsc. Ecol.* **2011**, *26*, 1247–1256, doi:10.1007/s10980-011-9639-6.

385. Do Nascimento, L.A.; Campos-Cerqueira, M.; Beard, K.H. Acoustic metrics predict habitat type and vegetation structure in the Amazon. *Ecol. Indic.* **2020**, *117*, 106679, doi:10.1016/j.ecolind.2020.106679.

386. Buxton, R.T.; Agnihotri, S.; Robin, V. V.; Goel, A.; Balakrishnan, R. Acoustic indices as rapid indicators of avian diversity in different land-use types in an Indian biodiversity hotspot. *J. Ecoacoustics* **2018**, *2*, 1–1, doi:10.22261/jea.gwpzvd.

387. Retamosa Izaguirre, M.I.; Ramírez-Alán, O. Acoustic indices applied to biodiversity monitoring in a Costa Rica dry tropical forest. *J. Ecoacoustics* **2018**, *2*, 1–1, doi:10.22261/jea.tnw2np.

388. Moreno-Gómez, F.N.; Bartheld, J.; Silva-Escobar, A.A.; Briones, R.; Márquez, R.; Penna, M. Evaluating acoustic indices in the Valdivian rainforest, a biodiversity hotspot in South America. *Ecol. Indic.* **2019**, *103*, 1–8, doi:10.1016/j.ecolind.2019.03.024.

389. Jorge, F.C.; Machado, C.G.; da Cunha Nogueira, S.S.; Nogueira-Filho, S.L.G. The effectiveness of acoustic indices for forest monitoring in Atlantic rainforest fragments. *Ecol. Indic.* **2018**, *91*, 71–76, doi:10.1016/j.ecolind.2018.04.001.

390. Campos, I.B.; Fewster, R.; Truskinger, A.; Towsey, M.; Roe, P.; Vasques Filho, D.; Lee, W.; Gaskett, A. Assessing the potential of acoustic indices for protected area monitoring in the Serra do Cipó National Park, Brazil. *Ecol. Indic.* **2021**, *120*, 106953, doi:10.1016/j.ecolind.2020.106953.

391. Machado, R.B.; Aguiar, L.; Jones, G. Do acoustic indices reflect the characteristics of bird communities in the savannas of Central Brazil? *Landsc. Urban Plan.* **2017**, *162*, 36–43, doi:10.1016/j.landurbplan.2017.01.014.

392. Farina, A.; Righini, R.; Fuller, S.; Li, P.; Pavan, G. Acoustic complexity indices reveal the acoustic communities of the old-growth Mediterranean forest of Sasso Fratino Integral Natural Reserve (Central Italy). *Ecol. Indic.* **2021**, *120*, 106927, doi:10.1016/j.ecolind.2020.106927.

393. Gómez, W.E.; Isaza, C. V.; Daza, J.M. Identifying disturbed habitats: A new method from acoustic indices. *Ecol. Inform.* **2018**, *45*, 16–25, doi:10.1016/j.ecoinf.2018.03.001.

394. Fairbrass, A.J.; Rennert, P.; Williams, C.; Titheridge, H.; Jones, K.E. Biases of acoustic indices measuring biodiversity in urban areas. *Ecol. Indic.* **2017**, *83*, 169–177, doi:10.1016/j.ecolind.2017.07.064.

395. Rajan, S.C.; Athira, K.; Jaishanker, R.; Sooraj, N.P.; Sarojkumar, V. Rapid assessment of biodiversity using acoustic indices. *Biodivers. Conserv.* **2019**, *28*, 2371–2383, doi:10.1007/s10531-018-1673-0.

396. Bolgan, M.; Amorim, M.C.P.; Fonseca, P.J.; Di Iorio, L.; Parmentier, E. Acoustic complexity of vocal

fish communities: A field and controlled validation. *Sci. Rep.* **2018**, *8*, doi:10.1038/s41598-018-28771-6.

397. Staaterman, E.; Paris, C.B.; DeFerrari, H.A.; Mann, D.A.; Rice, A.N.; D'Alessandro, E.K. Celestial patterns in marine soundscapes. *Mar. Ecol. Prog. Ser.* **2014**, *508*, 17–32, doi:10.3354/meps10911.

398. Staaterman, E.; Ogburn, M.; Altieri, A.; Brandl, S.; Whippo, R.; Seemann, J.; Goodison, M.; Duffy, J. Bioacoustic measurements complement visual biodiversity surveys: preliminary evidence from four shallow marine habitats. *Mar. Ecol. Prog. Ser.* **2017**, *575*, 207–215, doi:10.3354/meps12188.

399. Decker, E.; Parker, B.; Linke, S.; Capon, S.; Sheldon, F. Singing streams: Describing freshwater soundscapes with the help of acoustic indices. *Ecol. Evol.* **2020**, *10*, 4979–4989, doi:10.1002/ece3.6251.

400. Desjonquères, C.; Rybak, F.; Depraetere, M.; Gasc, A.; Le Viol, I.; Pavoine, S.; Sueur, J. First description of underwater acoustic diversity in three temperate ponds. *PeerJ* **2015**, *3*, e1393, doi:10.7717/peerj.1393.

401. Ceraulo, M.; Papale, E.; Caruso, F.; Filiciotto, F.; Grammauta, R.; Parisi, I.; Mazzola, S.; Farina, A.; Buscaino, G. Acoustic comparison of a patchy Mediterranean shallow water seascape: *Posidonia oceanica* meadow and sandy bottom habitats. *Ecol. Indic.* **2018**, *85*, 1030–1043, doi:10.1016/j.ecolind.2017.08.066.

402. Carriço, R.; Silva, M.; Vieira, M.; Afonso, P.; Menezes, G.; Fonseca, P.; Amorim, M. The Use of Soundscapes to Monitor Fish Communities: Meaningful Graphical Representations Differ with Acoustic Environment. *Acoustics* **2020**, *2*, 382–398, doi:10.3390/acoustics2020022.

403. Harris, S.A.; Shears, N.T.; Radford, C.A. Ecoacoustic indices as proxies for biodiversity on temperate reefs. *Methods Ecol. Evol.* **2016**, *7*, 713–724, doi:10.1111/2041-210X.12527.

404. Dimoff, S.A.; Halliday, W.D.; Pine, M.K.; Tietjen, K.L.; Juanes, F.; Baum, J.K. The utility of different acoustic indicators to describe biological sounds of a coral reef soundscape. *Ecol. Indic.* **2021**, *124*, 107435, doi:10.1016/j.ecolind.2021.107435.

405. Bohnenstiehl, D.R.; Lyon, R.P.; Caretti, O.N.; Ricci, S.W.; Eggleston, D.B. Investigating the utility of ecoacoustic metrics in marine soundscapes. *J. Ecoacoustics* **2018**, *2*, 1–1, doi:10.22261/JEA.R1156L.

406. Peck, M.; Tapilatu, R.F.; Kurniati, E.; Rosado, C. Rapid coral reef assessment using 3D modelling and acoustics: acoustic indices correlate to fish abundance, diversity and environmental indicators in West Papua, Indonesia. *PeerJ* **2021**, *9*, e10761, doi:10.7717/peerj.10761.

407. Zhao, Z.; Xu, Z.; Bellisario, K.; Zeng, R.; Li, N.; Zhou, W.; Pijanowski, B.C. How well do acoustic indices measure biodiversity? Computational experiments to determine effect of sound unit shape, vocalization intensity, and frequency of vocalization occurrence on performance of acoustic indices. *Ecol. Indic.* **2019**, *107*, 105588, doi:10.1016/j.ecolind.2019.105588.

408. Minello, M.; Calado, L.; Xavier, F.C. Ecoacoustic indices in marine ecosystems: a review on recent developments, challenges, and future directions. *ICES J. Mar. Sci.* **2021**, doi:10.1093/icesjms/fsab193.

409. Villanueva-Rivera, L.J.; Pijanowski, B.C.; Doucette, J.; Pekin, B. A primer of acoustic analysis for landscape ecologists. *Landsc. Ecol.* **2011**, *26*, 1233–1246, doi:10.1007/s10980-011-9636-9.

410. Krause, B. *The great animal orchestra: finding the origins of music in the world's wild places*; Parsley, J., Ed.; Little, Brown and Company, 2012; ISBN 978-0316086875.

411. Eldridge, A.; Guyot, P.; Moscoso, P.; Johnston, A.; Eyre-Walker, Y.; Peck, M. Sounding out ecoacoustic metrics: Avian species richness is predicted by acoustic indices in temperate but not tropical habitats. *Ecol. Indic.* **2018**, *95*, 939–952, doi:10.1016/j.ecolind.2018.06.012.

412. Ross, S.R.-J.; Friedman, N.R.; Yoshimura, M.; Yoshida, T.; Donohue, I.; Economo, E.P. Utility of acoustic indices for ecological monitoring in complex sonic environments. *Ecol. Indic.* **2021**, *121*, 107114, doi:10.1016/j.ecolind.2020.107114.

413. Williams, B.; Lamont, T.A.C.; Chapuis, L.; Harding, H.R.; May, E.B.; Prasetya, M.E.; Seraphim, M.J.; Jompa, J.; Smith, D.J.; Janetski, N.; et al. Enhancing automated analysis of marine soundscapes using ecoacoustic indices and machine learning. *Ecol. Indic.* **2022**, *140*, 108986, doi:10.1016/j.ecolind.2022.108986.

414. Indraswari, K.; Bower, D.S.; Tucker, D.; Schwarzkopf, L.; Towsey, M.; Roe, P. Assessing the value of acoustic indices to distinguish species and quantify activity: A case study using frogs. *Freshw. Biol.* **2020**, *65*, 142–152, doi:10.1111/fwb.13222.

415. Farina, A.; Lattanzi, E.; Piccioli, L.; Pieretti, N. The SoundscapeMeter 2012, http://www.disbef.uniurb.it/biomia/soundscapemeter.

416. Gasc, A.; Francomano, D.; Dunning, J.B.; Pijanowski, B.C. Future directions for soundscape ecology: The importance of ornithological contributions. *Auk* **2017**, *134*, 215–228, doi:10.1642/AUK-16-124.1.

417. Nedelec, S.L.; Simpson, S.D.; Holderied, M.; Radford, A.N.; Lecellier, G.; Radford, C.; Lecchini, D. Soundscapes and living communities in coral reefs: Temporal and spatial variation. *Mar. Ecol. Prog. Ser.* **2015**, *524*, 125–135, doi:10.3354/meps11175.

418. Gasc, A.; Pavoine, S.; Lellouch, L.; Grandcolas, P.; Sueur, J. Acoustic indices for biodiversity assessments: Analyses of bias based on simulated bird assemblages and recommendations for field surveys. *Biol. Conserv.* **2015**, *191*, 306–312, doi:10.1016/j.biocon.2015.06.018.

419. Donaldson, T.J. High Islands Versus Low Islands: A Comparison of Fish Faunal Composition of the Palau Islands. *Environ. Biol. Fishes* **2002**, *65*, 241–248, doi:10.1023/A:1020067931910.

420. Wagner, D.; Kosaki, R.K.; Spalding, H.L.; Whitton, R.K.; Pyle, R.L.; Sherwood, A.R.; Tsuda, R.T.; Calcinai, B. Mesophotic surveys of the flora and fauna at Johnston Atoll, Central Pacific Ocean. *Mar. Biodivers. Rec.* **2014**, *7*, e68, doi:10.1017/S1755267214000785.

421. Pinheiro, H.T.; Goodbody-Gringley, G.; Jessup, M.E.; Shepherd, B.; Chequer, A.D.; Rocha, L.A. Upper and lower mesophotic coral reef fish communities evaluated by underwater visual censuses in two Caribbean locations. *Coral Reefs* **2016**, *35*, 139–151, doi:10.1007/s00338-015-1381-0.

422. Vigliola, L.; Galzin, R.; Harmelin-Vivien, M.L.; Salvat, B. Les Heterocongrinae (Teleostei:Congridae) de la pente externe de Moorea (Ile de la Société, Polynésie Française): distribution et biologie. *Cybium* **1996**, *20*, 379–393, doi:10.26028/cybium/1996-204-004.

423. Bertucci, F.; Lejeune, P.; Payrot, J.; Parmentier, E. Sound production by dusky grouper Epinephelus marginatus at spawning aggregation sites. *J. Fish Biol.* **2015**, *87*, 400–421, doi:10.1111/jfb.12733.

424. Mélotte, G.; Raick, X.; Vigouroux, R.; Parmentier, E. Origin and evolution of sound production in Serrasalmidae. *Biol. J. Linn. Soc.* **2019**, *128*, 403–414, doi:10.1093/biolinnean/blz105.

425. Jost, L. Partitioning diversity into independent alpha and beta components. *Ecology* **2007**, *88*, 2427–2439, doi:10.1890/06-1736.1.

426. Alvarez, I.; Rasmuson, L.K.; Gerard, T.; Laiz-Carrion, R.; Hidalgo, M.; Lamkin, J.T.; Malca, E.; Ferra, C.; Torres, A.P.; Alvarez-Berastegui, D.; et al. Influence of the Seasonal Thermocline on the Vertical Distribution of Larval Fish Assemblages Associated with Atlantic Bluefin Tuna Spawning Grounds. *Oceans* **2021**, *2*, 64–83, doi:10.3390/oceans2010004.

427. Chambers, J.M. Linear Models. In *Statistical Models*; Chambers, S.J.M., Hastie, T.J., Eds.; Wadsworth & Brooks/Cole, Pacific Grove, California, 1992.

428. Bray, J.R.; Curtis, J.T. An Ordination of the Upland Forest Communities of Southern Wisconsin. *Ecol. Monogr.* **1957**, *27*, 325–349, doi:10.2307/1942268.

429. Warton, D.I.; Wright, S.T.; Wang, Y. Distance-based multivariate analyses confound location and dispersion effects. *Methods Ecol. Evol.* **2012**, *3*, 89–101, doi:10.1111/j.2041-210X.2011.00127.x.

430. Anderson, M.J. Permutational Multivariate Analysis of Variance (PERMANOVA). In *Wiley StatsRef: Statistics Reference Online*; Wiley, 2017; pp. 1–15.

431. ter Braak, C.J.F. Canonical Correspondence Analysis: A New Eigenvector Technique for Multivariate Direct Gradient Analysis. *Ecology* **1986**, *67*, 1167–1179, doi:10.2307/1938672.

432. Lammers, M.O.; Au, W.W.L.; Herzing, D.L. The broadband social acoustic signaling behavior of spinner and spotted dolphins. *J. Acoust. Soc. Am.* **2003**, *114*, 1629–1639, doi:10.1121/1.1596173.

433. Bolgan, M.; Soulard, J.; Di Iorio, L.; Gervaise, C.; Lejeune, P.; Gobert, S.; Parmentier, E. Sea

chordophones make the mysterious /Kwa/ sound: identification of the emitter of the dominant fish sound in Mediterranean seagrass meadows. *J. Exp. Biol.* **2019**, *222*, jeb196931, doi:10.1242/jeb.196931.

434. Parmentier, E.; Bouillac, G.; Dragičević, B.; Dulčič, J.; Fine, M.; Dragicevic, B.; Dulcic, J.; Fine, M. Call properties and morphology of the sound-producing organ in *Ophidion rochei* (Ophidiidae). *J. Exp. Biol.* **2010**, *213*, 3230–3236, doi:10.1242/jeb.044701.

435. Müller, J. Ueber die Fische, welche Töne von sich geben und die Entstehung dieser Töne. *Arch Anat Physiol wiss Med.* **1857**, 249–279.

436. Mann, D.A.; Lobel, P.S. Passive acoustic detection of sounds produced by the damselfish, *Dascyllus albisella* (Pomacentridae). *Bioacoustics* **1995**, *6*, 199–213, doi:10.1080/09524622.1995.9753290.

437. Ruppé, L.; Clément, G.; Herrel, A.; Ballesta, L.; Décamps, T.; Kéver, L.; Parmentier, E. Environmental constraints drive the partitioning of the soundscape in fishes. *Proc. Natl. Acad. Sci.* **2015**, *112*, 6092–6097, doi:10.1073/pnas.1424667112.

438. Kaplan, M.B.; Mooney, T.A.; Partan, J.; Solow, A.R. Coral reef species assemblages are associated with ambient soundscapes. *Mar. Ecol. Prog. Ser.* **2015**, *533*, 93–107, doi:10.3354/meps11382.

439. Faure, G.; Laboute, P. L'atoll de Tikehau, Premiers résultats. Formations récifales: I Définition des unités récifales et distribution des principaux peuplements de Scléractiniaires. *ORSTOM Océanographie, Notes Doc.* **1984**, *22*, 108–136.

440. Donaldson, T.J. Fishes of the remote Southwest Palau Islands: a zoogeographic perspective. *Pac. Sci.* **1996**, *50*, 285–308.

441. Kulbicki, M. First observations on the fish communities of fringing reefs in the region of Maumere (Flores-Indonesia). *Atoll Res. Bull* **1996**, *437*, 1–21.

442. Pyle, R.L.; Kosaki, R.K.; Pinheiro, H.T.; Rocha, L.A.; Whitton, R.K.; Copus, J.M. Fishes: Biodiversity. In *Mesophotic Coral Ecosystems*; Loya, Y., Puglise, K.A., Bridge, T.C.L., Eds.; Springer Cham, 2019; pp. 749–777 ISBN 978-3-319-92734-3.

443. Goodbody-Gringley, G.; Noyes, T.; Smith, S.R. Bermuda. In *Mesophotic Coral Ecosystems*; Loya, Y., Puglise, K.A., Bridge, T.C.L., Eds.; Springer Cham, 2019; pp. 31–45 ISBN 978-3-319-92734-3.

444. Montgomery, A.D.; Fenner, D.; Kosaki, R.K.; Pyle, R.L.; Wagner, D.; Toonen, R.J. American Samoa. In *Mesophotic Coral Ecosystems*; Loya, Y., Puglise, K.A., Bridge, T.C.L., Eds.; Springer Cham, 2019; pp. 387–407 ISBN 978-3-319-92734-3.

445. Sinniger, F.; Harii, S.; Humblet, M.; Nakamura, Y.; Ohba, H.; Prasetia, R. Ryukyu Islands, Japan. In *Mesophotic Coral Ecosystems*; Loya, Y., Puglise, K.A., Bridge, T.C.L., Eds.; Springer Cham, 2019; pp. 231–247 ISBN 978-3-319-92734-3.

446. Kahng, S.E.; Garcia-Sais, J.R.; Spalding, H.L.; Brokovich, E.; Wagner, D.; Weil, E.; Hinderstein, L.; Toonen, R.J. Community ecology of mesophotic coral reef ecosystems. *Coral Reefs* **2010**, *29*, 255–275, doi:10.1007/s00338-010-0593-6.

447. Armstrong, R.A.; Pizarro, O.; Roman, C. Underwater Robotic Technology for Imaging Mesophotic Coral Ecosystems. In *Mesophotic Coral Ecosystems*; Loya, Y., Puglise, K., Bridge, T., Eds.; Springer, Cham, 2019; pp. 973–988 ISBN 978-3-319-92734-3.

448. Luczkovich, J.J.; Mann, D.A.; Rountree, R.A. Passive Acoustics as a Tool in Fisheries Science. *Trans. Am. Fish. Soc.* **2008**, *137*, 533–541, doi:10.1577/T06-258.1.

449. Picciulin, M.; Bolgan, M.; Codarin, A.; Fiorin, R.; Zucchetta, M.; Malavasi, S. Passive acoustic monitoring of *Sciaena umbra* on rocky habitats in the Venetian littoral zone. *Fish. Res.* **2013**, *145*, 76–81, doi:10.1016/j.fishres.2013.02.008.

450. Higgs, D.M.; Humphrey, S.R. Passive acoustic monitoring shows no effect of anthropogenic noise on acoustic communication in the invasive round goby (*Neogobius melanostomus*). *Freshw. Biol.* **2020**, *65*, 66–74, doi:10.1111/fwb.13392.

451. Wall, C.C.; Simard, P.; Lembke, C.; Mann, D.A. Large-scale passive acoustic monitoring of fish sound production on the West Florida Shelf. *Mar. Ecol. Prog. Ser.* **2013**, *484*, 173–188,

doi:10.3354/meps10268.

452. Lombard, E. Le signe de l'élévation de la voix. *Ann. des Mal. l'oreille, du larynx, du nez du pharynx* **1911**, *37*, 101–119.

453. Brumm, H.; Slabbekoorn, H. Acoustic Communication in Noise. *Adv. Study Behav.* **2005**, *35*, 151–209, doi:10.1016/S0065-3454(05)35004-2.

454. Holt, D.E.; Johnston, C.E. Evidence of the Lombard effect in fishes. *Behav. Ecol.* **2014**, *25*, 819–826, doi:10.1093/beheco/aru028.

455. Carriço, R.; Silva, M.A.; Menezes, G.M.; Vieira, M.; Bolgan, M.; Fonseca, P.J.; Amorim, M.C.P. Temporal dynamics in diversity patterns of fish sound production in the Condor seamount (Azores, NE Atlantic). *Deep. Res. Part I Oceanogr. Res. Pap.* **2020**, *164*, doi:10.1016/j.dsr.2020.103357.

456. Connaughton, M.A.; Taylor, M.H. Seasonal and daily cycles in sound production associated with spawning in the weakfish, *Cynoscion regalis*. *Environ. Biol. Fishes* **1995**, *42*, 233–240, doi:10.1007/BF00004916.

457. Locascio, J. V; Mann, D.A. Diel and seasonal timing of sound production by black drum (*Pogonias cromis*). *Fish. Bull.* **2011**.

458. Nelson, M.; Koenig, C.C.; Coleman, F.C.; Mann, D.A. Sound production of red grouper Epinephelus morio on the West Florida Shelf. *Aquat. Biol.* **2011**, *12*, 97–108, doi:10.3354/ab00325.

459. McCauley, R.D.; Cato, D.H. Patterns of fish calling in a nearshore environment in the Great Barrier Reef. *Philos. Trans. R. Soc. B Biol. Sci.* **2000**, *355*, 1289–1293, doi:10.1098/rstb.2000.0686.

460. Bolgan, M.; Di Iorio, L.; Dailianis, T.; Catalan, I.A.; Lejeune, P.; Picciulin, M.; Parmentier, E. Fish acoustic community structure in Neptune seagrass meadows across the Mediterranean basin. *Aquat. Conserv. Mar. Freshw. Ecosyst.* **2022**, *32*, 329–347, doi:10.1002/aqc.3764.

461. Farina, A. *Soundscape Ecology Principles, Patterns, Methods and Applications*; Springer Dordrecht, 2014; ISBN 978-94-007-7373-8.

462. Krause, B. The Niche Hypothesis: A virtual symphony of animal sounds, the origins of musical expression and the health of habitats. In Proceedings of the Soundscape Newsletter (World Forum for Acoustic Ecology); 1993.

463. Popp, J.W.; Ficken, R.W.; Reinartz, J.A. Short-term temporal avoidance of interspecific acoustic interference among forest birds. *Auk* **1985**, *102*, 744–748, doi:10.1093/auk/102.4.744.

464. Chitnis, S.S.; Rajan, S.; Krishnan, A. Sympatric wren-warblers partition acoustic signal space and song perch height. *Behav. Ecol.* **2020**, *31*, 559–567, doi:10.1093/beheco/arz216.

465. Hart, P.J.; Ibanez, T.; Paxton, K.; Tredinnick, G.; Sebastián-González, E.; Tanimoto-Johnson, A. Timing Is Everything: Acoustic Niche Partitioning in Two Tropical Wet Forest Bird Communities. *Front. Ecol. Evol.* **2021**, *9*, doi:10.3389/fevo.2021.753363.

466. Duellman, W.E.; Pyles, R.A. Acoustic Resource Partitioning in Anuran Communities. *Copeia* **1983**, *1983*, 639, doi:10.2307/1444328.

467. Sinsch, U.; Lümkemann, K.; Rosar, K.; & C.S.; Dehling, J.M. Acoustic Niche Partitioning in an Anuran Community Inhabiting an Afromontane Wetland (Butare, Rwanda). *African Zool.* **2012**, *47*, 60–73, doi:10.3377/004.047.0122.

468. Allen-Ankins, S.; Schwarzkopf, L. Spectral overlap and temporal avoidance in a tropical savannah frog community. *Anim. Behav.* **2021**, *180*, 1–11, doi:10.1016/j.anbehav.2021.07.024.

469. SUEUR, J. Cicada acoustic communication: potential sound partitioning in a multispecies community from Mexico (Hemiptera: Cicadomorpha: Cicadidae). *Biol. J. Linn. Soc.* **2002**, *75*, 379–394, doi:10.1046/j.1095-8312.2002.00030.x.

470. Henry, C.S.; Wells, M.M. Acoustic niche partitioning in two cryptic sibling species of *Chrysoperla* green lacewings that must duet before mating. *Anim. Behav.* **2010**, *80*, 991–1003, doi:10.1016/j.anbehav.2010.08.021.

471. Wilson, K.; Semmens, B.; Pattengill-Semmens, C.; McCoy, C.; McCoy, C. Potential for grouper acoustic competition and partitioning at a multispecies spawning site off Little Cayman, Cayman Islands. *Mar. Ecol. Prog. Ser.* **2020**, *634*, 127–146, doi:10.3354/meps13181.

472. Raick, X.; Collet, P.; Under The Pole, C.; Lecchini, D.; Bertucci, F.; Parmentier, E.; Raick1, X.; Collet, P.; Under The Pole, C.; Lecchini, D.; et al. Diel cycle of two recurrent fish sounds from mesophotic coral reefs. *Sci. Mar.* **2023**, *87*, e078, doi:10.3989/scimar.05395.078.

473. Amorim, M.C.P.; Hawkins, A.D. Growling for food: Acoustic emissions during competitive feeding of the streaked gurnard. *J. Fish Biol.* **2000**, *57*, 895–907, doi:10.1111/j.1095-8649.2000.tb02200.x.

474. Raick, X.; Koussa, A.; Zawadzki, C.H.; Kurchevski, G.; Godinho, A.L.; Parmentier, É. Sounds and associated morphology of *Hypostomus* species from South-East Brazil. *J. Zool.* **2022**, *317*, 77–91, doi:10.1111/jzo.12967.

475. Puebla-Aparicio, M.; Ascencio-Elizondo, C.; Vieira, M.; Amorim, M.; Duarte, R.; Fonseca, P. Characterization of the fish acoustic communities in a Mozambican tropical coral reef. *Mar. Ecol. Prog. Ser.* **2024**, *727*, 143–158, doi:10.3354/meps14450.

476. Adlerstein, S.A.; Welleman, H.C. Diel variation of stomach contents of North Sea cod (*Gadus morhua*) during a 24-h fishing survey: an analysis using generalized additive models. *Can. J. Fish. Aquat. Sci.* **2000**, *57*, 2363–2367, doi:10.1139/f00-249.

477. Buscaino, G.; Picciulin, M.; Canale, D.E.; Papale, E.; Ceraulo, M.; Grammauta, R.; Mazzola, S. Spatio-temporal distribution and acoustic characterization of haddock (*Melanogrammus aeglefinus*, Gadidae) calls in the Arctic fjord Kongsfjorden (Svalbard Islands). *Sci. Rep.* **2020**, *10*, 18297, doi:10.1038/s41598-020-75415-9.

478. Bischof, R.; Ali, H.; Kabir, M.; Hameed, S.; Nawaz, M.A. Being the underdog: an elusive small carnivore uses space with prey and time without enemies. *J. Zool.* **2014**, *293*, 40–48, doi:10.1111/jzo.12100.

479. Colwell, R.K.; Futuyma, D.J. On the Measurement of Niche Breadth and Overlap. *Ecology* **1971**, *52*, 567–576, doi:10.2307/1934144.

480. Rice, A.N.; Soldevilla, M.S.; Quinlan, J.A. Nocturnal patterns in fish chorusing off the coasts of Georgia and eastern Florida. *Bull. Mar. Sci.* **2017**, *93*, 455–474, doi:10.5343/bms.2016.1043.

481. Mooney, T.A.; Kaplan, M.B.; Izzi, A.; Lamoni, L.; Sayigh, L. Temporal trends in cusk eel sound production at a proposed US wind farm site. *Aquat. Biol.* **2016**, *24*, 201–210, doi:10.3354/ab00650.

482. Suthers, R.A.; Fay, R.R. *Vertebrate Sound Production and Acoustic Communication*; 2016; Vol. 53; ISBN 978-3-319-27719-6.

483. Rountree, R.A.; Juanes, F.; Bolgan, M. Air movement sound production by alewife, white sucker, and four salmonid fishes suggests the phenomenon is widespread among freshwater fishes. *PLoS One* **2018**, *13*, e0204247, doi:10.1371/journal.pone.0204247.

484. Rowell, T.J.; Aburto-Oropeza, O.; Cota-Nieto, J.J.; Steele, M.A.; Erisman, B.E. Reproductive behaviour and concurrent sound production of Gulf grouper *Mycteroperca jordani* (Epinephelidae) at a spawning aggregation site. *J. Fish Biol.* **2019**, *94*, 277–296, doi:10.1111/jfb.13888.

485. Rowell, T.J.; D'Spain, G.L.; Aburto-Oropeza, O.; Erisman, B.E. Drivers of male sound production and effective communication distances at fish spawning aggregation sites. *ICES J. Mar. Sci.* **2020**, *77*, 730–745, doi:10.1093/icesjms/fsz236.

486. Parmentier, E.; Lecchini, D.; Mann, D.A. Sound Production in Damselfishes. In *Biology of Damselfishees*; Frederich, B., Parmentier, E., Eds.; Taylor & Francis: Boca Raton, 2016; pp. 204–228.

487. Amorim, M.C.P.; Vasconcelos, R.O. Variability in the mating calls of the Lusitanian toadfish *Halobatrachus didactylus*: cues for potential individual recognition. *J. Fish Biol.* **2008**, *73*, 1267–1283, doi:10.1111/j.1095-8649.2008.01974.x.

488. Wilson, L.J.; Burrows, M.T.; Hastie, G.D.; Wilson, B. Temporal variation and characterization of grunt sounds produced by Atlantic cod *Gadus morhua* and pollack *Pollachius pollachius* during the spawning season. *J. Fish Biol.* **2014**, *84*, 1014–1030, doi:10.1111/jfb.12342.

489. Drubbel, R.V.; Folia Primatologica, E. On the Occurrence of Nocturnal and Diurnal Loud Calls, Differing in Structure and Duration, in Red Howlers (*Alouatta seniculus*) of French Guyana. *Folia Primatol.* **1993**, *60*, 195–209, doi:10.1159/000156693.

490. Mossbridge, J.A.; Thomas, J.A. An "acoustic niche" for antartic killer whale and leopard seal sounds. *Mar. Mammal Sci.* **1999**, *15*, 1351–1357, doi:10.1111/j.1748-7692.1999.tb00897.x.

491. Villanueva-Rivera, L.J. *Eleutherodactylus* frogs show frequency but no temporal partitioning: implications for the acoustic niche hypothesis. *PeerJ* **2014**, *2*, e496, doi:10.7717/peerj.496.

492. Lima, M.S.C.S.; Pederassi, J.; Pineschi, R.B.; Barbosa, D.B.S. Acoustic niche partitioning in an anuran community from the municipality of Floriano, Piauí, Brazil. *Brazilian J. Biol.* **2019**, *79*, 566–576, doi:10.1590/1519-6984.180399.

493. Polechová, J.; Storch, D. Ecological niche. In *Encyclopedia of ecology*; 2008; pp. 1088–1097.

494. Hanski, I.; Koskela, H. Stability, abundance, and niche width in the beetle community inhabiting cow dung. *Oikos* **1978**, *31*, 290, doi:10.2307/3543653.

495. Sugai, L.S.M.; Llusia, D.; Siqueira, T.; Silva, T.S.F. Revisiting the drivers of acoustic similarities in tropical anuran assemblages. *Ecology* **2021**, *102*, doi:10.1002/ecy.3380.

496. Rice, A.N.; Farina, S.C.; Makowski, A.J.; Kaatz, I.M.; Lobel, P.S.; Bemis, W.E.; Bass, A.H. Evolutionary Patterns in Sound Production across Fishes. *Ichthyol. Herpetol.* **2022**, *110*, doi:10.1643/i2020172.

497. Tower, R.W. The production of sound in the drumfishes, the sea-robin and the toadfish. *Ann. N. Y. Acad. Sci.* **1908**, *18*, 149–180, doi:10.1111/j.1749-6632.1908.tb55101.x.

498. Rice, A.N.; Bass, A.H. Novel vocal repertoire and paired swimbladders of the three-spined toadfish, Batrachomoeus trispinosus: Insights into the diversity of the Batrachoididae. *J. Exp. Biol.* **2009**, *212*, 1377–1391, doi:10.1242/jeb.028506.

499. Connaughton, M.A. Sound generation in the searobin (Prionotus carolinus), a fish with alternate sonic muscle contraction. *J. Exp. Biol.* **2004**, *207*, 1643–1654, doi:10.1242/jeb.00928.

500. Sörensen, W. Are the Extrinsic Muscles of the Air-bladder in some Siluroidae and the "Elastic Spring" Apparatus of others Subordinate to the Voluntary Production of Sounds? What is, according to our Present Knowledge, the Function of the Weberian Ossicles?: A Contribu. *J. Anat. Physiol.* **1895**, *29*, 205–229.

501. Parmentier, E.; Diogo, R. Evolutionary trends of swimbladder sound mechanisms in some teleost fishes. In *Communication in fishes, vol 1*; Ladich, F., Collin, S.P., Moller, P., Kapoor, B.G., Eds.; Science Publisher Inc: Enfield, 2006; pp. 45–70.

502. Kaatz, I.M.; Stewart, D.J. Bioacoustic variation of swimbladder disturbance sounds in Neotropical doradoid catfishes (Siluriformes: Doradidae, Auchenipteridae): Potential morphological correlates. *Curr. Zool.* **2012**, *58*, 171–188, doi:10.1093/czoolo/58.1.171.

503. Mélotte, G.; Vigouroux, R.; Michel, C.; Parmentier, E. Interspecific variation of warning calls in piranhas: a comparative analysis. *Sci. Rep.* **2016**, *6*, 36127, doi:10.1038/srep36127.

504. Ono, R.D.; Poss, S.G. Structure and innervation of the swim bladder musculature in the weakfish, *Cynoscion regalis* (Teleostei: Sciaenidae). *Can. J. Zool.* **1982**, *60*, 1955–1967, doi:10.1139/z82-253.

505. Lagardère, J.P.; Mariani, A. Spawning sounds in the meagre Argyrosomus regius recorded in the Gironde estuary, France. *J. Fish Biol.* **2006**, *69*, 1697–1708, doi:10.1111/j.1095-8649.2006.01237.x.

506. Longrie, N.; Van Wassenbergh, S.; Vandewalle, P.; Mauguit, Q.; Parmentier, E. Potential mechanism of sound production in *Oreochromis niloticus* (Cichlidae). *J. Exp. Biol.* **2009**, *212*, 3395–3402, doi:10.1242/jeb.032946.

507. Lugli, M.; Pavan, G.; Torricelli, P.; Bobbio, L. Spawning vocalizations in male freshwater gobiids (Pisces, Gobiidae). *Environ. Biol. Fishes* **1995**, *43*, 219–231, doi:10.1007/BF00005853.

508. Barber, S.B.; Mowbray, W.H. Mechanism of Sound Production in the Sculpin. *Science (80-.).* **1956**,

124, 219–220, doi:10.1126/science.124.3214.219.

509. Malavasi, S.; Collatuzzo, S.; Torricelli, P. Interspecific variation of acoustic signals in Mediterranean gobies (Perciformes, Gobiidae): comparative analysis and evolutionary outlook. *Biol. J. Linn. Soc.* **2008**, *93*, 763–778, doi:10.1111/j.1095-8312.2008.00947.x.

510. Parmentier, E.; Colleye, O.; Fine, M.L.; Frédérich, B.; Vandewalle, P.; Herrel, A. Sound Production in the Clownfish *Amphiprion clarkii*. *Science (80-.).* **2007**, *316*, 1006–1006, doi:10.1126/science.1139753.

511. Colleye, O.; Parmentier, E. Overview on the Diversity of Sounds Produced by Clownfishes (Pomacentridae): Importance of Acoustic Signals in Their Peculiar Way of Life. *PLoS One* **2012**, *7*, doi:10.1371/journal.pone.0049179.

512. Burkenroad, M.D. Notes on the sound-producing marine fishes of Louisiana. *Copeia* **1931**, *1*, 20–28, doi:10.2307/1436789.

513. Tavolga, W.N. Sound Production and Detection. In *Fish Physiology*; Hoar, W., Randall, D., Eds.; New York, 1971; pp. 135–205.

514. Parmentier, E.; Marucco Fuentes, E.; Millot, M.; Raick, X.; Thiry, M. Sound production, hearing sensitivity, and in-depth study of the sound-producing muscles in the cowfish (*Lactoria cornuta*). *J. Anat.* **2021**, *238*, 956–969, doi:10.1111/joa.13353.

515. Elise, S.; Urbina-Barreto, I.; Pinel, R.; Mahamadaly, V.; Bureau, S.; Penin, L.; Adjeroud, M.; Kulbicki, M.; Bruggemann, J.H. Assessing key ecosystem functions through soundscapes: A new perspective from coral reefs. *Ecol. Indic.* **2019**, *107*, 105623, doi:10.1016/j.ecolind.2019.105623.

516. Elise, S.; Bailly, A.; Urbina-Barreto, I.; Mou-Tham, G.; Chiroleu, F.; Vigliola, L.; Robbins, W.D.; Bruggemann, J.H. An optimised passive acoustic sampling scheme to discriminate among coral reefs' ecological states. *Ecol. Indic.* **2019**, *107*, 105627, doi:10.1016/j.ecolind.2019.105627.

517. Parmentier, E.; Stainier, G.; Boistel, R.; Fine, M.L.; Kéver, L.; Di Iorio, L.; Bolgan, M. Sound production and mechanism in the cryptic cusk-eel *Parophidion vassali*. *J. Anat.* **2022**, *241*, 581–600, doi:10.1111/joa.13691.

518. Bradbury, J.; Vehrencamp, S. *Principles of animal communication*; Sinauer As.; Sunderland, UK, 1998; ISBN 978-0878931002.

519. Kasumyan, A.O. Sounds and sound production in fishes. *J. Ichthyol.* **2008**, *48*, 981–1030, doi:10.1134/s0032945208110039.

520. Amorim, M.C.P.; Pedroso, S.S.; Bolgan, M.; Jordão, J.M.; Caiano, M.; Fonseca, P.J. Painted gobies sing their quality out loud: acoustic rather than visual signals advertise male quality and contribute to mating success. *Funct. Ecol.* **2013**, *27*, 289–298, doi:10.1111/1365-2435.12032.

521. Fish, M.P.; Kelsey, A.S.J.; Mowbray, W.H. Studies on the production of underwater sound by north atlantic coastal fishes. *J. Mar. Res.* **1952**, *11*, 180–193.

522. Fish, M.P. The character and significance of sound production among fishes of the Western North Atlantic. *Bingham Oceanogr. Collect.* **1954**, *14*, 1–109.

523. Samber, B. De; Renders, J.; Elberfeld, T.; Maris, Y.; Sanctorum, J.; Six, N.; Liang, Z.; Beenhouwer, J. De; Sijbers, J. FleXCT: a flexible X-ray CT scanner with 10 degrees of freedom. *Opt. Express* **2021**, *29*, 3438, doi:10.1364/OE.409982.

524. Lugli, M.; Yan, H.Y.; Fine, M.L. Acoustic communication in two freshwater gobies: the relationship between ambient noise, hearing thresholds and sound spectrum. *J. Comp. Physiol. A* **2003**, *189*, 309–320, doi:10.1007/s00359-003-0404-4.

525. Looby, A.; Cox, K.; Bravo, S.; Rountree, R.; Juanes, F.; Reynolds, L.K.; Martin, C.W. A quantitative inventory of global soniferous fish diversity. *Rev. Fish Biol. Fish.* **2022**, doi:10.1007/s11160-022-09702-1.

526. Moulton, J.M. The acoustical behavior of some fishes in the Bimini area. *Biol. Bull.* **1958**, *114*, 357–374, doi:10.2307/1538991.

527. De Jong, K.; Bouton, N.; Slabbekoorn, H. Azorean rock-pool blennies produce size-dependent calls in a courtship context. *Anim. Behav.* **2007**, *74*, 1285–1292, doi:10.1016/j.anbehav.2007.02.023.

528. Coers, A.; Bouton, N.; Vincourt, D.; Slabbekoorn, H. Fluctuating noise conditions may limit acoustic communication distance in the rock-pool blenny. *Bioacoustics* **2008**, *17*, 63–65, doi:10.1080/09524622.2008.9753765.

529. Tavolga, W.N. Underwater Sounds Produced by Males of the Blenniid Fish, Chasmodes bosquianus. *Ecology* **1958**, *39*, 759–760, doi:10.2307/1931619.

530. Marshall, N.B. Sound-producing mechanisms and the biology of deep-sea fishes. In *Marine Bio-Acoustics*; Press, P., Ed.; Oxford, 1967; pp. 123–133.

531. Yokoyama, K.; Kamei, Y.; Toda, M.; Hirano, K.; Iwatsuki, Y. Reproductive behavior, eggs, and larvae of a caesionine fish, *Pterocaesio diagramma*, observed in an aquarium. *Japanese J. Ichtyology* **1994**, *41*, 261–274.

532. Fish, M.P. *Sonic fishes of the Pacific (technical report n°2).*; Office of.; Woods Hole (USA), 1948;

533. Steinberg, J.C.; Cummings, W.C.; Brahy, B.D.; MacBain Spires, J.Y. Further bio-acoustic studies off the west coast of North Bimini, Bahamas. *Bull. Mar. Sci.* **1965**, *15*, 942–963.

534. Tavolga, W.N. *Marine animal data atlas (American Museum of Natural History and U.S. Naval Training Device Center)*; 1968;

535. Kaparang, F.E.; Matsuno, Y.; Yamanaka, Y.; Fujieda, S. Studies on underwater sounds produced by yellowtail *Seriola quinqueradiata* and amberjack *Seriola dumerili* in net pens at culture grounds in middle Kagoshima Bay. *Fish. Sci.* **1998**, *64*, 353–358, doi:10.2331/fishsci.64.353.

536. Fujieda, S.; Fujieda, Shigeru; Matsuno, Yasuhisa; Yamanaka, Yuichi; Chung, Yong-jin; Kishimoto, C. Feature of the Swimming Sound for Fishes in the Netting Cages at the Culture Ground. *Kagoshima Daigaku Suisan Gakubu Kiyo* **1993**, *42*, 1–9.

537. Uchida, K. On the sound-producing fishes of Japan. In *Nihon Gakujitsu Kyokai Hokoku*; 1934; p. vol. 9, n°2.

538. Savchenko, N. V.; Gusar, A.G.; Getmantsev, V.A. On the locomotory activity of fish under conditions of low light intensity. *Vopr. Ikhtiologii* **1981**, *21*, 180–182.

539. Shishkova, E. V. [Notes and Investigations on Sound Produced by Fishes]. *Tr. Vses. Inst. Ribn. Hozaist. Okeanogr.* **1958**, *36*, 280–294.

540. Moulton, J.M. Swimming Sounds and the Schooling of Fishes. *Biol. Bull.* **1960**, *119*, 210–223, doi:10.2307/1538923.

541. Taylor, M.; Mansueti, R.J. Sounds produced by very young Crevalle Jack, Caranx hippos, from the Maryland seaside. *Chesap. Sci.* **1960**, *1*, 115–116, doi:10.2307/1350930.

542. Cummings, W.C.; Brahy, B.D.; Herrnkind, W.F. The occurence of underwater sounds of biological origin off the west coast of Bimini, Bahamas. In *Marine Bio-Acoustics*; Tavolga, W.N., Ed.; Pergamon Press: New-York, 1964; pp. 27–43.

543. Tricas, T.C.; Boyle, K.S. Diversity and evolution of sound production in the social behavior of *Chaetodon* butterflyfishes. *J. Exp. Biol.* **2015**, *218*, 1572–1584, doi:10.1242/jeb.114256.

544. Tricas, T.C.; Kajiura, S.M.; Kosaki, R.K. Acoustic communication in territorial butterflyfish: test of the sound production hypothesis. *J. Exp. Biol.* **2006**, *209*, 4994–5004, doi:10.1242/jeb.02609.

545. Dufossé, M. Recherches sur les bruits et les sons expressifs que font entendre les poissons d'Europe et sur les organes producteurs de ces phénomènes acoustiques ainsi que sur les appareils de l'audition de plusieurs de ces animaux. *Ann. des Sci. Nat.* **1874**, *5*, 1–53.

546. Amorim, M.C.P.; Neves, A.S.M. Acoustic signalling during courtship in the painted goby Pomatoschistus pictus. *J. Mar. Biol. Assoc. United Kingdom* **2007**, *87*, 5682/1–7, doi:10.1017/S0025315407056822.

547. Parmentier, E.; Vandewalle, P.; Brié, C.; Dinraths, L.; Lecchini, D. Comparative study on sound production in different Holocentridae species. *Front. Zool.* **2011**, *8*, article number 12, doi:10.1186/1742-9994-8-12.

548. Horch, K.; Salmon, M. Adaptations to the acoustic environment by the squirrelfishes *Myripristis violaceus* and *M. pralinius*. *Mar. Behav. Physiol.* **1973**, *2*, 121–139, doi:10.1080/10236247309386920.

549. Salmon, M. Acoustical behavior of the menpachi, *Myripristis berndti*, in Hawaii. *Pacific Sci.* **1967**, *21*, 364–381.

550. Carlson, B.A.; Bass, A.H. Sonic/Vocal Motor Pathways in Squirrelfish (Teleostei, Holocentridae). *Brain. Behav. Evol.* **2000**, *56*, 14–28, doi:10.1159/000006674.

551. Gainer, H.; Kusano, K.; Mathewson, R.F. Electrophysiological and mechanical properties of squirrelfish sound-producing muscle. *Comp. Biochem. Physiol.* **1965**, *14*, 661–671, doi:10.1016/0010-406X(65)90253-7.

552. Winn, H.E.; Marshall, J.A. Sound-Producing Organ of the Squirrelfish, *Holocentrus rufus*. *Physiol. Zool.* **1963**, *36*, 34–44.

553. Locascio, J. V.; Burton, M.L. A passive acoustic survey of fish sound production at Riley's Hump within Tortugas South Ecological Reserve; implications regarding spawning and habitat use. *Fish. Bull.* **2016**, *114*, 103–116, doi:10.7755/FB.114.1.9.

554. Boyle, K.S.; Cox, T.E. Courtship and spawning sounds in bird wrasse *Gomphosus varius* and saddle wrasse *Thalassoma duperrey*. *J. Fish Biol.* **2009**, *75*, 2670–2681, doi:10.1111/j.1095-8649.2009.02459.x.

555. Steinberg, J.; Cummings, W.; Brahy, B.; MacBain (Spires), J. Further Bio-Acoustic Studies off the West Coast of North Bimini, Bahamas. *Bull. Mar. Sci.* **1965**, *15*, 942–963.

556. Bordeau, B. Influences of the Acoustic Environment on the Marine and Freshwater Fishes. Application to Fisheries, PhD Dissertation, Université de Paris, 1982.

557. Protasov, V.R.; Romanenko, E. V. Sounds emitted by some fishes and their importance as signals. *Zool. Zurn.* **1962**, *41*, 1516–1528.

558. Yamada, T. Sea Where Fishes Croak. *Kaiyo no Kagaku* **1941**, *1*.

559. Moulton, J.M. Acoustic behaviour of fishes. In *Acoustic behaviour of animals*; Busnel, R.G., Ed.; Elsevier: New-York, 1964; pp. 655–693.

560. Staaterman, E.; Paris, C.B.; Kough, A.S. First evidence of fish larvae producing sounds. *Biol. Lett.* **2014**, *10*, 20140643, doi:10.1098/rsbl.2014.0643.

561. Marshall, N.. B. Systematic and biological studies of the Macrourid fishes (Anacanthini-Teleostii). *Deep Sea Res. Oceanogr. Abstr.* **1965**, *12*, 299–322, doi:10.1016/0011-7471(65)90004-5.

562. McCauley, R.D.; Cato, D.H. Evening choruses in the Perth Canyon and their potential link with Myctophidae fishes. *J. Acoust. Soc. Am.* **2016**, *140*, 2384–2398, doi:10.1121/1.4964108.

563. Parmentier, E.; Boistel, R.; Bahri, M.A.; Plenevaux, A.; Schwarzhans, W. Sexual dimorphism in the sonic system and otolith morphology of *Neobythites gilli* (Ophidiiformes). *J. Zool.* **2018**, *305*, 274–280, doi:10.1111/jzo.12561.

564. Kéver, L.; Lejeune, P.; Michel, L.N.; Parmentier, E. Passive acoustic recording of *Ophidion rochei* calling activity in Calvi Bay (France). *Mar. Ecol.* **2016**, *37*, 1315–1324, doi:10.1111/maec.12341.

565. Kéver, L.; Boyle, K.S.; Dragičević, B.; Dulčić, J.; Parmentier, E. A superfast muscle in the complex sonic apparatus of *Ophidion rochei* (Ophidiiformes): histological and physiological approaches. *J. Exp. Biol.* **2014**, doi:10.1242/jeb.105445.

566. Kéver, L.; Boyle, K.S.; Bolen, G.; Dragičević, B.; Dulčić, J.; Parmentier, E. Modifications in call characteristics and sonic apparatus morphology during puberty in *Ophidion rochei* (Actinopterygii: Ophidiidae). *J. Morphol.* **2014**, *275*, 650–660, doi:10.1002/jmor.20245.

567. Kéver, L.; Boyle, K.S.; Dragičević, B.; Dulčić, J.; Casadevall, M.; Parmentier, E. Sexual dimorphism of sonic apparatus and extreme intersexual variation of sounds in *Ophidion rochei* (Ophidiidae): first evidence of a tight relationship between morphology and sound characteristics in Ophidiidae. *Front. Zool.* **2012**, *9*, 34, doi:10.1186/1742-9994-9-34.

568. Parmentier, E.; Fontenelle, N.; Fine, M.L.; Vandewalle, P.; Henrist, C. Functional morphology of the sonic apparatus in Ophidion barbatum (Teleostei, Ophidiidae). *J. Morphol.* **2006**, *267*, 1461–1468, doi:10.1002/jmor.10496.

569. Mann, D.A.; Grothues, T.M. Response of fish sound production to short-term ocean upwelling events at the LEO-15 (Long-term Ecosystem Observatory at 15 m depth) ocean observatory. *J. Acoust. Soc. Am.* **2009**, *125*, 2485–2485, doi:10.1121/1.4783288.

570. Anderson, K.A.; Rountree, R.A.; Juanes, F. Soniferous Fishes in the Hudson River. *Trans. Am. Fish. Soc.* **2008**, *137*, 616–626, doi:10.1577/T05-220.1.

571. Mann, D.; Grothues, T. Short-term upwelling events modulate fish sound production at a mid-Atlantic Ocean observatory. *Mar. Ecol. Prog. Ser.* **2009**, *375*, 65–71, doi:10.3354/meps07720.

572. Sprague, M.W.; Luczkovich, J.J. Do striped cusk-eels Ophidion marginatum (Ophidiidae) produce the "chatter" sound attributed to weakfish Cynoscion regalis (Sciaenidae)? *Copeia* **2001**, *3*, 854–859, doi:10.1643/0045-8511(2001)001[0854:DSCEOM]2.0.CO;2.

573. Rountree, R.A.; Bowers-Altman, J. Soniferous behaviour of the striped cusk-eel *Ophidion marginatum*. *Bioacoustics* **2002**, *12*, 240–242, doi:10.1080/09524622.2002.9753709.

574. Mann, D.A.; Bowers Altman, J.; Rountree, R.A.; Bowers-Altman, J.; Rountree, R.A. Sounds produced by the striped cusk-eel *Ophidion marginatum* (Ophidiidae) during courtship and spawning. *Copeia* **1997**, *1997*, 610, doi:10.2307/1447568.

575. Courtenay, W.R. Sexual dimorphism of the sound producing mechanism of the striped cusk-eel, *Rissola marginata* (Pisces: Ophidiidae). *Copeia* **1971**, *1971*, 259, doi:10.2307/1442826.

576. Fine, M.L.; Lin, H.; Nguyen, B.B.; Rountree, R.A.; Cameron, T.M.; Parmentier, E. Functional morphology of the sonic apparatus in the fawn cusk-eel *Lepophidium profundorum* (Gill, 1863). *J. Morphol.* **2007**, *268*, 953–966, doi:10.1002/jmor.10551.

577. Wielsen, J.G. On the genera *Acanthonus* and *Typhlonus* (Pisces, Brotulidae). *Galathea Rep.* **1965**, *8*, 33–47.

578. Carter, H.J.; Musick, J.A. Sexual dimorphism in the deep-sea fish *Barathrodemus manatinus* (Ophidiidae). *Copeia* **1985**, *1985*, 69, doi:10.2307/1444791.

579. Parmentier, E.; Bahri, M.A.; Plenevaux, A.; Fine, M.L.; Estrada, J.M. Sound production and sonic apparatus in deep-living cusk-eels (*Genypterus chilensis* and *Genypterus maculatus*). *Deep Sea Res. Part I Oceanogr. Res. Pap.* **2018**, *141*, 83–92, doi:10.1016/j.dsr.2018.09.009.

580. Nguyen, T.K.; Lin, H.; Parmentier, E.; Fine, M.L.; Hsung, L.; Parmentier, E.; Fine, M.L. Seasonal variation in sonic muscles in the fawn cusk-eel *Lepophidium profundorum*. *Biol. Lett.* **2008**, *4*, 707–710, doi:10.1098/rsbl.2008.0383.

581. Ali, H.A.; Mok, H.K.; Fine, M.L. Development and sexual dimorphism of the sonic system in deep sea neobythitine fishes: The upper continental slope. *Deep. Res. Part I Oceanogr. Res. Pap.* **2016**, *115*, 293–308, doi:10.1016/j.dsr.2016.07.010.

582. Lobel, P.S. Spawning sound of the trunkfish, Ostracion meleagris (Ostraciidae). *Biol Bull* **1996**, *191*, 308–309, doi:10.1086/BBLv191n2p308.

583. Moyer, J.T. Mating Strategies and Reproductive Behavior of Ostraciid Fishes at Miyake-jima, Japan. *Japanese J. Ichthyol.* **1979**, *26*, 148–160, doi:10.11369/jji1950.26.148.

584. Frédérich, B.; Olivier, D.; Litsios, G.; Alfaro, M.E.; Parmentier, E. Trait decoupling promotes evolutionary diversification of the trophic and acoustic system of damselfishes. *Proc. R. Soc. London B - Biol. Sci.* **2014**, *281*, doi:10.1098/rspb.2014.1047.

585. Picciulin, M.M.; Constantini, M.; Hawkins, A.D.; Ferrero, E.A. Sound emission of the Mediterranean

Damselfish Chromis chromis (Pomacentridae). *Bioacoustics* **2001**, *12*, 236–237, doi:10.1080/09524622.2002.9753707.

586. Moulton, J.M. Marine animal sounds of the Queensland coast. *Am. Zool.* **1962**, *2*, 542.

587. Walls, P.D. The anatomy of the sound-producing apparatus of some Australian fishes, Bowdoin College, 1964.

588. Salmon, M.; Winn, H.E. Sound production by priacanthid fishes. *Copeia* **1966**, *4*, 869–872, doi:10.2307/1441415.

589. Allen, S.; Demer, D.A. Detection and characterization of yellowfin and bluefin tuna using passive-acoustical techniques. *Fish. Res.* **2003**, *63*, 393–403, doi:10.1016/S0165-7836(03)00096-1.

590. Hallacher, L.E. The comparative morphology of extrinsic gasbladder musculature in the scorpionfish genus *Sebastes* (Pisces: Scorpaenidae). *Proc. Calif. Acad. Sci. Fourth Ser.* **1974**, *40*, 59–86.

591. Beattie, M.; Nowacek, D.P.; Bogdanoff, A.K.; Akins, L.; Morris, J.A. The roar of the lionfishes *Pterois volitans* and *Pterois miles*. *J. Fish Biol.* **2017**, *90*, 2488–2495, doi:10.1111/jfb.13321.

592. Laxminarsimha Chary, K.; Sreekanth, G.B.; Deshmukh, M.K.; Sharma, N. Marine soundscape and fish chorus in an archipelago ecosystem comprising bio-diverse tropical islands off Goa Coast, India. *Aquat. Ecol.* **2020**, *54*, 475–493, doi:10.1007/s10452-020-09754-0.

593. Mann, D.A.; Locascio, J. V.; Schärer, M.; Nemeth, M.I.; Appeldoorn, R.S.; Schärer-Umpierre, M.T.; Nemeth, M.I.; Appeldoorn, R.S. Sound production by red hind *Epinephelus guttatus* in spatially segregated spawning aggregations. *Aquat. Biol.* **2010**, *10*, 149–154, doi:10.3354/ab00272.

594. Rowell, T.; Schärer, M.; Appeldoorn, R.; Nemeth, M.; Mann, D.; Rivera, J. Sound production as an indicator of red hind density at a spawning aggregation. *Mar. Ecol. Prog. Ser.* **2012**, *462*, 241–250, doi:10.3354/meps09839.

595. Ibrahim, A.K.; Chérubin, L.M.; Zhuang, H.; Schärer Umpierre, M.T.; Dalgleish, F.; Erdol, N.; Ouyang, B.; Dalgleish, A. An approach for automatic classification of grouper vocalizations with passive acoustic monitoring. *J. Acoust. Soc. Am.* **2018**, *143*, 666–676, doi:10.1121/1.5022281.

596. Schärer, M.; Rowell, T.J.; Nemeth, M.I.; Appeldoorn, R.S.R.; Schärer-Umpierre, M.T.; Rowell, T.J.; Nemeth, M.I.; Appeldoorn, R.S.R. Sound production associated with reproductive behavior of Nassau grouper *Epinephelus striatus* at spawning aggregations. *Endanger. Species Res.* **2012**, *19*, 29–38, doi:10.3354/esr00457.

597. Chérubin, L.M.; Dalgleish, F.; Ibrahim, A.K.; Schärer-Umpierre, M.; Nemeth, R.S.; Matthews, A.; Appeldoorn, R. Fish Spawning Aggregations Dynamics as Inferred From a Novel, Persistent Presence Robotic Approach. *Front. Mar. Sci.* **2020**, *6*, doi:10.3389/fmars.2019.00779.

598. Mann, D.; Locascio, J. V; Coleman, F.C.; Koenig, C.C. Goliath grouper *Epinephelus itajara* sound production and movement patterns on aggregation sites. *Endanger. Species Res.* **2009**, *7*, 229–236, doi:10.3354/esr00109.

599. Koenig, C.; Bueno, L.; Coleman, F.; Cusick, J.; Ellis, R.; Kingon, K.; Locascio, J.; Malinowski, C.; Murie, D.; Stallings, C. Diel, lunar, and seasonal spawning patterns of the Atlantic goliath grouper, *Epinephelus itajara*, off Florida, United States. *Bull. Mar. Sci.* **2017**, *93*, 391–406, doi:10.5343/bms.2016.1013.

600. Malinowski, C.; Coleman, F.; Koenig, C.; Locascio, J.; Murie, D. Are Atlantic goliath grouper, *Epinephelus itajara*, establishing more northerly spawning sites? Evidence from the northeast Gulf of Mexico. *Bull. Mar. Sci.* **2019**, *95*, 371–391, doi:10.5343/bms.2018.0062.

601. Wall, C.C.; Lembke, C.; Hu, C.; Mann, D.A. Fish Sound Production in the Presence of Harmful Algal Blooms in the Eastern Gulf of Mexico. *PLoS One* **2014**, *9*, e114893, doi:10.1371/journal.pone.0114893.

602. Wall, C.C.; Simard, P.; Lindemuth, M.; Lembke, C.; Naar, D.F.; Hu, C.; Barnes, B.B.; Muller-Karger, F.E.; Mann, D.A. Temporal and spatial mapping of red grouper *Epinephelus morio* sound production. *J. Fish Biol.* **2014**, *85*, 1470–1488, doi:10.1111/jfb.12500.

603. Wall, C.C.; Simard, P.; Mann, D.A. Distribution and Potential Impact of Boat Noise on Fish Sound

Production From an Autonomous Acoustic Array in the Eastern Gulf of Mexico. *Adv Exp Med Biol* **2012**, *730*, 403–406, doi:10.1007/978-1-4419-7311-5_92.

604. Rowell, T.; Nemeth, R.; Schärer, M.; Appeldoorn, R. Fish sound production and acoustic telemetry reveal behaviors and spatial patterns associated with spawning aggregations of two Caribbean groupers. *Mar. Ecol. Prog. Ser.* **2015**, *518*, 239–254, doi:10.3354/meps11060.

605. Sanchez, P.J.; Appeldoorn, R.S.; Schärer-Umpierre, M.T.; Locascio, J. V. Patterns of courtship acoustics and geophysical features at spawning sites of black grouper (*Mycteroperca bonaci*). *Fish. Bull.* **2017**, *115*, 186–195, doi:10.7755/FB.115.2.5.

606. Schärer, M.T.; Nemeth, M.I.; Rowell, T.J.; Appeldoorn, R.S. Sounds associated with the reproductive behavior of the black grouper (*Mycteroperca bonaci*). *Mar. Biol.* **2014**, *161*, 141–147, doi:10.1007/s00227-013-2324-3.

607. Schärer, M.T.; Nemeth, M.I.; Mann, D.; Locascio, J.; Appeldoorn, R.S.; Rowell, T.J. Sound production and reproductive behavior of yellowfin grouper, *Mycteroperca venenosa* (Serranidae) at a spawning aggregation. *Copeia* **2012**, *2012*, 135–144, doi:10.1643/CE-10-151.

608. Fish, M.P. The production of underwater sound by the Northern seahorse, Hippocampus hudsonius. *Copeia* **1953**, *2*, 98–99, doi:10.2307/1440134.

609. Colson, D.J.; Patek, S.N.; Brainerd, E.L.; Lewis, S.M. A mechanism of sound production during feeding in *Hippocampus* seahorses (Syngnathidae). *Am. Zool.* **1996**, *36*, 84A-84A.

610. Onuki, A.; Somiya, H. *Two types of sounds and additional spinal nerve innervation to the sonic muscle in John Dory*, Zeus faber *(Zeiformes: Teleostei)*; 2004; Vol. 84; ISBN 0025315404.

611. Radford, C.A.; Putland, R.L.; Mensinger, A.F. Barking mad: The vocalisation of the John Dory, *Zeus faber*. *PLoS One* **2018**, *13*, 1–11, doi:10.1371/journal.pone.0204647.

612. Bass, A.H.; Bodnar, D.A.; Marchaterre, M.A. Complementary explanations for existing phenotypes in an acoustic communication system. In *Neural Mechanisms of Communication*; Hauser, M., Konishi, M., Eds.; MIT Press: Cambridge, 1999; pp. 493–514.

613. Lugli, M.; Torricelli, P.; Pavan, G.; Mainardi, D. Sound production during courtship and spawning among freshwater gobiids (pisces, gobiidae). *Mar. Freshw. Behav. Physiol.* **1997**, *29*, 109–126, doi:10.1080/10236249709379003.

614. Lagardère, J.P.; Millot, S.; Parmentier, E. Aspects of sound communication in the pearlfish Carapus boraborensis and Carapus homei (Carapidae). *J. Exp. Zool. Part A Comp. Exp. Biol.* **2005**, *303*, 1066–1074, doi:10.1002/jez.a.230.

615. Service de la pêche Les paru ou poissons de profondeur. *Te Vea Tautai* **2004**, *15*.

616. Howes, G.J. Notes on the anatomy and classification of ophidiiform fishes with particular reference to the abyssal genus Acanthonus Gunther, 1878. *Bull. Br. Museum* 1978, *58*, 95–131.

617. Casadevall, M.; Matallanas, J.; Carrasson, M.; Munoz, M.; Muñoz, M.; Munoz, M. Morphometric, meristic and anatomical differences between *Ophidion barbatum* L., 1758 and *O. rochei* Muller, 1845 (Pisces, Ophidiidae). *Publicaciones Espec. - Inst. Esp. Oceanogr.* **1996**, *21*, 45–61.

618. Siebold, P.F. von; Haan, W. de; Schlegel, H.; Temminck, C.J. *Fauna japonica, sive, Descriptio animalium, quae in itinere per Japoniam, jussu et auspiciis, superiorum, qui summum in India Batava imperium tenent, suscepto, annis 1823-1830*; Apud Auctorem: Lugduni Batavorum, 1833;

619. Hubbs, C.L. Species of the circumtropical fish genus *Brotula*. *Copeia* **1944**, *1944*, 162, doi:10.2307/1437812.

620. McNeill Alexander, R. Tendon elasticity and muscle function. *Comp. Biochem. Physiol. Part A Mol. Integr. Physiol.* **2002**, *133*, 1001–1011, doi:10.1016/S1095-6433(02)00143-5.

621. Skoglund, C.R. Functional analysis of swim-bladder muscles engaged in sound production of the toadfish. *J. Biophys. Biochem. Cytol.* **1961**, *10*, 187–200, doi:10.1083/jcb.10.4.187.

622. Bass, A.H.; McKibben, J.R. Neural mechanisms and behaviors for acoustic communication in teleost

fish. *Prog. Neurobiol.* **2003**, *69*, 1–26, doi:10.1016/S0301-0082(03)00004-2.

623. Amorim, M.C.P.; Hawkins, A.D. Ontogeny of Acoustic and Feeding Behaviour in the Grey Gurnard, *Eutrigla gurnardus*. *Ethology* **2005**, *111*, 255–269, doi:10.1111/j.1439-0310.2004.01061.x.

624. Crawford, J.D.; Huang, X. Communication signals and sound production mechanisms of mormyrid electric fish. *J. Exp. Biol.* **1999**, *202*, 1417–1426, doi:10.1242/jeb.202.10.1417.

625. Young, D. Do cicadas radiate sound through their ear-drums? *J. Exp. Biol.* **1990**, *151*, 41–56, doi:10.1242/jeb.151.1.41.

626. Bennet-Clark, H.C.; Young, D. A model of the mechanism of sound production in cicadas. *J. Exp. Biol.* **1992**, *173*, 123–153, doi:10.1242/jeb.173.1.123.

627. Parmentier, E.; Lagardère, J.-P.; Braquegnier, J.-B.; Vandewalle, P.; Fine, M.L. Sound production mechanism in carapid fish: first example with a slow sonic muscle. *J. Exp. Biol.* **2006**, *209*, 2952–2960, doi:10.1242/jeb.02350.

628. Gleason, M.G. Effects of disturbance on coral communities: bleaching in Moorea, French Polynesia. *Coral Reefs* **1993**, *12*, 193–201, doi:10.1007/BF00334479.

629. De Loma, T.L.; Osenberg, C.W.; Shima, J.S.; Chancerelle, Y.; Davies, N.; Brooks, A.J.; Galzin, R. A framework for assessing impacts of marine protected areas in Moorea (French Polynesia). *Pacific Sci.* **2008**, *62*, 431–441, doi:10.2984/1534-6188(2008)62[431:AFFAIO]2.0.CO;2.

630. L'Heureux, M.L.; Takahashi, K.; Watkins, A.B.; Barnston, A.G.; Becker, E.J.; Di Liberto, T.E.; Gamble, F.; Gottschalck, J.; Halpert, M.S.; Huang, B.; et al. Observing and Predicting the 2015/16 El Niño. *Bull. Am. Meteorol. Soc.* **2017**, *98*, 1363–1382, doi:10.1175/BAMS-D-16-0009.1.

631. Eakin, C.M.; Sweatman, H.P.A.; Brainard, R.E. The 2014–2017 global-scale coral bleaching event: insights and impacts. *Coral Reefs* **2019**, *38*, 539–545, doi:10.1007/s00338-019-01844-2.

632. Hédouin, L.; Rouzé, H.; Berthe, C.; Perez-Rosales, G.; Martinez, E.; Chancerelle, Y.; Galand, P.E.; Lerouvreur, F.; Nugues, M.M.; Pochon, X.; et al. Contrasting patterns of mortality in Polynesian coral reefs following the third global coral bleaching event in 2016. *Coral Reefs* **2020**, *39*, 939–952, doi:10.1007/s00338-020-01914-w.

633. Edmunds, P.J. Unusually high coral recruitment during the 2016 El Niño in Mo'orea, French Polynesia. *PLoS One* **2017**, *12*, e0185167, doi:10.1371/journal.pone.0185167.

634. Burgess, S.C.; Johnston, E.C.; Wyatt, A.S.J.; Leichter, J.J.; Edmunds, P.J. Response diversity in corals: hidden differences in bleaching mortality among cryptic *Pocillopora* species. *Ecology* **2021**, *102*, doi:10.1002/ecy.3324.

635. Faurea, G. Degradation of Coral Reefs at Moorea Island (French Polynesia) by *Acanthaster planci*. *J. Coast. Res.* **1989**, *5*, 295–305.

636. Harmelin-Vivien, M.L.; Laboute, P. Catastrophic impact of hurricanes on atoll outer reef slopes in the Tuamotu (French Polynesia). *Coral Reefs* **1986**, *5*, 55–62, doi:10.1007/BF00270353.

637. Williams, E.H.; Bunkley-Williams, L. The world-wide coral reef bleaching cycle and related sources of coral mortality. *Atoll Res. Bull.* **1990**, *335*, 1–71, doi:10.5479/si.00775630.335.1.

638. Salvat, B. Blanchissement et mortalité des scléractiniaires sur les récifs de Moorea (Archipel de la Société) en 1991. *Comptes Rendus l'Académie des Sci.* **1992**, *314*, 105–111.

639. Adjeroud, M.; Michonneau, F.; Edmunds, P.J.; Chancerelle, Y.; de Loma, T.L.; Penin, L.; Thibaut, L.; Vidal-Dupiol, J.; Salvat, B.; Galzin, R. Recurrent disturbances, recovery trajectories, and resilience of coral assemblages on a South Central Pacific reef. *Coral Reefs* **2009**, *28*, 775–780, doi:10.1007/s00338-009-0515-7.

640. Hoegh-Guldberg, O.; Salvat, B.; Hoegh Guldberg, O.; Salvat, B. Periodic mass-bleaching and elevated sea temperatures:bleaching of outer reef slope communities in Moorea, French Polynesia. *Mar. Ecol. Prog. Ser.* **1995**, *121*, 181–190, doi:10.3354/meps121181.

641. Adjeroud, M.; Chancerelle, Y.; Schrimm, M.; Perez, T.; Lecchini, D.; Galzin, R.; Salvat, B. Detecting

the effects of natural disturbances on coral assemblages in French Polynesia: A decade survey at multiple scales. *Aquat. Living Resour.* **2005**, *18*, 111–123, doi:10.1051/alr:2005014.

642. Penin, L.; Adjeroud, M.; Schrimm, M.; Lenihan, H.S. High spatial variability in coral bleaching around Moorea (French Polynesia): patterns across locations and water depths. *C. R. Biol.* **2007**, *330*, 171–181, doi:10.1016/j.crvi.2006.12.003.

643. de Loma, T.L.; Chancerelle, Y.; Lerouvreur, F. *Evaluation des densités d'*Acanthaster planci *sur l'île de Moorea*; 2006;

644. Pratchett, M.S.; Trapon, M.; Berumen, M.L.; Chong-Seng, K. Recent disturbances augment community shifts in coral assemblages in Moorea, French Polynesia. *Coral Reefs* **2011**, *30*, 183–193, doi:10.1007/s00338-010-0678-2.

645. Kayal, M.; Vercelloni, J.; Lison de Loma, T.; Bosserelle, P.; Chancerelle, Y.; Geoffroy, S.; Stievenart, C.; Michonneau, F.; Penin, L.; Planes, S.; et al. Predator crown-of-thorns starfish (*Acanthaster planci*) outbreak, mass mortality of corals, and cascading effects on reef fish and benthic communities. *PLoS One* **2012**, *7*, e47363, doi:10.1371/journal.pone.0047363.

646. Penin, L.; Vidal-Dupiol, J.; Adjeroud, M. Response of coral assemblages to thermal stress: are bleaching intensity and spatial patterns consistent between events? *Environ. Monit. Assess.* **2013**, *185*, 5031–5042, doi:10.1007/s10661-012-2923-3.

647. Donovan, M.K.; Adam, T.C.; Shantz, A.A.; Speare, K.E.; Munsterman, K.S.; Rice, M.M.; Schmitt, R.J.; Holbrook, S.J.; Burkepile, D.E. Nitrogen pollution interacts with heat stress to increase coral bleaching across the seascape. *Proc. Natl. Acad. Sci.* **2020**, *117*, 5351–5357, doi:10.1073/pnas.1915395117.

648. Salvat, B.M.; Aubanel, A.; Adjeroud, M.; Bouisset, M.; Calmet, D.; Chancerelle, Y.; Cochennec, N.; Davies, N.; Fougerousse, A.; Galzin, R.; et al. Monitoring of French Polynesia coral reefs and their recent development. *Rev. d'Ecologie* **2008**, *63*, 145–177.

649. Mellin, C.; Aaron MacNeil, M.; Cheal, A.J.; Emslie, M.J.; Julian Caley, M. Marine protected areas increase resilience among coral reef communities. *Ecol. Lett.* **2016**, *19*, 629–637, doi:10.1111/ele.12598.

650. Salm, R. V; Smith, S.E.; Llewellyn, G. Mitigating the impact of coral bleaching through marine protected area design. In Proceedings of the 9th International Coral Reef Symposium; 2000; pp. 81–89.

651. Gaspar, C.; Bambridge, T. Territorialités et aires marines protégées à Moorea (Polynésie française). *J. Soc. Ocean.* **2008**, 231–246, doi:10.4000/jso.2462.

652. Galzin, R.; Kulbicki, M.; Petit, J.; Wickel, J. *Réflexions de biologistes sur les "effets réserve" en partant du cas d'étude de la Polynésie Française*; 2009;

653. Lindseth, A. V; Lobel, P.S. Underwater soundscape monitoring and fish bioacoustics : a review. *Fishes* **2018**, *3*, 36, doi:10.3390/fishes3030036.

654. Rowell, T.J.; Demer, D.A.; Aburto-oropeza, O.; Cota-nieto, J.J.; Hyde, J.R.; Erisman, B.E. Estimating fish abundance at spawning aggregations from courtship sound levels. *Sci. Rep.* **2017**, *7*, 1–14, doi:10.1038/s41598-017-03383-8.

655. Caiger, P.E.; Dean, M.J.; DeAngelis, A.I.; Hatch, L.T.; Rice, A.N.; Stanley, J.A.; Tholke, C.; Zemeckis, D.R.; van Parijs, S.M. A decade of monitoring atlantic cod *Gadus morhua* spawning aggregations in Massachusetts bay using passive acoustics. *Mar. Ecol. Prog. Ser.* **2020**, *635*, 89–103, doi:10.3354/MEPS13219.

656. Gannon, D.P. Passive Acoustic Techniques in Fisheries Science: A Review and Prospectus. *Trans. Am. Fish. Soc.* **2008**, *137*, 638–656, doi:10.1577/T04-142.1.

657. Galzin, R. Structure of fish communities of French Polynesian coral reefs. II. Temporal scales. *Mar. Ecol. Prog. Ser.* **1987**, *41*, 137–145, doi:10.3354/meps041137.

658. Loya, Y. Plotless and transect methods. In *Research Methods*; Stoddart, D.R., Johannes, R.F., Eds.; 1978; pp. 197–217.

659. Winn, H.E.; Marshall, J.A.; Hazlett, B. Behavior, diel activities, and stimuli that elicit sound production and reactions to sounds in the longspine squirrelfish. *Copeia* **1964**, *1964*, 413, doi:10.2307/1441036.

660. Kropp, R.K. Descriptions of Some Endolithic Habitats for Snapping Shrimp (Alpheidae) in Micronesia. *Bull. Mar. Sci.* **1987**, *41*, 204–213.

661. Ferreira, C.E.L.; Gonçalves, J.E.A.; Coutinho, R.; Peret, A.C. Herbivory by the Dusky Damselfish *Stegastes fuscus* (Cuvier, 1830) in a tropical rocky shore: effects on the benthic community. *J. Exp. Mar. Bio. Ecol.* **1998**, *229*, 241–264, doi:10.1016/S0022-0981(98)00056-2.

662. Malakoff, D. A Push for Quieter Ships. *Science (80-.).* **2010**, *328*, 1502–1503, doi:10.1126/science.328.5985.1502.

663. Ilyina, T.; Zeebe, R.E.; Brewer, P.G. Future ocean increasingly transparent to low-frequency sound owing to carbon dioxide emissions. *Nat. Geosci.* **2010**, *3*, 18–22, doi:10.1038/ngeo719.

664. Hester, K.C.; Peltzer, E.T.; Kirkwood, W.J.; Brewer, P.G. Unanticipated consequences of ocean acidification: A noisier ocean at lower pH. *Geophys. Res. Lett.* **2008**, *35*, L19601, doi:10.1029/2008GL034913.

665. Lecchini, D.; Shima, J.; Banaigs, B.; Galzin, R. Larval sensory abilities and mechanisms of habitat selection of a coral reef fish during settlement. *Oecologia* **2005**, *143*, 326–334, doi:10.1007/s00442-004-1805-y.

666. Igulu, M.M.; Nagelkerken, I.; Fraaije, R.; van Hintum, R.; Ligtenberg, H.; Mgaya, Y.D. The potential role of visual cues for microhabitat selection during the early life phase of a coral reef fish (*Lutjanus fulviflamma*). *J. Exp. Mar. Bio. Ecol.* **2011**, *401*, 118–125, doi:10.1016/j.jembe.2011.01.022.

667. Huijbers, C.M.; Nagelkerken, I.; Lössbroek, P.A.C.; Schulten, I.E.; Siegenthaler, A.; Holderied, M.W.; Simpson, S.D. A test of the senses: Fish select novel habitats by responding to multiple cues. *Ecology* **2012**, *93*, 46–55, doi:10.1890/10-2236.1.

668. Dittman, A.; Quinn, T. Homing in Pacific salmon: mechanisms and ecological basis. *J. Exp. Biol.* **1996**, *199*, 83–91, doi:10.1242/jeb.199.1.83.

669. Staaterman, E.; Paris, C.B. Modelling larval fish navigation: The way forward. *ICES J. Mar. Sci.* **2014**, *71*, 918–924, doi:10.1093/icesjms/fst103.

670. Paris, C.B.; Atema, J.; Irisson, J.-O.; Kingsford, M.; Gerlach, G.; Guigand, C.M. Reef Odor: A Wake Up Call for Navigation in Reef Fish Larvae. *PLoS One* **2013**, *8*, e72808, doi:10.1371/journal.pone.0072808.

671. Brewer, P.; Hester, K. Ocean Acidification and the Increasing Transparency of the Ocean to Low-Frequency Sound. *Oceanography* **2009**, *22*, 86–93, doi:10.5670/oceanog.2009.99.

672. Gazioğlu, C.; Müftüoğlu, A.E.; Demir, V.; Aksu, A.; Okutan, V. Connection between Ocean Acidification and Sound Propagation. *Int. J. Environ. Geoinformatics* **2015**, *2*, 16–26, doi:10.30897/ijegeo.303538.

673. Kingsford, M.J. Diel patterns of abundance of presettlement reef fishes and pelagic larvae on a coral reef. *Mar. Biol.* **2001**, *138*, 853–867, doi:10.1007/s002270000455.

674. Thorrold, S.R.; Shenker, J.M.; Wishinski, E.; Mojica, R.; Maddox, E.D. Larval supply of shorefishes to nursery habitats around Lee Stocking Island, Bahamas. I. Small-scale distribution patterns. *Mar. Biol.* **1994**, *118*, 555–566, doi:10.1007/BF00347502.

675. Tolimieri, N.; Haine, O.; Jeffs, A.; McCauley, R.; Montgomery, J. Directional orientation of pomacentrid larvae to ambient reef sound. *Coral Reefs* **2004**, *23*, doi:10.1007/s00338-004-0383-0.

676. Dufour, V.; Galzin, R. Colonization patterns of reef fish larvae to the lagoon at Moorea Island, French Polynesia. *Mar. Ecol. Prog. Ser.* **1993**, *102*, 143–152, doi:10.3354/meps102143.

677. Montgomery, J.C.; Tolimieri, N.; Haine, O.S. Active habitat selection by pre-settlement reef fishes. *Fish Fish.* **2001**, *2*, 261–277, doi:10.1046/j.1467-2960.2001.00053.x.

678. Kingsford, M.; Finn, M. The influence of phase of the moon and physical processes on the input of presettlement fishes to coral reefs. *J. Fish Biol.* **1997**, *51*, 176–205, doi:10.1111/j.1095-8649.1997.tb06099.x.

679. Milicich, M.J.; Meekan, M.G.; Doherty, P.J. Larval supply: a good predictor of recruitment of three

species of reef fish (Pomacentridae). *Mar. Ecol. Prog. Ser.* **1992**, *86*, 153–166, doi:10.3354/meps086153.

680. McCauley, R.D. *Aspects of marine biological sound in northern Australia III: reef associated fish choruses (Report for the Defence Science and Technology Organization)*; 1995;

681. Jones, G.P. Some interactions between residents and recruits in two coral reef fishes. *J. Exp. Mar. Bio. Ecol.* **1988**, *114*, 169–182, doi:10.1016/0022-0981(88)90136-0.

682. Booth, D.J. Larval settlement patterns and preferences by domino damselfish *Dascyllus albisella* Gill. *J. Exp. Mar. Bio. Ecol.* **1992**, *155*, 85–104, doi:10.1016/0022-0981(92)90029-A.

683. Baker, E..; Puglise, K.A.; Harris, P.T. *Mesophotic Coral Ecosystems - A Lifeboat for Coral Reefs?*; The United.; 2016; ISBN 978-82-7701-150-9.

684. Frederic Sinniger; Masaya Morita; Saki Harii "Locally extinct" coral species *Seriatopora hystrix* found at upper mesophotic depths in Okinawa. *Coral Reefs* **2013**, *32*, 153–153, doi:10.1007/s00338-012-0973-1.

685. Sinniger, F.; Prasetia, R.; Yorifuji, M.; Bongaerts, P.; Harii, S. *Seriatopora* diversity preserved in upper mesophotic coral ecosystems in Southern Japan. *Front. Mar. Sci.* **2017**, *4*, doi:10.3389/fmars.2017.00155.

686. Holstein, D.M.; Paris, C.B.; Vaz, A.C.; Smith, T.B. Modeling vertical coral connectivity and mesophotic refugia. *Coral Reefs* **2016**, *35*, 23–37, doi:10.1007/s00338-015-1339-2.

687. Hammerman, N.M.; Rivera-Vicens, R.E.; Galaska, M.P.; Weil, E.; Appledoorn, R.S.; Alfaro, M.; Schizas, N. V. Population connectivity of the plating coral *Agaricia lamarcki* from southwest Puerto Rico. *Coral Reefs* **2018**, *37*, 183–191, doi:10.1007/s00338-017-1646-x.

688. Soares, M. de O.; Araújo, J.T. de; Ferreira, S.M.C.; Santos, B.A.; Boavida, J.R.H.; Costantini, F.; Rossi, S. Why do mesophotic coral ecosystems have to be protected? *Sci. Total Environ.* **2020**, *726*, 138456, doi:10.1016/j.scitotenv.2020.138456.

689. Rocha, L.A.; Pinheiro, H.T.; Shepherd, B.; Papastamatiou, Y.P.; Luiz, O.J.; Pyle, R.L.; Bongaerts, P. Mesophotic coral ecosystems are threatened and ecologically distinct from shallow water reefs. *Science (80-.).* **2018**, *361*, 281–284, doi:10.1126/science.aaq1614.

690. Kosaki, R.K.; Pyle, R.L.; Leonard, J.C.; Hauk, B.B.; Whitton, R.K.; Wagner, D. 100% endemism in mesophotic reef fish assemblages at Kure Atoll, Hawaiian Islands. *Mar. Biodivers.* **2017**, *47*, 783–784, doi:10.1007/s12526-016-0510-5.

691. Loya, Y.; Eyal, G.; Treibitz, T.; Lesser, M.P.; Appeldoorn, R. Theme section on mesophotic coral ecosystems: advances in knowledge and future perspectives. *Coral Reefs* **2016**, *35*, 1–9, doi:10.1007/s00338-016-1410-7.

692. Laverick, J.H.; Andradi-Brown, D.A.; Rogers, A.D. Using light-dependent scleractinia to define the upper boundary of mesophotic coral ecosystems on the reefs of Utila, Honduras. *PLoS One* **2017**, *12*, e0183075, doi:10.1371/journal.pone.0183075.

693. Laverick, J.H.; Piango, S.; Andradi-Brown, D.A.; Exton, D.A.; Bongaerts, P.; Bridge, T.C.L.; Lesser, M.P.; Pyle, R.L.; Slattery, M.; Wagner, D.; et al. To what extent do mesophotic coral ecosystems and shallow reefs share species of conservation interest? A systematic review. *Environ. Evid.* **2018**, *7*, 15, doi:10.1186/s13750-018-0127-1.

694. Guerin, A. Comparaison des communautés acoustiques ichtyologiques de Moorea (Polynésie Française) en fonction du statut de protection, University of Liège, 2024.

695. Bianco, M.J.; Gerstoft, P.; Traer, J.; Ozanich, E.; Roch, M.A.; Gannot, S.; Deledalle, C.-A. Machine learning in acoustics: Theory and applications. *J. Acoust. Soc. Am.* **2019**, *146*, 3590–3628, doi:10.1121/1.5133944.

696. Malfante, M.; Mars, J.I.; Dalla Mura, M.; Gervaise, C. Automatic fish sounds classification. *J. Acoust. Soc. Am.* **2018**, *143*, 2834–2846, doi:10.1121/1.5036628.

697. Parsons, M.J.G.; Lin, T.H.; Mooney, T.A.; Erbe, C.; Juanes, F.; Lammers, M.; Li, S.; Linke, S.; Looby,

A.; Nedelec, S.L.; et al. Sounding the Call for a Global Library of Underwater Biological Sounds. *Front. Ecol. Evol.* **2022**, *10*, 1–20, doi:10.3389/fevo.2022.810156.

698. Vieira, M.; Fonseca, P.J.; Amorim, M.C.P.; Teixeira, C.J.C. Call recognition and individual identification of fish vocalizations based on automatic speech recognition: An example with the Lusitanian toadfish. *J. Acoust. Soc. Am.* **2015**, *138*, 3941–3950, doi:10.1121/1.4936858.

699. Sattar, F.; Cullis-Suzuki, S.; Jin, F. Acoustic analysis of big ocean data to monitor fish sounds. *Ecol. Inform.* **2016**, *34*, 102–107, doi:10.1016/j.ecoinf.2016.05.002.

700. Mouy, X.; Rountree, R.; Juanes, F.; Dosso, S.E. Cataloging fish sounds in the wild using combined acoustic and video recordings. *J. Acoust. Soc. Am.* **2018**, *143*, EL333–EL339, doi:10.1121/1.5037359.

701. Harakawa, R.; Ogawa, T.; Haseyama, M.; Akamatsu, T. Automatic detection of fish sounds based on multi-stage classification including logistic regression via adaptive feature weighting. *J. Acoust. Soc. Am.* **2018**, *144*, 2709–2718, doi:10.1121/1.5067373.

702. Monczak, A.; Ji, Y.; Soueidan, J.; Montie, E.W. Automatic detection, classification, and quantification of sciaenid fish calls in an estuarine soundscape in the Southeast United States. *PLoS One* **2019**, *14*, e0209914, doi:10.1371/journal.pone.0209914.

703. Lin, T.-H.; Tsao, Y.; Akamatsu, T. Comparison of passive acoustic soniferous fish monitoring with supervised and unsupervised approaches. *J. Acoust. Soc. Am.* **2018**, *143*, EL278–EL284, doi:10.1121/1.5034169.

704. Laplante, J.-F.; Akhloufi, M.A.; Gervaise, C. Fish recognition in underwater environments using deep learning and audio data. In Proceedings of the Ocean Sensing and Monitoring XIII; Hou, W., Ed.; SPIE, 2021; p. 15.

705. Ibrahim, A.K.; Zhuang, H.; Chérubin, L.M.; Schärer-Umpierre, M.T.; Erdol, N. Automatic classification of grouper species by their sounds using deep neural networks. *J. Acoust. Soc. Am.* **2018**, *144*, EL196–EL202, doi:10.1121/1.5054911.

706. Stolkin, R.; Radhakrishnan, S.; Sutin, A.; Rountree, R. Passive acoustic detection of modulated underwater sounds from biological and anthropogenic sources. In Proceedings of the OCEANS 2007; IEEE, 2007; pp. 1–8.

707. Le Bot, O.; Mars, J.I.; Gervaise, C.; Simard, Y. Rhythmic analysis for click train detection and source separation with examples on beluga whales. *Appl. Acoust.* **2015**, *95*, 37–49, doi:10.1016/j.apacoust.2015.02.005.

708. Ruff, Z.J.; Lesmeister, D.B.; Appel, C.L.; Sullivan, C.M. Workflow and convolutional neural network for automated identification of animal sounds. *Ecol. Indic.* **2021**, *124*, 107419, doi:10.1016/j.ecolind.2021.107419.

709. Ruff, Z.J.; Lesmeister, D.B.; Duchac, L.S.; Padmaraju, B.K.; Sullivan, C.M. Automated identification of avian vocalizations with deep convolutional neural networks. *Remote Sens. Ecol. Conserv.* **2020**, *6*, 79–92, doi:10.1002/rse2.125.

710. Williams, B.; Belvanera, S.M.; Sethi, S.S.; Lamont, T.A.C.; Jompa, J.; Prasetya, M.; Richardson, L.; Chapuis, L.; Weschke, E.; Hoey, A.; et al. Unlocking the soundscape of coral reefs with artificial intelligence. *Prepr. BioRxiv* **2024**, doi:10.1101/2024.02.02.578582.

711. Munger, J.; Herrera, D.; Haver, S.; Waterhouse, L.; McKenna, M.; Dziak, R.; Gedamke, J.; Heppell, S.; Haxel, J. Machine learning analysis reveals relationship between pomacentrid calls and environmental cues. *Mar. Ecol. Prog. Ser.* **2022**, *681*, 197–210, doi:10.3354/meps13912.

712. Hsu, T.-Y.; Shao, Y.-T.; Lin, T.-H. Using Passive Acoustic Monitoring and Source Separation for Analyzing the Inter-annual and Seasonal Variability of Fish communities. In Proceedings of the XXVIII International Bioacoustics Congress IBAC 2023 (poster presentation); 2023.

713. Lin, T.-H.; Fang, S.-H.; Tsao, Y. Improving biodiversity assessment via unsupervised separation of biological sounds from long-duration recordings. *Sci. Rep.* **2017**, *7*, 4547, doi:10.1038/s41598-017-04790-7.

714. Lin, T.; Tsao, Y. Source separation in ecoacoustics: a roadmap towards versatile soundscape information

retrieval. *Remote Sens. Ecol. Conserv.* **2020**, *6*, 236–247, doi:10.1002/rse2.141.

715. Mishachandar, B.; Vairamuthu, S. Diverse ocean noise classification using deep learning. *Appl. Acoust.* **2021**, *181*, 108141, doi:10.1016/j.apacoust.2021.108141.

716. Kim, E.B.; Frasier, K.E.; McKenna, M.F.; Kok, A.C.M.; Peavey Reeves, L.E.; Oestreich, W.K.; Arrieta, G.; Wiggins, S.; Baumann-Pickering, S. SoundScape learning: An automatic method for separating fish chorus in marine soundscapes. *J. Acoust. Soc. Am.* **2023**, *153*, 1710–1722, doi:10.1121/10.0017432.

717. Stefanoudis, P. V.; Gress, E.; Pitt, J.M.; Smith, S.R.; Kincaid, T.; Rivers, M.; Andradi-Brown, D.A.; Rowlands, G.; Woodall, L.C.; Rogers, A.D. Depth-Dependent Structuring of Reef Fish Assemblages From the Shallows to the Rariphotic Zone. *Front. Mar. Sci.* **2019**, *6*, doi:10.3389/fmars.2019.00307.

718. Stefanoudis, P. V.; Rivers, M.; Smith, S.R.; Schneider, C.W.; Wagner, D.; Ford, H.; Rogers, A.D.; Woodall, L.C. Low connectivity between shallow, mesophotic and rariphotic zone benthos. *R. Soc. Open Sci.* **2019**, *6*, 190958, doi:10.1098/rsos.190958.

719. Sieber, A.; Pyle, R. A review of the use of closed-circuit rebreathers for scientific diving. *Underw. Technol.* **2010**, *29*, 73–78, doi:10.3723/ut.29.073.

720. Galzin, R. La faune ichtyologique d'un récif corallien de Moorea, Polynésie Française: Echantillonnage et premiers résultats. *Terre Vie, Rev. Ecol.* **1979**, *33*, 623–644.

721. Arrêté n° 932 C M du 4 juillet 2007.

722. Marines, D. des ressources *Zones maritimes réglementées en Polynésie française 2021*; Papeete, 2021;

723. Kuwamura, T. Social and reproductive behavior of three mouthbrooding cardinalfishes, *Apogon doederleini*, *A. niger* and *A. notatus*. *Environ. Biol. Fishes* **1985**, *13*, 17–24, doi:10.1007/BF00004852.

724. Almada, V.C.; de Oliverira, R.F.; Barata, E.N.; Gonçalves, E.J.; Rito, A.P. Field observations on the behaviour of the breeding males of *Lipophrys pholis* (Pisces: Blenniidae). *Port. Zool.* **1990**, *1*.

725. Bridge Fishes, ascidians, etc. In *Cambridge Natural History*; 1904; pp. 355–365.

726. Tricas, T.C.; Kajiura, S.M.; Kosaki, R.K. Acoustic communication in territorial butterflyfish: test of the sound production hypothesis. *J. Exp. Biol.* **2006**, *209*, 4994–5004, doi:10.1242/jeb.02609.

727. Fine, M.L.; Ali, H.A.; Nguyen, T.K.; Mok, H.K.; Parmentier, E. Development and sexual dimorphism of the sonic system in three deep-sea neobythitine fishes and comparisons between upper mid and lower continental slope. *Deep. Res. Part I Oceanogr. Res. Pap.* **2017**, *131*, 41–53, doi:10.1016/j.dsr.2017.11.009.

728. Parmentier, E.; Herrel, A.; Banse, M.; Hornstra, H.; Bertucci, F.; Lecchini, D. Diving into dual functionality: Swim bladder muscles in lionfish for buoyancy and sonic capabilities. *J. Anat.* **2023**, 249–259, doi:10.1111/joa.13963.

729. Gill, T. The life history of the sea-horses (hippocampids). *Proc. United States Natl. Museum* **1905**, *28*, 805–814.

730. Lim, A.C.O.; Chong, V.C.; Chew, W.X.; Muniandy, S. V.; Wong, C.S.; Ong, Z.C. Sound production in the tiger-tail seahorse *Hippocampus comes*: Insights into the sound producing mechanisms. *J. Acoust. Soc. Am.* **2015**, *138*, 404–412, doi:10.1121/1.4923153.

731. Oliveira, T.P.R.; Ladich, F.; Abed-Navandi, D.; Souto, A.S.; Rosa, I.L. Sounds produced by the longsnout seahorse: a study of their structure and functions. *J. Zool.* **2014**, *294*, 114–121, doi:10.1111/jzo.12160.

732. Mikhailenko, N.A. Organ of sound formation and electro generation in the Black Sea stargazer *Uranoscopus scaber* (Uranoscopidae). *Zool. Zhurnal* **1973**, *52*, 1353–1359.

APPENDICES

Appendix to Chapter 1

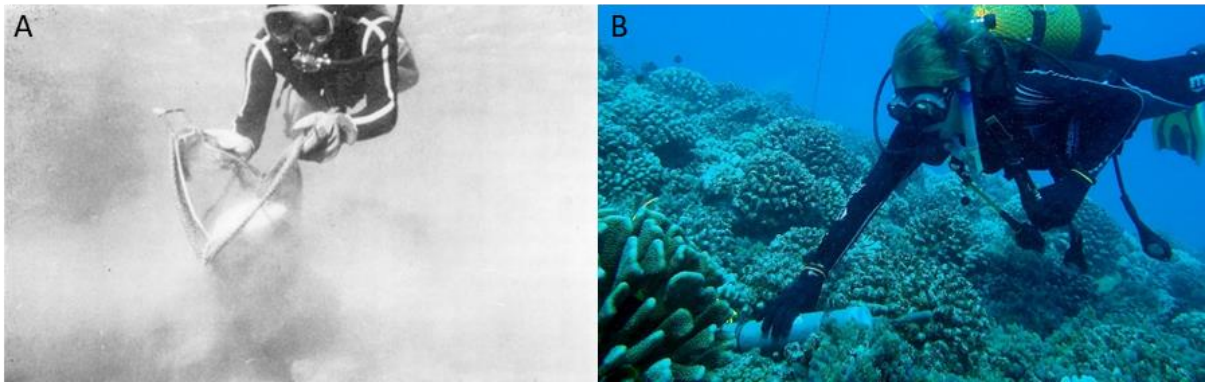

Figure SP1 - 1 Diver at the North-West coast of Moorea Island in (A) the 70's and (B) 2021, illustrating the evolution of sampling techniques. Both studies had the objective of gathering information on the diversity of species present. The left image, originally published in 1979 with the caption 'Sampling by poisoning. In the lower part of the photograph we can still distinguish the cloud of rotenone' [720]. The right image shows an acoustic recorder placed on the external slope as part of this thesis. Photographers: C. Rivers and K. Eustache.

A B C D

Figure SP1 - 2 (A) Introduction to acoustic values, (B) introduction to acoustic propagation in the ocean, (C) introduction to hearing in marine animals, and (D) mechanisms of fish sound production.

Table SP1 - 1 Main marine protected areas *lato sensu* in French Polynesia. Marine educative areas (MEAs) are not included in this classification. P = fishing prohibited, R = fishing restrictions, N = net fishing prohibited, S = fishing restrictions for specific fish species, G = giant clams protection, T = special protection for turtles and birds, RA = rahui [230,721,722]. res. = reserve. MPA = Marine protected area. ZPR = Specific fishing regulations area. NT = Natural tourist area. RA = Traditional alternating fishing area. HP = Protected habitat area. NP = Protected natural area. RI = integral reserve. I to VI: levels of the Environmental Code (Integral reserve and wilderness area, Territorial park, Natural monument, Habitat and species managed area, Protected countryside, and Managed area).

Municipality	Island	Name	Category	Year of protection	Fishing
Society Archipelago					
Maupiti	Manuae and Motu One	Scilly et Bellinghausen	I	(1971), 1992	P
Moorea Maio	Moorea	Tiahura	MPA (PGEM) + scientific res.	2004	P
		Tetaiuo	MPA (PGEM)	2004	P
		Taotaha	MPA (PGEM)	2004	P
		Pihaena	MPA (PGEM)	2004	P
		Aroa	MPA (PGEM)	2004	P
		Nuarei	MPA (PGEM)	2004	R
		Ahi	MPA (PGEM)	2004	R
		Maatea	MPA (PGEM)	2004	R
		Maharepa	ZPR (PGEM)	2004	R
		Papetoai	ZPR (PGEM)	2004	R
	Maio	-	rahui	-	R

Arue	Tahiti	Baie de Matavai	ZPR	2007	S
Mahina	Tahiti	Baie de Muriavai	ZPR	1997	N
	Tahiti	Hotu Ora	ZPR	2015	P
Pirae	Tahiti	Baie du Taaone	ZPR	2003	N
Faa'a	Tahiti	Moana nainai	ZPR	2006	P
Punaauia	Tahiti	Tata'a	ZPR	2016	R
	Tahiti	Nuuroa	ZPR	2016	R
	Tahiti	Atehi	ZPR	2016	R, P
Papara and Teva I Uta	Tahiti	Atimaono	ZPR	2019-2021	R, P
Papara	Tahiti	Pointe Patere	ZPR	2020-2021	R, P
Teva I Uta	Tahiti	Teva I Uta	ZPR	2015	S
		Lagon de Mataiea	rahui	In progress	RA
Tairapu-Ouest	Tahiti	Teahupoo	VI	2014	-
Taiarapu-Est	Tahiti	Rahui Pueu	ZPR	2018-2022	P
	Tahiti	Motu Nono	ZPR	2018-2022	P
	Tahiti	Anse de Teihipa	ZPR	2018-2020	P
	Tahiti	Tautira	ZPR	2018-(2022)	P, S
Arue	Tetiaroa	-	-	2014	N
		Nord	ZPR	2014	R
		Sud	ZPR	2014	P
Taputapuatea	Raiatea	Puohine	ZPR	2020-2021	R & P
Huahine	Huahine	Lagune de Faauna Rahi	-	1970	R
		Lagon de Haapu	rahui	2012	RA
Tuamotu Archipelago					
Tatakoto	Tatakoto	Hopue	ZPR	2004	G
		Pokego	ZPR	2014	G
		Tahuna Arearea	ZPR	2014	G
		Kivakiva Tekoroa	ZPR	2014	G
Rangiroa	Rangiroa	Te Roto Uri Fa'ahotu	ZPR	2015	R
	Mataiva	Village de Pahua	ZPR	2018	N, R
		Hoa Hitirari	ZPR	2018	N, R
		Hoa Ruatao	ZPR	2018	N, R
		Hoa Ohutu	ZPR	2018	N, R
		Tiatiaia	ZPR	2018	N, R
		Est du lagon et Motu Manu	ZPR	2018	N, R
	Makatea	-	Rahui		RA crustaceans
Manihi	Manihi	Manihi	ZPR (including the 'zone de reserve' of Tairapa)	2017-2022	N, R
Reao	Reao	Hakahiri	ZPR	2016	G
		Tegagiefanaugatua	ZPR	2016	G
Anaa	Anaa	Gânaa Tâku-Tua Gânaa Tâku-Aro	ZPR	2020-2024	R
Arutua	Arutua	Roren	ZPR	2021-2025	R, P
Direct authority of the French government	Moruroa	-	Military site	1964 (1980)	-
	Fangataufa	-	Military site	1964 (1980)	-
Tuamotu Archipelago: *Commune of Fakarava Biosphere Reserve* (since 1977) with a central area, buffer area, and transition zone					
Fakarava	Taiaro	W. A. Robinson	I & MPA	1972, 2007	*Almost* P
		-	VI	2016	R
	Raraka	-	HP, IV	2007, 2016	R, T

		-	rahui	2007	RA crustaceans 1 year
		-	VI	2016	R
	Fakarava	Fakarava	NP & IV or VI	2007	P, R
			rahui	2007	RA fish 2 years
			rahui		RA crustaceans 2 years
			NT & V	2007	R
	Niau	Niau	Rahui	2007	RA fish 6 months
			Rahui		RA crustaceans and mollusks 6 months
			I	2016	P
			VI	2016	R
	Aratika	Aratika	NP, IV	2007, 2016	P
			VI	2016	R
	Kauehi	Tupaka	HP, IV	2007, 2016	P, T
		Tupanui	HP, IV	2007, 2016	P, T
		Vairatea	HP, IV	2007, 2016	P, T
		Mahuehue	HP, IV	2007, 2016	P, T
		-	NT	2007	-
		-	VI	2016	R
	Toau	Otokau	NP, IV	2007, 2016	R
		Puanea	NP, IV	2007, 2016	R
		-	NT	2007	-
		-	NT, VI	2007, 2016	R
		-	IV	2016	R
		-	VI	2016	R
Marquesas Archipelago					
Ua Huka	Ua Huka	Tokatai	ZPR	2020-2023	P
		Teuaua	ZPR	2020-2023	P
Nuku Hiva	Eiao	Eiao	IV	1971, 1992	P
	Hatutu	Hatutu	IV	1971, 1992	P
	Motu One	Motu One	IV	1971, 1992	P
Hiva-Oa	Motane = Moho Tani	Motane = Moho Tani	IV	1971, 1992	P
Ua Pou	Ua Pou	-	Rahui	In progress	RA
Austral Archipelago					
Rapa	Rapa	-	rahui	-	RA
Tubuai	Tubuai	Taahueia	ZPR	In progress	RA?
Tubuai	Tubuai	Mahu	ZPR	In progress	RA?
Tubuai	Tubuai	Mataura	ZPR	In progress	RA?
Raivavae	Raivavae	?	ZPR	In Progress	?
All archipelagos					
-	-	Tainui Atea	VI	2018	-

Appendix to Chapter 2

Table SP2 - 1 Sampling sites used in the thesis.

Island	Site	Depth (m)	Month	Year	Replicates	Mission	Type	Chapter
Bora-Bora		20, 60, and 120	09	2018	1 replicate of 72 h	UTP3	Acoustic	4 and 5
		100-400	07-08	2022	N/A	ULIEGE-22	Fishing	8
Mangareva		20 and 60	04	2019	1 replicate of 72 h	UTP3	Acoustic	4 and 5
Moorea	Open ocean	5	05	2016	78 stations between 50 m and 10 km from the reef crest	CHORUS-16	Acoustic	3
	Ta'ahiamanu	0-28	07-08	2022	N/A	ULIEGE-22	Fishing	8
	E2B	10		2015	1 replicate of 24 h	CRIOBE-15	Acoustic	9
		10	01-02	2021	2 replicates of 7 days	ULIEGE-20/21	Acoustic	9
		20, 60, and 120	09	2018	1 replicate of 72 h	UTP3	Acoustic	4 and 5
		12	05	2016	1 replicate of 5 days	CHORUS-16	Acoustic	3
		300	07	2021	1 replicate of 10 days	ULIEGE-22	Acoustic	10
	Tetaiuo	10		2015	1 replicate of 24 h	CRIOBE-15	Acoustic	9
		10	01	2021	2 replicates of 7 days	ULIEGE-20/21	Acoustic	9
	Gendron	10		2015	1 replicate of 24 h	CRIOBE-15	Acoustic	9
		10	01	2021	2 replicates of 7 days	ULIEGE-20/21	Acoustic	9
	Tiahura	10		2015	1 replicate of 24 h	CRIOBE-15	Acoustic	9
		10	01	2021	2 replicates of 7 days	ULIEGE-20/21	Acoustic	9
	Papetoai	10		2015	1 replicate of 24 h	CRIOBE-15	Acoustic	9
		10	01	2021	2 replicates of 7 days	ULIEGE-20/21	Acoustic	9
	Pihaena	10		2015	1 replicate of 24 h	CRIOBE-15	Acoustic	9
		10	01-02	2021	2 replicates of 7 days	ULIEGE-20/21	Acoustic	9
	Aroa	10	01-02	2021	2 replicates of 7 days	ULIEGE-20/21	Acoustic	10
	Nuarei	10		2015	1 replicate of 24 h	CRIOBE-15	Acoustic	9
		10	01-02	2021	2 replicates of 7 days	ULIEGE-20/21	Acoustic	9
	Temae	0-4	12-01	2020-21	5 replicates of 90 min	ULIEGE-20/21	Acoustic	7
		10		2015	1 replicate of 24 h	CRIOBE-15	Acoustic	9
		10	01-02	2021	2 replicates of 7 days	ULIEGE-20/21	Acoustic	9
Rangiroa		20, 60, and 120	10-11	2018	1 replicate of 72 h	UTP3	Acoustic	4, 5, and 6
Raroia		20, 60, and 120	03	2018	1 replicate of 72 h	UTP3	Acoustic	4, 5, 6, and 7
Tikehau		20, 60, and 120	10	2018	1 replicate of 72 h	UTP3	Acoustic	4, 5, and 6

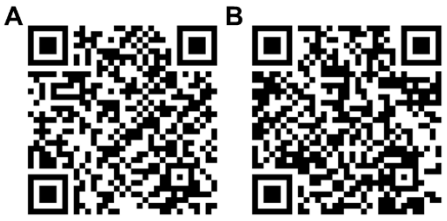

Figure SP2 - 1 Supplementary information on (A) FFT, overlap, frequency resolution, and type of window; (B) Sample rate, number of bits, subsampling, and aliasing.

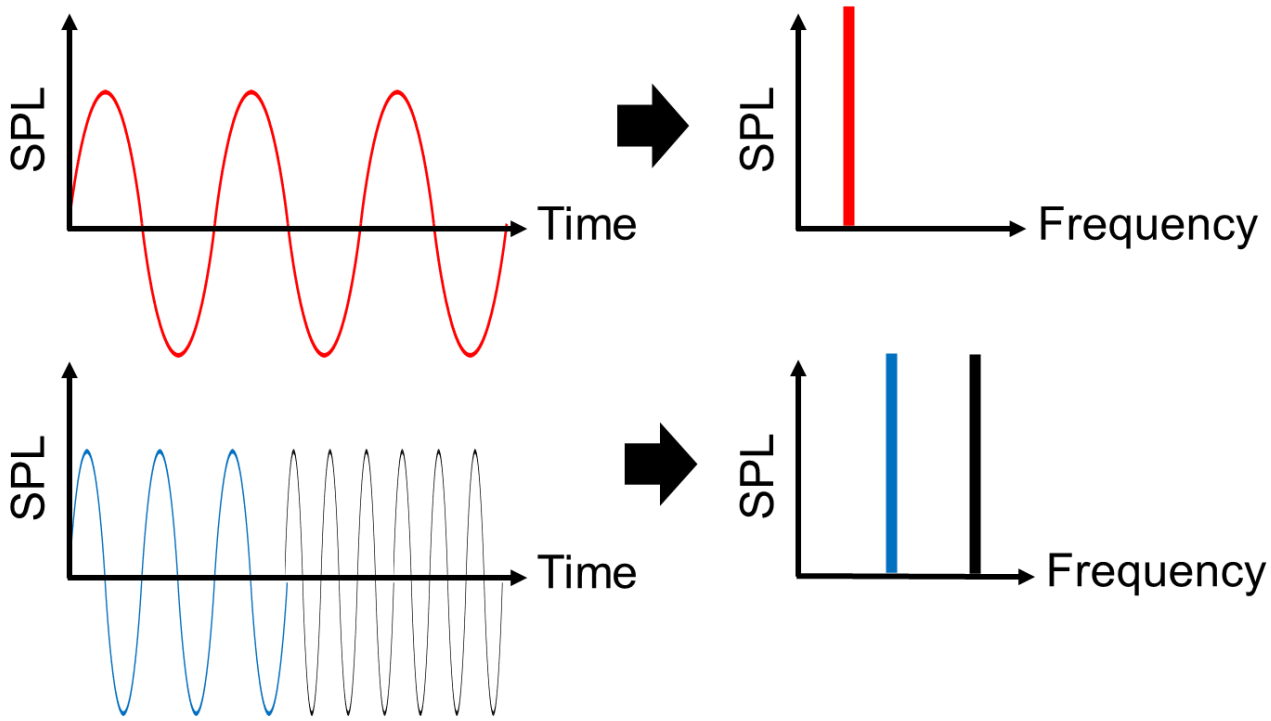

Figure SP2 - 2 Passage from the temporal domain (oscillogram) to the frequency domain (power spectrum) for two distinct signals: a single-frequency signal (in red) and a dual-frequency signal (in blue and black).

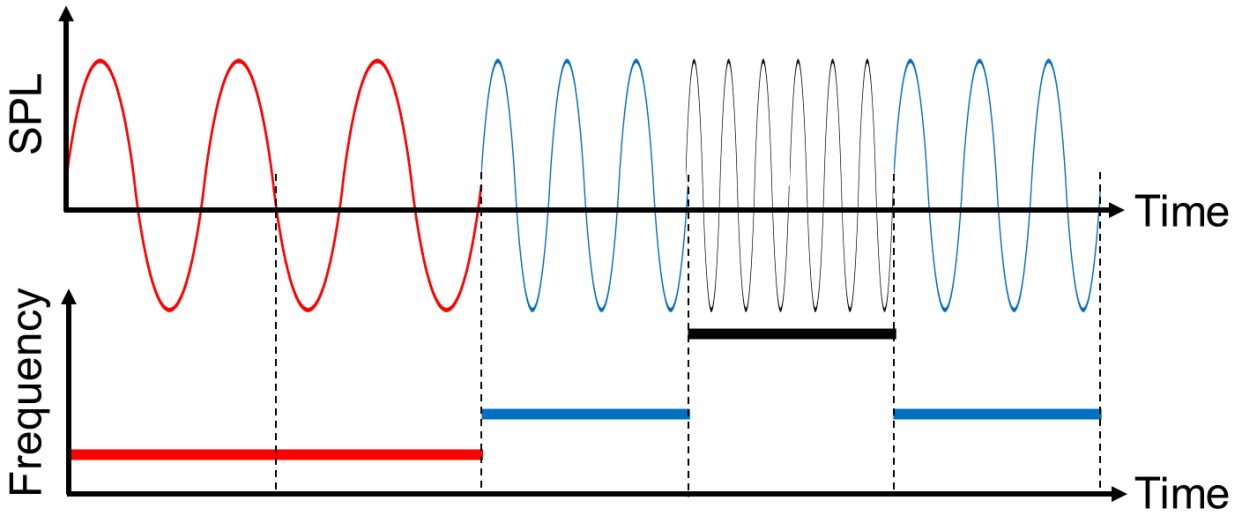

Figure SP2 - 3 Construction of a spectrogram by applying an FFT to small segments of an oscillogram.

Appendix to Chapter 3

The following are available online at https://www.mdpi.com/article/10.3390/jmse9040420/s1.

Table SP3 - 1 Propagation distance of the '570–2000 Hz band' for different levels of Wenz background noise for wind speeds between 0 and 18 kn and different ship traffic index.

Table SP3 - 2 Regressions of the sound of the barrier reef for audiogram frequencies from the literature.

Table SP3 - 3 Maximal distances of detection for each considered species.

Appendix to Chapter 4

Table SP4 - 1 Comparison of the Power Spectral Density associated to the peak frequency (PSD_{Fpeak}) at different depths. Significative *P*-values are in bold. α = 0.05

Island	Test	Dunn *Post-hoc*		
		Comparison	**Z**	**Adjusted *P***
Bora Bora	Kruskal-Wallis	20 and 120 m	−5	**< 0.0001**
	χ^2 = 25, df = 2, *P* < 0.0001	60 and 120 m	−2	0.055
		20 and 60 m	3	**0.003**
Mangareva	Mann-Whitney U, W = 102, *P* = 0.007	20 and 60 m		
Moorea	Kruskal-Wallis	20 and 120 m	−5	**< 0.0001**
	χ^2 = 119, df = 2, *P* < 0.0001	60 and 120 m	−3	**0.003**
		20 and 60 m	2	0.06
Rangiroa	Kruskal-Wallis	20 and 120 m	−3	**0.005**
	χ^2 = 10, df = 2, *P* = 0.006	60 and 120 m	−1	0.2
		20 and 60 m	2	0.09
Raroia	Kruskal-Wallis	20 and 120 m	−5	**< 0.0001**
	χ^2 = 23, df = 2, *P* < 0.0001	60 and 120 m	−1	0.2
		20 and 60 m	3	**0.001**
Tikehau	Kruskal-Wallis	20 and 120 m	−5	**< 0.0001**
	χ^2 = 25, df = 2, *P* < 0.0001	60 and 120 m	−2	**0.04**
		20 and 60 m	3	**0.005**

Table SP4 - 2 Comparison of BTS SPL at different depths. Significative *P*-values are in bold. α = 0.05

Island	Test	Dunn *Post-hoc*		
		Comparison	**Z**	**Adjusted *P***
Bora Bora	Kruskal-Wallis	20 and 120 m	20	**< 0.0001**
	χ^2 = 421, df = 2, *P* < 0.0001	60 and 120 m	−9	**< 0.0001**
		20 and 60 m	12	**< 0.0001**
Mangareva	Mann-Whitney U, W =32400 , *P* < 0.0001	20 and 60 m		
Moorea	Kruskal-Wallis	20 and 120 m	−21	**< 0.0001**
	χ^2 = 442, df = 2, *P* < 0.0001	60 and 120 m	−10	**< 0.0001**
		20 and 60 m	11	**< 0.0001**
Rangiroa	Kruskal-Wallis	20 and 120 m	−21	**< 0.0001**
	χ^2 = 458, df = 2, *P* < 0.0001	60 and 120 m	−10	**< 0.0001**
		20 and 60 m	11	**< 0.0001**
Raroia	Kruskal-Wallis	20 and 120 m	−22	**< 0.0001**
	χ^2 = 473, df = 2, *P* < 0.0001	60 and 120 m	−11	**< 0.0001**
		20 and 60 m	11	**< 0.0001**
Tikehau	Kruskal-Wallis	20 and 120 m	−19	**< 0.0001**
	χ^2 = 381, df = 2, *P* < 0.0001	60 and 120 m	−8	**< 0.0001**
		20 and 60 m	11	**< 0.0001**

Table SP4 - 3 Biplot information and scores of the redundancy analysis testing for a link between cover features and acoustic features.

	RDA1	RDA2
Eigenvalue	4.02	1.10
Proportion explained	0.67	0.18
Cumulative proportion	0.67	0.85
Cover features	**RDA1**	**RDA2**
Macroalgae including *Halimeda* algae	−0.64	0.0069
Non encrusting sponges	0.70	−0.13
Encrusting algae	−0.26	0.27
Fleshy algae	−0.24	−0.051
Rubble	−0.39	−0.18
Hydroids	0.67	−0.033
Turf	0.059	0.17
Dead coral	−0.50	0.018
Anthoathecatae	−0.075	−0.14
Sand	0.67	−0.13
Black coral and gorgonians	0.58	−0.20
Consolidate substrate	−0.32	−0.085
Sessile invertebrates	0.62	0.018
Encrusting sponges	−0.19	0.40
Scleractinian	−0.55	0.17
Calcifying algae	−0.075	0.22
Acoustic features	**RDA1**	**RDA2**
PSD	−1.17	−0.40
Fpeak	−0.70	0.85
Delta20	−1.23	−0.11
BTS Fpeak	1.08	0.34
NoBTS	−0.72	0.86
BTS SPL	−1.22	−0.20
Sites	**RDA1**	**RDA2**
Bora Bora 20 m	−0.98	−1.03
Bora Bora 60 m	0.38	0.33
Bora Bora 120 m	1.08	−0.65
Mangareva 20 m	−0.69	−0.085
Mangareva 60 m	−0.42	−0.042
Moorea 20 m	−0.74	0.20
Moorea 60 m	−0.076	−1.15
Moorea 120 m	1.83	0.077
Rangiroa 20 m	−0.63	−0.28
Rangiroa 60 m	−0.11	−0.033
Rangiroa 120 m	0.32	−0.99
Raroia 20 m	−0.68	−0.24
Raroia 60 m	−0.077	1.76
Raroia 120 m	0.62	0.76
Tikehau 20 m	−0.78	0.61
Tikehau 60 m	−0.027	1.21

Tikehau 120 m	1.00	−0.44

Table SP4 - 4 Temporal comparison of the Power Spectral Density associated to the peak frequency (PSD_{Fpeak}) at 120 m. Significative *P*−values are in bold. α = 0.05

Island	Test	Dunn *Post−hoc*		
		Comparison	**Z**	**Adjusted *P***
Bora Bora	Kruskal−Wallis	Day and night	−1.75	0.16
	χ^2 = 6.29, df = 3, *P* = 0.098	Day and sunrise	0.30	0.91
		Night and sunrise	2.29	0.13
		Day and sunset	−0.083	0.93
		Night and sunset	1.86	0.19
		Sunrise and sunset	−0.43	0.997
Moorea	Kruskal−Wallis	Day and night	2.60	0.056
	χ^2 = 7.26, df = 3, *P* = 0.064	Day and sunrise	1.27	0.30
		Night and sunrise	−1.48	0.28
		Day and sunset	1.00	0.38
		Night and sunset	−1.79	0.22
		Sunrise and sunset	−0.31	0.76
Rangiroa	Kruskal−Wallis	Day and night	−0.91	0.43
	χ^2 = 9.33, df = 3, *P* = 0.025	Day and sunrise	0.69	0.49
		Night and sunrise	1.80	0.14
		Day and sunset	−1.91	0.17
		Night and sunset	−1.12	0.40
		Sunrise and sunset	−2.91	**0.022**
Raroia	Kruskal−Wallis	Day and night	−2.81	**0.029**
	χ^2 = 9.45, df = 3, *P* = 0.024	Day and sunrise	−0.83	0.41
		Night and sunrise	2.22	0.079
		Day and sunset	−1.82	0.14
		Night and sunset	1.11	0.32
		Sunrise and sunset	−1.11	0.40
Tikehau	Kruskal−Wallis	Day and night	−2.48	0.078
	χ^2 = 7.06, df = 3, *P* = 0.070	Day and sunrise	−0.77	0.53
		Night and sunrise	1.91	0.17
		Day and sunset	−0.99	0.48
		Night and sunset	1.67	0.19
		Sunrise and sunset	−0.25	0.80

Table SP4 - 5 Temporal comparison of the Δ20 at 120 m. Significative *P*−values are in bold. α = 0.05.

Island	Test	Dunn *Post−hoc*		
		Comparison	**Z**	**Adjusted *P***
Bora Bora	Kruskal−Wallis χ^2 = 5.91, df = 3, *P* = 0.1162			
Moorea	Kruskal−Wallis χ^2 = 8.60, df = 3, *P* = 0.035	Day and night	2.81	**0.030**
		Day and sunrise	1.60	0.22
		Night and sunrise	−1.35	0.26
		Day and sunset	1.05	0.35
		Night and sunset	−1.97	0.15
		Sunrise and sunset	−0.62	0.54
Rangiroa	Kruskal−Wallis χ^2 = 9.50, df = 3, *P* = 0.023	Day and night	−0.83	0.41
		Day and sunrise	0.83	0.49
		Night and sunrise	1.85	0.19
		Day and sunset	−1.82	0.14
		Night and sunset	−1.11	0.40
		Sunrise and sunset	−2.96	**0.018**
Raroia	Kruskal−Wallis χ^2 = 5.50, df = 3, *P* = 0.14			
Tikehau	Kruskal−Wallis χ^2 = 8.60, df = 3, *P* = 0.035	Day and night	2.04	0.12
		Day and sunrise	0.83	0.49
		Night and sunrise	−1.35	0.26
		Day and sunset	2.59	0.058
		Night and sunset	0.62	0.54
		Sunrise and sunset	1.97	0.10

Table SP4 - 6 Temporal comparison of the number of BTS at 20 m. Significative *P*−values are in bold.

Island	Test	Dunn *Post−hoc*		
		Comparison	**Z**	**Adjusted *P***
Bora Bora	Kruskal−Wallis	Day and night	15.39	**< 0.0001**
	χ^2 = 242.84, df = 3, *P* < 0.0001	Day and sunrise	7.85	**< 0.0001**
		Night and sunrise	−1.78	**0.090**
		Day and sunset	6.83	**< 0.0001**
		Night and sunset	−2.84	**0.0067**
		Sunrise and sunset	−0.82	0.41
Mangareva	Kruskal−Wallis	Day and night	14.42	**< 0.0001**
	χ^2 = 208.22, df = 3, *P* < 0.0001	Day and sunrise	6.13	**< 0.0001**
		Night and sunrise	−3.25	**0.0017**
		Day and sunset	6.25	**< 0.0001**
		Night and sunset	−3.13	**0.0021**
		Sunrise and sunset	0.095	0.92
Moorea	Kruskal−Wallis	Day and night	11.96	**< 0.0001**
	χ^2 = 148.75, df = 3, *P* < 0.0001	Day and sunrise	3.29	**0.0012**
		Night and sunrise	−4.81	**< 0.0001**
		Day and sunset	3.77	**0.00024**
		Night and sunset	−4.29	**< 0.0001**
		Sunrise and sunset	0.40	0.69
Rangiroa	Kruskal−Wallis	Day and night	12.47	**< 0.0001**
	χ^2 = 238.34, df = 3, *P* < 0.0001	Day and sunrise	0.13	0.90
		Night and sunrise	−8.00	**< 0.0001**
		Day and sunset	11.24	**< 0.0001**
		Night and sunset	3.61	**0.00037**
		Sunrise and sunset	8.99	**< 0.0001**
Raroia	Kruskal−Wallis	Day and night	13.95	**< 0.0001**
	χ^2 = 208.8, df = 3, *P* < 0.0001	Day and sunrise	2.80	**0.0062**
		Night and sunrise	−6.34	**< 0.0001**
		Day and sunset	6.57	**< 0.0001**
		Night and sunset	−2.54	**0.011**
		Sunrise and sunset	3.02	**0.0038**
Tikehau	Kruskal−Wallis	Day and night	−2.24	**0.030**
	χ^2 = 30.44, df = 3, *P* < 0.0001	Day and sunrise	2.90	**0.0057**
		Night and sunrise	4.53	**< 0.0001**
		Day and sunset	−3.14	**0.0033**
		Night and sunset	−1.82	0.069
		Sunrise and sunset	−4.92	**< 0.0001**

Table SP4 - 7 Temporal comparison of the number of BTS at 60 m. Significative *P*−values are in bold.

Island	Test	Dunn *Post−hoc*		
		Comparison	**Z**	**Adjusted *P***
Bora Bora	Kruskal−Wallis	Day and night	12.48	**< 0.0001**
	χ^2 = 158.28, df = 3, *P* < 0.0001	Day and sunrise	3.85	**0.00014**
		Night and sunrise	−4.37	**< 0.0001**
		Day and sunset	4.13	**< 0.0001**
		Night and sunset	−4.06	**< 0.0001**
		Sunrise and sunset	0.23	0.81
Mangareva	Kruskal−Wallis	Day and night	14.32	**< 0.0001**
	χ^2 = 209.03, df = 3, *P* < 0.0001	Day and sunrise	6.11	**< 0.0001**
		Night and sunrise	−3.35	**0.0012**
		Day and sunset	7.80	**< 0.0001**
		Night and sunset	−1.54	0.15
		Sunrise and sunset	1.40	0.16
Moorea	Kruskal−Wallis	Day and night	11.25	**< 0.0001**
	χ^2 = 130.65, df = 3, *P* < 0.0001	Day and sunrise	3.93	**0.00013**
		Night and sunrise	−4.27	**< 0.0001**
		Day and sunset	6.07	**< 0.0001**
		Night and sunset	−1.79	0.073
		Sunrise and sunset	1.90	0.070
Rangiroa	Kruskal−Wallis	Day and night	6.08	**< 0.0001**
	χ^2 = 95.32, df = 3, *P* < 0.0001	Day and sunrise	−2.64	**0.0083**
		Night and sunrise	−6.82	**< 0.0001**
		Day and sunset	6.71	**< 0.0001**
		Night and sunset	2.99	**0.0033**
		Sunrise and sunset	7.63	**0.0014**
Raroia	Kruskal−Wallis	Day and night	9.07	**< 0.0001**
	χ^2 = 106.47, df = 3, *P* < 0.0001	Day and sunrise	−0.18	0.85
		Night and sunrise	−6.64	**< 0.0001**
		Day and sunset	2.21	**0.040**
		Night and sunset	−4.11	**< 0.0001**
		Sunrise and sunset	2.01	0.054
Tikehau	Kruskal−Wallis	Day and night	−13.57	**< 0.0001**
	χ^2 = 210.32, df = 3, *P* < 0.0001	Day and sunrise	−3.38	**0.00086**
		Night and sunrise	5.73	**< 0.0001**
		Day and sunset	−9.28	**< 0.0001**
		Night and sunset	−0.35	0.73
		Sunrise and sunset	−4.80	**< 0.0001**

Table SP4 - 8 Temporal comparison of the number of BTS at 120 m. Significative *P*−values are in bold. α = 0.05

Island	Test	Dunn *Post−hoc*		
		Comparison	**Z**	**Adjusted *P***
Bora Bora	Kruskal−Wallis χ^2 = 2.21, df = 3, *P* = 0.53			
Moorea	Kruskal−Wallis χ^2 = 126.41, df = 3, *P* < 0.0001	Day and night	−11.19	**< 0.0001**
		Day and sunrise	−3.81	**0.00028**
		Night and sunrise	2.70	**0.010**
		Day and sunset	−5.64	**< 0.0001**
		Night and sunset	1.78	**0.090**
		Sunrise and sunset	−0.96	0.33
Rangiroa	Kruskal−Wallis χ^2 = 206.89, df = 3, *P* < 0.0001	Day and night	10.30	**< 0.0001**
		Day and sunrise	−1.33	0.18
		Night and sunrise	−8.86	**< 0.0001**
		Day and sunset	10.50	**< 0.0001**
		Night and sunset	4.25	**< 0.0001**
		Sunrise and sunset	10.03	**< 0.0001**
Raroia	Kruskal−Wallis χ^2 = 11.83, df = 3, *P* = 0.0080	Day and night	−2.93	**0.020**
		Day and sunrise	−2.65	**0.024**
		Night and sunrise	−0.80	0.50
		Day and sunset	−0.57	0.57
		Night and sunset	1.36	0.26
		Sunrise and sunset	1.68	0.18
Tikehau	Kruskal−Wallis χ^2 = 191.38, df = 3, *P* < 0.0001	Day and night	−12.85	**< 0.0001**
		Day and sunrise	−1.71	0.10
		Night and sunrise	7.37	**< 0.0001**
		Day and sunset	−7.92	**< 0.0001**
		Night and sunset	1.01	0.31
		Sunrise and sunset	−5.12	**< 0.0001**

Table SP4 - 9 Temporal comparison of the BTS SPL at 20 m. Significative *P*−values are in bold. α = 0.05

Island	Test	Dunn *Post−hoc*		
		Comparison	**Z**	**Adjusted *P***
Bora Bora	Kruskal−Wallis	Day and night	−15.29	**< 0.0001**
	χ^2 = 243.59, df = 3, *P* < 0.0001	Day and sunrise	−7.59	**< 0.0001**
		Night and sunrise	1.98	0.071
		Day and sunset	−8.14	**< 0.0001**
		Night and sunset	1.41	0.19
		Sunrise and sunset	−0.45	0.66
Mangareva	Kruskal−Wallis	Day and night	−14.38	**< 0.0001**
	χ^2 = 217.91, df = 3, *P* < 0.0001	Day and sunrise	−7.63	**< 0.0001**
		Night and sunrise	1.64	0.15
		Day and sunset	−8.47	**< 0.0001**
		Night and sunset	0.75	0.55
		Sunrise and sunset	−0.69	0.49
Moorea	Kruskal−Wallis	Day and night	−14.48	**< 0.0001**
	χ^2 = 213.99, df = 3, *P* < 0.0001	Day and sunrise	−6.31	**< 0.0001**
		Night and sunrise	3.33	**0.0013**
		Day and sunset	−8.02	**< 0.0001**
		Night and sunset	1.48	0.17
		Sunrise and sunset	−1.43	0.15
Rangiroa	Kruskal−Wallis	Day and night	−13.82	**< 0.0001**
	χ^2 = 281.61, df = 3, *P* < 0.0001	Day and sunrise	−1.42	0.16
		Night and sunrise	7.53	**< 0.0001**
		Day and sunset	−12.72	**< 0.0001**
		Night and sunset	−4.28	**< 0.0001**
		Sunrise and sunset	−9.14	**< 0.0001**
Raroia	Kruskal−Wallis	Day and night	−15.08	**< 0.0001**
	χ^2 = 241.44, df = 3, *P* < 0.0001	Day and sunrise	−3.40	**0.00080**
		Night and sunrise	6.44	**< 0.0001**
		Day and sunset	−8.06	**< 0.0001**
		Night and sunset	1.72	0.085
		Sunrise and sunset	−3.72	**0.00030**
Tikehau	Kruskal−Wallis	Day and night	−15.75	**< 0.0001**
	χ^2 = 254.49, df = 3, *P* < 0.0001	Day and sunrise	−4.63	**< 0.0001**
		Night and sunrise	5.57	**< 0.0001**
		Day and sunset	−7.75	**< 0.0001**
		Night and sunset	2.29	**0.022**
		Sunrise and sunset	−2.54	**0.013**

Table SP4 - 10 Temporal comparison of the BTS SPL at 60 m. Significative *P*−values are in bold. α = 0.05.

Island	Test	Dunn *Post−hoc*		
		Comparison	**Z**	**Adjusted *P***
Bora Bora	Kruskal−Wallis	Day and night	−14.29	**< 0.0001**
	χ^2 = 209.95, df = 3, *P* < 0.0001	Day and sunrise	−6.70	**< 0.0001**
		Night and sunrise	2.57	**0.015**
		Day and sunset	−7.90	**< 0.0001**
		Night and sunset	1.30	0.23
		Sunrise and sunset	−0.98	0.32
Mangareva	Kruskal−Wallis	Day and night	−14.07	**< 0.0001**
	χ^2 = 209.93, df = 3, *P* < 0.0001	Day and sunrise	−7.47	**< 0.0001**
		Night and sunrise	1.72	0.13
		Day and sunset	−8.78	**< 0.0001**
		Night and sunset	0.32	0.75
		Sunrise and sunset	−1.09	0.33
Moorea	Kruskal−Wallis	Day and night	−13.06	**< 0.0001**
	χ^2 = 176.9, df = 3, *P* < 0.0001	Day and sunrise	−5.60	**< 0.0001**
		Night and sunrise	3.80	**0.00022**
		Day and sunset	−8.25	**< 0.0001**
		Night and sunset	0.74	0.46
		Sunrise and sunset	−2.35	**0.025**
Rangiroa	Kruskal−Wallis	Day and night	−13.43	**< 0.0001**
	χ^2 = 269.51, df = 3, *P* < 0.0001	Day and sunrise	−1.12	0.26
		Night and sunrise	7.78	**< 0.0001**
		Day and sunset	−12.39	**< 0.0001**
		Night and sunset	−4.05	**< 0.0001**
		Sunrise and sunset	−9.19	**< 0.0001**
Raroia	Kruskal−Wallis	Day and night	−14.29	**< 0.0001**
	χ^2 = 218.13, df = 3, *P* < 0.0001	Day and sunrise	−3.29	**0.0012**
		Night and sunrise	6.58	**< 0.0001**
		Day and sunset	−7.41	**< 0.0001**
		Night and sunset	2.22	**0.027**
		Sunrise and sunset	−3.43	**0.00096**
Tikehau	Kruskal−Wallis	Day and night	−15.19	**< 0.0001**
	χ^2 = 237.87, df = 3, *P* < 0.0001	Day and sunrise	−4.57	**< 0.0001**
		Night and sunrise	5.61	**< 0.0001**
		Day and sunset	−7.76	**< 0.0001**
		Night and sunset	2.31	**0.021**
		Sunrise and sunset	−2.60	**0.011**

Table SP4 - 11 Temporal comparison of the BTS SPL at 120 m. Significative *P*−values are in bold. α = 0.05.

Island	Test	Dunn *Post−hoc*		
		Comparison	**Z**	**Adjusted *P***
Bora Bora	Kruskal−Wallis	Day and night	−11.17	**< 0.0001**
	χ^2 = 124.89, df = 3, *P* < 0.0001	Day and sunrise	−3.96	**0.00015**
		Night and sunrise	3.14	**0.0026**
		Day and sunset	−4.45	**< 0.0001**
		Night and sunset	2.71	**0.0080**
		Sunrise and sunset	−0.36	0.72
Moorea	Kruskal−Wallis	Day and night	0.74	0.55
	χ^2 = 8.52, df = 3, *P* = 0.036	Day and sunrise	−0.37	0.71
		Night and sunrise	−0.84	0.60
		Day and sunset	−2.21	0.081
		Night and sunset	−2.89	**0.023**
		Sunrise and sunset	−1.35	0.36
Rangiroa	Kruskal−Wallis	Day and night	−11.18	**< 0.0001**
	χ^2 = 222.17, df = 3, *P* < 0.0001	Day and sunrise	0.62	0.54
		Night and sunrise	8.72	**< 0.0001**
		Day and sunset	−10.91	**< 0.0001**
		Night and sunset	−4.27	**< 0.0001**
		Sunrise and sunset	−9.85	**< 0.0001**
Raroia	Kruskal−Wallis	Day and night	−14.96	**< 0.0001**
	χ^2 = 238.84, df = 3, *P* < 0.0001	Day and sunrise	−3.65	**0.00032**
		Night and sunrise	6.41	**< 0.0001**
		Day and sunset	−8.19	**< 0.0001**
		Night and sunset	1.35	0.18
		Sunrise and sunset	−3.84	**0.00018**
Tikehau	Kruskal−Wallis	Day and night	−13.86	**< 0.0001**
	χ^2 = 198.42, df = 3, *P* < 0.0001	Day and sunrise	−3.68	**0.00035**
		Night and sunrise	6.10	**< 0.0001**
		Day and sunset	−6.71	**< 0.0001**
		Night and sunset	2.93	**0.0040**
		Sunrise and sunset	−2.53	**0.012**

Table SP4 - 12 Temporal comparison of the F_{peak} at 20 m. Significative *P*−values are in bold. α = 0.05.

Island	Test	Dunn *Post−hoc*		
		Comparison	**Z**	**Adjusted *P***
Bora Bora	Kruskal−Wallis	Day and night	−11.05	**< 0.0001**
	χ^2 = 129.64, df = 3, *P* < 0.0001	Day and sunrise	−1.80	0.087
		Night and sunrise	5.19	**< 0.0001**
		Day and sunset	−2.69	**0.011**
		Night and sunset	4.27	**< 0.0001**
		Sunrise and sunset	−0.71	0.47
Mangareva	Kruskal−Wallis	Day and night	8.51	**< 0.0001**
	χ^2 = 80.05, df = 3, *P* < 0.0001	Day and sunrise	5.49	**< 0.0001**
		Night and sunrise	0.035	0.97
		Day and sunset	5.17	**< 0.0001**
		Night and sunset	−0.31	≈ 1
		Sunrise and sunset	−0.27	0.95
Moorea	Kruskal−Wallis	Day and night		
	χ^2 = 4.49, df = 3, *P* = 0.21			
Rangiroa	Kruskal−Wallis	Day and night	6.81	**< 0.0001**
	χ^2 = 74.84, df = 3, *P* < 0.0001	Day and sunrise	−0.21	0.83
		Night and sunrise	−4.66	**< 0.0001**
		Day and sunset	6.33	**< 0.0001**
		Night and sunset	2.16	**0.036**
		Sunrise and sunset	5.29	**< 0.0001**
Raroia	Kruskal−Wallis	Day and night	11.68	**< 0.0001**
	χ^2 = 146.16, df = 3, *P* < 0.0001	Day and sunrise	2.14	**0.039**
		Night and sunrise	−5.54	**< 0.0001**
		Day and sunset	5.71	**< 0.0001**
		Night and sunset	−1.83	0.067
		Sunrise and sunset	2.90	**0.0056**
Tikehau	Kruskal−Wallis	Day and night	4.21	**0.00015**
	χ^2 = 20.11, df = 3, *P* = 0.00016	Day and sunrise	1.41	0.32
		Night and sunrise	−1.31	0.28
		Day and sunset	3.01	**0.0077**
		Night and sunset	0.37	0.70
		Sunrise and sunset	1.31	0.23

Table SP4 - 13 Temporal comparison of the F_{peak} at 60 m. Significative *P*−values are in bold. α = 0.05.

Island	Test	Dunn *Post−hoc*		
		Comparison	**Z**	**Adjusted *P***
Bora Bora	Kruskal−Wallis	Day and night	3.88	**0.00062**
	χ^2 = 18.46, df = 3, *P* = 0.00035	Day and sunrise	3.18	**0.0044**
		Night and sunrise	0.75	0.68
		Day and sunset	2.10	0.071
		Night and sunset	−0.23	0.81
		Sunrise and sunset	−0.75	0.55
Mangareva	Kruskal−Wallis	Day and night	9.56	**< 0.0001**
	χ^2 = 93.13, df = 3, *P* < 0.0001	Day and sunrise	3.71	**0.00062**
		Night and sunrise	−2.63	**0.010**
		Day and sunset	2.77	**0.0085**
		Night and sunset	−3.56	**0.00073**
		Sunrise and sunset	−0.75	0.45
Moorea	Kruskal−Wallis	Day and night	−7.80	**< 0.0001**
	χ^2 = 64.15, df = 3, *P* < 0.0001	Day and sunrise	−2.22	**0.031**
		Night and sunrise	3.52	**0.0013**
		Day and sunset	−3.10	**0.0038**
		Night and sunset	2.49	**0.019**
		Sunrise and sunset	−0.78	**0.43**
Rangiroa	Kruskal−Wallis			
	χ^2 = 6.16, df = 3, *P* = 0.10			
Raroia	Kruskal−Wallis	Day and night	10.61	**< 0.0001**
	χ^2 = 116.98, df = 3, *P* < 0.0001	Day and sunrise	2.88	**0.0060**
		Night and sunrise	−4.40	**< 0.0001**
		Day and sunset	4.44	**< 0.0001**
		Night and sunset	−2.86	**0.0050**
		Sunrise and sunset	1.26	**0.21**
Tikehau	Kruskal−Wallis	Day and night	6.84	**< 0.0001**
	χ^2 = 52.42, df = 3, *P* < 0.0001	Day and sunrise	0.86	0.47
		Night and sunrise	−3.76	**0.00050**
		Day and sunset	3.71	**0.00041**
		Night and sunset	−0.82	0.41
		Sunrise and sunset	2.32	**0.030**

Table SP4 - 14 Temporal comparison of the F_{peak} at 120 m. Significative *P*−values are in bold. α = 0.05.

Island	Test	Dunn *Post−hoc*		
		Comparison	**Z**	**Adjusted *P***
Bora Bora	Kruskal−Wallis χ^2 = 0.93, df = 3, *P* = 0.82			
Moorea	Kruskal−Wallis χ^2 = 15.72, df = 3, *P* = 0.0013	Day and night	−3.93	**0.00051**
		Day and sunrise	−1.64	0.20
		Night and sunrise	0.65	0.77
		Day and sunset	−2.24	0.075
		Night and sunset	0.43	0.80
		Sunrise and sunset	−0.24	0.81
Rangiroa	Kruskal−Wallis χ^2 = 20.23, df = 3, *P* = 0.00015	Day and night	2.99	**0.0056**
		Day and sunrise	0.090	0.93
		Night and sunrise	−2.05	**0.048**
		Day and sunset	3.85	**0.00071**
		Night and sunset	2.24	**0.038**
		Sunrise and sunset	3.28	**0.0031**
Raroia	Kruskal−Wallis χ^2 = 148.57, df = 3, *P* < 0.0001	Day and night	11.78	**< 0.0001**
		Day and sunrise	2.12	**0.041**
		Night and sunrise	−5.78	**< 0.0001**
		Day and sunset	3.19	**0.0022**
		Night and sunset	−4.26	**< 0.0001**
		Sunrise and sunset	0.97	0.33
Tikehau	Kruskal−Wallis χ^2 = 88.26, df = 3, *P* < 0.0001	Day and night	9.18	**< 0.0001**
		Day and sunrise	2.76	**0.0087**
		Night and sunrise	−3.48	**0.0010**
		Day and sunset	5.14	**< 0.0001**
		Night and sunset	−1.09	0.27
		Sunrise and sunset	1.92	0.066

Table SP4 - 15 Temporal comparison of the number of BTS (NoBTS) around 7 PM at 120 m. Significative *P*−values are in bold. α = 0.05.

Island	Test	Dunn *Post−hoc*		
		Comparison	**Z**	**Adjusted *P***
Bora Bora	Kruskal−Wallis	before vs. after	−1.97	**0.049**
	χ^2 = 60.64, df = 2, *P* < 0.0001	‘7 PM’ vs. after	−7.52	**< 0.0001**
		‘7 PM’ vs. before	−5.50	**< 0.0001**
Moorea	Kruskal−Wallis	before vs. after	3.21	**0.0013**
	χ^2 = 55.06, df = 2, *P* < 0.0001	‘7 PM’ vs. after	−4.44	**< 0.0001**
		‘7 PM’ vs. before	−7.39	**< 0.0001**
Rangiroa	Kruskal−Wallis	before vs. after	3.66	**0.00075**
	χ^2 = 15.27, df = 2, *P* = 0.00048	‘7 PM’ vs. after	3.10	**0.0029**
		‘7 PM’ vs. before	−0.78	0.43
Raroia	Kruskal−Wallis			
	χ^2 = 1.10, df = 2, *P* = 0.58			
Tikehau	Kruskal−Wallis	before vs. after	2.62	**0.0088**
	χ^2 = 53.1, df = 2, *P* < 0.0001	‘7 PM’ vs. after	−4.28	**< 0.0001**
		‘7 PM’ vs. before	−7.27	**< 0.0001**

Table SP4 - 16 Temporal comparison of the BTS F_{peak} around 7 PM at 120 m. Significative *P*−values are in bold. α = 0.05.

Island	Test	Dunn *Post−hoc*		
		Comparison	**Z**	**Adjusted *P***
Bora Bora	Kruskal−Wallis			
	χ^2 = 1.97, df = 2, *P* = 0.37			
Moorea	Kruskal−Wallis	before vs. after	0.19	0.85
	χ^2 = 29.25, df = 2, *P* < 0.0001	‘7 PM’ vs. after	4.78	**< 0.0001**
		‘7 PM’ vs. before	4.48	**< 0.0001**
Rangiroa	Kruskal−Wallis			
	χ^2 = 3.94, df = 2, *P* = 0.14			
Raroia	Kruskal−Wallis	before vs. after	−3.91	**0.00028**
	χ^2 = 18.17, df = 2, *P* = 0.00011	‘7 PM’ vs. after	−0.41	0.68
		‘7 PM’ vs. before	3.52	**0.00066**
Tikehau	Kruskal−Wallis	before vs. after	−1.84	0.066
	χ^2 = 53.72, df = 2, *P* < 0.0001	‘7 PM’ vs. after	4.93	**< 0.0001**
		‘7 PM’ vs. before	7.04	**< 0.0001**

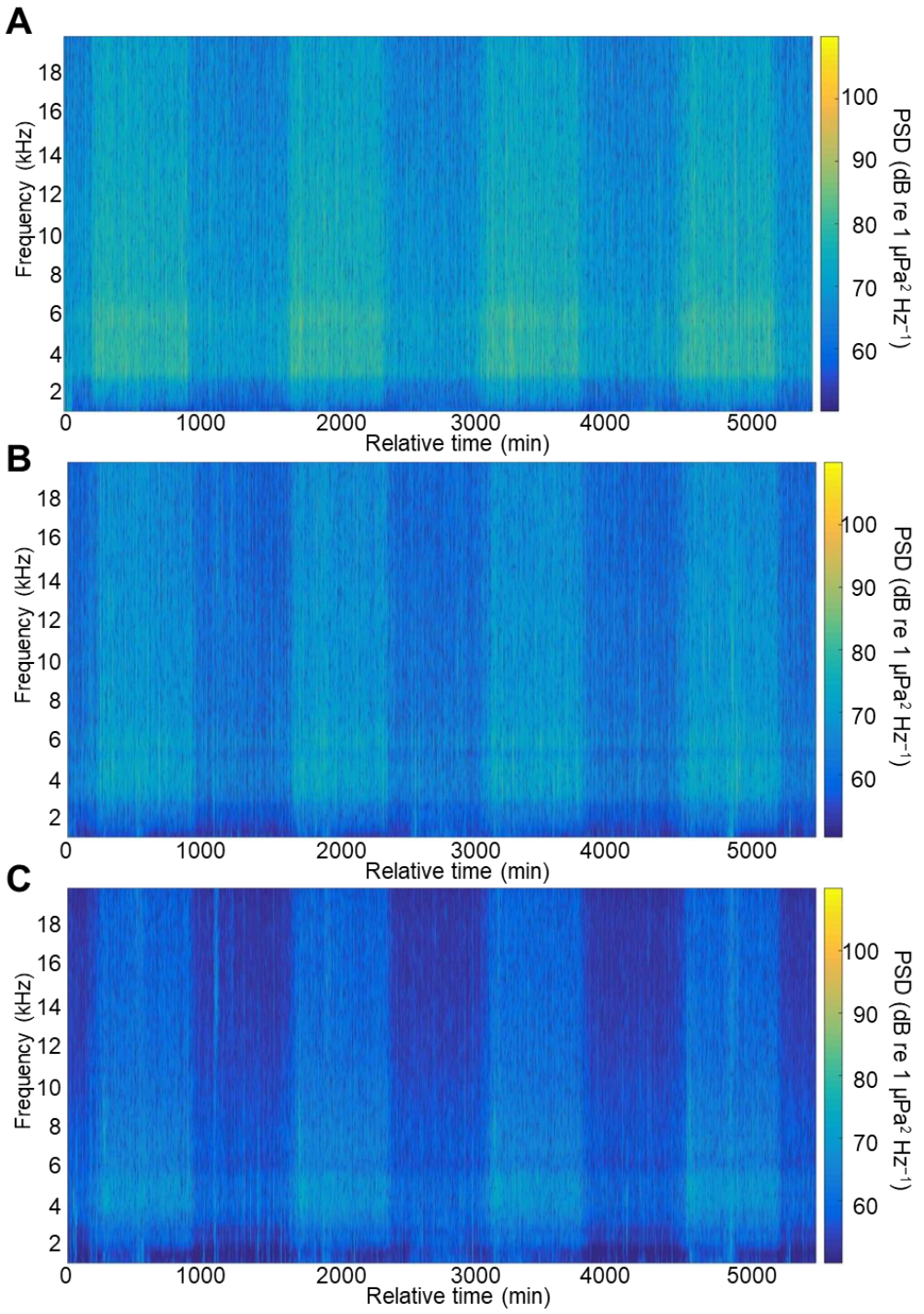

Figure SP4 - 1 Spectrograms of the soundscape between 1 and 20 kHz at Rangiroa at (A) 20 m, (B) 60 m and (C) 120 m. The diel cycle is illustrated as an 'on/off' pattern of changing color intensities.

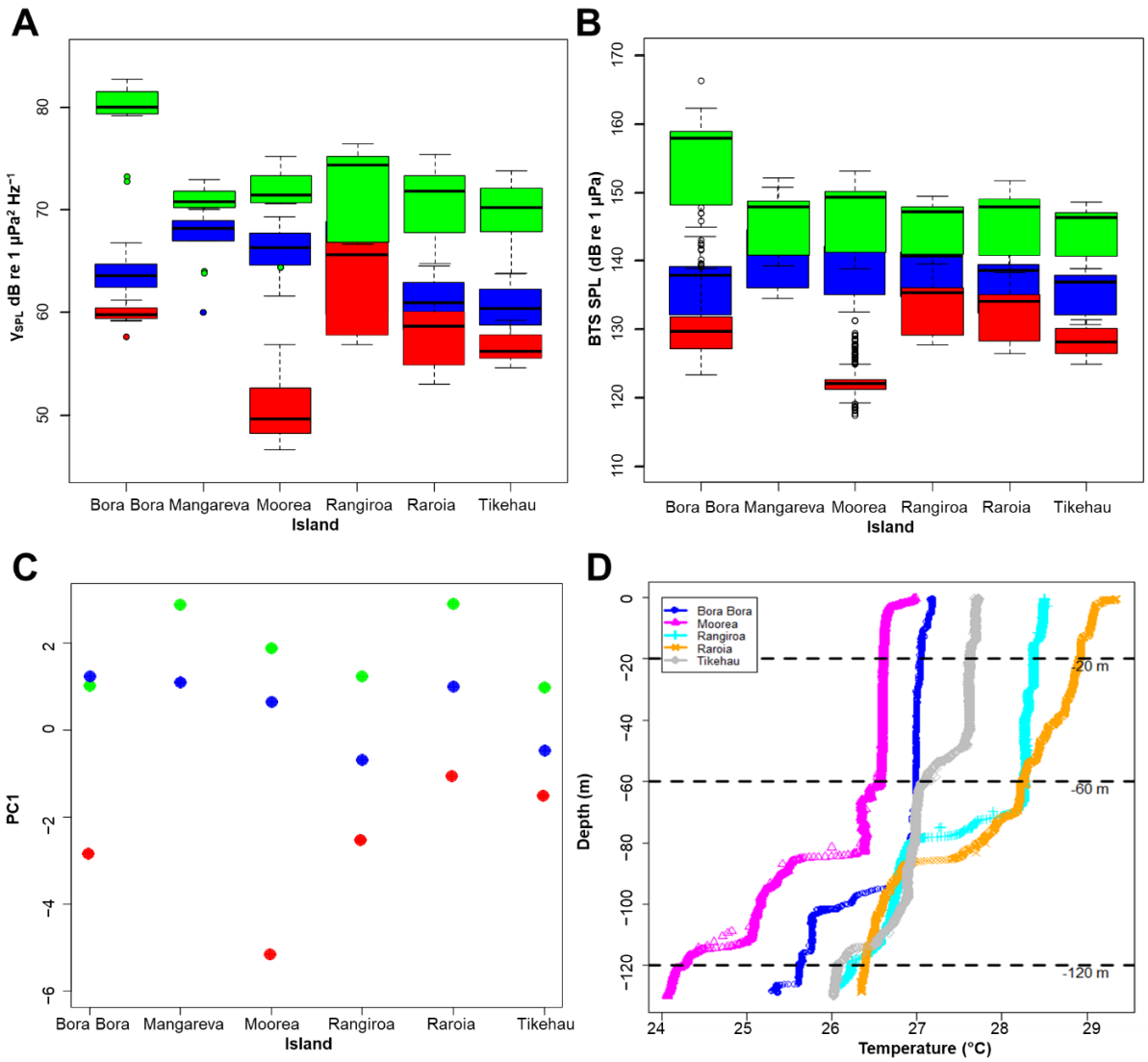

Figure SP4 - 2 (A) Power Spectral Density (PSD) *per* island, (B) BTS SPL *per* island, (C) mean value of PC1 from the Principal Components Analysis (PCA) carried out on environmental features, and (D) temperature profile per island. For **A**, **B**, and **C**: 20 m (green), 60 m (blue) and 120 m (red).

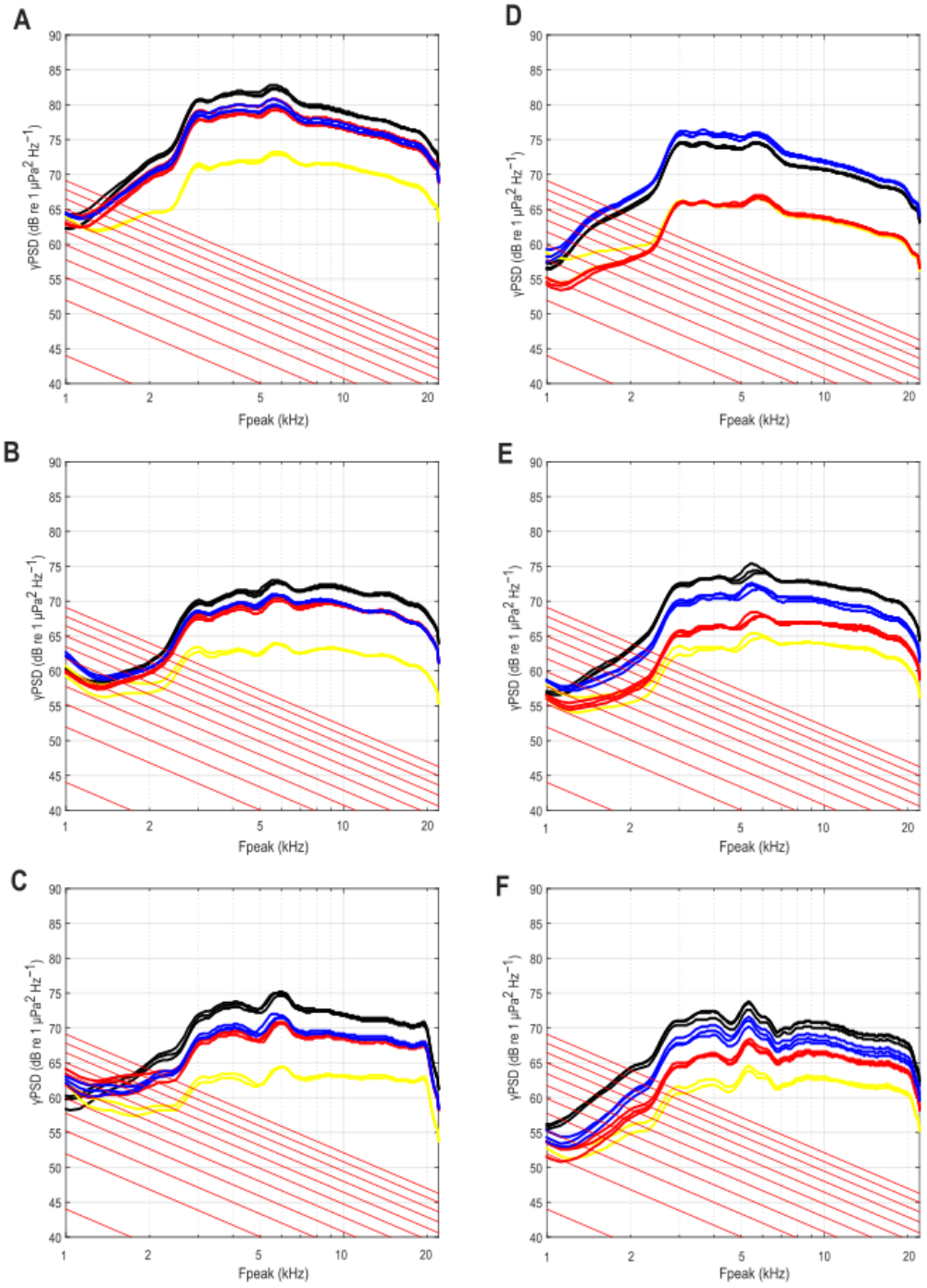

Figure SP4 - 3 Median Power Spectral Density at 20 m per island. (A) Bora Bora, (B) Mangareva, (C) Moorea, (D) Rangiroa, (E) Raroia, and (F) Tikehau. In black: night, in blue: sunset, in red: sunrise and in yellow: day. Each line is a replicate (e.g. first night, second night, and third night). Thin red lines represent Wenz ambient noise (wind levels of 0, 3, 6, 9, 12, 15, 18, 21, 24, 27 and 30 knots from bottom to top).

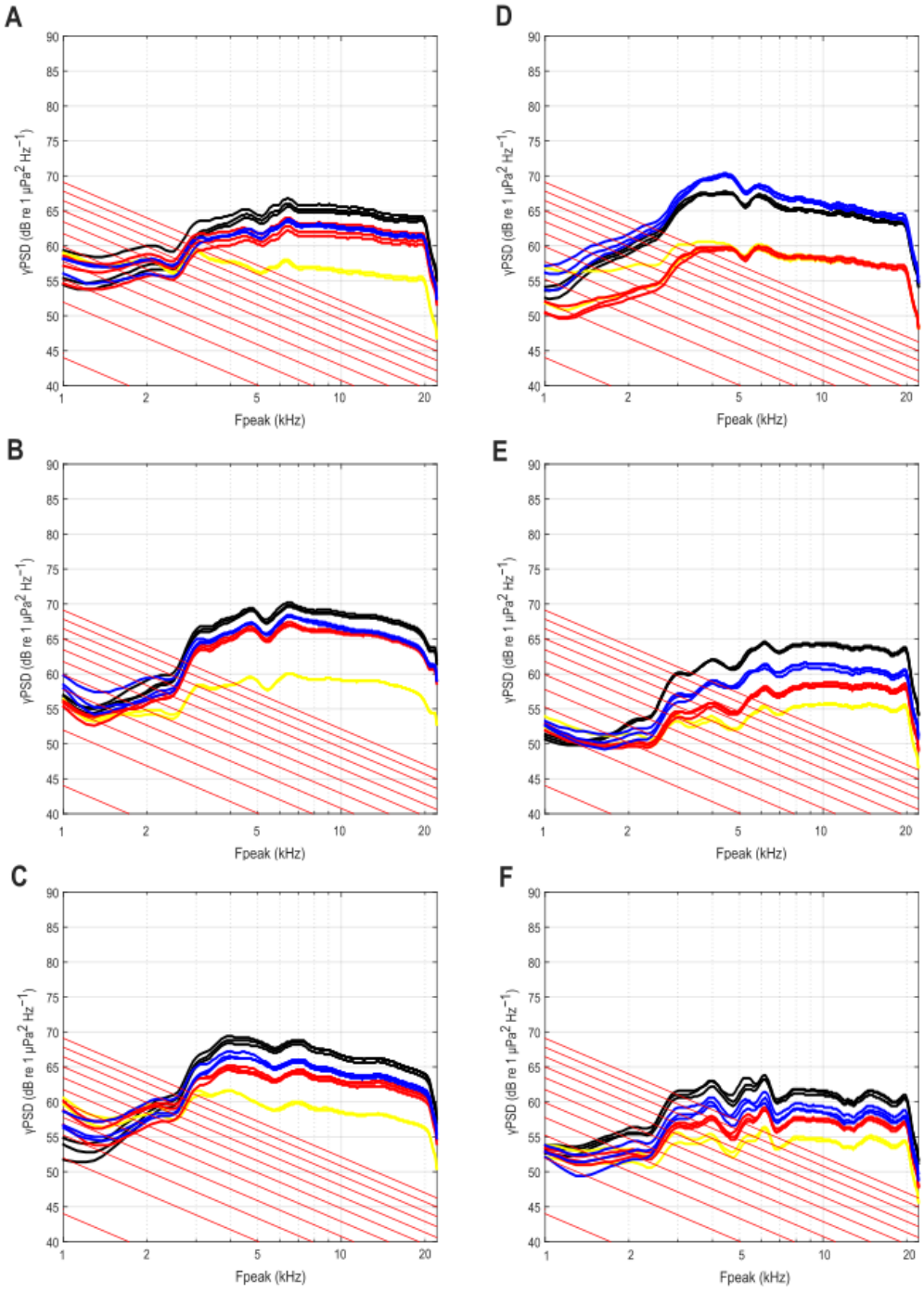

Figure SP4 - 4 Median Power Spectral Density at 60 m per island. (A) Bora Bora, (B) Mangareva, (C) Moorea, (D) Rangiroa, (E) Raroia, and (F) Tikehau. In black: night, in blue: sunset, in red: sunrise and in yellow: day. Each line is a replicate (e.g. first night, second night, and third night). Thin red lines represent Wenz ambient noise (wind levels of 0, 3, 6, 9, 12, 15, 18, 21, 24, 27 and 30 knots from bottom to top).

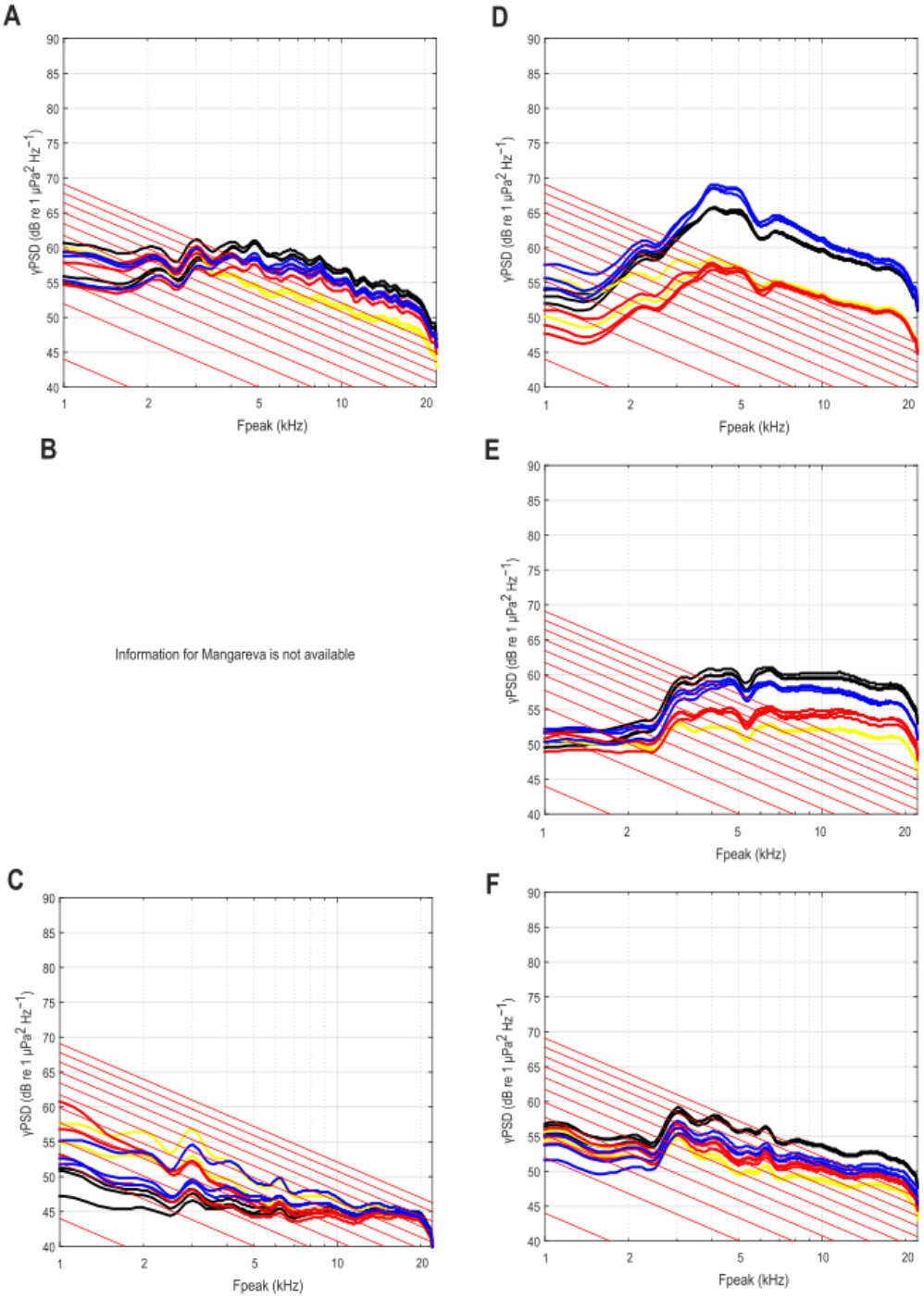

Figure SP4 - 5 Median Power Spectral Density at 120 m per island. (A) Bora Bora, (B) Mangareva: no data, (C) Moorea, (D) Rangiroa, (E) Raroia, and (F) Tikehau. In black: night, in blue: sunset, in red: sunrise and in yellow: day. Each line is a replicate (e.g. first night, second night, and third night). Thin red lines represent Wenz ambient noise (wind levels of 0, 3, 6, 9, 12, 15, 18, 21, 24, 27 and 30 knots from bottom to top).

Appendix to Chapter 5

The following are available online at https://zenodo.org/records/10090721 or at

https://journals.jams.pub/user/manuscripts/displayFile/643fd555cd2d08fa84fb14c0f4418aa5/supplementary.

Figure SP5 - 1 H values for three different abundances (20, 60 and 100 fish sounds min^{-1}) with the loudspeaker silent and with the loudspeaker emitting 1, 2 or 3 different fish sound types.

Table SP5 - 1 Abundance and sound type species richness of each sound stimuli file created.

Table SP5 - 2 Location of sampling sites in the lagoon of Temae (Moorea, French Polynesia).

Table SP5 - 3 Correlation coefficients and associated P-values between the ADI, abundance, and sound type richness in the controlled environment.

Table SP5 - 4 Correlation coefficients and associated P-values between the AEI, abundance, and sound type richness in the controlled environment.

Table SP5 - 5 Correlation coefficients and associated P-values between α-acoustic indices, artificial (= introduced) abundance and artificial sound type species richness with in situ playbacks.

Table SP5 - 6 Correlation coefficients and associated P-values between α-acoustic indices, abundance, and sound type richness with in situ playbacks (delta sounds).

Table SP5 - 7 Correlation coefficients and associated P-values between the ADI, artificial (= introduced) abundance, and artificial sound type richness with in situ playbacks.

Table SP5 - 8 Correlation coefficients and associated P-values between the ADI, abundance, and sound type richness per minute (natural + introduced) with in situ playbacks.

Table SP5 - 9 Correlation coefficients and associated P-values between the ADI, abundance, and sound type richness with in situ playbacks (delta sounds).

Table SP5 - 10 Correlation coefficients and associated P-values between the AEI, artificial (= introduced) abundance, and artificial sound type richness with in situ playbacks.

Table SP5 - 11 Correlation coefficients and associated P-values between the AEI, abundance, and sound type richness per minute (natural + introduced) with in situ playbacks.

Table SP5 - 12 Correlation coefficients and associated P-values between the AEI, abundance, and sound type richness with in situ playbacks (delta sounds).

Table SP5 - 13 Correlation coefficients and associated P-values between the ADI, abundance, and sound type richness in the natural environment.

Table SP5 - 14 Correlation coefficients and associated P-values between the AEI, abundance, and sound type richness in the natural environment.

And five supplementary equations (from Equation SP5 - 1 to Equation SP5 - 5).

Appendix to Chapter 6

The following are available online at

https://static-content.springer.com/esm/art%3A10.1007%2Fs00338-022-02343-7/MediaObjects/338_2022_2343_MOESM1_ESM.pdf

Table SP6 - 1 Location and period of sampling for each island.

Table SP6 - 2 Detail of the Pulse Series *stricto sensu* sounds.

Table SP6 - 3 Detail of the frequency modulated and arched sounds.

Table SP6 - 4 Number of sound types per 1 min per (pseudo-)replicate, i.e., for each sunset period, for each depth and for each island (n = 51).

Table SP6 - 5 Most abundant type of fish sounds for each depth and each island.

Table SP6 - 6 Median and IQR of the acoustic fish α-diversity (Shannon) per depth and per island.

Table SP6 - 7 Acoustic fish Shannon diversity, overlap and results of the variance model per depth and type of island and results of the linear model to test the influence of benthic cover features on Shannon diversity.

Table SP6 - 8 Output of the permutation based-test of multivariate homogeneity of group variances on the β diversity.

Table SP6 - 9 Results of the PerMANOVAstests based on Bray-Curtis dissimilarities for the influence of the depth and type of island on acoustic communities composition.

Table SP6 - 10 Results of the Canonical correspondence analysis testing for a link between acoustic communities and cover features.

Table SP6 - 11 Biplot information and scores for constraining variables of the Canonical correspondence analysis testing for a link between acoustic communities and cover features.

Figure SP6 - 1 Pictures inside a quadrat of 1 m^2 in Moorea (left) and Rangiroa (right).

Figure SP6 - 2 Plot of the temperature according to the depth.

Figure SP6 - 3 Oscillogram (top) and power-spectrum (bottom) of Pulse Series stricto sensu sounds.

Figure SP6 - 4 Oscillogram (top) and power-spectrum (bottom) of frequency modulated and arched sounds.

Figure SP6 - 5 Spectrograms of a fragment of soundscape between 6:50 and 7:00 PM at Raroia Island.

Figure SP6 - 6 Number of the ten most abundant fish sounds at each depth.

Figure SP6 - 7 100% stacked column of the abundance of fish sounds for each depth.

Figure SP6 - 8 Plot of the acoustic fish β-diversity between the islands.

KeySP6 - 1 Sound identification key for the frequencies bellow 2 kHz based on spectrograms.

Appendix to Chapter 7

KeySP7 – 1 Sound identification key for biological sounds below 2 kHz from mesophotic reefs in French Polynesia. Available at https://zenodo.org/records/10592329.

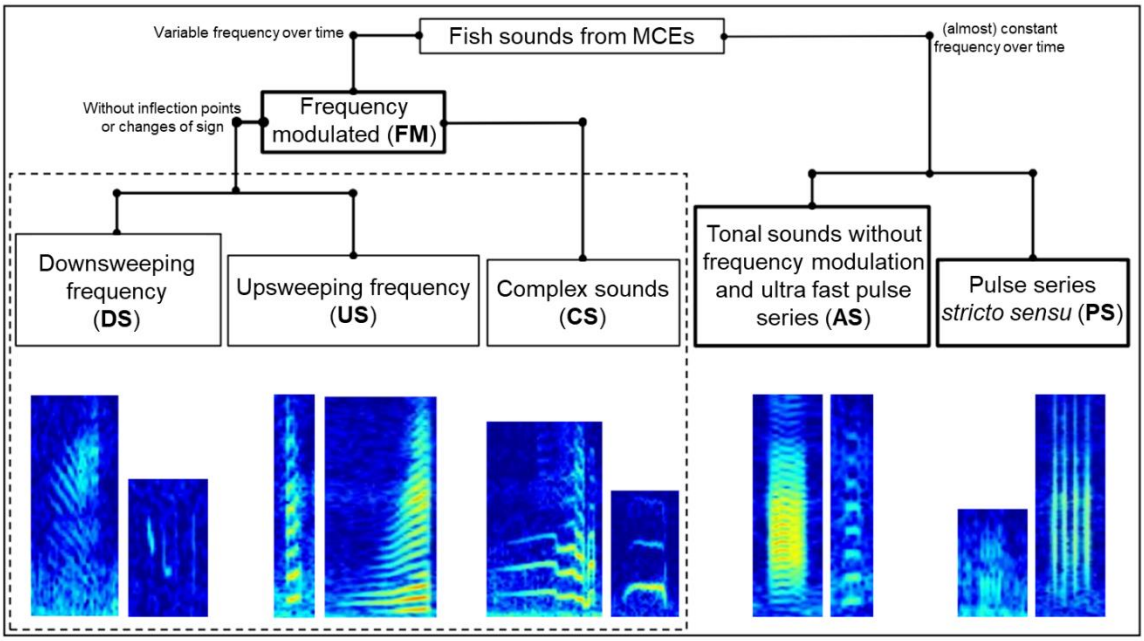

Figure SP7 - 1 Classification of fish sounds from Polynesian MCEs with spectrogram captions (FFT = 256) to illustrate various sound types. AS and PS can be grouped as 'Pulse series *lato sensu*'. Bold boxes represent acoustic categories, while non-bold boxes represent acoustic sub-categories of sound types. Adapted from Chapter 6.

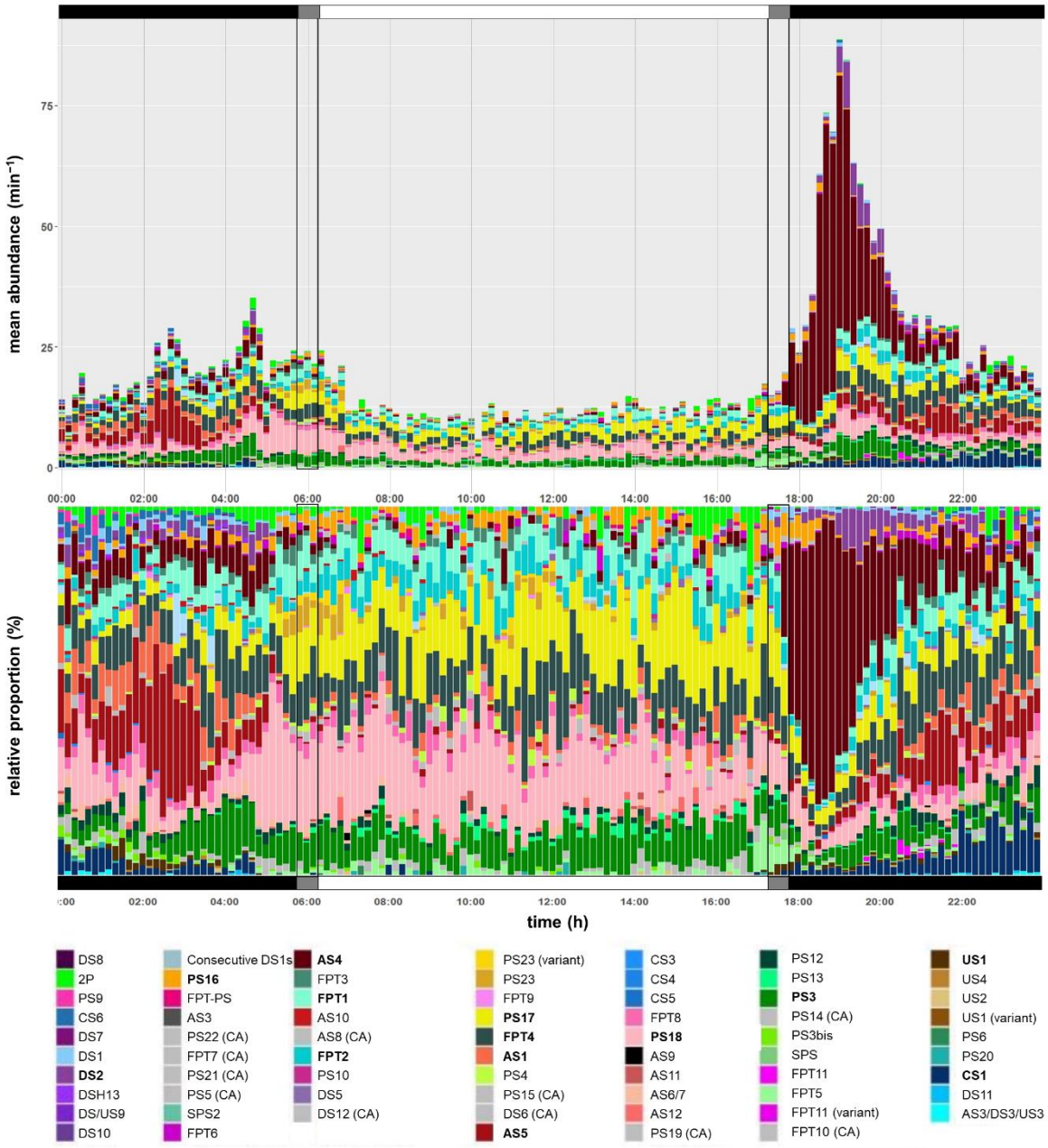

Figure SP7 - 2 Cumulative graph of mean abundance over time for all sound types at 60 m depth: absolute values (A) and relative proportion (B). Less abundant sound types lacking a clear diel cycle are colored in grey for ease of interpretation. The legend includes the annotation 'CA' (Cycle Absent) for such sounds. The 13 most abundant sound types, utilized in the models, are highlighted in bold.

Table SP7 - 1 Summary of GAM model results for the 13 most abundant sound types. '/' = insufficient number of sounds to perform the model.

	GAM Model	Adjusted R^2	Edf		P-value		Dispersion of residuals	N
			60 m	120 m	60 m	120 m		
AS4	NB	0.75	8.70	8.63	< 0.001	< 0.001	0.77	11550
AS5	NB	0.09	6.90	6.63	< 0.001	< 0.001	0.59	4067
AS1	Poisson	0.42	8.42	7.02	< 0.001	0.00069	0.65	1039
PS3	Poisson	0.64	8.10	9.00	< 0.001	< 0.001	1.23	6168
PS17	Poisson	0.47	7.29	8.12	< 0.001	< 0.001	1.085	4446
PS16	Poisson	0.20	7.35	7.32	< 0.001	< 0.001	1.19	1665
PS18	Poisson	0.64	8.98	6.90	< 0.001	< 0.001	1.16	2967
FPT1	Poisson	0.40	7.40	/	< 0.001	/	0.82	1352
FPT2	Poisson	0.30	6.30	8.48	< 0.001	< 0.001	0.83	1599
FPT4	Poisson	0.55	7.80	7.58	< 0.001	< 0.001	1.12	3563

CS1	Poisson	0.40	8.89	8.88	< 0.001	< 0.001	1.05	1883
DS2	Poisson	0.62	8.74	/	< 0.001	/	0.68	1098
US1	Poisson	0.48	/	8.45	/	< 0.001	0.86	1181

Table SP7 - 2 Mean abundance per minute predicted by the GAM models for the 13 most abundant sound types. '-' = no peak abundance detected. '/' = insufficient number of sounds to perform the model.

Sound type	**Depth (m)**	**Time of peak 1**	**Corresponding abundance**	**Time of peak 2**	**Corresponding abundance**
AS4	60	7:10 PM	33.15	-	-
AS4	60	9:10 PM	2.95	02:30 AM	4.14
AS1	60	10:20 PM	0.92	02:40 AM	1.40
PS3	60	7:30 PM	2	04:40 AM	2
PS17	60	7:00 PM	2.13	06:20 AM	1.68
PS16	60	06:30 PM	0.86	05:40 AM	0.54
PS18	60	06:30 PM	3.31	06:00 AM	6.75
FPT1	60	09:10 PM	1.20	05:00 AM	1.02
FPT2	60	08:00 PM	1.55	06:30 AM	0.92
FPT4	60	08:40 PM	4.01	04:30 AM	2.60
CS1	60	11:10 PM	2.35	03:50 AM	0.44
DS2	60	07:30 PM	4.01	04:10 AM	0.70
US1	60	/	/	/	/
AS4	120	07:00 PM	48.8	-	-
AS4	120	11:50 PM	10.92	01:10 AM	3.84
AS1	120	-	-	04:00 AM	0.30
PS3	120	07:20 PM	6.16	04:20 AM	4.81
PS17	120	06:40 PM	2.30	05:10 AM	1.90
PS16	120	11:50 PM	2	02:40 AM	1.76
PS18	120	-	-	04:40 AM	0.80
FPT1	120	/	/	/	/
FPT2	120	03:40 PM	0.75	06:20 AM	1.17
FPT4	120	-	-	06:10 AM	1.14
CS1	120	11:50 PM	2.70	04:20 AM	1.34
DS2	120	/	/	/	/
US1	120	06:30	3.3	4:00 AM	1.78

Table SP7 - 3 Width of the realized acoustic niches for each sound type. NB_{temp}* = standardized niche width for the temporal axis; NB_{freq}* = standardized niche width for the frequency axis; NB_{pp}* = standardized niche width for the pulse period axis; and NB_{tot}* = overall standardized niche width.

	NBtemp*		**NBfreq***		**NBpp***		**NBtot***	
	60 m	**120 m**	**60 m**	**120 m**	**60 m**	**120 m**	**60 m**	**120 m**
AS4	0.14	0.12	0.21	0.16	0.12	0.11	0.17	0.15
AS5	0.30	0.30	0.41	0.29	0.11	0.09	0.26	0.23
AS1	0.58	0.56	0.18	0.14	0.12	0.14	0.30	0.30
PS3	0.64	0.44	0.11	0.13	0.10	0.07	0.30	0.22
PS17	0.72	0.65	0.13	0.15	0.17	0.17	0.37	0.33
PS16	0.63	0.50	0.22	0.40	0.20	0.27	0.36	0.40
PS18	0.67	0.58	0.07	0.11	0.15	0.15	0.33	0.30
FPT1	0.77	0.71	0.12	0.22	0.17	0.12	0.38	0.36
FPT2	0.73	0.54	0.13	0.10	0.19	0.25	0.37	0.33
FPT4	0.60	0.68	0.16	0.18	0.08	0.08	0.29	0.34
DS2	0.13	0.30	0.38	0.35	0.15	0.16	0.22	0.28
US1	0.33	0.37	0.11	0.09	0.10	0.14	0.20	0.23
CS1	0.27	0.34	0.13	0.12	0.13	0.11	0.20	0.22
Community level	0.40	0.32	0.31	0.43	0.41	0.40	0.38	0.40

Appendix to Chapter 8

Note SP8 - 1 Sonic morphology of the other Serranidae species.

Variola louti, Cephalopholis spp.*, Epinephelus tauvina,* and *Liopropoma lunulatum*

In *Cephalopholis* the swim bladder was closely associated with ribs 3 to 6, which were notably longer than the first two ribs. Ligaments were inserted on the consecutive ribs, and longer ligaments were also attached to the anterior portion of ribs 5 and 6. The first rib was connected to the neurocranium by a muscle. Similarly, muscles were found between consecutive ribs, at least for the three first ribs.

In *E. tauvina*, intercostal ligaments were not observed. Instead, a long ligament was inserted into the first rib, extending over the second and third ribs before attaching to the fourth rib. Another portion of the ligament was inserted into the second rib, extended over the third rib, and inserted to the fourth rib. As in the other species, two types of muscles were identified: one muscle connecting the first rib to the neurocranium, and muscles connecting the adjacent ribs, at least between the first two ribs.

Plectranthias taylori

The inter-costal ligament system associated with the ribs and the muscle connecting the first rib to the neurocranium are similar to the one described in *S. powelli*. The swim bladder in *P. taylori* is elongated, appearing white to transparent, and had very thin walls. The swim bladder was positioned adjacent to the rib bases, with no muscle directly inserted into it. Similar to other species, a muscle was inserted into the first rib and the neurocranium (Figure 59). However, this muscle was also attached to the ventral process of the posttemporal in the pectoral girdle, in addition to its attachment to the neurocranium. This muscle formed a distinct bundle that passed through the Baudelot's ligament. A peculiar ligament connected the internal part of the supracoracoid to the anterior part of the ventro-lateral extremity of the first pair of ribs, a feature not observed in other examined species. Multiple intercostal ligaments were observed (Figure 59). L1A is inserted into the first rib, passes under the second rib, and attaches to the third rib. L1B is also inserted into the first rib, passes under the second rib, above the third ribs, and is attached to the fourth rib. L2 is attached to the second rib, goes above the third and fourth ribs, and attached to the vertebrae between the fourth and fifth ribs. L3 is attached to the third rib, extended above the fourth rib and attached to the fifth rib. L4, L5, and L6 were positioned between consecutive ribs. Beneath the intercostal ligaments, intercostal muscles were observed

between consecutive ribs, at least up to the fourth rib. These muscles exhibited fibers oriented parallel to the vertebral column, whereas the intercostal ligaments displayed a more exterior orientation.

Table SP8 - 1 Sound description of the sonic families found in the deeper part of Polynesian mesophotic reefs.

Family	Genus or species of interest	Genus or species from the litterature	Sonic mechanism	Sound description	Source
Acanthuridae	*Naso hexacanthus*	*Acanthurus bahianus*		Raspy sounds, grunts, knocks, occasionally series of knocks, espace sounds (some double)	[21]
				'Pop-like' sound	[533]
		Acanthurus chirurgus	Dorsal fin spine stridulation?	(Weak) knocks, weak escape sounds,	[21]
		Acanthurus coeruleus	Dorsal fin spine stridulation?	Single grunt,escape sounds, scratches, knocks, weak clicks	[21]
		Acanthurus olivaceus		Pulse	[138]
		Ctenochaetus hawaiiensis		Pulse train Long pulse	[138]
		Ctenochaetus strigosus		Pulse	[138]
		Paracanthurus hepatus	With the strong-spined dorsal fin	Stridulatory sound	[532]
		Zebrasoma flavescens		Pulse, collision	[138]
Apogonidae	*Foa fo*	*Apogonichthyoides niger*	The fish tremble	'Sound'	[723]
Balistidae	*Xanthichthys auromarginatus*	*Xanthichthys auromarginatus*		Pulse or pulse train with 4.8 + 1.1 events	[138]
	Xanthichthys caeruleolineatus				
Blenniidae	*Petroscirtes xestus*	*Chasmodes bosquianus*	Synchronized with a quick sidewise shake of the head.	Non-harmonic low-pitched grunting or thumping sound.	[529]
		Lipophrys pholis	Head raised and mouth opened.	Clacking sound	[724]
		Parablennius parvicornis		Calls solely and repeatedly made of three parts (central part = grunt) with a harmonic structure	[527]
				Call	[528]
Bythitidae	*Tuamotuichthys bispinosus*	*Cataetyx messieri*	Sonic muscles		[530]
Caesionidae	*Caesionidae*	*Caesio caerulaurea*			[531]
	Pterocaesio sp.				
Caproidae	*Antigonia capros*	*Capros aper*	Dorsal and pelvic fin	Stridulatory noise	[532,725]
Carangidae	*Alectis indica*	*Alectis ciliaris*		Sharp bark or scratchy burst	[21,522]

Atule mate *Decapterus macarellus* *Decapterus tabl* *Uraspis helvola*	*Carangoides bartholomaei*	Swim bladder?	Knocs and thumps	[21]
	Caranx crysos	Swim bladder and adjacent pharyngeal teeth	Low-pitched thump, loud rasps (sometimes prolonged like scraping of rought file), loud bursts of grating, no tooth sounds during feeding, weak scraping followed by loud bursts, weak scraping	[21,521,522]
			Pharyngeal stridulation	[540]
			Horn-like sounds?	[534,555]
	Caranx hippos	Stridulation of weel-toothed mouth reinforced by large swim bladder	Series if grunts, sustained croaking with a marked scratchy quality	[21,532]
		Pharyngeal teeth	Stridulation	[526]
			Series of short, rapid, rasping croaks	[541]
	Caranx latus	Pharyngeal teeth stridulation amplified by swim bladder, swim bladder vibrate also by body muscle contraction	Thumps, escape sounds, feeding sounds, toothy grunts, thump-like	[21]
			Thump, volleys of thump-like sounds, pharyngeal stridulation	[540]
	Caranx ruber	Swim bladder in conjunction with teeth	High-pitched grunts	[21]
		Pharyngeal stridulation	Stridulation	[540]
		Movements of fish bodies in the water	Low-pitched swimming and veering sounds	
		Swimming sound of individuals or schools	‘Blast’	[542]
	Chloroscombrus chrysurus	Swim bladder and pharyngeal teeth	Low-knocking, series of short fast grunts, tiny knocks, raspy grunts	[21]
		Scraping the upper and lower pharyngeal patches together	Stridulatory sound, a harsh, almost continuous croak	[512]
	Elagatis bipinnulata	Swim bladder and pharyngeal teeth	Escape grunts similar to other carangids	[21]

Naucrates ductor	Pharyngeal teeth stridulation augmented by adjacent swim bladder	Tumping sound? Production of characteristic carangid stridulation possible.	[21,521,522]
Oligoplites saurus	Swim bladder?	Escape thumps, weak knock	[21]
Selene brevoortii	Air bladder resonance? Pharyngeal stridulation?	'Grunt like a young pig'	[532]
Selene peruviana	Scrape upper and lower pharyngeal patches	Almost continuous rasping sound	[532]
Selene setapinnis	Swim bladder and pharyngeal teeth	Almost continuous pig-like grunting, loud scratchy grunting	[21]
	Scrapping the upper and lower pharyngeal patches together	Stridulatory sound: harsh almost continuous croak	[512]
Selene vomer	Swim bladder and pharyngeal teeth	Loud grunts	[21]
Seriola dumerili	Similar to *S. zonata*	Knocks, thumps	[21]
		Tuba-like sound	[533,534]
		Bait-eating and swimming sound	[535]
Seriola lalandi			[536]
Seriola quinqueradiata		Bait-eating and swimming sound	[535]
Seriola rivoliana		Similarity with an unknown sound from the field.	[164]
Seriola zonata	Sound production synchronized with opening of mouth, in which position pharyngeal teeth scraped in close proximity to swim bladder.	Sharp knocks	[21]
Trachinotus falcatus	Similar to *T. goodei*	Consistent weak escape sounds.	[21]
Trachinotus goodei	Swim bladder and pharyngeal teeth in young, mostly swim bladder in older fish	Weak knocks, escape knocks, weak chewing sounds during feeding, escape knocks in rapid series with violent body twisting.	[21]
Trachinotus paitensis	Hitting together of dorsal fins	Grinding and clicking noises	[532]

		Trachurus japonicus	Pharyngeal teeths while feeding	Harsh grating	[532]
			Quick vibrations of the body immediately behind the pectorals, short stretching movements of the lower jaw => friction of pharyngeal teeth and airbladder vibrations	Low snoring, low-pitched sound	[537]
				Bait-eating and swimming sound	[535]
		Trachurus mediterraneus			[538]
		Trachurus trachurus			[539]
		+ *Selar* and *Alectis* species			
	Selar boops	*Selar crumenophthalmus*		Sustained or irregular series of toothy grating sounds and a few knocks	[21]
Carapidae	*Carapus mourlani*	*Carapus mourlani*	Central constriction in their swim bladder	Single and double-pulsed calls	[146]
				Train of 2-6 pulses	[145]
				Suite of double pulses	
				Staccatos of 2-17 weak pulses	
				Hums (rare) usually preceded by a knock	
Chaetodontidae	*Chaetodon* sp.	*Chaetodon auriga*	Vertical elevation of the head and a strong protrusion of the jaws	Head bob–jaw protrusion pulse: pulses and less frequently two-pulse train	[543]
		Chaetodon kleinii	Jaw protusion	Short pulse sound	[543]
				HF pulse	[138]
		Chaetodon multicintus	Motion of the whole body directed at the nearby conspecific	Tail slap	[543]
				Body shake	
			Movements of the caudal peduncle and/or extension of the pelvic fins	Body motion	
				Body motion pulse train	
				Pulse	[138]
				Tail slap	[726]
				Low frequency pulse	

				High frequency click	
				Jump	
				Dorsal-anal fin erect	
				Pelvic fin flick	
				Grunt train	
		Chaetodon ocellatus		Small thumps and knocks, some double and with toothy clicks	[21]
		Chaetodon ornatissimus	Movements of the caudal peduncle and/or extension of the pelvic fins	Body motion = pulse	[543]
			Motion of the whole body directed at the nearby conspecific	Tail slap	
				Pulse	[138]
		Chaetodon striatus		Small knocks, almost inaudible but definite	[21]
		Chaetodon unimaculatus	Clear extension and retraction movement of the jaws	Head-bob-jaw protusion	[543]
			Motion of the whole body directed at the nearby conspecific	Tail slap	
	Heniochus singularius	*Heniochus chrysostomus*	Extrinsic sonic drumming muscles in association with the articulated bones of the ribcage	Isolated pulses	[149]
				Trains of 4 to 11 pulses sometimes preceded by an isolated pulse	
Congridae	*Ariosoma scheelei* *Ariosoma sereti* *Bathyuroconger vicinus* *Congriscus marquesaensis* *Uroconger* sp.	*Conger conger*		Mechanical noise	[521,522]
Dactylopteridae	*Dactyloptena sp.*	*Dactylopterus volitans*		Bursts of barking	[21]
			Intrinsic muscles	*Sons commensurables*	[545]
Diodontidae	Diodontidae	*Diodon hystrix*	Stridulation	Loud toothy scrapes during feeding, jaw stridulation	[21]
				Toothplate stridulation	[526]

		Chilomycterus schoepfii	Stridulation	Toothy whines, pronounced thump	[21,521,522]
		Chilomycterus reticulatus	Stridulation	Erking series, rasps, toothy sounds	[21]
		Chilomycterus spinosus	Grating of the incisor teeth, during and after inflation	Stridulatory sound: high-pitched nasal whining scrape	[512]
Gobiidae	*Gnatholepis anjerensis* *Gunnellichthys monostigma* *Kraemeria bryani* *Oxyurichthys notonema* *Priolepis farcimen* *Priolepis sp.* *Valenciennea strigata*	**Numerous species from genera *Bathygobius, Gobiosoma, Gobius, Gobiusculus, Knipowitschia, Neogobius, Padogobius, Periophthalmodon, Pomatoschistus, Ponticola,* and *Zosterisessor* emit low-intensity sounds.**			
Holocentridae	*Myripristis chryseres*	*Myripristis jacobus*	Sonic muscles	Grunts, singly produced or in bursts, toothy clicks, short bursts of grunting	[21]
		Myripristis parlinia *Myripristis violacea*		Grunts	[548]
		Myripristis berndti	Sonic muscles	Knocks, growls, grunts, and staccatos	[549]
				Knock, growl, grunt, staccato	[138]
		Myripristis amaena		Growl, grunt, staccato	[138]
		Myripristis kuntee *Myripristis violacea*	Extrinsic sonic muscles	Harmonic train of pulses = grunts	[547]
	Ostichthys archiepiscopus *Ostichthys ovaloculus* *Pristilepis* sp.	*Holocentrus adcensionis*	Vibration by body musculature of very large swim bladder	Series of grunts, isolated grunts, prolonged grunting, thumps, bursts of 2-5 grunts, low grumbling, single and volleyed grunts?	[21]
			Stridulation of pharyngeal teeth reinforced by swim bladder	Higher-pitched rasping grunts	
			Swim bladder embraced by modified ribs expanded and	Thumps repeated singly at irregular intervals or volleyed (4-20), volleys (3-20)	[526]

	flattened to serve as drumheads activated by attached musculature		
		Narrow-band, short pulses, regularly repeated in short bursts of 10-20, fundamental frequency ca. 75 Hz	[534]
	Sonic muscles		[551]
Holocentrus rufus	Swim bladder vibrate by simultaneous contractions of paired bilateral muscles		[552]
	Fast-contracting sonic muscles.	Harmonic sounds made of a variable number of pulses with gradually increasing periods towards the end of the call.	[547]
			[553]
	Sonic muscles		[550,551]
Neoniphon aurolineatus		Grunt, knock, staccato, train of grunts, train of staccato Growl= rapid series of contiguous pulses that decreased in rate over time	[138]
Neoniphon sammara		Growl, knock, staccato, train of staccato	[138]
	Fast-contracting sonic muscles.	Harmonic sounds made of a variable number of pulses with gradually increasing periods towards the end of the call.	[547]
	Sonic muscles		[550]
Sargocentron cornutum	Sonic muscles		[550]
Sargocentron diadema	Fast-contracting sonic muscles.	Harmonic sounds made of a variable number of pulses with gradually increasing periods towards the end of the call.	[547]
Sargocentron seychellense	Sonic muscles		[550]
Sargocentron spiniferum		Sounds	[138]
	Fast-contracting sonic muscles.	Harmonic sounds made of a variable number of pulses with gradually increasing periods towards the end of the call.	[547]
Sargocentron tiere		Growl, grunt, knock, series of growl, series og knock	[138]
	Fast-contracting sonic muscles.	Harmonic sounds made of a variable number of pulses with	[547]

				gradually increasing periods towards the end of the call.	
		Sargocentron wantherythrum	Sonic muscles		[550]
		+ *Myripristis* species.			
Labridae	*Bodianus bilunulatus*	*Bodianus rufus*		Only feeding noises	[21]
	Bodianus paraleucostictic us				
	Cirrhilabrus claire *Oxycheilinus lineatus* *Polylepion russelli*	*Gomphosus varius*		Pulse I, pulse II, buzz, train of pulse I, train of pulse II	[138]
				Pulse train (type I and II)	[554]
		Halichoeres bivittatus	Swibladder? Strong teeth?	Feeble knocks and thumps, small toothy feeding sounds	[21]
			Moving contact of teeth on rock, conchs etc during feeding	Stridulatory rasping	[555]
		Halichoeres garnoti		Feeding noises	[21]
		Halichoeres radiatus	Swibladder? Strong teeth?	Thumps, knocks, toothy feeding noises	[21]
				Feeding sounds	[526]
		Labrux mixtus *Symphodus melops*			[556]
		Labrus viridis			[539]
		Lachnolaimus maximus	Large swim bladder? Strong jaw and pharyngeal teeth?	Escape sounds, knocks coincident with body twist	[21]
		Symphodus cinereus *Symphodus ocellatus* *Symphodus tinca*			[557]
		Tautogra onitis	Swim bladder vibrates by violent contraction of skeletal muscles, slight striking or possible rubbing of ribs, and drum-beating motion of opercula	Deep thumps, bark-like grunts, loud noise from crushing and dragging shells on bottom, escape sounds, thumps, mechanical noise incident to feeding, loud thumps	[21,521,522]
		Tautogolabrus adspersus	Swim bladder compressed by violent contraction	Low-frequency knocks synchronized with muscular twinge and vibratory shudder,	[21,521,522]

			of skeletal muscles; teeth in jaws and granular pharyngeals adapted for crushing	loud scrunching noise during feeding	
		Thalassoma bifasciatum		Feeding noise	[21]
		Thalassoma duperrey		Pulse I, pulse I blended, pulse II, train of pulse I, train of pulse II	[138]
				Pulse train (type I and II)	[554]
		And *Bodianus*			
Leiognathidae	*Deveximentum insidiator*	*Leiognathus equula*		Soniferous	[558]
	Gazza minuta		Friction of premaxilla and frontal	Noise	[537]
Lethrinidae	*Gymnocranius confer grandoculis* *Lethrinus rubrioperculatus*	*Lethrinidae*			[559]
Lutjanidae	*Lutjanus kasmira*	*Lutjanus kasmira*		Pulse	[138]
	Lutjanus argentimaculatus	*Lutjanus griseus*	‘Swim bladder’	Low thumps and knocks, sometimes followed by growls	[21]
	Lutjanus sp.	*Lutjanus jocu*	‘Swim bladder’	Thumps	
		Lutjanus apodus	‘Swim bladder’	Thumps, knocks, singly or in short series, booms	
		Lutjanus analis	‘Swim bladder’	Knock, thump, toothy scraping	
		Lutjanus synagris	‘Swim bladder’	Knocks	
		Lutjanus mahogoni	‘Swim bladder’	Possibly thump	
	Aphareus furca *Aphareus rutilans* *Etelis carbunculus* *Etelis coruscans* *Etelis radiosus* *Aphareus furca* *Parapristipomoides squamimaxillaris*	*Hoplopagrus guentherii*		Maybe sound during feeding	[21]
		Ocyurus chrysurus	Swim bladder?	Low-pitched thrumps, escape sounds, toothy clicks, weak knocks, weak knocks, some louder bumps, very feeble thumps	[21]
		Rhomboplites aurorubens	Swim bladder?	Feeble knocks and thumps	[21]

	Pristipomoides argyrogrammicus *Pristipomoides auricilla* *Pristipomoides filamentosus* *Pristipomoides flavipinnis* *Pristipomoides sieboldii* *Pristipomoides zonatus* *Randallichthys filamentosus*	And ***Lutjanus*** species.			
Macrouridae	*Malacocephalus laevis*	*Malacocephalus laevis*	Drumming muscles (swim bladder to body wall)		[561]
	Malacocephalus nipponensis *Malacocephalus sp.*	*Malacocephalus laevis* *Malacocephalus occidentalis*			
			Drumming muscles		
Mullidae	*Mulloidichthys pfluegeri*	*Mulloidichthys flavolineatus*		One poor quality sound	[138]
	Mulloidichthys sp. *Mulloidichthys vanicolensis*	*Mulloidichthys martinicus*	Muscles + teeth	Thumps, knocks, scratchy sounds	[21]
	Parupeneus sp.	*Parupeneus insularis*		Pulse, pulse train	[138]
		Parupeneus multifasciatus		Pulse, pulse train, HF pulse	
		Parupeneus porphyreus		Pulse, pulse train	
Myctophidae	*Benthosema fibulatum* *Diaphus splendidus* *Lampadena luminosa* *Symbolophorus evermanni*	Myctophidae		The most likely chorus source is considered to be fishes of the family Myctophidae foraging in the water column	[562]
Ophidiidae	*Brotula multibarbata*	*Acanthonus armatus*	The swim bladder is apparently unfit as a soundproducing organ, but perhaps the pharyngeal teeth can produce sound by stridulation		[577]
		Barathrodemus manatinus	Two pairs of sonic muscles:		[578]

	ventrolateral sound producing muscles (skull => swim bladder) and ventromedial muscles (skull => ribs attached to the 4th vertebra) in males, in females: only 1 pair (ventromedial)		
Bathyonus pectoralis	Single pair of ventral medial muscles that connects to a smaller and thinner swim bladder via a long tendon, Larger muscle fibers suggesting an adaptation to facilitate rapid bladder movement for sound production		[727]
Dicrolene introniger	Four pairs of sonic muscles: two ventral muscles (ventral medial and ventral lateral) and two intermediate muscles (intermediate medial and intermediate lateral)		[727]
Genypterus chilensis	Modified vertebra, three pairs of sonic muscles and the swim bladder	Calls made of 7-19 units	[579]
Genypterus maculatus		Sound 1 = train of pulses that vary in amplitude and pacing	[579]
		Call 2 = growl (harmonic, tonal)	
Hoplobrotula armata	Four pairs of sonic muscles	Sounds suggested to be more intense than in Neobytites	[581]
Lepophidium jeannae		Maybe produce 100 Hz Pulsing	[451]

	Lepophidium profundorum	Ventral and dorsal antagonistic sonic muscles		[576,580]
	Monomitopus metriostoma	Sonic muscles		[530]
	Neobythites longipes		Sounds suggested to be longer than in *Hoplobrotula armata*	[581]
	Neobythites unimaculatus			[581]
	Parophidion vasali			[517]
	Neobythites gilli	Four pairs of sonic muscles (ventral and intermediate)		[563]
	Neobythites steatiticus	Sonic muscles		[530]
	Porogadus miles	Single pair of ventral medial muscles that connects to a smaller and thinner swim bladder via a long tendon		[727]
	Typhlonus nasus	Might be able to produce sound by stridulation with the teeth		[577]
	And ***Ophidion*** species			
Ophidion muraenolepis	*Ophidion rochei*		Long, multiple-pulsed calls	[564]
		Three pairs of sonic muscles		[565]
		Sonic muscles and rocker bone	Mate calls	[566]
		Differences in morphology of sonic muscles, swim bladder, supraoccipital crest, first vertebrae and associated ribs (rocker bone present vs. absent)	Males: Non harmonic multiple-pulsed sounds Females and juveniles harmonic sounds	[567]
		Three pairs of sonic muscles, rocker bone, modified neural arch	Male courtship calls = train of pulses that increase in amplitude and decrease in rate	[434]
			Long trains of Low-frequency pulses	[90]

				Pulses series with alternating pulse period (APPPS)	[163]
		Ophidion barbatum	Three pairs of sonic muscles		[568]
		Ophidion marginatum			[569,570]
				Mainly crepuscular repeated pulses	[571]
			Sonic muscles associated with the swim bladder and vertebral components.	Chatter sound	[572]
				Croaking sound	[573]
			2 or 3 pairs of sonic muscles	Broad-band pulsed calls at dusk	[574]
			Specialized musculature, swim bladder and modified anterior vertebral components		[575]
Ostraciidae	*Lactoria* sp.	*Lactoria cornuta*	Extrinsic and intrinsic sonic muscles	Hums (= long train of pulses) and clicks	[514]
		Lactoria fornasini		Spawning sound (= a highpitched hum),	[583]
	Ostracion sp.	*Ostracion cubicus*	Extrinsic and intrinsic sonic muscles	Hums (= long train of pulses) and clicks	[150]
		Ostracion meleagris	Extrinsic and intrinsic sonic muscles	Spawning sound, bump, and buzz. Hums (= long train of pulses) and clicks	[150,582]
	Tetrosomus sp.	*Acanthostracion quadricornis*	Swim bladder and associated muscles, stridulating teeth	Short growls, some in long series, clicks, sustained rasping, chewing noise, loud growling	[21]
				Chorus of nocturnal ‘frog-like’ sounds (1000-3400 Hz) tentatively attributed to this species?	[533]
		Lactophrys bicaudalis	Vibration of swim bladder anticipated, stridulation of teeth.	Clicks, scrapes, toothy grunts during feeding, clicks, scrapes	[21]
		Lactophrys trigonus	Swim bladder and associated muscles, stridulating teeth	Feeding noise only, low-frequency groans, toothy scrapes singly or in combination, groans, rasps, scrapes	[21]

		Lactophrys triqueter	Swim bladder and associated muscles, stridulating teeth	Single faint clicks, low-pitched growls, loud scrapes	[21]
		See *Ostracion* and *Lactoria* species			
Peristediidae	*Satyrichthys* sp.	*Satyrichthys rieffeli* *Satyrichthys welchi*	Not reported sonic family but close relationship to known sound-makers.		[532]
Pleuronectidae	*Nematops nanosquama*	*Hippoglossoides platessoides*		Mechanical noise	[521,522]
		Pseudopleuronectes americanus		Mechanical noise	[521,522]
Pomacanthidae	*Centropyge boylei*	*Centropyge loriculus*		Pulse	[138]
	Centropyge narcosis				
	Genicanthus bellus	*Apolemichthys arcuatus*		Pulse	[138]
		Holacanthus bermudensis	Swim bladder?	Thumps, rasps, series of scratchy grunts	[21]
		Holacanthus ciliaris	Swim bladder? Body twist	Knocks, (small) thumps	[21]
				Grunt single or repeated (vibrant, deep grunts not easily distinguished from those of serranids)	[526]
		Holacanthus tricolor	Swim bladder?	Escape sounds, weak knocks	[21]
		Pomacanthus arcuatus	Swim bladder?	Thumps, knocks, quick escape	[21]
		Pomacanthus paru		Thumps, (low) knocks, escape sounds, feeding sounds	[21]
			Swim bladder vibrate by adjacent axial muscles	Grunts (change of signals from short grunt to moan-like sound?)	[526]
		See *Centropyge*			
Pomacentridae	*Chromis* sp. 2 (Tahiti Island)	*Chromis chromis*		Pop made of a single pulse	[585]
		Chromis hanui		Pulse	[138]
		Chromis ovalis			
		Chromis verater		Pulse Pulse train	
		Chromis atripectoralis *Chromis viridis*			[584]
	Pomacentridae sp. (Rapa Is.)	**See *Chromis* species in addition to numerous sonic species from *Dascyllus, Hypsypops, Plectroglyphidodon, Pomacentrus, Premnas, Stegastes, Pomatomus, Abudefduf, Similiparma* and *Amphiprion*.**			

Priacanthidae	*Cookeolus japonicus*	*Heteropriacanthus cruentatus*	Muscle (swim bladder – body wall)	Sounds composed of a rapid series of pulses	[588]
		See *Priacanthus* species			
	Priacanthus hamrur	*Priacanthus meeki*	Muscle (swim bladder – body wall)	Sounds composed of a rapid series of pulses	[588]
		Priacanthus macracanthus	Muscles		[586,587]
Scombridae	*Thunnus maccoyii* *Thunnus obesus*	*Thunnus albacares* *Thunnus thynnus*	Possibly caused by contraction of muscles about the swim bladder	Low-frequency pulses usually single, double pulses, quadruple pulse train, high frequency (= jaw snap sounds)	[589]
Scorpaenidae	*Neomerinthe naevosa*	*Neomerinthe beanorum*	Similar to *Aleutianus-zacentrus* type 1 (cranium, vertebral parapophyses)		[590]
	Pontinus macrocephalus	*Pontinus longispinis*	*Aleutianus-zacentrus* type 1 extrinsic gasblader muscle, attached to vertebra 8, 9 and 10 and the cranium		[590]
	Pteroidichthys amboinensis *Pteroidichthys caussei*	*Brachypterois serrulifer*	Two large gasbladder muscles (type II, Taczanowskii subdivision) originating on the cranium and inserting usually on the swim bladder. No connection to the pectoral girdle.		[590]
		Dendrochirus zebra	Two large gasbladder muscles (type II, Taczanowskii subdivision) originating on the cranium and inserting usually on the swim bladder. No connection to the pectoral girdle.	Train of 4 to 25 pulses	[590,728]

	Iracundus signifer	Possibly caused by contraction of muscles about the swim bladder		[590]
	Pterois miles	Similar to *Aleutianus-zacentrus* type 1 (cranium, vertebral parapophyses)	Repetitive pulse call (1 to 4 pulses = knocks) with occasional occurrences of up to 8 pulses Hum + intermittent pulses	[591]
	Pterois radiata	Two large gasbladder muscles (type II, Taczanowskii subdivision) originating on the cranium and inserting usually on the swim bladder. No connection to the pectoral girdle.	Knocks and hums	[590,728]
	Pterois volitans	Muscles closely associated with the swim bladder	Repetitive pulse call (1 to 4 pulses = knocks) with occasional occurrences of up to 8 pulses Hum + intermittent pulses	[591,728]
	Scorpaenodes parvipinnis	Two large gasbladder muscles (type II, Taczanowskii subdivision) originating on the cranium and inserting usually on the swim bladder. No connection to the pectoral girdle.		[590]
	Sebastapistes cyanostigma	Similar to *Aleutianus-zacentrus* type 1 (cranium, vertebral parapophyses)		[590]
	+ *Scorpaena, Scorpaenopsis, Pontinus*, and *Neomerinthe* species			
Scorpaena lacrimata	*Scorpaena plumieri*		Low-pitched growl (questionable)	[21]
	Scorpaena agassizii	Similar to *Aleutianus-zacentrus* type 1 (cranium, vertebral		[590]
	Scorpaena brasiliensis			
	Scorpaena elongata			
	Scorpaena guttata			

		Scorpaena mystes	parapophyses) with 4 tendons, one attached to each of the parapophyses of the 6th, 7th, 8th, 9th vertebrae		
		Scorpaena russula			
		Scorpaena porcus			
			Muscles that originate on the exoccipital bone and insert on the anterior part of the backbone, from the sixth to the ninth vertebrae. The complete apparatus consists of bilaterally symmetric muscular bundles (three muscular bundles on each side), connected to four long tendons, which insert on lateral branches of the haemal arch (vertebrae VI and VII) or on haemal spines (vertebrae VIII and IX) underneath different vertebral bodies No swim bladder	/kwa/	[433]
		Scorpaena scrofa *Scorpaena notata*		/kwa/	[433]
	Scorpaenopsis pusilla	*Scorpaenopsis gibbosa*		Low grinding noise	[21,532]
Serranidae	*Cephalopholis aurantia* *Cephalopholis igarashiensis* *Cephalopholis sexmaculata*	*Cephalopholis formosa*			[592]
		Cephalopholis cruentata	Swim bladder vibrate by contraction of body muscles.	Thumps, rumbles, knocks?	[21]
		Cephalopholis fulva	Swim bladder vibrate by	Boom, thumps, knocks, escape sounds	

		contraction of associated axial muscles.		
	Cephalopholis argus		Pulse	[138]
Epinephelus morrhua *Epinephelus retouti* *Epinephelus tuamotuensis*	*Epinephelus adscensionis*	Swim bladder vibrate by axial muscles	Long loud bursts of vibrant grunting, single thumps, knocks, grunts	[21,526]
	Epinephelus drummondhayi	Swim bladder vibrate by associated muscles	Vibrant grunting	[21]
	Epinephelus erythrurus			[592]
	Epinephelus guttatus		Low-frequency series of pulses repeated at a variable rate, one or moreportions of the call had a high pulse rate, whichappears tonal	[593]
		Swim bladder vibrate by associated musles	Series of grunts during feeding, deep grunt, boom, thump, escape sounds	[21]
			Narrow-band short pulses (grunt-like sounds) single or in irregular groups	[534]
				[471,553, 594,597]
	Epinephelus itajara	Swim bladder and associated musles	Boom sometimes followed by two grunts, bursts	[21]
			Single-pulse calls with a low dominant frequency	[598]
				[599,600]
	Epinephelus marginatus		Single booms, serial booms (rarely recorded), growls (= short multi-harmonic calls with a slight downward frequency modulation)	[423]
			Low-frequency downsweep (LDS)	[163]
			Low-frequency pulse sequence (LPS)	
	Epinephelus polyphekadion			[154]
	Epinephelus morio	Swim bladder vibrate by associated muscles	One loud boom	[21]
			Low-frequency pulses, short calls (=1 to 4 brief pulses followed by a growl), pulse train calls (=a short call immediately followed by a	[458]

			rapid series of broadband bursts)	
				[93,553,601–603]
	Epinephelus striatus		Deep booms, sustained rumbles, loud grunts, loud grinding of teeth, low grunts, vibrant grunts (single or in rapid series), serranid-like grunts	[21]
		Swim bladder vibrate by contraction of attached axial muscle fibers.	Vibrant grunt (single or repeated)	[526]
			Deep booms, sustained rumbles, loud grunts, loud grinding of teeth, low grunts	[521]
		Single bilateral muscle vibrate inact swim bladder.		[352]
			Mooing-like sound maybe produced by this species.	[533]
				[471,553,597,604]
			Pulse train	[596]
			Tonal sound	
Hyporthodus octofasciatus	*Hyporthodus nigritus*	Swim bladder vibrated by associated muscles	Booms, thumps	[21]
Belonoperca pylei	*Alphestes afer*	Swim bladder and associated muscles	Escape sounds, knocks and low thumps	[21]
Liopropoma erythraeum	*Anthias anthias*		Potentially sonic	[164]
Liopropoma lunulatum	*Centropristis striata*	Swim bladder vibrates by general body contraction and striking of opercula against body, pharyngeal teeth stridulation	Single weak grunts, small thumps, low thumps, possible scrapes	[21,521,522]
Odontanthias tapui				
Plectranthias bennetti				
Plectranthias kamii	*Diplectrum formosum*	Swim bladder vibrate by contraction of body musculature	Single escape sound, rasp, burst of one-five low grunts	[21]
Plectranthias rubrifasciatus				
Plectranthias sp.	*Hypoplectrus unicolor*	Contraction of the abdominal musculature externally observed.	Series of sound pulses	[89]
Plectranthias taylori			Short duration frequency modulated downward (600 Hz to 200 Hz) tonal sweep followed by a longer broadband noise	
Pogonoperca punctata				
Saloptia powelli	*Mycteroperca bonaci*	Swim bladder vibrate by sudden	Spontaneous single booms, sustained thundering rolls, loud	[21]

			contraction of body musculature	feeding noises, loud percussive sound	
				Ocassional single, 4-beat and 6-beat but usually 5-beat burst of sounds. Each of the five 'drum-beats' consists of five sound pulses with rapidly dropping pitch	Tavolga 1958 IN [21]
				Pulse train undulation	[605]
				Series of pulses followed by a longer tonal section, Not all signals included the discrete pulses prior to the tonal section	[606]
					[471,553]
		Mycteroperca interstitialis	Swim bladder and associated muscles	Low-pitched serranid grunt	[21]
		Mycteroperca jordani		Short and long tonal sounds, as well as multiple combinations, preceded and followed by a variable number of short, low frequency, repeated pulses	[484,485]
		Mycteroperca microlepis	Swim bladder and associated muscles	Weak typical serranid thump	[21]
		Mycteroperca venenosa	Swim bladder and associated muscles	Feeding noise Loud deep booms similar to other groupers	[21]
					[604]
					[471,553, 597]
				Pulse train calls, tonal call and sequential combination	[607]
		Rypticus bistrispinus	As other serranids	Very weak knocks	[21]
		Rypticus saponaceus	As other serranids	Small hollow knocks	[21]
		Serranus tigrinus	Probably swim bladder vibrate as in other serranids	Weak knocks and thumps	[21]
		See *Cephalopholis, Epinephelus, Hyporthodus* and *Pseudanthias,*			
	Pseudanthias privitera	*Pseudanthias bicolor*		Pulse	[138]
	Pseudanthias ventralis				
Setarchidae	*Setarches guentheri*	*Setarches guentheri*	Two large gasbladder muscles (type II, Taczanowskii subdivision) originating on the cranium and inserting usually on the swim		[590]

			bladder. No connection to the pectoral girdle.		
Sphyraenidae	*Sphyraena acutipinnis*	*Sphyraena viridensis*		Sounds maybe produced by this species.	[164]
		Sphyraena barracuda		Thumps, knocks during swift motion	[21]
		Sphyraena guachancho	As *S. barracuda*		[21]
Syngnathidae	*Hippocampus kuda* *Hippocampus* sp.	*Hippocampus erectus*	Sharp flexion of head and rapid movement of mouth parts	Loud clicks similar to snapping of finger against thumb, snaps	[21,521,522,608]
			Supraoccipital-coronet articulation (stridulation)	Clicks	[609]
		Hippocampus sp.	Muscular closing and sudden expansion of lower jaw	Snaps, resembled in strength and tone the snapping sound produced by *Alpheus ruber*.	[729]
		Hippocampus hippocampus		Tambour-like	[545]
		Hippocampus zosterae	Supraoccipital-coronet articulation (stridulation)	Feeding clicks	[609]
		Hippocampus comes	Likely come from two sound producing mechanisms	Click	[730]
			Vibration observed at the cheek	Growling	
		Hippocampus guttulatus			[557]
		Hippocampus reidi		Click	[731]
			Body vibrations	Growl (= serie of sound pulses)	
Tetraodontidae	*Sphoeroides pachygaster*	*Sphoeroides nephelus*	Grating of the incisor teeth	Stridulatory sound (high-pitched, nasal, whining scrape)	[512]
		Sphoeroides testudineus	Jaw stridulation	Loud single scrapes, erks, rapid paris of low-high pitch	[21]
		Sphoeroides maculatus	Grinding of upper and lower plates in mouth. Possible participation of swim bladder	Long bursts of creaking erk-erks, scrapes, erls, low dull thumps, double erks	[21,521,522]
		Sphoeroides spengleri	Jaw stridulation		[21]
			Toothplate stridulation		[526]
Uranoscopidae	*Genyagnus monopterygius*	*Uranoscopus scaber*	Sonic morphology		[732]

Zanclidae	*Zanclus cornutus*	*Zanclus cornutus*		Pulse, pulse train (2 events per train)	[138]
Zeidae	*Cyttomimus affinis*	*Zeus faber*		Barks	[610,611] [545]

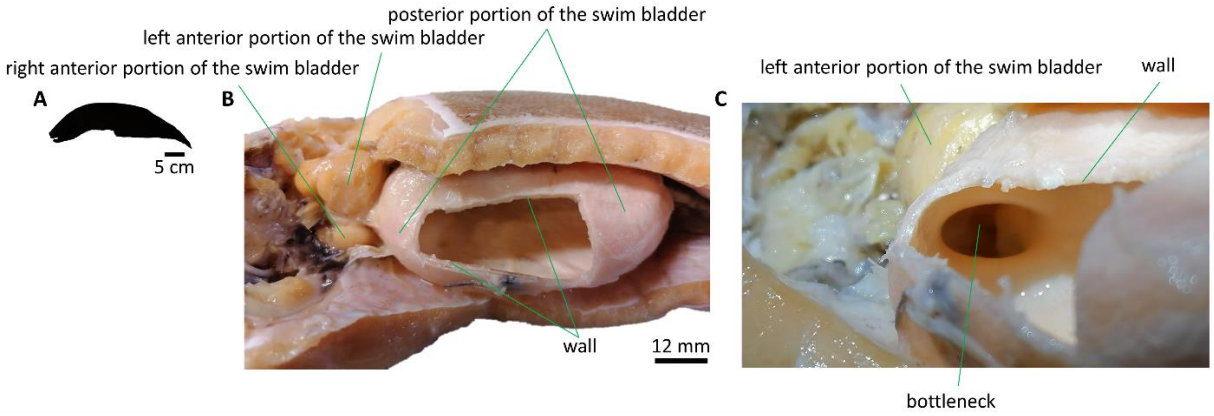

Figure SP8 - 1 Illustration of the swim bladder of *Brotula multibarbata*. (**A**) Schematization of the dissected specimen. (**B**) Zoom on the swim bladder of the dissected specimen. Part of the swim bladder wall was removed. (**C**) Illustration of the bottleneck between the anterior and posterior parts of the swim bladder.

Appendix to Chapter 9

Table SP9 - 1 Location of the sampling sites. MPA = Marine Protected Area. nMPA= non Marine Protected Area. E2B= 'entre deux baies'.

Name		Site	GPS		Date	
Status	**Coast**		**latitude**	**longitude**	**2015**	**2021**
MPA	West	Tetaiuo	-17.5052	-149.9275	07/04	31/01
nMPA	West	Gendron	-17.4995	-149.9276	03/03	27/01
MPA	North-West	Tiahura	-17.4830	-149.8998	09/04	01/02
nMPA	North-West	Papetoai	-17.4829	-149.8861	05/03	28/01
MPA	North	Pihaena	-17.4765	-149.8291	06/05	04/02
nMPA	North	E2B	-17.4751	-149.8372	18/03	09/02
MPA	East	Nuarei	-17.5006	-149.7546	02/04	04/02
nMPA	East	Temae	-17.5067	-149.7600	10/03	04/02

Table SP9 - 2 Details concerning the categories used for coral cover according to Lison de Lima (2008).

Live coral	Broken living fragments larger than 15 cm were considered.
Dead coral	Only recently dead coral (less than one year) still standing or recently broken were considered. The polyp structure must be visible and algal cover must be slight.
Macroalgae	Only noncalcareous algae of large size were considered.
Pavement	Hard compacted substrate even when covered with fine turf (smaller than 5 mm) or encrusting algae. In addition, old dead coral (for more than one year) was included.
Rubble	Small fragments of biogenic calcium carbonate between 0.2 and 15 cm.
Sand	Fine sediment with particles < 0.2 cm that do not stay suspended when disturbed (contrarly to the mud).

Table SP9 - 3 Nested Analyses of covariance outputs for the data from 2021.

	Frequency band	**Temporal period**	**response**	χ^2	**Df**	***P***
Moon	high	night	PSD_{Fpeak}	4.99	1	**0.025**
protection				0.27	1	0.60
Moon	high	night	γFpeak	1.73	1	0.19
protection				145.74	1	< **0.0001**
Moon	high	day	PSD_{Fpeak}	0.069	1	0.79
protection				1.69	1	0.19
Moon	high	day	γFpeak	1.28	1	0.26
protection				103.84	1	< **0.0001**
Moon	low	night	PSD_{Fpeak}	51.06	1	< **0.0001**
protection				19.00	1	< **0.0001**
Moon	low	night	γFpeak	0.44	1	0.50
protection				0.033	1	0.86
Moon	low	day	PSD_{Fpeak}	0.015	1	0.90
protection				110.51	1	< **0.0001**
Moon	low	day	γFpeak	0.97	1	0.32
protection				111.62	1	< **0.0001**

Table SP9 - 4 Nested Analyses of variance outputs for the data from 2021.

	Value nMPA	Value MPA	χ^2	Df	P
Fish abundance	259.89	276.75	0.31	1	0.58
Fish species richness	63	68	4.45	1	**0.035**
Total Sleractinia	0.15	0.22	21.86	1	< **0.0001**
Total Algae	0.058	0.063	48.47	1	< **0.0001**
Asparagopsis	0.040	0.057	2.83	1	0.092
Halimeda	0.0089	0.0067	30.85	1	< **0.0001**
Others macroalgae	0.0044	0.00	5.71	1	**0.017**
Turbinaria	0.0044	0.00	1.43	1	0.23
Pavement	0.60	0.64	0.077	1	0.78
Rubble	0.16	0.063	1.94	1	0.16
Sand	0.038	0.017	2.94	1	0.087

Table SP9 - 5 Mean and standard deviation (SD) acoustic features for each frequency band and temporal period.

Frequency band	Temporal period	Year	protection	PSD_{Fpeak}			γFpeak (Hz)		
				mean	SD	n	mean	SD	n
high	night	2015	MPA	76.32	2.80	8	5514.75	1120.24	8
			nMPA	77.12	2.14	8	4871.25	816.52	8
		2021	MPA	79.20	1.40	56	4595.75	508.07	56
			nMPA	79.08	1.06	56	5281.91	233.16	56
high	day	2015	MPA	69.85	3.33	4	5514.75	1282.37	4
			nMPA	69.75	2.70	4	4917.50	1075.84	4
		2021	MPA	69.88	2.04	56	4961.89	574.21	56
			nMPA	70.16	0.82	56	5549.59	369.84	56
low	night	2015	MPA	66.38	0.82	8	197.54	13.44	8
			nMPA	68.48	2.53	8	208.71	42.25	8
		2021	MPA	70.92	1.90	56	207.37	17.19	56
			nMPA	72.05	1.97	56	206.86	25.03	56
low	day	2015	MPA	71.40	2.19	4	324.62	33.58	4
			nMPA	72.50	2.23	4	349.50	11.48	4
		2021	MPA	71.36	0.91	56	292.02	68.44	56
			nMPA	73.23	1.43	56	355.50	41.67	56

Table SP9 - 6 Nested Analyses of covariance outputs for the data from 2015 and 2021.

	Frequency band	Temporal period	response	χ^2	Df	*P*
Moon	high	night	PSD_{Fpeak}	12.38	1	**0.00043**
Year				23.35	1	**< 0.0001**
Protection				0.031	1	0.86
Year:protection				0.79	1	0.37
Moon	high	night	γFpeak	3.00	1	0.083
Year				5.62	1	**0.018**
Protection				42.33	1	**< 0.0001**
Year:protection				32.64	1	**< 0.0001**
Moon	high	day	PSD_{Fpeak}	0.32	1	0.57
Year				0.088	1	0.77
Protection				1.30	1	0.25
Year:protection				0.23	1	0.63
Moon	high	day	γFpeak	2.06	1	0.15
Year				0.013	1	0.91
Protection				40.90	1	**< 0.0001**
Year:protection				14.79	1	**0.00012**
Moon	low	night	PSD_{Fpeak}	44.79	1	**< 0.0001**
Year				44.82	1	**< 0.0001**
Protection				20.27	1	**< 0.0001**
Year:protection				0.20	1	0.66
Moon	low	night	γFpeak	0.41	1	0.52
Year				0.28	1	0.60
Protection				0.092	1	0.76
Year:protection				1.75	1	0.19
Moon	low	day	PSD_{Fpeak}	0.24	1	0.62
Year				1.06	1	0.30
Protection				88.60	1	**< 0.0001**
Year:protection				0.89	1	0.35
Moon	low	day	γFpeak	1.32	1	0.25
Year				0.41	1	0.52
Protection				104.27	1	**< 0.0001**
Year:protection				2.25	1	0.13

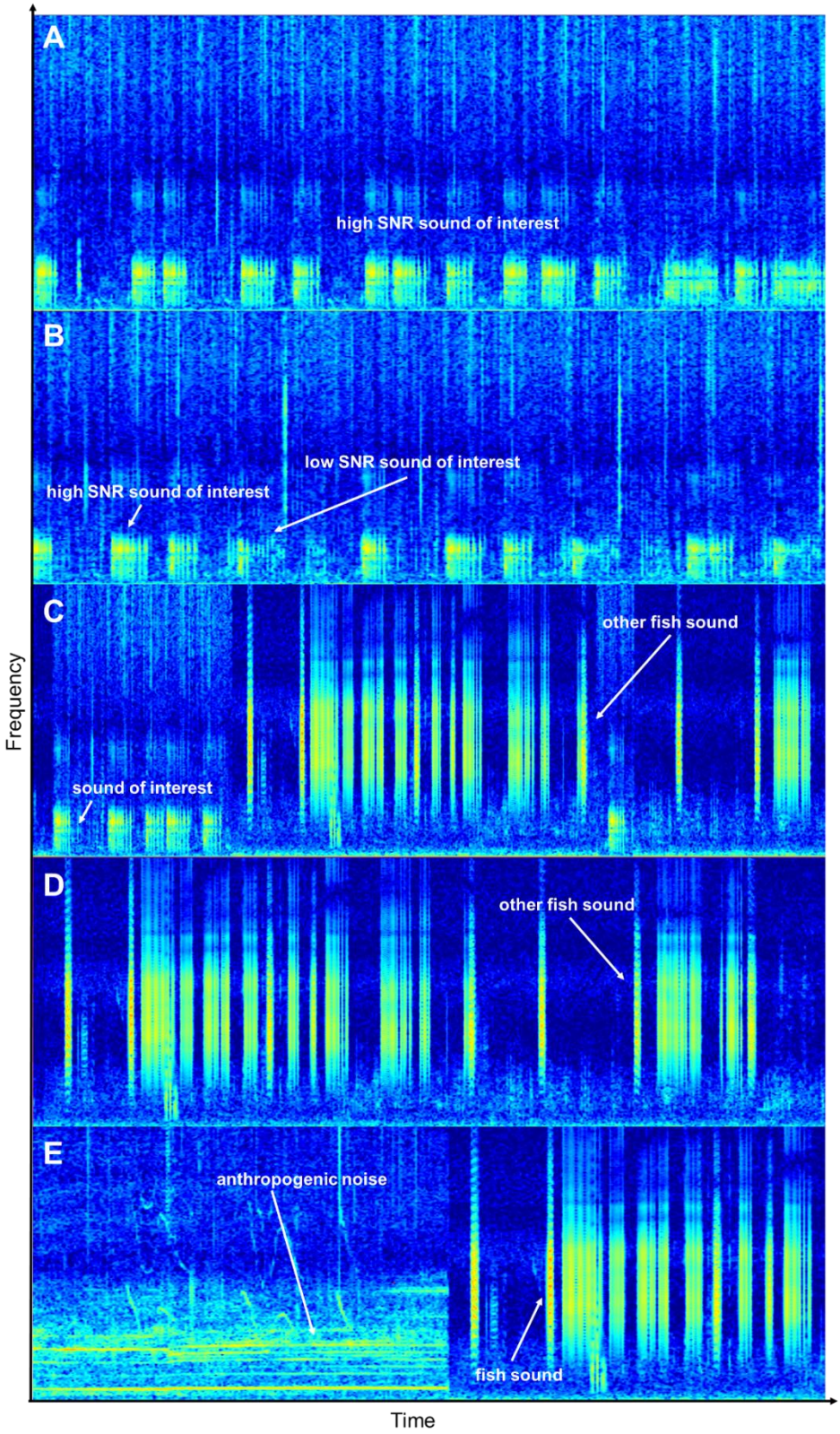

Figure SP10 - 1 Conditions employed to test the detection algorithm: (A) only high SNR sounds of interest, (B) a mix of low and high SNR sounds of interest, (C) a mix of sounds of interest and other fish sounds, (D) only other fish sounds, and (E) a mix of fish sounds and anthropogenic noise. SNR = signal-to-noise ratio.

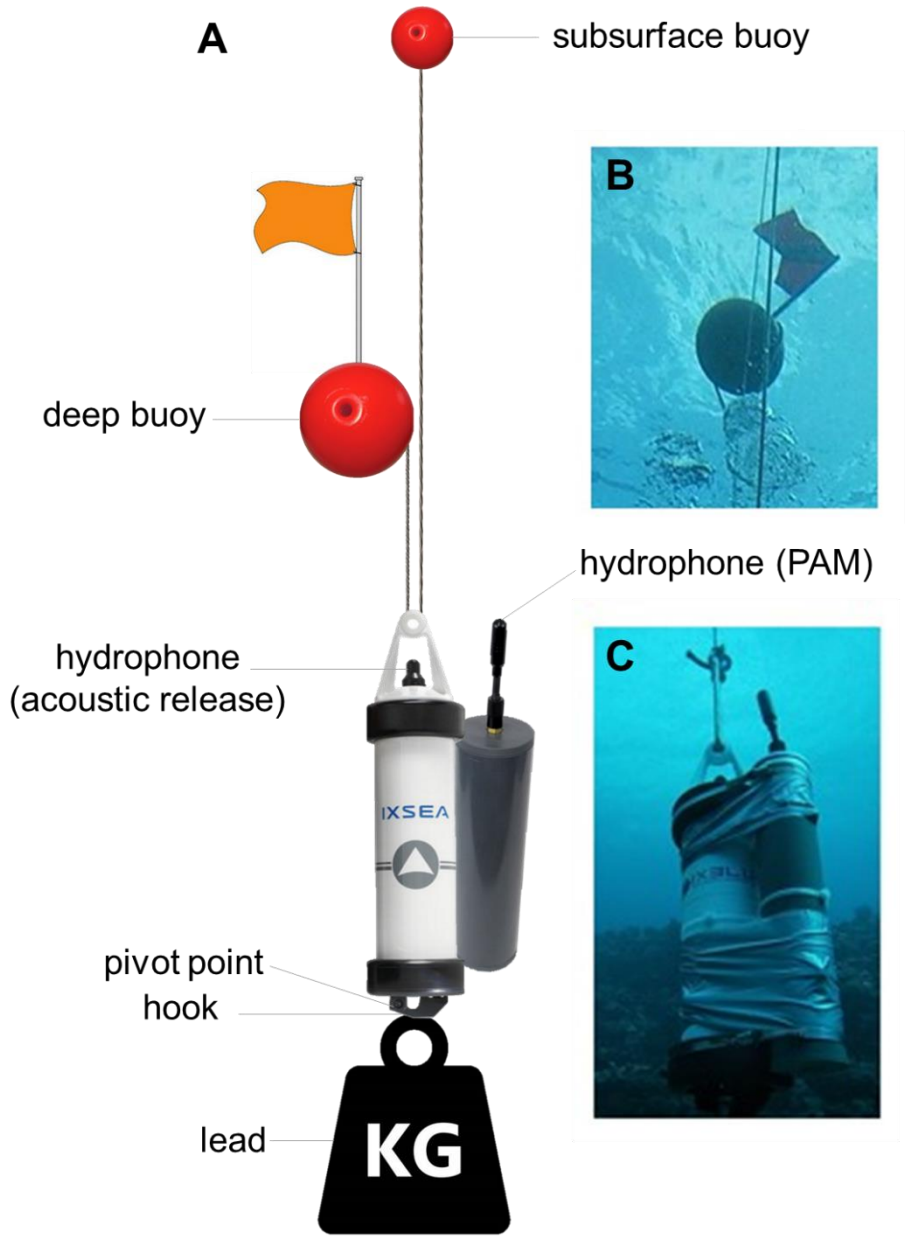

Figure SP10 - 2 Schematization of the acoustic release and the acoustic recorder used to record the biophony at 300 m at Moorea Island. (**B**) Zoom on the deep buoy. (**C**) Zoom on the acoustic release and the acoustic recorder. The picture was taken at a shallower depth for illustration purposes.

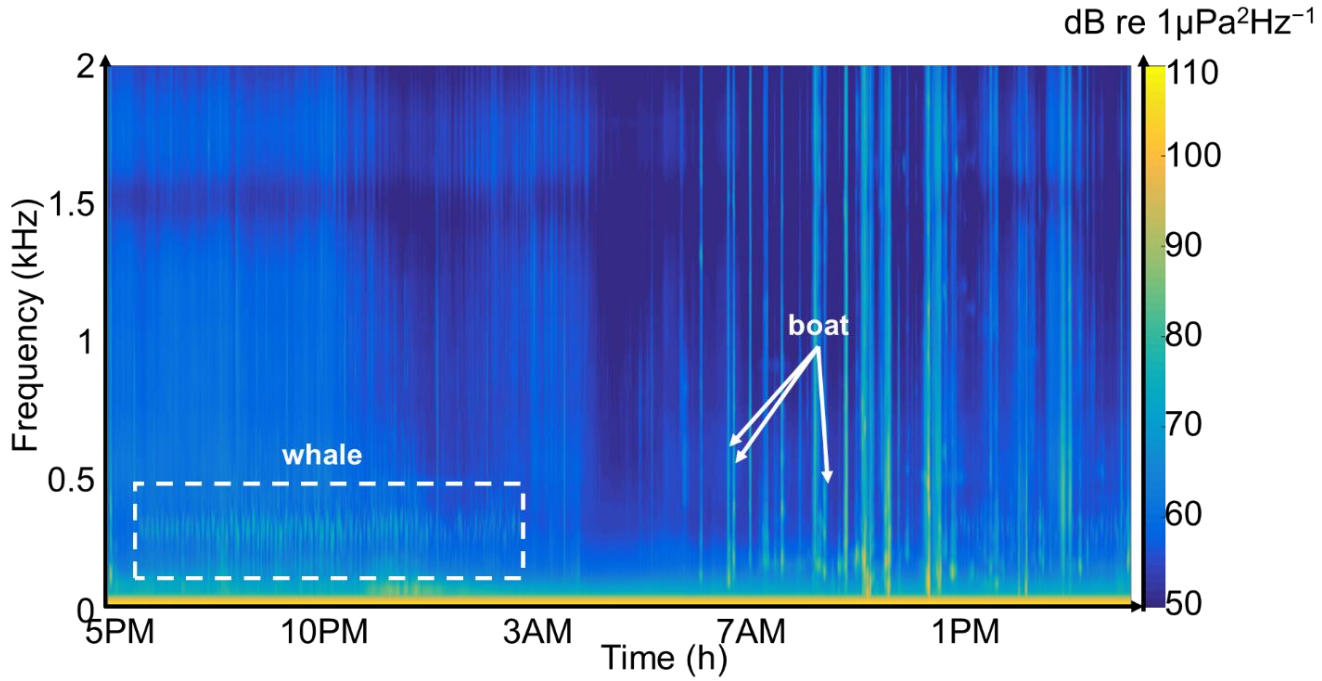

Figure SP10 - 3 Spectrogram of the soundscape under 2 kHz recorded at 300 m at Moorea (24h, from 5PM to 4:59 PM). LFFT = 256, overlap = 75%, window = Kaiser.

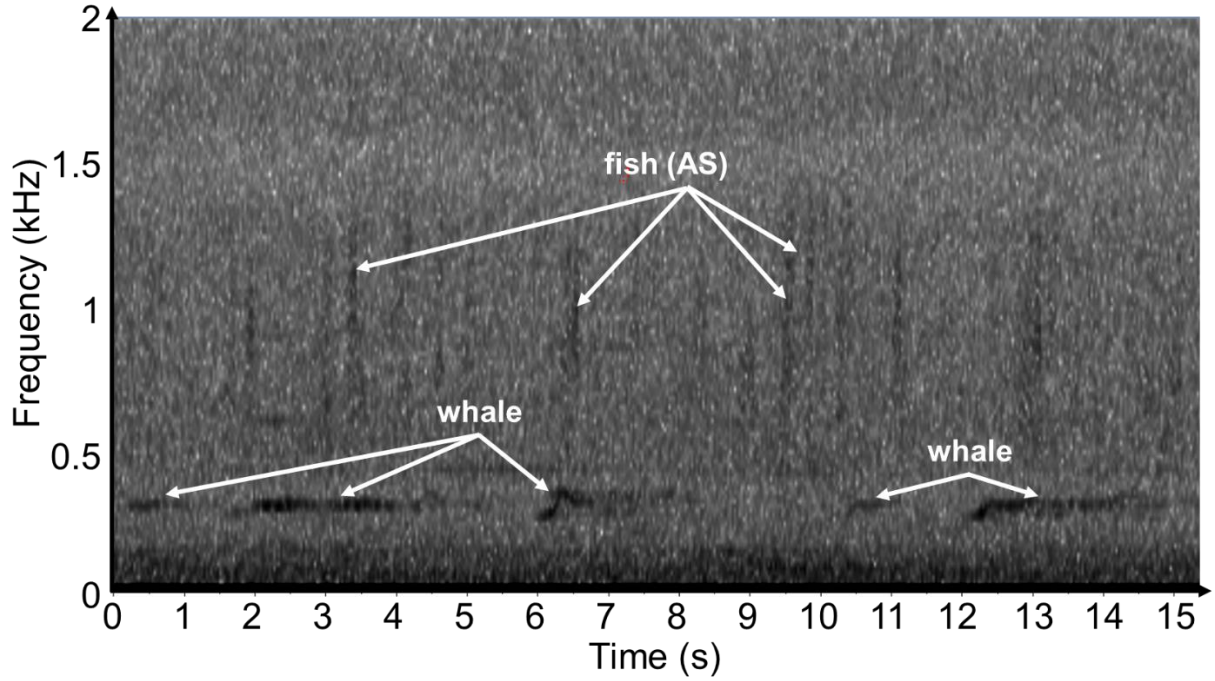

Figure SP10 - 4 Spectrogram of the soundscape under 2 kHz recorded at 300 m at Moorea. FFT = 256.